Methods of Dendrochronology

Applications in the Environmental Sciences

Edited by

E. R. Cook and L. A. Kairiukstis

LUWER ACADEMIC PUBLISHERS

AL INSTITUTE FOR APPLIED SYSTEMS ANALYSIS

THE INTERNATIONAL INSTITUTE FOR APPLIED SYSTEMS ANALYSIS

is a nongovernmental research institution, bringing together scientists from around the world to work on problems of common concern. Situated in Laxenburg, Austria, IIASA was founded in October 1972 by the academies of science and equivalent organizations of twelve countries. Its founders gave IIASA a unique position outside national, disciplinary, and institutional boundaries so that it might take the broadest possible view in pursuing its objectives:

To promote international cooperation in solving problems from social, economic, technological, and environmental change

To create a network of institutions in the national member organization countries and elsewhere for joint scientific research

To develop and formalize systems analysis and the sciences contributing to it, and promote the use of analytical techniques needed to evaluate and address complex problems

To inform policy advisors and decision makers about the potential application of the Institute's work to such problems

The Institute now has national member organizations in the following countries:

Austria
The Austrian Academy of Sciences

Bulgaria
The National Committee for Applied Systems Analysis and Management

Canada
The Canadian Committee for IIASA

Czechoslovakia
The Committee for IIASA of the Czechoslovak Socialist Republic

Finland
The Finnish Committee for IIASA

France
The French Association for the Development of Systems Analysis

German Democratic Republic
The Academy of Sciences of the German Democratic Republic

Federal Republic of Germany
Association for the Advancement of IIASA

Hungary
The Hungarian Committee for Applied Systems Analysis

Italy
The National Research Council

Japan
The Japan Committee for IIASA

Netherlands
The Foundation IIASA–Netherlands

Poland
The Polish Academy of Sciences

Sweden
The Swedish Council for Planning and Coordination of Research

Union of Soviet Socialist Republics
The Academy of Sciences of the Union of Soviet Socialist Republics

United States of America
The American Academy of Arts and Sciences

Methods of Dendrochronology

Applications in the Environmental Sciences

Edited by

E. R. Cook

Tree-Ring Laboratory, Lamont-Doherty Geological Observatory, Columbia University, New York, U.S.A.

and

L. A. Kairiukstis

IIASA, Laxenburg, Austria and Lithuanian Academy of Sciences, U.S.S.R.

KLUWER ACADEMIC PUBLISHERS
DORDRECHT / BOSTON / LONDON

INTERNATIONAL INSTITUTE FOR APPLIED SYSTEMS ANALYSIS

Library of Congress Cataloging in Publication Data

Methods of dendrochronology : applications in the environmental
science / E. Cook and L. Kairiukstis, editors.
p. cm.
Includes bibliographical references.
ISBN 0-7923-0586-8
1. Dendrochronology. 2. Ecology. I. Cook, E. (Edward)
II. Kairiūkštis, Leonardas.
QK477.2.A6M48 1989
582.16'0372--dc20 89-48124

ISBN 0-7923-0586-8

Published by Kluwer Academic Publishers,
P.O. Box 17, 3300 AA Dordrecht, The Netherlands.

Kluwer Academic Publishers incorporates
the publishing programmes of
D. Reidel, Martinus Nijhoff, Dr W. Junk and MTP Press.

Sold and distributed in the U.S.A. and Canada
by Kluwer Academic Publishers,
101 Philip Drive, Norwell, MA 02061, U.S.A.

In all other countries, sold and distributed
by Kluwer Academic Publishers Group,
P.O. Box 322, 3300 AH Dordrecht, The Netherlands.

Printed on acid-free paper

Printed in the Netherlands

Schweingruber : Starkmann Ofe 180.—
11.7.1990

Preface

This book is a review and description of the state-of-the-art methods of tree-ring analysis with specific emphasis on applications in the environmental sciences. Traditionally, methods of tree-ring analysis, or more properly in this case *methods of dendrochronology*, were developed and used for dating archaeological and historical structures and for reconstructing past climates. The classic book *Tree Rings and Climate*, by H.C. Fritts, published in 1976, provided a superb introduction to the science and an in-depth description of techniques useful for extracting climatic information from tree rings. This book, which was published by Academic Press, is sadly out of print and, even though only 12 years old, limited in its methods and applications. This is owing to the extremely rapid development of the science since the 1970s.

Only recently have tree rings as environmental sensors been fully recognized as a valuable tool in detecting environmental change. For example, tree-ring measurements have been critically important in studies of forest decline in Europe and North America. There are also attempts to use tree-ring analysis for ecological prognosis to solve large-scale regional problems including the sustainability of water supplies, prediction of agricultural crops, and adoption of silvicultural measures in response to ecological changes. More speculatively, dendrochronological methods are also used for dating and evaluating some astrophysical phenomena and for indicating possible increase in the biospheric carrying capacity due to increased atmospheric carbon dioxide.

Such a wide range of application of modern dendrochronology beyond its traditional field has resulted in the development of various approaches. This has placed heavy demands on methodological unification and improvement. However, the principles and methods of tree-ring analysis are not widely known by scientists outside the field. In addition, papers on the application of tree-ring analysis are not always easily accessible as they are scattered in a wide range of journals, many of which are non-English. Therefore, an attempt to meet these

demands is being made through international cooperative efforts among the International Institute for Applied Systems Analysis (IIASA) and leading dendrochronological bodies, such as the International Tree-Ring Data Bank (ITRDB), the Dendrochronological Commission of the Academy of Sciences of the USSR, the International Project in Dendrochronology (IPID), as well as leading dendrochronology laboratories in countries around the world.

As a result of these activities, an international network has been established, East–West collaboration of scientists has been fascilitated, several international workshops on dendrochronology (Albena, Bulgaria, 1985; Cracow, Poland, 1986; Irkutsk, USSR, 1987) have been organized, and, finally, this book – an international multi-author monograph, *Methods of Dendrochronology: Applications in the Environmental Sciences* – has been prepared. The book begins by describing the historical development of dendrochronology in countries in the West and East, and in the Northern and Southern Hemispheres. Chapter 2 introduces and defines the most important principles and methods for primary data collection and sample treatment. Chapters 3 and 4 cover the basic principles of tree-ring chronology development and methods of climatic reconstruction. Chapter 5 treats tree-ring/environment interactions and detection. Chapter 6 describes applications of dendrochronology in the study of future environmental changes. Therefore, this book fills existing gaps by bringing together, in one volume, an updated range of principles, concepts, and methods that will introduce the reader to the vast possibilities of tree-ring analysis. The emphasis is on reviewing old and new methods for extracting environmental information from tree rings. Considerable effort has been made to provide examples of the different methods especially when they are new or not well known.

The book is international in scope. Each chapter includes contributions from several scientists around the world with experience in the Northern and Southern Hemispheres. Scientists from the United States, the Soviet Union, the United Kingdom, the Federal Republic of Germany, and France are chapter leaders.

The authors and editors hope that this book will become a reference for foresters, climatologists, and broad-profile environmental scientists who are interested in applying the techniques of tree-ring analysis. As the importance of the science continues to expand in parallel with increasing global concerns about anthropogenic alterations of the environment, this book should appeal to a wide audience.

This publication on dendrochronology so wide in scope, particularly with respect to the East–West dimension, is a first, and the authors and editors are aware that some gaps or inequalities in the reviews of separate methods or preferences given to their applications may occur. That is why a truly international bibliography is included to direct readers to the most recent data sources or method descriptions, and to provide more in-depth reading for the interested scientist.

The editors remain indebted to colleagues at IIASA, particularly to Olivia Völker. Also, we are grateful for the help provided by two tree-ring laboratories in the USA: Lamont-Doherty Geological Observatory (G.C. Jacoby) of Columbia University and the University of Arizona Laboratory of Tree-Ring Research (H.C. Fritts, W.J. Robinson, and M.K. Hughes). In addition, we are indebted to colleagues from the Dendroclimatological Commission of the Academy of Sciences of the USSR, who have played a very important role in the preparation of this book.

The following people deserve special mention for their important contributions to the development, preparation, and critical review of this book. They are: R.E. Munn, former Leader of the Environment Program, IIASA; T.M.L. Wigley, Director of the Climatic Research Unit, University of East Anglia; and J.R. Pilcher, Palaeoecology Laboratory, Queen's University, Belfast. We are also indebted to J. Barnard, Director of the National Vegetation Survey, and V. Adamkus, Great Lakes National Program Manager of the Environmental Protection Agency, both in the USA, for the financial support that made the final preparation of this manuscript possible.

Leonardas A. Kairiukstis
IIASA, Laxenburg, Austria
on leave from the
Lithuanian Academy of
Sciences, USSR

Edward R. Cook
Tree-Ring Laboratory
Lamont-Doherty
Geological Observatory
Columbia University, New York, USA

Contents

Preface v

1. Some Historical Background on Dendrochronology
W.J. Robinson, E. Cook, J.R. Pilcher, D. Eckstein, L. Kairiukstis, S. Shiyatov, and D.A. Norton 1

1.1. Dendrochronology in Western North America: The Early Years
W.J. Robinson 1
1.2. Dendrochronology in Eastern North America
E. Cook 8
1.3. Dendrochronology in Western Europe
D. Eckstein and J.R. Pilcher 11
1.4. Dendrochronology in the USSR
L. Kairiukstis and S. Shiyatov 13
1.5. Dendrochronology in the Southern Hemisphere
D.A. Norton 17

2. Primary Data
Chapter Leader: J.R. Pilcher
Chapter Contributors: F.H. Schweingruber, L. Kairiukstis, S. Shiyatov, M. Worbes, V.G. Kolishchuk, E.A. Vaganov, R. Jagels, and F.W. Telewski 23

2.1. Sample Selection
F.H. Schweingruber, L. Kairiukstis, and S. Shiyatov 23
2.2. Site and Sample Selection in Tropical Forests
M. Worbes 35

2.3. Sample Preparation, Cross-dating, and Measurement
J.R. Pilcher 40
2.4. Dendroclimatological Study of Prostrate Woody Plants
V.G. Kolishchuk 51
2.5. Radiodensitometry
F.H. Schweingruber 55
2.6. The Tracheidogram Method in Tree-Ring Analysis and Its Application
E.A. Vaganov 63
2.7. Computer-Aided Image Analysis of Tree Rings
R. Jagels and F.W. Telewski 76
2.8. Radioactive Isotopes in Wood
J.R. Pilcher 93

3. Data Analysis
Chapter Leaders: E. Cook and K. Briffa
Chapter Contributors: S. Shiyatov, V. Mazepa, and P.D. Jones 97

3.1. Introduction
E. Cook and K. Briffa 97
3.2. A Conceptual Linear Aggregate Model for Tree Rings
E. Cook 98
3.3. Tree-Ring Standardization and Growth-Trend Estimation
E. Cook, K. Briffa, S. Shiyatov, and V. Mazepa 104
3.4. Estimation of the Mean Chronology
E. Cook, S. Shiyatov, and V. Mazepa 123
3.5. Correcting for Trend in Variance Due to Changing Sample Size
S. Shiyatov, V. Mazepa, and E. Cook 133
3.6. Basic Chronology Statistics and Assessment
K. Briffa and P.D. Jones 137
3.7. A Comparison of Some Tree-Ring Standardization Methods
E. Cook and K. Briffa 153

4. Methods of Calibration, Verification, and Reconstruction
Chapter Leaders: H.C. Fritts and J. Guiot
Chapter Contributors: G.A. Gordon and F. Schweingruber 163

4.1. Introduction
H.C. Fritts 163
4.2. Methods of Calibration
J. Guiot 165
4.3. Verification
H.C. Fritts, J. Guiot, and G.A. Gordon 178

4.4. Comparison of the Methods
J. Guiot 185
4.5. Statistical Reconstruction of Spatial Variations in Climate Using 65 Chronologies from Semiarid Sites
H.C. Fritts 193
4.6. Visual Analysis
F. Schweingruber 211
4.7. Conclusions
H.C. Fritts 214

5. Tree-Ring/Environment Interactions and Their Assessment
Chapter Leader: D. Eckstein
Chapter Contributors: J. Innes, L. Kairiukstis, G.E. Kocharov, T.H. Nash, W.B. Kincaid, K. Briffa, E. Cook, F. Serre-Bachet, L. Tessier, D.J. Downing, S.B. McLaughlin, H. Visser, J. Molenaar, F.H. Schweingruber, D.A. Norton, and J. Ogden 219

5.1. Introduction
D. Eckstein 219
5.2. Qualitative Assessment of Past Environmental Changes
D. Eckstein 220
5.3. General Aspects in the Use of Tree Rings for Environmental Impact Studies
J. Innes 224
5.4. Measuring the Chemical Ingredients in Tree Rings
L. Kairiukstis and G.E. Kocharov 229
5.5. Statistical Methods for Detecting Environmental Changes
T.H. Nash and W.B. Kincaid 232
5.6. Methods of Response Function Analysis
K. Briffa and E. Cook 240
5.7. Response Function Analysis for Ecological Study
F. Serre-Bachet and L. Tessier 247
5.8. Detecting Shifts in Radial Growth by Use of Intervention Detection
D.J. Downing and S.B. McLaughlin 258
5.9. Detecting Time-Dependent Climatic Responses in Tree Rings Using the Kalman Filter
H. Visser and J. Molenaar 270
5.10. Dendroecological Information in Pointer Years and Abrupt Growth Changes
F.H. Schweingruber 277
5.11. Problems with the Use of Tree Rings in the Study of Forest Population Dynamics
D.A. Norton and J. Ogden 284

6. Tree Rings in the Study of Future Change 289
Chapter Leaders: L. Kairiukstis and S.G. Shiyatov
Chapter Contributors: G.E. Kocharov, V. Mazepa, J. Dubinskaite, E. Vaganov, T. Bitvinskas, and P.D. Jones

6.1. Tree Rings: A Unique Source of Information on Processes on the Earth and in Space 289
G.E. Kocharov
6.2. Outline of Methods of Long-Range Prognosis on the Basis of Dendrochronological Information 296
L. Kairiukstis and S.G. Shiyatov
6.3. Spectral Approach and Narrow Band Filtering for Assessment of Cyclic Components and Ecological Prognoses 302
V. Mazepa
6.4. Harmonic Analysis for Ecological Prognoses 308
L. Kairiukstis and J. Dubinskaite
6.5. Examples of Dendrochronological Prognoses 323
L. Kairiukstis, E. Vaganov, and J. Dubinskaite
6.6. Prognosis of Tree Growth by Cycles of Solar Activity 332
T. Bitvinskas
6.7. Possible Future Environmental Change 339
P.D. Jones

Appendix A 341
Appendix B 345
Appendix C 349
References 351
The Authors 393

CHAPTER 1

Some Historical Background on Dendrochronology

Chapter Contributors: W.J. Robinson, E. Cook, J.R. Pilcher, D. Eckstein, L. Kairiukstis, S. Shiyatov, and D.A. Norton

1.1. Dendrochronology in Western North America: The Early Years

W.J. Robinson

The systematic study of tree rings in western North America began with an intuitive insight by an astronomer, Andrew Ellicott Douglass. He was, before the turn of the 20th century, working at the Lowell Observatory in Flagstaff, Arizona, and was interested in the cyclic nature of solar activity, particularly sunspots, and its relation to terrestrial climate. Since the written record of solar activity extended further back in time than the record of terrestrial weather, he envisioned tree growth as a proxy measure of climate. Douglass' investigation began in 1901 and was based on the following premises: that the rings of a tree are a measure of its food supply; that the food supply depends largely on the amount of available moisture, especially in drier climates where the quantity of moisture is limited and the life struggle of the tree is against drought rather than competing vegetation; and that therefore the rings are a measure of precipitation (Douglass, 1914, page 321). His method involved first the preparation of a tree-growth curve, and for this purpose pine (*Pinus*) trees growing in the environs of Flagstaff were chosen. In addition to convenience, these trees had two obvious advantages. First, the moisture available to the trees was primarily in the form of precipitation and, second, the average age of the trees was nearly 350 years, with some more than 500 years old (Douglass, 1914, page 322). This latter quality allowed a large backward extension of the growth curve in the record of a single tree.

As he worked on the growth curve, Douglass noticed that the same pattern of thick and thin rings could be identified in different trees that grew during the

E. R. Cook and L. A. Kairiukstis (eds.), Methods of Dendrochronology, 1–21.

same time period. He also noticed that the same patterns were evident in trees growing near Prescott, Arizona, which was nearly 100 miles southwest of Flagstaff and more than 300 m lower in elevation. The recognition of the recurrent patterns in the rings was the first step in the formation of the fundamental principle of all tree-ring investigation, which is referred to as cross-dating.

Cross-dating was first established experimentally by Douglass in 1904 when he recognized the ring pattern in a dead stump that allowed him to specify the actual date of cutting – a fact that was verified by the man who had cleared the land. For the next decade Douglass continued his work on rings as climatic indicators and on the establishment of long growth curves. He succeeded in cross-dating living trees growing as far away as southern Arizona (Douglass, 1914, page 325) and devoted much effort in the investigation of the Sequoia of California, which at that time held promise of extremely long growth records. It was during this period that Douglass' long association with the University of Arizona began in 1906.

At the end of this period of the development of the basic principle of dendrochronology, the cross-dated sequence extended back in time nearly 500 years, based mainly on Flagstaff-area trees.

Archaeological Studies

Although Douglass never lost sight of tree growth as a climatic indicator, an event occurred in 1914 that led him off on a tangent. This was the potential application of the dating of tree growth to past events in man's history. In that year Douglass delivered a paper to the Carnegie Institution of Washington on the relationships between tree growth and climatic cycles. The substance of the paper came to the attention of Clark Wissler of the American Museum of Natural History who offered Douglass some beams for his general inspection (Douglass, 1935a, page 10). These materials were received in 1916 and were sections of living trees growing near prehistoric ruins. As a result of his examination of the sections, Douglass became convinced that trees from as far as northwestern New Mexico had a potential of cross-dating with his Flagstaff trees (Douglass, 1921, page 27).

A few years later Earl H. Morris sent Douglass a small selection of prehistoric beams from the Aztec Ruin and from Pueblo Bonito in Chaco Canyon. The sections from Aztec were immediately cross-dated among themselves, but not those from Pueblo Bonito. In hopes of obtaining an exact age correspondence of the Aztec beams, Douglass tried futilely to match them to the three-millennia Sequoia record. Later in 1919, Douglass visited Morris at the Aztec Ruin and secured 37 additional specimens. These, with the original pieces, formed the basis for the first relative, often referred to as *floating*, chronology. As a result of this initial success, Douglass formulated the dating technique that ultimately proved successful. In a letter to Wissler in 1919, he stated that the technique "consists in obtaining groups of timbers of different ages so that one group will overlap another, and after combining them by cross-dating, we may bridge over a great many hundred years in the past." Wissler's response to this

suggestion was to send more beams from Pueblo Bonito, collected many years earlier during excavations by the Hyde Expedition. Without undue effort these sections cross-dated well with each other.

But a great step forward was achieved when it was found that the Pueblo Bonito logs cross-dated with the sections from Aztec. Thus Douglass was able to announce that Aztec was constructed 40 to 45 years later than Pueblo Bonito (Douglass, 1921, page 28).

In 1922, Neil M. Judd, who had begun work under the National Geographic Society auspices at Pueblo Bonito the previous year, encouraged the Society to support the approach that Douglass had suggested in 1919. Thus a program was established to gather successively older groups of beams back from the present with the specific objective of dating Pueblo Bonito (Judd, 1930, pages 169–171).

The First Beam Expedition, sponsored by the National Geographic Society, operated in 1923 under the field leadership of J.A. Jeancon, of the State Historical and Natural History Society of Colorado, and O.G. Ricketson, of the Carnegie Institution of Washington. They collected about 100 beam specimens from the Hopi Mesas to the Rio Grande and to Mesa Verde. Douglass in the meantime obtained additional beams from Wupatki, a ruin north of Flagstaff, Arizona. It was hoped that the sections from the Hopi villages and from the mission churches would cross-date at the early end of the chronology developed from living trees and, in turn, extend back far enough to cross-date with the outer rings of the prehistoric specimens. Although the desired result was not immediately achieved, it was recognized by the nature of the cross-dating of many of the specimens that the entire area of collection acted as a climatic unit in regard to tree growth. This cross-dating also resulted in placing other ruins within the relatively dated chronology first developed from the Aztec and Pueblo Bonito beams. One ruin so placed was Wupatki. The link with the living-tree chronology remained elusive, however.

In addition, a second relative or floating chronology was developed from Wupatki specimens that did not immediately cross-date with the established relative chronology. This was termed *Citadel dating*, as it included the ring record of a specimen from the Citadel, a ruin near Wupatki. Other ruins also fit into this second chronology, including samples from Mummy Cave Tower in Canyon de Chelly and sections from the classic cliff dwellings of Mesa Verde.

This second chronology was approximately 140 years long without any suggestion of its proper placement in time. On the basis of ceramic seriation, however, Judd assured Douglass that it should fall between the living-tree chronology and the one developed from Aztec and Pueblo Bonito beams.

As analyses proceeded on the collections made by the First Beam Expedition, more and more specimens gradually yielded to cross-dating within one or the other of the two relative chronologies. These two were ultimately merged, in 1928, to form a single chronology of prehistoric ruins with a length of 585 years. The status of chronology building in early 1928 consisted of two long records. The absolute chronology extended from the present back to about 1400 with confidence, and weakly – because it was based on few trees – to about 1300. The other was a floating chronology of 585 years of unknown absolute age based on specimens from approximately 30 prehistoric ruins.

In an attempt to strengthen the chronology before 1400, the Second Beam Expedition was organized in the summer of 1928 under the field supervision of Lyndon L. Hargrave. Because it was already known that material in the early end of the known time scale was present at the Hopi Village of Oraibi, the expedition concentrated on early historic beams throughout the Hopi villages. Emphasis was placed on the abandoned sections of Oraibi and on beams that exhibited stone-ax-cut ends. In all, more than 200 specimens were collected from Oraibi and other Hopi villages.

Because the chronology had already been developed for most of the period represented by the new specimens, more than 140 were quickly cross-dated by Douglass into the known sequence, and he succeeded in extending the chronology back to near 1300 with confidence. A single specimen seemed to carry the series even farther back to about 1260. Still no cross-dating was evident with the floating chronology of the prehistoric ruins.

Toward the end of the summer Hargrave collected from ruins in the Jeddito area, just east of the Hopi villages, with the hope that the material there would predate Oraibi. Earl H. Morris was excavating at Kawaikuh and was encouraged to look for and send back charcoal or wood from his excavations to Douglass. In October of that year a piece of charcoal from Morris' excavations cross-dated with the living-tree series in the 15th century. Thus, Kawaikuh has a double distinction: it was the first prehistoric ruin tied to calendar dates by the tree-ring method, and it provided the first charcoal for dating. This latter success opened up a new and less-restrictive source of material.

Shortly afterward, material from three other ruins was successfully cross-dated into the known chronology. These were Turkey Hill near Flagstaff, Kokopnyama in the Jeddito area, and Chaves Pass southeast of Flagstaff.

The Second Beam Expedition, then, provided the first prehistoric ruin dates and served to extend and strengthen the known chronology, but no overlap was yet established with the 585-year-long relative chronology that included the chronology from Pueblo Bonito.

It was evident by the end of 1928 that the collection of the proper material to close the gap, as it became known, would have to change from more or less random, easily obtainable, collections to excavation. Late in the 1928 Beam Expedition much attention was paid to the pottery assemblage of the sites, and it soon became evident to Hargrave, Judd, and Douglass that the latest sites in the relative dating chronology were characterized by red background polychrome pottery, whereas the earliest sites in the known chronology had orange and yellow background pottery. The search was then on for sites that fulfilled a threefold qualification: first, a site must be ceramically placed between ruins with orange and yellow pottery at the early end of the known chronology and the latest prehistoric ruins such as Kiet Siel, in Tsegi Canyon, with red background polychrome; second, a site must contain evidence of burning in order for preservation to be possible in the form of charcoal; and third, a site must lie in or near pine forests. Of all the candidates, the ruins at Pinedale, Showlow, Kin Tiel, and Kokopnyama were chosen as the most likely.

Excavations were begun in June 1929 at the Showlow Ruin by Hargrave and Emil W. Haury (Haury, 1962, page 12). On completing that work, Haury

went on to excavate at the Pinedale Ruin while Hargrave undertook Kin Tiel and Kokopnyama (Haury and Hargrave, 1931).

The solution to the problem came soon. Toward the end of June, Douglass and Judd visited Haury and Hargrave at Showlow to check on the progress. One charred log, designated in the field as HH-39, seemed very promising. It had an outside ring near 1380 and extended back to 1237 (Haury, 1962, page 13). It did not, however, immediately cross-date with the prehistoric sequence. That night Douglass, whose memory for ring sequences was phenomenal, mentally reviewed HH-39 against the known and relative chronologies and by the next morning was satisfied that it cross-dated with the relative chronology in such a way that the gap was closed between the two series. Actually, no gap had existed. Rather, an overlap of about 25 years had been present but unrecognized because only one specimen (BE-269) on the known chronology extended inside 1300 and because of the extreme variability of the growth pattern between 1276 and 1299 – a period soon characterized as the Great Drought. Later many pieces of charcoal from both Showlow and Pinedale verified the merging of the two series and strengthened this segment of the total chronology.

Thus, nearly 40 prehistoric Southwestern ruins were dated in terms of the Christian calendar (Douglass, 1935a, pages 41–45), and an absolute chronology was developed based on tree-ring patterns from 1929 back to about 700.

Since the joining of the two chronologies into a single one of over 1,200 years, much of the effort of the succeeding years has been directed toward extending the chronology back in time and toward strengthening and detailing many segments of the established chronology. Both efforts have helped to date thousands of prehistoric ruins.

Shortly after the gap was closed a charcoal specimen was submitted by Morris in 1931 from the LaPlata district (Morris, 1939) that bound together several short floating chronologies into a longer, but unplaced, series of 356 years. As has happened so many times before and after, this floating chronology did not cross-date with any known sequence. Shortly thereafter, however, in 1932, a piece from the ruin of Chetro Ketl in Chaco Canyon was dated from roughly A.D. 650 to 800 and, on its inner series, cross-dated with the unplaced series. This, then, extended the continuous chronology back to 475. The cross-dating was confirmed by an excellent specimen excavated from a ruin at Allantown, Arizona.

As early as 1927 Douglass had recognized yet another floating chronology, which he termed the *Early Pueblo dating* based on specimens from Mummy Cave in Canyon del Muerto (Douglass, 1946, page 9). Further collections were made in 1930 and 1931 by Morris from Mummy Cave and from caves – notably Broken Flute and Obelisk – in the Red Rock district of northeastern Arizona. These were high-quality datings and soon allowed Douglass to identify the ring patterns in the known chronology and again make a leap back to A.D. 11. Thus by 1933 the tree-ring chronology in southwestern USA had attained a length of nearly 2,000 years.

The last significant work until recently on the backward extension was achieved by Edmund Schulman. Just before World War II, Douglass received a number of specimens from Morris from very early sites in the area of Durango,

Colorado (Morris and Burgh, 1954). Although Douglass was able to date some of these back to the first few centuries A.D., the war interrupted complete analysis. After the war Schulman took up the work where Douglass had left it (Schulman, 1949a, 1949b). Schulman's work was greatly aided by a long piece from Mummy Cave that extended the known chronology to 59 B.C. Although this piece still held the distinction of containing the oldest dated ring, its series allowed placement of many of the specimens from the Durango area. As a consequence, the earliest outside, and therefore archaeological, date was placed at 20 B.C., and the earliest established bark, or actual death, date at A.D. 46 (Schulman, 1952a).

In the midst of this activity, the Laboratory of Tree-Ring Research was formally established at the University of Arizona in December 1937. Douglass was joined by Haury, Anthropology, and E.F. Carpenter, Astronomy, on the initial staff. Douglass continued to serve as Director nearly until his death in 1962 as both research interests and staff grew with increasing applications of dendrochronology.

In the two decades between 1930 and 1950, other individuals and institutions also became involved in tree-ring studies in western North America, particularly from the archaeological point of view. At the Museum of Northern Arizona, John C. McGregor, who had been trained by Douglass, engaged in independent tree-ring studies from 1930 to 1940. Basing his work on that begun by Douglass in the areas around Flagstaff and in the Tsegi Canyon (Marsh Pass area), McGregor (1934, 1936a, 1936b, 1938) established chronologies and dated many ruins under investigation by the Museum of Northern Arizona.

Douglass recognized certain discrepancies in the ring patterns of material from east of the Continental Divide in New Mexico as early as the First Beam Expedition. He suggested, therefore, shortly after 1930 that an independent chronology-building program should be based at a New Mexico institution to pursue the so-called Rio Grande chronology with the same methodology that had culminated in success west of the Divide. W.S. Stallings, Jr., another of Douglass' students, was soon at work at the Laboratory of Anthropology in Sante Fe. He used the method suggested and started to build back from growing trees to Spanish missions and historic pueblos, to late-prehistoric ruins, and so on. Stallings began in 1931 and, perhaps because of the lessons in chronology building already learned, had soon extended the Rio Grande chronology back to A.D. 930 (Stallings, 1939, page 16). Again, World War II interfered with the research program, and the study of Stallings' collection was continued and completed by Smiley, Stubbs, and Bannister (1953).

The fourth and last institution to engage seriously in tree-ring studies was Gila Pueblo in Globe, Arizona, under the direction of Harold S. Gladwin. The first dating of material was done by Haury (1931, 1934, 1936) using Douglass' methods. Soon, however, Gladwin embarked on different techniques inspired by his lack of confidence in, and inability to use, Douglass' methods (Gladwin, 1940, page 9). He was concerned mainly with employing subjective judgments on relative ring widths and sought a more quantitative method of recording and manipulating ring widths. These efforts led to a series of disputes with archaeological sequences and chronological associations that had been established by followers

of Douglass (Gladwin, 1943, 1944, 1946, 1947); however, Douglass never directly refuted the methods used by Gladwin. Nevertheless, Douglass' methods have survived the test of time and are in general use today.

Most of the dating work produced by Gladwin and those associated with his method was never published. A large collection of tree-ring specimens was accumulated at Gila Pueblo through excavation and, in 1940 and 1941, through the collection activities of Deric O'Bryan, then a member of the Gila Pueblo staff.

By 1950 all these institutions had ceased their efforts in tree-ring dating, and ultimately the collections were transferred to the Laboratory of Tree-Ring Research for preservation and further analysis. As a result of the efforts of the Laboratory of Tree-Ring Research, only Smiley (1951, page 6) was able to compile tree-ring data that listed more than 5,600 individual dated specimens from 365 southwestern sites. This valuable work served for more than a decade as the basic reference to prehistoric chronology in southwestern USA. Three years later, a similar summary was published (Smiley, Stubbs, and Bannister, 1953) based on the collections made by Stallings for the Laboratory of Anthropology and concentrated on the northern Rio Grande.

Dendroclimatic Studies

Douglass maintained his interest in sunspots and weather cycles throughout his long career. His paper (Douglass, 1914) on estimating rainfall by the growth of trees was only the first of many publications revealing his continuing efforts. A review of his bibliography (Anonymous, 1962, pages 5–10) lists numerous works related to tree rings and climate. These researches were most fully explicated in a monumental book series entitled *Climatic Cycles and Tree Growth* (Douglass 1919, 1928, 1936).

Beginning in 1932, Douglass was joined at the University of Arizona, first as a student and later as a colleague, by Schulman. He aided Douglass at first with the development of the methods of tree-ring analysis, but soon shifted his interests to dendroclimatic work. Schulman twice returned to Harvard University for advanced degrees (1938–1939; 1942–1944) where his doctoral thesis was on a precipitation and runoff reconstruction for the Colorado River basin.

Schulman, in his way, was a pioneer in two areas of dendrochronology. The focus on dendrohydrology evidenced in his Harvard thesis was presented extensively (Schulman, 1945a) for the Colorado River basin and supplemented by similar studies for the South Platte River basin (Schulman, 1945b), southern California (Schulman, 1950), and the Bryce Canyon area of southern Utah (Schulman, 1950). He was the first to apply methods of analysis in tree-ring studies with climatic reconstruction as a direct goal. Given the nature of instrumented records at the time and his emphasis on drought-sensitive sites and trees, it is logical that his reconstructions were limited to precipitation and stream flow.

Throughout his career, Schulman advocated a fundamental advance in dendroclimatology involving the derivation of more reliable and extensive tree-ring data. His strategy for the "successive 'improvement' of tree-ring indices" was

"(1) the finding and sampling of trees with ring growth more sensitive to fluctuations in the limiting climatic variable, (2) an increase in the number of such sampled trees, and (3) an increase in the length of the individual tree records" (Schulman, 1956, page 7). This led him, in the late 1940s, to extensive field collection in western North America and as far away as South America. The culmination of these years was Schulman's discovery of the bristlecone pine (*Pinus aristata*) in California, still acknowledged as the world's oldest living trees. Unfortunately, Schulman's premature death left exploitation of the bristlecone to others.

Thus, this development period in dendrochronology – from its beginning with cross-dating to its end with the death of Douglass and Schulman – provided a firm foundation in data, methods, and analyses that still forms the basis for dendrochronology in western North America.

1.2. Dendrochronology in Eastern North America
E. Cook

The earliest account of tree-ring analysis in eastern North America is that of Stewart (1913). He studied the annual rings of a single oak (*Quercus*) tree growing in New York. He noted a correspondence between annual growth and June–July precipitation. No relationship could be found for temperature however.

Douglass (1919), while passing through New England, collected 11 increment cores from hemlock (*Tsuga*) trees growing in central Vermont. He identified cross-dating between the trees and constructed an average ring-width chronology. However, he failed to identify a relationship between the tree rings and precipitation.

Marshall (1927) correlated decadal means of hemlock radial growth and annual precipitation data collected in Massachusetts. Using hemlock growth rates from a well-drained site, he found a correlation coefficient of 0.70. For hemlock growing on a poorly drained site, the correlation was −0.06.

In 1935, Charles J. Lyon initiated a very intensive period of tree-ring research in the northeast with the paper entitled "Rainfall and Hemlock Growth in New Hampshire." He obtained two hemlock cross sections, cross-dated each to assure correct dating, and constructed an average ring-width chronology based on three radii per section. Lyon found that his chronology cross-dated well with Douglass' Vermont series. He also noted a strong visual agreement between the annual variation in his ring series and April–August total rainfall for the years 1857–1927.

Lyon (1936) expanded his previous study to include a total of six hemlock site chronologies from Vermont and New Hampshire. Despite a noted diversity in site characteristics, he found strong cross-dating among all six series. He, again, identified a direct relationship between April–August rainfall and annual growth. Lyon concluded that the hemlocks were responding to the regional physiological dryness of the growing season.

Lyon (1939) defined several objectives and methods of tree-ring research in New England. He stressed that cross-dating is the key for developing a chronology that is free of dating errors and is based on trees with a similar growth response to climate. He strongly advocated that replicated measurements be made along three radii of each specimen to average out any lack of circuit uniformity.

These six studies represent some of the pioneering work that helped establish the feasibility of doing tree-ring research in the eastern temperate forests of North America.

Site Selection Studies

The development of site-selection criteria for tree-ring research in temperate, forested regions has yet to be fully studied. Lyon (1939) suggested that, based on his experience, almost any trees other than those growing in swamps were potentially usable for dendrochronological studies in New England.

Avery, Creighton, and Hock (1940) compared the ring-width chronologies of hemlock trees growing on adjacent wet and well-drained sites. They found that while the trees on the moist site consistently produced wider rings than those on the more xeric site, the two groups of trees cross-dated well.

Lutz (1944) analyzed radial sections of white pine (*Pinus strobus*) and hemlock trees growing in a swamp in Connecticut. He found that cross-dating existed both within and between the species. He also noted that he could cross-date the trees with the same species growing on sites in Massachusetts and New Hampshire. Lutz concluded that swamp-grown trees could be used as dendrochronologic material in the northeast.

Lyon (1949) compared the ring-width patterns of white pines growing in bog and upland environments in New Hampshire. He noted that prior to major release from growth suppression, the bog trees tended to produce wide or narrow rings a year before or a year after the upland trees. However, after release the bog-tree chronology cross-dated perfectly with the upland-tree chronology. Lyon hypothesized that changes affecting root aeration in the bog after release may have altered the trees' growth response to climate.

Dendroclimatic Studies

Goldthwait and Lyon (1937) studied the secondary growth of white pine from four sites in New England in relation to water supply. They found that radial growth correlated best with precipitation during the growing season. They noted that only in years of pronounced drought or rainfall abundance did this relationship consistently hold up, however.

Schumacher and Day (1939) used some advanced statistical techniques to identify significant relationships between radial growth and monthly precipitation. Using, among others, a hemlock chronology supplied by Lyon, they removed the non-climatic growth trends from the data with a polynomial curve. The resulting residuals served as the dependent variable for subsequent regression analysis. The independent variables were derived from monthly

precipitation records of growth from the prior June to the current August. Specifically, they were the coefficients of sixth degree orthogonal polynomials fit to each 15-month rainfall period for the years 1836–1855 and 1868–1934. The authors were unable to identify any significant precipitation effect on hemlock radial growth, although they did note that additional rainfall during the previous July–August and current July months tended to augment the current annual ring. They felt that the unusual tolerance of hemlock to competition may have "overshadowed the benefit of precipitation rather thoroughly."

Lyon (1940) studied the relationship between the tree-ring chronologies of six species and monthly temperature and precipitation data. He developed chronologies for black pine (*Pinus nigra*), Scots pine (*P. sylvestris*), Norway spruce (*Picea abies*), European larch (*Larix decidua*), white pine (*P. strobus*), and red oak (*Quercus rubra*), all based on a minimum sample of five trees – three radii per tree. After constructing a mean ring-width chronology for each species, Lyon fit a growth-trend line to the data to standardize each series and remove non-climatic noise. He then used the standard correlation coefficient to identify significant relationships between tree growth and climate. Lyon found that red oak, Scots pine, and white pine growth correlated significantly with April–August total precipitation. He also found that precipitation of the previous September–November period had some impact on growth, particularly for white pine. Surprisingly, no precipitation effect could be found with the other species. March–April mean temperature proved to be the most significant temperature variables for all species except oak.

Meyer (1941) used analysis of variance to partition the ring-width variation owing to climate from non-climatic factors for two hemlock chronologies developed from sites in northern Pennsylvania. He found that only 19.5% and 17.5% of the annual growth fluctuations were in common with all specimens within the sites. But of this remaining common variance, 91.0% and 79.2% were due to what he thought to be fluctuations in weather. Meyer then attempted to identify some significant growth–climate relationships. Surprisingly, he could find none.

Lyon (1943) studied the annual growth rates of white pine and hemlock in relation to water supply around Boston, Massachusetts. After constructing an average ring-width chronology for 11 sites, he compared the growth departures with nearby precipitation data using a simple sign test. For white pine, the best relationship proved to be with May–July total precipitation. Hemlock response proved to be less well defined. Both May–July and May–August summed rainfall correlated well with radial growth. Additionally, one of the hemlock sites responded strongly to January–July total precipitation. Lyon suggested that factors of exposure, topography, and soil probably determine how important winter precipitation is to a site's growing-season water supply.

Miscellaneous Studies

Lyon (1941) computed the cross-correlation coefficients for 13 hemlock, white pine, and red spruce chronologies from northern New England to study how well the species growth responses were related. He found that the variations in

hemlock and white pine rates were not quite significantly correlated, those in hemlock and red spruce were significantly correlated, and those in white pine and red spruce were almost zero. He concluded that except for the total lack of correlation between white pine and red spruce, the growth departures for all three species tended to be alike.

Schulman (1944) examined the ring series of several tree species growing in the Arnold Arboretum near Boston, Massachusetts. He noted good cross-dating in hemlock trees, but failed to find it in eastern red cedar (*Juniperus virginiana*). Other species lacked sufficient ring-width variation for cross-dating.

Lyon (1946) compared the growth rates of hemlock throughout New England. The agreement among sites was uncertain at best, with only a few years of growth minima found in common. Thus, cross-dating with a structural wood must depend on a few widely scattered rings.

In addition, Lyon (1953) studied the vertical uniformity within hemlock, white pine, and red spruce trees growing in New England. Using graphical and statistical techniques, he demonstrated that a very high degree of ring-width uniformity existed within each species.

These early dendrochronological investigations in eastern North America by Lyon and others provided a sound basis for expanding the science out from the semiarid confines of western North America.

1.3. Dendrochronology in Western Europe

D. Eckstein and J.R. Pilcher

Dendrochronology in Europe can be traced back to the 19th century. The history of dendrochronology for dating applications is recorded in several publications, e.g., by Eckstein (1972), Baillie (1982), and Schweingruber (1983).

From all of its conventional applications, dendrochronology has been used most extensively to study the impact of industrial pollution on the environment. More than 100 years ago, tree-ring analysis was already being used to recognize and quantify forest damage caused by air pollution (Stoeckhardt, 1871). Since then a large number of studies have demonstrated a correlation between atmospheric concentrations of certain pollutants and reductions in increment (Clevenger, 1913; Bakke, 1913). Although it was already known that missing rings are a common feature for trees growing under stress conditions (Hartig, 1891), it was Vinš (1961) who pointed out the necessity of seriously taking them into account. Pollanschutz (1962) used tree-ring analyses to determine the area and the temporal development of forest damage by air pollution. Until that time pollution from point sources such as smelters and refineries near a forest was the only aspect considered to be of importance.

Over the last 10 to 15 years, however, long-range pollution from large numbers of rather small and diffuse sources has become a more urgent problem. It is this pollution that is currently causing widespread concern in Europe and North America. In reality there is a degree of overlap, as a single source may contribute to both local and long-range pollution. The most recent development in the field is not only to take tree-ring width as a measure of tree vitality but

also to include the tree-ring density and the content of heavy metals in the annual xylem layers, and to treat each source of information as a time series.

Dendrochronology in its original narrow sense as a dating method developed more or less independently from environmental studies. In the 1880s the Dutch forester Kapteyn (1914) measured oak (*Quercus*) trees from Holland and Germany and cross-dated them. His chronologies extended back for several centuries. However, it was not until the early 1940s that the German forest botanist Huber (1941) laid the foundation for the further development and systematic application of the method in Europe. Huber could not simply take the method as it was developed by Douglass (1919, 1928). With temperate tree species it proved necessary to measure and plot the width of every ring, because the year-to-year variation is not as pronounced as it is for semiarid zone trees. Huber found that it was not sufficient to rely on narrow rings alone for dating, so he introduced a statistical test of similarity (the Coefficient of Parallel Variation) to back up the visual cross-dating. More recently other statistical aids to cross-dating have been introduced based on correlation coefficients (Baillie and Pilcher, 1973; Aniol, 1983; Munro, 1985; Wigley *et al.*, 1986).

Long-range and wide-area chronologies have been constructed in many parts of Europe. Oak chronologies that include natural subfossil timber extend back many millennia (Becker, 1986; Brown *et al.*, 1986; Leuschner and Delorme, 1984) and their application has been proved from Ireland in the west to Czechoslovakia in the east. These and many other chronologies have been very useful for dating archaeological, architectural, and art–historical objects. The method has also been useful for dating geomorphological processes such as alteration in river valleys. Furthermore, the long European oak chronologies have provided much of the precisely dated timber that has been used as the standard for calibration of the radiocarbon dating method (Pearson and Stuiver, 1986).

In contrast to this long tradition in classical dendrochronology, dendroclimatology is still a young discipline in Europe. This accounts for the slow development of science. Nevertheless, during this time the instrumental climate database in Europe has grown to become the best in the world.

There are some valuable older studies and observations on the relationship between tree growth and climate, particularly in North and East Europe. These studies were completed without the help of modern data processing and therefore could not make use of large amounts of complex data and multivariate statistical procedures. Many studies suggest that the overall climatic information obtainable from tree-ring analysis of deciduous tree species is low. More climatic information is apparently extractable from coniferous species in the Alpine region and in Scandinavia and East Europe. In this case, wood density has proved a better recorder of climate, particularly summer temperature, than ring width. Preliminary studies suggest that, if rainfall is to be considered more precisely, the vessel system of deciduous trees may contribute a suitable parameter.

There are a number of general points to be considered in the evaluation of dendroclimatology in Europe: the largest part of the area has relatively few tree species. Although the Mediterranean region is rich in tree species, only a few have so far proved suitable for dendroclimatology. The trees are mostly short-

lived. The forests have been influenced by man since prehistoric times. Moreover, many of the current chronologies that were constructed for dating purposes are unsuitable for climatic studies as they are based on timbers from too wide a geographical area. Only their youngest parts are based on trees from known sites. The trees that form the older parts of the chronology are nonliving trees from a large area and in many cases from habitats that today do not support trees. This is particularly true of the long oak chronologies that are formed from subfossil oaks grown on developing fens for which there are no modern analogs.

1.4. Dendrochronology in the USSR

L. Kairiukstis and S. Shiyatov

In contrast to West European approaches, dendrochronology in East Europe started from dendroclimatology. The first notable dendroclimatological work was carried out by F. Shvedov in 1882 on two black locust trees (*Robinia pseudoacacia*) growing in Odessa in the Ukraine (Shvedov, 1892). He showed that, in this region, the width of annual wood layers depends to a large extent on annual precipitation, and the narrowest layers form in very dry years. The narrow layers are regularly repeated at three-to-nine-year intervals. On the basis of the periodicity revealed in these tree-ring variations, he gave a prognosis of droughts (in 1882 and 1891) that was proved correct. In this work Shvedov demonstrated very well the possibility of the *dendrometric* method for reconstructing climatic conditions of the past. He should be rightfully considered as one of the founders of dendroclimatology.

From the first half of the 20th century, the work of Zaozersky (1934) should be noted. In a paper entitled "Towards the Methods of Retrospective Revealing of Climatic Conditions by the Tree Growth Study," he reported the significance of tree-ring information for the solution of a wide range of problems, especially hydrological ones, and gave valuable methodological advice for collecting field samples. He also provided quantitative and qualitative reconstructions of some environmental factors influencing annual tree-ring variability. Tolsky (1936) gave a survey of works devoted to the influence of climate on tree growth, reconstruction of climatic conditions of the past, and practical recommendations about the choice of the most valuable regions, sites, and species for dendroclimatological investigations. Analysis of drought periodicity in the Voronezh region in terms of annual growth of European ash (*Fraxinus exelsior*) was given by Kostin (1940). At this time the abstracts about the works of American dendrochronologists were first published in the USSR. In abstracts by Jashnov (1925), Krishtofovitsh (1934), and Chrgian (1938), the works of Douglass and his students on the relationships between growth and heliogeophysical and climatic factors, the reconstruction of climatic conditions, and the study of the cyclicity in tree growth were reviewed.

Intensive development of dendrochronological investigations in the USSR began only in 1950–1960. Rudakov (1951, 1958, 1961) is credited with popularizing of the dendroclimatological method. In particular, he advocated the moving average method for estimating the time trend in ring-width series. Important

work on the reconstruction of humidity in Central Asia during the last millenium on the basis of a study of ring width in Turkestan juniper (*Juniperus turkestanica*) was carried out by Gursky *et al.* (1953). Tree rings were extensively used by Galazy for reconstruction of climatic conditions and the upper-timberline dynamics in Transbaikal (Galazy, 1954) and reconstruction of the dates of high water levels in Lake Baikal (Galazy, 1955, 1967). Periodic recurrence of dry and moist periods have also been studied from tree rings in the Karelian Neck (Dmitrieva, 1959) and in the central Chernozem region (Kostin, 1960, 1963). And, significant dendroclimatological investigations, particularly on tree response to solar activity, were carried out in the Latvian SSR by Zviedris and Sacinieks (1958) and Zviedris and Matuzanis (1962).

At the same time, dendrochronological methods were first used for dating historical and architectural monuments and relics. Zamotorin (1959, 1963) and Zacharieva (1974) carried out a relative dating of Sajan–Altai barrows. In 1959 the first Dendrochronological Laboratory in the USSR was established at the Institute of Archaeology of the USSR Academy of Sciences. The researchers at the Institute studied absolute dating of medieval wood buildings in the northwest of the Soviet Union. Today the laboratory contains more than 800 wood samples collected from 18 old Russian towns, from 12 ancient monuments, and from living trees. On the basis of this collection, a tree-ring chronology 1,200 years long was obtained (Kolchin and Chernych, 1977). Dating of historic and architectural monuments and relics by dendrochronological methods has been accomplished by Shiyatov (1980) and Komin (1980) in the north of western Siberia, by Kolishchuk *et al.* (1984) in the Ukraine, and by Brukstus (1986) in the Lithuanian SSR.

During the last two decades, dendrochronological methods have been used extensively in different regions of the country to study cyclical forest ecosystem dynamics and different natural processes, the reconstruction of climatic conditions and catastrophic phenomena, and the evaluation of forest management measures.

Quite a number of dendrochronological investigations were also carried out in the Urals and the adjacent plains. Adamenko (1963a, 1963b) engaged in the reconstruction of climate and glacierization in the polar Urals. Dendrochronological information has been used by Shiyatov (1965, 1975, 1979, 1986) for climatic reconstruction and for investigations of the upper and polar timberline dynamics. Komin (1963, 1969, 1970a) carried out his studies in the taiga and forest-steppe zones on the eastern slope of the Urals and in the west Siberian plain. Olenin (1976, 1977) used tree-ring analysis for the investigation of forest cyclic dynamics on the western slope of the Urals and the eastern part of the Russian plain. Pugachev (1975) worked in the steppe zone of the northern Kazakhstan. Ural dendrochronologists are paying close attention to establishing methods to obtain more reliable dendroclimatic series, to reveal cyclic components in tree-ring chronologies, and to work out long-term prognoses of tree-ring indices and forest-growth conditions (Komin, 1963, 1970b; Shiyatov, 1972, 1986; Olenin, 1974; Mazepa, 1982, 1986).

Since 1953, research on dendrochronology has been carried out in the Lithuanian SSR. The Dendroclimatochronological Laboratory at the Institute of

Botany of the Academy of Sciences at present is the biggest specialized scientific subdivision in the Soviet Union operating in the field of dendrochronology (Bitvinskas, 1978a,b,c). Scientists at this laboratory are investigating dendrochronology in the European part of the USSR, Siberia, and the Far East. They are giving much prominence to revealing the relationships between tree growth and some astrophysical–geophysical phenomena and hydroclimatic factors, establishing a chronology several thousand years long, studying cyclicity in tree growth, reconstructing the radiocarbon content of the Earth's atmosphere, and estimating forest management effectivity (Bitvinskas, 1964, 1965, 1974, 1978, 1984, 1987; Pakalnis, 1972; Bitvinskas and Kairaitis, 1975; Stupneva and Bitvinskas, 1978; Karpavichus, 1981; Dergachev and Kocharov, 1981). Along with the research problems mentioned above, various fields of application, including dendrochronological investigations near the Baltic Sea, are also dealt with at the Lithuanian Research Institute of Forestry (Kairiukstis, 1968; Kairiukstis and Juodvalkis, 1972; Stravinskene, 1981; Kairiukstis and Dubinskaite, 1986; Kairiukstis *et al.*, 1987a), the Latvian Research Institute of Forest Management Problems (Zviedris and Sacinieks, 1958; Zviedris and Matuzanis, 1962; Shpalte, 1971), as well as the Tartu State University (Läänelaid, 1981).

In the western Ukraine, Kolishchuk (1966, 1979) is studying the process of the recognition of factors influencing tree-growth variability. On the basis of the study of radial growth regularities in prostrate trees, he has worked out a method of obtaining standardized tree-ring chronologies (Chapter 2).

In the area of the European part of the USSR, dendroclimatic investigations have been carried out also by Liseev (1962), Gortinsky (1968), Lovelius (1979), Feklistov (1978), Evdokimov (1979), Barsut (1984), and Molchanov (1970). Dendrochronological methods have been used for dating such catastrophic phenomena as snow avalanches, mud flows, and landslides (Turmanina, 1972, 1979). Kovalev *et al.* (1984) have carried out dendroclimatic investigations in the Caucasus Mountains.

In Siberia, dendrochronological investigations are carried out at the V.N. Sukachev Institute of Forest and Wood of the Siberian Division of the USSR Academy of Sciences (Glebov and Pogodina, 1972; Glebov and Litvinenko, 1976; Buzikin, Dashkowskaya, and Chlebopros, 1986). They are focusing attention on a study of dendroclimatic relationships in forest-bog ecosystems and on the regularities of radial growth in forest stands. Their colleagues at the Institute of Biophysics have made a significant contribution to recognizing the mechanisms of annual tree-layer formation (Spirov and Terskov, 1973; Vaganov, Smirnov, and Terskov, 1975; Vaganov and Terskov, 1977; Vaganov *et al.*, 1985). In 1970, a microphotometric analyzer of wood was constructed, which allows the examination of annual ring structure automatically on the basis of diffused–reflected light recording. In 1977, a measuring instrument of ring structure (MSR-2M) was constructed for use with a minicomputer, which allows the semiautomatic recording of the number and dimensions of cells within the growth ring and allows the obtained information to be processed quickly. By these devices, the procedures of investigation of microanatomical heterogeneity of annual wood rings were worked out. This established the importance of regularities of seasonal tree growth and projected ways and means of using photometric curves

and tracheidograms for dendrochronological needs. Cyclic oscillations in tree growth in connection with climatic changes and solar activity have been investigated by Polushkin (1979) and Polushkin *et al.* (1977). Adamenko (1978, 1986) is using dendrochronological methods for reconstructing the thermal regime of summer months and glacierization in the Altai Mountains.

A comparatively small number of dendrochronological investigations have been carried out in the Soviet Far East. In this region, works on cyclic oscillations in tree growth and the influence of hydroclimatic and phytocoenotic factors in tree-ring variability have been produced (Tarankov, 1973; Malokvasov, 1974, 1986; Sabirov, 1986).

In Central Asia, annual growth variability of Turkestan juniper (*Juniperus turkestanica*) was studied by Muchamedshin (1974). This species is the most long-lived in the USSR (up to 1,500–2,000 years) and is very sensitive to climatic changes. Interesting dendroclimatological investigations on Schrenka spruce (*Picea schrenkiana*) were carried out in the Tien Shan Mountains (Borshova, 1981, 1986).

Coordination of dendrochronological investigations in the USSR is conducted by the Commission for Dendroclimatology of the USSR Academy of Sciences. Every five years the Commission organizes an All-Union Meeting on problems of dendrochronology and dendroclimatology (Vilnius, 1968; Kaunas, 1972; Archangelsk, 1978; Irkutsk, 1983, 1987). With the assistance of the Commission, the Dendrochronological Bank of the Soviet Union (DBSU) was organized in 1980 at the Dendroclimatochronological Laboratory and the Lithuanian Research Institute of Forestry (Kaunas). Also the proceedings, *Dendroclimatological Scales of the Soviet Union* (1978, 1981, 1984, 1987), and the bibliographical pointer, *Dendroclimatochronology, 1900–1970* (Vilnius, 1978), have been published.

Four basic points should be mentioned that are essential for evaluating dendroclimatology in the USSR.

- Having access to a large territory covering several vegetation zones for sampling in natural forests, Soviet scientists have arrived at the general conclusion that dendroclimatological investigations are best based on a precisely understood ecological background and carried out on a large spatial scale by means of the dendrochronological profile method: north–south and east–west. Comparisons of similar data both by site conditions and by species composition allow them to reveal, under such conditions, zonal differences in tree-ring-climate relationships.
- Dendroclimatological investigations involve problems of high complexity and are analyzed with the participation of different specialists, particularly climatologists and traditionally also those dealing with astrophysical and geophysical phenomena. Studies are based on carbon isotope measurements of exactly dated tree rings; carbon content variations in tree rings are observed to be extremely valuable indices of Earth biosphere changeability under the influence of cosmic and geophysical factors. Variation of solar activity and its strong influence on atmospheric circulation has been used for indication of extreme behavior of trees in separate regions.

- Variation in rhythms of tree-ring increment and their significance for indication of background climatic changeability (complex hydrothermic indices, cosmic and geophysical factors) in a given territory have been considered important subjects of investigation. Cyclicity in dendrochronologies provided a basis for the subdivision of regions on a dendroclimatic basis. In this field there remains a need for a high degree of rigorous testing and verification.
- Finally, dendroclimatology in the Soviet Union, particularly owing to prognostic activities, has become an important tool in forestry and regional planning (timing of soil reclamation, application of fertilizers, stand thinning).

1.5. Dendrochronology in the Southern Hemisphere

D.A. Norton

1.5.1. Introduction

Dendrochronological research started relatively late in the Southern Hemisphere, and it has only been in the last 10–15 years that large numbers of chronologies have been developed. This late start undoubtedly reflects, at least in part, the small land area and population compared with the Northern Hemisphere and the often limited knowledge about the ecology and botany of the southern forests. Much of the impetus for Southern Hemisphere dendrochronology has come from visiting northern scientists: in the 1950s Schulman in South America and Bell in New Zealand and in the 1970s LaMarche, Holmes, and others. Today active groups of dendrochronologists work in Argentina, Australia, New Zealand, and South Africa.

The historical development of Southern Hemisphere dendrochronology is briefly discussed here. Earlier reviews have been provided by Dyer (1982), Holmes (1982), and Ogden (1982).

South America

The first published chronologies for South America were presented by Schulman (1956) for Chilean incense cedar (*Austrocedrus chilensis*) and Chile pine (*Araucaria araucana*) from Argentina. *A. chilensis* was found to be the easier species to work with, although relationships between growth and climate were ambiguous for both species. Further sampling of *A. chilensis* in Chile in the early 1970s lead to the development of a well-replicated chronology that was used to develop a preliminary reconstruction of Santiago precipitation back to A.D. 1010 (LaMarche, 1975). This reconstruction is still the longest developed for the Southern Hemisphere, although the calibration regression was not verified. The study was followed by an extensive sampling program that resulted in the development of 32 chronologies from three species (*Austrocedrus chilensis*, *Araucaria araucana*, and *Pilgerodendron uviferum*) in Chile and Argentina (LaMarche *et al.*, 1979a, 1979b). Climatic analyses of these chronologies have, however,

been limited; only two paleoclimate reconstructions have been published (for river flow in Argentina, Holmes *et al.*, 1979).

Other species have also been investigated. Preliminary analysis of *Nothofagus pumilo* suggests that chronology development should be possible with this species (Boninsegna, 1982). The conifer *Fitzroya cupressoides* was sampled by Schulman (1956) and LaMarche *et al.* (1979a, 1979b) but cross-dating was not achieved. Reanalysis of this material has, however, resulted in the development of a 1,534-year chronology from western Argentina (Boninsegna and Holmes, 1985), the longest Southern Hemisphere chronology to date. Lamprecht (1984) had investigated the potential of trees from Chile and Brazil for radiodensitometric analysis but with only limited success. Some chronology was developed in Chile for *Podocarpus nubigenus*, and cross-dating observed in *F. cupressoides*, but no statistical links with the climate were found.

South Africa

Tree-ring research in southern Africa appears to have been hampered by a lack of suitable trees (Lilly, 1977; Dyer, 1982). Problems encountered include indistinct ring boundaries, severe ring wedging, short-life spans, and scarcity of potentially useful species. More recent sampling (LaMarche *et al.*, 1979e) suggests that the conifer genera *Podocarpus* and *Widdringtonia* (especially *P. falcatus* and *W. cedarbergensis*) offer the most potential. Progress with *P. falcatus* has not been possible because of severe ring wedging and lobate growth (Hall, 1976; Curtis *et al.*, 1978; McNaughton and Tyson, 1979; LaMarche *et al.*, 1979e). Study on *W. cedarbergensis* has proved more successful, and a 413-year chronology developed (Dunwiddie and LaMarche, 1980a). Statistically significant links between ring width and spring and early-summer precipitation have been identified.

Australia

The predominant Australian tree genus, *Eucalyptus*, has shown little promise for dendrochronology (Ogden, 1978a), although limited cross-dating has been achieved between subalpine *E. pauciflora* trees (Ogden, 1982). The only chronology developed for an angiosperm tree in Australia is for *Nothofagus gunnii* from Tasmania (LaMarche *et al.*, 1979d). More success had been achieved with Australian conifers. Results from several studies of the arid-zone conifer *Callitris* (Lange, 1965; Pearman, 1971; Johnston, 1975; Dunwiddie and LaMarche, 1980b) suggest that ring width is dependent on precipitation. However, the potential of this species is limited by the generally young age of the trees; the two published chronologies (LaMarche *et al.*, 1979d) are 43 and 64 years long. The greatest potential for dendrochronology in Australia appears to lie with the genera *Arthrotaxis*, *Phyllocladus*, and *Lagarostrobos* (Ogden, 1978a, 1978b; LaMarche *et al.*, 1979d; Dunwiddie and LaMarche, 1980b; Francey *et al.*, 1984). Preliminary work with the Tasmanian *Arthrotaxis cupressoides* and *A. selaginoides* (Ogden, 1978b) showed that cross-dating could be achieved, and four chronologies have now been published (LaMarche *et al.*, 1979d). The longest, for *A. cupressoides*,

covers the period 1028–1974. Ten chronologies have also been developed for *Phyllocladus asplenifolius* (LaMarche *et al.*, 1979e), the longest extending back to 1310.

Chronology development is also underway with the very long-lived *Lagarostrobos franklinii* (Francey *et al.*, 1984). This species, which may live up to 2,000 years, is also the subject of a detailed study of carbon isotopes (McPhail *et al.*, 1983; Francey *et al.*, 1984). Buried wood, dating from throughout the last 8,000 years (McPhail *et al.*, 1983), offers the potential for developing a long historical chronology comparable with those developed for oak and bristlecone pine, in the Northern Hemisphere.

Preliminary reconstructions of temperature and river flow have been developed using some of the Tasmanian chronologies (Campbell, 1982; LaMarche and Pittock, 1982) and illustrate the potential of these long-lived conifers for developing paleoclimate reconstructions.

New Zealand

Early dendrochronological research in New Zealand was largely unsuccessful, and a pessimistic attitude developed toward this technique (Bell, 1958; Bell and Bell, 1958; Cameron, 1960; Scott, 1964, 1972; Wardle, 1963; Franklin, 1969; Wells, 1972). However, since the mid-1970s considerable progress had been made in New Zealand. A total of 65 chronologies have now been developed. Initial sampling in 1977 and 1978 resulted in the development of 21 chronologies from seven conifer species (*Libocedrus bidwillii*, *Phyllocladus alpinus*, *P. glaucus*, *P. trichomanoides*, *Lagarostrobos colensoi*, *Halocarpus biformis*, and *Agathis australis*) (LaMarche *et al.*, 1979c; Dunwiddie, 1979). Several of these chronologies date back further than 1500 – the longest, for *L. bidwillii*, extending back to 1256.

Subsequent research with *A. australis* has resulted in the development of an additional eight modern chronologies (Ahmed and Ogden, 1985) and one subfossil chronology (Bridge and Ogden, 1986) for the period 3500–300 B.P. The presence of substantial amounts of buried wood presents the opportunity of developing a long subfossil tree-ring chronology. In the South Island, substantial progress has made with two species of *Nothofagus*, *N. solandri* and *N. menziesii*. Thirty chronologies have been developed (Norton, 1983a, 1983b, 1985, 1987), the oldest, for *N. menziesii*, extending back to 1580. Two additional *L. bidwillii* chronologies have also been developed. Climatic analyses have so far been restricted to *Nothofagus* where strong links with both temperature and precipitation have been identified (Norton, 1984, 1987). Reconstructions of temperature, precipitation, and river flow have been derived from these chronologies (Norton *et al.*, 1989; Norton, 1987).

Tropical Southern Hemisphere

A number of difficulties occur in applying dendrochronological techniques to tropical areas (Ogden, 1981), but nevertheless some progress has been made. The major difficulty encountered has been in ascertaining if growth rings are formed annually. Early work in Java (Berlage, 1936) suggested that the widths

of *Tectona grandis* growth rings were correlated with precipitation. In the Australian tropics cross-dating among trees and correlations between ring widths and precipitation have been observed in several species including *Araucaria cunninghamii* (Booth and Ryan, 1985), *Callitris columellaris* (Perlinski, 1983), *C. macleayana* (Ash, 1983b), *Diospyros spo* (Duke *et al.*, 1981, but see Ash, 1983a), and *Pisonia grandis* (Ogden, 1981). So far no chronologies have been formally presented.

Research had also been undertaken with tropical South American species (Villalba *et al.*, 1985). Four chronologies have been developed from *Juglans australis* and *Cedrela angustifolia* in northern Argentina. Good cross-dating was achieved and preliminary correlations with climate were promising.

1.5.2. Discussion

Probably the most serious limitation in Southern Hemisphere dendrochronology is a lack of knowledge on the ecology and life history of many of the tree species investigated. Phenological information is necessary to identify accurately the periods of radial growth and to gain an understanding of the climatic conditions influencing growth. For example, Palmer and Ogden (1983) found that in *Agathis australis*, although growth at the start and end of the growing season was temperature dependent, soil moisture deficits were important limitations on growth in midsummer. Such phenological information is, however, sparse. For example, in New Zealand phenological information for mature trees is available for only two of the nine species from which chronologies have been developed.

A similar lack of information on the ecological requirements of the different species is apparent. Ecological information is particularly important for assessing long-term trends in tree-ring series. For example, species like *Libocedrus bidwillii*, *Arthrotaxis selaginoides*, and *Araucaria araucana* regenerate after disturbance (Ogden, 1978b; Veblen, 1982; Veblen and Stewart, 1982; Norton, 1983c; Cullen, 1987). It is likely that for at least the first 100 years of the tree's life, growth is strongly influenced by competition rather than climate. Although a large network of chronologies has been developed, with a commendable amount of work being involved in this, these chronologies have significant limitations. First, replication is poor in several chronologies. For example, a long Chilean *Austrocedrus chilensis* chronology (ELA479, LaMarche *et al.*, 1979b), although using a total of 42 radii from 24 trees, has only nine radii prior to 1425, and only one for the first 200 years. Similarly, for a long New Zealand *Libocedrus bidwillii* chronology (CRC601, Norton, unpublished), only two ring-width series are used for the first 177 years. Clearly the early periods of these chronologies are not necessarily representative of the modern periods used in calibrating and verifying transfer functions. The use of statistics such as the subsample signal strength (Wigley *et al.*, 1984) will be essential in assessing the reliability of the early part of these chronologies and thus their suitability for use in paleoclimate reconstruction.

Low correlations among trees within chronologies are another characteristic feature of some Southern Hemisphere chronologies. For example, the 11

Libocedrus bidwillii chronologies have an average mean correlation of 0.30, while in some species (e.g., for the PRA799) chronology mean correlation is 0.07, LaMarche *et al.* (1979b). These very low values could be indicative of poor cross-dating (a chronology developed from random number series had a mean correlation of 0.09, Norton, unpublished). However, it is more likely that the influence of low-frequency variance (e.g., from stand dynamics) is masking climatic influences. The use of filtering techniques such as Gaussian filters (Chapter 3) in standardization may help enhance the climate signal.

Autocorrelation values are very high in many Southern Hemisphere chronologies (e.g., mean of 0.68 in *Libocedrus bidwillii*), and again suggest that careful standardization will be necessary before any climate signal can be identified. The opposite situation also occurs where, for example, some New Zealand *Phyllocladus* chronologies have very low and often negative autocorrelation values. In these trees this is a result of alternating wide and narrow growth rings and is best seen in *P. glauca* (Dunwiddie, 1979). Other New Zealand species also exhibit this alternation of ring widths (e.g., *Beilschmieda tawa*, Ogden and West, 1981), and there is no reason why this should not occur elsewhere. The phenomenon may relate to the phenology of the trees, in particular to biennial flowering (Ogden, 1982).

The potential for Southern Hemisphere dendrochronology is considerable, but the lack of knowledge on the ecology and life histories of many of the trees needs to be overcome before extensive climatic reconstructions are undertaken. The failure to reconstruct the Southern Oscillation using Southern Hemisphere tree-ring chronologies (Lough and Fritts, 1985) may reflect a lack of information on the ecology of the trees being used. Despite this, I see considerable potential for Southern Hemisphere dendrochronology, especially with the angiosperm genus *Nothofagus* and with several southern conifer genera.

CHAPTER 2

Primary Data

Chapter Leader: J.R. Pilcher
Chapter Contributors: F.H. Schweingruber, L. Kairiukstis, S. Shiyatov, M. Worbes, V.G. Kolishchuk, E.A. Vaganov, R. Jagels, and F.W. Telewski

2.1. Sample Selection

F.H. Schweingruber, L. Kairiukstis, and S. Shiyatov

2.1.1. Introduction

The search and selection of suitable regions, sites, species, and trees are fundamentally important in dendrochronological studies. Practically every dendrochronological study states the locality from which the material is taken and the number of tree rings contained in the samples and the chronologies. However, only in dendroecological papers are the principles of site and specimen selection described (e.g., Mueller-Stoll, 1951; Jazewitsch, 1961; Fritts, 1965; Shiyatov, 1973, 1986; Bitvinskas, 1974; Lovelius, 1979). LaMarche *et al.* (1982) point out the potentials and limits of dendrochronological studies in historical and ecological fields. These depend primarily on the aims and the tasks of the investigator, and their accuracy determines the quality of the tree-ring chronologies obtained. This section focuses on the importance of the sampling strategies for various applications of dendrochronology.

2.1.2. Selection of a study area

The most appropriate regions for dendroclimatological investigations are those where trees grow at their climatic distribution limit and where climatic factors greatly affect tree-ring variability (e.g., northern, southern, upper, and lower distribution limits of forest communities and tree species). However, in many cases

E. R. Cook and L. A. Kairiukstis (eds.), Methods of Dendrochronology, 23–96.

reliable climatic information may be obtained from growth variations of trees growing under more favorable conditions.

Regions with optimal tree-growth conditions are also well suited for reconstructing such non-climatic factors as competition between species and individuals, forest fires, pest attack, etc. Therefore, at an early stage of study, an investigator should become acquainted with schemes of botanical and geographical subdivision of large territories and with detailed zonation of the study area. The principles of geobotanical zonation are different in various countries, which presents difficulties for a comparative evaluation of general conditions of forest vegetation growth at widely separated regions. Geobotanical characteristics of the large regions, for example, the Soviet Union, may be taken from monographs like *Vegetation Cover of the USSR: Explanations to the Geobotanical Map, Scale 1:4,000,000 1956* and *Vegetation of the European Part of the USSR, 1980.* Most areas of the globe now have some similar broad-scale vegetation descriptions (e.g., Rowe, 1972, for Canada; or Loucks, 1962, for the Maritime Provinces).

2.1.3. Selection of sites

Within the limits of certain regions one may choose sites with the maximum tree growth response to changes in the factors of interest. For example, to study precipitation reconstruction, tree samples should be taken from the driest sites where moisture would most probably be the limiting factor. To reconstruct thermal conditions, the most appropriate sites would be those where trees do not have a limited water supply. Selection of proper sites permits a climatic signal to be revealed in the rings of trees growing in regions optimal for forest development.

This is a principle that at first glance seems to run contrary to statistical considerations requiring random sampling. However, tree and site selection is an extension of the principle of limiting factors, the concept of ecological amplitude and replication. Differences in site lead to differences in the most important limiting factors. Thus, it is important to choose the specific site and to replicate within this site, so that all the sampled trees will have the same or similar signals (LaMarche *et al.*, 1982).

In many areas promising sites for dendrochronological studies are found in mountainous regions, where contrasts may be found in a small territory and where diverse catastrophic factors (such as snow avalanches, mud flows, rock avalanches, glacier advance) greatly influence tree growth. However, dendroclimatic relationships are often difficult to establish here owing to a lack of long climate records and the great variety of microclimatic, mesoclimatic, and macroclimatic conditions. In all areas, site selection for ecological and climatic studies may be influenced by the location of climatic-recording stations. Environmental gradients are examined by selecting specific sites along the environmental gradient (Fritts *et al.*, 1969; Norton, 1983a) and by building strong site chronologies so that any differences reflecting the gradient may be statistically tested. Two general principles should be considered when selecting sites:

Site homogeneity largely determines the quality of the chronology. A site chronology should only be constructed from trees from the same class of site. In the most opportune cases it is possible to find sufficient trees within a small area. Often, however, it is necessary to group together trees from different places but with the same site conditions to obtain a chronology. The units of collection are best identified by means of phytosociological relevés or at least floristic descriptions. These surveys also permit an understanding of the relationship of ecological conditions on sites far from each other, which is not possible on the basis of topographical or geological descriptions alone.

Stand development affects cambial activity. Wherever possible, only trees of the same social status (e.g., dominant, codominant) should be grouped into a site chronology. The variability owing to competition is thus reduced, although it cannot be completely eliminated, particularly in intensively managed forests where a number of silvicultural operations are conducted within a relatively short time. If, however, the study concerns stand development, then trees of each social status should be examined.

2.1.4. Selection of species

In some areas of the world, dendrochronology is not possible because appropriate trees are not available. Trees in these areas may show an absence of annual rings, insufficient variability from ring to ring for cross-dating to be established, missing rings, or interannual growth bands. In many areas there are no trees of sufficient age for useful dendrochronology. Many trees growing in the tropics do not produce distinct annual layers, or, if they do, there is no visible pattern common among trees that can be used for cross-dating (Eckstein *et al.*, 1981).

Appendix A lists the species for which tree-ring chronologies have been published or for which it appears dendrochronology has been possible. Many are represented by chronologies that are held in the International Tree-Ring Data Bank. The majority of chronologies from the USSR is from species of *Pinus*, *Picea*, and *Larix*. In western North America *Pinus* also supplies many of the chronologies together with *Pseudotsuga*, *Libocedrus*, and *Juniperus*.

The longest-lived species of dendrochronological interest are *Pinus aristata* and *P. longaevea* (up to 4,000 years) (Ferguson, 1969) growing in western North America and *Juniperus turkestanica* (up to 2,000 years) growing in Middle Asia (Mukhamedshin, 1968). The most sensitive tree-ring chronologies in the Eastern Hemisphere have been obtained from *Larix* species. This can be attributed to their ecological and biological peculiarities: light-loving, yearly defoliation, and efficient use of environmental resources in biomass accumulation (Shiyatov, 1967, 1986).

Of the angiospermous species, the most widely used are of *Quercus*, particularly in Europe and eastern North America. The second longest chronology in the world, after the bristlecone pine (*Pinus aristata*), is from English oak (*Quercus robur*) (Pilcher *et al.*, 1984). Oak has been widely used for archaeological dating, dendroclimatology, radiocarbon calibration, and dendroecology

(Eckstein, 1972; Brown *et al.*, 1986; Becker, 1986; Kostin, 1963; Bitvinskas and Kairaitis, 1975; Leuschner and Delorme, 1984). In the Southern Hemisphere, *Nothofagus* has proved a valuable broadleaf genus (Ogden, 1982; Norton, 1983b,c).

In conclusion any tree or shrub species that meets the following requirements can be used for a dendrochronological study:

- It produces distinguishable rings for most years.
- It possesses ring features that can be cross-dated dendrochronologically
- It attains sufficient age to provide the time control required for a particular investigation.

2.1.5. Selection of stands

The selection of stands is dependent on the purpose of the scientific investigation. When climate is to be reconstructed it is desirable to minimize the effect of competition in dendrochronological series by taking samples from open forests or scattered trees. Where possible it is better to sample in old growth rather than secondary forest. Therefore, a detailed description of the community with special attention to origin and development stage of the stand is preferred. Undisturbed stands that fulfill requirements of age, year-to-year ring-width variability, and cross-dating are sometimes difficult to find, so some disturbances made by man in stand structure may be unavoidable. However, it is important that the sampled forest communities have not been similarly damaged by fires, wind, or other catastrophic factors to extract reliable climatic information from tree rings. Having said this, in some areas such as the Mediterranean and Western Europe there are no trees that can truly be considered free from the influence of man or fire or both. In such cases, special care must be made to remove as best as possible these non-climatic effects. Chapter 3 discusses some methods of removing such non-climatic noise.

A quite different stand selection strategy may be used for dendroecological studies. Here, stands are selected that are likely to be influenced by specific factors, be they natural or man-made. Examples are forest fires, insect defoliations, and pollution.

2.1.6. Selection of trees

There are two ways to select sample trees. First, they may be randomly chosen from small (up to 0.5–1.0 ha) sample plots that are usually set up for forestry purposes. Though maximum homogeneity of the conditions in each plot is maintained, it is not always possible to find a sufficient number of old trees suitable for dendroclimatic studies. This procedure is more frequently used for studies of non-climatic factors where randomness in the statistical sampling design may be crucial to the success of the study.

The principles of tree selection for dating and reconstructing non-climatic factors are quite different from those used for selecting trees in dendroclimatic studies. For example, timing of a snow avalanche is primarily based on the dating of mechanically damaged, dead, or leaning trees. Each tree should be described in detail and numbered in some cases so that it will be possible to extend the chronology by future sampling. Brubaker and Greene (1979) and Swetnam *et al.* (1985) chose replicated samples from host and non-host species to evaluate differences in growth associated with the effects of periodic insect attacks on trees. For an investigation of pollution impacts on the forest, different principles of tree selection must also be used.

In the second main sampling strategy, trees are selected from the same site type but from a considerably greater area, the size depending on the homogeneity of the region and the aims of the study. The sampling site should be climatically and geobotanically homogeneous. In this case, it is possible to select a sufficient number of old trees to obtain a chronology of maximum duration. This method is mainly used for dendroclimatic studies. To obtain a mean tree-ring chronology, 20–30 trees are usually used. In regions and sites where tree growth depends very much on one or another limiting factor, a reliable chronology may be constructed using five to seven trees.

For densitometric studies, two cores from at least 12 trees are usually sufficient. For ring-width analysis, a sample of two cores from each of 20 trees is recommended. Studies on individual features such as frequency of wounding or abrupt growth changes require samples from more than 20 trees. If circuit uniformity of the ring widths within a tree is very high compared with the differences in annual growth among trees, then single core samples of more trees are preferable. In extreme growth conditions, for example, at the upper distribution limit of scattered trees with flaglike crowns and eccentric annual rings, measurement and dating of rings are possible only on a single radius (from the lee side of the trunk) where annual ring widths are widest. Dead or fallen trees may be sampled from the upper or middle parts of the trunk as the peripheral rings are very narrow at the base of the trunk.

Dominant trees provide the most reliable climatic information and reflect growth dynamics of the whole stand with more precision (Dmitrieva, 1959; Komin, 1970a). Trees with a relatively sparse crown, massive and irregularly tapering trunk, few but heavy branches, and a general unsymmetric appearance are usually the oldest with the strongest year-to-year ring-width variability, which is associated with a strong climatic response (Fritts, 1976). As peripheral rings in the oldest dying trees are usually very narrow, with slight variation in width, trees of different ages should be used to get sensitive and homogeneous chronologies. Using uneven-aged tree specimens may assist cross-dating of the oldest trees (Shiyatov, 1986).

2.1.7. Sampling a single tree

Growth varies within an individual tree. This variability is greatest at the base of the stem and smallest in the crown section. To obtain the longest possible

ring sequences with a minimum of individual variability, samples are taken at breast height. Where stem disks are available, it is possible to exclude all the irregularities (compression wood, tension wood, abrupt or localized changes in ring width, and wound tissue). However, samples are usually obtained with an increment borer. With two cores per tree, a large part of the individual variability can be eliminated through averaging.

For our own studies we apply the following criteria for sampling:

- Avoid sampling in the vicinity of a wound.
- Avoid sampling in the vicinity of reaction wood.
- Avoid buttresses and the upslope and downslope sides of trees growing on sloping ground (to avoid reaction wood). The absolute compass direction does not appear to be of any great importance.

However, not all irregularities are predictable. Consequently, it is best to sample a few more trees than necessary so that anomalous cores may be discarded. In studies on slope or snow movements or on the influence of wind, attention must be paid to the side of the trunk with compression wood in conifers or tension wood in broadleaves. In this case, the anomalies being avoided using the above criteria are of interest. Individual variability in the final chronology decreases with an increasing number of samples. For this reason several trees are cored on each site. In densitometric studies, variability owing to technical processing can be greatly reduced by taking cores as nearly perpendicular to the fiber orientation as possible. This requires the use of a support for the increment borer (Schweingruber, 1983). The more carefully and appropriately the sites and trees are selected, the fewer the trees that have to be sampled and thus the less the work involved.

It should be borne in mind that coring injures the tree. Even with careful work, a bore hole is left. The hole becomes sealed and grown over within a few years. In the case of conifers, treatment is seldom necessary. Broadleaves, however, react physiologically, the result being radial disk-shaped discolorations around the bore hole. Furthermore, fungal infection often follows. As a minimum preventative measure, the holes should be plugged with wax to prevent the entry of spores. Opinions on the effectiveness of this and further treatments vary, but the dendrochronologist should follow the wishes of the tree owner if in doubt.

2.1.8. Search for ancient wood

To extend tree-ring chronologies beyond the limits of old living trees, historical, archaeological, or subfossil timbers must be sought. Such wood can be found in old buildings, in works of art, and in the ground as natural and cultural remains. It is most frequently discovered in human settlements and burial places, in river, lake, and marine deposits, and in peat bogs and permafrost soils.

Based on wood from Holocene deposits, continuous tree-ring chronologies covering all or part of the last eight millennia have been constructed (Ferguson,

1970; LaMarche and Harlan, 1973; Pilcher *et al.*, 1984; Becker, 1986; Leuschner and Delorme, 1984). Ancient wood is preserved when its weathering is hindered, for example, in dry air or in waterlogged or frozen ground. In some regions with a continental climate at the upper tree line, trunk and root remains are preserved on the surface for more than 1,000 years (Ferguson, 1968; Shiyatov, 1986), and in one instance for some 45 million years (Basinger, 1984). The layered annual structure of charred wood is also well preserved.

The bulk of subfossil wood is available from alluvial deposits, and a search for it is easier as rivers wash away their banks. One should bear in mind that exact estimation of growth conditions of the past is not always possible if the wood was used for buildings or works of cultural and everyday use. Even buried wood may have traveled some distance before preservation.

2.1.9. Site recording

The importance of good site recording cannot be too strongly stressed. The data generated by a particular project may be of value to other projects not envisaged by the sampler, but only if the site information recorded is adequate. Appendix B gives examples of two site-recording sheets to suggest a desirable and a minimum standard (the minimum being based on the entry requirements for the International Tree-Ring Data Bank). In addition to factual information about the site, the record sheet should include a brief description of the site, e.g., "old pine stand with earlier pasturage, with dense undergrowth, on deep brown soil, on gentle south facing slope. Stand possibly planted." The site notes should also include the aims of the study or reason for sampling, e.g., "part of a climatological sampling network" or "study of Mayfly epidemics."

2.1.10. Preliminary assessment of samples

Every study begins with a search phase. At this stage, the optimum information should be obtained with the least effort. To that end those features of the core that are easy to identify visually are examined. These are:

- Mean ring width.
- Sensitivity (frequency of visually recognizable signatures or pointer years).
- Frequency and date of abrupt changes in ring width.
- Rot, wounds, compression wood.

The final decisions on the selection of sites are made in the course of this work.

During sample collection, the basic assumptions of the research problem may be tested by visual inspection of each core. Aberrant cores may be discarded when it is possible to detect what feature of the tree or the site caused the abnormality. However, care should be taken not to bias unintentionally the collection in a way that will invalidate later analyses. This phase of selection is often ignored once the samples reach the laboratory, with the outcome that good

results may be obscured and the amount of work increased. Many statistical misfits can be recognized as such in the field. Samples collected previously may be unsuitable for certain studies if they were collected with different aims in mind. Samples from rigid networks may also be unsuitable, as the sites may not be homogeneous and may fail to meet the criteria for a valid ecological study.

2.1.11. Examples of sampling strategies

Dendrochronology can be applied to a wide spectrum of fields, and the range of sampling strategies is correspondingly broad. The basic principles are illustrated by the following three examples.

Example 1: Dendroclimatology Using Continental Networks

Fritts (1965), Kutzbach and Guetter (1980), and LaMarche *et al.* (1982) have shown how ring-width chronologies from ecologically different sites in the western USA and the Southern Hemisphere can be analyzed statistically to obtain reconstructions of the climate for given areas and years.

Selection of sites and trees. By selecting trees growing at their altitudinal, elevational, and latitudinal range limits, it is possible to maximize particular ecological factors in the tree rings. Trees growing near the northern or upper timberlines contain most information on temperature, while those growing near the lower-elevation, arid timberline provide more information on precipitation (see *Figure 2.1*).

The density of sites within a network can be increased within a study area by including local extreme sites. In deciduous forests, for instance, sites in hollows affected by cold air drainage may be climatically more sensitive than those in the surrounding normal sites; at the upper timberline in arid areas only those trees growing on north-facing slopes with deep soils contain worthwhile information on temperature. In every case, phytosociological findings indicate the special features and suitability of a site. Through strict application of this ecological principle of selection, it is possible to eliminate diffuse ecological effects, particularly those that are not limiting every year, and to emphasize those that are most commonly limiting each year.

Methods. Where applicable, densitometry is one of the most suitable methods for the reconstruction of summer temperatures in the Northern Hemisphere. Determination of maximum density allows year-by-year reconstruction for large areas. Additional information from ring widths may also be included in some cases. For the reconstruction of precipitation, ring width is often used (Fritts, 1976; Fritts *et al.*, 1979; Kienast, 1985). Most hardwoods, Araucariaceae, certain Cupressaceae, and five-needled pines are less suitable for densitometric analysis.

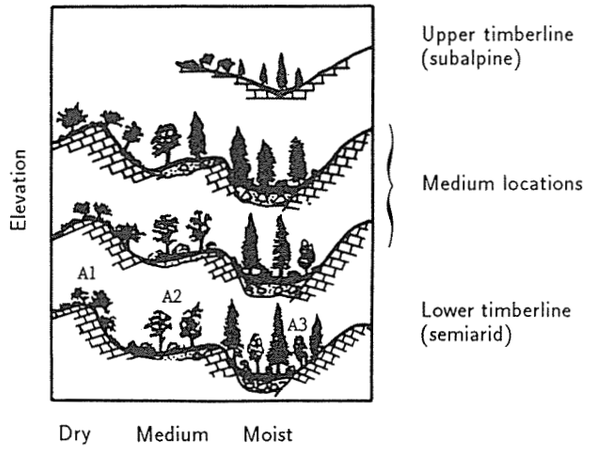

Figure 2.1. By selecting trees growing at their altitudinal and latitudinal range limits, it is possible to maximize particular ecological factors in the tree rings. Trees growing near the northern or upper timberlines contain most information on temperature, while those growing near the lower-elevation, arid timberline provide more information on precipitation.

Example 2: Dendroecology

The aim of dendroecology is the determination of the year-by-year interplay of relationships among climate, site conditions, and tree growth to assess exogenous and endogenous factors that influence the growth of a plant community.

Selection of sites, species, and trees. Definition of the research program is made on the basis of geobotanical, climatological, topographical, and geological characteristics assessed from maps, aerial photographs, and field inspections.

For investigations of changes of interaction between factors, such as climate and plant-community reactions in the Soviet Union, the profile method was used (Bitvinskas, 1978b; Lovelius, 1979). In one example of a north–south profile, 41 study areas (2,692 trees) were chosen for sampling in typical parts of Kolapechora, Valdai–Onega, Baltic–Belorussian subprovinces, North European taiga province, Polessje subprovince as well as in the Carpathian subprovince of the Central European province (see *Figure 2.2*). Such studies enabled a distinction to be made between differences in climate and plant community interactions. For example, it is possible to find small vegetation zones within an area that are distinct and may be similar to the plant communities many hundreds of kilometers away. Hence, to assess the biological productivity, typical sites of each region and subprovince should be selected. For the identification of typical sites in terms of geobotanical site characteristics for dendrochronological studies, local geobotanical or forest-site classifications can be used. The selection of typical trees can be made according to the descriptions above.

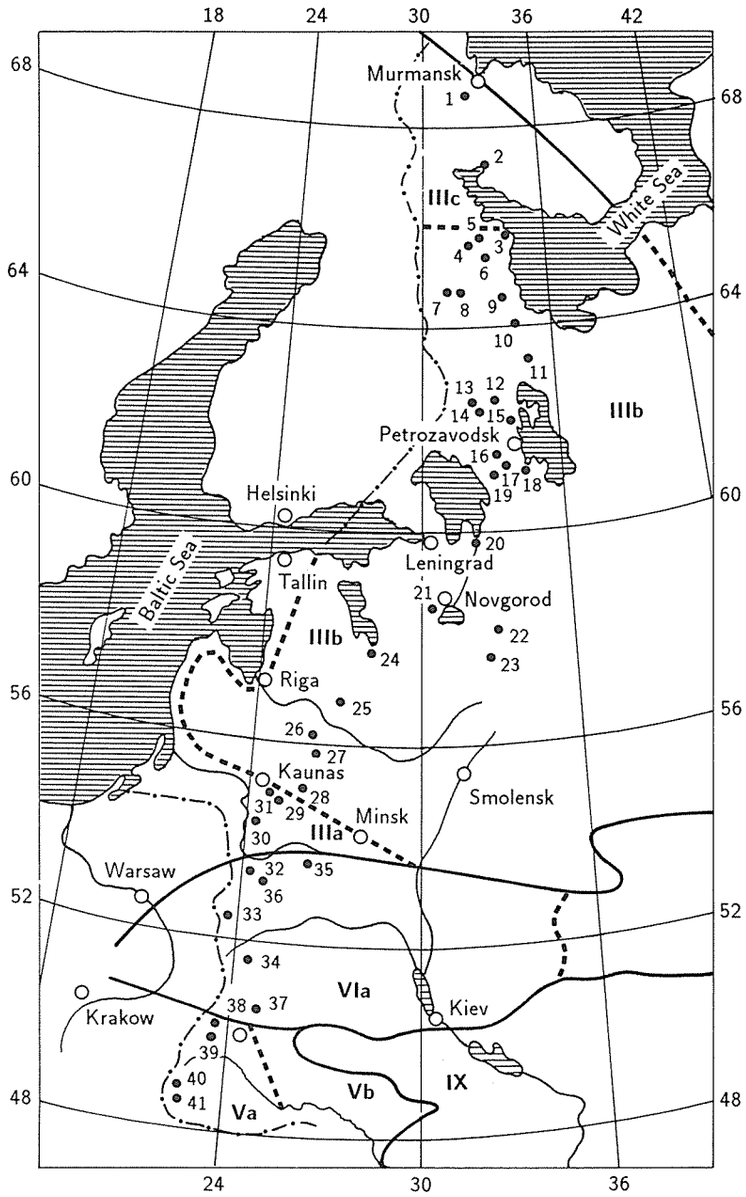

Figure 2.2. A north–south profile in which 41 study areas (2,692 trees) were chosen for sampling in typical parts of Kolapechora, Valdai–Onega, Baltic–Belorussian subprovinces, North European taiga province, Polessje subprovince as well as in the Carpathian subprovince of the Central European province.

Methods. Simple methods should be used at first, e.g., registration of pointer years as well as long-term and abrupt growth changes (see Chapter 5). Measurements of ring width and density can naturally also be used. This involves considerably more work, but may be more appropriate for some species.

Example 3: Pollution Research

Since dendrochronology is practically the only discipline that can provide the long-term historical dimension in pollution research on forested ecosystems, the range of applications is very wide and, in almost every case, politically important. The following problem areas can be investigated:

- Local: damage to trees and forests in the immediate vicinity of an emission source (Thompson, 1981; Fox *et al.*, 1986). Damage to and the state of health of trees in cities (Joos, 1987).
- Regional/national: comparison of the state of health of forests in areas with different population densities or exposure to different anthropogenic hazards (McLaughlin *et al.*, 1987).
- Continental/hemispheric: investigation of tree growth in relation to climatic and environmental changes caused by CO_2, acid rain, nitrogen oxides, and other very large-scale mechanisms (Hughes, 1987b).

Selection of sites and trees. Vinš and Markva (1972), Stravinskiene (1981), Thompson (1981), and Fox *et al.* (1986) obtained replicate samples of trees at increasing distances from a pollution source to study the relative growth effects attributed to proximity of pollution sources. Stands free of pollution were sampled for controls. Selection of trees of different species but with the same social status (16–20 per species and site) on homogeneous sites is desirable. Selection is based primarily on ecological gradients: dry to moist, acidic to basic, low to high elevation, outside and inside inversion layers, close to or far from suspected emission sources. Loss of radial increment owing to pollution as expressed in dendrochronological indices seems to be enough for increment calculations in forestry. In such studies, it may be necessary to compare a large number of trees and sites. Several hundred trees may not be sufficient, depending on the strength of the suspected pollution signal being investigated.

As the spatial scale progresses from the local effects of high pollution to chronic effects of regional background levels of pollution, the required number of sites and sampled trees may increase enormously. This is because of the lower level of impact that chronic, low-level pollution may have on trees. However, additional sampling design problems occur because regional studies may cross through vegetation, climate, and soil gradients that could confound the subsequent analyses. McLaughlin *et al.* (1987) provide an example of this kind of study.

With regard to continental and hemispheric studies, no sampling design has been satisfactorily formulated. However, the first attempts at hemispheric-scale investigations are in progress using existing tree-ring data collected for other purposes (Hughes, 1987b).

Method. When very large sample numbers are required, the use of the simplest methods may be necessary. The classic skeleton plot or the shortened version using pointer years may be used to record the onset, duration, and intensity of abrupt growth changes (see Chapter 5). At a higher level of analysis the influence of climate on ring width of trees in polluted areas may be factored out using the ring width from trees in unpolluted areas as controls (*Figure 2.3*; Thompson, 1981) or can be calculated by and removed from the tree-ring widths (Cook *et al.*, 1987; Cook, 1987a,b).

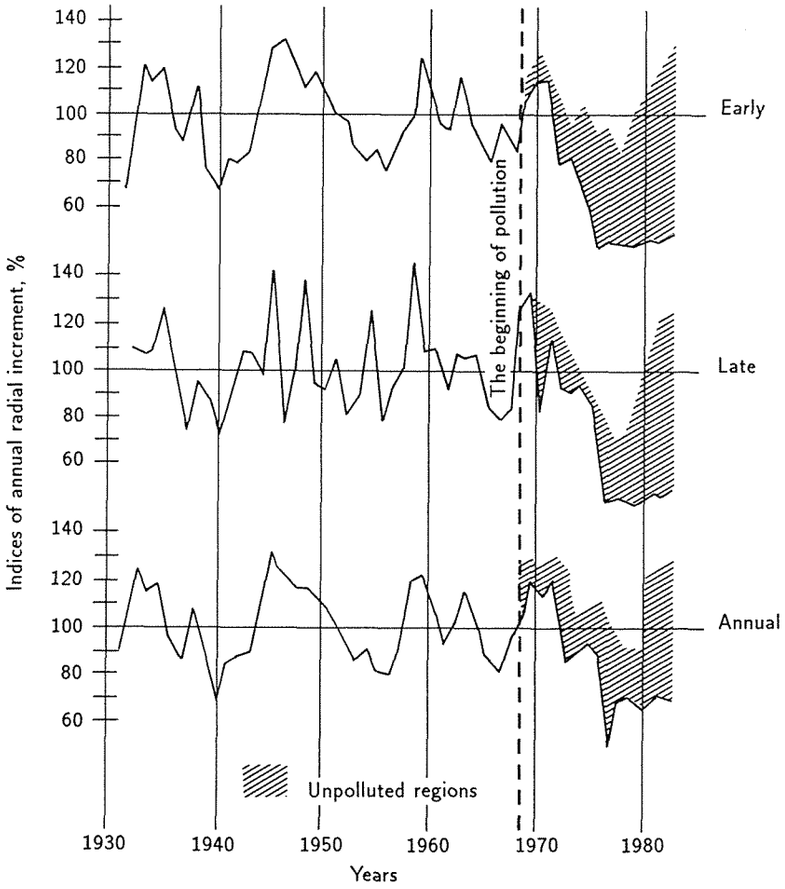

Figure 2.3. Variation of early, late, and annual ring width of *Pinus sylvestris* growing in a considerably polluted region. The hatched area is the loss of radial increment when compared with tree-ring widths from comparatively unpolluted regions.

It is difficult to understand pollution-induced growth changes because knowledge about translocation and fixation of elements in different parts of the tree is incomplete. It is known that pollution reduces cambial activity, increases K+ ion permeability, and increases the potassium residue in annual rings (Kairiukstis *et al.*, 1987b). It is not clear, however, how much time it will take before pollution causes abrupt growth changes. Regional and continental damage attributed to air pollution is more difficult to assess. The selection of sites can be the same as that of dendrochronological studies. A simple but powerful tool was introduced by Schweingruber *et al.* (1983). Severe growth reductions were recorded directly on the core or timber slice from thousands of trees from central Switzerland and the results mapped. All non-climatically caused tree-ring variations (aging, woodland management, etc.) were statistically eliminated as much as possible. All tree-ring series of a site that cross-date were then averaged, and the climatic impact was reconstructed according to the methods described in Chapter 4. The pollutant damage may then be assessed. In the case where the tree-growth baseline manifests distinct regularities (rhythmical, cyclical, etc.), dendrochronological prediction of increment damages can also be made (Kairiukstis *et al.*, 1987b,c).

2.1.12. Conclusion

The basis of every good dendrochronological study is the selection of samples according to biological–ecological criteria. The first important step in the somewhat lengthy process of dendrochronological analysis therefore takes place in the forest itself. Neither the most accurate measurements nor the most sophisticated statistical treatment can compensate for errors made here. The selection of trees, sites, and methods should primarily be made according to the aims of the study. One case may involve the use of complicated methods for the analysis of a single tree, while another may require simple observations of 5,000 trees. Dendrochronology today offers many methods, and it is important to decide which is the most appropriate for the task at hand.

2.2. Site and Sample Selection in Tropical Forests
M. Worbes

2.2.1. Introduction

Annual growth rings have been shown to occur in many tree species throughout the entire tropical zone (*Figure 2.4*; Coster, 1927, 1928; Mariaux, 1981; Worbes, 1986). Nevertheless, the idea still persists that tree growth under the "uniform tropical climate" is continuous. The growth rings frequently observed in tropical wood are often attributed to endogenous rhythms. Review articles tend to emphasize the difficulties of research on growth periodicity in tropical tree species rather than the successes achieved. Such research has generally been

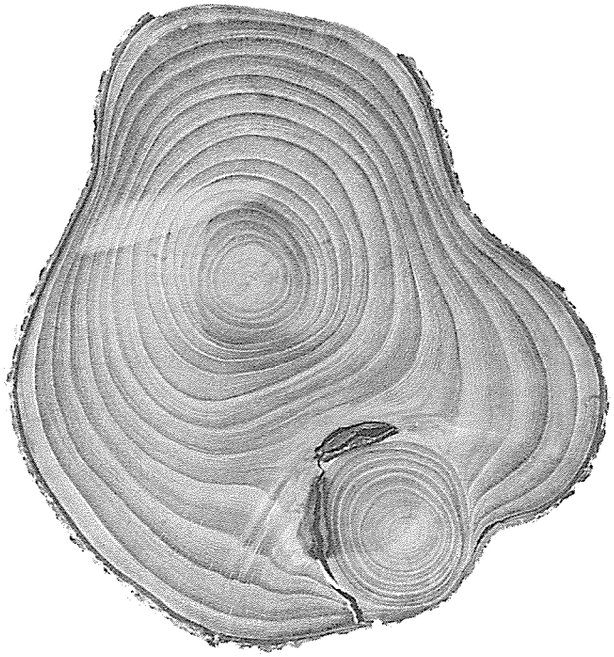

Figure 2.4. Cross section of a tropical hardwood *Tabebula bowbata* showing the appearance of annual tree rings.

conducted from an economic viewpoint. However, good commercial timber does not necessarily exhibit distinct growth bands.

2.2.2. Site selection

Our knowledge of the great variability of site conditions in the Tropics is currently increasing, particularly through large-scale ecological research projects. New information on both climatic and edaphic factors is available in connection with very diverse forms of vegetation and particular species composition.

Some factors that periodically limit tree growth in the Tropics are described below. On sites where these factors influence growth, annual rings either have been found or can be expected to be found.

Drought. Periods of pronounced drought are known to induce cambial dormancy. Though many reports maintain the opposite, marked dry periods do occur annually in many areas of the humid Tropics. For instance, Manaus, in the Amazon basin, experiences a phase of at least one to two months with less than 50 mm precipitation (*Figure 2.5*). Similar dry periods also occur in tropical Africa and parts of Southeast Asia.

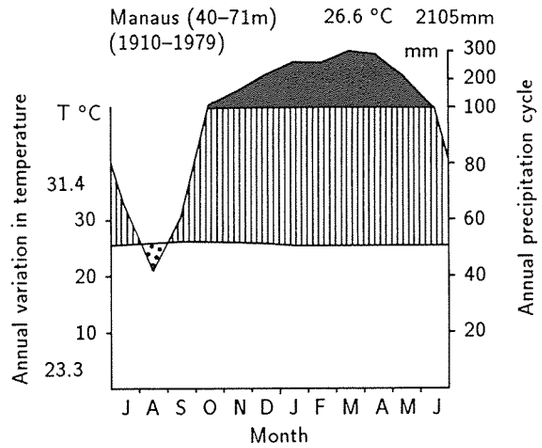

Figure 2.5. Monthly temperature and precipitation profiles for Manaus, Brazil, for the period 1910–1979. Note virtually no annual variation in temperature (left y-axis), but a clear dry period in the annual precipitation cycle (right y-axis) during the month of August. Such dry spells in the Tropics may allow trees to go dormant and, thus, produce annual rings.

Timberline. So far, no definite explanation has been found for the timberline in the Tropics. Walter (1973) lists a number of possible limiting factors, most of which are seasonal in nature, including the number of days with frost, the volume of precipitation, and the soil temperature.

Periodic inundation. One of the indirect effects of the climate is the annual inundation of large river systems. Such floods may inundate vast areas of forest stands, for example, in the Amazon basin. In circumstances of long-term flooding, anoxic conditions in the soil induce a dormant phase in tree growth and the formation of annual growth rings.

Chemical stress. Several stress factors occurring simultaneously at one site may mutually amplify each other's growth-limiting effects. The influence of periodic water shortage, for instance, may be intensified by an extremely low supply of nutrients, such as that which occurs in the Guayanas of Venezuela.

In the Tropics, as in temperate zones, the effect of climatic factors may be intensified by local conditions:

- Precipitation in the lee of mountain ranges is lower than the nationwide average.
- Water stress is higher on shallow, well-drained slopes than on plains.
- Floods exert their greatest influence in areas of low altitude.

Sites exposed to such extreme conditions may be expected to bear a greater number of species and more individuals with clearly defined growth rings than sites experiencing more uniform conditions.

Bearing in mind the great variation in site conditions and the present stage of research, large-scale sampling networks based purely on geographic coordinates offer even less promise in the Tropics than in temperate zones. Much more information can be obtained by compiling the results of various ecological research projects currently being conducted throughout the world, which provide data on climate, soil conditions, species composition, and ecological relationships. Indeed, the factors affecting tree growth can often be recognized solely through such comprehensive studies.

2.2.3. Sampling strategies

In view of the great site and species diversity and the difficulties of growth-ring analysis, dendrochronological studies in the Tropics require specially designed, multistaged sampling strategies.

Stage I: Selection of species. The first stage is selecting, from the multitude of tree species, one suitable for dendrochronological studies. A careful site selection is advantageous here, since it is apparent that on extreme sites the pressure of adaptation and specialization reduce the number of species.

It is also useful to consult lists of species already investigated (Fahn *et al.*, 1981; Worbes, 1985) and focus attention on genera or families common in these lists. In zones where annual flooding occur, the Annonaceae, Bignoniaceae, and Leguminosae [Papillionaeae], in particular, tend to form distinct growth rings. Furthermore, it is helpful to examine the deciduous species or stands, bearing in mind that deciduous species do not always form definite growth rings – for instance, those blooming or bearing fruit while bare of foliage.

In this stage, the main goal is to find trees with clearly defined growth rings. To achieve this, cores should be taken from two or three individuals of each species, because the distinctness of growth rings often varies within one species.

Stage II: Macroscopic analysis of growth rings. Having found trees with distinct growth rings, the next step is to examine whole stem disks for tapering, missing, or disappearing rings, and to determine whether the rings are uniformly evident over the entire cross section. Tapering rings often occur in the vicinity of branches, while rings are often found missing in regions between buttress roots. In trees of the lower story, with poor light conditions, growth rings are often narrow and indistinct.

Stage III: Determination of age and periodicity of growth rings. Before further investigations are initiated, the basic question of the periodicity of the growth rings should be clarified. When the study extends over a number of years, the easiest method is that of marking the cambium. If research is conducted on felled trees, a combination of independent methods is both essential and fruitful:

- Anatomical studies to identify the structure of growth-ring boundaries.
- Macroscopic examination of carefully prepared stem disks so a basic picture of the periodicity of the growth may be obtained. Applied to conifers from the timberline zone, the skeleton-plot method has proved suitable (Eckstein *et al.*, 1981). For analysis of trees growing on annually flooded sites, ring-width measurements have proved successful (Worbes, 1985).
- Once the structure of the growth rings has been determined, the findings should be confirmed through radiocarbon analysis (the 1960s nuclear weapon spike in ^{14}C). Such analyses, however, are both time-consuming and expensive; for wood with clearly defined growth rings, one analysis is sufficient, provided that the growth ring from the year with the highest radiocarbon can be isolated. The exact dating of samples with indistinct ring boundaries requires at least two or three analyses.

Stage IV: Particular dendrochronological problems. Once careful preliminary studies are completed, sites and species for dendrochronological, dendroclimatological, or dendroecological studies can be selected and a decision made as to whether cores or whole stem disks should be used. Disturbance of the forest environment can sometimes be avoided by taking samples from trees that have been felled for other reasons; in such cases it is necessary to define clearly the site conditions. Fresh botanical material should be collected for exact determination of the species sampled. Because of the great diversity, caution must be exercised in identifying species and, where possible, an expert in taxonomy should be consulted. Local names are particularly tricky, since they are often applied to several different species or even whole genera.

The selection of a species for certain studies may also be influenced by the method employed:

- Ring-width measurements should only be undertaken on species with clearly defined ring boundaries (e.g., Leguminosae).
- Densitometric studies are best conducted on species with the simplest anatomical structure. Species with a regular arrangement of parenchyma and fibrous tissues (Annonaceae) or little parenchyma (some Lauraceae) are most useful.
- Elemental and isotopic analyses often require a relatively large quantity of material. For such studies, fast-growing species or species from open stands (wide rings) are preferable. Species meeting all these requirements (e.g., *Swartzia laevicarpa*) may be difficult to find. Nevertheless, studies should be restricted to as few species as possible.

2.2.4. Conclusion

A survey of the literature and our own investigations show that the number of tropical species exhibiting distinct growth rings is much larger than generally

assumed. Dendrochronological studies on tropical species require not only refined techniques, but also a great deal of patience. Tropical species are certainly more difficult to work with than those trees from the temperate zones. Nevertheless, through careful choice of species, site, and method, dendrochronological studies can rapidly and extensively broaden our knowledge of the functioning of tropical forest ecosystems. It is to be hoped that this new branch of research will not only promote better utilization of wood in the endangered tropical forests, but also and above all contribute to the preservation of these unique forests.

2.3. Sample Preparation, Cross-dating, and Measurement

J.R. Pilcher

2.3.1. Introduction

This section deals with wood samples once they reach the laboratory. All samples collected by corer or by saw require some surface preparation before the rings are readable. Instructions for the handling of cores from increment corers may be found in Phipps (1985), Schweingruber (1983), and Bitvinskas (1974). Much was written in the early days of dendrochronology on preparation technique, and some of the methods used then deserve more attention. It has always been a common failing among students of dendrochronology that not enough effort is applied to sample preparation. No amount of fancy computerized equipment will produce satisfactory measurements and dating if the sample preparation is inadequate.

Once the surface is prepared it may be cross-dated first or measured first then cross-dated using the measured ring widths. The method used should be conditioned by the nature of the ring pattern, but in practice it tends to depend on the traditional habits of a particular laboratory. In general, the European laboratories, following the Huber tradition, measure first and then carry out the cross-dating on the measured ring widths; the US laboratories, following the Douglass tradition, cross-date first. Regardless of the method used, cross-dating is the single most important step in dendrochronology and the step that distinguishes dendrochronology from ring counting.

2.3.2. Sample preparation

Core mounting. Stokes and Smiley (1968) describe the mounting of increment cores in wooden supports. Further details may be found in Phipps (1985). The most important aspect of the mounting is the correct alignment of the cells in the core. If the core is twisted it may be softened in a jet of steam and gently twisted back to the correct alignment. Cores should be fixed to the mount using a water-soluble glue, so that they can be realigned if necessary. It is essential to clamp the core or to hold it in place with adhesive tape while the glue sets otherwise the core will bend and spring free of the mount at the ends.

Blade methods. Many dendrochronologists use a razor blade or scalpel to trim cores in the field to check core orientation and timber quality as a guide to further sampling. In early dendrochronological research, razor trimming was the main preparation method in the laboratory also. Douglass was very concerned about the perfection of surface preparation, and in a series of articles in *Tree-Ring Bulletin* (Douglass, 1940, 1941a, 1941b, 1943) he describes in great detail the correct methods of sample preparation. He considered that superior resolution of surface detail was obtained by cutting the wood at 35 degrees to the long axis of the cells as shown in *Figure 2.6.*

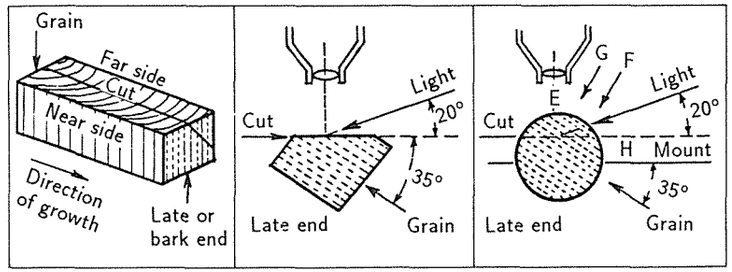

Figure 2.6. Cutting angle in relation to the grain of the wood (1 and 2). Observation and illumination angles in relation to the grain (3). (From Douglass, 1941a, page 31.)

The preparation of cores using a razor demands a fair degree of skill, but is still the simplest and fastest method for soft timbers. Several laboratories have recently modified sledge microtomes to enable long thin sections of cores to be obtained. The microtome leaves a superb surface on the core as well as provides thin sections that can be used for transmission microscopy and image analysis (Telewski *et al.*, 1987; Spirov and Terskov, 1987).

Sanding methods. Most laboratories now use sanding methods for routine sample preparation. Simple orbital or rotary-sanding tools using a range of grit size from 280 to 600 are quite satisfactory for most purposes, although most workers consider hand finishing of cores essential even for those sanded mechanically with the finest grit sizes. Where blocks of wood are available, considerable preparation time can be saved by using a sharp tungsten carbide-tipped, circular saw to cut the sample before sanding. These blades leave a surface that requires minimal sanding. In fact, the special blades used to prepare slices for X-ray densitometry give a surface suitable for ring-width measurement without further treatment (Schweingruber, 1983). Bowers (1964) describes a belt-sanding machine with a small contact area that avoids the common problem of overheating of the wood (*Figure 2.7*). Because of the time taken to change the sanding belts, this machine is only suitable for the bulk finishing of large numbers of samples in a batch.

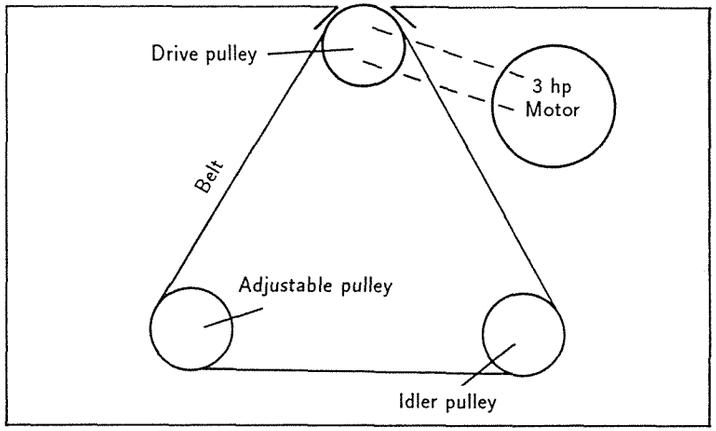

Figure 2.7. Essentials of the sanding machine as described by Bowers (1964).

If sanding methods are used, attention must be given to the dangers of breathing wood dust. Recent studies have linked hardwood dust inhalation to cancer of the nose and lungs. Suitable masks should be worn and dust extraction equipment installed in workshops.

Surface enhancements. Douglass describes the use of kerosene as a wetting agent to enhance the clarity of rings particularly on a saw-cut surface. At various times different pigments have been used to increase the contrast between cell wall and lumen on a wood surface. Powdered alumina was used by Douglass, and anthracene – which fluoresces under ultraviolet light – was used for photography. Phloroglucinol has been used to highlight the ring boundaries of diffuse porous hardwoods. Parker *et al.* (1976) describe ring enhancement using zinc oxide, which has the advantage that it can be removed easily using dilute acid. Many workers dating both ring-porous and diffuse-porous species use some form of chalk to fill the spring wood vessels to make them clearer. Ordinary blackboard chalk is suitable and convenient for this purpose.

Tropical woods. Tropical woods pose many problems to the dendrochronologist that are beyond the scope of this article. Not least of these is the problem of determining whether any observed rings in the wood are annual. This must be tested empirically, for example, by coring the same trees on two occasions separated by a few years (Villalba *et al.*, 1985). In many tropical woods, boundaries between rings (annual or otherwise) are often marked by parenchyma cells. Oblique lighting of razor-cut surfaces may highlight these cells.

Decayed wood and charcoal. Douglass (1941b) gives instructions for handling charcoal specimens. A cleanly broken surface usually gives the clearest picture of the rings, but will have a surface too uneven for photography. Hall (1939, 1946) gives full details of a paraffin-embedding method for charcoal, including how to trim the surface and remove the paraffin by heat treatment to leave a flat surface for photography. The dendrochronological laboratory in Sheffield (UK), which dates a lot of rotten and waterlogged oak wood, freezes the timber and prepares a surface using a multibladed surfacing tool (Surform) while still frozen. The measurement is carried out with the sample frozen or partially frozen.

Unorthodox methods. Occasionnally, necessity forces less satisfactory solutions for measurement problems. Failure to get permission to sample either living trees or felled logs in a forest in France forced me to photograph the chain-saw-cut ends of a number of felled trees. The rings were measured on the resulting color slides, and a satisfactory chronology developed (for most applications of dendrochronology the absolute ring widths are not important because the chronology is developed in the form of indices). Onoe (1987) describes a computed X-ray tomographical technique for imaging the rings in a solid object without any destructive sampling. The technique was developed to look at wood rot in utility poles, but satisfactory ring patterns were also obtained from dead wood and living trees. The technique could be applied to the analysis of museum objects.

2.3.3. Cross-dating

In 1943 Douglass stated, "To reach a feeling of security in cross-dating there is no substitute for minute personal comparisons between actual ring records in different trees." Later he stated, "There is no mechanical process, no rule of thumb, no formula, no correlation coefficient, to take the place of this personal comparison between different ring records; the operator does not dare to seek relief from his responsibility." The situation has not changed. There are many aids to cross-dating available, but the ultimate test remains the personal judgment of the dendrochronologist.

As noted above, cross-dating can be carried out either *on the wood* before measurement or using the measured ring widths.

Cross-dating on the wood. This is the classic method of cross-dating as performed by Douglass and his pupils. The dendrochronologist with many years of experience carries the patterns of hundreds of years of chronology in his head and can compare an observed pattern with this mental reference. The advantage of this method is its speed. Although it may seem rather subjective, the key to success of this and all other forms of cross-dating is replication. Even if a comparison of two pieces of wood appears satisfactory it would only be acceptable if replicated by comparison with other samples of the same age.

The skeleton plot as an aid to cross-dating. The skeleton plot is a graphic representation of those rings considered important in cross-dating. In the case of the stress-grown conifers, for which the method is normally most suited, these indicator years are the narrow rings. The method is explained in detail by

Douglass and by Stokes and Smiley (1968). Swetnam *et al.* (1985) give excellent examples of photographs of cores and of the skeleton plots derived from them. They even provide strips of graph paper so that the examples may be used as a tutorial. The skeleton plot method has been computerized by Cropper (1979) as shown in *Figure 2.8.*

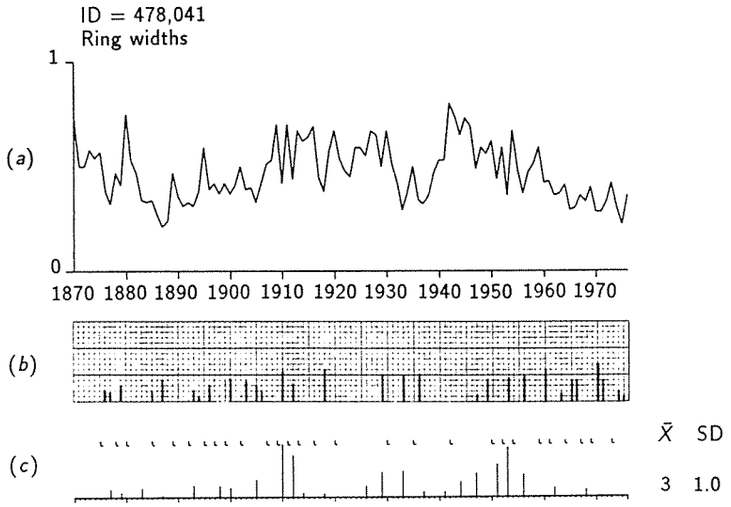

Figure 2.8. An example of a ring-width series (*a*), a hand-drawn skeleton plot of that series (*b*), and a computer-generated skeleton plot of the same series (*c*). (From Cropper, 1979.)

2.3.4. Measurement of ring widths

Measurement of ring widths can be carried out using any system that is sufficiently accurate. Much early work used the traditional traveling microscope of the physics laboratory. These are very slow to use as each measurement requires the reading of a vernier scale. Satisfactory measurement and dating of wide-ringed species can be carried out using a hand lens and transparent ruler. I routinely use this simple method in undergraduate classes. The main requirement for any serious dendrochronology, however, is a microscope of sufficient quality to enable measurement to continue without eyestrain and a system that does not require the operator to write down the measurements. The system most commonly used is one in which the measuring stage is electronically interfaced with a microcomputer that serves as the data recorder and editor.

The sample must not be held rigidly during the measurement stage because it is necessary to move the wood during the process to keep the line of measurement parallel to the rays. In some woods this adjustment needs to be done

between each ring. As part of the measurement process, it is normal to mark the wood to enable the operator to retrace his steps and to enable other dendrochronologists to see what has been measured. The standard marking system is to use a single mark for each decade, a double mark for each 50 years, and three marks for each century. In addition, special marks may be used to indicate the position of missing rings, frost rings, and other anomalies (see Swetnam *et al.*, 1985). When choosing or designing a computerized system, the researcher must keep in mind the need to record wood anatomical features while measuring.

Accuracy and precision of measurement. There are two sorts of accuracy in tree-ring dating. First, there is the accuracy of the annual record. This was the topic of the initial articles in the first two issues of *Tree-Ring Bulletin* (Douglass, 1934, 1935b) and has been central to the subject ever since. The ring record must be correct. There is no scope in dendrochronology for a plus or minus error as in radiocarbon dating. One year of error in the ring record will destroy the cross-dating and invalidate the result. Errors of this type are normally detected at the cross-dating stage. Apart from errors caused by missing and false rings, the most common source of error is a 9 or 11 year *decade* caused by careless observation or careless recording of the sample. For this reason it is important to mark the wood so that the error may be detected easily. One of the best checks on dating error is to ensure that samples of different sites are processed independently so that site chronologies may be used to check each other.

The second type of accuracy concerns the precision of measurement. As with any measurement system, there is the possibility of machine error and human error. The tree-ring measurement depends on the operator's judgment of the ring boundary. Machine error may come from poor quality screw threads or slippage on moving stage measurement machines. Many laboratories employ a quality-control system in which a proportion of all samples are measured by two operators and the results checked. In examples given by Fritts (1976), the sums of squares of differences is used as a criterion for the rejection of replicate measurements. One laboratory, using undergraduate labor, requires all samples to be measured by two workers and keeps an accuracy league displayed in the laboratory! The importance of accuracy depends on the purpose of the project. For dating, the accuracy of measurement is not of great importance. Where the measurements are the main end product, as in climatic studies, then the accuracy of measurement may be critical.

Cross-dating using measured ring widths. The usual procedure is to plot the ring width on a linear scale representing the years of growth for the x-axis and either a linear or logarithmic y-axis for the width of each ring. The log scale is often used in European laboratories and is justified on the grounds that it emphasizes the importance of narrow rings, which in some material may be important for dating. Log chart recorder paper may be obtained in rolls and used for manual plotting. Now that many laboratories use computer-driven plotters, the choice of scaling for the y-axis may be easily made to suit the material being dated. The dating is carried out on a light box by superimposing one or more graphs.

Use of computers in cross-dating. From the early days of dendrochronology workers have looked to computational methods to assist with cross-dating. Although the human brain is very efficient at cross-dating, the process lacks the objectivity demanded of a scientific discipline. Douglass mentions the use of correlation coefficients but rightly stressed the importance of the dendrochronologist's judgment. Any correlation method requires that the sample be measured first. Schulman (1952b) describes a coefficient of cross-dating quality for a batch of samples based on the mean sensitivity. Fritts (1963) gives a suite of computer programs for tree-ring research and shows the use of the correlation coefficient "to date series that cannot be conclusively dated by skeleton plot techniques."

The German dendrochronologists used the coefficient of parallel variation (Gleichläufigkeits-Koeffizient), which is a simple, but powerful, nonparametric test. While it can be calculated simply without a computer, a computer version is first described by Eckstein and Bauch (1969). In 1973, Baillie and Pilcher published a FORTRAN program for the calculation of a correlation coefficient and Student's t for all positions of overlap of two series. The program was designed to mimic the action of sliding one graph or skeleton plot past another to look for a position of coincidence. In the construction of the very long oak chronologies that have been used for radiocarbon calibration (Pilcher *et al.*, 1984; Brown *et al.*, 1986), the use of such a program to indicate likely cross-dating has been essential. The length of time spanned by the chronologies is such that it is practically impossible to find cross-dating without computer assistance. The graph of plotted ring widths of a chronology may be many meters long. The computer can scan all positions very quickly and indicate to the dendrochronologist the highest correlation that can then be examined visually.

In the last 10 years there has been a proliferation of computer programs for tree-ring research; the major ones will be described later. Some programs specifically concerned with cross-dating have been published. Wendland (1975) gives a program for locating missing rings in series being cross-dated. In 1983, Holmes published COFECHA, which is a valuable checking program that is designed to be used to check the cross-dating of a number of samples before they are combined into a chronology. In 1984, Munro reexamined the CROS program of Baillie and Pilcher and suggested improvements to the algorithm used in the calculation. Further discussions of cross-dating methods and recommendations for data transformations are given by Wigley *et al.* (1987a). Many of the cross-dating programs have been built into compact suites of programs for use on microcomputers. Some of these are described in Section 2.3.5.

Cross-dating of short sequences. Cross-dating depends on recognition of unique patterns of wide and narrow rings. It is clear that the chances of a pattern repeating in time and hence being *undatable* increase as the length of the pattern decreases. There is no single minimum number of rings that can be cross-dated, although experience in many laboratories suggests that reliable cross-dating should not be expected for sequences of less than about 40 years. Ideally, every dendrochronologist should establish a minimum for his or her own area and type of timber. This may be established by subdividing a long cross-dating series into

smaller and smaller sections and recording where cross-dating breaks down (Pilcher and Baillie, 1987). There are many examples in the literature of cross-dating on timbers of less than 50 years (e.g., Hollstein, 1980). Most of these must be treated with considerable caution. The dating is normally only possible by making assumptions about the likely age or contemporaneity of timbers. In other words, the dating is not true dendrochronology but is tree-ring-assisted dating or even tree-ring-assisted guesswork.

2.3.5. Microcomputers in dendrochronology

Dendrochronology was successful before computers were available and can still be carried out without computers. The use of a computer does not make the cross-dating or the dendrochronology in any way better, it merely makes the process faster and easier.

One of the main requirements for an automated measurement system is that the operator needs to be able to record the measured width without looking up from the microscope. Douglass recommended having an assistant write down the measurements as the operator calls them out. Recording the measurements is now the job of the computer. The computer may also be required to give warning of values that are outside a preset range and can signify the end of a decade to enable the operator to mark the wood. Normally, the measurements are stored on some form of disk storage system. Once in this form, printing, plotting, editing, cross-dating, and the formation of chronologies can be carried out without any further manual handling of the data.

One of the advantages of this type of system is the reduction in errors from data transcription. In the early stages of computerization most laboratories used some form of punch-card system to input information into the computer, but errors occurred in the manual transfer of data from recording sheets to the punch cards. This stage has been eliminated with the microcomputer systems. However, these systems have several disadvantages. Because of the large amounts of data that can be stored on floppy disks or hard disks, the potential loss from accidental damage is considerable. A single floppy disk may contain the data from more than 100 trees and represent a month of measurement time. Clearly, it is essential to keep backup copies of data disks.

Another more subtle danger is that the microcomputer can become a substitute for dendrochronological skill. It is easy to measure rings and use a computer cross-dating program without plotting the rings and examining the cross-dating visually. This is not dendrochronology. Equally, the speed with which measurement and cross-dating can be completed often leads to neglecting careful observation of the timber. In particular, the careful observation and recording of tree centers, presence of sapwood, ring anomalies, and other details of the wood can easily be overlooked to the great detriment of the interpretation of the result. There is justification for training all dendrochronologists to cross-date and process samples entirely without a computer until they are familiar with the fundamental methods.

Microcomputer Systems Commonly Used

Purchasing information of measurement machines and software mentioned below is given in Appendix C.

CompU-TA. This is a series of programs for measurement, listing, plotting, editing, and cross-dating for use on an Apple microcomputer. It is written in BASIC and is designed for data capture from an incremental measurement machine. The programs are professionally written and are well equipped with error traps. New users can become familiar with the system in a few hours. The programs are described by Robinson and Evans (1980).

TRIMS. This system is similar in concept to the *CompU-TA* programs but is designed for IBM and IBM compatible machines. Some idea of the scope of the programs can be gained from the main menu and edit menu illustrated in *Figure 2.9.*

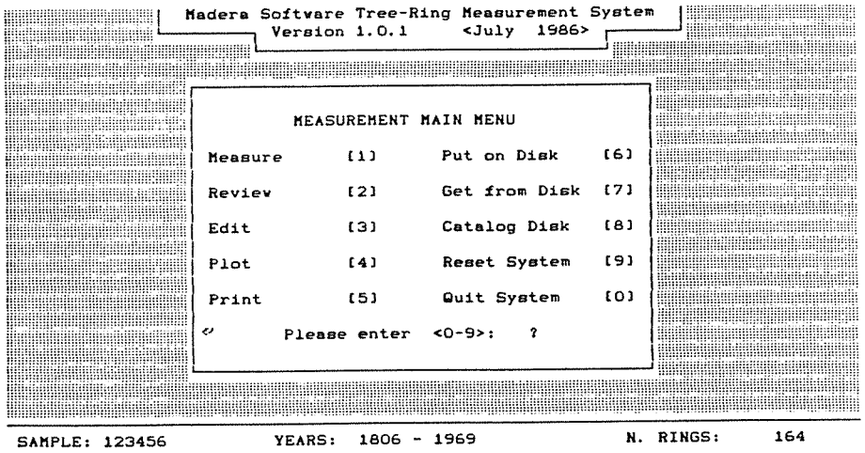

Figure 2.9. Main menu from the *TRIMS* computer package showing the range of options available.

Belfast Tree-Ring Programs. A suite of programs with a rather similar concept to the *CompU-TA* system has been produced by the Belfast tree-ring laboratory. This is also for use with an Apple II microcomputer and Henson measuring machine and has options for measurement, listing, plotting, editing, forming chronologies, and various other facilities. While not professionally programmed, the *Belfast* programs are easy to operate and are widely used. Data conversion between the *CompU-TA* and *Belfast* systems on Apple computers is simple.

CATRAS. The other widely used professional system is *CATRAS* (Computer Aided Tree-Ring Analysis System). This program is modeled somewhat differently, being built around a database system as illustrated in *Figure 2.10.* This system is fully described by Aniol (1983). It runs under the CP/M operating system, which is widely available. It has been implemented on Kontron PSI-80, Intersystems DPS-1, and DEC PDP 11/70 where it is used in a multi-user system. It has recently become available for use on IBM computers. *CATRAS* is a friendly system requiring no knowledge of the internal working of the programs. It has been widely used for archaeological dating and in climatological and ecological research.

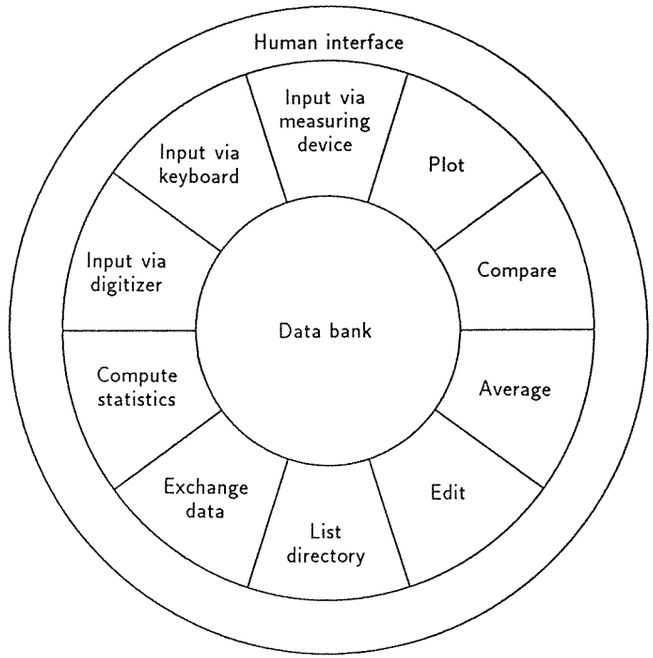

Figure 2.10. The schematic structure of *CATRAS.* (From Aniol, 1983.)

Many laboratories have invented their own wheels. Some have attempted to mechanize the process of measurement further by adding a stepping motor to drive the sample across the field of view of the microscope. While some operators have become used to such a system others feel more in control and more relaxed if the sample movement is by hand.

2.3.6. Archiving the primary data

With the advent of the microcomputer measurement systems described above, a large amount of tree-ring data is now kept on computer disks. The life of these disks is not known, but they are certainly not of archive quality and are very easily destroyed by magnetic fields, heat, mechanical damage – or coffee. Any laboratory carrying out dendrochronological research should consider the problems of long-term data storage. There is still a good case to be made for keeping one copy of all primary data on paper in addition to any backup copies of the magnetic storage medium that might be kept. Data on magnetic tape has a life of only about five years, and under adverse conditions tape may become unreadable before that. For the long-term safekeeping of primary data the International Tree-Ring Data Bank forms the obvious repository.

Archiving the Wood: The Ideal and the Reality

Wood samples are bulky, occupy a lot of expensive space, and are a fire hazard. It is possible to reduce all tree-ring samples to 1–2 mm slices and to file these in some storage such as that used for photographic negatives. The Tree-Ring Laboratory at Marseille keeps all increment cores in this form. In this way thousands of samples may be stored on an office bookshelf or more sensibly in a fire-resistant filing cabinet. However, such storage does not preserve enough material for future studies of isotopes, radiocarbon, heavy metals, etc. Bulk samples for such a purpose pose a more serious problem. The work on bog and river oaks in Ireland and the Federal Republic of Germany has resulted in many thousands of samples each of several kg weight. The permanent labeling of such samples also poses a problem. Embossed plastic tape is convenient but not very permanent. Embossed stainless steel tape securely nailed to the log is probably the best solution.

There is no point in keeping the wood if no one knows where it is – the same applies to the numerical data. Reports and publications should state where the wood and the data are stored.

The International Tree-Ring Data Bank

The ITRDB is a professional organization that provides a central storehouse for dendrochronological data around the world. It was formed to encourage international cooperation among the various branches of dendrochronology, especially dendroclimatology. Its holdings include computerized records of dated tree-ring width measurements and site chronologies that can be used for dendroclimatic studies. These data are available to all researchers in the field. The Data Bank is housed in the Laboratory of Tree-Ring Research, University of Arizona, Tucson, Arizona 85721, USA. The Data Bank is independent of the Laboratory of Tree-Ring Research and the University of Arizona and is administered by a director and a board selected from members representing different countries that have contributed data. The Data Bank has information from more than 500 sites in 27 countries, representing 60 species of tree and contributed by more

than 45 individuals or institutions. Further information may be obtained from the Director at the address given above.

2.4. Dendroclimatological Study of Prostrate Woody Plants

V.G. Kolishchuk

2.4.1. Introduction

Prostrate woody plants, which include prostrate trees, prostrate shrubs, and prostrate dwarf shrubs, make up a specific group of plant life forms. They are found among the gymnosperms and angiosperms in different families and genera. According to incomplete data there are more than 1,200 species of prostrate woody plants in the world flora. Many species of prostrate woody plants grow in forests, but more commonly they are distributed at high altitudes, in forest tundra, in the tundra, on the seashore, and also in arid regions where they often form a closed canopy over vast territories. Being protected by snow in winter and because of a short vegetative period, prostrate woody plants spread farther than erect trees at their northern and altitudinal limits. Dendrochronological investigations can be considerably enlarged in such regions if prostrate plants are studied.

The longevity of prostrate woody plants is quite often no less than that of erect trees, shrubs, and dwarf shrubs, and as a rule even exceeds it. The stable correlation of increment with limiting ecological factors is vividly expressed in prostrate woody plants on the upper and northern limits of woody vegetation. The sensitivity of their increment is also no less than that of erect forest trees. Their individual increment variability is also smaller, which can be explained by the greater stability of the plant communities with time.

The numerous attempts to use cross sections of the basal trunk parts of prostrate woody plants for their increment analysis and the definition of their age gave no positive results. For instance, according to Grosset (1959), the number of annual rings in any part of the prostrate trunk of *Pinus pumila* was approximately the same, which contradicted the age calculated from the increment of the trunk length.

2.4.2. Prostrate growth and missing rings

All the difficulties of using prostrate woody plants in dendrochronology are caused by the peculiarities of the formation of wood increment along the trunk (Kolishchuk, 1966, 1967, 1968a). To understand this better it is expedient to start with the well-known phenomenon of missing rings in the basal part of the trunk. Missing annual rings for one or more years usually occur in the years most unfavorable for tree growth. In such years the volume of the annual increment of wood decreases to such a degree that assimilates are not available to form a growth layer along the whole trunk. As the cambial activity starts from the top of the tree, the annual ring is able to form only in the upper part of the

trunk. Missing rings in the lower part of the trunk cause considerable difficulties, and the size of tree increment in such years cannot be compared with the size of the increment in the previous and following years. In fact, the increment for the period of the missing rings cannot be measured. If the frequency of missing rings is great, such trees are difficult to use for dendrochronology.

For prostrate woody plants having both unlimited growth of trunk length and limited growth in thickness, missing annual rings in the basal part of the trunk are common. Consequently, normal layers of increment are found only in the upper part of the trunks. With age the trunks become longer and the vegetative growth moves further from the roots and the basal zone of the trunk. This is promoted by the formation of adventitious roots. Thus the zone of formation of normal annual rings moves away from the base of the trunk. This is why further growth of the trunk diameter in its basal part does not take place, and the diameter along most of the length of the trunk remains approximately the same (*Figure 2.11*).

2.4.3. Methods

To find the real age of prostrate woody plants and to investigate the dynamics of their growth, we applied the method of serial sectioning of the trunk at equal intervals from the top to the base (Kolishchuk, 1966, 1967). Depending on the type of plant, its life form, and the size of increment in height (length), it is necessary to take sections at 1, 0.5, 0.25, or even 0.1 m intervals. The length of the wood increment zone in prostrate trees is three to five or more m, in prostrate shrubs one to three m, and in prostrate dwarf shrubs about one m. When choosing the distance between cuts the most important factor is to provide sufficient overlap of ring-width curves of neighboring sections and to cover the formation zone of the normal annual increment by at least three or four sections. On each section, the annual rings are widest in the central part, because their formation takes place near the apex of the trunk (*Figure 2.11*). To the periphery of the sections the width of the annual rings decreases steadily until indistinct rings are formed by a few cells of secondary xylem and then the rings are missing. It should be noted that the phloem part of the trunk remains viable up to the last living roots at the basal end of the trunk.

Each section of the prostrate woody plant under investigation is numbered according to the number of the parent plant and the number of the trunk of this plant, and the distance to the top is measured. It is also identified according to the part of the world from which it was acquired. The sections taken from rising overground parts and prostrate parts are also distinguished. The calculation of the annual rings, their division into five-year periods (as is normal silvicultural practice in some areas), and measurement of their widths are started from the cut nearest the top, moving from the periphery to the center. On sections with very narrow outer rings, the measurement of the rings should start from the center, referring the central ring arbitrarily to a certain year. The precision of the ring-width measurement should be 10 times more than the minimum value of their width (usually 0.01 mm). On the basis of the measured widths on each

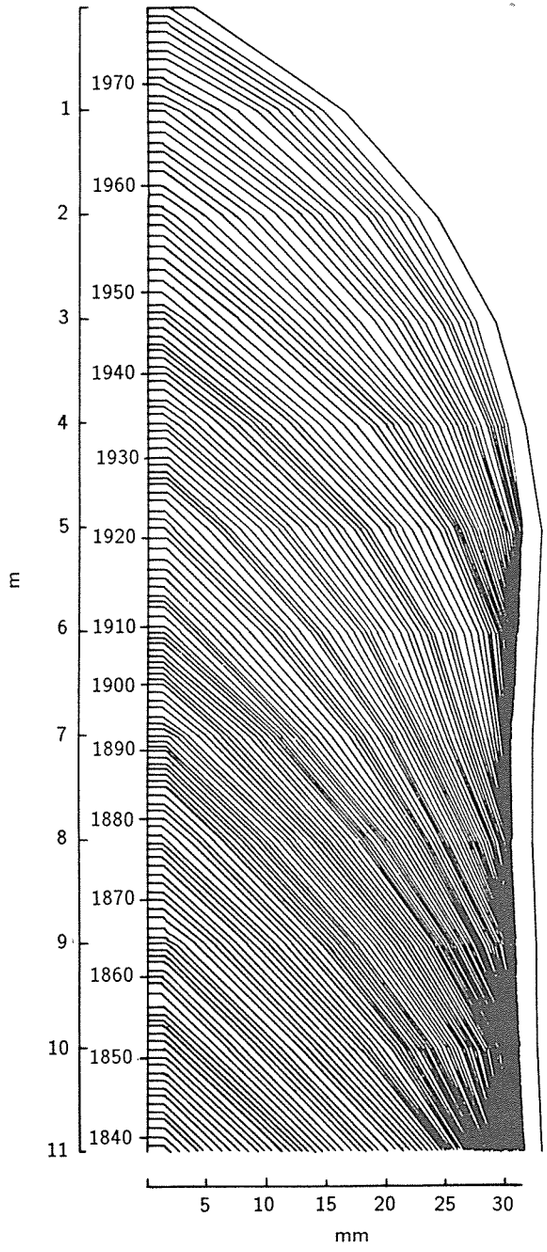

Figure 2.11. Longitudinal section of the trunk of *Pinus mugo* showing the widths of the annual ring profiles with height.

radius, we construct graphs by which we follow the synchronism of changes of the ring widths on all the radii of the section and thus prevent possible error. Only after that do we calculate the average values from four radii for each calendar year of the given section. The successive overlapping of the curves of separate sections from the top to the basal part of the trunk helps to refer the curve of each section to a definite time period during which the radial growth of the trunk took place (*Figure 2.12*). Cross-dating the changes of ring width from year to year allows accurate dating of all annual rings that have been recorded and measured on all sections of the trunk. Thus the age of the whole trunk is obtained.

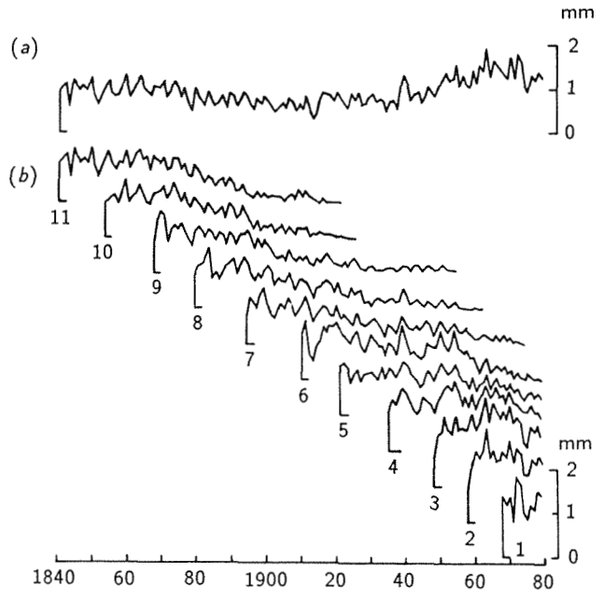

Figure 2.12. Curves of the annual ring widths of the whole trunk averaged across sections (*a*) and separate cross sections (1–11) (*b*).

The average width of the annual increment for each calendar year is calculated by the values of three or four neighboring sections moving from the top to the basal part of the trunk. The central ring and several (two or three) following ones should not be included in the calculation of the average values of ring width. The average values reflect the dynamics of the radial increment of the prostrate woody-plant trunk for the period of its growth. To obtain a tree-ring chronology that accurately reflects the growth of the species under study in a specific habitat, about 10 individuals must be analyzed. The difference in the increment of separate individuals being small, the chronology of the absolute values of radial increment can be constructed. If the difference in the value of

the radial increment of separate individuals is more than 30%, it is necessary to calculate indices of increment for each tree (see Chapter 3) and construct a tree-ring chronology from these indices.

In the chronologies from prostrate woody plants of many years length, cycles of different duration are clearly evident (Kolishchuk, 1966). The variety of the length of the increment accumulation zone along the trunk is also noticeable. From investigations in the Carpathians, in the Caucasus, and in the Baikal region, prostrate trees (*Pinus mugo*, *Dushekia viridis*, *Quercus pontica*, *Pinus pumila*) show stable positive correlations of increment with the average temperature during the period of active growth.

Prostrate woody plants deserve a wider application in dendrochronology. Using these plants we can obtain information about the dynamics of increment growth and ecological factors under the least favorable conditions for woody plants.

2.5. Radiodensitometry

F.H. Schweingruber

2.5.1. Introduction

Wood density is an important parameter in wood technology. The density of fairly large wood samples may be determined through volumetric-gravimetric methods, i.e., weighing and volume measurement, and is then termed gravimetric density. As the measurement of this density presents methodological problems where small objects are concerned, a number of processes for tracing density variations within annual rings have been developed. Those that have proved most practicable are described below.

Photometry. Wood density may be determined by measuring the light passing through a microsection or reflected from a transverse section (*Figure 2.13*). Because of differing wood colors and uneven dye absorption, errors often occur. The new electronic image analyzers seem to eliminate several of the problems (Yanosky *et al.*, 1986). Possibly they could be used to determine gray levels on radiographs. If so they will replace the densitometer used in the X-ray technique. Photometric methods have been described by several authors (e.g., Muller-Stoll, 1947; Green, 1965; Vaganov and Terskov, 1977).

Morphometry. As cell wall density is practically constant at 2.56 g/cc in most species (Eckstein *et al.*, 1977; Jagels and Dyer, 1983), wood density can be very accurately determined through the measurement of cell wall thickness and cell lumen size in microsections or well-polished transverse sections. The results are comparable with those obtained through X-ray analysis.

Radiographic methods. Since the early 1960s a number of radiographic methods have been developed, e.g., beta radiography (Phillips *et al.*, 1962), gamma radiography (Woods and Lawhon, 1974), and X-ray radiography. Only the last

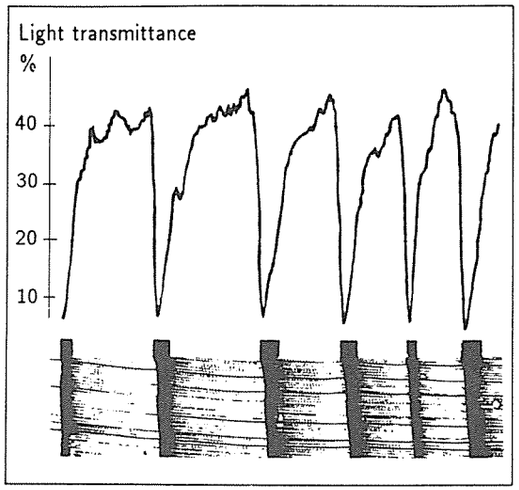

Figure 2.13. Wood density may be determined by measuring the light passing through a microsection or reflected from a transverse section. Note that the amount of light that has been transmitted through this wood specimen is lowest (<10%) for the more dense latewood and highest (>40%) for the less dense earlywood.

of these has proved suitable. Today it is generally termed X-ray densitometry, although Polge (1963) used the term xylochronology. All the literature on densitometry has been compiled up to 1982 by Sauvala (1982).

X-ray densitometry. This technique was invented by Polge (1963, 1966) and further developed by Lenz *et al.* (1976) and Jacoby and Perry (1981). The basic steps and the possible sources of error are described below. Detailed descriptions may be found in Polge (1963, 1966), Parker (1970), and Schweingruber (1983). The main steps are illustrated in *Figure 2.14*.

2.5.2. Sample collection and preparation

The technique is basically the same as that used in ring-width measurement (increment borer of 5 mm diameter, special dry wood borers, stem disks). The cores must be taken as nearly perpendicular to the stem axis as possible so that the maximum density values obtained through radiography are not distorted. To ensure correct orientation, a corer support is used. The cores are stored in air-dry conditions after labeling with a very soft pencil.

Elimination of heartwood substances. Resins and heartwood substances are more or less mobile compounds whose X-ray absorption rates differ from those of cell wall components. Consequently, they must be chemically removed. This is done

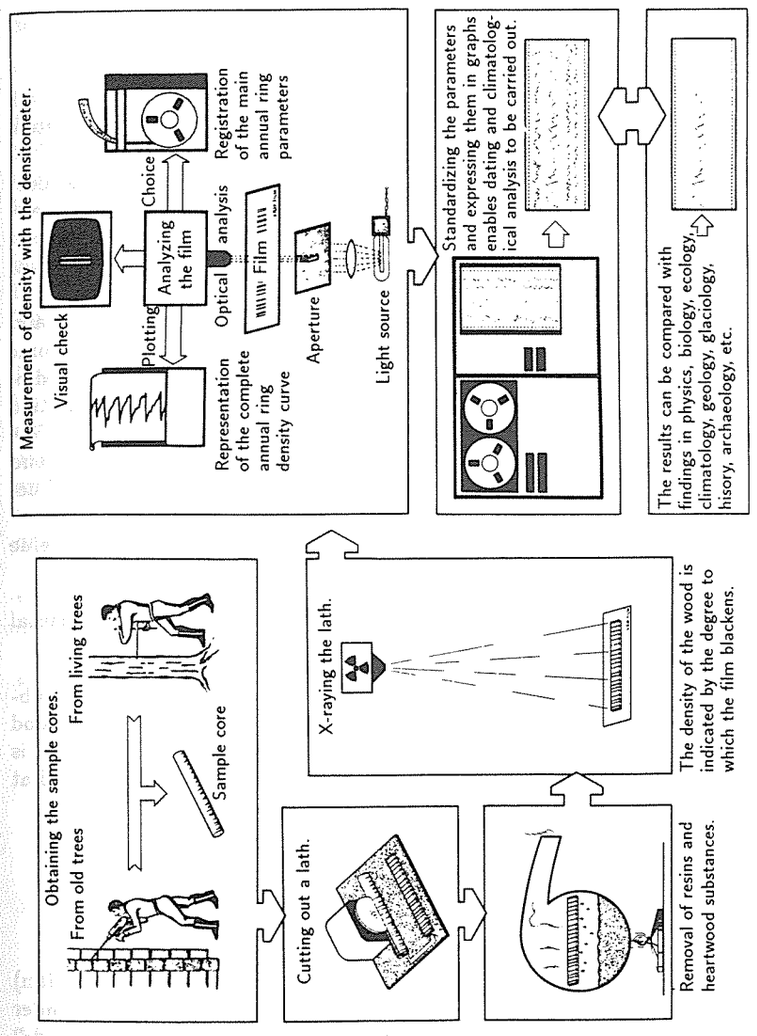

Figure 2.14. The basic steps of X-ray densitometry from sample collection to specimen preparation and, finally, to the measurement and analysis of wood density profiles. At each step, care must be taken to ensure that errors are eliminated.

through distillation in a Soxhlett device; resins are extracted with alcohol, heartwood substances with water. It is difficult to know when extraction is complete. Some woods such as *Larix* require long extraction (e.g., more than one week in xylene). The dangers of using carcinogenic solvents such as benzene and xylene in extraction equipment must be considered in the design of a procedure.

Cutting. Laths of equal thickness have to be cut from the round cores. Four methods are currently in use.

- The core is glued between two wooden supports and a two-mm-thick lath cut out with a twin-bladed circular saw. This is the Vancouver system (Kusec, 1972).
- The core is glued to a wooden support with the radial surface uppermost and a 1.25-mm-thick lath cut out with a small twin-bladed circular saw. This is the Birmensdorf system. With this method it is possible to cut obliquely bored cores into several pieces, so that the radiograph is clear over the whole length of each lath.
- The core is glued to a support with the transverse surface uppermost, and microsections of 80–100 microns are cut with a very steady microtome using a very thick knife. Thanks to the fineness of the sections, the radiographs are clear even where the fibers run obliquely. The preparation involves much work, and the technical problems are not easy to solve. The technique was developed at the Lamont-Doherty Geological Laboratory and is also in use by Telewski in the Laboratory of Tree-Ring Research in Tucson (see Telewski *et al.*, 1987).
- In the Nancy system the sample is held by clamps when being cut. No glue is used.

The first two methods have proved valuable; the third is still in the experimental stage.

Climatization. Water absorbs X-rays to a greater degree than cell wall substances. To obtain comparable density values, the moisture content of the wood must be kept constant. In Birmensdorf, for example, the moisture content is adjusted to 9% by placing the samples in the X-ray booth, which is climatized at 20 °C and 50% relative humidity, for two to four hours before radiography.

2.5.3. Radiography

Three methods are currently in use.

- Irradiation of a film (Kodak, Type R, single-coated industrial X-ray film) resting on the moving stage. The film is transported at five cm/min under the radiation source, which is 31 cm above, and irradiated at 20kVh and 2 mA (Parker and Jozsa, 1973; Vancouver system).
- Irradiation of a film (Kodak, Type X-Omat TL, double-coated medical X-ray film) resting on a stationary stage at 11 kVh and 20 mA for 90 min. The source is 250 cm above the film (Nancy system).

- Irradiation of the wood samples on a moving stage. The radiation passing through the samples is measured directly thus eliminating the production of radiographs (Jozsa and Myronuk, 1987).

The first two methods provide radiographs forming a database that can be preserved and rechecked at any time; they have both proved useful. The third technique does not supply any optical database and is still in the experimental stage.

Film development. The development of the film is of great importance (Polge, 1966). Most laboratories use their own semiautomatic processors. The laboratory in Birmensdorf develops its films in an automatic processor with standardized processing belonging to a city hospital, where proper maintenance is guaranteed. Nonstandardized processing, hand developing, and often developing in semiautomatic processors result in uneven blackening of the film caused by irregular movement in the developer tank or the use of old inactive solutions. The wood density values obtained from such films cannot be used.

Measurement of density. The different gray levels produced on the radiograph by the wood samples are converted to wood density values. The basic instrument used is the densitometer. Different systems are in current use and new ones are being developed (see Parker *et al.*, 1976; Lenz *et al.*, 1976; Schweingruber, 1986). Calibration is extremely important. At present different laboratories seem to use different standards (Evertsen, 1982). The principle is described below.

- A stepped calibration wedge is made from a homogeneous material with similar X-ray absorption properties to wood. The density and thickness of the wedge are known.
- The wedge is irradiated together with the samples. As the optical density does not increase linearly with increasing thickness of the steps, it has to be mathematically converted to gravimetric density. That is, each step on the wedge corresponds to a gravimetric density. The radiographic densities of the wedge are converted to gravimetric wood densities through comparison of the known densities of the wood and the material of which the wedge is made and the radiographic densities. The difference between the radiographic and gravimetric values is used as a correction factor. Each species seems to have its own absorption coefficient. On average, the radiographic density is higher than the volumetric–gravimetric density by 12.9% in *Picea abies* and by 7.2% in *Pinus sylvestris*, *P. cembra*, and *Larix decidua*.

2.5.4. Selection of parameters from density profiles

For both technological and biological–climatological studies it is necessary to measure a selection of parameters within the density profile. Analog or digital processing of the actual measurements (every 10 microns) produces a density

profile. From this certain parameters are registered, either optically or, more commonly today, with a computerized system. In the Birmensdorf system this is done by a computer directly linked to the densitometer. In other systems all the values are stored first and the parameters selected from the digitized density profile. The parameters found to be important by the Birmensdorf laboratory (*Figure 2.15*) are described below.

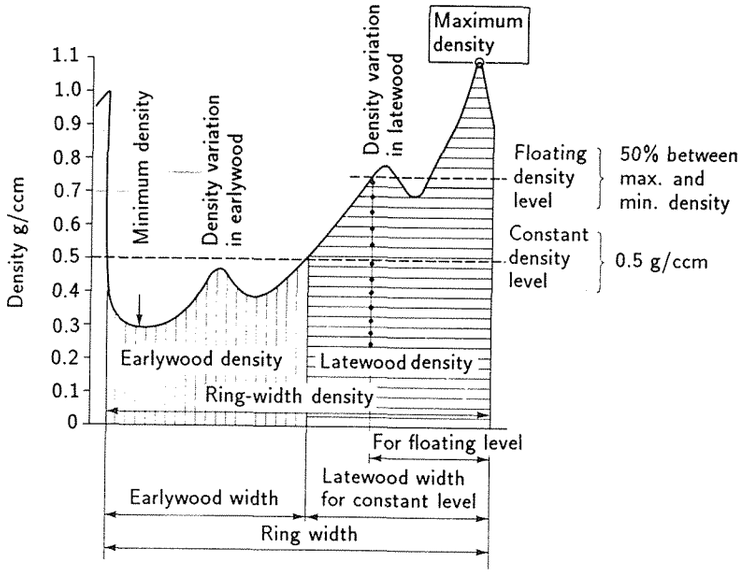

Figure 2.15. Ring parameters that are measured when analyzing tree rings using X-ray densitometry.

Maximum density. Important for the reconstruction of temperature in cool–moist zones.

Minimum density. Important for the reconstruction of precipitation in drier zones.

Total ring width. Important for all dating work. Ring width is particularly suitable for the reconstruction of precipitation in semiarid zones.

Earlywood width, latewood width. These, especially latewood width, seem to react strongly to limiting environmental factors in temperate zones. The distinction between earlywood and latewood is always arbitrary. For European woods, the following density thresholds have been found appropriate: larch 0.55, spruce 0.5, cembran pine 0.45 g/cc. Recently, a sliding threshold has come into use; it

remains halfway between the minimum and maximum density values of each ring. There has been a lot of research on the interpretation of density profiles, and many different systems have been studied.

Proportion of latewood. This varies from species to species and from site to site. It seems particularly suitable for the investigation of silvicultural measures.

Earlywood density, latewood density, total ring density. The use of these parameters in biological–climatological research has barely been explored. At the moment they are only important in technological wood research where they are used to characterize the wood.

Intra-annual density variations are important for the determination of short-term climatic changes during the vegetation period in arid, temperate, and subtropical zones. They rarely occur in cool–moist climates (boreal zone and mountain locations).

The statistical processing of the results is in principle the same as in all ring-width studies. However, standardization to remove age trend is usually different from that used for ring-width series. Because several parameters are measured for each ring, the volume of data in densitometry is very great, consequently standard computer programs for the statistical processing of tree-ring data need modification.

2.5.5. Limits of radiodensitometry

The applications of densitometrical techniques are limited by the anatomical characteristics of the wood. For example, hardwoods are rarely suitable for dendroecological studies. Irregular distributions of pores (vessels) and rays distort the general density pattern of the wood. Densitometric investigations involve much work and, from the technical viewpoint, are not easy to conduct. Consequently, such studies should only be undertaken where other, simpler methods prove inadequate, e.g., the determination of maximum density or mean earlywood and latewood densities. Since none of the densitometric systems has been industrially manufactured on a large scale, they all have their weak points. At the moment it is not possible to compare the absolute values measured at the different laboratories directly with each other (Evertsen, 1982).

Within each system many possible sources of error can considerably distort the results. They can, however, be avoided through appropriate measures.

- Oblique fiber direction may lead to unclear radiographs, i.e., the earlywood and latewood zones are mixed.
- Great care must be taken in data acquisition to avoid technical errors such as oblique positioning of the measuring slit at ring boundaries, lack of attention to cracks in the sample, misinterpretation of resin ducts, density fluctuations, fungal attack, heartwood substances, reaction wood, or decay. In each case the operator must decide what should be included in the data file. Automation of this process seems impossible.

The invention of radiodensitometry has provided dendrochronological research with a superb technical instrument. Over the first 20 years, its usefulness and applications had to be demonstrated through pioneer studies. Today it can be employed on a broad basis in many subdisciplines of dendrochronology.

To give an example for climatology: samples were taken from conifers on cool–moist sites throughout Europe and used to construct 104 chronologies of maximum latewood density and ring width (Schweingruber, 1985). The area of significant similarity between the curves is considerably greater for maximum density than for ring width (*Figure 2.16*). This indicated that external factors have a more uniform influence on cell wall growth in latewood than on cambial activity. In trees of the northern and subalpine timberlines, maximum density is essentially a measure of mean summer temperature (Schweingruber, 1985). It looks as if it will be possible to use these results to reconstruct the annual summer temperature distributions in the Northern Hemisphere over the past 300–400 years with great accuracy. These results constitute an important basis for

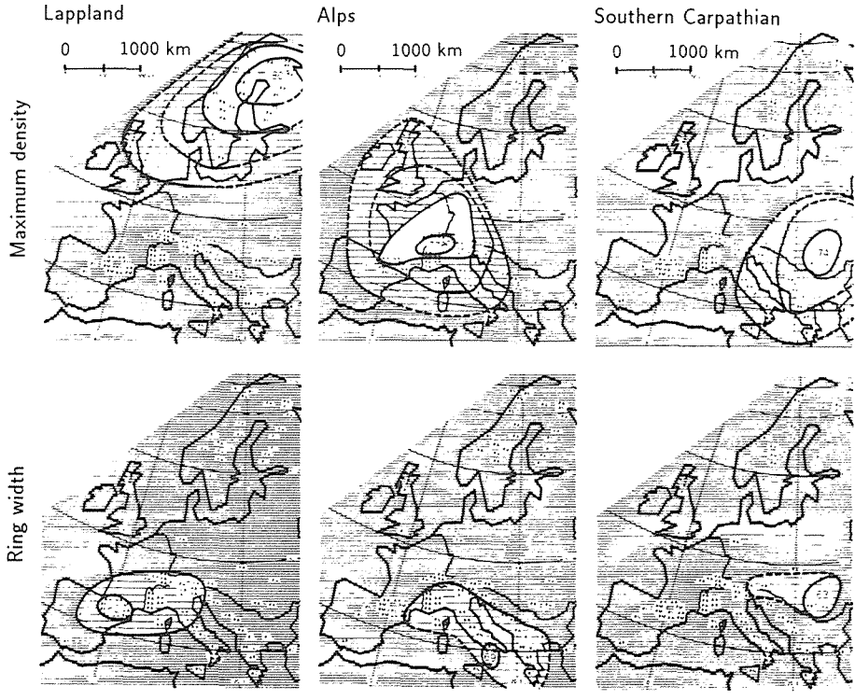

Figure 2.16. Maximum latewood density and ring-width patterns obtained from conifers growing on 104 cool–moist sites throughout Europe. The area of significant similarity between the curves is considerably greater for maximum density than for ring width. This indicated that external factors such as climate have a more uniform influence on cell wall growth in latewood than on cambial activity.

prognoses of climatic development in the light of the suspected global warming due to the greenhouse effect.

2.6. The Tracheidogram Method in Tree-Ring Analysis and Its Application

E.A. Vaganov

2.6.1. Introduction

Data on the anatomical structure of tree rings are currently being applied more and more intensively. This fact is confirmed by the development of new equipment and methods for this kind of analysis (Polge, 1966, 1978; Schweingruber, 1983; Vaganov and Terskov, 1977) and by the vast volume of ecologically based information concerning woody-plant growth. Also a more precise interpretation of this information on the basis of statistical models describes the interrelations between annual ring structure and climate.

Indirect physical indices of tree-ring structure (such as density and its distribution, porosity, and the reflection and transmission of light) possess a quite distinct structural basis, i.e., they integrate the anatomical differences of cells in intra-seasonal zones. For instance, the changes in density as well as incident light or porosity changes in conifers may in practice be defined by the ratio between the size of the cell lumen and the width of tracheid wall in different parts of the annual ring. In other words, histological heterogeneity of xylem results in differences in the physical parameters of the annual ring structure.

The aim of this section is to describe original, semiautomated methods dealing with histometric data analysis, to discuss some problems concerning the relationships between the kinetic parameters of seasonal growth and the structure of tree rings, to estimate the ecological factors (climate ones first of all) influencing the formation of anatomical ring structure of conifers, and to evaluate the possibilities of identifying growth conditions on the basis of histometric data. The case with conifers (pine and larch mainly) in different growth conditions has been investigated. Radial sizes of tracheids have been analyzed as the principal characteristic.

2.6.2. The method of tracheidograms

Tracheidograms are curves of cell size variations in radial files of xylem cells. They are produced by the automated measurement of tracheid radial sizes on cross sections. The radial cell size varies considerably within the tree rings of a single tree as well as between tree rings of trees from different growth conditions. As a first approximation this variability can be attributed to three causes: an average seasonal trend, specific detail of the season trend, and endogenous factors. The average seasonal trend is responsible for a cell size decrease from earlywood to latewood. The detail of the seasonal trend causes the difference between the tracheidograms of tree-rings. The endogenous factor is connected

with growth heterogeneity of a separate stand and the interrelation of growth changes in the absence of displacement (sliding) growth of neighboring cell files, etc.

The sample preparation is standard: microtome sections are cut from chosen core segments up to five or six cm long, stained, and fixed in glycerin–gelatine or cedar balsam (Canada balsam). The samples are then analyzed in an automated system.

2.6.3. Measurement system

The system (which was devised in the Institute of Biophysics, Siberian Branch, Academy of Science of USSR) includes semiautomated equipment to obtain tree-ring tracheidograms (*Figure 2.17*). It consists of a mechanical part (a drive and a carriage to move the sample at a uniform speed), an optical part (microscope for transmitted and reflected light), an electronic part (to convert time intervals to electronic signals), a recorder (to register the initial tracheidograms on paper tape), and a microcomputer (for further processing of the information). When a sample moves in a radial direction the operator successively records cell boundaries of separate files of cells when they cross the cursor. The electronic interface provides three parameters: cell size, time of its crossing the cursor, and the value of the electronic impulse, which is recorded by a potentiometer or on paper tape. As a result, a curve (the tracheidogram) is obtained, which has several peaks. The ordinate of each peak corresponds to the cell size.

The instrument is connected to a computer, which is programmed to convert the time intervals into cell size values, to store them, and to process the initial information. The data are then recorded on magnetic tape and transmitted to a printer. The system can be used in a number of ways: to produce data on cell sizes and to total ring width and earlywood and latewood separately. The data obtained can be processed with the computer during the recording process (for example, the calculation of smoothed means, tree-ring indices). In the range of cell sizes typical of the majority of conifers (15–70 microns), the accuracy of measurement is ± 6%. The working parameters of the system when the minicomputer is connected are such that the sizes of some 600 cells are measured and processed in 30 minutes.

For one measuring regime, the computer is programmed so that each cell (tracheid) is assigned to a size category according to its radial size (usually each size interval is two or three microns). After scanning several sequential tree rings and processing the data with the computer, the discrete curve of cells according to their size distribution is obtained as a histogram, and statistical features of the histogram are estimated (mean size, dispersion, asymmetry, and excess coefficients). Since tree rings of a single tree as well as of many trees have different numbers of cells and these are of different widths, the comparative analysis of their structure becomes difficult. Therefore, the second measurement regime standardizes the initial tracheidograms. Standardization [*Figure 2.17(d)*] *decreases* or *increases* the initial tracheidogram along the abscissa leaving the

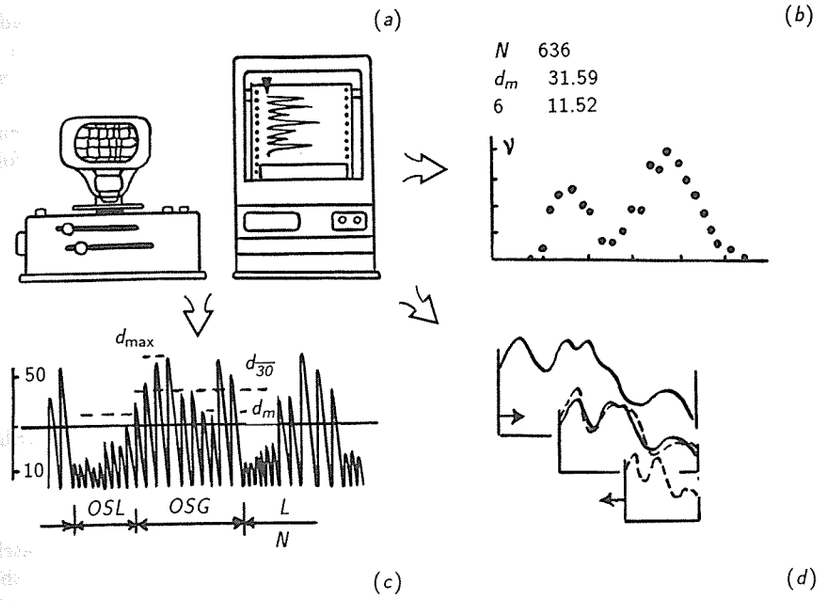

Figure 2.17. The semiautomated system used to obtain tree-ring tracheidograms. It consists of a drive and a carriage to move the sample at a uniform speed, a microscope for transmitted and reflected light, an electronic part to convert time intervals to electronic signals, a recorder to register the initial tracheidograms on paper tape, and a computer to estimate and standardize the tracheidograms.

ordinate unchanged. As a standard, 30 cells of different growth seasons can be used.

The standard tracheidogram is produced after transformation of the initial sequence of cell sizes in a radial file $\{d_i\}$, $i = 1,\ldots, N$ firstly into the sequence: $\{d_i{}^*\}$, $i = 1,\ldots, K$ with $K = \varepsilon N$, where ε is the number of cells of the standard, and then into the sequence: $\{d_i^H\}$, $i = 1,\ldots, \varepsilon$, which includes ε terms.

The general form of the intermediate sequence is:

$$\{d_i{}^*\} = \frac{d_1,\ldots, d_1}{\varepsilon} \quad , \quad \frac{d_2,\ldots, d_2}{\varepsilon} \quad ,\ldots, \quad \frac{d_N,\ldots, d_N}{\varepsilon} \quad .$$

The terms of the standardized tracheidogram are obtained by the formula:

$$d_i^* = \frac{1}{N} \sum_{j=N(j-1)+1}^{N_i} d_j^* \quad ,$$

where $i = 1,\ldots, \varepsilon$.

The mathematical treatment of the standardized tracheidogram is made after the measurement and takes 10–15 seconds of computer time. To obtain a standardized tracheidogram that shows the variations of cell size in different parts of a tree ring, six random radial files of cells in each ring are measured.

The third measuring regime is meant for quantitative evaluation of peculiarities of the tracheidogram of a tree ring. In the course of recording, the following characteristics of the radial curve are calculated [see *Figure 2.17(c)*]:

(1) The number of cells in a radial file (mean).
(2) The number of cells in the tree-ring (N).
(3) The ring width (L).
(4) Maximum cell size (dmax).
(5) Mean cell size (dm).
(6) Minimum cell size (dmin).
(7) Mean intra-annual cell sizes ($d\overline{30}$ and $d\underline{30}$).
(8) The dimension of zones with cells of more than (OSG) or less than (OSL) 30 microns (this divides the ring into earlywood and latewood).
(9) The relative position of the cell size maximum (ONM).

The application of these parameters makes it possible to present multiparametrically the structural peculiarities of the tree ring, and hence the peculiarity of the seasonal variability of cell sizes in different radial files is seen in the mean tracheidogram. To estimate the accuracy with which the tree-ring structure is registered by the mean tracheidogram, the following series of measurements were carried out. For several pine tree rings, tracheidograms for 100 cell files were recorded, and the cell size histogram was obtained (for cells of the same number or position in the tracheidogram). The estimation proved the histograms to be of the normal form. For earlywood (45–55 microns) the difference between cell sizes in the mean tracheidogram obtained for six random radial files and the mean tracheidogram obtained from 100 radial files does not exceed 2.5 microns with a probability of 0.95. For latewood (15–25 microns) this difference does not exceed one micron with the same probability. Thus, the difference between the tracheidograms is not more than 5%.

The mean tracheidogram for six radial files of cells reliably characterizes the cell size changes for a tree ring of a given year. However, when considering the changes of growth conditions and their effect on the annual ring structure it becomes important to establish the reliability of the difference between the tracheidograms of the same tree for different seasons.

Let us estimate the variability of the tracheidogram shape from year to year. For several pines and larches it was shown that the variability from year to year considerably exceeded the intra-annual variability. Hence, the change of the tracheidogram form can be reliably used to find out the peculiarities of seasonal growth of trees in seasons when growth conditions were different.

As an example of the cell size variability in different parts of the tree rings of trees from different sites, the values of the variation coefficients are presented in *Figure 2.18*. The coefficients have been calculated for the cell sizes of several pines from dry and wet sites. After eliminating variation caused by measurement error one can see that cell size variations for pine from wet sites (where the variations are caused mainly by temperature) are less than those for pine from dry sites. The maximum value of the variation coefficient for trees from a dry site was obtained for the cells of the transition zone and the beginning of the latewood zone of a ring (this is the 15th to 23rd cells in the standardized tracheidogram). This fact is not due to chance since, during the formation of these cells in a ring, moisture deficit is at a maximum for trees from dry sites.

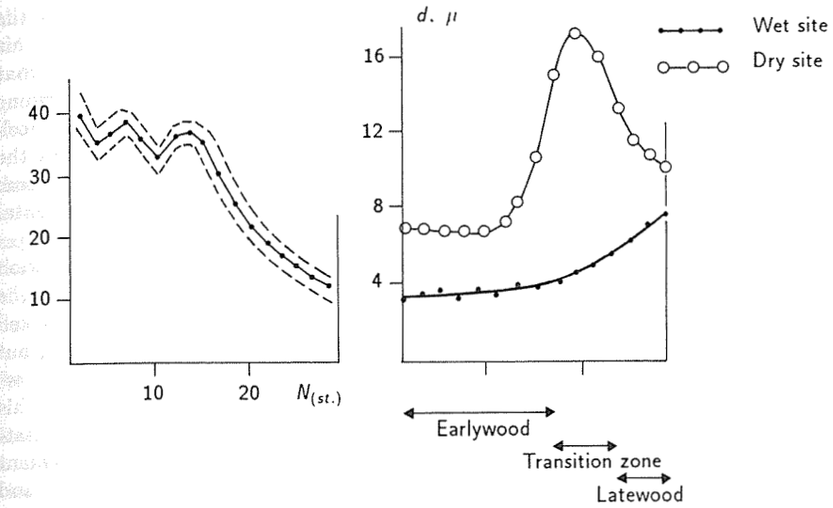

Figure 2.18. Variation coefficients from the tracheidogram calculated for the cell sizes of several pines from dry and wet sites. Cell size variations for pine from wet sites, where the variations are caused mainly by temperature, are less than those for pine from dry sites.

Thus, each component of cell size variability in tree rings is a characteristic of tree growth (peculiarities of cell growth in a file, seasonal changes in growth rate, and the effect of growth-rate conditions on the seasonal growth rate). Therefore, the analysis of tracheidograms is the method that can be used for determination of corresponding changes in the growing conditions.

2.6.4. Tracheidograms in the analysis of growth mechanisms and seasonal differentiation of xylem cells

Once a cell differentiates from the cambium, enlarges, and reaches its full size, further changes in cell size do not occur. However, the mature tracheids of conifers, forming in different intervals of seasonal growth, differ appreciably in lumen size and cell wall thickness. Therefore, if the number of cells and the annual ring width account for the whole seasonal increment, then the anatomical

indices (i.e., radial size of tracheids) can be used for a more detailed characterization of the seasonal growth process and, hence, for the determination of the factors affecting the growth rate in different seasonal intervals. However, this approach demands solving three problems. First, it is necessary to identify what aspects of xylem growth (cell production rate, rate of elongation, etc.) determine the final size of the cells. Second, since the tracheidogram is the sequence of cell sizes, it is important to establish the season in which the given cell passes the maturing phase, i.e., in which it may reflect an environmental influence to some extent. And finally, as a result the mechanism of influence of the environmental factor and growth phase on cell radial size must be established.

Special investigations of seasonal growth kinetics and annual ring formation of trees with different growth potential were carried out in field conditions in the region of the Angara River, with the following results. Growth kinetics of cell number for the same year in trees of different growth potential is identical, but the growth kinetics of ring-width increment differs (*Figure 2.19*). In slow-growing trees the cells move into the zone of enlargement after some delay. This is why the cells in the same relative position in a ring become enlarged in fast- and slow-growing specimens in different seasons, yet have the same enlargement period and do not differ in size. The duration of cell production in slow- and fast-growing trees is not significantly different in the same year. The increase in the total production is conditioned by the increase in the cambial zone as long as a positive correlation ($r = 0.6$–0.7) exists between these kinetic parameters.

Additional information on the ratio of cell production and cell enlargement can be obtained from the analysis of *instant* tracheidograms, i.e., the ones

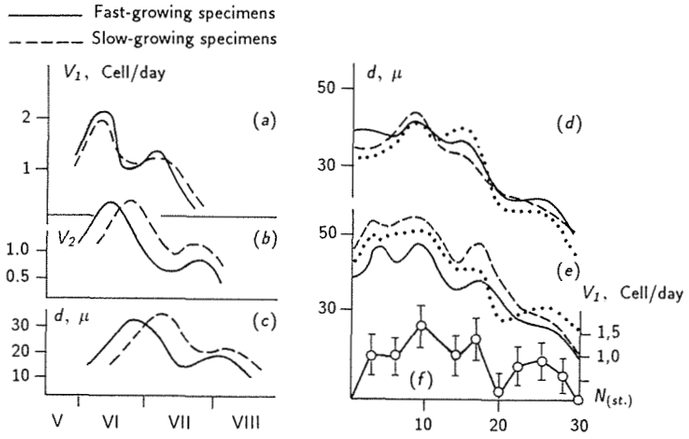

Figure 2.19. Seasonal dynamics of cell production rate (*a*), the rate of transition to enlargement (*b*), the average cell size in the enlargement zone (*c*) in fast- and slow- growing specimens. Cell production rate comparison (*f*) with tracheidograms of fast- (*d*) and slow- (*e*) growing pines.

obtained on the forming of annual rings under certain seasonal conditions. That the formation of the local maxima and minima of cell size changes within the ring is clearly observed. These changes are seen to be tied to the same ring zones, though the cells forming them in the annual rings in slow- and fast-growing trees are enlarged at different times (see also Vaganov *et al.*, 1985; Terskov *et al.*, 1981).

From the above results, we can conclude that the final size of tracheids depends on the kinetic characteristics during the season which change in fast- and slow-growing trees identically and simultaneously. The analysis of the experimental data shows that the final size of tracheids is determined at the earliest stage of cell differentiation – at a level of change in production rate. Thus, the tracheidograms of the annual rings reflect the specificity of growth-rate curves of cell quantity (*Figure 2.19*). The similarity of rate of cell production in annual rings of different trees also accounts for the similarity in tracheidograms for the same year of radial growth [*Figure 2.19*(*d*)].

The analysis of seasonal kinetics of annual ring formation and its structure leads to an important conclusion for dendroclimatology: since the production season is far shorter in duration than the season of growth and xylem maturation, the correlation between the histometric characteristics of tree rings and climate conditions should be searched for only during the cell production period and the time preceding it. The number of cells in the cambial zone is largely predetermined at the beginning of the season (Wilson, 1964), i.e., the number of cells, but not the cell size, is determined by the previous year. The cambium assigns the total cell number production for 80–90% and the annual ring width for 60–70%. The current changes in production will depend on the conditions of this period (e.g., 2–2.5 months in this study). Therefore, attempting to establish close relationships between any histometric characteristics of the annual rings and weather conditions in the period following cell production is hardly useful.

Data on the kinetics of the annual ring formation and on the relationship between the kinetic and morphological characteristics of xylem cells are described in terms of a simple computerized model (Vaganov *et al.*, 1985). This allows the reconstruction of the seasonal dynamics of cell production and ring width. The following statements are the basis of the model:

- Cell size and relative rate of production are proportional.
- There exists a delay in time between cell division and enlargement of 8–10 days based on experimental evidence.
- The kinetics of cell enlargement of earlywood and latewood cells conforms with the equation of monomolecular reactions with similar kinetic coefficients.

The comparison of the calculated and experimental data for various materials, including one not used in the construction of the model, showed them to be in good agreement not only in terms of a quantitative estimation of cell production, enlargement, and total wood increment, but also with the dynamics of the instant tracheidograms. It is not only the indirect proof of the correctness of the initial premises of the model, but an immediate indication of the close

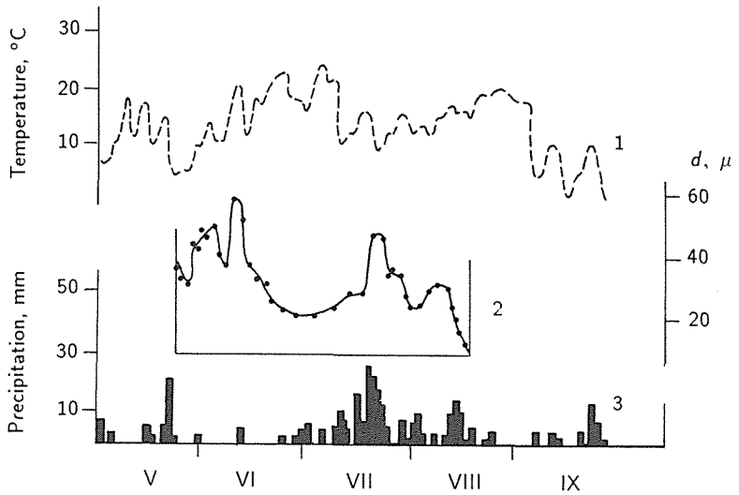

Figure 2.20. The seasonal variations of temperature (1) and precipitation (3) along with changes in cell size (2) of pine in a given year. As can be seen, the fluctuations of cell size in the first half of the season follow the temperature fluctuations. Precipitation deficiency at the end of June caused a soil-moisture deficit and a sharp decrease in cell production rate and size.

relationship between the intra-seasonal growth rate and cell size in conifers. The practical result of the model is the possibility of relating every cell with the specific seasonal interval that conditioned its size. For example, *Figure 2.20* shows the seasonal variations of temperature and precipitation along with changes in cell size of pine in a given year. As can be seen, the fluctuations of cell size in the first half season follow the temperature fluctuations. Precipitation deficiency at the end of June caused a soil-moisture deficit and a sharp decrease in cell production rate and size. Only the rains of July reinforced increment production and promoted the increase in cell size (a weak *semifalse* ring was formed). Thus, the model is applicable in different aspects. The possibility appears, first, to fix the tracheidogram in time (i.e., to mark a time scale on the tracheidogram). Second, the direct comparison of annual ring growth rate with meteorological factors is possible, thus clarifying the reasons for intra-seasonal growth changes. Third, it is possible to establish the quantitative relationships between increment and the main weather factors influencing it. These are of paramount importance for the interpretation of dendroclimatological information for the given year.

2.6.5. Tracheidogram use in the analysis of weather conditions on seasonal growth rate and cell size

The comparative analysis of annual rings in trees of one stand, but of different growth potential, showed their similarity (*Figure 2.19*). Standardized

tracheidograms are more suitable for visual comparison. Their likeness testifies to one type of increment reaction in different trees in response to the dynamics of the external conditions (weather effects mainly) in a given year. This uniformity manifests itself in a high degree of synchronism of changes in tracheidogram quantitative indices.

The annual ring tracheidograms of trees even in the same region differ greatly. For instance, the annual rings of pines from dry sites reveal a clear transition from earlywood to latewood. The transition to the formation of latewood cells is observed earlier in the annual ring as the moisture deficit increases in the first half of the season.

Let us consider tracheidogram applications in the quantitative evaluation of the relationship between cell size and weather factors in the course of the growing season. *Table 2.1* presents the correlations of annual ring structure

Table 2.1. Correlation coefficients of indices in tree-ring tracheidograms of pines and larches growing in different locations. Rows 1 and 2 – larch growing in dry and moderate moisture areas; row 3 – pine growing on dry sites; row 4 – larch growing at the northern forest border.

Index		*N*	d_m	d_{max}	*OSL*	*ONM*	$d\overline{30}$	$d\underline{30}$
N	1							
	2	1.000						
	3							
	4							
d_m	1	.386						
	2	.345	1.000					
	3	.765						
	4	.506						
d_{max}	1	.297	.735					
	2	.607	.685	1.000				
	3	.759	.949					
	4	.435	.700					
OSL	1	−.253	.300	.011				
	2	.080	−.629	.155	1.000			
	3	−.686	−.725	−.642				
	4	−.242	−.714	−.460				
ONM	1	−.094	−.639	−.672	−.232			
	2	.329	−.007	−.145	.038	1.000		
	3	−.273	−.151	−.255	−.094			
	4	.060	.400	.330	−.490			
$d\overline{30}$	1	.578	.802	.447	−.510	.206		
	2	.371	.788	.747	−.031	.016	1.000	
	3	.605	.514	.793	−.431	.133		
$d\underline{30}$	1	.156	.316	.097	.336	.114	.467	
	2	.406	.529	.512	−.083	−.053	.519	1.000
	3	.521	.783	.667	−.597	−.074	.345	

indices for trees at different localities. Depending on the conditions (dry or humid), the correlation between the same indices may be different in sign. Limiting conditions of either temperature or moisture may cause one factor to have a prevailing influence on growth, thus enhancing the correlation with annual ring structure. The annual increment of cell number is in agreement with the increase of average or maximum cell size in a ring and also correlates with the increase of average cell size in early and late zones. This correlation is not spurious because the production inhibition also affects the intra-seasonal dynamics of growth and cell size. It is an important fact that the correlation between the relative width of the latewood zone and cell production and their average size is normally negative, i.e., growth acceleration causes a deterioration in wood quality.

Apparently, the cell size in different parts of the annual ring in trees from dry and humid sites would react to the temperature regime and some months of precipitation in different ways. The data presented in *Figure 2.21* illustrates this. The temperature increase adversely affects the cell size of pine growing in dry conditions; May and June temperatures appreciably influence the cell size. The changes in correlation coefficient show the positive relationship between cell size and precipitation in May and June and the negative relationship between cell size of transition and late zones and the precipitation in July.

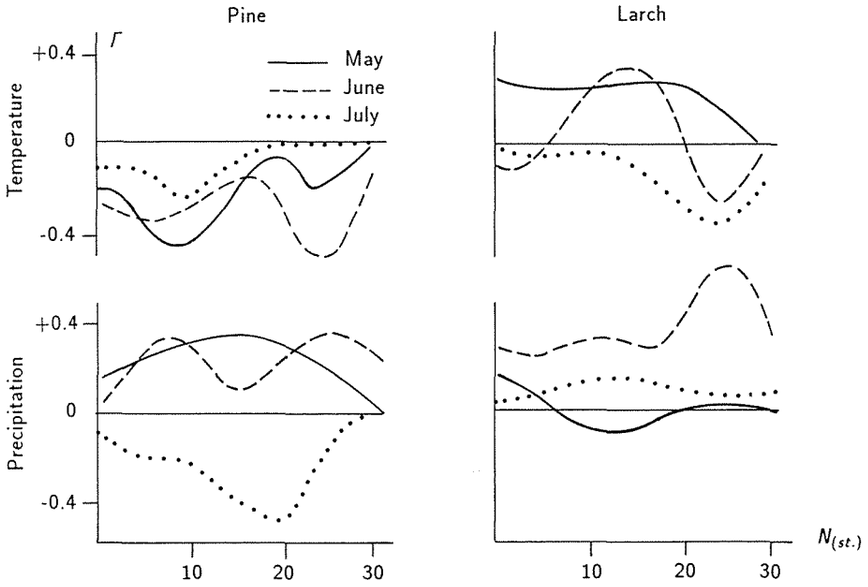

Figure 2.21. Correlation in cell size of pine and larch annual rings from different moisture regimes during May, June, and July according to temperature and precipitation.

Quite different correlation coefficients between cell size and weather conditions are observed for a larch growing in moderate humidity conditions [*Figure 2.21*(*b*)]. The increase in May temperatures positively affects the cell size of the early and transition zones. The temperatures in June account for the cell size only in the central part of the ring forming mainly during this month. The temperatures of July influence the cell size only in the late zone. The changes in May and July precipitation have little or no effect on cell size in these zones. The increase of rains in June results in the size increase of the cells completing the early and starting the late zones. These conclusions are supported by further analysis reported by Vaganov *et al.* (1985).

The correlation analysis of ring structure parameters and weather factors leads to the conclusion that changes in weather conditions of certain months in different locations unequally influence the cell size and morphology, the cells being formed in growth rings at different times in the growing season.

2.6.6. Annual ring tracheidograms in the reconstruction of weather conditions

The analysis of the data showed that the cell size and seasonal growth rate of the trees that were growing in conditions with some factor constantly limiting growth were essentially influenced by the conditions preceding the beginning of growth. On the contrary, woody plants grown in more favorable climatic conditions are more sensitive to changes. The indices of seasonal ring structure depend on different factors, and weather conditions of different months influence these index values. So the connection between the weather factors and seasonal ring structure indices is multivariate in most cases. This makes it possible for dendroclimatological reconstruction to use the methods of multiple regression, where tracheidogram indices are presented as independent variables and the weather factors as dependent ones. The preliminary correlation analysis and the quantitative estimation of the influence of weather conditions of certain months on cell size in different ring parts assist in carrying out the regression analysis. *Figure 2.22* presents the instrumental values and the values obtained from the equations of linear multiple regression of some weather factors on the basis of the data on annual ring fine structure. This example demonstrates the unique abilities of dendroclimatological reconstruction using tracheidograms: a single ring provides the evaluation of several weather factors that have influenced the growth of the tree.

Even more informative is the use of histometric information in the reconstruction of weather conditions with the help of differential tracheidograms. Tracheidograms have their characteristic patterns for each year. If the standardized tracheidograms of many growth years are plotted on one graph, then the spread in values of cell size in one and the same part of a seasonal ring would be considerable. Moreover, the standardized tracheidograms serve as the summarized estimate of seasonal growth conditions, whatever the weather conditions and duration of the season were. In this sense the standardized tracheidogram can be considered as the ecological equivalent of the growth season.

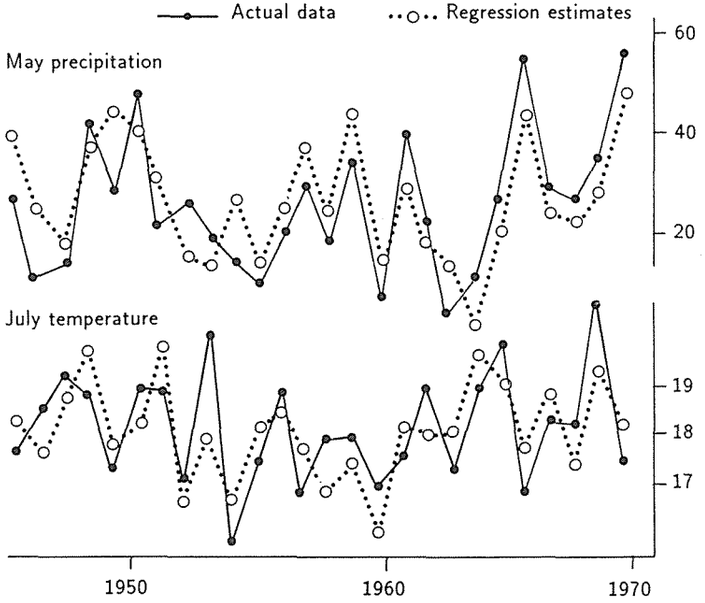

Figure 2.22. Examples of how tracheidograms can be used to reconstruct weather conditions. Using the tracheidogram method, a single ring provides information on several weather variables that have influenced tree growth.

By unifying the standardized tracheidograms of many years one can obtain, first, the optimal tracheidogram of the whole growth period under study. This will correspond to the maximum possible cell growth that could be caused by the optimal combination of moisture and temperature conditions. Second, the differential tracheidogram for a specific year can be derived. This will show how much smaller the individual tracheidogram cell size is than that of the maximum one in different seasons. Differential tracheidograms of trees growing in abundant moisture locations will show differences owing to variations in temperature. Differential tracheidograms of trees growing in dry locations will summarize the growth deviations from optimal in both temperature and moisture. If both differential curves are brought in line for an individual year then one can determine the limiting factors and the seasonal intervals when they occurred (*Figure 2.23*). For example, in 1963 and in 1964 the seasonal growth of pines in this locality was limited only by temperature (differential growth curves practically coincide); in 1967 and 1969 the lack of moisture was noticeable, but nevertheless the fluctuations in cell size and growth rate are mainly conditioned by temperature. However, the 1965 and 1966 years reveal the essential difference in the curves, showing the influence of a strong drought on pine growth in those years.

The application of differential tracheidograms provides a quantitative characterization of weather conditions and helps to elucidate which factor is mainly

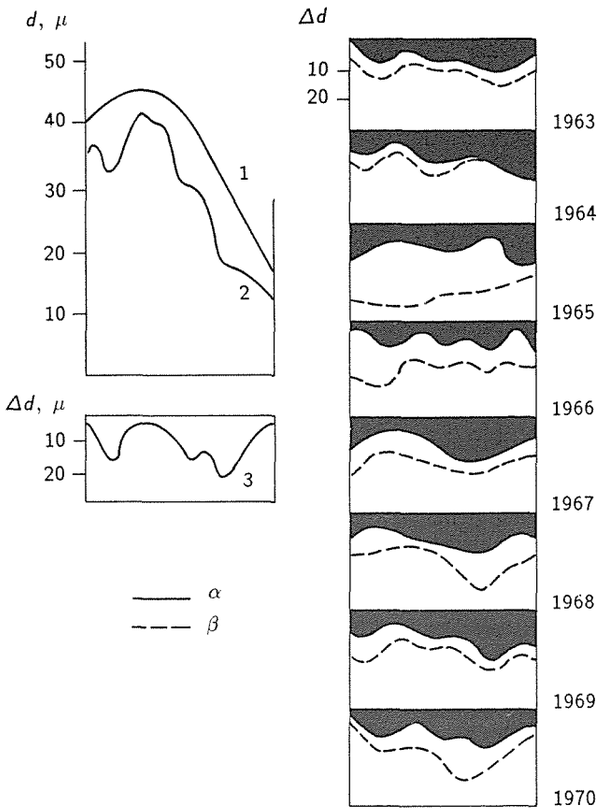

Figure 2.23. The differential tracheidograms for specific years. Differential tracheidograms of trees growing in abundant moisture locations will show differences owing to variations in temperature. Differential tracheidograms of trees growing in dry locations will summarize the growth deviations from optimal in both temperature and moisture. If both differential curves are brought in line for an individual year then one can determine the limiting factors and the seasonal intervals when they occurred.

responsible for the variations in cell size and growth rate. One of the features of a differential tracheidogram is its ability to reflect a tree's reaction not only to changes in current conditions but also to proceeding ones. The effect of moisture deficit at the start of the season can be different from that at the end of the season. If the soils are at field capacity, short periods of precipitation deficit will not show up in the tracheidogram. A decrease of cell size and growth rate can be ascribed to moisture deficit in some cases and in others to a considerable decrease in temperature. Differential tracheidograms allow a distinction to be made between these two cases.

In conclusion, the application of histometric data makes a valuable contribution to dendroclimatology and develops the biological principles of the

methods in the use of annual ring structure. The method opens up the possibility of new kinds of analysis and new approaches to dendroclimatological reconstruction.

2.7. Computer-Aided Image Analysis of Tree Rings

R. Jagels and F. W. Telewski

2.7.1. Introduction

Radial increment width is one measure of cambial activity in a tree, and as such is a record of forest growth. The use of tree-ring width measurements to assess environmental changes or anthropogenic stresses on trees assumes that the secondary cambium will respond in a single quantitative way to external perturbations. But, in fact, the cambium may respond in several different quantitative and qualitative ways that can be monitored morphometrically in conifers in the radial files of xylem cells produced (Bannan, 1967; Elliot and Brook, 1967; Larson, 1969; Diaz-Vaz *et al.*, 1975; Ford *et al.*, 1978; Jagels and Dyer, 1983; Telewski *et al.*, 1983; Merkel, 1984).

Since radial increment provides only one measure of cambial activity, it is difficult to ascertain the particular environmental trigger for a growth decline response. A decrease in radial increment may reflect one or a combination of events such as drought, frost damage, insect attack, or airborne pollutants (Mott *et al.*, 1957; Glerum and Farrar, 1966; Yokobori and Ohta, 1983). Similarly, an increase in radial increment may reflect increased growth owing to one or a combination of factors, such as fertilization effects due to increased NO_x, SO_2, or CO_2, or changes in forest-management practices. Morphometric analysis of individual, key growth rings might provide a way of establishing *fingerprints* or unique patterns within growth rings as a response to meteorological or other natural stresses, anthropogenic pollutants, or forest-management practices.

Early attempts at morphometric analysis with wood cross sections focused on earlywood (springwood) and latewood (summerwood) boundaries, to determine the percentages of each produced in a growth ring. In abrupt transition conifers such as southern hard pines or Douglas fir (*Pseudotsuga menziesii*), this boundary is reasonably distinct and may be further defined by Mork's index (Mork, 1928). Larson (1969) has pointed out, however, that Mork's index is not appropriate for gradual transition conifers (such as spruce and fir). Staining techniques have had only limited success in differentiating earlywood from latewood in such species. More recently, techniques in X-ray densitometry were developed to provide an additional level of sensitivity (Lenz, 1957; Polge, 1966; Fletcher and Hughes, 1970; Parker and Kennedy, 1973; Parker, 1976; Schweingruber, 1983, 1989).

Research has also focused on particular cell features such as tracheid diameter or wall thickness as ways of indirectly assessing environmental influences such as photoperiod and drought in seedlings or young trees (Larson, 1963, 1964). During the 1950s and 1960s, Bannan (1967) developed his theory for the relationships between cambial activity, ring width, and tracheid length, based on the relative frequencies of periclinal and pseudotransverse divisions. Richardson

(1964) carried this to the next stage by investigating the effects of temperature, light intensity, and length of day on tracheid length, cell wall thickness, and lumen diameter in conifer seedlings. He concluded that all were affected to varying degrees, but that length of day, presumably by mediating auxin flow, had the greatest influence on the change from earlywood to latewood, and temperature (but not light intensity) was also positively correlated with lumen diameter. Ford *et al.* (1978) found a strong positive correlation between daily solar radiation and daily production of earlywood tracheids in 12-year-old Sitka spruce (*Picea sitchensis*).

Another important milestone was the development of a model for cell production of coniferous cambia by Wilson (1964). The major contribution from this model was the demonstration of the direct relationship between the width of the cambial zone, formed in early spring, and the width of the latewood, formed at the end of the season. Subsequent models of xylem production and development in conifers (Howard and Wilson, 1972; Wilson and Howard, 1968) do not simulate the direct effects of the environmental and physiological conditions directly on cambial activity, but focus on rate of cell enlargement, rate of cell wall thickening, and cell size at three levels of tracheid development (cell division, cell enlargement, and cell wall thickening). Wilson (1973) incorporated the physiological aspect of annual xylem production by adding an unspecified growth substance to the model. Ford (1981) discusses the possibility of developing a model of xylem production that includes the direct effects of environmental and physiological conditions on cambial activity. He emphasizes the need for morphometric and densitometric analyses coupled with cambial marking to generate the data needed to develop a model of xylem production.

Morphometric analyses of xylem are also important in interpreting wood quality and strength. The measure of fiber and tracheid length (Micko *et al.*, 1982), proportions of cellular types (Jayme and Krause, 1963; Ladell, 1959), and proportion of cell wall material to cell lumen space (Tsoumis, 1964) are of value to the forest-products industry. The measure of the amount of cell wall substance can be directly related to the relative density or specific gravity of the xylem (Tsoumis, 1964; Smith, 1965; Quirk, 1975). Smith and Miller (1964), Smith (1967), and Quirk (1984) review several of the morphometric or optometric methods for determining wood density.

These methods would appear to be very appropriate for dendrochronological research. In some instances of very narrow tree rings, where a growth ring may be represented by very few earlywood or latewood cells, the morphometric method of determining wood density would be more accurate than the more widely used method of X-ray densitometry. However, quantitative studies that entail measuring areas and dimensions of cells can be extremely tedious and time-consuming if a large number of individual growth rings and tree radii are to be measured. Instead, the relatively faster microradiographic methods of determining wood densities (Lenz, 1957; Polge, 1966; Schweingruber, 1983, 1989) have been widely applied to dendrochronological research. A relationship between X-ray densitometry and optical morphometry, using cell wall thickness and tracheid diameters (not cell wall and lumen areas), has been established, but not widely used in dendrochronological studies (Diaz-Vaz *et al.*, 1975; Merkel, 1984).

The development of sophisticated computer systems and digital image analyzers makes it possible to measure quickly the anatomy of biological systems, both quantitatively and qualitatively, and to plot graphically the changes that occur in space or time (Fisher, 1972; Gahm, 1972; Sells, 1978; Quirk, 1981; McMillan, 1982; Micko *et al.*, 1982; Round *et al.*, 1982; Jagels and Dyer, 1983; Telewski *et al.*, 1983; Yanosky and Robinove, 1986). When these approaches are applied to coniferous xylem, one can distinguish zones of earlywood, transition latewood, and latewood (as defined by Larson, 1969) or simply let the plotted curves serve as fingerprints for cambial zone activity as manifested in cell division, enlargement, and differentiation (Jagels, 1984). These sophisticated instruments not only greatly reduce the time required for the measurement of dimensional parameters, but, perhaps of even greater value, permit one to devise and process complex analyses beyond those most commonly performed.

The following discussion describes the different instruments and methods used, develops two case studies (the first using a semiautomated image-analysis system and the second using an automated system), expands the discussion to other conifer woods, and finally suggests possibilities for morphometric analysis of wood structure.

2.7.2. Image-analysis systems

Image-analysis systems can be separated into three types according to the principles on which they are based (Weibel *et al.*, 1972). These are source-plane-scanning systems that include the flying spot scanners and moving slit scanners, specimen-plane-scanners, and image-plane-scanners. The focus of this section will be on the third group of image analyzers, for it is this system upon which all video-image-analyzing systems are based.

Video-image-analysis systems were developed in the early 1960s. The early systems, based on mainframe computers, were used mostly by industry and medical research owing to limited availability and high cost. With the development of the minicomputer and the microcomputer, a wider range of applications has been reported. Reviews of the history and development of these video-image-analysis systems can be found in Gore (1979), Anonymous (1985), and Inoué (1986).

Sells (1978), Micko *et al.* (1982), McMillan (1982), and Telewski *et al.* (1983) have used video-image-analysis systems to determine the size and area of various tissues and cells and cell wall material in xylem. Fukazawa and Imagawa (1981) determined the amount of lignin in cell walls across several tree rings using a UV microscopic image analyzer. Yanosky and Robinove (1986) used image analysis to determine the total area of a growth ring in transverse section and to determine the cell wall to cell lumen ratio. Swain (1987) reported a strong correlation between wood density determined by X-ray densitometry and cell wall area determined using video-image analysis. Jagels and Dyer (1983) determined cell lumen area and cell shape, and Vaganov *et al.* (1985, 1989) used image analysis to determine tracheid diameters across a growth ring in a tree-ring analysis.

Before conducting a dendrochronological analysis using a video-image-analysis system, one should be aware of the two different systems available and the limitations to their use. To develop such an understanding, it is important to have basic knowledge of how a system works. Such reviews can be found in Gore (1979), McMillan (1982), Telewski *et al.* (1983), Jaffe *et al.* (1985), Anonymous (1985), Inoué (1986), and will be presented briefly below.

The two systems can be separated into automated and semiautomated image analyzers. Both systems first convert an analog video signal to a digital signal. Digitization of the video image can be accomplished by a direct method in which the video signal is fed to a video digitizer or frame grabber or both that digitizes the entire image. This method is used in all automated and some semiautomated systems. Digitization can also be accomplished in some semiautomated systems using a graphics tablet, electronic drawing board, or digitizing tablet (digi-pad). In this type of analyzer, the image is projected onto the pad and digitization occurs as the object to be analyzed in the image is outlined with an electromagnetic or radio-signal stylus or cursor.

In automated systems the digitizer divides the image into a matrix of squares or rectangles, termed *pixels*. Each pixel has three coordinates: X and Y values that define the position of the pixel in the image and a Z value that represents the gray level or degree of brightness. In most systems a Z value of 0 represents absolute black and the highest value represents absolute white. The size of the pixel matrix will depend upon the digitizer or the video camera or both. Digitizers most commonly divide a video image into a matrix of 256 $\times$ 256, 512 $\times$ 512, or 1,024 $\times$ 1,024. (Some manual digi-pad systems have denser pixel arrays, such as 1,000 $\times$ 1,000 pixels per inch, and are not limited by video signals.) Most standard video cameras in the USA produce 525 horizontal lines of video and can be used as an input for both 256 $\times$ 256 and 512 $\times$ 512 digitizers. Unfortunately, only 480 to 485 lines of video are active, thus reducing the 512 $\times$ 512 pixel matrix to a maximum of 512 $\times$ 485 pixels. This is not a problem in Europe because most standard European video cameras generate 625 horizontal lines of video. To take advantage of the higher-resolution digitizers, special high-resolution video cameras must be used that generate a minimum of 1,079 horizontal lines of video (resolutions of up to 1,225 horizontal lines are readily available).

Both automated and semiautomated image analyzers have specific advantages and limitations in the type of analyses to which they can be applied. The automated image-analysis system will differentiate an object in a field of view from the background based on differences in gray levels. The threshold for defining an object or series of objects is set by the operator. Once set, the image analyzer will record all pixels that are equal to or beyond the gray-level threshold (Telewski *et al.*, 1983). Contiguous pixels are considered as a single object unless directed otherwise by the software or user-driven editing subroutines. The array of pixels that displays a specific object can be analyzed for area, perimeter, weighted center (centroid), shape, average gray level of all pixels in the object, and a number of other parameters of the object depending on the software package.

To maximize the use of an automatic system, images should be of high contrast. Video-image contrast can be increased with stains; oblique, dark field, or phase contrast lighting; microscope condenser aperture or video camera lens; light filters; externalized gain and gamma controls on the video camera; and contrast of the digitizer (usually an external adjustment). The exact boundary of low-contrast images are difficult for the image analyzer to determine. Improperly set gray-level thresholds will also bias area determinations (*Figure 2.24*).

For the most part, wood is an ideal object to analyze using the automatic system. The boundary between the cell wall and the cell lumen is distinct in well-prepared samples, and the cell wall can be easily stained to increase contrast. Determinations of cell wall to cell lumen area can be obtained quickly across an entire tree ring or within specific regions of the tree ring (*Figure 2.25*). Problems of parallax will develop in the analysis of tree rings in sections where transmitted light is used if the cell walls of the axial tracheids are not perpendicular to the viewing surface. This problem can be overcome by using a dark field, incident light system on a wood surface, which enhances contrast between the cell wall and the filled lumen space.

Depending on the flexibility of the software driving the automated system, profiles of double cell wall thickness to lumen diameter can be determined across a tree ring. Such an analysis would be conducted by reducing the amount of image being scanned to a line of one or a few pixels in height and the entire length of the video screen.

The second type of video-image analyzer is the semiautomated type and uses an electronic drawing board or digitizing tablet. This system requires the operator to identify and outline the object to be studied with a stylus or cursor (Gore, 1979; Quirk, 1981; Jagels *et al.*, 1982; Micko *et al.*, 1982) or to trace the object on the video screen using a light pen, joystick, or mouse. These systems can be used in conjunction with a video camera, projection system with 2 × 2 slides, photomicrographs, or a transmitted light or incident light microscope with drawing tube. The option allowing the user to identify and outline the object is important because some quantitative problems can only be solved using the high level of discrimination achieved by the eye and brain. An example of this can be found in the application of morphometry to tree-ring analysis. The determination of total cell size (not lumen size), cannot be easily determined on the basis of gray-level density on automatic analysis systems. Using the semi-automated system, the operator can identify the middle lamella between adjacent cell walls and outline it using the stylus on the electronic drawing board or digitizing tablet or by moving a cursor on a high-resolution video monitor.

Calibration of a video-image-analysis system is critical and easy to check. If the area of an object determined by the image analyzer changes as it is rotated 90° in the field of the video camera, the system is not calibrated properly. One cause of inaccurate area determinations is an improperly set aspect ratio in the video camera. Video cameras used for commercial applications have an 4:3 aspect ratio. Unless compensated for by the hardware or software of the image-analysis system, the aspect ratio should be 1:1. One needs to consult the manufacturer of the system to correct the problem. Another common cause of inaccurate area determinations is optical distortion of an image due to improper

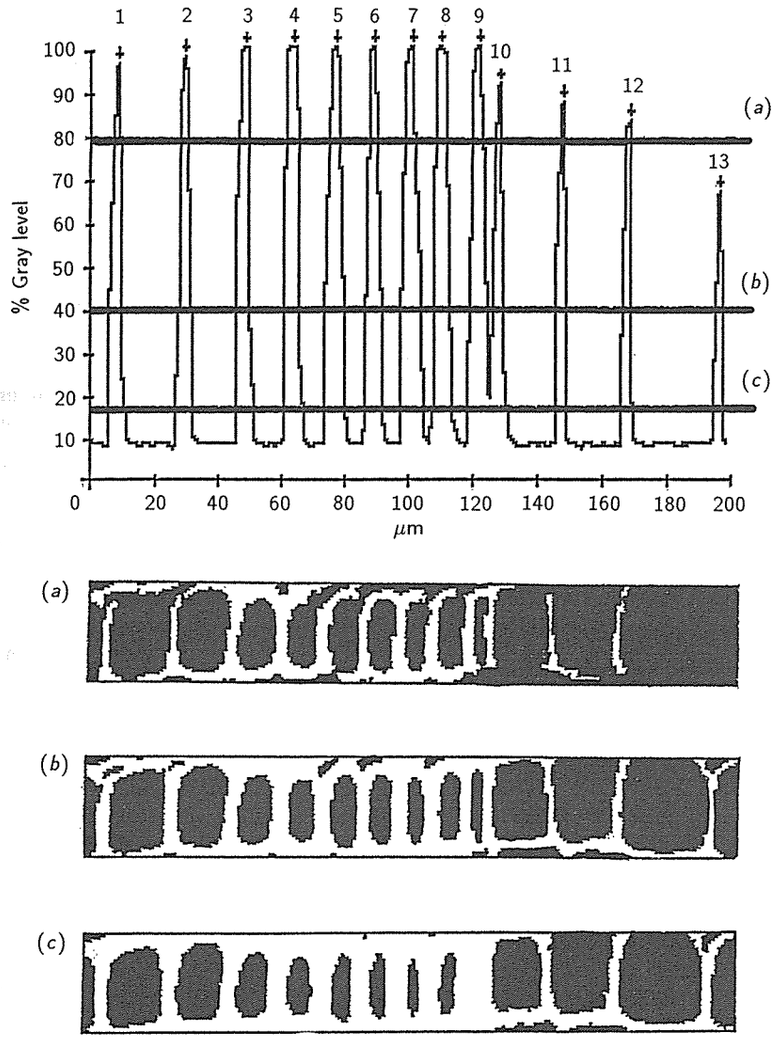

Figure 2.24. An automatic image analyzer (Telewski *et al.*, 1983) generated gray-level profile along a radial file of conifer cells (*Pinus sylvestris*) including a latewood-earlywood boundary. The position of three [(*a*), (*b*), and (*c*)] gray-level thresholds (density slices) are presented, and the respective reconstructions of lumens included below the gray-level profile. Threshold (*a*) is too high, resulting in an overestimation of lumen size and a failure to differentiate cell wall #13. Threshold (*b*) is the proper setting, producing the most accurate determination of lumen area. Threshold (*c*) is too low, producing an underestimation of lumen size and a failure to differentiate the cell lumen between cell walls 9 and 10.

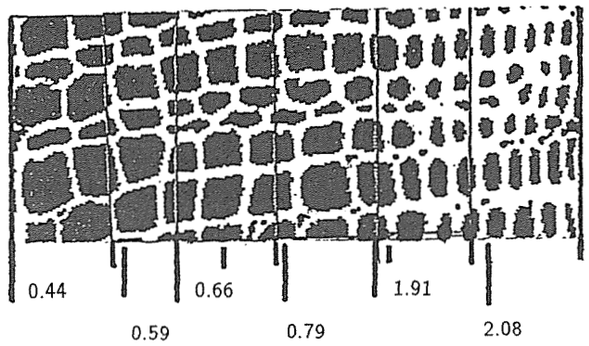

Figure 2.23. Automatic image analyzer generated mosaic of 6,100 μm $\times$ 200 μm, images across a tree ring of *Pinus sylvestris*. The calculation of the cell wall area to cell lumen area ratio (CAW:CAL) for each image is presented below the mosaic. The lumen area, circumference, and circularity index were calculated for the entire lumens in the mosaic, but are not presented.

lens systems. A polygon-analysis system can be incorporated into the computer program to correct for projection system distortions (Jagels *et al.*, 1982).

There are two types of video cameras presently available. One type uses a tube that derives an image from a photoconductor coating (antimony trisulfide in vidicon tube cameras). Vidicon and neuvicon tubes are the most common. As the video camera tube ages, the tube begins to show signs of erosion of the photoconductor. Unless compensated for by the software, the erosion of the photoconductor will result in a gradient of brightness across the monitor screen, presenting a problem in automated image-analysis systems. This is best detected by placing a monochromatic surface in front of the video camera and giving it uniform illumination. If there is a gradient of brightness from the upper-left corner to the lower-right corner, the video tube may be worn. Images of intense brightness may also permanently damage a video tube by burning in the image on the photoconductor surface of the tube. Sometimes a ghost image may appear to be burned into the video tube. This image can be removed or reduced by allowing the camera to view a well-illuminated uniform white surface for several hours. If the image persists, the tube may be permanently damaged. Over time the sensitivity of a photoconductor tube camera decreases.

Video cameras that use photoconductor tubes can also use a solid-state photoconducting tube known as a Silicon Diode Array tube. This type of video tube will not have the problems of photoconductor erosion, burn in, or loss of sensitivity due to use.

Many of the problems associated with tube-based video cameras will be solved with the introduction and use of higher-resolution solid-state video cameras. The most common solid-state video camera is the Charged Coupled Device (CCD) camera, and the most commonly available CCD at present has a pixel array of 380 $\times$ 488. In 1986, a CCD camera was introduced with a pixel array of 754 $\times$ 488, resulting in a horizontal resolution of 565 TV lines per picture height.

Experimental CCDs have much higher resolution; however, they are costly. Two less common solid-state cameras are also available commercially. These include the Charged Injection Device (CID camera) and the Color Metal Oxide Semiconductor (Color MOS camera). The Silicon Injection Device (SID) video camera is no longer available and considered obsolete.

2.7.3. Strategies and case studies

Morphometric Analysis of Earlywood to Latewood Transitions

Coniferous woods, particularly those displaying a gradual transition between earlywood and latewood, pose special problems when attempting to analyze seasonal variations in wood production. Mork (1928) presented a method to assess the boundary between earlywood and latewood, but, as Larson (1969) has pointed out, this method was not designed for gradual transition species. Staining techniques have been utilized to differentiate earlywood from latewood (Haasemann, 1963; Wiksten, 1954), but these have limitations and provide only a rough estimate of the boundary.

The formation of latewood involves two independent events: cell wall thickening and the cessation of radial enlargement of tracheids (Larson, 1969). The independence of the two events can be demonstrated by the anomaly of transition latewood, which exhibits only one of the two characteristics. Mork's index (1928) permits some transition latewood to qualify as true latewood (Larson, 1969).

The use of radiodensitometry has provided a method for rapid assessment of earlywood-latewood percentages in growth rings. However, the determination of the earlywood-latewood boundary using radiodensitometry is currently arbitrary. Schweingruber (1983) compares two methods of determining the earlywood-latewood boundary based on density values within the tree ring. The first is to use a constant density value as a threshold to determine the boundary in all tree rings within a series. This method is not satisfactory since the maximum latewood density in some rings may fall below the arbitrary density threshold set to determine the earlywood-latewood boundary. The second, more acceptable method is to determine the boundary of each ring as a percentage of the minimum earlywood density value. Schweingruber (1983) uses 20% over the minimum (120% of the minimum) earlywood density value in each ring. In this way, the boundary is determined specifically for each growth ring in the series based on its individual earlywood density. This method of determining the boundary can be misleading because the minimum earlywood density of a tree ring does not vary greatly compared with the latewood maximum density from ring to ring within a tree.

The two cross-sectional morphometric parameters of cell shape and cell wall thickness can be used to differentiate between earlywood and latewood. If one postulates that cell wall thickening is uniform around the cell, as supported by Smith (1967), then cell shape can be measured either at the lumen boundary

or at the middle lamella boundary. The lumen boundary is generally easier to define visually, and therefore, is the measurement of choice.

A simple way of quantifying shape is to reference the observed shape to a known regular geometric shape. An unhindered biological cell with symmetrical internal forces evenly distributed over a bounding membrane of uniform thickness will assume a spherical shape, and a plane section through that sphere will be a circle. For a given circumference, a circle encloses the greatest area. If an observed cell cross section is enclosed by a shape other than a circle, its area will be less than the area enclosed by a circle with the same circumference. The ratio of the two areas will be a measure of the degree of deviation from circularity, or what can be termed *circularity index*. The formula derived from this relationship is:

$$\mathrm{CI} = 4\,\pi\,A/C^2 \quad ,$$

where CI is circularity index, C is the circumference, and A is the area within the circumference. By definition, CI for any circle equals 1.0 and for any other shape is less than 1.0. A plot of CI, cell by cell, across a growth ring should provide some measure of the initiation of latewood since a rectangular shape has a lower CI than a square shape (CI for a perfect square = 0.785; CI for a rectangle with sides in the ratio of 1:2 = 0.698). A more thorough review of CI for quantifying shape in medical histology was presented by Biedenbach *et al.* (1975).

Cell wall thickness can be determined either by using the double-wall thickness method or by determining cell wall area by subtracting cell lumen area, in a progressive step pattern, along the radial file of cells, from the digitized outline of the radial file perimeter. The latter method requires a more sophisticated computer program but has the advantage of minimizing erroneous measurements created by pits or other inhomogeneities in the wall. Well-trained operators, however, can recognize these anomalies and digitize at appropriate points of the cell wall.

Cell area is another useful parameter for assessing cambial activity differences across the growth ring and can be classified into three categories: total cell area (CAT), which is equal to the total area within the middle lamella boundary; cell wall area (CAW), which is equal to the area circumscribed by the middle lamella and limited to the interior by the cell lumen boundary; and cell lumen area (CAL), which is equal to the area enclosed within the cell lumen boundary (*Figure 2.26*).

A decrease in CAL signals either an increase in CAW, a decrease in CAT (cell wall thickness remaining constant), or the concurrence of both (the possibility of both increasing is not likely in a radial file sequence for a coniferous wood). The independent increase of CAW or decrease of CAT each separately denotes transition latewood, while a synchronous increase of CAW and decrease of CAT signify the formation of true latewood. Therefore, the curve of CAL, plotted cell by cell across a radial file, should decline at a steeper angle at the beginning of true latewood than in transition latewood. A hypothetical curve illustrating these points is drawn in *Figure 2.26*. The portion of the curve that is horizontal

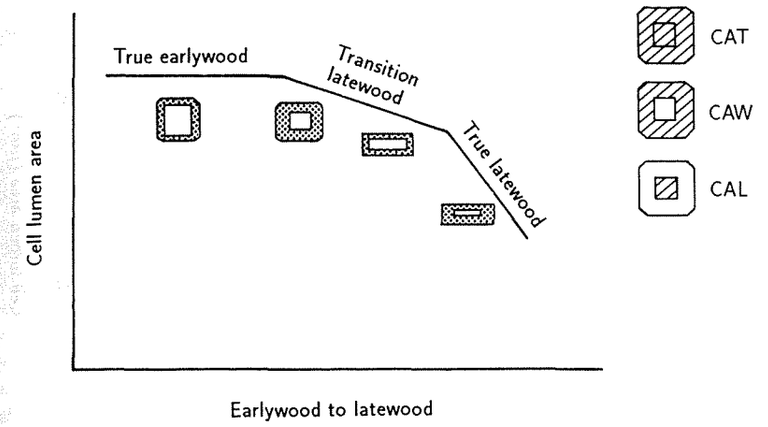

Figure 2.26. Modeled cell lumen area curve along a radial file of tracheids showing expected relative slopes associated with true earlywood, transition latewood, and true latewood. Shaded areas in key indicate measures for total cell area (CAT), cell wall area (CAW), and cell lumen area (CAL).

represents true earlywood, where shape and cell wall thickness do not change. Transition latewood is characterized by either a change in cell shape or cell wall thickness, but not both, and is depicted by the next portion of the curve where the slope is not steep. The final portion of the curve depicts true latewood, where both shape and wall thickness have changed, and the slope is steeper. The shapes of actual CAL curves can be referenced to this hypothetical curve.

An analysis of both the CI curve and CAL curve for a radial file of cells across a growth ring should provide information concerning the boundary between earlywood and latewood as well as the presence or absence of transition latewood. The CI curve is unit-less and, therefore, is strictly a measure of shape change. The CAL curve provides additional quantitative information. Both automated and semiautomated image-analysis systems provide the input data necessary to calculate both CI and CAL. At present, only semiautomated image-analysis systems can give accurate determinations of CAT and CAW of individual cells.

Case Study I: Effect of Fertilization on Wet Versus Dry Sites

Red spruce (*Picea rubens*) trees were fertilized with nitrogen on two different sites in northern Maine, USA. One was a poorly drained (*wet*) site and the other a well-drained (*dry*) site. The wood of red spruce is generally classified as a gradual transition softwood (Panshin and deZeeuw, 1980) and, therefore, the earlywood-latewood boundary is difficult to ascertain. The details of this morphometric analysis have been reported by Jagels and Dyer (1983).

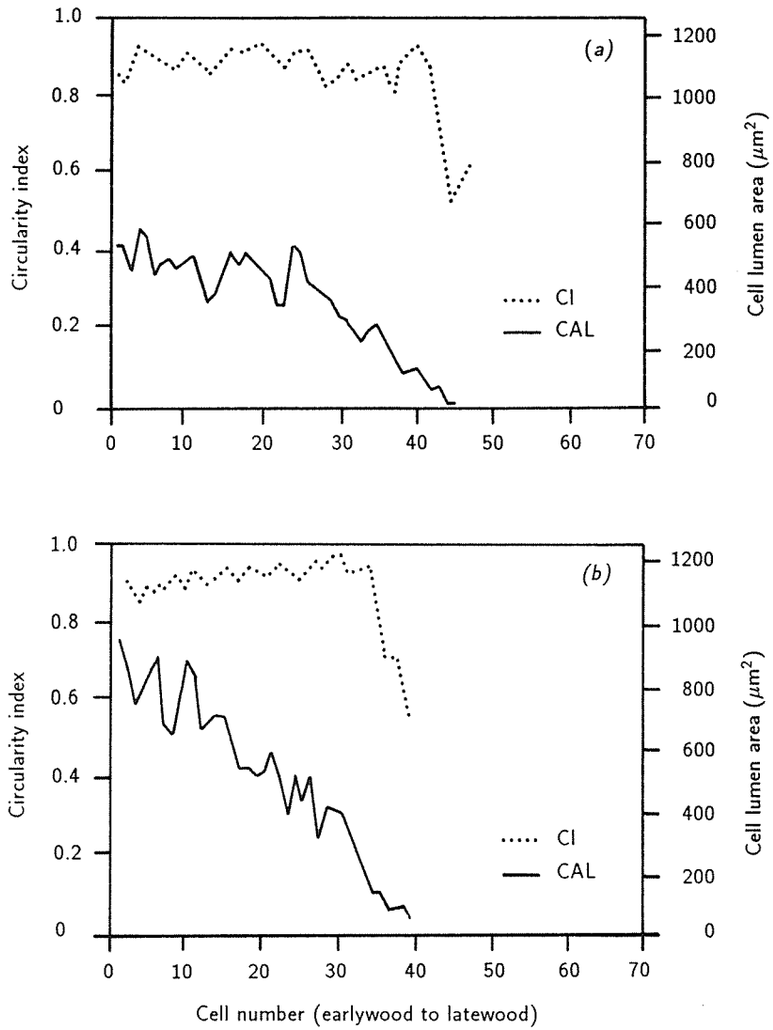

Figure 2.27. Circularity index (CI) and cell lumen area (CAL) curves for fertilized red spruce (*Picea rubens*) on a wet site (*a*) and on a dry site (*b*).

Figure 2.27 summarizes typical dry-site and wet-site trees. The CI curves are reasonably similar; the break point in the curves corresponds with Larson's definition for true latewood, but is often not coincidental with Mork's index (as might be anticipated for gradual transition species). Of 20 growth rings analyzed, three rings lacked a true latewood as defined by both Larson's (1969) criteria and CI curves. All were from wet-site trees: one was from a control

tree, and two were from a fertilized tree. All three were wide growth rings within their respective series. This suggests that on wet sites, when external factors favor increased growth, some factor may limit latewood production. Failure to produce true latewood is discussed in Section 2.7.4.

Previous research had shown that average wood-specific gravity did not change for fertilized trees and was similar on wet and dry sites (Shepard and Shottafer, 1979). However, the CAL curves for wet- and dry-site fertilized trees differ markedly. Dry-site growth rings have earlywood cells about one-third larger than earlywood cells of wet-site trees [compare *Figures 2.27*(*a*) and *2.27*(*b*)]. True earlywood comprises a much smaller percentage of the growth ring in dry-site trees. Transition latewood occupies a larger proportion of the growth ring on dry-site trees, but total cell wall area percentage for wet-site and dry-site trees is nearly identical – 49.0% and 50.3%, respectively. This agrees with the specific gravity data reported by Shepard and Shottafer (1979). These data indicate that the earlywood in the wet-site trees, which is composed of smaller cells, provides a summary (average) density similar to that produced by a brief zone of larger earlywood cells followed by a long transition latewood zone in the wood of dry-site trees. Thus, although summary density data suggest a similarity between fertilization response for wet- and dry-site trees, morphometric analysis reveals basic differences in cambial activity.

Wood density and morphometry. Wood density, the weight of a given volume of wood, and specific gravity (the ratio of wood density to the density of water) have often been determined by displacement volume and weight measurements of samples at a specific water content. Unfortunately, the determination of density by this method does not account for the presence of extractives in the sample and is limited to relatively large samples of wood. The procedure is not applicable to studies within growth rings.

During the late 1950s and early 1960s the methods of X-ray densitometry (Lenz, 1957; Polge, 1966) and wood morphometry (Tsoumis, 1964) were developed for determining wood density within a growth ring. X-ray densitometry can produce accurate determinations of wood density, and wood morphometry produces strong correlations between cell wall area and wood density. Both methods overcome many of the limitations of the displacement method, but both are time-consuming, demand precision, and depend on indirect measures (Lenz *et al.*, 1976; Quirk, 1975, 1984; Schweingruber, 1983; Smith, 1965; Tsoumis, 1964).

Wood density determined by X-ray densitometry is the absolute density of cell wall material (cellulose and lignin) and air spaces (represented by the cell lumens) after all soluble extractives have been removed. The true density of wood is a function of three aspects of wood structure: a basic estimate of wood density, within a species, can be accounted for by the ratio of cell wall area (CAW) to cell lumen area (CAL) (Smith, 1965; Swain, 1987; Tsoumis, 1964); wood density can also be affected by changes in the packing density, or the amount of cell wall material in a known volume of cell wall (Jayme and Krause, 1963); and the ratio of lignin to cellulose within the cell wall can modify actual density (Fukazawa and Imagawa, 1981). Thus, wood density determined by X-

ray densitometry can be thought of as a function of some combination of CAW:CAL, packing density, and lignin:cellulose.

Both wood density and CAW:CAL yield limited information about wood structure and may limit interpretation of environmental effects on cambial activity and xylogenesis. Cells of large diameter and thick cell walls can produce wood with a density equivalent to that of small diameter cells with thin cell walls. The two wood types may be produced under very different environmental conditions that cannot be determined from densitometric analysis alone. Morphometric determinations of cell size (lumen diameter or area) and cell wall thickness can overcome this limitation.

Case Study II: The Effect of Drought on Wood Density and Structure

Loblolly pine (*Pinus taeda*) seedlings were grown under both dry (water-stressed) and wet (non-water-stressed) conditions for three years. At the end of the third year, wood samples were analyzed to characterize latewood density, by X-ray densitometry, and morphometry (CAW:CAL ratios, lumen radial widths, and cell wall thicknesses), by video-image analysis. The video-image-analysis system used in this study has been reported elsewhere (Telewski *et al.*, 1983). It should be noted that the results of this study allow direct comparison between wet and dry conditions for seedlings, but extrapolation from this juvenile tissue to mature trees could result in erroneous conclusions.

Table 2.2. Latewood density determined by X-ray densitometry and morphometric parameters of last-formed latewood cells in three-year-old non-drought- and drought-stressed loblolly pine (*Pinus taeda*).

	Non-drought-stressed	*Drought-stressed*
Latewood density (gm/cc)	0.54	0.50
CAW:CAL	1.49[a]	1.25[a]
Radial width of lumens (μm)	25.30[a]	21.60[a]
Cell wall thickness (μm) latewood	3.60[a]	2.70[a]

[a]Indicates significance at $p = 0.05$.

Drought-stressed conditions decrease turgor pressure of a tree and thus reduce the amount of water available to expand newly formed xylem cells in the cambial zone during the phase of cell enlargement. As a result, xylem produced under drought-stressed conditions should consist of cells of smaller radial width than cells produced in the absence of drought-stress. A cell of smaller radial width should have a lumen of smaller cross-sectional area if the cell wall thickness remains constant or increases. A reduction in the radial width of cell lumens was observed in latewood cells produced under drought-stressed conditions (*Table 2.2*). Such a change in cell structure should result in an increase in wood density. However, as shown in *Table 2.2*, there is a decrease in the latewood density. This reduction in density is confirmed by the decrease in the CAW:CAL ratio determined by video-image analysis. The reduction in latewood

density and the CAW:CAL ratio is a result of significantly thinner tracheid cell walls in the drought-stressed seedlings when compared with non-drought-stressed seedlings (*Table 2.2*).

The information on cell size and structure in combination with values of wood density will be more important in interpreting cambial activity and the ecophysiological response of trees to environmental signals than wood density values alone.

2.7.4. Further studies

CI and CAL curves have now been generated for several coniferous species: *Thuja occidentalis*, *Pinus banksiana*, *Larix laricina*, and *Abies balsamea*. Each species tends to have a distinctive CAL curve, with species like *P. banksiana* and *L. laricina* having an abrupt transition between earlywood and latewood, as expected (*Figure 2.28*). In these trees, the onset of latewood corresponds well with Mork's index on the CAL curve, but often not as indicated by the CI curve. We are beginning to examine this more closely, and it appears that even in abrupt transition conifers the first formed latewood is, in fact, transition latewood as defined by Larson (1969).

The fact that true latewood fails to form in some growth rings on wet-site fertilized red spruce, as cited in Case Study I, has been investigated further on other, unperturbed, sites. *Figure 2.29* shows a typical double wall thickness (DWT) curve, in which DWT increases in the latewood zone. *Figures 2.30*, *2.31*, and *2.32* show DWT, CI, and CAL curves for a red spruce ring that lacks true latewood. The CAL (*Figure 2.32*) curve suggests the presence of a latewood zone, yet the DWT (*Figure 2.30*) and CI (*Figure 2.31*) curves confirm the absence of true latewood. An X-ray densitometry curve would erroneously indicate the presence of latewood in this ring based on the methods of determining earlywood-latewood boundaries described earlier.

At present the environmental cues that stimulate the production of this *false latewood* are not known, but clearly the cambial response is quite different and suggests a nutrient deficiency, change in the maturation rate of cells in the cambial zone, or some other block to cell wall thickening. This phenomenon needs to be explored further.

2.7.5. Discussion and summary

The introduction of computer-assisted image-analysis systems has removed the time-consuming and tedious aspect of using ocular micrometers and ocular grids in morphometric studies of tree rings. Both the planer measure of CAW:CAL ratios and the linear measure of radial cell wall thickness and radial cell diameter give accurate assessments of wood density in coniferous species at a level unobtainable using radiodensitometric methods. When used in conjunction with radiodensitometric methods, wood density can be analyzed to determine the contribution of packing density, lignin to cellulose ratios, and the CAW:CAL ratio

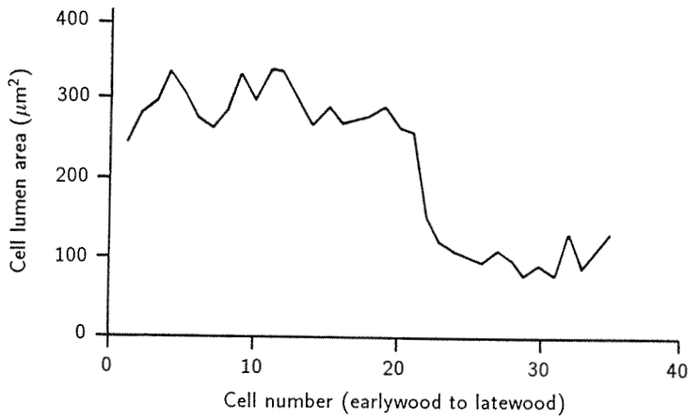

Figure 2.28. Cell lumen area (CAL) curves for jack pine (*Pinus banksiana*), an abrupt transition conifer.

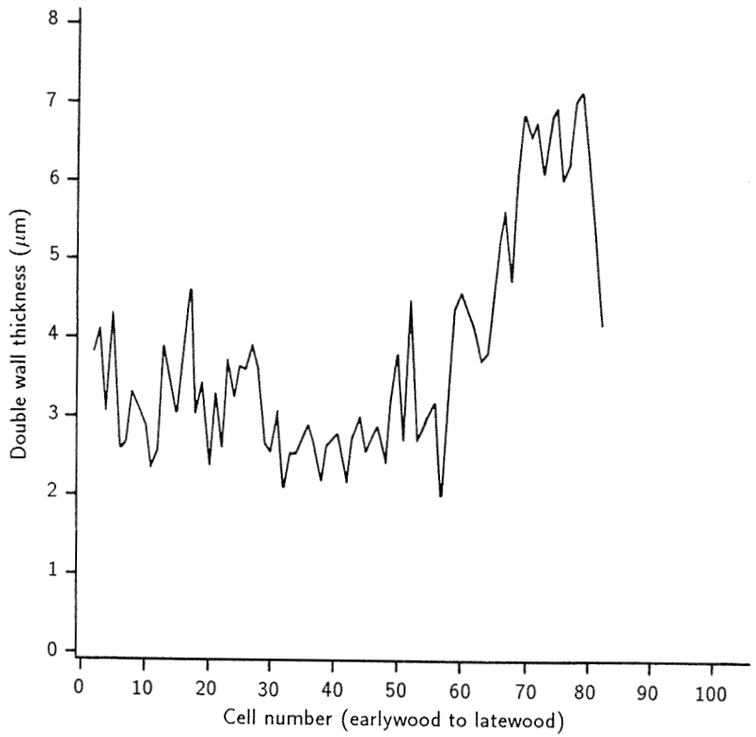

Figure 2.29. Double wall thickness (DWT) curve for typical red spruce (*Picea rubens*) with a true latewood.

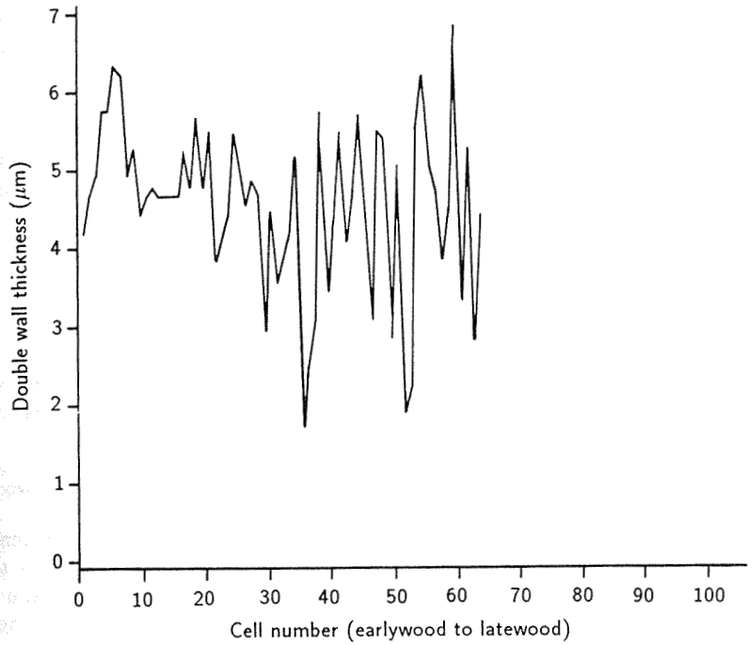

Figure 2.30. Double wall thickness (DWT) curve for typical red spruce (*Picea rubens*) lacking true latewood.

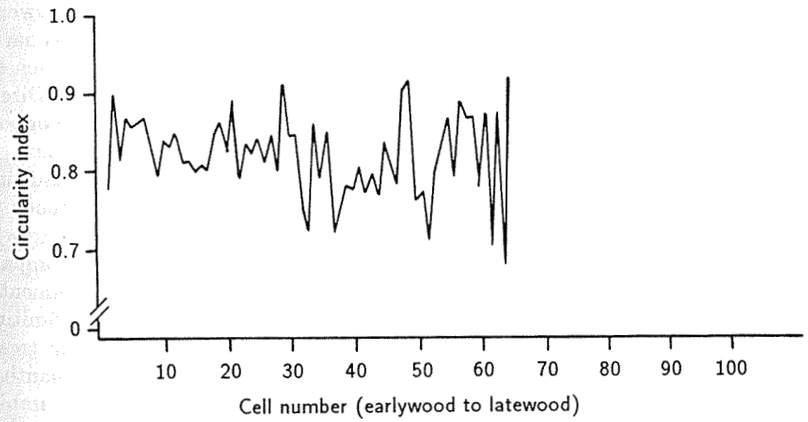

Figure 2.31. Circularity index (CI) curve for typical red spruce lacking true latewood.

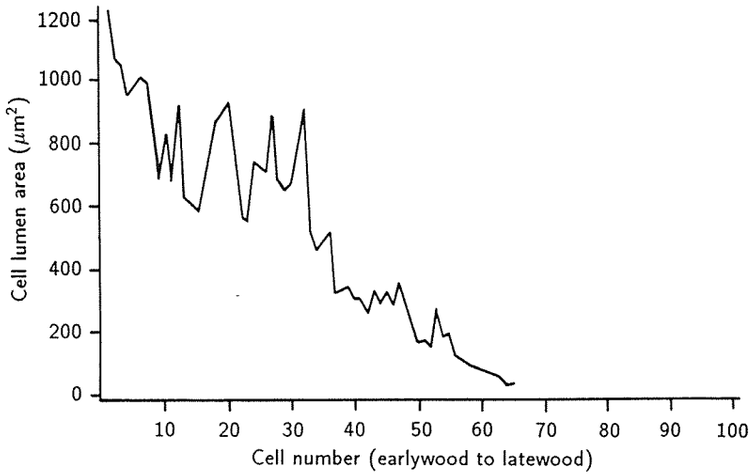

Figure 2.32. Cell lumen area (CAL) curve for typical red spruce lacking true latewood.

to total wood density. If morphometric methods of determining wood density are to be used in a dendrochronological study, the relationship between total wood density (determined by radiographic or displacement methods) and the morphometric determination of wood density should be established for species not tested previously. In many studies, morphometric analysis may replace radiographic methods of determining wood density.

Morphometric analysis across a growth ring provides a sensitive cell-by-cell record of cambial activity through CI, DWT, and CAL curves and obviates the necessity for artificial classifications of the growth ring. The terms earlywood and latewood clearly have different biological connotations in a ring porous hardwood versus a gradual transition softwood. But the categories may not even be comparable between abrupt transition and gradual transition softwoods. Direct plots of growth-ring curves based on morphometric analysis provide the opportunity for direct comparison among different species for interpretive analysis.

By plotting CAL, DWT, or CI curves on a 100% scale (i.e., standardizing the abscissa), rings of various widths can be compared by overlay methods to determine differences in area between two curves, to compare individual growth rings with an average curve determined for a set of tree rings, or to compare each growth ring with a hypothetical curve representing ideal environmental conditions for growth. These differences can be compared with different limiting factors in the environment. The curves can also be averaged for certain treatments for statistical comparison. From these kinds of analyses, a more quantitative basis can be established for assessing environmental influences on cambial activity and wood structure.

Morphometric techniques can also be applied to answer other basic wood structure questions. For instance, CI could be used to ascertain the limits of compression wood on a cross section. A CI value limit above that achieved in

the first-formed earlywood tracheids could be set on an automatic image analyzer, and compression wood areas would be automatically plotted. Circularity index may also have potential in assessing pit aperture shape changes, such as those associated with drying defects or biological degradation.

We are presently using CAL measurements to assess vessel volume in diffuse porous hardwoods in relation to site, silvicultural practices, or different levels of atmospheric CO_2. CI measurements could also be applied to hardwood vessels for studying physiological and pathological variation.

2.8. Radioactive Isotopes in Wood
J.R. Pilcher

The story of radioactive isotopes in wood is the story of radiocarbon dating. Of the chief constituents of wood, carbon has one radioisotope (^{14}C), oxygen has none, and hydrogen has one (tritium ^{3}H). Trace elements in plants or elements that might occur fortuitously in wood include some natural and artificial radioisotopes, but these have generated little research interest. Tritium has been extensively studied in groundwaters. However, it has been seldom studied in wood because the mobility of hydrogen atoms in organic molecules is likely to make such measurement valueless. This leaves us with ^{14}C – the basis of radiocarbon dating.

The literature on radiocarbon dating is spread widely over a number of diverse fields. The subject has its own journal, *Radiocarbon*, and also may be discussed in journals of geophysics and atmospheric physics and in the archaeological literature; archaeologists are among the most frequent users of the dating method. A simple review written for the nonspecialist may be found in a European Science Foundation *Handbooks for Archaeologists*, *Radiocarbon Dating* (Mook and Waterbolk, 1985). The early history of the subject is reviewed by Libby (1965), who was awarded the Nobel Prize for his discovery of natural radiocarbon and for his work on the development of the radiocarbon-dating method.

Wood has always been a favored material for radiocarbon measurement. In theory at least the carbon in each annual ring in wood largely represents the production of photosynthesis for that year. Some material is transported in wood rays from the phloem to older wood where it contributes to the formation of heartwood. There may be a small synthesis of cellulose in the formation of tyloses in the heartwood formation zone in some genera (e.g., *Quercus*), but most of the material transported to the heartwood is in the form of tannins, gums, and resins. Cain and Suess (1976) investigated the movement of substances into heartwood by tracing the ^{14}C from the 1963 nuclear weapon tests in wood from years before 1963. They detected a small peak of activity in the rings of the 1930s, but found that the contribution to the total carbon of the heartwood ring was small and was mostly in the extractable fraction. Most radiocarbon studies of wood employ some form of extraction to remove tannins and resins. Although the ^{14}C activity of each annual ring may thus be specific to the year of formation, the archaeologist or other *user* usually wants to know the time of use of the

piece of wood not the time of formation of the rings. Thus the problems of interpretation are much the same as those of dendrochronology where missing rings, decayed sapwood, etc., must be taken into account. In the case of radiocarbon dating this is further confused by the fact that the sample measured may span many years.

The first wood samples ever dated, apart from a series of living trees, were from Egyptian tombs that Libby measured in an attempt to provide confirmation for his early dating method. If he had known of the controversy that was to rumble on through Egyptological dating for the next 40 years (see, for example, Mellaart, 1979), he might have chosen some other material to test. However, this was the first attempt to use *known age* wood to check or calibrate the radiocarbon dating method. Since then an enormous research effort has been applied to the problem of calibrating the radiocarbon time scale.

Bristlecone Pine Calibrations

The bristlecone pine (*Pinus aristata* and *P. longaevea*) has provided for many years the longest tree-ring chronology in the world. Initially a chronology of 7,104 years was constructed using living-tree chronologies and only 17 samples of preserved old wood (Ferguson, 1969). Over most of its length this chronology has a replication of only four trees. This basic chronology was later extended to 7,484 years (Ferguson, 1970), and finally to 8,681 years (Ferguson and Graybill, 1983). Since 1969 there have been various attempts to discredit the bristlecone pine chronology or the radiocarbon work based on it. The most convincing proof of the chronology accuracy came from the independent chronology of LaMarche and Harlan (1973). The radiocarbon measurement of samples of wood from the bristlecone pine chronology was carried out in several laboratories. The history of this era of radiocarbon calibration is complicated by the personalities involved and the intense inter-laboratory rivalry for funding that developed. Some insight into this may be gained by reading the *Nobel Symposium*, Vol. 12, devoted to radiocarbon dating (Olsson, 1970) from which it is clear that the laboratories were not willing to collaborate or combine their results and did not trust the accuracy of each other's results.

The publication of the *Nobel Symposium* in 1970 was a turning point in radiocarbon calibration. Whether people did or did not believe the detail of the calibration results (see discussion of wiggles in Olsson, 1970, pages 309–311) there was no escaping the general conclusion that the ^{14}C ages and true ages could deviate by up to 800 years, thus demonstrating the need for a calibration curve. In most sciences calibration is something done by researchers in the privacy of their laboratories. The calibration of a spectrophotometer using standard solutions would be a part of the measurement procedure and would not normally be discussed with or even mentioned to the submitter of the sample. With radiocarbon dating the process of calibration has been left to the customer with the result that the literature of the 1970s and early 1980s is scattered with a variety of calibration curves and tables (for example, Clark, 1975; Watkins, 1975; Klein *et al.*, 1982) and with radiocarbon dates quoted with a variety of different calibrations or none at all. One can sympathize with the archaeologist who,

faced with this confusion, decided to have nothing to do with calibration at all. From 1970 the second series of calibration measurements started.

European Oak Calibrations

With the bristlecone pine chronology extending over 7,000 years in existence in 1970, one may wonder why an attempt was made to produce another long chronology for radiocarbon calibration. The work started mainly in response to three criticisms of the bristlecone pine calibration.

- It was not known whether the bristlecone pine calibration was applicable worldwide.
- It was not known whether other species or trees at lower altitudes would show the same variations.
- The accuracy of measurements on bristlecone pine were not adequate to resolve the controversial wiggles in the calibration curve published by Suess (1970). Bristlecone pine could not provide large enough samples for the necessary high-precision measurement.

The exercise of producing an alternative calibration based on a different species, from low altitude and geographically separated from California, demanded a huge dendrochronological effort in both Ireland and the Federal Republic of Germany that lasted from about 1970 to 1986. This work has itself generated a considerable literature. The early work in Europe is reviewed by Eckstein (1972) and Baillie (1976), and by Eckstein and Pilcher in Chapter 1. Key references to the work of the Belfast laboratory are Pilcher *et al.* (1977), Pilcher *et al.* (1984), and Brown *et al.* (1986). The work of the German laboratories is described by Becker and Schmidt (1982), Becker (1983a), Stuiver *et al.* (1986), and Leuschner and Delorme (1984). The German and Irish chronologies are based on deciduous oaks (*Quercus robur* and *Q. petraea*, which are not normally separated on the basis of wood anatomy).

Because of the relatively short age span of oaks compared with bristlecone pine, large numbers of individual trees are required to build a long chronology. For example, the 7,272-year Belfast chronology contains the ring records of more than 1,000 trees. The bulk of the radiocarbon calibration measurements have been made on oak samples dated by the Belfast chronology and the south German chronology of Bernd Becker.

Radiocarbon Measurement

Recent advances in radiocarbon measurement that have lead to the new era of high-precision measurements are described by Pearson (1979, 1980). For more information the reader should consult the special calibration volume of *Radiocarbon*, Vol. 28, A&B (1985). This provides a definitive calibration curve agreed to by the International Calibration Committee presented in both graphic and tabular form. This should mark the end of the calibration controversy.

Future advances are likely to include a modest extension of the chronologies dating perhaps as far back as 10,000 years (Becker and Kromer, 1986). Extension back to the start of the late Glacial period (about 14,000 years) would require almost doubling the length of existing chronologies. Because the first 7,000 years took about 15 years to complete, the next 7,000 years will not be an easy task. Refinement of radiocarbon measurement is unlikely to make any major changes to the calibration apart from a further extension back in time. Further significant improvement in precision seems unlikely. Advances in this field are normally reported at international radiocarbon conferences held every three years and in the journal *Radiocarbon*.

CHAPTER 3

Data Analysis

Chapter Leaders: E. Cook and K. Briffa
Chapter Contributors: S. Shiyatov, V. Mazepa, and P.D. Jones

3.1. Introduction

E. Cook and K. Briffa

The information contained in annual tree rings is a valuable resource for studying environmental change. Past climate can be reconstructed from the year-to-year changes in annual ring width and ring density (e.g., Fritts, 1976; Schweingruber *et al.*, 1978). The occurrence of previously unrecorded geomorphological events, such as earthquakes and landslides, can be inferred from anomalous changes in the ring-width pattern (e.g., Shroder, 1980; Jacoby and Ulan, 1983). Forest-stand disturbances and gap-phase dynamics can be inferred from suppression-release patterns in tree rings (Brubaker, 1987), and, anomalous changes in the forest environment, due perhaps to anthropogenic pollutants, can be examined based on the recent patterns of tree rings (e.g., Eckstein *et al.*, 1983, 1984; Cook, 1987a). This list of applications is not complete. It is only intended to show that tree rings can be used to study a variety of environmental changes.

Although the use of tree rings for studying environmental change is widespread, the extraction of the desired signal from the unwanted noise can be difficult and uncertain. *Signal* is defined here, in a hypothesis-testing sense, as the information derived from tree rings that is relevant to the study of a particular problem. In contrast, *noise* is defined as the information that is irrelevant to the problem being studied. Given this reality, a tree-ring series is more appropriately thought of as the aggregation of several signals that become signal or noise only within the context of a specific hypothesis test or application. It is from this basis that the problem of signal extraction in tree-ring research is more fundamentally related to the disaggregation of the observed ring widths into a finite number of signals that represent the sum of the environmental influences on tree growth.

E. R. Cook and L. A. Kairiukstis (eds.), Methods of Dendrochronology, 97–162.

To provide a conceptual framework for this signal extraction problem, a linear aggregate model for tree-ring series will be described.

3.2. A Conceptual Linear Aggregate Model for Tree Rings

E. Cook

Consider a tree-ring series as a linear aggregate of several unobserved subseries. Let this aggregate series be expressed as

$$R_t = A_t + C_t + \delta D1_t + \delta D2_t + E_t \quad ,$$

where:

R_t	=	the observed ring-width series;
A_t	=	the age-size-related trend in ring width;
C_t	=	the climatically related environmental signal;
$D1_t$	=	the disturbance pulse caused by a local endogenous disturbance;
$D2_t$	=	the disturbance pulse caused by a standwide exogenous disturbance; and
E_t	=	the largely unexplained year-to-year variability not related to the other signals.

This model is expressed in linear form to simplify the discussion of the concepts associated with each component of the model. It is known that certain ring-width properties are usually multiplicative (i.e., the relationship between the mean and standard deviation of ring widths). However, such nonlinear relationships can be easily linearized by transforming the ring widths to logarithms. In this sense, tree-ring series are intrinsically linear processes and the above formulation holds. The δ associated with $D1_t$ and $D2_t$ is a binary indicator of the presence ($\delta = 1$) or absence ($\delta = 0$) of either class of disturbance at some time t in the ring widths. Thus, A_t, C_t, and E_t are assumed to be continuously present in R_t, while $D1_t$ and $D2_t$ may or may not be present depending on whether the intervention of a disturbance has occurred at some time t. Some general properties of these subseries will now be described that are pertinent to the problem of estimating each one as a discrete process.

A_t is a nonstationary process that reflects, in part, the geometrical constraint of adding a volume of wood to a stem of increasing radius. When this constraint is the principal source of the trend, A_t will exhibit an exponential decay as a function of time once the juvenile period of increasing radial increment has passed. This form of trend is most commonly found in trees growing in open environments where competition and disturbance effects are minimal. *Figure 3.1(a)* shows one such ring-width series from an open-canopy, semiarid site, ponderosa pine (*Pinus ponderosa*). More frequently, the behavior of A_t is strongly influenced and distorted by competition and disturbances in the forest.

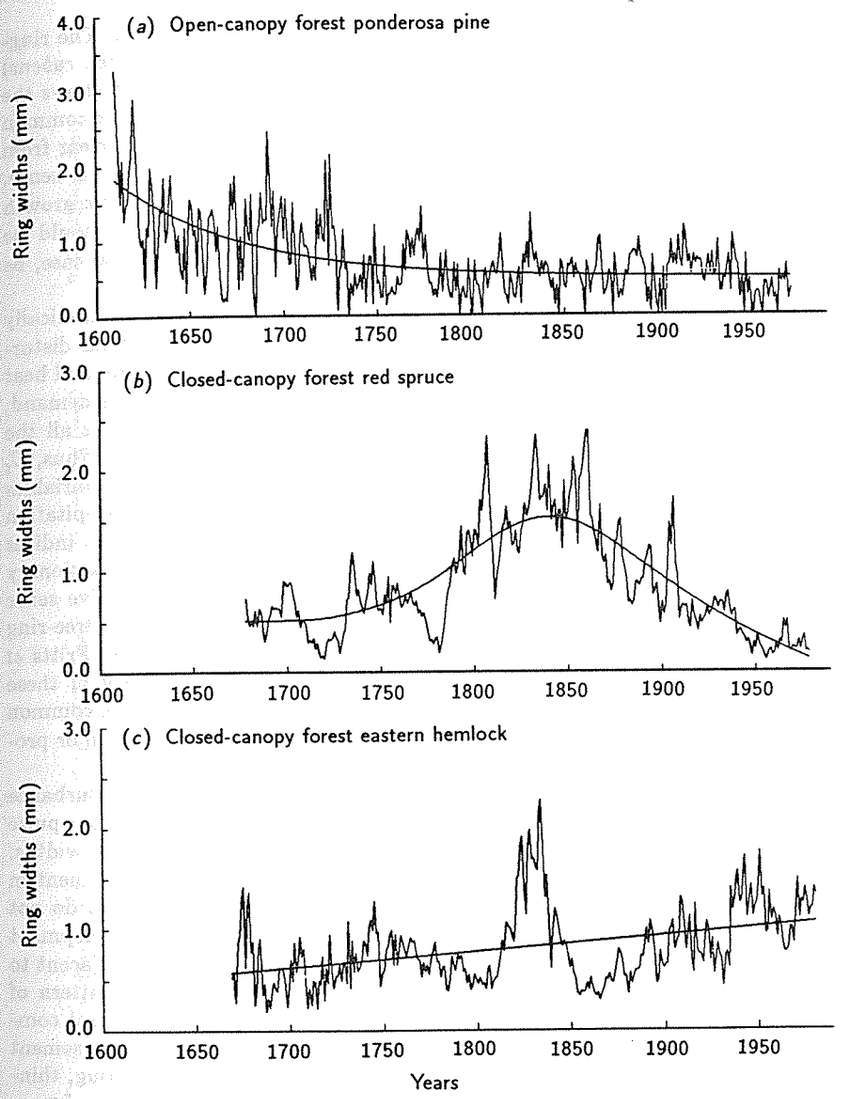

Figure 3.1. Three examples of the kinds of growth trends that can be found in ring-width data. Series (*a*) is from a semiarid site ponderosa pine (*Pinus ponderosa*), growing in an undisturbed, open-canopy environment. It shows the classic exponential decay of ring width that is expected when a tree ages, and when competition and disturbance are minimal. *Figures* (*b*) and (*c*) are from closed-canopy stands of red spruce (*Picea rubens*) and eastern hemlock (*Tsuga canadensis*). These latter two series show how the effects of competition and disturbance can radically alter the expected exponential decay of ring widths.

Figures 3.1(b) and *3.1(c)* show two typical examples of this problem. The ring-width series in *Figures 3.1(b)* and *3.1(c)* are from a red spruce (*Picea rubens*) and an eastern hemlock (*Tsuga canadensis*), respectively. Each series shows the effects of suppression and release due to competition. These effects are common in stands of shade-tolerant species such as spruce and hemlock. It is clear from *Figure 3.1* that there is no predictable shape for A_t in the most general sense. That is, A_t does not necessarily arise from any family of deterministic growth curve models such as the negative exponential curve. Rather, A_t should be thought of as a nonstationary, stochastic process that may, as a special case, be modeled as a deterministic process (e.g., Fritts *et al.*, 1969).

C_t represents the aggregate influence on tree growth of all climatically related environmental variables except for those associated with stand disturbances. Typical variables composing C_t are precipitation, temperature, and heat sums as they affect available soil-moisture supply, evapotranspiration demand, and phenology. These variables are assumed to be broad scale in that all the trees in a stand will be affected similarly by the same set of variables. Thus, C_t is a signal in common to all sampled trees in a stand. Some climatic variables that have been used to model C_t are monthly temperature and precipitation (Fritts, 1976), summer degree-days (Jacoby *et al.*, 1985), and drought indices (Cook and Jacoby, 1977). These variables can usually be regarded as stationary stochastic processes although they may be persistent in an autoregressive sense (Gilman *et al.*, 1963). Methods for modeling the composition of C_t in tree-ring chronologies, as response functions, are many and well researched (e.g., Fritts *et al.*, 1971; Meko, 1981; Guiot *et al.*, 1982b, Guiot, 1985a). A review of these methods is found in Chapter 5. Here, C_t will be regarded simply as the common climatic signal among all sampled trees without regard to its composition or properties.

The characteristic response of a tree to a local, or endogenous, disturbance in the forest is represented by $D1_t$. This response will be referred to as a pulse due to its expected transience and eventual disappearance in the ring widths. Endogenous disturbances are a consequence of gap-phase stand development in which individual trees are removed from the canopy by processes that do not affect the stand as a whole (White, 1979). This pattern of stand development creates patterns of suppression and release in the ring widths of trees adjacent to the trees removed from the canopy. See *Figure 3.1(b)* for a typical pattern of ring-width variation caused by gap-phase stand dynamics. Such natural competition effects are ubiquitous in closed-canopy forests. Forest management practices also fall within this class of disturbances when selective cutting, thinning, and the removal of undergrowth disturb only the local environment of trees in a stand.

An important property of endogenous disturbances, which is relevant to the disaggregation of R_t, is the likelihood that truly endogenous disturbances will be random events in both space and time within a forest stand of sufficient size. This means that the endogenous disturbance pulse in the ring widths of a given tree will be largely uncorrelated with endogenous disturbance pulses in other trees from the same stand. An example of this property is shown in *Figure 3.2*

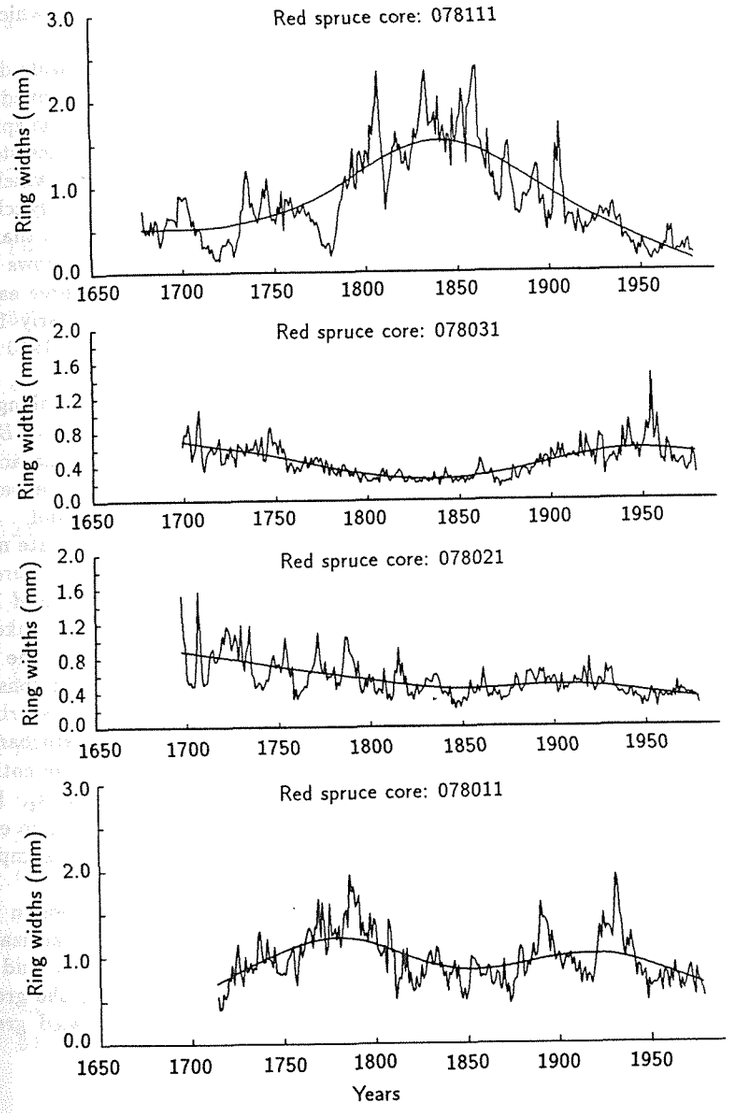

Figure 3.2. Four red spruce ring-width series from the same stand. Note the general lack of agreement in the long-term growth trends and also for shorter periods lasting 20–30 years. The lack of agreement is caused by differing competition and disturbance histories that alter the growth trends individually. These effects may be classified as endogenous disturbance effects due to the lack of synchrony among trees.

for four red spruce trees from the same stand. Each series has divergent or out-of-phase ring-width fluctuations lasting 20 or more years in length, which are likely to be due to endogenous disturbance events.

$D2_t$ represents the characteristic response of a tree to a standwide disturbance. Examples of non-climatic agents capable of producing a standwide disturbance are fire, insects, disease, logging, and perhaps pollution. Some episodic weather-related disturbance agents are severe frosts, high winds, and ice storms. The pertinent feature of the resultant exogenous disturbance pulse, which can differentiate it from that caused by an endogenous disturbance, is the synchrony in time of this event in all sampled trees from a stand. This indicates that $D2_t$ will be a common feature among all trees, unlike $D1_t$. *Figure 3.3* shows some examples of an exogenous disturbance pulse in the ring widths of three eastern hemlock trees, which were all influenced by logging activity in the early 1900s. Note the sudden and synchronous increase in ring widths after about 1910 in all three series.

E_t represents the unexplained variance in the ring widths after taking into account the contributions of A_t, C_t, $D1_t$, and $D2_t$. Some likely sources of E_t are, for example, microsite differences within the stand, gradients in soil characteristics and hydrology, and measurement error. E_t is assumed to be serially uncorrelated within and spatially uncorrelated between trees in the stand.

The conceptual model for ring widths based on the linear aggregate model indicates that a ring-width series may be broadly decomposed into a pure age trend component (A_t), two common stochastic signal components (C_t and $D2_t$), and two unique stochastic signal components ($D1_t$ and E_t). This breakdown into discrete classes assumes that there is no covariance between any of the components. That this assumption will not always hold is apparent when considering the problem of separating the trend component, A_t, from either disturbance pulse, $D1_t$ and $D2_t$. If the response time of a tree to either kind of disturbance is short relative to the length of the ring-width series, then A_t may be differentiated from $D1_t$ and $D2_t$ within the limits of the method used to estimate A_t. However, if the ring-width series is short relative to the transient response to either kind of disturbance, than the trend component may, in fact, be largely composed of $D1_t$, $D2_t$, or both.

In Section 3.3, methods of estimating and removing growth trends in ring-width data will be described, as part of the process of tree-ring standardization. Because of the potentially complicated character of these trends and the definition of what needs to be estimated as *trend*, the notation for the growth trend will be changed and generalized as follows. Let the estimated growth trend be defined as some deterministic or stochastic process

$$G_t = f(A_t, \delta D1_t, \delta D2_t) \quad ,$$

where the estimated growth trend G_t is a function of the pure age trend component, A_t, and the stochastic perturbers of pure age trend, $\delta D1_t$ and $\delta D2_t$. The δ again means that these endogenous and exogenous disturbance effects need not be present in the observed ring-width series.

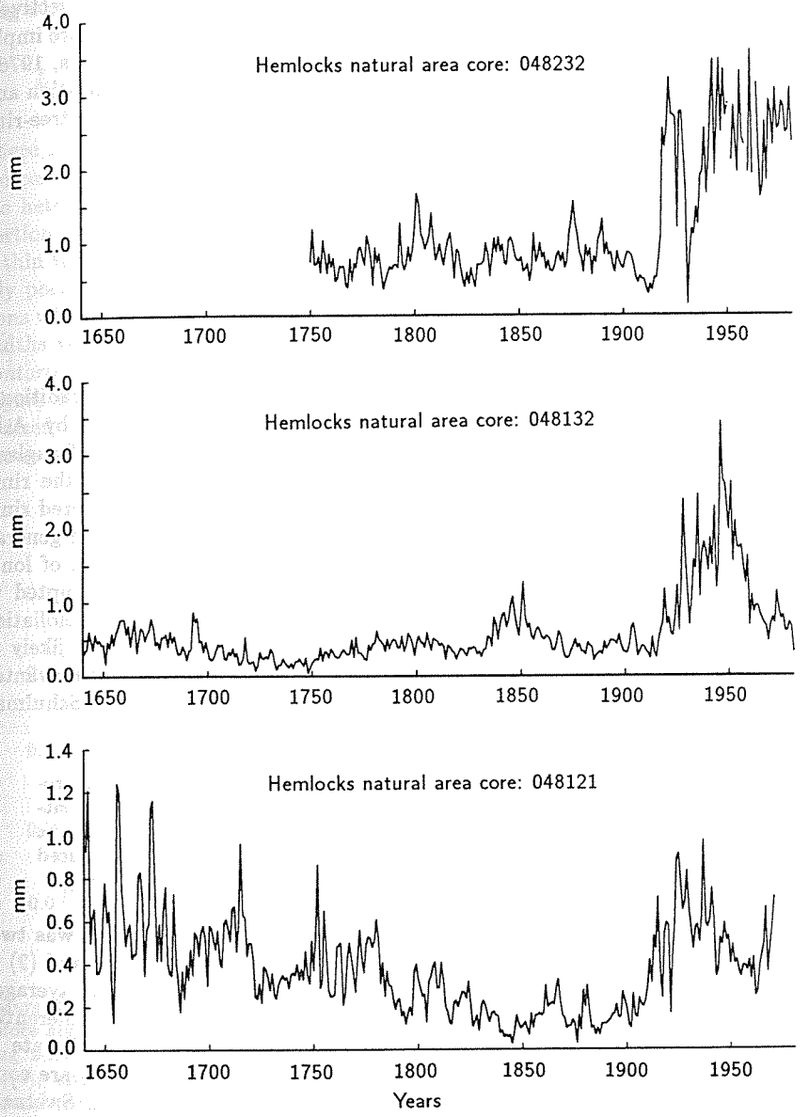

Figure 3.3. Three eastern hemlock ring-width series from a stand that has been affected by logging activity. It is known that the area around the hemlock stand was logged around 1910. Note the rapid increase in ring width in all three series at about that time. These synchronous changes in ring width due to a stand-level disturbance may be classified as exogenous disturbance effects.

This definition of G_t suggests that the common climatic component, C_t, may be the signal of interest, since A_t, $D1_t$, and $D2_t$ are considered collectively as non-climatic variance or noise. These definitions of signal and noise are implicit when standardizing tree-ring series for dendroclimatic studies (Fritts, 1976). They will be maintained throughout this section on tree-ring standardization and chronology development, with the realization that other applications of tree-ring analysis may define signal and noise differently.

3.3. Tree-Ring Standardization and Growth-Trend Estimation

E. Cook, K. Briffa, S. Shiyatov, and V. Mazepa

3.3.1. Introduction

The estimation and removal of G_t from a ring-width series has been a traditional procedure in dendrochronology since its modern-day development by A.E. Douglass (1914, 1919). This procedure is known as standardization (Douglass, 1919; Fritts, 1976). Early workers searching for climatic signals in the ring-width series of old conifers identified long-term growth trends in measured ring-width data that could confidently be attributed solely to tree aging. In general, many factors can influence tree growth. However, by careful selection of long-lived trees growing in climatically stressed sites, early workers attempted to ensure that non-climatic growth influences such as competition and defoliation were minimized (Douglass, 1914). In this way, the selected trees were likely to have a strong climate signal, and the ring-width series were such that unwanted noise (resulting from tree aging) could be unambiguously identified. Schulman (1945b) described the purpose of standardization as follows:

> To obtain a mean curve representing trees of various ages, the usual procedure is to "standardize" the individual tree curves by computing percentage departures from a trend line fitted to the curve and then to average the standardized values. Thus the large average growth rate of youth is reduced to conform with slower growth of maturity and old age.

From this quote, it is clear that the original intent of standardization was two-fold: (1) to remove non-climatic age trends from the ring-width series and (2) to allow the resultant standardized values of individual trees to be averaged together into a mean-value function by adjusting the series for differential growth rates due to differing tree ages and differences in the overall rate of growth. The "percentage departures" described by Schulman (1945b) are commonly known today as "tree-ring indices" (Fritts, 1976). Fritts and Swetnam (1986) provide an excellent description of the sequential process of trend removal, indexing, and averaging used in dendrochronology.

Standardization transforms the nonstationary ring widths into a new series of stationary, relative tree-ring indices that have a defined mean of 1.0 and a

relatively constant variance. This is accomplished by dividing each measured ring width by its expected value, as estimated by G_t. That is,

$$I_t = R_t / G_t \tag{3.1}$$

where I_t is the relative tree-ring index. When standardizing ring-width data, the indices are produced by division instead of differencing because ring-width series are heteroscedastic. That is, the local variance of ring widths is generally proportional to the local mean, where local is defined as some subinterval of time within the time span covered by the ring widths. The actual relationship is usually positive and linear between the ring-width means and their standard deviations when compared over time. *Figure 3.4(a)* shows a plot of 10-year mean ring widths versus their standard deviations for a collection of lodgepole pine (*Pinus contorta*) ring-width series. The positive correlation ($r = .67$) is quite apparent. *Figure 3.4(b)* shows the same data after the ring-width series have been standardized using negative exponential and linear regression curves. The correlation between mean and standard deviation ($r = .10$) is now largely gone.

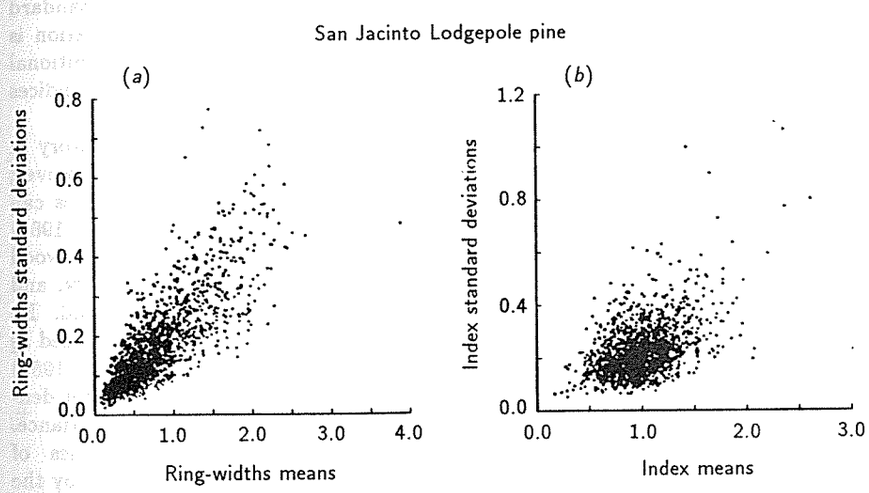

Figure 3.4. The relationship between the mean and standard deviation of tree-ring data before and after standardization. *Figure 3.4(a)* shows the scatter-plot of 10-year mean ring widths versus their standard deviations. The correlation is $r = .67$. In *Figure 3.4(b)*, after standardization and reduction of the ring widths to indices, the linear dependence between the mean and standard deviation is for the most part gone ($r = .10$).

Another way of stabilizing the variance is by transforming the ring widths to logarithms. In this case, the resultant indices are computed by subtracting $\log_e G_t$ from $\log_e R_t$, not by dividing as above. That is,

$$\log_e I_t = \log_e R_t - \log_e G_t \quad . \tag{3.2}$$

Problems arise in employing the logarithmic transformation to ring widths when the series has locally absent rings, which are typically coded as zero when using equation (3.1) to estimate I_t. Since the logarithm of zero does not exist, it has been suggested (e.g., Warren, 1980) that some arbitrarily small positive number replace the zero. This procedure may impart a statistically significant negative skew to the probability distribution of $\log_e I_t$ if the chosen number is too small. In addition, a logarithmic transformation of the form in equation (3.2) may overcorrect the heteroscedasticity and impart a negative dependence between the mean and standard deviation. Preliminary research indicates that the correct transformation of ring-width series to stabilize the variance is $\log_e(R_t + c)$, where c is a constant estimated from the series being transformed. That a simple logarithmic transformation will not be correct all of the time is illustrated in *Figure 3.5* for two white oak (*Quercus alba*) ring-width series. The lower series shows the typical linear dependence between the local 10-year means and their standard deviations [$r = .77$, *Figure 3.5(b)*]. A logarithmic transformation is clearly justified. In contrast, the upper ring-width series from the same stand of trees has no significant linear dependence between the local means and standard deviations [$r = .08$, *Figure 3.5(a)*]. Therefore, a logarithmic transformation is not justified in this case. These examples indicate the need for additional research to determine the best way to stabilize the variance of tree-ring indices by transformation.

The method of computing tree-ring indices as ratios has a long history in dendrochronology (Douglass, 1936; Schulman, 1956; Fritts, 1976). However, with the development of X-ray densitometry, additional tree-ring variables can be measured that also require some form of standardization. Bräker (1981) analyzed the properties of six tree-ring variables (total ring width, earlywood width, latewood width, latewood percentage, minimum earlywood density, and maximum latewood density) for conifer tree species growing in Switzerland. He found that latewood percentages and density data were properly standardized as differences from the estimated growth trend, not as ratios. Bräker (1981) justified the computation of differences because latewood percentages and density data do not usually show a clear dependence between mean and variance. However, Cleaveland (1983) found that maximum latewood densities of semiarid-site conifers in the western United States still required indexing by the ratio method to stabilize the variance. As more experience is gained in standardizing these comparatively new tree-ring variables, a preferred method of computing indices may be determined.

Because tree-ring indices are stationary processes having a defined mean and homogeneous variance, the index series of many trees from a site can be averaged together to form a mean-value function. Strictly speaking, it is not valid to average together nonstationary processes, like the majority of ring-width series, because such processes do not possess a defined mean or variance. While it is possible to compute the mean and variance of a ring-width series for a specific time period, it is incorrect to use these statistics as expectations for other

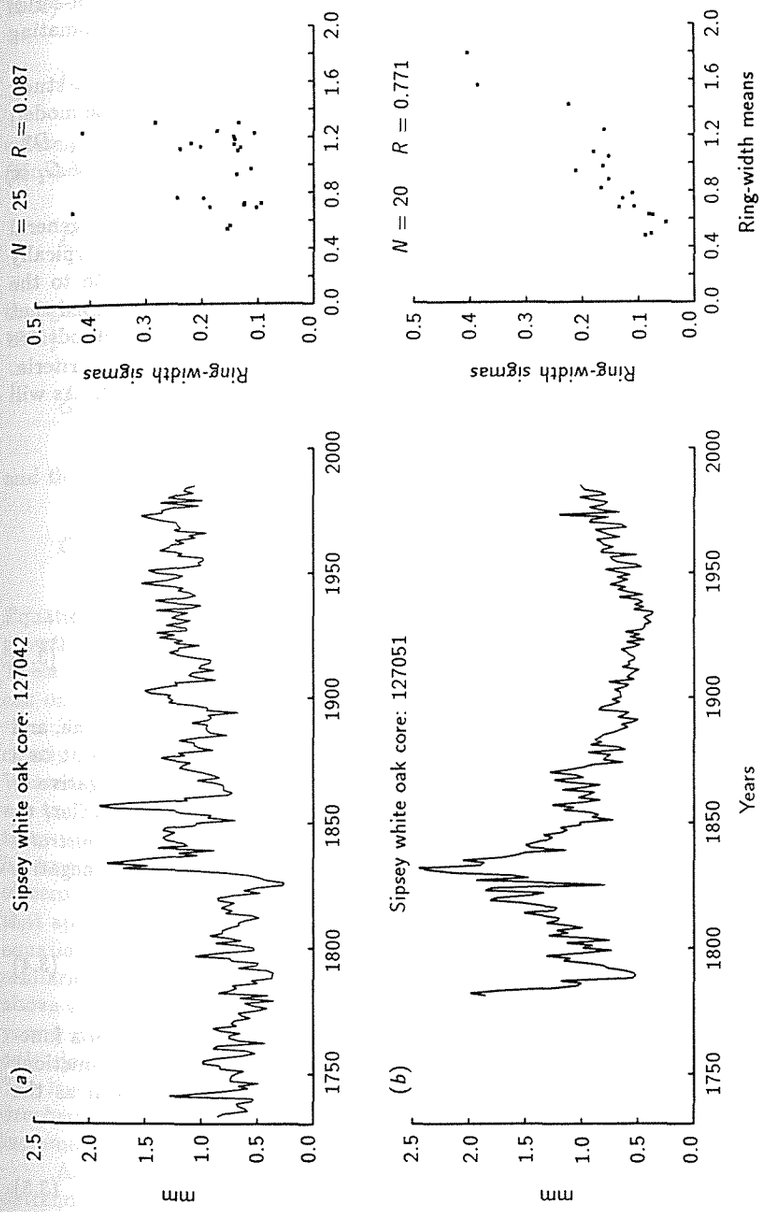

Figure 3.5. The variability in the mean-to-standard deviation relationship in two white oak (*Quercus alba*) ring-width series from the same stand. The bottom series (*b*) has the normally expected linear dependence, while the upper series (*a*) has no significant relationship. A logarithmic transformation to stabilize the variance would be appropriate for the lower series, but not for the upper series.

time periods or to use them as within-series estimates of the population parameters. This same problem carries through in a cross-sectional or between-series sense, where the lack of a defined sample mean makes the concept of estimating the between-series population mean invalid.

The mean-value function of tree-ring indices is frequently used to study past climate (Fritts, 1976). When climate (i.e., C_t in the linear aggregate model) is the signal of interest, all other information in the ring widths (i.e., A_t, $D1_t$, $D2_t$, and E_t) is considered as noise and discarded as a compound form of G_t or minimized through averaging into the mean-value function.

Many methods are available for estimating G_t. They fall into two general classes: deterministic and stochastic. The deterministic methods typically involve fitting an *a priori* defined mathematical model of radial growth to the ring-width series, by the method of least squares. Ordinarily, it is assumed that $G_t = f(A_t)$, with $D1_t$ and $D2_t$ absent or negligible. The stochastic methods are more data-adaptive, and often are chosen by *a posteriori* selection criteria. These methods allow for the more general case, $G_t = f(A_t, \delta D1_t, \delta D2_t)$. As will be seen, each class of models has its advantages and disadvantages.

3.3.2. Deterministic methods of growth-trend estimation

The simplest deterministic model is the linear trend model, *viz.*,

$$G_t = b_0 + b_1 t \quad , \tag{3.3}$$

where b_0 is the y-intercept, b_1 is the slope of the fitted linear regression line, and t is time in years from 1 to n. *Figure 3.1(c)* shows a linear trend line fit to a ring-width series. The slope coefficient, b_1, may be constrained to be negative or zero if the *a priori* expectation of G_t requires it. However, as noted earlier, G_t may also be negative exponential in form because of the *geometrical constraint* argument. Therefore, Fritts *et al.* (1969) suggest fitting the modified negative exponential curve of the form

$$G_t = a \exp^{-bt} + k \quad , \tag{3.4}$$

where a, b, and k are coefficients of this nonlinear regression function, all a function of time t. *Figure 3.1(a)* shows an example of this curve fit. Other functions have been used for estimating the age trend of ring-width series, such as the negative exponential curve (Fritts, 1963)

$$G_t = a \exp^{-bt} \quad , \tag{3.5}$$

which is a special case ($k = 0$) of equation (3.4); the hyperbolic function (Eklund, 1954)

$$1/G_t = a + b\,(t - k) \quad , \tag{3.6}$$

where k is the middle year (i.e., $k = n/2$) of the series; the power function (Kuusela and Kilkki, 1963)

$$G_t = at^{-b} \quad , \tag{3.7}$$

the generalized exponential or "Hugershoff" function (Warren, 1980; Bräker, 1981)

$$G_t = at^b \exp^{-gt} \quad ; \tag{3.8}$$

and the Weibull probability density function (Yang *et al.*, 1978)

$$G_t = at^{a-1}b^{-a} \exp[-(t/b)^a] \quad . \tag{3.9}$$

Equations (3.8) and (3.9) are able to fit both the juvenile increase in radial growth and the subsequent exponential decay of ring width as trees mature. These functions are more theoretically complete than the other models, which can only fit the maturation phase of declining radial growth.

These deterministic models produce monotonic or unimodal curves, which clearly require that the observed growth trend be simple in form. However, Warren (1980) made his fitting procedure much more general by allowing the age trend to be modeled as a temporal aggregate of generalized exponential functions. This allowed Warren (1980) to fit a series of suppression-release events in his tree rings. And, except for equations (3.3) and (3.4), all have a limiting value of zero for G_t as t grows large. This property is unsatisfactory for many trees that approach a constant level of ring width in old age, hence the preference for equation (3.4) over equation (3.5) by Fritts *et al.*, (1969) for standardizing semiarid-site, old-age conifers. The deterministic growth-trend models described above are most appropriate for open-canopy stands of undisturbed trees and for young trees with strong juvenile age trends. It is also clear that these models only depend on time t for predictive purposes. Thus, they are deterministic. The last two models [equations (3.8) and (3.9)] have not been widely used in dendrochronology, although their use in forest mensuration to estimate growth increment functions is more common.

Another family of deterministic growth-trend models is found in polynomial detrending (Jonsson and Matern, 1974; Fritts, 1976; Graybill, 1979). This model for G_t has the form

$$G_t = b_0 + b_1 t + b_2 t^2 + \cdots + b_p t^p \quad . \tag{3.10}$$

The linear-trend model is just a special case of this polynomial model. This method of growth-trend estimation is not based on any *a priori* age-trend model. Rather, a best-fit, order-p polynomial, which is initially unknown, is fit to a ring-width series based on the behavior of that series alone. It is far more *ad hoc* and data adaptive than the previous models, although it still maintains its dependence on time alone for predictive purposes. Polynomial detrending of the form above suffers from problems of order selection, potentially severe end-fitting problems, and poor local goodness-of-fit (Cook and Peters, 1981; Briffa, 1984; Cook, 1985). In spite of their wide usage in the past, polynomials of the form of equation (3.10) are not recommended as a general method for detrending ring-width series.

In the rare situations where the age trend is known to have a simple deterministic form based on theoretical considerations, the best approach is to describe that trend with an appropriate mathematical model. This is the most concise and directly communicable way of describing and explaining the character of the age trend. Nevertheless, assuming a mathematical function for describing trends in tree growth may be unnecessarily restrictive. Problems increasingly arise when this approach is used in situations where trends are complex or where it is necessary to remove relatively medium or short time scale variation in tree-ring data during standardization. Functional growth equations are often too simple.

A more basic weakness of the method is that the goodness-of-fit varies with time because of time-dependent stochastic departures from the theoretical model. Thus, noise-related medium-frequency variance may be retained in some parts of the series, yet removed in others. This may introduce spurious medium frequency variations into the standardized series.

Given the inherent limitations and potential problems of deterministic growth-trend models in fitting the low- and middle-frequency stochastic perturbations commonly found in ring-width series (see *Figures 3.1–3.3*), stochastic methods of growth-trend estimation have been investigated. These methods fall within the realms of low-pass digital filtering (Parker, 1971; Cook and Peters, 1981; Briffa *et al.*, 1983), exponential smoothing (Barefoot *et al.*, 1974), and differencing (Box and Jenkins, 1970). These methods will be described next.

3.3.3. Stochastic methods of growth-trend estimation

Low-Pass Digital Filtering

Low-pass digital filtering typically involves passing an odd-numbered set of symmetrical, low-pass filter weights over a ring-width series to produce a smoothed estimate of the actual series. This is accomplished as

$$G_t = \sum_{i=-n}^{+n} w_i R_{t+i} \Big/ \sum_{i=-n}^{+n} w_i \quad , \tag{3.11}$$

where G_t is the tth filtered value and where w_i is the weight by which the value of the series i units removed from t is multiplied. There are $2n+1$ filter weights. Equation (3.11) clearly shows that this digital filter is a centrally weighted moving average of the actual data. The w_i tapers off equally on both sides of the maximum central weight until the outermost weights are arbitrarily close to zero. These weights may be derived from the Gaussian probability distribution function and tailored to have a particular frequency response (Mitchell *et al.*, 1966; Briffa, 1984). Alternately, the cubic-smoothing spline can be used as a symmetrical, low-pass digital filter (Cook and Peters, 1981), without the need to compute explicitly the filter weights.

Symmetrical filters of this type preserve the original phase information of the unfiltered time series in the filtered values. In the past, equally weighted (i.e., $w_i = 1.0$ for all i) moving averages have been advocated for standardizing tree-ring series (e.g., Bitvinskas, 1974). This form of digital filter cannot be recommended under any circumstances because it causes undesirable phase shifts in the smoothed age-trend estimates and distortion in the power spectrum of the resultant standardized tree-ring indices. Fritts (1976) and Briffa (1984) detail the use of digital filters in tree-ring analysis.

The degree of smoothness of the low-pass filter estimates of G_t depends on the characteristic frequency response of the filter. For the Gaussian filter, the response is approximately

$$u(f) = \exp(-2\pi^2 s_G f^2) \quad , \tag{3.12}$$

where s_G equals $L/6$ and L is the length of the filter (Briffa, 1984). For the cubic-smoothing spline (Cook and Peters, 1981), the frequency-response function is computed as

$$u(f) = 1 - \frac{1}{1 + \dfrac{p\,(\cos 2\pi f + 2)}{6\,(\cos 2\pi f - 1)^2}} \quad , \tag{3.13}$$

where p is the Lagrange multiplier that uniquely defines the frequency response of the spline. The 50% frequency-response cutoff, which is the frequency at which 50% of the amplitude of a signal is retained (or removed), is typically used to define the degree of smoothing by a digital filter. For the smoothing spline, it can be defined in terms of p as

$$p = \frac{6(\cos 2\pi f - 1)^2}{\cos 2\pi f + 2} \quad . \tag{3.14}$$

Equations (3.12)–(3.14) assume a sampling interval of one year, which is typical for tree-ring series. *Figure 3.6* shows some characteristic frequency-response functions of the Gaussian filter and smoothing spline. The transition bandwidth

of each filter, which is defined as the bandwidth of frequencies between $u(f) = 0$ and $u(f) = 1$, is rather broad in each case. The response of the spline filter is steeper than that of the Gaussian filter, which means that the latter will leave in slightly more low-frequency variance for a given 50% response cutoff. Although the transition bandwidths in *Figure 3.6* could be criticized for being too broad, they are probably satisfactory for estimating G_t – given the considerable uncertainty in knowing what degree of smoothing to use.

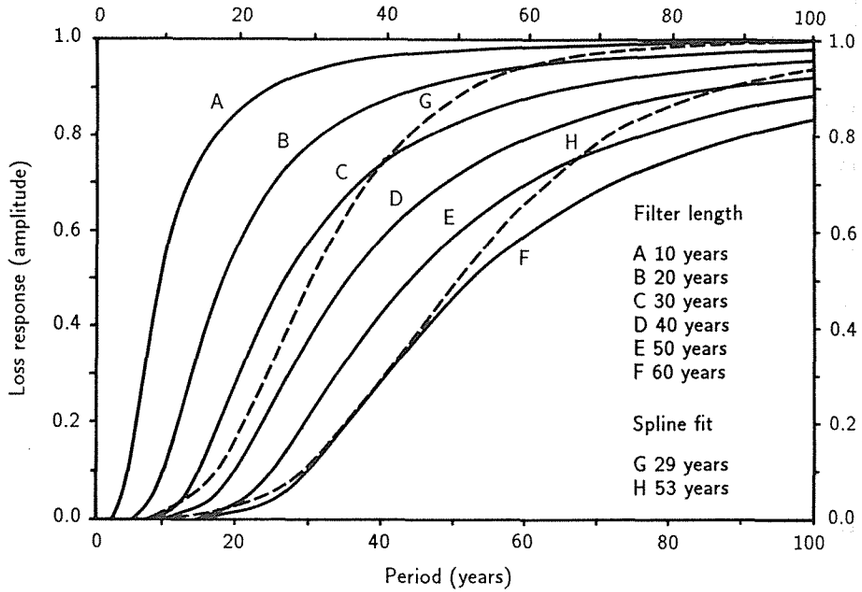

Figure 3.6. Some characteristic frequency-response functions of the Gaussian filter (solid curves) and the cubic-smoothing spline (dashed curves). The 50% frequency-response cutoff in years is given for each filter. (Modified from Briffa, 1984.)

There is often little theoretical basis for selecting the *proper* degree of curve flexibility or data smoothing when using digital filters. For this reason, a chosen digital filter can be rather difficult to justify. Briffa *et al.* (1983) used *a priori* information about stand-management practices in Europe to select the frequency response for their low-pass filter used in estimating G_t. Their selection criterion is based on the concept that the unwanted noise in the ring widths is frequency dependent (Briffa *et al.*, 1986). In this case, it was felt that the noise was largely restricted to wavelengths longer than about 50 years. A similar determination was made by Cook and Peters (1981) and Blasing *et al.* (1983), based on using the cubic-smoothing spline as a digital filter on ring widths from North American trees. However, the filters advocated by these studies may be too flexible for general use.

Given that the frequency dependent properties of the noise (i.e., the band-limited spectral properties of the age trend and stochastic disturbance effects) will be unknown *a priori* in many situations, how might the *appropriate* or *optimal* frequency response be selected objectively? One possible criterion is based on the signal-to-noise ratio (SNR) (Wigley *et al.*, 1984). The SNR is defined as

$$\mathrm{SNR} = N\bar{r}/(1-\bar{r}) \quad , \tag{3.15}$$

where $\bar{r}$ is the average correlation between trees and N is the number of trees in the ensemble of standardized tree-ring indices. SNR is an expression of the strength of the observed common signal among trees in the ensemble. Tuning the frequency response of the digital filter to maximize the SNR would seem to be one optimal and objective criterion. Two examples, in *Table 3.1*, show how the SNR of tree-ring indices can change as the frequency response of a Gaussian filter is tuned to maximize that criterion. In example A, a peak in SNR is indicated for the filter with a 50% frequency response of 40 years. However, for example B, the SNR increases all the way to the minimum 50% frequency response of 10 years. This result indicates that there may not be a clear maximum SNR in the low-to-intermediate frequencies of some tree-ring chronologies, which will make the application of the maximum SNR criterion more difficult. The maximum SNR criterion is also flawed because it assumes, in the derivation of equation (3.15), that the series being cross-correlated is serially random. This means that the SNR is best suited for measuring the strength of the observed high-frequency signal in the tree-ring indices, not the persistent, low-frequency signal that may of interest in the study of climatic change. Thus, the maximum SNR criterion may be biased toward selecting a digital filter that removes an excessive amount of low-frequency variance during standardization.

Table 3.1. The effect of different Gaussian low-pass filters on the fractional common variance ($\bar{r}$) and signal-to-noise ratio (SNR) of an ensemble of standardized tree-ring indices (Briffa, 1984). The tree-ring data are from oak sites in the United Kingdom. The 50% frequency response of each filter is given in years. Each analysis is based on 14 trees for the time period 1880–1979.

Example A			*Example B*		
Filter length	$\bar{r} \times 100$	*SNR*	*Filter length*	$\bar{r} \times 100$	*SNR*
10 years	30.09	6.03	10 years	46.54	20.03[a]
20 years	30.90	6.26	20 years	41.93	16.61
30 years	32.08	6.61	30 years	39.18	14.81
40 years	32.83	6.84[a]	40 years	38.06	14.14
50 years	32.77	6.83	50 years	37.53	13.82
60 years	32.42	6.72	60 years	36.94	13.47

[a]Denotes the maximum $\bar{r}$ and SNR.

Blasing *et al.* (1983) examined another objective criterion for choosing the optimum filter response of the smoothing spline. They selected a filter for standardization that produced the best tree-ring chronology for dendroclimatic reconstruction. In their example, Blasing *et al.* (1983) reconstructed total annual precipitation for Iowa from white oak (*Quercus alba*) tree-ring chronologies standardized with splines of differing frequency response. They determined the optimum frequency response from the chronology, which produced the reconstruction that verified best against independent data. In this case, the optimum spline had a 50% frequency response of about 50 years, a value similar to example A in *Table 3.1.* It is not clear whether this technique will be widely applicable, however, because it depends on having long, homogeneous climatic records for reconstruction and verification. This will not be the case for many regions of the world where tree-ring analysis can be done. In addition, this optimization rule depends on having tree-ring data that can strongly model the climatic data. This may not be the case in many mesic forest environments where climate has a weaker and less-direct impact on tree growth than was the case for the Iowa oaks.

Another possible criterion for objectively selecting an optimal digital filter for standardization is related to the concept of "trend in mean" (Granger, 1966). From the theory of spectral analysis (Jenkins and Watts, 1968), the lowest-frequency harmonic that can be be theoretically resolved in a time series has a frequency $f = 1/n$, where n is the length of the series. This is the fundamental frequency of the process (Jenkins and Watts, 1968). The fundamental frequency corresponds to one complete sine wave with a cycle length of n years. According to the definition of trend in mean, any variance at wavelengths longer than the observed time series ($f < 1/n$) cannot be differentiated from pure trend ($f = 0.0$), unless strong *a priori* information on climatic variability and the properties of the ring-width data allow for it. For example, if it is known that the sampled trees are temperature sensitive and that the trend in temperature for the recent past has been positive for the region where the trees were sampled, then any positive trend in ring width may be related to the positive trend in temperature. In this case, ring-width series with positive trends should be standardized with deterministic curves that are constrained to be non-positive in trend. Obviously, care must be taken to ensure that the observed positive trend in ring width is not due to non-climatic effects, such as a release from competition. However, for the majority of cases, trend in mean can be used as the basic definition of the theoretical resolvable limit of climatic information in tree-ring chronologies.

Given the above definition of trend in mean, another objective criterion for selecting the optimal frequency response of a digital filter is as follows. Select a 50% frequency-response cutoff in years for the filter that equals some large percentage of the series length, n. This is the $\%n$ criterion described in Cook (1985). The results of Cook (1985) suggest that the percentage is 67%n to 75%n based on using the cubic-smoothing spline as a digital filter. The $\%n$ criterion ensures that little low-frequency variance, which is resolvable in the standardized tree rings, will be lost in estimating and removing the growth trend. This criterion also has a bias of sorts because of the stiff character of the low-pass filter estimates of the growth trend. It will not necessarily guarantee and, in fact, will

rarely possess any kind of optimal goodness-of-fit. Thus, the SNR of an ensemble of tree-ring indices standardized by the $\%n$ criterion will usually be inferior to those standardized by the maximum SNR criterion. The SNR of $\%n$ standardized indices can, of course, be increased by adding additional trees to the ensemble. Additional increases in SNR are also possible by prewhitening the detrended indices as autoregressive processes and by using a robust mean in estimating the mean-value function (Cook, 1985). The last two approaches will be described in Sections 3.4.2 and 3.4.3. Either way, the drawback of lower SNR for the $\%n$ method can be ameliorated.

Figure 3.7 compares cubic-smoothing spline estimates of G_t for three red spruce ring-width series using a 67%n criterion (solid line) and a fixed, 50% frequency-response cutoff of 60 years (dashed line). The 60-year cutoff is not the exact maximum SNR criterion, but it is much closer to it than the 67%n curves. The differences in the curve fits are readily apparent. The 67%n criterion does a poor job in tracking medium-frequency (10–30 years) fluctuations within each series that sometimes disagree with contemporaneous fluctuations in the other series. Examples of this lack of synchrony are found in the 1850s and 1950s of series (*b*). If signal is defined as information in the tree rings that is common to all trees in the ensemble, then the 67%n criterion does not eliminate noise as well as the 60-year cutoff. On the basis of noise reduction performance alone, the adequacy of the 67%n criterion will usually depend more on sufficient replication to average out endogenous-style growth fluctuations and on additional noise reduction techniques such as robust mean estimation and autoregressive modeling. All of these noise reduction techniques assume that common, exogenous non-climatic variance ($D2_t$) is not present in the ensemble. If $D2_t$ variance is known to be present either *a priori* or by strong inference, then more flexible filters may be necessary to remove that component.

The $\%n$ and maximum SNR criteria represent two reasonable and objective limits for selecting the frequency response of the digital filter and, therefore, the degree of flexibility of the resultant low-pass filter estimates of the age trend. If high-frequency information is of sole interest in a tree-ring chronology, then the latter criterion will probably be preferred if other noise reduction techniques, such as autoregressive modeling, are not used. However, if tree-ring series are to be used to study climatic and environmental change at virtually all resolvable wavelengths in a tree-ring chronology, then the $\%n$ criterion should be considered as a criterion of smoothness for the digital filter.

Although digital filtering, as described above, is attractive for estimating the non-climatic growth trend in ring-width series, a theoretical drawback of this method should be noted. The symmetry of the filter weights in equation (3.11) requires both past and future ring widths to estimate the central smoothed value for each year. This model for low-frequency changes in ring width is obviously incorrect because trees cannot possibly anticipate radial growth performance of future years in developing an expectation for ring width for the current year. The predisposition to grow at a certain potential rate must come only from the past. This means that one-sided or causal filters (Robinson and Treital, 1980) of the general form

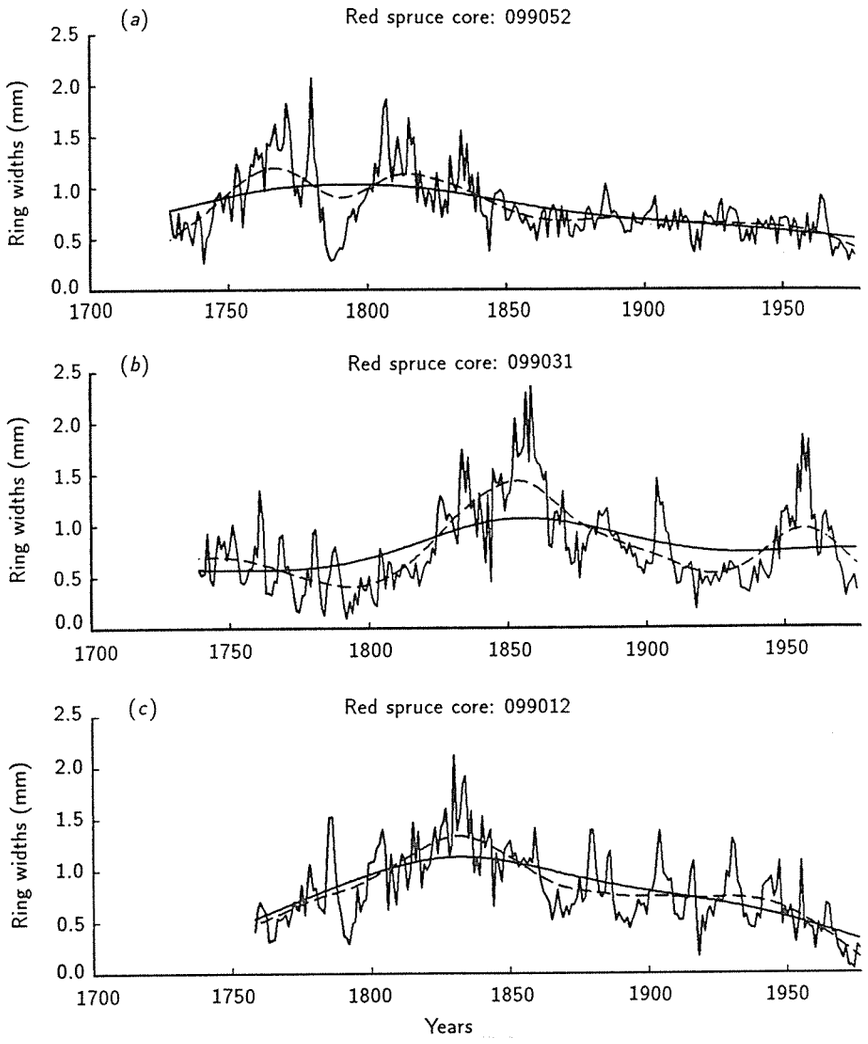

Figure 3.7. A comparison of two selections of smoothing ring-width data using the cubic-smoothing spline. The solid lines indicate spline values based on a 50% frequency-response cutoff of 67%n, where n is the series length in years. The dashed lines indicate splines with fixed 50% frequency-response cutoffs of 60 years. The more flexible curve fit is clearly superior on an individual series basis. However, with sufficient replication and the use of other noise reduction techniques, the %n criterion may be used if the need to preserve potentially resolvable long-term climatic variance is important.

$$Z_t = \sum_{i=1}^{-\infty} \Psi_i e_{t-i} + e_t \tag{3.16}$$

are more appropriate for modeling certain aspects of the persistence or predictability in ring width from year to year. Equation (3.16) is the general linear process, which serves as the foundation for autoregressive-moving average (ARMA) time series modeling (Box and Jenkins, 1970). The general linear process and its finite ARMA derivatives are causal filters because only current and past information is necessary for the evolution of the observed process. The use of ARMA models in tree-ring chronology development will be described more fully, later.

Exponential Smoothing

A quite different stochastic estimate of G_t is possible by using exponential smoothing (Barefoot *et al.*, 1974). The smoothing function chosen by Barefoot *et al.* (1974) consists of two components: an average, $\bar{R}_t$, and a lag correction for trend, $\tilde{R}_t$. This is expressed as

$$G_t = \alpha \bar{R}_t + (1 - \alpha)\, \alpha \tilde{R}_t \quad , \tag{3.17a}$$

where G_t is the smoothed estimate for year t,

$$\bar{R}_t = \alpha\,(R_t - 1) + (1 - \alpha)\,(\bar{R}_{t-1}) \quad , \tag{3.17b}$$

and

$$\tilde{R}_t = \alpha\,(R_t - R_{t-1}) + [(1 - \alpha)/\alpha]\,(\tilde{R}_{t-1}) \quad . \tag{3.17c}$$

The quantity α is a weighting factor that determines the degree of smoothing or how much past information on ring width enters into the current estimate. The influence of past ring widths decays exponentially as $(1 - \alpha)^n$, where n is the number of years prior to the current estimate. Barefoot *et al.* (1974) selected $\alpha = 0.2$ to smooth their ring widths, which allows the previous 10–15 years of data to influence the current estimate of G_t. In contrast to the symmetrical digital filter, exponential smoothing operates as a one-sided, causal filter (Robinson and Treital, 1980) that only relies on current and prior values in its estimation. As noted earlier, this is a desirable property in that the estimates of G_t evolve through time in the same way that trees grow. However, the selection of α may be series dependent and difficult to select. In this sense, it has the same problem as digital filtering.

Abraham and Ledolter (1983) review exponential smoothing techniques and suggest selecting an α that minimizes the one-step ahead prediction error variance. This criterion for α, if adequate, will produce a series of random residuals from the smoothing function. Except in rare cases where a serially random tree-ring series is of interest, an α based on minimizing the prediction mean-square error will remove too much low-frequency variance for climatic studies. The one-sided form of equation (3.17a) is conceptually appealing, but additional research is needed on developing objective guidelines for choosing the smoothing constant for tree-ring standardization.

Differencing

Another method of stochastic detrending is based on differencing (Box and Jenkins, 1970; Van Deusen, 1987). In this approach, a ring-width series is considered to be a random walk with deterministic drift. This process has the form

$$R_t = R_{t-1} + e_t + \delta \quad , \tag{3.18}$$

where R_t is the observed ring width, e_t is a serially uncorrelated random shock, and δ is the deterministic drift of the process that may also be thought of as a constant slope parameter. By taking first differences of R_t (usually after logarithmic transformation) as

$$\nabla R_t = R_t - R_{t-1} \quad , \tag{3.19}$$

the deterministic drift, which imparts linear trend to the R_t, is nothing more than the arithmetic mean of ∇R_t. However, the trend that is removed by differencing is actually stochastic, rather than deterministic. This is easily seen by noting that the conditional expectation of R_t given R_{t-1}, $R_{t-2}, \ldots$ is $E(R_t) = R_{t-1} + \delta$. Since R_{t-1} is subject to random shocks in the form of e_t, the deterministic trend component of $E(R_t)$ is also subjected to random shocks. Thus, the trend changes stochastically.

The advantage of differencing lies in its simplicity, causal structure, and total objectivity. There are no parameters to estimate, and the method is insensitive to ring widths more than one year apart. The latter property makes differencing especially attractive when old tree-ring collections are updated. The addition of new rings to each series will have no effect on the way that the detrended tree rings are produced. In this sense, differencing is locally robust as a detrending method when new data are added, which is not the case for deterministic least squares methods of detrending.

The disadvantage of differencing is the way in which the method acts as a high-pass filter. Virtually all low-frequency variance is attenuated and the high, year-to-year variance is emphasized. This property follows from the notion that the differenced series is nothing more than a numerical estimate of the 1st-

derivative of the process (Van Deusen, 1987). Thus, each differenced value is the relative rate of change in ring width from one year to the next. The severe attenuation of low-frequency variance in the first differences means that the resultant tree-ring chronology will not exhibit the year-to-year persistence commonly seen both in climate (Gilman *et al.*, 1963; Mitchell *et al.*, 1966) and in tree rings standardized by other detrending methods (Rose, 1983; Monserud, 1986). This deficiency can be ameliorated through the use of ARMA time series modeling techniques, which are described in the next section.

Differencing has only recently been applied to the problem of tree-ring detrending and standardization (Van Deusen, 1987; Guiot, 1987a). Because of this and its importance in autoregressive-integrated moving average (ARIMA) time series modeling (Box and Jenkins, 1970), it deserves additional research and testing.

3.3.4. Other methods of estimating growth trends

Other techniques can be used for estimating growth trends that do not clearly fit into the simple categories of techniques just described.

Graphic techniques. In the precomputer era of dendrochronology, growth trends were frequently estimated visually using flexible rulers (Schulman, 1956; Stokes and Smiley, 1968). Although this method has an inherently subjective aspect to it, it can be applied with a high degree of uniformity by experienced individuals when the growth trend is simple in form (i.e., negative exponential and linear). However, with the availability of digital computers and programs for estimating satisfactory growth trends, this method is rarely applied today.

Stand-level growth trends based on the biological age of trees. Another method of growth-trend estimation has been described by Erlandsson (1936), Mitchell (1967), and Komin (1987). It is based on collecting ring-width material from a large range of age classes of a given tree species. The ring-width measurements of each sample are aligned with those of the other samples according to the biological age of the rings, not the chronological age. For example, year five of a 200-year-old tree is aligned with year five of a 50-year-old tree by this method. Once the biological age alignment is done, the ring widths of all samples are averaged together to produce a tree-based, average biological growth trend. The averaging process greatly attenuates the yearly fluctuations in ring width due to environmental factors because of the chronological misalignment of the tree rings. Consequently, the underlying growth curve is emphasized. The degree to which the environmental effects are attenuated will depend on the sample size for each year, the distribution of tree ages in the collection, and the level of randomness through time of the environmental factors. The estimation of the mean growth curve also assumes that the structural form of the curve at any biological age is independent of the time period during which it is produced. There seems to be little room for endogenous and exogenous disturbance effects in this model.

Once the mean growth curve is estimated, a smooth mathematical function is fit to the curve and used to standardize the individual series from the site (Mitchell, 1967; Komin, 1987). Fritts (1976, page 280) points out that this method is flawed as a technique of tree-ring standardization. He notes:

> All individuals of a species rarely attain optimum growth at the same age, and individual trees differ in their growth rates because of differences in soil factors, competition, microclimate, and other factors governing the productivity of the site. Therefore, individual trees will deviate markedly and systematically from the mean growth curve.

These reasons are sufficient to reject the method as a standardizing tool for dendroclimatic studies. However, where the signal of interest is the variance within each series that deviates from the mean growth curve of the stand, this method is appropriate.

The corridor method. Shiyatov (1987) describes another approach to standardization called the corridor method. It is based on the construction of a maximum possible growth curve and a minimum possible growth curve for each ring-width series. These two curves form a growth corridor within which the range in ring-width variability fluctuates. *Figures 3.8(a)*, *3.8(c)*, and *3.8(e)* illustrate some common forms of the corridor, which is usually constrained to evolve smoothly through time. The maximum growth curve is based on a few ring widths that define the local maxima in the ring-width series. Typically, it displays the most pronounced growth trend and is usually constrained to have only one peak (Shiyatov and Mazepa, 1987). The minimum growth curve is based on a few ring widths that define the local minima in the series. It tends to have a less pronounced growth trend and may be constrained to repeat the bends of the maximum curve (Shiyatov and Mazepa, 1987). Where the ring widths get very small or when there is a high frequency of locally absent rings, the minimum curve approaches or equals zero [e.g., *Figures 3.8 (a)* and *3.8(c)*].

The tree-ring indices are calculated from the corridor estimates as

$$I_t = \frac{R_t - G1_t}{G2_t - G1_t} * 100\ (200) \quad , \tag{3.20}$$

where I_t is the index, R_t is the ring width, $G1_t$ is the minimum growth-curve estimate, and $G2_t$ is the maximum growth-curve estimate, all for year t. The 100 (200) are scaling factors that transform the index into either percentages (* 100) of the corridor width or 2 × percentages (* 200).

A comparison of equation (3.20) with the more commonly used formula for computing indices, equation (3.1) reveals the difference in the techniques. The indices computed from equation (3.1) are (effectively) percentage departures from an expectation of growth (G_t). This is equivalent to using a time-dependent mean for standardizing ring widths. In contrast, indices computed from equation (3.20) are (effectively) percentages of the corridor width ($G2_t$ −

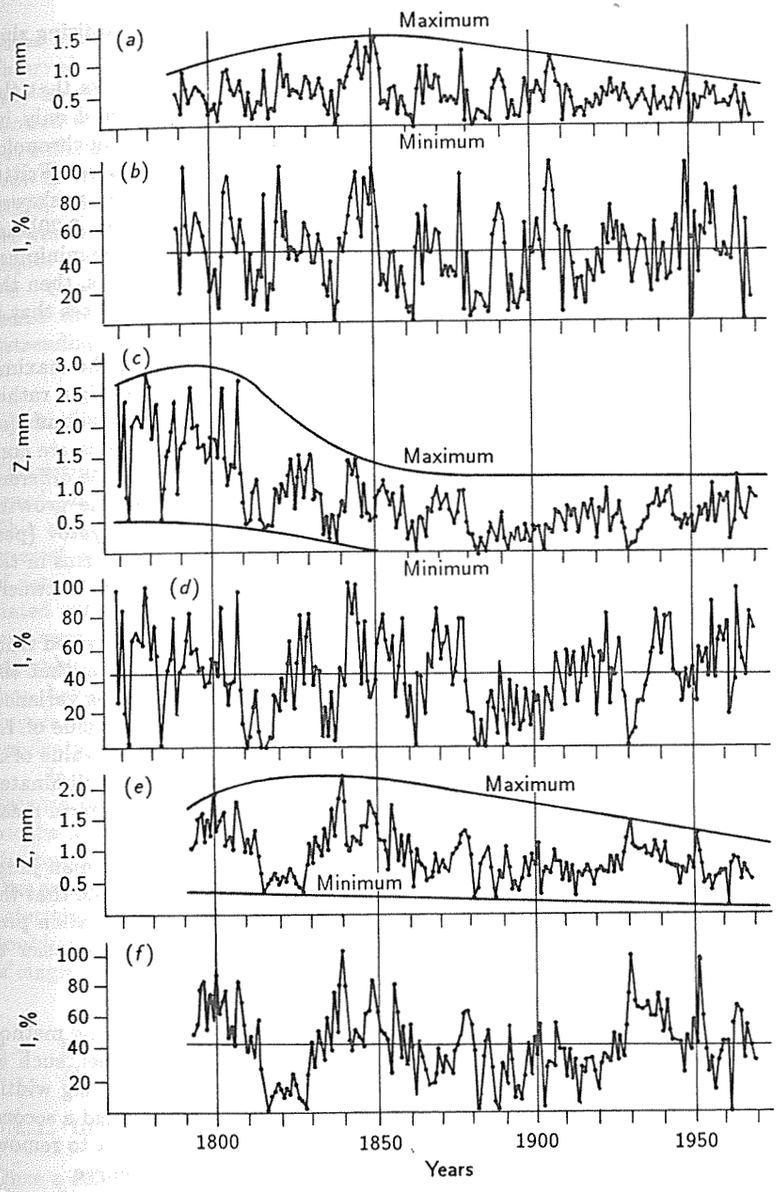

Figure 3.8. Examples of the *corridor* method of tree-ring standardization. The curves of maximum and minimum possible growth, which define the corridor, are shown for three Siberian larch (*Larix sibirica*) ring-width series [(*a*), (*c*), and (*e*)]. The standardized tree-ring indices derived from their respective corridors and equation (3.20) in the text are shown [(*b*), (*d*), and (*f*)].

$G1_t$), which is equivalent to using a time-dependent range for standardizing ring widths.

Whether one selects the mean or the range may affect the limits that the resultant indices take. Indices computed by equation (3.1) are bound only by zero and have an unbound maximum. Although standardized tree-ring chronologies developed from equation (3.1) are usually normally distributed (Fritts, 1976), the lower bound means that the potential exists for a truncated or skewed probability distribution. In contrast, indices computed by equation (3.20) are bound by both the minimum and the maximum growth curves. If the minimum and maximum curves pass through an excessive number of ring widths, then the possibility exists for creating a probability distribution function of indices that is truncated at either or both ends of the distribution.

The corridor method also assumes that the time variations in the maxima and minima, which define the corridor, are principally biological in origin rather than climatic. This assumption follows from the way that the maximum (or minimum) values in the early and later segments of a ring-width series are constrained to be identical in indexed form, even though they may be quite different in absolute ring width. This constraint implicitly assumes that the growth-limiting factors owing to climate were identical for those years. Shiyatov (personal communication) notes that these issues are not likely to be problems in the mean-value function of corridor-indexed series because of the inherent between-tree variability of the ring widths used to define the corridors.

Figures 3.8(b), *3.8(c)*, and *3.8(f)* show the resultant indices computed from the estimated corridors in *Figure 3.8* and equation (3.20). It is clear that the technique produces indices having a stationary mean and homogeneous variance. Unlike indices computed from equation (3.1) that have an expected value of 1.0 or 100%, indices computed by the corridor method have an expected value of .5 or 50%. Shiyatov and Mazepa (1987) note that this difference can be eliminated simply by re-standardizing each corridor-indexed series using its long-term mean and equation (3.1).

The corridors shown in *Figure 3.8* were drawn by hand and human judgment using a flexible ruler. However, Shiyatov and Mazepa (1987) note that the technique can also be solved mathematically. They describe an estimation procedure that should make the corridor method more objective and far easier to implement as a standardization option.

Double-detrending. Holmes *et al.* (1986) describe a two-stage detrending method that they call *double-detrending.* A deterministic growth-trend model, such as the negative exponential curve, first estimates the observed trend in ring width. The tree-ring indices are computed from this curve and then detrended a second time using a cubic-smoothing spline. The second detrending is meant to remove any residual growth trend that is not modeled by the deterministic curve.

Holmes *et al.* (1986) justified double-detrending by illustrating that the negative exponential curve can fit the highly variable, steeply descending juvenile portion of the ring-width trend better than the less variable, flatter portion associated with maturity and old age. This is a consequence of least squares fitting, which can be dominated by the high-variance, juvenile portion of ring-width

series and of the inadequacy of the negative exponential curve as a model for the observed growth trend. In such cases, the outer portion of a ring-width series may be systematically underfit or overfit for decades. Holmes *et al.* (1986) also showed that a stiff spline fit alone to the same series by the 67%n criterion was not sufficiently flexible to track the sharp curvature of the juvenile portion of the growth trend, even though it was quite adequate for the mature phase of the trend. Since each method of detrending was better for different portions of the growth trend, Holmes *et al.* (1986) reasoned that the sequential use of both techniques would correct the deficiencies of each method.

Cook (1985) examined the spectral properties of double-detrending and found that linear or negative exponential detrending followed by 67%n spline detrending worked well without removing too much low-frequency variance.

3.3.5. Concluding remarks on growth-trend estimation

The estimation and removal of growth trends from tree-ring series should be based, as much as possible, on the intended application of the tree-ring data. This means that there should be an *a priori* expectation of what the signal of interest is in the ring-width measurements. Given this expectation, the method of detrending should be chosen that will reduce the low-frequency noise not associated with that signal. It is difficult to accomplish this task within an objective framework because of the uncertainty distinguishing signal from noise in a given ensemble of ring-width data. Inevitably, some assumptions must be made that may have a great effect on the final standardized tree-ring chronology. It is imperative that these assumptions are carefully considered and justified in any application of standardized tree rings.

In general, stochastic methods are preferable to deterministic methods because of the freedom that the former possess in fitting the behavior of ring widths as they are observed, not as theory would have them behave. However, the consequence of this added flexibility are the problems of *ad hoc* model selection and overfitting, which are more likely to occur for stochastic models than for deterministic models. There also seems to be some utility in using a hybrid double-detrending approach, which can compensate for local lack-of-fit problems of single detrending methods.

3.4. Estimation of the Mean Chronology

E. Cook, S. Shiyatov, and V. Mazepa

3.4.1. Introduction

Once a collection of ring-width series has been detrended and indexed into a new ensemble of tree-ring indices, the estimation of the common signal, C_t, can proceed. As mentioned earlier, tree-ring indices can be treated as stationary, stochastic processes that allow them to be treated as a collective ensemble of realizations containing both a common signal in the form of C_t (and perhaps $D2_t$) and individual signals unique to the series ($D1_t$ and E_t).

3.4.2. Methods of computing the mean-value function

Three methods will be described that have been used in tree-ring studies: the arithmetic mean, the biweight robust mean that discounts outliers, and a mean based on testing for a mixture of normal distributions in the sample.

The Arithmetic Mean

The classical method of estimating C_t is by averaging the ensemble of detrended tree-ring indices across series for each year using the arithmetic mean (Fritts, 1976). This produces a time series mean-value function that concentrates the signal (C_t) and averages out the noise ($D1_t$ and E_t). The arithmetic mean of m indices available in year t is computed as

$$\bar{\mathrm{I}}_t = \sum_{j=1}^{m} I_t/m \quad . \tag{3.21}$$

This is an estimate of the signal in the tree-ring indices for year t. The variance or spread of the frequency distribution of m indices about the mean is computed as

$$\mathrm{S}_t^2 = \sum_{j=1}^{m} (I_t - \bar{\mathrm{I}}_t)^2/(m-1) \quad . \tag{3.22}$$

The square root of S_t^2 is the standard deviation of m indices for year t. And, the variance of the mean, which is a measure of the noise or uncertainty in the estimation of the mean, is computed as

$$\mathrm{S}_{\bar{\mathrm{I}}}{}^2 = \mathrm{S}_t^2/m \quad . \tag{3.23}$$

The square root of equation (3.23) is the standard error of the mean. These statistics are described in virtually all basic statistics textbooks and in Fritts (1976). A measure of the strength of the resultant estimate of C_t is the signal-to-noise ratio (SNR) (Wigley *et al.*, 1984; Briffa *et al.*, 1987), an estimate of which is given in equation (3.15). The SNR can only provide information about the quality of the observed signal, but says nothing about its relationship to the expected signal, which is not known at this stage (Briffa *et al.*, 1987).

The Biweight Robust Mean

Other more involved methods are available for computing the mean-value function. If there are suspected outliers, or extreme values, in the tree-ring indices, than a robust mean such as the biweight mean (Mosteller and Tukey, 1977) can

be used in place of the arithmetic mean. When outliers are present, the arithmetic mean is no longer a minimum variance estimate of the population mean, and it is not guaranteed to be unbiased. In contrast, robust means automatically discount the influence of outliers in the computation of the mean and, thus, reduce the variance and bias caused by the outliers. The use of a robust mean tacitly admits the likelihood of contamination by endogenous disturbance effects and other sources of noise having long-tailed, not normally distributed properties. Endogenous disturbance effects are likely to act as outliers because, as defined earlier, endogenous disturbances tend to behave as random events in space and time. The biweight mean for year t is computed by iteration as

$$\bar{\mathrm{I}}_t^{\,*} = \sum_{j=1}^{m} w_t I_t \quad , \tag{3.24}$$

where

$$w_t = \left[1 - \left(\frac{I_t - \bar{\mathrm{I}}_t^{\,*}}{c\mathrm{S}_t^{\,*}}\right)^2\right]^2 \quad ,$$

when

$$\left(\frac{I_t - \bar{\mathrm{I}}_t^{\,*}}{c\mathrm{S}_t^{\,*}}\right)^2 < 1 \quad ,$$

otherwise 0. The weight function, w_t, is symmetric, and, therefore, unbiased in its estimation of central tendency when the data are symmetrically distributed (Cook, 1985). $\mathrm{S}_t^{\,*}$ is a robust measure of the standard deviation of the frequency distribution, which will be the median absolute deviation (MAD)

$$\mathrm{S}_t^{\,*} = \text{median}\,\{|I_t - \bar{\mathrm{I}}_t^{\,*}|\} \quad , \tag{3.25}$$

and c is a constant, often taken as six or nine (Mosteller and Tukey, 1977). The constant c determines the point at which a discordant value is given a weight of zero. When this is the case, the outlier is totally discounted in computing the mean and, thus, has no influence on the estimation of the mean index. A constant c equal to 9 was used by Cook (1985) in developing a new tree-ring standardization procedure. From Mosteller and Tukey (1977), c equal to 9 is equivalent to totally rejecting any value exceeding ± 6 standard deviations from the mean, as estimated by equations (3.25) and (3.24), respectively. To start the iteration for computing the final $\bar{\mathrm{I}}_t^{\,*}$, the arithmetic mean or median can be used as an initial estimate. Ordinarily, only three to four iterations are needed to

converge on an estimate of $\bar{I}_t^*$ that does not change by more than 10^{-3}. A robust estimate of the variance, analogous to equation (3.22), is also available for the biweight mean as

$$mS_t^{*2} = \frac{m\Sigma'(I_t - \bar{I}_t^*)^2(1-u_t^2)^4}{[\Sigma'(1-u_t^2)(1-5u_t^2)][-1+\Sigma'(1-u_t^2)(1-5u_t^2)]} \quad , \qquad (3.26)$$

where $u_t = (I_t - \bar{I}_t^*) \; / \; 9(\text{MAD})$ and Σ' indicates summation for $u_t^2 \leq 1$, only (Mosteller and Tukey, 1977). Similarly, a robust estimate of the variance of the biweight mean, analogous to equation (3.23), is also available as

$$S_{\bar{I}_t}^{*2} = \frac{\Sigma'(I_t - \bar{I}_t^*)^2(1-u_t^2)^4}{[\Sigma'(1-u_t^2)(1-5u_t^2)][-1+\Sigma'(1-u_t^2)(1-5u_t^2)]} \quad , \qquad (3.27)$$

where u_t and Σ' are defined as above.

Aside from its added computational complexity, the biweight mean has a potential cost or premium associated with it. When the sample of indices is devoid of outliers and approximates a Gaussian distribution, the variance of the biweight mean will be greater than that of the arithmetic mean. That is,

$$S_{\bar{I}_t}^{*2} > S_{\bar{I}_t}^{2} \quad .$$

This means that the biweight mean is less efficient in estimating the common signal when the assumed presence of outliers is false. However, when outliers are present in the sample, the variance of the biweight mean will be less than that of the arithmetic mean. That is,

$$S_{\bar{I}_t}^{*2} < S_{\bar{I}_t}^{2} \quad .$$

In this case, the biweight mean is more efficient at estimating the common signal. A measure of statistical efficiency of the biweight mean relative to the arithmetic mean is (Mosteller and Tukey, 1977)

$$\text{Efficiency} = S_{\bar{I}_t}^{2} \; / \; S_{\bar{I}_t}^{*2} \quad , \qquad (3.28)$$

which is the ratio of the lowest variance feasible, under the Gaussian assumption, to the actual variance of the biweight mean. Under the Gaussian assumption and for moderate to large sample sizes (say $m > 10$), the efficiency of the biweight mean exceeds 90% of the arithmetic mean. This is a small premium to pay for protection from outliers and is very difficult to see in practice. When the

sample size drops below 6, the simpler median can replace the biweight as the robust mean (Cook, 1985).

Extensive use of the biweight mean on closed-canopy forest tree-ring data (Cook, 1985) revealed that approximately 45% of the yearly means of 66 tree-ring chronologies showed some reduction in error variance using the biweight mean. This resulted in an average error variance reduction of about 20% in the robust mean-value functions compared with those based on the arithmetic mean. These results reveal the high level of outlier contamination in closed-canopy forest tree-ring data that can corrupt the estimated common signal if left unattended.

Mean-Values from a Mixture of Normal Distributions

Shiyatov and Mazepa (1987) and Mazepa (1982) describe another method of computing the mean-value function, which is based on examining the frequency distribution of the individual indices for each year. If the distribution is symmetrical and unimodal, the arithmetic mean is computed. However, if the distribution appears to be bimodal or multimodal, then the distribution is tested for a mixture of normal distributions. If mixed normal distributions are detected in the sample, then the mode of the grouping of largest indices is used as the best estimate of central tendency for that year. The selection of the grouping of largest indices is based on the notion that non-climatic effects, such as fruiting, will cause the ring widths of the affected trees to be narrower than the ring widths of the unaffected trees for the same years (Danilov, 1953; Kolischuk *et al.*, 1975). Therefore, the grouping of largest indices should more faithfully record the influence of climate.

In addition, the Law of Limiting Factors suggests that these anomalous effects are more likely to be seen when climate is less limiting to growth in a given year. That is, any expression of bimodality or multimodality in the sample distribution of tree-ring indices in a given year is more likely to be found when growth is not severely limited by climate. *Figure 3.9* shows six frequency histograms of tree-ring indices derived from Siberian larch (*Larix sibirica*) growing in the Ural Mountains, USSR. Four of the six examples show a clear indication of bimodality or multimodality, which tends to increase as the mean increases. The dispersion of the histograms increases as the mean level increases. This reflects the typical positive correlation between the means and standard deviations of tree-ring indices, which has been described by Fritts (1976).

Figure 3.10 provides an illustration of the proposed technique of Shiyatov and Mazepa (1987). Because of the limited sample size for each year (usually < 30), Shiyatov and Mazepa (1987) restricted the test for mixtures of normal distributions to two distributions. The authors than tested four different tree-ring chronologies for climatic signal enhancement by modeling the climatic signal in each chronology after estimation by their new method and by the arithmetic mean alone. The percentage of years in which skewness or multimodality was indicated was approximately 25%. Shiyatov and Mazepa (1987) found a statistically significant ($\alpha = .15$) increase in the strength of the modeled climatic signal in three of the four chronologies developed by their procedure. This encouraging

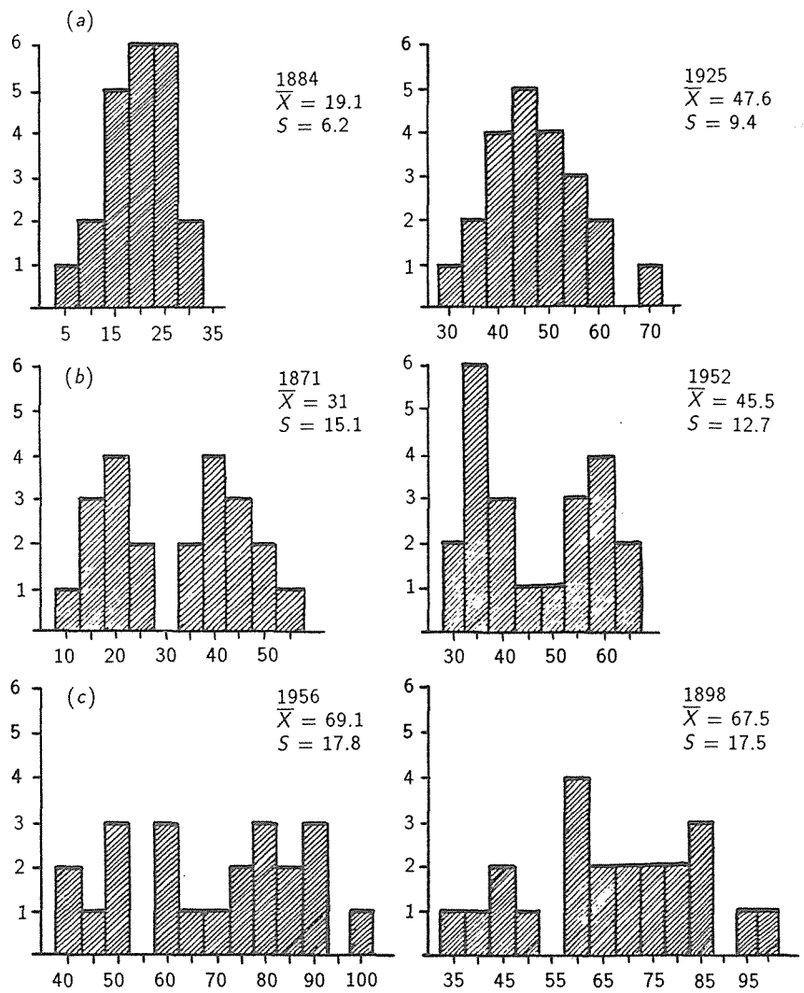

Figure 3.9. Some characteristic frequency distributions of *Larix sibirica* tree-ring indices for separate years. Note the clearly bimodal distributions in *3.9(b)* and the more multimodal forms in *3.9(c)*. $\overline{X}$ is the arithmetic mean, and S is the standard deviation for each distribution.

result is probably conservative because it is based on using all years, not just those years in which a mixture of normal distributions was detected.

As noted by Shiyatov and Mazepa (1987), their method has not yet dealt with the problem of serial dependence between the yearly sample distributions of indices and how it may affect any mixtures of normal distributions in each

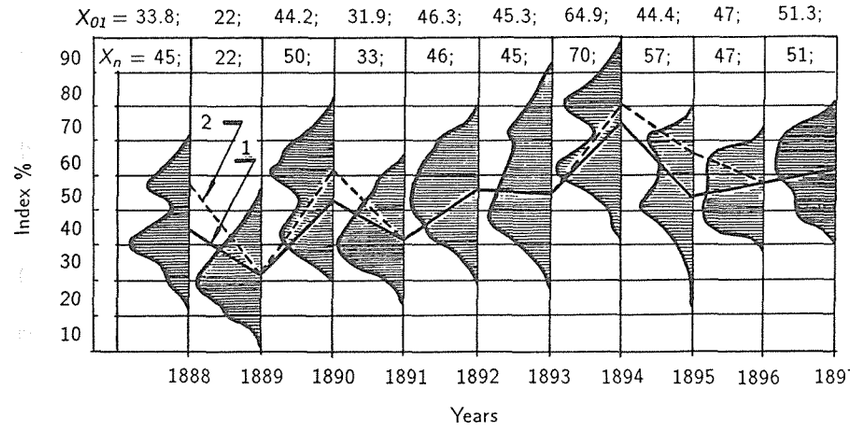

Figure 3.10. An illustration of the method of computing the mean-value function based on modeling the distributions of sample indices as mixtures of normal distributions. The mean-value function is computed using the arithmetic mean of all samples (1); the mean-value function is computed by testing for the presence of a mixture of normal distributions and adjusting the estimate of the mean, accordingly (2). (From Shiyatov and Mazepa, 1987.)

sample. Therefore, further research is needed before the method can be routinely used for estimating mean-value functions. There is almost certainly some overlap between the expected performance of the biweight robust mean and the method of Shiyatov and Mazepa (1987). This performance overlap is likely when the frequency distribution is principally skewed or long-tailed, rather than bimodal or multimodal. When the former condition is present, either method may provide outlier-resistant measures of central tendency. However, when the latter condition occurs, the biweight mean will iterate toward the mode of highest frequency or to a compromise position between balanced modes, without regard to biological considerations. In this case, the performance of the two techniques will diverge.

3.4.3. The use of autoregressive-moving average models in estimating the common signal

The computation of the mean-value function, by any of the above methods, is easily done with the tree-ring indices. However, if the autocorrelation within each series is high, then a more statistically efficient estimate of the mean-value function (i.e., a higher SNR) is possible, in many cases, through the use of time series modeling and prewhitening techniques. Tree-ring series have an autocorrelation structure that allows the estimation of C_t to be broken down into a

two-stage procedure (Cook, 1985; Guiot, 1987a), based on ARMA time series modeling (Box and Jenkins, 1970).

Tree-ring indices can be expressed, in difference equation form, as an ARMA process of order p and q, *viz.*,

$$I_t = \phi_p I_{t-p} + \cdots + \phi_1 I_{t-1} + e_t - \theta_1 e_{t-1} - \cdots - \theta_q e_{t-q} \quad , \tag{3.29}$$

where the values for e_t are serially random inputs or shocks that drive the tree-growth system as reflected in the tree rings, the ϕ_i values are the p autoregressive (AR) coefficients, and the θ_i values are the q moving average (MA) coefficients that produce the characteristic persistence or memory seen in the I_t. Equation (3.29) can be economically re-expressed in polynomial form using the backshift operator, B, as

$$I_t = [\theta(B)/\phi(B)]\, e_t \quad , \tag{3.30}$$

where

$$\phi(B) = 1 - \phi_1 B - \cdots - \phi_p B^p$$

and

$$\theta(B) = 1 - \theta_1 B - \cdots - \theta_q B^q$$

(Box and Jenkins, 1970). On an individual series basis, the values for e_t are assumed to be composed of inputs owing to climate (C_t) and those owing to disturbances and random variability ($D1_t$ and E_t). Component A_t is assumed to be nonexistent either in the raw ring-width series in total or for certain periods (Guiot, 1987a) (i.e., $I_t = R_t$), or to have been removed by detrending or differencing. Extensive ARMA modeling of tree-ring chronologies by Rose (1983) and Monserud (1986) indicates that western North American conifers are most commonly ARMA(1,1) processes, with the best competing models falling in the AR(1)–AR(3) classes. Cook (1985) restricted his analyses of eastern North American conifer and hardwood tree-ring chronologies to the AR process and found that AR(1)–AR(3) models were satisfactory, in most cases.

ARMA processes are examples of causal feedback-feedforward filters (Robinson and Treital, 1980) that are used extensively in geophysical signal analysis. The AR part of the process operates as a feedback filter, while the MA part operates as a feedforward filter. That is, the current I_t is a product of the current e_t plus past I_{t-i} inputs, which are fed back into the process, and past e_{t-i} inputs, which are fed forward upon the arrival of the current e_t. In this way, the potential for current growth is largely affected by previous radial growth (I_{t-i}) and by reflections of antecedent environmental inputs (e_{t-i}).

Thus, the ARMA process is an elegant mathematical expression of *physiological preconditioning* (Fritts, 1976).

An important concept of ARMA processes is the way in which they can operate as signal amplifiers. The amplifier mechanism can be seen in the variance formula of AR(p) processes, *viz.*,

$$\sigma_y^{\,2} = \frac{\sigma_e^{\,2}}{1 - \rho_1\phi_1 - \rho_2\phi_2 - \cdots - \rho_p\phi_p} \quad , \tag{3.31}$$

where $\sigma_y^{\,2}$ is the variance of the observed AR process, $\sigma_e^{\,2}$ is the variance of the unobserved random shocks, and ρ_i and ϕ_i are the theoretical autocorrelation and autoregression coefficients of the process. If both the ρ_i and ϕ_i are positive, which is usually the case for tree-ring indices, then $\sigma_y^{\,2}$ will always be greater than $\sigma_e^{\,2}$. A reflection of this amplifier mechanism is transience. That is, the effect of a given e_t in a tree-ring series, whether climatic or from disturbance, will last for several years or, in extreme cases, decades before it disappears (Cook, 1985). The consequence of transience, when endogenous disturbance shocks are present in the e_t, is a degradation of the SNR of the C_t in the mean-value function of tree-ring indices.

To remove the effects of unwanted, disturbance-related transience on the common signal among trees, the tree-ring indices can be modeled and prewhitened as AR(p) (Cook, 1985) or ARMA(p, q) (Guiot, 1987a) processes before the mean-value function is computed. The order of the process can be determined at the time of estimation using the Akaike Information Criterion (AIC) (Akaike, 1974). Once the ARMA(p, q) coefficients are estimated, the prewhitening is carried out as

$$e_t = I_t - \phi_1 I_{t-1} - \cdots - \phi_p I_{t-p} + \theta_1 e_{t-1} + \cdots + \theta_q e_{t-q} \tag{3.32}$$

in difference equation form, or

$$e_t = [\phi(B)/\theta(B)]\, I_t \tag{3.33}$$

in backshift operator form. The tree-ring series are now *white noise.*

The resulting e_t represent the contributions of C_t, $D1_t$, and E_t, with $D2_t$ assumed to be absent at this stage. The reduction of the transient effects of endogenous disturbance pulses results in an increase in fractional common variance (Wigley *et al.*, 1984) or $\%Y$ (Fritts, 1976) and in an improved SNR in the mean-value function of the e_t, denoted $\mathbf{e_t}$. This results in an improved estimate of C_t, especially if the biweight robust mean is also used in computing $\mathbf{e_t}$. Cook (1985) found that the average absolute increase in fractional common variance between sampled trees was about 7% for 66 tree-ring chronologies developed from closed-canopy forest stands. The average relative increase in fractional common variance, compared with that of a mean-value function developed

without using AR modeling, was about 25%. There are no comparable figures for ARMA-based models.

The estimate of C_t, in the form of $\mathbf{e_t}$, is incomplete because it is missing the natural persistence owing to climate and tree physiology. To have a complete model of the common signal within the ensemble, an estimate of the common persistence structure among all detrended tree-ring series is necessary. For the pure AR model, a pooled estimate of autoregression, denoted $\Phi(\mathbf{B})$, can be computed directly from lag-product sum matrices of the ensemble that include information on persistence both within and among series (Cook, 1985). The method appears to be quite robust in the face of high levels of out-of-phase fluctuations among series that are caused by endogenous disturbances. Unfortunately, this pooling procedure is difficult to apply to the ARMA case because of the highly nonlinear MA coefficients.

Guiot (1987a) addressed the estimation of the common ARMA model by first creating a mean-value function of raw ring-width series from very old trees, which were selected by principal components and cluster analysis of the corresponding white-noise series. The common ARMA(p, q) model, denoted $\Theta(\mathbf{B})/\Phi(\mathbf{B})$, was then estimated for stationary subperiods in the mean ring-width series. However, this approach may be difficult to apply to the general closed-canopy forest where stationary subperiods rarely exist for any length of time (e.g., *Figures 3.1* and *3.2*). As an alternative, the ring-width series could be detrended first, a robust mean-value function created, and the mean series modeled as an ARMA process to produce $\Theta(\mathbf{B})/\Phi(\mathbf{B})$. This method would depend upon sufficient replication to diminish the effects of endogenous disturbance effects. Experiments in detrending ring-width series (Cook, 1985) indicate that the choice of the detrending method will have little effect on the order and coefficients of the mean ARMA process as long as the variance removed by the trend line is effectively all trend, as defined by Granger (1966).

The estimation of the common signal components is now complete. A final tree-ring chronology, $\mathbf{I_t}$, containing both common signal components, can be easily created by simply convolving the pooled AR, $\Phi(\mathbf{B})$, or the ARMA $[\Theta(\mathbf{B})/\Phi(\mathbf{B})]$ operators with the $\mathbf{e_t}$ (Cook, 1985; Guiot, 1987a), once suitable starting values are obtained. The q starting values for the MA component will ordinarily be set to zero, the unconditional expected value of $\mathbf{e_t}$. The p starting values for the AR component may be obtained from the I_t lost through prewhitening (Cook, 1985), by back-forecasting of the I_t past the beginning of the I_t (Box and Jenkins, 1970), or by using the unconditional expected value of the I_t. If the characteristic transience of the AR component decays rapidly, then the choice of starting values will have little effect on the final series.

For the full ARMA case, the final estimate of C_t is

$$\mathbf{I_t} = [\Theta(\mathbf{B})/\Phi(\mathbf{B})]\mathbf{e_t} \quad . \tag{3.34}$$

Aside from producing an efficient estimate of C_t, knowledge of $[\Theta(\mathbf{B})/\Phi(\mathbf{B})]$ and $\mathbf{e_t}$ are also useful for estimating $D1_t$ and E_t in the individual tree-ring series.

3.5. Correcting for Trend in Variance Due to Changing Sample Size

S. Shiyatov, V. Mazepa, and E. Cook

With the possible exception of tree-ring chronologies developed from even-aged stands or narrow-age classes of trees, the yearly sample size of m indices in a tree-ring chronology can be expected to diminish backward in time as younger trees drop out of the series. As the sample size decreases below some threshold, commonly between 5 and 10, a perceptible increase in the variance of the mean-value function can be discerned when compared with better replicated time intervals. This increase in variance is largely a function of decreasing sample size, which is independent of changes in the variance owing to environmental influences on radial growth. This problem of nonuniform variance owing to changing sample size was recognized by Schulman (1956). He suggested deleting the early, poorly replicated portions of chronologies because of this non-climatic, statistical artifact. To date, this method of deletion is commonly used in dendroclimatic studies to avoid spurious conclusions concerning past climatic variability.

The change in time series variance, described above, is related to the change in variance of the arithmetic mean, equation (3.23), which is proportional to $1/m$. As m gets small (say, $m < 10$), additional reductions in m result in rapid increases in $1/m$. The change in the standard error of the mean, square root of equation (3.23), is even more dramatic because it is proportional to $1/\sqrt{m}$. How quickly this effect will manifest itself in the mean-value function will depend upon the variance of the sample of m indices, equation (3.22), and the signal-to-noise ratio (SNR) of the chronology, equation (3.15). The SNR and a related measure called the subsample signal strength (SSS) (Wigley *et al.*, 1984) will be described in more detail in Section 3.6. As will be shown, SSS can be used to determine the point in time where a chronology loses too much accuracy to be useful, owing to reduced sample size. For now, it is sufficient to illustrate the sample-size effect on the variance of tree-ring chronologies and describe a method developed by Shiyatov and Mazepa (1987) for correcting this effect.

Figure 3.11 (Shiyatov and Mazepa, 1987) shows the way in which the coefficient of variation of a tree-ring chronology can vary as a function of sample size. These plots were created, from an ensemble of 22 indexed *Picea obovata* tree-ring series, by randomly selecting many subsets of size $m = 1 - 20$ from the total and by computing the coefficient of variation of each mean series. Below about $m = 7$, there is a clear increase in the plots of the mean and maximum coefficients of variation. This reflects the increase in variance owing to decreasing sample size. The plot of minima remains much more constant in the range of $m = 2 - 10$. This probably reflects a subset of series in the ensemble that are highly correlated and, therefore, have high SNR. Nonetheless, *Figure 3.11* indicates that a trend in variance from decreasing sample size should be expected most of the time.

Shiyatov and Mazepa (1987) note that there are times when it is important to use as much of a tree-ring chronology as possible. Given this circumstance, they suggest the following method for correcting the trend in variance caused by

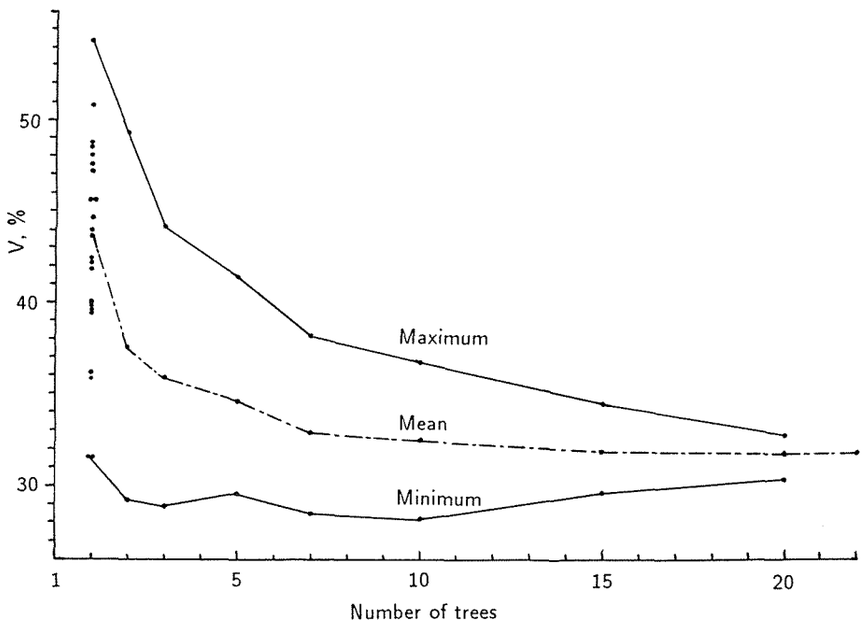

Figure 3.11. The maximum, mean, and minimum values of the coefficient of variation (CV) obtained from a different number of sampled *Picea obovata* trees from the same site. The dots (·) on the left of the chart indicate the range of the CV of the individual series.

changing sample size. For the time interval of maximum sample size, m_{max}, compute the coefficient of variation for the mean series as

$$CV_{std} = s_{std}/\bar{x}_{std} \quad , \tag{3.35}$$

where s_{std} and $\bar{x}_{std}$ are the standard deviation and mean, respectively, of that series. CV_{std} is the standard used for contracting the variance in other time periods having smaller sample sizes. Having estimated CV_{std}, new coefficients of variation CV_k are then computed using equation (3.35) for the total time period of the longest series, the entire period of overlap of the mean of the two oldest series, the entire period of overlap of the mean of the three oldest series, and so on up to the time interval and sample size covered by CV_{std}. The variance corrections for the time intervals not having maximum sample size are then computed as

$$I_t^{cor} = (I_t^{act} - I) * k + I \quad , \tag{3.36}$$

where I_t^{cor} is the corrected tree-ring index, I_t^{act} is the uncorrected index for year t, I is the the mean of the entire mean series, and k is the coefficient of contraction estimated as $k = CV_{std}/CV_k$, which is the ratio of the coefficient of variation of the m_{max} time period to that for a sample size $m < m_{max}$.

Table 3.2 shows the way in which CV_k varies in an ensemble of tree-ring indices of 24 *Picea obovata*. The last value for all sampled trees is CV_{std}. These values reinforce the example in *Figure 3.11* and, again, indicate that sample-size effects on variance are likely to occur at some point below $m = 10$. Having estimated the necessary CV_{std} and CV_k in *Table 3.2*, Shiyatov and Mazepa (1987) used this information in equation (3.36) to produce a corrected tree-ring chronology. The uncorrected and corrected series are shown in *Figure 3.12*. There is a clear contraction in the variance of the corrected series below $m = 5$, in accordance with the values in *Table 3.2*.

Table 3.2. Change in the coefficient of variation (CV) of a mean chronology (*Picea obovata*) owing to changing sample size. The % deviation of each CV from the standard value is used to correct variance of the mean series for changing sample size.

Sample size	*Time interval*	*Years*	*CV in %*	*% Deviation of CV from the standard*
1	1829–1968	140	58.5	+20.3
2	1837–1968	132	57.2	+19.0
3	1854–1968	115	49.9	+11.7
5	1876–1968	93	46.0	+7.8
6	1878–1968	91	43.6	+5.4
7	1879–1968	90	42.4	+4.2
8	1881–1968	88	41.2	+3.0
9	1882–1968	87	39.5	+1.3
10	1884–1968	85	38.4	+0.2
11	1885–1968	84	38.8	+0.6
12	1893–1968	76	37.1	−1.1
All sampled trees – The standard				
13–24	1894–1968	75	38.2	0.0

A trend in variance, which is independent of changing sample size, can also be expected in tree-ring chronologies of ring-porous tree species, such as *Quercus*. The active xylem vessels of ring-porous species are almost totally restricted to the newly formed vessels of each growing season. These large *springwood* vessels are formed from stored carbohydrates before the flush of new leaves each year. Their contribution to each total ring width varies little from year to year, compared with the subsequently formed *summerwood* vessels, and declines more slowly with age than the summerwood width. Thus, the contribution of springwood vessels to the total ring width often increases with age. This causes the yearly variance of ring-porous radial increments to decrease with age in a way that is independent of sample size.

As a means of correcting this problem in *Quercus* tree-ring chronologies, Cook (unpublished) included in the tree-ring standardization program ARSTND

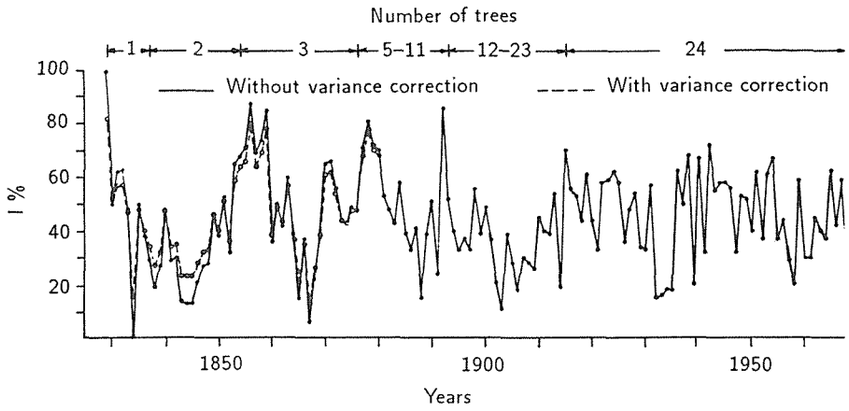

Figure 3.12. The mean chronology of 24 *Picea obovata* tree-ring series without (solid line) and with (dashed line) the variance correction based on the coefficient of variation. The change in sample size in the chronology is indicated by the number of trees at the top of the plot. The most obvious contraction of variance occurs below a sample size of five trees.

(Cook and Holmes, n.d.) an option for removing the trend in variance in tree-ring chronologies. This method is distinctly different from that of Shiyatov and Mazepa (1987) and does not rely on the coefficient of variation. It is based on fitting a smoothing spline to the absolute values of the mean-corrected, standardized tree-ring indices. The spline is used to track the trend in the standard deviation of the indices, as revealed by the low-frequency fluctuations in the absolute values. Each absolute value is divided by its respective spline value. The corrected absolute values are than back-transformed into normal tree-ring indices and scaled to have the same overall variance as the original, uncorrected indices. This technique can be used on both single series and the mean-value function. In the latter case, it will correct for both the trend in variance caused by ring-porous wood anatomy and the changing sample size, if the variance correction is not made on the individual series.

Given that the method of Shiyatov and Mazepa (1987) or the method in the *ARSTND* program (Cook and Holmes, n.d.) can be used to correct for a trend in variance owing to changing sample size, a word of caution must be made. The increase in variance when m gets small is a consequence of the noise in the ensemble that is not adequately reduced by averaging. As a result, those mean values based on small m are considerably less precise and probably less accurate then the mean indices derived from larger sample sizes. Correcting the variance for changing sample size will not necessarily improve the accuracy. It merely adjusts those means based on $m < m_{\max}$ to behave as if they were based on the maximum sample size. As a consequence, the loss of accuracy is masked by the variance correction. Additional information on the accuracy of the small

m segment of tree-ring chronologies can be obtained by computing the SSS (sub-sample signal strength) and should be made available if corrections are made to the variance for changing sample size.

3.6. Basic Chronology Statistics and Assessment

K. Briffa and P.D. Jones

3.6.1. Measuring the statistical quality of a chronology

This section is concerned with the problem of assessing the statistical confidence of a chronology. Up to this point we have described various approaches and techniques that are used to produce tree-ring chronologies from such variables as ring widths or maximum latewood density data. We have discussed in some detail the ways in which measured series of these data may be standardized during chronology production so that the unwanted index time series, thought to obscure those variations representing the hypothesized forcing with which we are concerned, has been removed. In other words, we have described the production of chronologies in terms of a noise-reduction process, and the concepts of signal and noise have been clearly framed in terms of specific hypotheses or applications.

Here, we will investigate the concept of a chronology signal. This signal is a statistical quantity representing the common variability present in all of the tree-ring series at a particular site. The strength of this signal is estimated empirically, and here it is not necessary to speculate on the forcing(s) of which the signal is the manifestation. We merely assume that a group of tree-ring series from a site make up one sample from a hypothetical population whose average would be the *perfect* chronology – one that fully represents the underlying forcing(s). The variance of any series of tree-ring indices will contain this common forcing signal (though it will be modified according to how the data are standardized), but in any one core it will be obscured by variability common only to the specific tree and core – the statistical noise. By definition, this noise is uncorrelated from core to core and, therefore, will cancel out in a chronology to an extent that depends on the number of series being averaged. Therefore, the question of the statistical quality of a chronology may be phrased as follows: To what degree does the chronology represent the hypothetical population chronology? To answer this question, it is necessary, first, to estimate the strength of the signal and, second, to quantify how clearly this signal is expressed in the chronology. We shall discuss these points in turn.

3.6.2. Estimating the chronology signal strength

The Analysis of Variance Technique

Traditionally, dendroclimatologists haved used the Analysis of Variance (ANOVA) technique to estimate signal and noise within groups of standardized

tree-ring series (indices) by measuring common variability within and between trees. Considered sampling design also allows the dendrochronologist to judge the relative importance of various environmental influences acting on the growth of trees. A discussion of this use of ANOVA can be found in Fritts (1976).

Table 3.3 (Fritts, 1976) illustrates how the relative importance of within-tree and between-tree signals is calculated by computing the variance components, $V(Y)$, etc., associated with specific groups of standardized series that make up the final chronology. In this example, the analysis involves indices Y_{ijk}, where $i = 1$ to t trees, each with $j = 1$ to c cores (hence, the total number of cores is

$$C = \sum_{i=1}^{t} c_i \quad .$$

All data series run from $k = 1$ to n years. The various fractional variance components are calculated as shown in *Table 3.3*.

The fractional variance component for the chronology, $V(Y)$, according to Fritts (1976), shows how much of the variance is common among all trees and cores. This, he says, represents the overall growth forcing(s) at the site and, as such, it is a measure of the chronology signal.

The component *chronologies of trees*, $V(YT)$, measures that part of the overall variance that is common to cores within trees but not common between trees. This is the between-tree noise. The *chronologies of cores within trees* component, $V(YCT)$, is a measure of the variance not common among individual cores within any one tree, the within-tree noise. Subtracting this value from 1, therefore, defines the within-tree signal.

The Mean Correlation Technique and a New Definition of the Chronology Signal

When producing a chronology of a tree-ring variable, it is a simple matter to calculate a correlation matrix displaying the relationships between all series of indices for individual cores. Given such a matrix, several mean correlation values can be calculated. This represents an alternative approach to estimating the quantities that arise in the ANOVA.

First, we should define the correlation matrix grand mean, i.e., the mean of all correlations among different cores – both within and between trees. This can be termed

$$\bar{r}_{\text{tot}} = \frac{1}{N_{\text{tot}}} \sum_{i=1}^{t} \sum_{\substack{l=1 \\ i \neq l}}^{t} \sum_{j=1}^{c_i} r_{ilj} \quad , \tag{3.37}$$

where

$$N_{tot} = \frac{1}{2} \left(\sum_{i=1}^{t} c_i \right) \left[\left(\sum_{i=1}^{t} c_i \right) - 1 \right] \quad .$$

An estimate of the within-tree signal is given by averaging the correlation coefficients between series of indices from the same tree over all trees. This within-tree signal can be denoted as

$$\bar{r}_{wt} = \frac{1}{N_{wt}} \sum_{i=1}^{t} \left[\sum_{j=2}^{c_i} r_{ij} \right] \quad , \tag{3.38a}$$

where

$$N_{wt} = \sum_{i=1}^{t} \frac{1}{2} c_i (c_i - 1) \quad . \tag{3.38b}$$

The expression $1 - \bar{r}_{wt}$ is equivalent to $V(YCT)$ in *Table 3.3*.

We can also calculate a between-tree signal, $\bar{r}_{bt}$, defined as the mean inter-series correlation calculated between all possible pairs of indexed series drawn from different trees:

$$\bar{r}_{bt} = \frac{1}{N_{bt}} \left(\bar{r}_{\text{tot}} N_{\text{tot}} - \bar{r}_{wt} N_{wt} \right) \quad , \tag{3.39a}$$

where

$$N_{bt} = N_{\text{tot}} - N_{wt} \quad . \tag{3.39b}$$

Fritts (1976, page 294) noted, using empirical evidence, that $V(Y)$ defined in *Table 3.3* is invariably close to $\bar{r}_{bt}$. Wigley *et al.* (1984) have shown that $V(Y)$ and $\bar{r}_{bt}$ are in fact identical provided that both estimates are calculated using data normalized over the common period of analysis. The normalization of individual series of indices is not common practice in chronology development. However, both the ANOVA and correlation approaches to estimating chronology-population signals tacitly assume that there is no difference between the means of individual core series. Generally, standardization ensures that there is little difference. If, however, each indexed series is normalized over its whole length prior to averaging, then this generally ensures that the means of the core indices over the common period are not significantly different from zero [i.e., that $V(YC)$ is very close to zero]. This is recommended. The between-tree noise, $V(YT)$ in *Table 3.3*, is conveniently calculated as the difference between $\bar{r}_{wt}$ and $\bar{r}_{bt}$.

Wigley *et al.* (1984) derived the relationship between $\bar{r}_{bt}$ and $V(Y)$ using data from only one core per tree and confirmed the result empirically. In fact, $\bar{r}_{bt}$ defined by equation (3.39a) and $V(Y)$ in *Table 3.3* are also equivalent for multiple cores per tree (identical if the data are normalized over the common

Analysis of variance table showing how the different sources of chronology variation are calculated. Equivalent mean corre-
es described in the text are also shown. ANOVA table adapted from Fritts (1976).

	Corrected sum of squares		*Degrees of freedom*
	$\frac{1}{tn}\left[\sum_{j=1}^{c}\left[\sum_{i=1}^{t}\sum_{k=1}^{n} Y_{ijk}\right]^2\right]-K$	$= C$	$(c-1)$
s	$\frac{1}{cn}\left[\sum_{i=1}^{t}\left[\sum_{j=1}^{c}\sum_{k=1}^{n} Y_{ijk}\right]^2\right]-K$	$= T$	$(t-1)$
s s	$\frac{1}{n}\left[\sum_{i=1}^{t}\sum_{j=1}^{c}\left[\sum_{k=1}^{n} Y_{ijk}\right]^2\right]-C\ {}^{-T}_{-K}$	$= CT$	$(c-1)(t-1)$
ces logy	$\frac{1}{tc}\left[\sum_{k=1}^{n}\left[\sum_{i=1}^{t}\sum_{j=1}^{c} Y_{ijk}\right]^2\right]-K$	$= Y$	$(n-1)$
ies	$\frac{1}{c}\left[\sum_{k=1}^{n}\sum_{i=1}^{t}\left[\sum_{j=1}^{c} Y_{ijk}\right]^2\right]-Y\ {}^{-T}_{-K}$	$= YT$	$(n-1)(t-1)$
ies asses	$\frac{1}{t}\left[\sum_{k=1}^{n}\sum_{j=1}^{c}\left[\sum_{i=1}^{t} Y_{ijk}\right]^2\right]-Y\ {}^{-C}_{-K}$	$= YC$	$(n-1)(c-1)$
ies s	$\left[\sum_{k=1}^{n}\sum_{i=1}^{t}\sum_{j=1}^{c}\left(Y_{ijk}\right)^2\right]\ {}^{-Y-C\ -CT}_{-YC-YT}_{-K}$	$= YCT$	$(n-1)(c-1)(t-1)$

able 3.3. Continued.

ariance urce	*Mean square*	*Variance component*	*Fractional variance component*	*Equivalent mean correlation*
ore class neans	$MS(C) = \frac{C}{(c-1)}$			
ree means	$MS(T) = \frac{T}{(t-1)}$			
ore means with trees	$MS(CT) = \frac{CT}{(t-1)(c-1)}$			
lean indices n chronology	$MS(Y) = \frac{Y}{(n-1)}$	$\frac{MS(Y)-MS(YT)}{ct} = V\{Y\}$	$\frac{V(Y)}{\text{Total } V} = V\{Y\}$	$\bar{r}_{bt}$
hronologies of trees	$MS(YT) = \frac{YT}{(n-1)(t-1)}$	$\frac{MS(YT)-MS(YCT)}{c} = V\{YT\}$	$\frac{V(YT)}{\text{Total } V} = V\{YT\}$	$\bar{r}_{wt}-\bar{r}_{bt}$
hronologies of core classes	$MS(YC) = \frac{YC}{(n-1)(c-1)}$	$\frac{MS(YC)-MS(YCT)}{t} = V\{YC\}$	$\frac{V(YC)}{\text{Total } V} = V\{YC\}$	Zero
hronologies of cores with trees	$MS(YCT) = \frac{YCT}{(n-1)(c-1)(t-1)}$	$MS(YCT) = V(YCT)$	$\frac{V(YCT)}{\text{Total } V} = V\{YCT\}$	$1-\bar{r}_{wt}$

he correction factor, $K = \frac{1}{tcn}\left[\sum_{i=1}^{t}\sum_{j=1}^{c}\sum_{k=1}^{n} Y_{ijk}\right]^2$,

where $i = 1,2,\ldots,t$ t = number of trees
$j = 1,2,\ldots,c$ c = number of cores per tree
$k = 1,2,\ldots,n$ n = number of years

otal $V = V\{Y\} + V\{YT\} + V\{YC\} + V\{YCT\}$

period). However, $\bar{r}_{bt}$ is not the best estimate of the chronology signal where more than one core series per tree are involved. Though $V(Y)$ (and the equivalent $\bar{r}_{bt}$) is commonly used to represent the chronology signal, it is not an ideal measure of the forcing that is common between and within all trees at a site. This is because $V(Y)$ incorporates noise associated with differences among cores within trees – noise that is reduced by averaging. It is possible to define a chronology signal that makes allowance for this.

In seeking to generalize the results of their paper, Wigley *et al.* (1984, page 211) stated:

> Our analysis only considers the case of one core per tree but it can be adapted to more general cases. For example, multiple cores may be averaged to produce a single time series for each tree, or $\bar{r}$ ... can be determined using only a single core per tree if the early parts of a chronology suggest that such a strategy is more appropriate.

The second option they suggest will give an estimate of $\bar{r}_{bt}$ (and one which does not use all of the available data). Importantly, the potential for measuring the within-tree signal will be wasted. Their first suggestion, though it too does not give a value for $\bar{r}_{wt}$, gives a better estimate of the chronology signal, one that is less obscured by within-tree noise and involves calculating the mean correlation between series of previously averaged core series. We can denote this as $\bar{r}_{mt}$, the mean-tree correlation mean, i.e.,

$$\bar{r}_{mt} = \frac{2}{t(t-1)} \sum_{i=1}^{t} \sum_{\substack{l=i \\ i \neq l}}^{t} r_{il}^{*} \quad , \tag{3.40}$$

where r_{il}^{*} is the correlation coefficient between the mean of all core time series for tree i and the mean for tree i. It can be shown that $\bar{r}_{mt}$ is given by

$$\bar{r}_{mt} = \frac{\bar{r}_{bt}}{\bar{r}_{wt} + \dfrac{1 - \bar{r}_{wt}}{c}} \tag{3.41}$$

where $\bar{r}_{bt}$ is given by equation (3.39a), $\bar{r}_{wt}$ is given by equation (3.38a), and c is the number of cores per tree and must be the same for all trees. If an unequal number of cores per tree are averaged, instead of c, an effective number of cores, c_{eff}, should be used such as

$$\frac{1}{c_{\text{eff}}} = \frac{1}{t} \sum_{i=1}^{t} \frac{1}{c_i} \quad , \tag{3.42}$$

where t is the number of trees and c is the number of cores in tree i. Hence, we can define a chronology-signal estimate that incorporates both within- and between-tree signals, which we will call the effective chronology signal, $\bar{r}_{\text{eff}}$,

$$\bar{r}_{\text{eff}} = \frac{\bar{r}_{bt}}{\bar{r}_{wt} + \dfrac{1 - \bar{r}_{wt}}{c_{\text{eff}}}} \quad . \tag{3.43}$$

From this point on we will refer to $\bar{r}_{\text{eff}}$, but it should be remembered that, when studying the same number of cores per tree, $\bar{r}_{\text{eff}}$ is equal to $\bar{r}_{mt}$. When the number of cores per tree are unequal, equation (3.43) gives a chronology-signal estimate that is still extremely close to the one derived from equation (3.40). As $\bar{r}_{wt}$ has, by definition, a lower limit equal to $\bar{r}_{bt}$ it can be shown that equation (3.43) gives a measure of the chronology signal that is almost invariably greater than $\bar{r}_{bt}$ and implies that, to date, the strength of common forcing has been generally underestimated by quoting chronology $V(Y)$ or $\bar{r}_{bt}$ values. *Figure 3.13* illustrates how the degree of underestimation depends on $\bar{r}_{bt}$ and $\bar{r}_{wt}$. If as an example we say that $\bar{r}_{wt}$ is often in the range 0.6–0.7 and chronologies often comprise two cores per tree, the $\bar{r}_{\text{eff}}$ value for the chronology signal may well be 20% to 30% greater than the $\bar{r}_{bt}$ value. The difference is less where $\bar{r}_{wt}$ is higher and greater where it is lower. The difference is also less marked when $\bar{r}_{wt}$ values are based on more cores per tree.

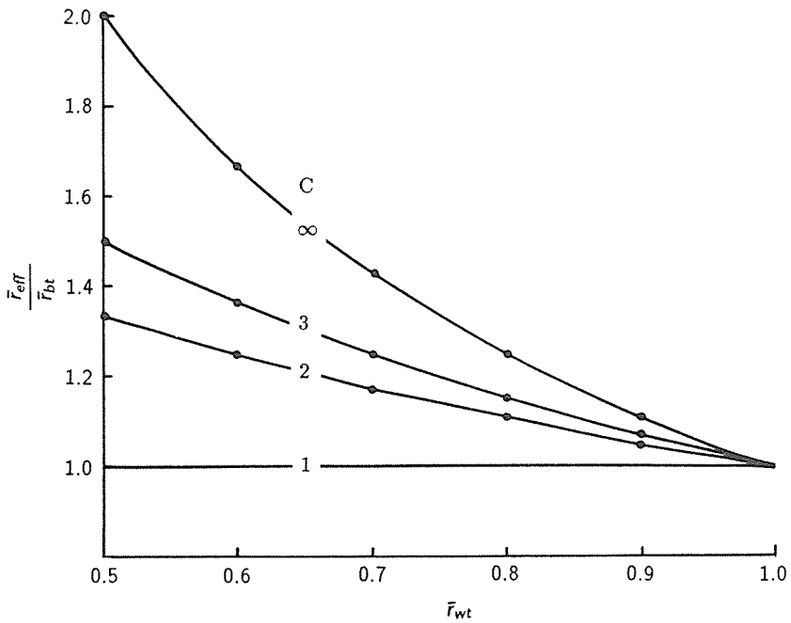

Figure 3.13. The ratio of $\bar{r}_{\text{eff}}$ and $\bar{r}_{bt}$ plotted as a function of $\bar{r}_{wt}$ and the number of cores per tree, c.

Relative Advantages of the Correlation Versus the ANOVA Method

As generally implemented, the ANOVA requires that all series must span a common set of years and that each tree must be represented by the same number of cores. Restrictions, such as trees of different ages or core samples of unequal numbers, may limit the period of analysis when using ANOVA or they might necessitate the exclusion of a number of cores from the analysis. In extreme cases, there might not be a common overlap of sufficient length in the series to make a useful analysis.

An advantage of the correlation-based technique is that it allows all series of indices to be used, including the case where the number of series varies from tree to tree. Furthermore, it is not necessary for all of the series to have a common period of overlap. A correlation matrix can be computed using the maximum overlap period between each pair of series and the signal parameters estimated from this. (In practice, one would set a minimum limit on the length of the overlap required to calculate a correlation coefficient, e.g., 30 years.)

Illustrative Examples

Table 3.4 gives some examples of the calculation of the quantities discussed above. In this simplified illustration, two correlation matrices are shown – each involving four trees: two with two cores, one with a single core, and one with three cores. (These numbers are in fact taken from the full correlation matrix of data for the chronology *Twisted Tree-Heartrot Hill* described in Section 3.7. The data used here have been standardized using the modified negative exponential option.) The top matrix is calculated over the overall common period, 1807–1974. The mean of the values without a footnote is the between-tree signal, $\bar{r}_{bt}$, [$V(Y)$ in *Table 3.3*] and is 0.39 in this case. The within-tree signal, $\bar{r}_{wt}$, is the mean of the values with a footnote, 0.76; the within-tree noise, $V(YCT)$, is given by subtracting $\bar{r}_{wt}$ from 1 to give 0.24. The between-tree noise, $V(YT)$, calculated as the difference between $\bar{r}_{wt}$ and $\bar{r}_{bt}$, is 0.37. The chronology signal, $\bar{r}_{\text{eff}}$, calculated using equation (3.43), is 0.43 for the top matrix. All of the values in the top matrix are based on a common 168-year period.

The lower matrix in *Table 3.4* is calculated using the maximum overlaps between individual pairs of series. These overlaps range from 205 to 463 years. Use of the values in this matrix gives a lower value of $\bar{r}_{bt}$ of 0.30. The core-to-core variability of $\bar{r}_{bt}$ is also reduced from a standard deviation of 0.21 to 0.12. The $\bar{r}_{wt}$ value is very similar to the previous one at 0.77, but again it has a smaller standard deviation. The $\bar{r}_{\text{eff}}$ value for this matrix is 0.33.

On this evidence the second matrix seems to give more conservative (i.e., lower) estimates of the signal parameters. Experiments have been made where very short-period correlations are excluded and where the mean correlations are computed by preferentially weighting those based on longer overlaps, but such modifications do not seem to affect the results significantly.

Both the ANOVA-derived and correlation-based signal estimates are unbiased estimates of the population parameters (Wigley *et al.*, 1984) and give

Table 3.4. Alternative correlation matrices for calculating the different signal estimates. The column and row headings identify the different tree (1st figure) and core (2nd figure) series, i.e., 4.3 indicates the third core series from tree 4.

Maximum period common to all cores (1807–1974)

	1.1	1.2	2.1	2.2	3.1	4.1	4.2	4.3
1.1	–	0.47[a]	-0.01	0.32	0.44	0.33	0.28	0.26
1.2		–	-0.10	0.50	0.43	0.27	0.21	0.28
2.1			–	0.46[a]	0.23	0.63	0.67	0.61
2.2				–	0.57	0.68	0.64	0.68
3.1					–	0.41	0.33	0.39
4.1						–	0.96[a]	0.96[a]
4.2							–	0.96[a]
4.3								–

$\bar{r}_{bt}$ = 0.39 (standard deviation = 0.21)
$\bar{r}_{wt}$ = 0.76 (standard deviation = 0.27)
$\bar{r}_{\text{eff}}$ = 0.43 from equation (3.43)

Maximum individual pair overlaps (years shown in parenthesis)

	1.1	1.2	2.1	2.2	3.1	4.1	4.2	4.3
1.1	–	0.53(285)[a]	0.26(304)	0.48(294)	0.43(205)	0.26(304)	0.25(304)	0.10(304)
1.2		–	0.06(285)	0.46(285)	0.38(205)	0.28(285)	0.21(285)	0.15(285)
2.1			–	0.60(294)[a]	0.19(205)	0.29(325)	0.41(325)	0.21(325)
2.2				–	0.52(205)	0.41(294)	0.42(294)	0.28(294)
3.1					–	0.37(205)	0.26(205)	0.32(205)
4.1						–	0.92(445)[a]	0.92(463)[a]
4.2							–	0.89(445)[a]
4.3								–

$\bar{r}_{bt}$ = 0.30 (standard deviation = 0.12)
$\bar{r}_{wt}$ = 0.77 (standard deviation = 0.19)
$\bar{r}_{\text{eff}}$ = 0.33 from equation (3.43)

[a]Indicates correlations among core series from the same tree.

quite accurate values provided a reasonable number of series and a reasonable span of annual values are used to calculate them. Empirical experiments, based on single-core-per-tree data, suggest that at least five series and a minimum of 30 years should be used (Briffa, 1984). Obviously, the more cores and, more importantly, the longer the period of analysis, the more representative the estimates will be of the population parameters. However, one important characteristic of tree-ring time series (indexed or not) is that the statistical quantities defined above are not constant in time. Indeed, they frequently vary markedly on decadal and century time scales.

Given a chronology with an equal number of cores per tree and uniform replication throughout its length, there will be little difference in results achieved using either the ANOVA method or a correlation matrix. However, if core depth is variable and the number of cores varies per tree, or if the time span varies greatly between individual cores, the method of estimating the signal parameters based on the matrix of maximum individual pair overlaps will be easier to apply.

As it is based on almost all, if not all, the data, it will go further toward overcoming the temporal instability in parameter estimation inherent in analyses based on restricted numbers of cores or years.

3.6.3. Estimating the chronology confidence

Expressed Population Signal, Signal-to-Noise Ratio, and Subsample Signal Strength

After estimating the strength of the statistical signals and their related noise parameters for a number of tree-ring series, it is necessary to quantify the degree to which the chronology signal is expressed when series are averaged.

Uncommon variance (noise) will cancel in direct proportion to the number of series averaged. In a simple example where a chronology comprises t trees with only a single core per tree, the variance of each series of indices is made up of the common signal, $\bar{r}_{bt}$ (in this case also equivalent to $\bar{r}_{\text{eff}}$, and $V(Y)$ in ANOVA), and noise, $1 - \bar{r}_{bt}$. Averaging reduces the noise to $(1 - \bar{r}_{bt})/t$ while the common variance is unaffected. Therefore, the mean chronology has a total variance (signal + residual noise) of $\bar{r}_{bt} + (1 - \bar{r}_{bt})/t$. The chronology signal, expressed as a fraction of the total chronology variance, then quantifies the degree to which this particular sample chronology portrays the hypothetically perfect chronology. This has been termed the Expressed Population Signal or EPS (Briffa, 1984; Wigley *et al.*, 1984):

$$\text{EPS}(t) = \frac{\bar{r}_{bt}}{\bar{r}_{bt} + (1 - \bar{r}_{bt})/t} = \frac{t\ \bar{r}_{bt}}{t\ \bar{r}_{bt} + (1 - \bar{r}_{bt})} \quad , \tag{3.44}$$

where t is the number of tree series averaged – one core per tree – and $\bar{r}_{bt}$ is the mean between-tree correlation.

A more general expression for EPS, where a chronology has more than one core per tree, can be obtained by replacing $\bar{r}_{bt}$ with $\bar{r}_{\text{eff}}$ in equation (3.44) and using the number of trees sampled as t.

In a sample group of trees such as that used to produce *Table 3.4* where in any one year four trees with 2, 2, 1, and 3 cores, respectively, might be averaged, c_{eff} would be 1.7. Using the lower matrix estimates from *Table 3.4* of 0.30 and 0.77 for $\bar{r}_{bt}$ and $\bar{r}_{wt}$, respectively, equation (3.40) gives $\bar{r}_{\text{eff}} = 0.33$ and, hence, an EPS value, based on $t = 4$ trees, of 0.66.

EPS is formally equivalent to the $R_N{}^2$ (the expected correlation between the t-series average and the hypothetical population average) derived from first principles by Wigley *et al.* (1984) for the case of one core per tree. In this instance, it is also equivalent to the *percent common signal* defined by Cropper (1982) as

$$\text{PERCENT COMMON SIGNAL} = \frac{\text{SNR}}{1 + \text{SNR}} \quad , \tag{3.45a}$$

where

$$\text{SNR} = \frac{tV(Y)}{1 - V(Y)} \quad , \tag{3.45b}$$

where t is the number of series, and $V(Y)$ defined in *Table 3.3* is used as the measure of the chronology signal. Because it uses $\bar{r}_{bt}$ as the chronology signal, the percent common signal is not the same as EPS in which there is more than one core per tree.

SNR values (invariably the maximum value for a chronology, i.e., the value relating to the section of the chronology composed of the maximum number of cores) are often quoted as a measure of chronology quality (e.g., De Witt and Ames, 1978). This is clearly a difficult quantity to interpret because it has no upper bounds and its use for comparing chronologies is problematical. SNR behaves in a markedly nonlinear fashion – as a function of the number of trees. For large SNR, large increases in SNR lead to only minimal changes in EPS. The latter is easier to interpret.

However, EPS (or SNR) is not often a constant over the different parts of a chronology. It is important to appreciate the degree to which EPS varies through time as a function of variations in r and series replication. [It is not generally realized how variable all r values can be. However, the most important source of EPS variations is series replication, as equation (3.44) is relatively insensitive to variations in $\bar{r}_{\text{eff}}$.] *Figure 3.14* illustrates how EPS varies as a function of tree replication for a range of underlying $\bar{r}_{\text{eff}}$ signals. The horizontal axis shows the number of trees in the chronology and three EPS curves are shown, each representing a different $\bar{r}_{\text{eff}}$ value, equation (3.43). EPS rises asymptotically toward 1.0 as the number of trees tends to infinity. It rises very quickly as the number of trees increases from 1 to around 10 (for all values of $\bar{r}_{\text{eff}}$), but progressively slowing for more than 10.

When $\bar{r}_{\text{eff}}$ or tree numbers are already fairly high, EPS can still be improved through $\bar{r}_{\text{eff}}$, which can be increased by changing the type or level of standardization. This, however, produces only a slight improvement in EPS. The increase is more rapid with increasing $\bar{r}_{\text{eff}}$ when tree numbers are low (as might be the case in early years of a chronology), so here it is clearly helpful to use an optimal standardization method.

Figure 3.14 clearly shows that the law of diminishing returns is relevant when considering what range of EPS values constitute acceptable statistical quality. A value of 0.85 is one reasonable choice suggested by Wigley *et al.* (1984). Chronologies with $\bar{r}_{\text{eff}}$ values of around 0.6 [$\bar{r}_{bt}$ values of around 0.6 are typical for arid-site conifers in the western United States, e.g., De Witt and Ames (1978)] require as few as four trees to achieve this value. At the other end of the range, chronologies with $\bar{r}_{\text{eff}}$ values of 0.2 (at the lower end of the range found in deciduous sites in the UK), approximately 25 trees are required to reach an EPS of 0.85.

No specific value of EPS can be thought of as adequate or minimum to ensure that a chronology is suitable for climate reconstruction. The common

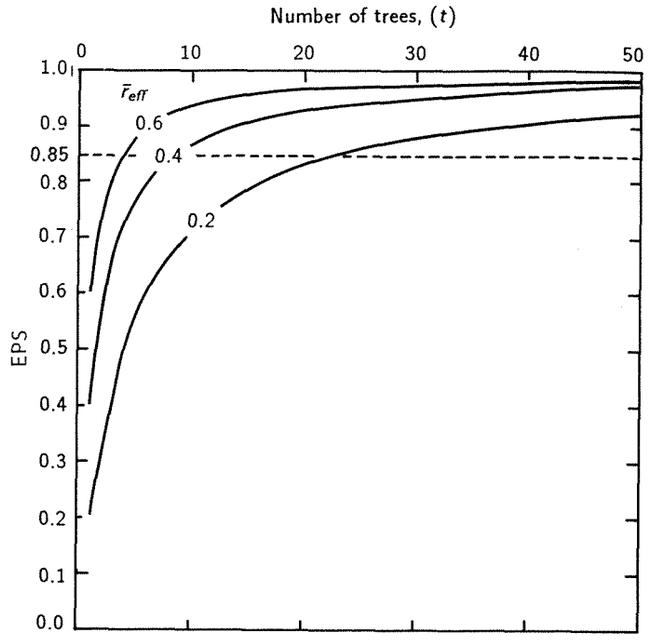

Figure 3.14. EPS values plotted as a function of the number of trees in a chronology for several example $\bar{r}_{eff}$ values.

signal does not necessarily reflect only climate forcing (i.e., other common factors could include management, pests, pollution). Nonetheless, the use of some critical threshold can provide an objective, statistical benchmark for inter-chronology comparisons and for making quantitative judgments on the likely confidence of regression-based estimates made using chronologies with or without variable replication. One way of doing this is to select a value of EPS that is considered high enough to represent an acceptable level of chronology confidence and then quote the range of years for which EPS values equal or exceed this.

Relationships Between the EPS and the Chronology Standard Error

Fritts (1976, page 290) discusses the way in which chronology error can be gauged using the standard error (SE) calculated from the component variances of an ANOVA analysis (c.f. *Table 3.3*). He defined the SE as

$$SE^2 = \frac{V(YT)}{t} + \frac{V(YCT)}{ct} \quad , \tag{3.46}$$

where the $V(YT)$ is the variance component due to differences in trees, the $V(YCT)$ is the component due to differences in individual core chronologies (i.e., the between-tree and within-tree noise components), and t and c are the numbers of trees and cores per tree, respectively [note, equation (3.46) assumes $V(YC) = 0$]. SE can easily be written in terms of $\bar{r}_{eff}$ as shown below.

Fritts calculated SE values for different numbers of trees and different numbers of cores per tree for a small sample of *Pinus longaeva* indices to illustrate that on purely statistical grounds, given the same overall number of cores, the chronology with least error is always achieved by taking one core per tree rather than by sampling trees more than once. There are, however, as he points out, sometimes good practical reasons for adopting the latter strategy.

Fritts' SE values (1976, page 291) were calculated using absolute variance components, rather than the more easily compared values based on fractional variances (which can be calculated by dividing Fritts' SE values by the square root of the total variance component). If the fractional variance components are used, the equivalence between the EPS and the SE (for normalized core indices) can be shown to be

$$SE^2 = \frac{1 - EPS}{t(1 - EPS) + EPS} \tag{3.47}$$

in terms of the number of trees, t. From this, an EPS of 0.85 is equivalent to an SE^2 of $1/(t + 5.67)$. Alternatively, SE can be expressed as

$$SE^2 = \frac{\bar{r}_{eff}(1 - EPS)}{EPS} \quad . \tag{3.48}$$

An EPS of 0.85 is therefore equivalent to an SE of 0.325 for a relatively high $\bar{r}_{eff}$ value of 0.6, but is equivalent to an SE of 0.188 when $\bar{r}_{eff}$ is only 0.2. By replacing EPS in equation (3.48) with equation (3.44) using $\bar{r}_{eff}$, the SE can be expressed as

$$SE^2 = \frac{1 - \bar{r}_{eff}}{t} \tag{3.49}$$

in terms of the chronology signal, $\bar{r}_{eff}$, and the number of trees, t. *Figure 3.15* illustrates equation (3.49) plotted for a range of $\bar{r}_{eff}$ values.

The Subsample Signal Strength (SSS)

The EPS is an absolute measure of chronology error that determines how well a chronology based on a finite number of trees approximates the theoretical population chronology from which it is assumed to have been drawn. It may not, however, always represent the most relevant estimate of chronology confidence

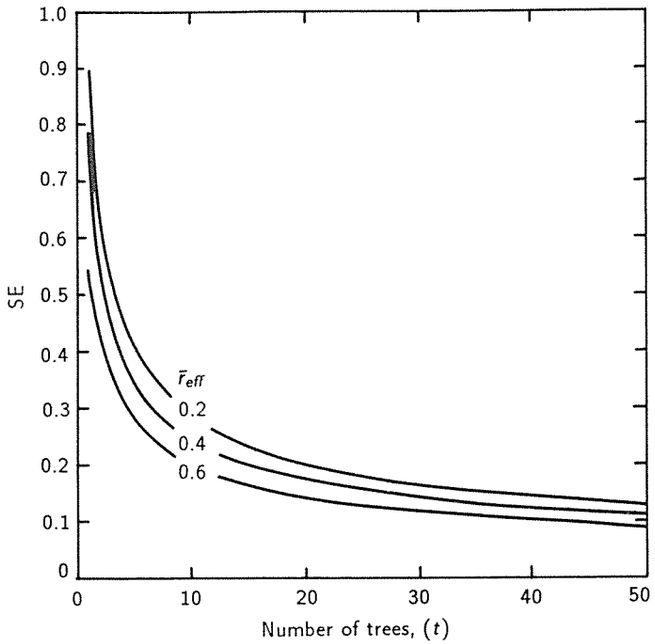

Figure 3.15. The standard error of a chronology plotted as a function of the number of constituent trees for several $\bar{r}_{\text{eff}}$ values.

as a function of decreasing tree number. In dendroclimatology, a statistical link between climate and one or more chronologies is usually established by regression analysis. Frequently, this link is calibrated against a recent section of chronology data often made up of the maximum number of individual tree series (t). Reconstruction estimates can then be made using earlier sections of chronology data. These tend to be made up of few tree series (t'), generally even fewer as one goes further back in time. As t' becomes smaller there must be an absolute increase in chronology error (measured by the falling EPS) and hence an additional reduction of reconstruction confidence beyond that quantified in the calibration equation.

To measure this additional uncertainty, we can pose a general question: How representative is a t'-tree chronology of a t-tree chronology where t' is less than t? The question may be answered by quantifying how well a chronology based on a subset of t'-tree series estimates a larger t-series chronology.

Wigley *et al.* (1984) derived an equation that describes the variance in common between a t'-core subsample and the t-core chronology, assuming that there is only one core per tree. They define a quantity, the subsample signal strength (SSS), as

$$\text{SSS} = \frac{t'[1 + (t - 1)\bar{r}]}{t[1 + (t' - 1)\bar{r}]} \quad . \tag{3.50}$$

The t and t' are the number of cores in the sample and subsample, respectively. In the case where only one core per tree was involved, the $\bar{r}$ is the $\bar{r}_{bt}$ described earlier, equation (3.39a). Equation (3.50) has been validated empirically by comparing the theoretical estimates with those obtained by averaging individual values of subsample chronology correlations over large numbers of randomly chosen subsets (Briffa, 1984; Wigley *et al.*, 1984). Where multiple cores are available, $\bar{r}_{\text{eff}}$ should be used, and t' and t become the number of trees in the subsample and reference chronologies, respectively.

The SSS can also be calculated as

$$\text{SSS} = \frac{\text{EPS}(t')}{\text{EPS}(t)} \quad . \tag{3.51}$$

In calculating SSS using equation (3.51), the EPS values should be defined using equation (3.44) with $\bar{r}_{bt}$ replaced by $\bar{r}_{\text{eff}}$ (note that $\bar{r}_{bt} = \bar{r}_{\text{eff}}$ when there is only one core per tree).

Defining Acceptable Chronology Confidence Based on the SSS

As with the EPS, just what constitutes an acceptable SSS level must ultimately be a subjective choice, and different criteria may be applied in different applications. Wigley *et al.* (1984) suggest that in climate reconstruction work, SSS values should be sufficiently large to ensure that any reconstruction uncertainty arising from decreasing core numbers should be *considerably less* than that quantified in the calibration of the chronology–climate link. In effect, this would require a critical or threshold SSS value for defining acceptable chronology uncertainty, substantially above that of the amount of climate variance explained by the fitted equation(s).

As an illustration, they show that for a climate reconstruction with 50% explained variance an SSS threshold of 0.85 (equivalent to allowing a maximum additional reconstruction uncertainty of 15%) would reduce the explained climate variance to around 43% (50% × 0.85). Their choice of an SSS of 0.85 was given only as an illustration. A general acceptance of this figure would ensure that additional chronology error was always restricted to a maximum of 15%.

It would not always be desirable or practicable to withhold potentially useful chronologies in climatic reconstruction solely on the basis of poor chronology confidence. Chronologies, or sections of chronologies, with only moderately high EPS or SSS values might still be highly correlated with climate parameters. It is important, however, to be aware of the true extent of uncertainty that is inherent in the estimates of past climate based on such chronologies. In any particular reconstruction case, the magnitude of regression coefficients define which specific chronologies are most important to the reconstructions. Provided these

specific chronologies are of good statistical quality, then lower EPS or SSS values could be accepted for others.

Alternatively, one could use a single SSS cutoff for defining usable portions of chronologies such as the figure of 0.85 used to construct *Figure 3.16*. This shows, for a t-tree chronology with a particular $\bar{r}_{eff}$ signal, the minimum number of trees required for a t'-tree subset to maintain an SSS above 0.85. Reconstructions based on these portions of chronologies are subject to additional reconstruction uncertainty (over that of the calibration estimates) of no more than 15%. The points on *Figure 3.16* illustrate the minimum number of trees required to maintain an SSS above 0.85 in the same chronologies used in the following comparison of standardization methods.

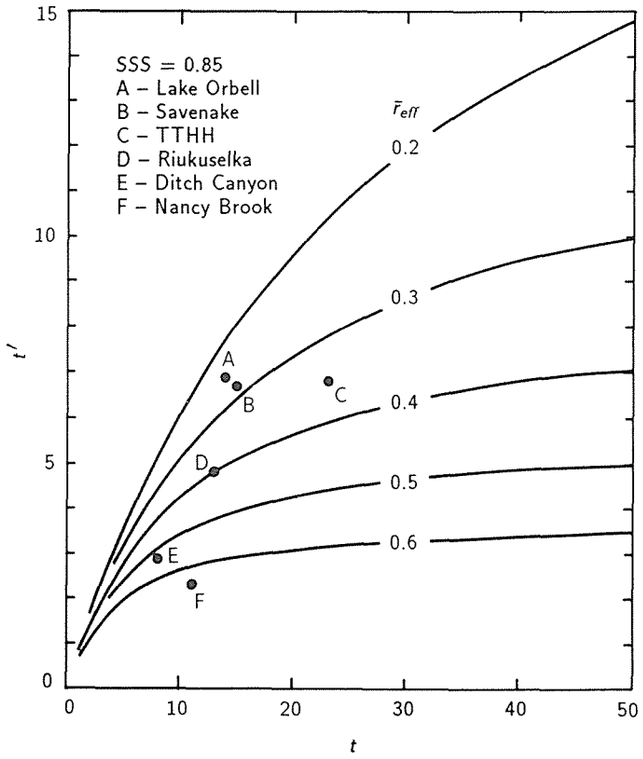

Figure 3.16. The number of trees (t') necessary in a subsample chronology to maintain the SSS above 0.85 where the reference chronology is composed of t trees. Curves are shown for several different $\bar{r}_{eff}$ values. The values for a number of chronologies are shown as examples. These are the same chronologies used in the comparison of standardization methods in Section 3.7. The minimum number of trees required to reach SSS equal to 0.85 varies from three to seven.

3.7. A Comparison of Some Tree-Ring Standardization Methods

E. Cook and K. Briffa

This chapter has described a large array of techniques that can be used for standardizing ring widths and creating a mean chronology of tree-ring indices. In this section, some of the methods will be applied to six different collections of ring-width data. The results will be compared with the known characteristics and history of each tree-ring site and the known statistical properties of the ring-width data. These comparisons will highlight the strengths and weaknesses of the methods of the known properties of the data being standardized. However, they are not intended to determine if one method is superior to the others. While some techniques may work well in many situations, there is probably no one method that is universally superior.

The strengths and weaknesses of any tree-ring standardization method will be largely determined by the properties of the data being standardized and by the intended use of the standardized data. The definition of the expected signal (Briffa *et al.*, 1987) in the tree-ring data must be considered prior to selecting the method of standardization. Only after the signal has been defined can an appropriate method of standardization be chosen to minimize the noise. Thus, the definition of noise will be determined by the prior definition of the signal. Once a method is chosen, the ring-width data can be standardized to produce an estimate of the expected signal, which we will call the observed signal (Briffa *et al.*, 1987). Unlike most statistical estimators of population parameters, no statistical theory tells us how well the observed signal in tree rings estimates the expected signal. In most cases, we must rely on statistical measures of signal strength, frequency domain definitions of signal and noise, and knowledge about sites, stand histories, and tree biology to guide us.

3.7.1. Ring-width data sets

The six data sets used in this study were selected to provide a range of stochastic properties and standardization problems. The data sets reflect differences owing to species biology, site character, and disturbance or management history. A brief description of each ring-width data set will be given next.

Ditch Canyon (DC)

The species is ponderosa pine (*Pinus ponderosa*). The site is in the low-elevation, discontinuous coniferous forest zone of the southwestern United States, which has produced some of the finest tree-ring chronologies for dendroclimatic studies. The sampled trees are in an open-canopy stand, with minimal competition among trees and no known disturbance history. A chronology developed from these ring-width series has excellent statistical properties for dendroclimatic studies (Fritts and Shatz, 1975). The growth trends of the ring-width series are largely negative exponential in form. High-frequency variations (time scale < 10

years) in ring width are large and only moderately autocorrelated. This collection has the fewest potential standardization problems of the six data sets and comes closest to a control for comparing the different methods.

Twisted Tree-Heartrot Hill (TTHH)

The species is white spruce (*Picea glauca*). The site is in the discontinuous forest-tundra ecotone region of the Yukon Territory, Canada, and has been described previously in Jacoby and Cook (1981). The sampled trees are in an open-canopy stand with low competition among trees and no known history of disturbance. The growth trends tend to be negative exponential or linear in form, with a high proportion of the latter trends being positive in slope. The yearly variations in ring width are relatively small and dominated by very strong low-frequency fluctuations (time scale > 50 years) that are usually common to all trees. As a consequence, the ring-width series are highly autocorrelated even after any apparent trend has been removed. Although this collection has few standardization problems, the very strong low-frequency fluctuations and high autocorrelation make the series more sensitive to the method of detrending and any manipulation of the persistence structure.

Riukuselka (RIUK)

The species is Scots pine (*Pinus sylvestris*). The site represents old, unmanaged coniferous forest, typical of northern Scandinavia. The sampled trees were in relatively open habitat at the top of a hill less than 100 meters below the natural timberline. The sampled trees range in age from about 250 to over 450 years, with the majority in the range of 250–350 years. Competition among trees is not a significant factor affecting the age trends of the individual ring-width series. Consequently, the ring widths show a classic deterministic-type age-related decline over the length of each series. However, other than this, the series show relatively little variance at low frequencies (time scales > 50 years). Medium-frequency fluctuations (time scales > 10 and < 50 years) appear to be synchronous among most series.

Nancy Brook (NB)

The species is red spruce (*Picea rubens*). The site is in a montane boreal forest, typical of the higher elevations of the northern Appalachian Mountains in eastern North America. The ring-width series range from about 200 to 370 years in age, with the majority in the range of 250–300 years. The sampled trees were growing in a closed-canopy, old-growth stand with no known cutting history. Competition for light among neighboring trees is great, and the structure of the stand is strongly affected by gap-phase stand dynamics. This is reflected in the medium-frequency fluctuations (10–50 year) of ring width, which are frequently out-of-phase between trees owing to competition and disturbances. These and the longer-term growth trends are highly stochastic in form and variable among trees. The yearly variations in ring width are dominated by these low- and

medium-frequency fluctuations. This collection is an excellent example of tree-ring data having a common signal that is strongly contaminated by competition effects in the stand. It is a more difficult standardization problem compared with the previous three cases.

Lake Orbell (OBL)

The species is silver beech (*Nothofagus menziesii*), a Southern Hemisphere evergreen beech. The collection of 20 ring-width series is from a site near the alpine timberline on the southern island of New Zealand. The ring-width series exceed 200 years of age. The site and stand have been described previously by Norton (1983a). It is a closed-canopy forest of mixed *Nothofagus* species where competition among trees is likely to be high. Consequently, the long-term growth trends tend to be disturbed by competition in the stand.

Savenake (SAV)

The species is the European pedunculate oak (*Quercus robur*). The site is typical of an *ancient* English parkland wood. It forms part of a royal forest, which has been managed for centuries, and is commercially managed today. The sampled trees were typically between 200–300 years of age. The sampled trees are growing in relatively open forest, but the density of trees is great enough to mean that competition will be a significant factor influencing the evolution of the *biological* or age-related growth curves of the individual trees. Sampling was restricted to an area of forest of about one hectare.

3.7.2. Methods of standardization and statistical assessment

Four methods of standardization were performed on each data set: linear and negative exponential detrending (LE), spline detrending using the 67%n criterion (SP), 67%n spline detrending and autoregressive modeling (AR), and filtering with a 60-year Gaussian low-pass filter (GF). Each method has been described earlier. The LE and GF methods represent the extremes in terms of growth-curve flexibility, with the former being the most rigid and the latter the most flexible. Thus, in terms of trend removal and its ultimate effect on low-frequency variance, the LE and GF methods should provide the sharpest contrasts, with the SP and AR methods falling somewhere in between. The SP and AR methods only differ in terms of autoregressive modeling, which may have more subtle effects on the final chronology.

The summary statistics used for comparing each standardization method are mean sensitivity (MS), standard deviation (SD), coefficient of skew (SK), coefficient of kurtosis (KT), lag-1 autocorrelation coefficient (R1), and the average correlation among trees for the common overlap period among series [RBar; equation (3.39a)]. The MS, SD, and R1 statistics are frequently used to assess the statistical-dendroclimatological quality of tree-ring chronologies (Fritts and Shatz, 1975; Fritts, 1976). The SK and KT statistics are included to assess any

higher-order effects on the probability distribution owing to the method of standardization. The time period used for all but the RBar comparisons was 1701–1975 for each data set – except Ditch Canyon, which was 1701–1971. No RBar values are included for the AR chronologies because this method uses prewhitened indices rather than simple detrended indices, which contain autocorrelation. Hence, the AR RBar may not be strictly comparable with that computed using the other standardization methods. In addition, the RBar for site SAV is a weighted average of the inter-series correlations over the maximum possible overlap period between series because the ring-width series do not overlap sufficiently.

Besides these summary statistics, we will look at the correlations among the chronologies developed by the different standardization methods and use spectral analysis to search for frequency-dependent effects. Each spectrum is computed from 55 lags of the autocorrelation function and smoothed with the Hamming window.

Table 3.5 shows the summary statistics for the six sites and four standardization methods. It is readily apparent that most of the statistics are extremely similar regardless of the method of standardization. The greatest differences are seen in R1 and RBar. Differences in R1 reflect how much low-frequency variance has been removed by each method. The LE method generally removes the least; the GF method, defined by the 50% cutoff of 60 years, removes the most. However, the way in which this low-frequency variance removal translates into the estimates of RBar is not predictable. In some cases (i.e., site DC and NB), the RBar increases from LE to GF; in other cases (i.e., TTHH and SAV), the RBar decreases from LE to GF. The differences in performance reflect the differences in the low-frequency properties of the raw data. For both DC and especially NB, most of the out-of-phase variance between series is in the wavelengths longer than about 60 years in duration. A 60-year low-pass filter performs better in removing this variance than does a negative exponential or linear regression curve, hence the increased RBar using the GF method. In contrast, both the TTHH and SAV ring-width collections have lower-frequency fluctuations that tend to be in phase. A 60-year low-pass filter removes most of this in-phase variance, which leads in these cases to a reduced RBar.

The correlations between chronologies as a function of the standardization method are shown in *Table 3.6*. The correlations are usually high and often greater then 0.95. However, some are quite low, i.e., 0.68 (LE versus GF) for site TTHH. The greatest differences are found between the LE, SP, and GF methods, with AR being very similar to SP. These differences largely reflect how much low-frequency variance has been left in the final chronology by each standardization method. This fact is graphically revealed in the variance spectra of the different chronologies [*Figures 3.17(a–f)*]. Virtually all of the significant ($\alpha = .20$) differences between chronologies are in the low frequencies, with the 60-year GF method being most different by far. This is not surprising considering that most of the variance in the original ring widths is composed of low-frequency growth trends and fluctuations. At wavelengths shorter than about 20 years in duration, more subtle differences are apparent. However, it is impossible to say to what extent they are meaningful with regard to the intended application.

Table 3.5. Within-series summary statistics for the tree-ring standardization tests: mean sensitivity (MS); standard deviation (SD); lag-1 autocorrelation (R1); coefficient of skew (SK); coefficient of kurtosis (KT); average correlation between trees for the common overlap period among series (RBar); linear–exponential detrending (LE); 67%n spline detrending (SP); autoregressive modeling (AR); 60-year Gaussian low-pass filter (GF).

Site: Ditch Canyon (DC)	*Standardization method*			
Statistics	LE	SP	AR	GF
MS	.382	.385	.387	.392
SD	.391	.374	.374	.367
R1	.416	.383	.367	.256
SK	.092	.009	−.028	−.038
KT	2.905	2.774	2.858	2.869
RBar	.598	.609	–	.721
Site: Twisted Tree-Heartrot Hill (TTHH)				
MS	.126	.125	.126	.125
SD	.224	.186	.185	.126
R1	.773	.655	.627	.223
SK	.079	−.074	−.077	.198
KT	2.394	2.879	2.866	3.215
RBar	.380	.399	–	.345
Site: Riukuselka (RIUK)				
MS	.169	.169	.176	.171
SD	.262	.250	.251	.201
R1	.692	.669	.635	.402
SK	−.026	−.014	−.096	−.019
KT	2.871	2.780	2.791	3.235
RBar	.454	.521	–	.526
Site: Nancy Brook (NB)				
MS	.114	.116	.118	.116
SD	.182	.142	.142	.133
R1	.708	.515	.465	.399
SK	.224	.017	.087	.053
KT	3.178	3.613	3.866	3.826
RBar	.218	.383	–	.363
Site: Lake Orbell (LO)				
MS	.263	.264	.272	.264
SD	.314	.295	.278	.260
R1	.398	.337	.211	.166
SK	.628	.457	.431	.222
KT	3.843	3.598	3.595	3.092
RBar	.270	.370	–	.316
Site: Savenake (SAV)				
MS	.148	.148	.161	.147
SD	.189	.178	.193	.166
R1	.506	.465	.474	.388
SK	.372	.201	.052	.017
KT	2.931	2.763	2.625	2.795
RBar	.397	.327	–	.344

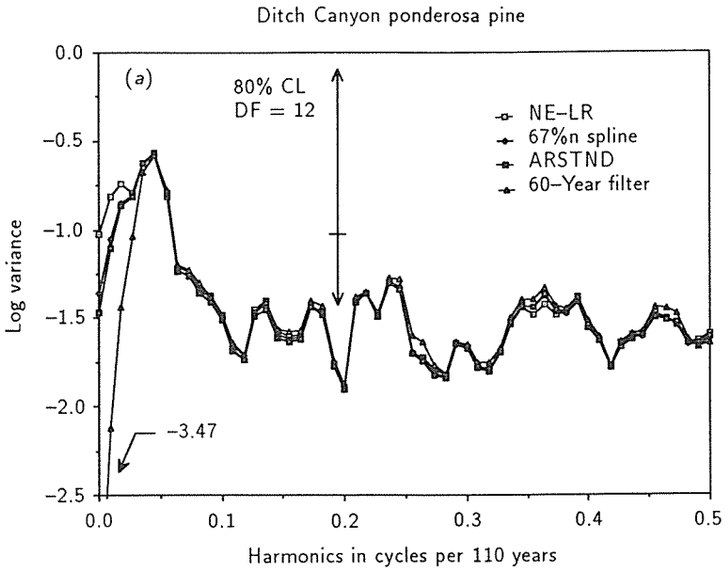

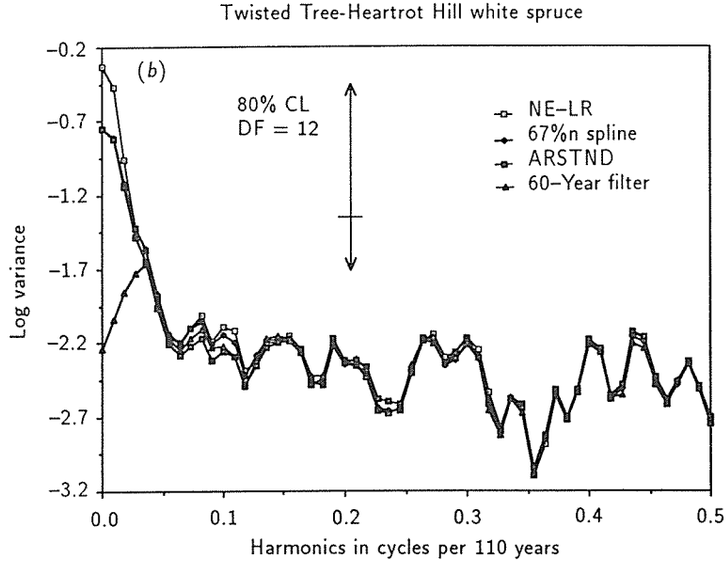

Figure 3.17. The variance spectra of the tree-ring chronologies for six sites produced by four different methods of standardization: (*a*) Ditch Canyon; (*b*) Twisted Tree-Heartrot Hill; (*c*) Nancy Brook; (*d*) Riukuselka; (*e*) Lake Orbell; (*f*) Savenake. Each spectrum is computed from 55 lags of the autocorrelation function and smoothed with the Hamming window.

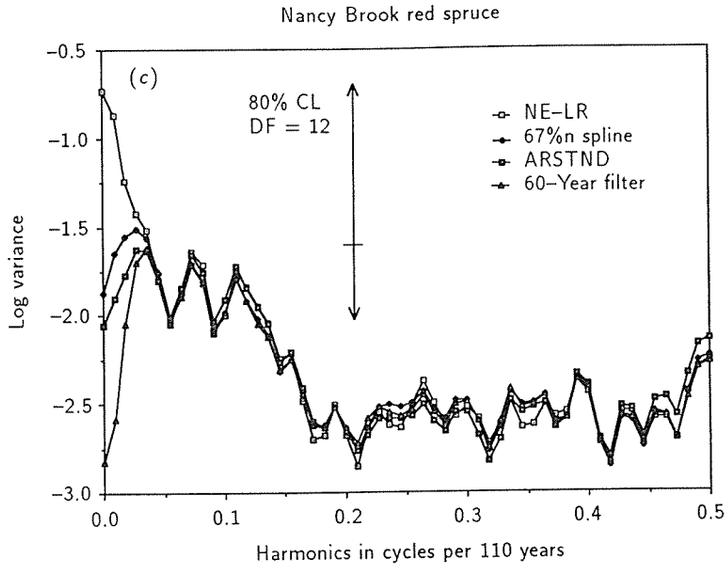

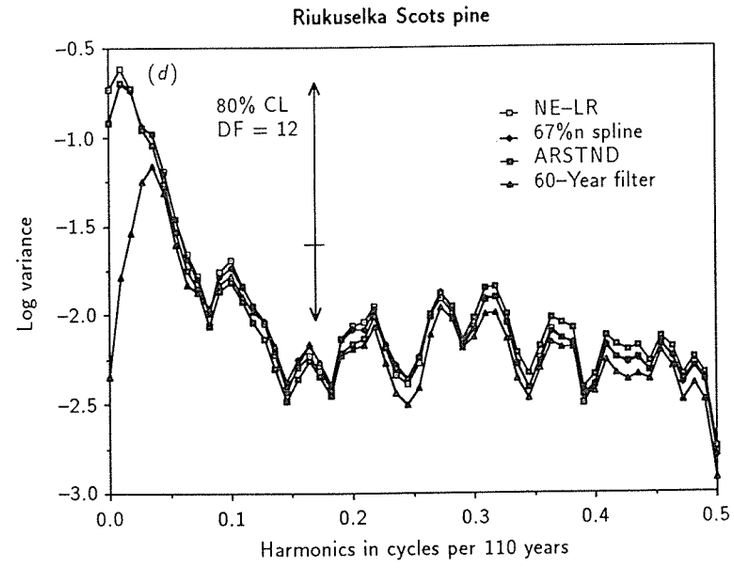

Figure 3.17. Continued.

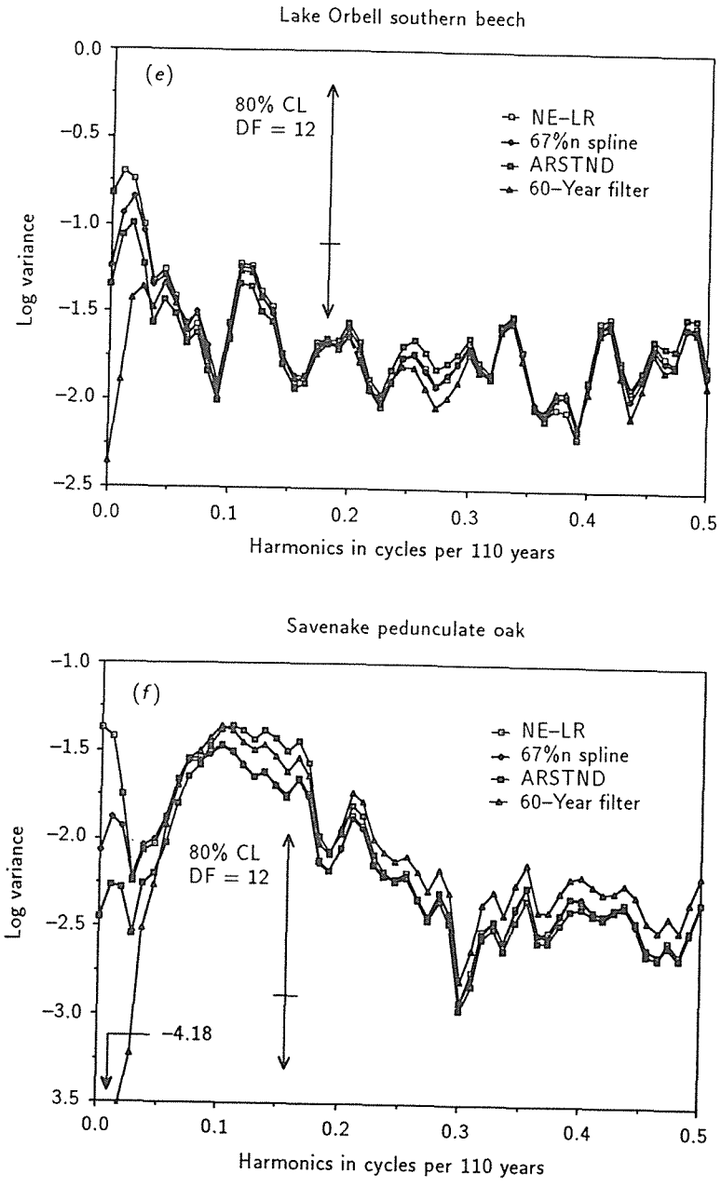

Figure 3.17. Continued.

Table 3.6. Correlations between the chronologies of each site developed by the four standardization methods. The standardization methods are linear–exponential detrending (LE); 67%*n* spline detrending (SP); autoregressive modeling (AR); 60-year Gaussian low-pass filter (GF).

	Ditch Canyon				*TTHH*			
	LE	SP	AR	GF	LE	SP	AR	GF
LE	1.00	0.99	0.98	0.94	1.00	0.95	0.94	0.68
SP		1.00	1.00	0.97		1.00	0.99	0.82
AR			1.00	0.97			1.00	0.81
GF				1.00				1.00
	Ruikuselka				*Nancy Brook*			
	LE	SP	AR	GF	LE	SP	AR	GF
LE	1.00	0.99	0.98	0.87	1.00	0.81	0.79	0.78
SP		1.00	0.99	0.90		1.00	0.98	0.96
AR			1.00	0.89			1.00	0.97
GF				1.00				1.00
	Lake Orbell				*Savenake*			
	LE	SP	AR	GF	LE	SP	AR	GF
LE	1.00	0.98	0.97	0.91	1.00	0.98	0.93	0.93
SP		1.00	0.99	0.95		1.00	0.96	0.97
AR			1.00	0.95			1.00	0.92
GF				1.00				1.00

The very small differences between the SP and AR chronologies reflect the fact that autoregressive modeling has its strongest effect on the error variance of the mean-value function, a characteristic that we have not reported on here because of the AR method.

3.7.3. Conclusions

These comparisons indicate that the method of standardization can have profound effects on the resultant chronology. These effects are most readily seen in the variance spectrum where they are largely restricted to the lowest frequencies. Depending on the application of the tree-ring chronology and the definition of signal and noise, an *a priori* decision must be made about what will be retained as signal (or discarded as noise) in the low frequencies of tree-ring data. We do not propose any guidelines for making this decision because it is likely to be completely data and application dependent. However, we strongly caution the user of any tree-ring standardization method to think carefully about the definitions of signal and noise, as they pertain to the tree-ring application at hand, the site from where the tree-ring data came, and the frequency-domain properties of the raw tree-ring data. And, never use any tree-ring standardization method or computer program as a *black box*.

This chapter has covered a wide range of concepts and statistical techniques useful in developing tree-ring chronologies for environmental studies.

Tree-ring series will be used increasingly in the future as monitors of environmental change for the simple reason that they are available where no other comparable long-term environmental sensors exist. In the process, the statistical methods used to analyze tree rings will change and improve. Thus, we do not claim any timelessness in the methods we have described. However, we hope that the chapter will provide a reference for the present and a basis for future developments in the science.

CHAPTER 4

Methods of Calibration, Verification, and Reconstruction

Chapter Leaders: H.C. Fritts and J. Guiot
Chapter Contributors: G.A. Gordon and F. Schweingruber

4.1. Introduction
H.C. Fritts

Often tree-ring variations can be correlated with the variations in one or more environmental factors that are known to influence growth. In such cases, it should be possible to find a statistical growth-environment relationship that can be used to deduce or reconstruct the past variations in the environment from past variations in tree-ring growth. The procedure that estimates the statistical growth-environment relationship is called ***calibration.*** The word calibration was originally applied to the process of finding the caliber (area of cross section) of a tube, as in calibrating a thermometer. The word has been extended to include the determination of absolute values appropriate to selected fixed points of an instrument (McIntosh, 1972). In paleoclimatology, calibration involves the fitting of a statistical equation or model that can be applied to one or more ***predictors*** to estimate or reconstruct one or more ***predictands.*** One set of predictor and predictand data, called the dependent set, is used to estimate the coefficients of the calibration equation. The remaining data are outside of the interval used for calibration, so they are referred to as independent data. If climate is the predictor and tree-ring variation is the predictand, then the equation is referred to as a ***response function.*** In response functions, the magnitudes and the signs of the coefficients of the statistical equation indicate the importance and signs of the tree-ring response to the calibrated variables of climate.

If tree-ring chronologies are the predictors and climate the predictand, then the equation is referred to as a ***transfer function.*** The signs and magnitudes of the transfer function coefficients are not usually interpreted, although they can be. Instead, the coefficients are applied to tree-ring data to obtain estimates or reconstructions of climate.

E. R. Cook and L. A. Kairiukstis (eds.), Methods of Dendrochronology, 163–217.

A model is a simplified picture of a functional relationship used to solve a problem (Jorgensen, 1986). The model will never include all features of a system, but it should include all characteristics that are essential to the problem to be solved (Jorgensen, 1986). Following the notation of Lofgren and Hunt (1982), one particular functional relationship discussed in this chapter can be conveniently stated as

$$g_t = f(c_t) \quad , \tag{4.1}$$

where g_t is a standardized tree-ring chronology value for year t and c_t is either a causally linked climate factor for year t or a factor correlated with a causally linked factor. If the relationship is linear, it can be estimated by the following statistical equation:

$$y = F(x) + \varepsilon \quad , \tag{4.2}$$

where F is a linear function between x and y, and ε is an error component that includes relationships, which are not modeled, that exist. Often, more than one factor may be involved in the relationship so that a multiple linear regression with m predictors may be a better model:

$$y = \sum_{j=1}^{m} x_j \beta_j + \varepsilon \quad . \tag{4.3}$$

Calibration involves certain assumptions that lead to important limitations:

- The relationships to be modeled are assumed to be time stable. Those that occur in the present are assumed to have occurred in the past (Fritts, 1976).
- Conditions in the past can be reconstructed from growth observations only if conditions in the calibration period are analogous to the conditions in the past (Webb and Clarke, 1977; Bryson, 1985).
- The relationship between the predictands and predictors must resemble the model structure that was applied (Lofgren and Hunt, 1982). For example, linear relationship are calibrated using linear equations, such as simple regression and multiple regression.
- When parametric statistics are tested for significance they assume that the data are normally distributed. Outliers and any other nonnormative form of the data can distort the significance testing. Graumlich (1985) and Graumlich and Brubaker (1986) examine each tree-ring chronology carefully for normal and extreme values before using it in a calibration. In addition, they also use detailed diagnostic tests on the model residuals to search for outliers and influential observations that can distort the calibration equation.

- Most statistical testing procedures also assume that the observations are independent of each other. The presence of dependence or autocorrelation among successive observations in time or among observations in space can seriously reduce the number of degrees of freedom used for statistical significance testing. Livezey and Chen (1983) provide guidelines for dealing with spatial correlation, and Mitchell *et al.* (1966) suggest a way of dealing with first-order autocorrelation in time series.

One feature of ring-width chronologies requires some additional comment. Very low index values corresponding to climatic stress are often more consistent (the error is less) among chronologies from neighboring trees than very high index values (Fritts, 1976). This produces one type of nonlinearity in which the error (or noise) in the climatic signal is directly proportional to the magnitude of the mean ring-width index.

4.2. Methods of Calibration

J. Guiot

The aim of the model using equation (4.3) is to estimate values of y when contemporary values of the variables x_j are known. We may generalize equation (4.3) to cases where p variables y_k are available. Climate reconstruction is of interest when the tree-ring series are long, with a common size denoted nx, and the climate series are shorter, with a size denoted ny ($ny << nx$). The aim is then to extrapolate (or reconstruct) matrix ${}_{ny}\mathbf{Y}_p$ from matrix ${}_{nx}\mathbf{X}_m$, where nx is the number of rows in the matrix $\mathbf{X}$, m is the number of columns in the matrix $\mathbf{X}$, ny is the number of rows in the matrix $\mathbf{Y}$, and p is the number of columns in the matrix $\mathbf{Y}$. To facilitate the discussion, we assume that the ny observations are common among the predictors and the predictands. In addition, ny is usually decomposed as:

$$ny = n + n' \quad ,$$

where n is the number of observations used for calibration and n' is the number of observations used for an independent verification (see Section 4.3).

The variables are standardized in the following equations so that the elements x_{ij} are replaced by

$$\begin{aligned} x_{ij} &\rightarrow (x_{ij} - \bar{x}_j)/sx_j \\ y_{ik} &\rightarrow (y_{ik} - \bar{y}_k)/sy_k \quad , \end{aligned} \tag{4.4}$$

where the bar denotes the mean and s denotes the standard deviation of x_j and y_k. Many useful books exist on the matter of regression. Draper and Smith

(1981), Wonnacott and Wonnacott (1981), and Tomassone *et al.* (1983) are a few of them.

4.2.1. Multiple regression analysis

The multiple regression may be written as follows:

$$ {}_n\mathbf{Y}_p = {}_n\mathbf{X}_m\mathbf{B}_p + {}_n\mathbf{E}_p \quad , \tag{4.5} $$

where ${}_m\mathbf{B}_p = (\mathbf{X}'\mathbf{X})^{-1}\,\mathbf{X}'\mathbf{Y}$ and ${}_n\mathbf{E}_p$ is the matrix of residuals. The matrices $\mathbf{X}$ and $\mathbf{Y}$ are assumed to be standardized as in equation (4.4). Note also that equation (4.5) is the general form of multiple regression because m predictors are simultaneously estimating p predictands.

Equation (4.5) states that the climate is linearly related to the variations of tree growth by coefficients b_{jk}, which are estimates of the population coefficients β_{jk}. Several conditions may limit the quality of the estimates: first, the number of observations (n) may be too small to provide realistic estimates of the population parameters; second, the actual relationship that is modeled may not necessarily be a linear one; third, it is sometimes impossible to isolate the effect of one climatic factor on the growth; and finally, the predictors may be highly correlated, which creates a problem when the matrix $\mathbf{X}'\mathbf{X}$ in equation (4.5) is inverted.

These limitations can sometimes be resolved by using another type of model. In most cases, it is necessary to examine the variability of $\mathbf{B}$ and to check if the relationships are stable using independent observations. The variability of the estimates of the regression coefficients is given by the covariance matrix $\mathbf{V}$ of the coefficients. For the kth predictand, it is

$$ {}_m\mathbf{V}(\mathbf{B}_k)_m = \mathbf{S}e_k{}^2\,(\mathbf{X}'\mathbf{X})^{-1} \quad , \tag{4.6} $$

where $\mathbf{S}e_k{}^2$ is the residual variance of the kth predictand, i.e., the portion of the variance ($\mathbf{S}y_k{}^2$) of the kth predictand, which is not explained by the predictors. The variance explained is given by

$$ \mathbf{EV}_k = (\mathbf{S}y_k{}^2 - \mathbf{S}e_k{}^2)/\mathbf{S}y_k{}^2 \quad . \tag{4.7} $$

When $\mathbf{EV}$ is multipled by 100, it gives the percentage of variance explained. To know if the coefficient b_{jk} is statistically significant, we have to compare b_{jk} with the jth diagonal element $\mathbf{S}b_{jk}$ of $\mathbf{V}(\mathbf{B}_k)$.

It is preferable to use multiple regression when the tree-ring series are not highly correlated or when only a few series are considered (Shiyatov, 1986; Hughes *et al.*, 1984; Aniol and Eckstein, 1984).

4.2.2. Selection of the predictors (screening)

The stepwise regression attempts to reduce the correlation between predictors by selecting a subset of them that are well correlated with the predictand, but not with each other. The procedure progressively improves the regression equation by adding and/or deleting predictors according to their ability to reduce the residual sum-of-squares for a given climatic variable. This reduction may be tested for significance using some predefined criterion, such as the F test for incoming variables (Draper and Smith, 1981). Examples of screening may be found in Cook and Jacoby (1983), Fritts (1962), or Berger *et al.* (1979).

Because the selection of the *best* predictors is largely dependent on the criterion that was predefined and because we are never sure that it is effectively the *best*, it is preferable in fact to try all possible subsets. The number of combinations is 2^m (32,768 for $m = 15$). Fast algorithms make this possible in practice (e.g., Furnival and Wilson, 1974).

Another method of screening is the backward-elimination procedure. It starts with a regression equation containing all candidate predictors. The one predictor variable that explains the least variance is eliminated, a new regression is calculated, and the next one that explains the least variance is eliminated. This procedure continues until the Fisher ratio (F) is as high or higher than a preselected significance level. The F ratio, based on the inclusion of j predictors in the model, is calculated as

$$ F = (Sy^2 - Se^2)(n - j - 1)/Se^2/j \quad , \tag{4.8} $$

where Se^2 is the mean residual variance computed over the p predictands and Sy^2 is the corresponding mean variance of the p predictands. This is used to find a compromise between maximizing the variance explained and minimizing the number of predictors used in the regression.

Briffa *et al.* (1983) have used another Fisher criterion to determine the subset of j predictors that explains most of the predictand variance within the total set of m candidate predictors, according to the respective loss of degrees of freedom. For one predictand, it is defined as

$$ F = (\mathrm{EV}_m - \mathrm{EV}_j)(n - m - 1)/(1 - \mathrm{EV}_j)/(m - j) \quad , \tag{4.9} $$

where EV_m is the variance explained with all m candidate predictors in the model and EV_j is the variance explained by the subset of j predictors.

4.2.3. Regression after extracting principal components

When the predictors are correlated or there are a very large number of them, they can be replaced and their number reduced by substituting a set of uncorrelated but equivalent variables. These are the principal components (PC) or the

empirical orthogonal functions. The PCs are the eigenvectors ($\mathbf{A}x$) of the matrix $\mathbf{X'X}/\mathbf{n}$ (the correlation matrix of the predictors). The relationship between the original predictors and their corresponding PCs is

$$1/n\mathbf{X'X}\,\mathbf{A}x = \mathbf{A}x\,\mathbf{L}x \quad , \tag{4.10}$$

where $\mathbf{L}x$ is the diagonal matrix of the eigenvalues. Because of the orthogonality properties of $\mathbf{A}x$, we have

$$(\mathbf{X'X})^{-1} = \mathbf{A}x\,\mathbf{L}x^{-1}\,\mathbf{A}x'/n \quad . \tag{4.11}$$

The correlation between the predictors has the consequence that the last eigenvalues are close to zero within the limits of computation accuracy. Thus $\mathbf{L}x^{-1}$ may have some very large elements that are poorly estimated. From equations (4.6) and (4.11), it also follows that these small eigenvalues lead to very large standard errors in the estimates of the regression coefficients. A way to avoid this problem is to use only $qx (qx < p)$ columns of $\mathbf{A}x$ and a submatrix (qx, qx) of $\mathbf{L}x$. The choice of the number qx varies with the method of selection.

- qx may be the number of PCs explaining together more than a certain percentage of the total variance. Ninety percent is a reasonable cutoff level. Fritts *et al.* (1979) and Fritts (forthcoming) used this test to select 15 out of a possible 65 tree-ring PCs, which amounted to only 69% of the total chronology variance.
- qx may be the number of PCs with an eigenvalue > 1 (i.e., greater than the average value of the eigenvalues extracted from a correlation matrix). An eigenvalue of 1 is also equal to the expected eigenvalue extracted from a correlation matrix of uncorrelated variables.
- qx may be selected using the *scree* line approach (Tatsuoka, 1974), in which the eigenvalues are plotted as a function of their order and qx is the number of eigenvalues above the point where the change in slope becomes nearly constant. Fritts (forthcoming) used this method, among others, for selecting the meaningful PCs of climate.
- qx may be selected using the PVP criterion (Guiot, 1981, 1985a), which is the point where the cumulative product of the eigenvalues falls just below 1. The cutoff for the PVP is at the point where the cumulative product is equivalent to the determinant of a correlation matrix of uncorrelated variables.
- Another objective criterion may be based on Monte Carlo analysis (Preisendorfer *et al.*, 1981). One hundred random data sets are generated with sizes equivalent to these of the original data set. From these random correlation matrices, 100 sets of random eigenvalues are computed. The means and standard deviations of these eigenvalues are calculated. The qx eigenvalues are retained that exceed the mean random eigenvalue trace by more than two standard deviations. This method provides a very strict criterion because only the very largest PCs are retained for analysis. The method is well suited for cases where only interpretation is important, because it reduces the number qx to only the largest and most important PCs.

A mixing of a simulation method and the PVP criterion will be presented in the discussion on the bootstrap method, Section 4.2.7. Briffa *et al.* (1983) compared several criteria for selecting qx in regression analysis. They found that the PVP criterion produced the most satisfactory results based on verification tests on the independent data withheld from regression analysis.

Finally ${}_m\mathbf{B}_p$ in equation (4.5) becomes

$${}_m\mathbf{B}_p = {}_m\mathbf{A}x_{qx}\mathbf{L}x_{qx}{}^{-1}{}_{qx}\mathbf{A}x'{}_m\mathbf{X'}_n\mathbf{Y}_p/n \quad . \tag{4.12}$$

If $qx = p$, equation (4.12) is identical to equation (4.5), given the equality between the eigenvectors and the original data shown in equation (4.11). The variability of the regression coefficients is estimated, from equations (4.6) and (4.11), as

$${}_m\mathbf{V}(\mathbf{B}_k)_m = \mathbf{S}e_k{}^2\,\mathbf{A}x\,\mathbf{L}x^{-1}\,\mathbf{A}x'/n \quad . \tag{4.13}$$

Because equation (4.13) has the eigenvalues in the denominator, the use of a PC with a small eigenvalue may considerably increase the variance of the regression coefficients. Although the removal of PCs with small eigenvalues may decrease the percentage of variance explained in the calibration interval, the higher precision of the resultant regression coefficients may increase the explained variance on the independent interval and produce more reliable reconstructions.

4.2.4. Canonical correlation and regression analysis

Canonical correlation analysis finds linear combinations of predictors and predictands that are the best correlated. When only one predictand is analyzed, this is the same as multiple regression.

We assume that all the variables are standardized. Details on canonical correlation are given by Clark (1975) and Dagnélie (1975). The canonical pairs are defined as linear combinations of matrices $\mathbf{X}$ and $\mathbf{Y}$:

$$\begin{aligned} {}_n\mathbf{U}\mathbf{x}_q &= {}_n\mathbf{X}_m\mathbf{V}\mathbf{x}_q \\ {}_n\mathbf{U}\mathbf{y}_q &= {}_n\mathbf{Y}_m\mathbf{V}\mathbf{y}_q \quad , \end{aligned} \tag{4.14}$$

where $\mathbf{Vx}$ and $\mathbf{Vy}$ are the coefficient matrices of the linear combinations (the canonical pairs or variates) and q is the number of canonical pairs $\leq \min(p, m)$.

The definition of the canonical pairs must satisfy three conditions:

$$
\begin{aligned}
{}_q\mathbf{Ux}'_n\mathbf{Ux}_q &= {}_q\mathbf{I}_q \\
{}_q\mathbf{Uy}'_n\mathbf{Uy}_q &= {}_q\mathbf{I}_q \\
{}_q\mathbf{Ux}'_n\mathbf{Uy}_q &= {}_q\mathbf{Uy}'_n\mathbf{Ux}_q = {}_q\mathbf{C}_q \quad ,
\end{aligned}
\tag{4.15}
$$

where $\mathbf{I}$ is the identity matrix of order q, having 1s on the main diagonal and 0s elsewhere, and $\mathbf{C}$ is the diagonal matrix of the canonical correlations. These three conditions mean that the two components of a canonical pair are correlated with a correlation equal to its corresponding element in $\mathbf{C}$, each canonical pair is independent (or uncorrelated) with every other canonical pair, and each pair has unit variance. In addition, the canonical pairs are sorted from highest to lowest canonical correlation.

The computation of canonical correlations requires the inversion of both the $\mathbf{X}$ and $\mathbf{Y}$ correlation matrices (Glahn, 1968). This means that canonical correlation analysis, like multiple regression analysis, may produce unstable results when there are high correlations within the predictor and predictand matrices. When such high correlations exist, or when there is the need to reduce the dimensions of either data set, principal components analysis on either or both data sets is recommended before proceeding with the canonical analysis. The PCs extracted from the $\mathbf{X}$ and $\mathbf{Y}$ matrices will have the necessary orthogonality, and the dimensions of the problem can be reduced through the use of a PC subset selection criterion such as the PVP.

The $\mathbf{Vx}$ and $\mathbf{Vy}$ matrices in equation (4.14) contain the canonical weights that maximally correlate the m predictors and p predictands. However, these weights may not be easily interpretable expressions of the original variables from which they were derived. However, the original variables fed into the canonical analysis may be estimated (Glahn, 1968; Fritts, 1976; Blasing, 1978) as

$$
{}_n\mathbf{Y}_p = {}_n\mathbf{X}_m\mathbf{Vx}_q\mathbf{C}_q{\mathbf{Vy}_p}^{-1} \quad . \tag{4.16}
$$

It is at this point that canonical analysis changes from a correlation model to a regression model. The canonical solution of the multiple regression coefficients in equation (4.5) is then given by

$$
{}_m\mathbf{B}_p = {}_m\mathbf{Vx}_q\mathbf{C}_q{\mathbf{Uy}_p}^{-1} \quad . \tag{4.17}
$$

Different ways are possible to determine q:

- If all q variate pairs of the original data are used, the analysis becomes standard multiple regression analysis. In this case, canonical regression would only be an expeditious way of regressing all predictors against each predictand, without any benefit of screening the candidate predictors.

- Select q by using the PVP criterion (or another) to determine the number of eigenvalues different from zero in the inversion of $\mathbf{X}'\mathbf{X}$, i.e., qx, and in the inversion of $\mathbf{Y}'\mathbf{Y}$, i.e., qy. In this case, q is then equal to min (qx, qy). This choice of q is based on the assumption that the PC selection criterion has screened out the noise in the predictors and predictands, therefore making all of the retained variance useful for canonical regression analysis.
- Another way is to test the canonical correlation using a chi-square test, based on the Wilks' lambda statistic, to determine the number of canonical correlations different from zero (Clark, 1975)

$$
\begin{aligned}
\Lambda(q) = \; & -[n - 0.5\,(m + p + 3)] \\
& \ln\{(1 + c_q^2)(1 + c_{q+2}^2)\cdots[1 + c_{min(p,m)}^2]\} \quad .
\end{aligned}
\tag{4.18}
$$

  The expression $\Lambda(q)$ is approximately χ^2-distributed with $(p - q + 1)$ and $(m - q + 1)$ degrees of freedom. Then, q is selected where $\Lambda(q) < \chi^2(1 - \alpha)$ and $\Lambda(q + 1) > \chi^2(1 - \alpha)$. This test can be applied either to the original variables or to a subset of retained PCs, but it measures only the degree of correlation without regard to the amount of variance reduced on the predictand variables in regression.
- An F test is a better test of regression relationships because it compares the variance reduced on the dependent data set by each canonical pair. Each pair may then be accepted or rejected depending upon whether the pair reduces a significant amount of the dependent data variance.

The canonical regression as presented by Blasing (1978) was first applied to tree-ring data by Fritts *et al.* (1971). The details on this kind of application are given in Fritts (1976), and an example (from Fritts, forthcoming) is presented in Section 4.5.

4.2.5. The best analogs method

This method differs from regression in that observations rather than the variables are compared. It is useful when variables with different distributions (i.e., tree rings and historical records) are to be analyzed for common information. While in regression, correlation coefficients between variables are calculated, here an observation vector i is compared with another observation vector k, using a weighted Euclidean distance:

$$
d_{ik}^2 = \sum_{j=1}^{m} [w_j(z_{ij} - z_{kj})]^2 \quad , \tag{4.19}
$$

where w_j is a coefficient used to weight the influence of the variable j in the distance: the w_j may be either equal to 1 (the unweighted case: UW) or not equal

to 1 (the weighted case: W). Canonical correlation analysis may suggest the choice of w_j. The loadings of the first canonical pair are used to represent the *optimal* weights to maximize the correlation between the m predictors and the p predictands, i.e., the first column of **Vx** (Guiot, 1985b). The distance measures z_{ij} are defined according to the standardization process chosen:

$$\begin{aligned}
&\text{US: } z_{ij} = x_{ij} && \text{(unstandardized case)}\\
&\text{SD: } z_{ij} = (x_{ij} - \bar{x}_j)/S_j && \text{(standardization by the}\\
&&& \quad\text{standard deviation)}\\
&\text{LG: } z_{ij} = \ln x_{ij} && \text{(natural logarithm transform)}\\
&\text{MN: } z_{ij} = x_{ij}/\bar{x}_j && \text{(standardization by the mean).}
\end{aligned} \tag{4.20}$$

Other cases are possible, but these four are sufficient in most analyses. The first one is well adapted when the variables are homoscedastic (i.e., with similar variance), and the second one is useful in most cases. When the variables are necessarily positive and the probability distributions are asymmetric, the two last cases are preferable.

A threshold, dc, must be chosen for this distance. If a tolerance of one standard deviation is acceptable for the variables, we have:

$$\begin{aligned}
&\text{US: } dc = \sum_{j=1}^{m} (w_j S_j)^2\\
&\text{SD: } dc = \sum_{j=1}^{m} w_j^2\\
&\text{LG: } dc = \sum_{j=1}^{m} 2w_j^2\\
&\text{MN: } dc = \sum_{j=1}^{m} (w_j S_j)/\bar{x}_j)^2 \quad .
\end{aligned} \tag{4.21}$$

The LG threshold is justified by the fact that the variance of the ratio of the logarithm of two random variables tends to two when the sample size increases.

The k_i observations, analog to the ith observation, i.e., d_{ik}^2 is less than dc, are analyzed exclusively in the subset $(1, n)$. The estimate of y_{ij} is then given by

$$\hat{y}_{ij} = \sum_{k=1}^{k_i} (y_{kj}/d_{ik}^2)/(\sum_{k=1}^{k_i} d_{ik}^{-2}) \qquad j = 1, \ldots, p \quad . \tag{4.22}$$

This method is not an extrapolative method, since it is not possible to obtain estimates forward or backward in time beyond the limits of the actual values.

4.2.6. Multivariate autoregressive analysis

Multivariate autoregressive (AR) models are a generalization of univariate AR models (Box and Jenkins, 1970). The normal formulation of the multivariate AR model allows for the prediction of several time series, each from its own past and from the past of the other causally linked series. Here, because we want to create a transfer function for reconstructing climate from tree rings, the formulation is one in which climate is estimated from its own past as well as contemporary climatic information contained in the tree rings. The information contained in the past represents the delay or lagged response of trees to climate and the autoregression (or internal predictability) of the climate series itself.

The general equation for this model is

$$y_{ik} = \sum_{l=1}^{s} a_{lk} y_{(i-l)k} + \sum_{j=1}^{m} \sum_{l=0}^{s} b_{ljk} x_{(i-l)j} + e_{ik} \tag{4.23}$$

for $k = 1, \ldots, p$ and for $i = 1, \ldots, n$, where the first summation concerns the lagged climate predictand (autoregressive terms) and the second summation concerns the lagged tree-ring predictors. In Guiot (1986), an equivalent model has been selected for the reconstruction of June–July temperature in Marseille from one tree-ring series (Vallee des Merveilles, French Alps):

$$\hat{y}_i = a_7 y_{i-7} + b_0 x_i \quad , \tag{4.24}$$

where the subscripts k and j are omitted because $p = m = 1$. Various combinations of ARMA analysis and regression analysis have been used by Cook and Jacoby (1983), Guiot *et al.* (1982c), Guiot (1984), Meko (1981), and Meko *et al.* (1980).

A method of estimation for such models is given by Jones (1978, 1985) for the case where $s_o = s_1 = \cdots = s_m = s$. The method given below uses an algorithm of nonlinear maximization (partial quadratization, in Legras, 1980). This method allows the nonsignificant lag (or delay) terms to be constrained to zero. Thus, only the most significant lags in each predictor are used to estimate climate.

4.2.7. The bootstrap method for estimating standard errors

The bootstrap method is a recent technique (Efron, 1979) developed for estimating standard errors of statistical estimators and related statistics. The idea behind the bootstrap method is that the available observations of a variable contain the necessary information to construct an empirical probability distribution of any statistic of interest. Its application does not require any theory about the true underlying probability distribution of the statistic. Therefore, the bootstrap can provide standard errors of statistical estimators even when no theory exists.

This is done is through techniques of Monte Carlo simulation. The original observations are sampled with replacement in a suitable way to construct new data (pseudo-data sets) on which the estimations of the statistical parameters are made. In the regression case, the technique is useful when the residuals are nonnormative, autocorrelated, or when the data set is too small for reliable theoretical standard errors. Even when all the assumptions of the standard parametric hypothesis tests are thought to be satisfied, it is often informative to verify that the standard errors of the estimates are not underestimated. Gordon (1982) has already suggested the use of *jackknife* (or other subsample) replication methods to assess the accuracy of the calibrated regression equation. The bootstrap method is in fact a generalization of jackknife replication.

Here we are not interested in the stochastic structure of the residuals, so the resampling may be independent of time. The size of the original data set is n. For a regression, n actual observations are randomly sampled, with replacement, using uniformly distributed pseudo-random numbers scaled to the interval $(1, n)$. The regression coefficients are then estimated for the pseudo-data set. A new pseudo-data set is then created, a new set of regression coefficients estimated, and so on for an arbitrary number (NC) of times (*Figure 4.1*). The mean of the regression coefficients and their standard deviation are then calculated from these NC trials. These parameters give an idea of the effective variability of the statistics used.

This process may be used also for the selection of PCs. The number q of PCs is determined using the PVP criterion of each pseudo-data set. In the example data set considered below, the mean of q, based on 100 bootstrap replications, is estimated as 12.3 and its standard deviation is ± 0.5. The value of q is thus close to the value of q found on the total data set (i.e., 12). The small standard deviation shows the stability of the PVP criterion and justifies it. The use of the Monte Carlo criterion of Preisendorfer *et al.* (1981) suggests that two PCs only are significant (95% level). Equivalent results are found with the bootstrap method; indeed, only the two first eigenvectors have mean loadings (more than 100 replications) greater than their respective standard deviations. Only the first two PCs are interpretable, but 12 are necessary to assure that most of the useful information in the original variables is contained in the PCs. This is why the PVP method is recommended over the Preisendorfer method.

The bootstrap method can be applied to the best analogs method as follows: for each observation to be estimated, NC pseudo-data sets are constructed, and the minimum distance is found for each one. So NC analogs to i are found, and the final estimation is given by

$$\hat{y}_{ij} = \sum_{k=1}^{NC} (y_{kj}/d_{ik}^2)/(\sum_{k=1}^{NC} d_{ik}^{-2}) \qquad j = 1, \ldots, p \quad . \tag{4.25}$$

The corresponding standard deviations are given by

$$Sy_{ij} = \sum_{k=1}^{NC} (y_{kj}/d_{ik}^2)/(\sum_{k=1}^{NC} d_{ik}^{-2}) - \hat{y}_{ij} \quad . \tag{4.26}$$

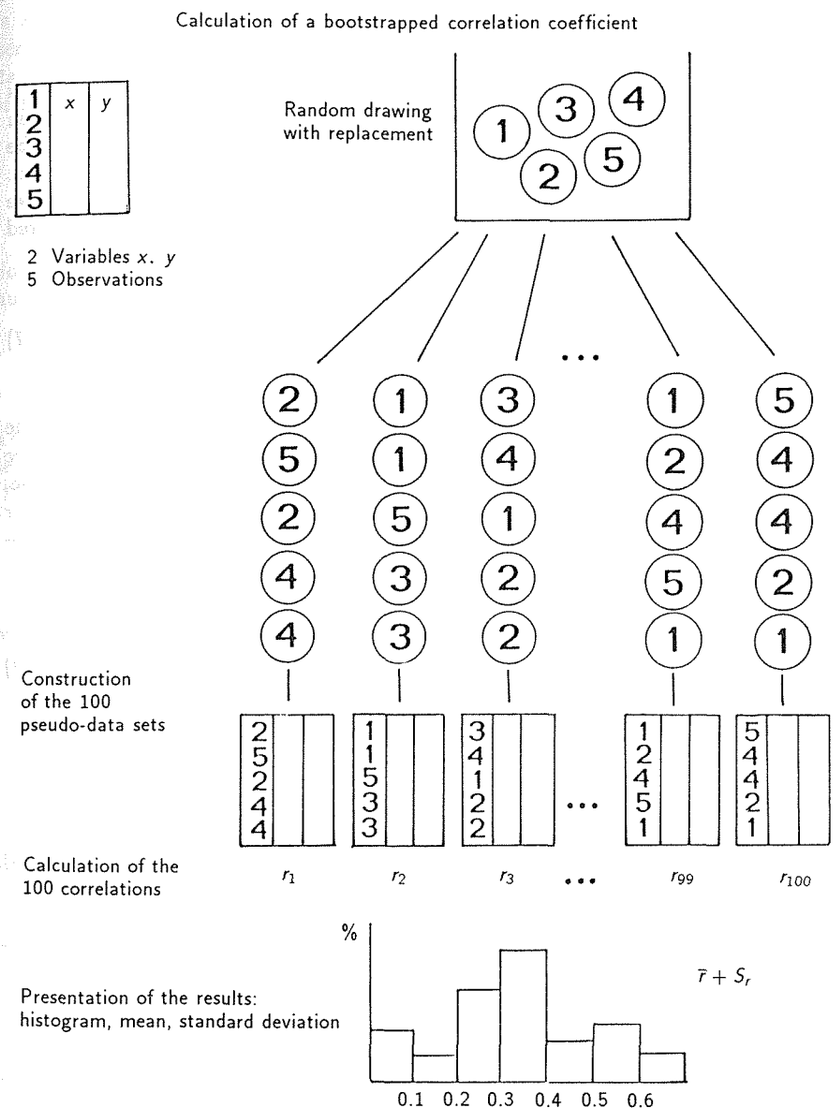

Figure 4.1. A schematic representation of the bootstrap method applied to the correlation coefficient.

Here the threshold dc [see equation (4.21)] is no longer necessary as the number NC replaces it.

4.2.8. Separation from low to high frequencies

Because tree rings may record the climatic signal differently when the forcing is confined to a single year or when it is persistent over several years, it has been suggested (Guiot 1981, 1984, 1985a) that low- and high-frequency variations be reconstructed separately by a method called canonical spectral regression. Canonical regression is applied to predictands and predictors after they have been filtered by complementary symmetric digital filters. If $x_{ij}{}^L$ is the filtered observation corresponding to x_{ij}, we have

$$x_{ij}^L = w_0 w_{ij} + \sum_{k=1}^{s} w_k \left[x_{(i+k)j} + x_{(i-k)j}\right] \quad . \tag{4.27}$$

The same notations can be used for the predictands y_{ij}. The idea to filter the time series to enhance the signal to be analyzed has always been widespread (see Douglass, 1936; Schulman, 1956; Fritts, 1976; Kairiukstis *et al.*, this volume, Chapter 5). Here, the idea is to structure such an approach. A low-pass filter may be defined by a frequency response function $R^L(f)$ with these characteristics:

$$\begin{aligned} R^L(f) &= 1 && \text{for } f \le f_1 \\ &= 0.5\,\{1 + \cos[\pi(f - f_1)/(f_2 - f_1)]\} && \text{for } f_1 < f < f_2 \\ &= 0 && \text{for } f_2 \le f < \pi \quad . \end{aligned} \tag{4.28}$$

By inverse Fourier transform, the weights are estimated as

$$W^L{}_k = \pi[\sin(kf_1) + \sin(kf_2)]/[2k\pi^2 - k^3(f_2 - f_1)^2] \quad . \tag{4.29}$$

A complementary high-pass filter is defined from the weights of the low-pass filter:

$$\begin{aligned} w^H{}_o &= 1 - w^L{}_o \\ w^H{}_k &= -\,w^L{}_k \qquad \text{for } k = 1, \ldots, s \quad . \end{aligned} \tag{4.30}$$

Its frequency response function is given by

$$R^H(f) = 1 - R^L(f) \qquad \text{for } 0 \le f \le \pi \quad . \tag{4.31}$$

The mean of a low-pass filtered series is preserved if the sum of the $2s+1$ weights is 1. In this case, the mean of the complementary high-pass filtered series is zero. The variance, however, is not preserved: it is multiplied by the sum of the $2s+1$ squared weights. The autocorrelation function of a filtered white-noise series is given by

$$r_l = \left(\sum_{k=-s}^{s-l} w_k w_{k+l}\right)/(\Sigma_k w_k^2) \qquad l = 0, \ldots, 2s \quad . \tag{4.32}$$

So the number ndf of degrees of freedom of a filtered series is not equal to the number n of observations. For a low-pass filtered series, it is given by

$$\text{ndf}^L = n(f_1 + f_2) \quad . \tag{4.33}$$

This is based on the fact that the largest frequency component of a white-noise series is π, whereas for a series filtered by equation (4.29), it is approximately $(2\pi f_1 + 2\pi f_2)/2$. For the complementary high-pass filter, we have

$$\text{ndf}^H = n - \text{ndf}^L \quad .$$

Matrices $\mathbf{X}$ and $\mathbf{Y}$ may be decomposed in such a way

$$\mathbf{X} = \mathbf{X}^L + \mathbf{X}^H \quad \text{and} \quad \mathbf{Y} = \mathbf{Y}^L + \mathbf{Y}^H \quad . \tag{4.34}$$

A reconstruction may be done in the two spectral bands:

$$\mathbf{Y}^L = \mathbf{X}^L\,\mathbf{B}^L + \mathbf{E}^L \quad \text{and} \quad \mathbf{Y}^H = \mathbf{X}^H\,\mathbf{B}^H + \mathbf{E}^H \quad . \tag{4.35}$$

The final reconstruction is given by

$$\mathbf{Y} = \mathbf{X}^L\,\mathbf{B}^L + \mathbf{X}^H\,\mathbf{B}^H + \mathbf{E} \quad \text{with} \quad \mathbf{E} = \mathbf{E}^H + \mathbf{E}^L \quad . \tag{4.36}$$

If $\mathbf{X}^L$ and $\mathbf{X}^H$ are expressed as a function of the weights of the filters using equation (4.28), it appears that equation (4.36) is also a function of the lagged predictors. The method may be generalized to a larger number of digital band-pass filters (Guiot, 1985a).

Equation (4.32) shows that the observations become autocorrelated using this method. It is difficult to know the variability of the regression coefficients

with autocorrelated observations. Adapted statistical models exist for such cases, but bootstrap methods make the problem easier to solve.

Instead of using symmetric digital filters of the form in equation (4.29), we may use ARMA coefficients that are in fact causal asymmetric filters (see Cook and Briffa, Chapter 3). The predictive part of the process is the low-frequency component, and the residuals are the high-frequency component. The sum gives the original series.

4.3. Verification

H.C. Fritts, J. Guiot, and G.A. Gordon

It is necessary to confirm that the modeled relationship has some universal properties, including a physical, biological, or statistical basis, so that it can be applied to predictor data outside the dependent period to obtain meaningful independent estimates (Gordon, 1982; Larson, 1931; Wherry, 1931; Anderson *et al.*, 1972; Stone, 1974).

The first consideration should be the development of a calibration model that matches current understanding of the biological and physical processes that link the predictors to the predictands. It may be necessary to obtain some biological measurements or to estimate some kind of response function that can filter out improper relationships, thus allowing one to concentrate on examining relationships that are reasonable and likely to exist. Such efforts help to limit, but do not eliminate, the possibility that a significant calibration could occur solely by chance. Additional independent calculations are required for this purpose.

The reliability of a particular statistical model can be assessed directly by calculating a number of verification statistics that measure the degree of similarity between independent estimates of climate made from the model and the corresponding instrumental data for time periods independent of the calibration (Gordon, 1982). A successful reconstruction must not only have significant calibration statistics, but also have significant verification statistics, which demonstrate that the independent estimates continue to be accurate at a level greater than would be expected solely by chance.

The process used to optimize the coefficients of the transfer function virtually ensures that the model will be more accurate for the dependent data than for any other body of data to which it may be applied. Thus, the predictive power of a regression model must decrease when the model is applied to independent data. This deterioration in accuracy should be measured whenever possible, and the results used either to evaluate the performance of the model or to provide the proper perspective with which to view the climate reconstruction. A successful model does not only mimic the calibration data. It also expresses a universal property relating the predictors and predictands so that it applies over all periods of time when analogs exist (Gordon, 1982).

A number of statistics can be used for verification. Some are parametric statistics, which involve assumptions about the underlying probability distributions of the data. These statistics are sensitive to any violations of the

assumptions. Other statistics are nonparametric and, therefore, not sensitive to these violations. Some statistics may be applied in more than one way to asses different attributes of the similarity. The statistics used by Fritts and Gordon are the product moment correlation or simply the correlation coefficient, the sign test, the reduction of error, and the product means (Fritts, 1976, forthcoming; Gordon, 1980). Guiot uses the goodness-of-fit of the means, the variance, and the mean variance of the regression coefficients.

4.3.1. Correlation coefficient

This statistic measures the relative variation (covariance) that is common to two data sets. It is totally insensitive to differences in the mean and variance between the two data sets. In addition, the correlation coefficient reflects the entire spectrum of variation, including both high and low frequencies, and its value can be affected markedly by trends in the two data sets.

The effect of trends can be eliminated by calculating a new correlation coefficient from the first differences of the two data sets. This correlation coefficient, r_d, measures only the high-frequency variation in common, as expressed by the year-to-year differences.

It is assumed that the data sets are normally distributed, so the values of r and r_d are tested by comparing them with the desired probability limit for a zero correlation calculated as:

$$r_{1-\alpha/2} = t_{n'-k,\,1-\alpha/2} \,/\, (n' - k + t^2_{n-k,\,1-\alpha/2})^{1/2} \quad , \tag{4.37}$$

where $t_{n'-k,\,1-\alpha/2}$ is student statistic at $1 - \alpha/2$ probability with $n' - k$ degrees of freedom ($k = 2$ for r and $k = 3$ for r_d).

A significant correlation is one that is greater than $r_{1-\alpha/2}$, which implies that the variance in the two data sets is linearly related. However, the correlation does not imply that the values in one data set lie near those in the other data set, nor does it imply that the scale of the variations, the amount of variance, in the two sets is similar. Other tests can be used to evaluate these types of differences.

4.3.2. Sign test

A nonparametric and less sensitive measurement of reliability is simply to count the number of times that the signs of the departures from the sample means agree or disagree. Inferences can be made about the probabilities of two dichotomous outcomes: (+1) that the estimate y_{ij} and the observation y_{ij} are on the same side of the dependent data mean (i.e., a success), and (–1) that they are not (i.e., a failure).

The number of positive signs expected by chance follows a binomial distribution and is $1/2\ n'$. For $n' < 45$, the cumulative distribution tables for the

binomial distribution with parameter $p = 0.5$ (Beyer, 1968, page 194) can be used to evaluate the critical value ($p = 0.95$). For $n' > 45$, the binomial distribution is well approximated by the normal distribution.

If the result of the sign test is a success, it can be concluded that the sign of the estimate is more often correct than would be expected from random numbers. The test measures the associations at all frequencies. In addition, a similar test is made using the first differences to test high frequencies.

4.3.3. Product Means test

The Product Means (PM) test (Fritts, 1976) was originally proposed by Terence J. Blasing and is not described in the statistical literature. However, it does have intuitive appeal as a diagnostic tool because the test is straightforward, and it does account for both the signs and the magnitudes of the similarities in two data sets. It emphasizes the larger deviations from the mean over the smaller ones.

The PM test calculates the products of the deviations and collects the positive and negative products in two separate groups based on their signs. The values of the products in each group are summed, and the means computed. The difference between the absolute values of the two means $M_+ - M_-$ can be tested for significance.

If the estimates bear no relationship to the observed values, then the positive and negative products will occur with about equal frequencies, the absolute values of the expected means will be the same with a zero difference. If there is a real relationship, the positive products will be more numerous; the mean of the positive products will be larger than the mean of the negative products; and the difference will be large and positive.

The t statistic for the difference of two means (see Dunn and Clark, 1974, page 53) is used for testing. The statistic can be expressed as:

$$t = (M_+ - M_-) \; / \; ({S_+}^2/n_+ + {S_-}^2/n_-)^{1/2} \tag{4.38}$$

where n_+ and n_- are the number of positive and negative products and ${S_+}^2$ and ${S_-}^2$ are the corresponding variances. The value of t computed from equation (4.39) can be compared with a critical value $t_{k,1-\alpha/2}$ from a Student's t statistic at $k = n_+ + n_- - 2$ degrees of freedom and $1 - \alpha/2$ probability (Beyer, 1968, page 282). For sample sizes smaller than 30, an adjustment is made in the degrees of freedom used (Bickel and Doksum, 1977, page 218).

The PM test, unlike the majority of the verification tests, is not a standard statistic with well-known characteristics. Therefore, Gordon and LeDuc (1981) used simulations to evaluate the PM statistic, and they reported that this test was much more likely to underestimate than to overestimate the value of the true relationship, especially when the relationship is a weak one. This appears to occur because the distributions of the observations are truncated at zero, so the data are skewed and, thus, do not approximate a normal distribution.

However, Gordon and LeDuc (1981) report that the error terms of the statistic are overestimated so that the PM test fails more often than would be expected if the data were normally distributed. If the test fails, one cannot be sure that no relationship exists. However, if the test passes, it indicates that a significant relationship exists with extreme values agreeing more often than values that are near the sample mean. Even with this limitation, the PM statistic can serve as a valuable diagnostic tool. It has been included as one of a group of verification tests to evaluate whether large departures from the mean are reconstructed any more reliably than small ones.

4.3.4. Reduction of error

The reduction of error (RE) statistic provides a highly sensitive measure of reliability. It has useful diagnostic capabilities (Gordon, 1980) and is similar, but not equivalent, to the explained variance statistic obtained with the calibration of the dependent data (Lorenz, 1956; 1977). Therefore, RE should assume a central role in the verification procedure. The equation used to calculate the RE can be expressed in terms of the $\hat{y}_i$ estimates and the y_i predictand that are expressed as departures from the dependent period mean value:

$$\mathrm{RE} = 1.0 - \sum_{i=1}^{n'} (y_i - \hat{y}_i)^2 / \sum_{i=1}^{n'} y_i^2 \quad . \tag{4.39}$$

The term on the right of (4.39) is the ratio of the total squared error obtained with the regression estimates and the total squared error obtained using the dependent period mean as the only estimate (Lorenz, 1956, 1977; Kutzbach and Guetter, 1980). This average estimation becomes a standard against which the regression estimation is compared. If the reconstruction does a better job at estimating the independent data than the average of the dependent period, then the total error of the regression estimates would be less, the ratio would be less than one, and the RE statistic would be positive.

The value of RE can range from negative infinity to a maximum value of 1.0, which indicates perfect estimation. A theoretical distribution for the RE statistic has not been determined, so its significance cannot be tested. Any positive value of RE indicates that the regression model on the average has some skill and that the reconstruction made with the particular model is of some value. However, the errors are unbounded so that one extreme error value in what was otherwise a nearly correct set of estimates could cause the RE statistic to be negative.

The RE can be partitioned into three components that express various attributes of the relationship (Gordon and LeDuc, 1981; Gordon, 1980). These components can be extremely useful as diagnostic tools for analyzing sources of error affecting a particular climatic reconstruction. The equations are

$$\mathrm{RE} = -\sum \hat{y}_i^2 / \sum y_i^2 + 2n'\bar{y}\bar{\hat{y}} / \sum y_i^2 + 2(n'-1)\widehat{\mathrm{cov}}(y,\hat{y}) \qquad (4.40a)$$

or

$$\mathrm{RE} = \mathrm{RISK} + \mathrm{BIAS} + \mathrm{COVAR} \quad . \qquad (4.40b)$$

The RISK term is always negative, and its absolute magnitude is a comparative measure of the variability of both the estimates and the actual observations used in testing. In one sense, this term represents the risk that the model takes in making the independent estimates. Ideally, it would be desirable to have equal variance in y_i and $\hat{y}_i$ with RISK = –1.0. Estimates with a small explained variance usually have RISK values between –0.5 and 0.0. Conversely, reconstructions that are overspecified with the variance of $\hat{y}_i$ > variance of y_i will have RISK terms < –1.0. Overspecification can be associated with an excessive number of predictors included in the transfer function.

To obtain a positive RE, the RISK term must be offset by the accuracy of the estimates as indicated by the second and third terms, representing the BIAS and COVARiation. The BIAS is positive when the mean of the estimates is on the same side of the calibration mean as the actual independent climatic data used for the verification testing. It is negative when the estimated mean is on the opposite side of the calibration mean as the mean of the instrumental data. Shifts in the mean are often insignificant; however, for a small sample, BIAS can be an important RE component. The covariation term, COVAR, reflects the strength of the correlation between $\hat{y}_i$ and y_i and measures the similarity of the temporal patterns in the estimates and observed predictands.

Having partitioned RE into these three components, it is possible to establish a lower limit for RE, below which the regression reconstructions will exhibit no skill at all in reproducing the variations in the instrumented data (Gordon, 1980). Such a model would be one where the mean of the estimates has not shifted, BIAS=0, and where the estimates and the actual data are independent, COVAR=0. In that case, the reduction of error would simply be the RISK term. The value of RE could certainly be less than the RISK term, if the COVAR term was negative for example, but the RISK does define a lower limit for an acceptable RE statistic. Values of RE that are negative, but greater than the RISK, indicate that the reconstructions may still contain some meaningful climatic information. However, negative RE statistics clearly indicate that some improvements are needed to make the estimates at least as good as substituting the dependent data mean value for the estimates.

The partitioned RE components can be used in the following ways to diagnose reconstruction characteristics. Some reconstructions can successfully duplicate the temporal patterns of variation in the actual observations but contain no appreciable amount of variability. The correlation coefficient would not differentiate such a reconstruction from one with more variability, but the RISK term would clearly reveal this difference. Cases frequently arise where regression estimates have a negative RE statistic and yet still pass a majority of other verification tests, especially the correlation statistics. When this occurs, the RISK term may reveal major differences in the reconstructed and instrumental

data variance, in the BIAS term differences in the reconstructed and instrumental mean, or when the COVAR term is small or negative.

Gordon and LeDuc (1981) show that the RE statistic does estimate the explained variance fairly accurately, but they also report that the size of the sample being analyzed, n', appears to affect its significance markedly. For $n' = 20$, an RE statistic of zero was roughly equivalent to a 0.95 confidence limit, but for $n' = 10$ or 15 an RE statistic would have to be greater than 0.25 or 0.12, respectively, to be significantly different from zero.

4.3.5. Summing verification statistics over several variables

These statistics are calculated and tested for each of the p predictand variables. They can then be summed or averaged over all variables to obtain the mean model verification results. In this section, the verification is summed over all p variables. This does not provide information on differences among the p variables but is an efficient method to obtain the overall model statistics. For example, the mean variance (MSSP) is calculated over the p predictands and over the calibration interval as

$$\mathrm{MSSP} = 1/(np) \sum_{j=1}^{p} \sum_{i=1}^{n} (y_{ij} - \bar{y}_j)^2 \quad . \qquad (4.41)$$

The mean sum of squares of the difference between actual and reconstructed means, which is related to MSSP, is given by

$$\mathrm{DM} = \sum_{j=1}^{p} (\bar{y}_j - \bar{\hat{y}}_j)^2 \,/\, \mathrm{MSSP} \quad . \qquad (4.42)$$

Measurements of DM can be used to verify if the mean of the series (or the trend) is well reconstructed. DM is zero for the calibration interval and becomes positive or negative depending on the drift of the mean in the verification period. DM is similar to the BIAS term in the reduction of error statistic, equation (4.40b).

The mean sum of squares of the difference between actual and reconstructed standard deviations, related to MSSP, is given by

$$\mathrm{DSD} = \sum_{j=1}^{p} (Sy_j - \widehat{Sy}_j)^2 \,/\, \mathrm{MSSP} \quad . \qquad (4.43)$$

DSD assesses whether the variability of the series is well reconstructed. A value that is too large, both for the calibration and for the verification intervals, shows a failure to reconstruct the high frequencies. It may be compared with the RISK in equation (4.40b).

The parametric statistics defined previously may be averaged on the p predictands:

$$\bar{R} = \sum_{j=1}^{p} r_j/p \quad \text{and} \quad \overline{RE} = \sum_{j=1}^{p} RE_j/p \tag{4.44}$$

where r_j and RE_j are the individual correlation coefficient and reduction of error statistics.

The fractional variance explained (EV) equation (4.7) may overestimate the variance in the *population* of climate values from which the sample came. The correction for this overestimate is made in proportion to the variance of predictor variates entered into regression and the degrees of freedom remaining in the residuals. The adjusted statistic, EV′, is calculated from the EV statistic, equation (4.7), following Kutzbach and Guetter (1980). The necessary computations, as modified by Fritts (forthcoming), are

$$EV' = [EV(npC) - p] \,/\, [npC - mq - p] \tag{4.45}$$

with n the number of observation used for the estimates p and m (respectively, the number of predictands and predictors), q the number of canonical pairs used (if canonical regression is not used, $q = p$), and C the correction factor for the first-order autocorrelation of the residuals:

$$C = (1 - r_1) \,/\, (1 + r_1) \quad .$$

For one predictand ($p = q = 1$), equation (4.45) becomes

$$EV' = EV[(n-1)/(n-m-1)] \quad , \tag{4.46}$$

which shows that the residual variance is divided by the number of degrees of freedom $n-m-1$ rather than by the number of observations n. When independent data are lacking, Kutzbach and Guetter (1980) propose the next statistic, RE′, computed on dependent data:

$$RE' = EV' - [mqC/(npC + p)]\,(1 - EV') \quad . \tag{4.47}$$

Bootstrap methods, described in Section 4.4, are an alternative way of testing regression stability.

4.3.6. Variance of the regression coefficients

When many predictors are entered into a regression equation, the percentage of variance explained may be overestimated. One way to correct for this problem is to calculate the mean squares and F ratio after adjusting for any losses in degrees of freedom. The regression coefficients are often large but not statistically different from zero. For this reason, it is necessary to compute their variances. The distributions of regression coefficients are often not Gaussian, but 95% of the coefficients are usually included inside an interval of ±2 standard deviations from the mean. Exact tests can be made, but in general a coefficient b_{jk} is considered significantly different from zero if it is exceeds the ±2 standard deviation limits.

$$SB = [\textstyle\sum_{jk} Sb_{jk}^2/(mp)]^{1/2} \quad . \tag{4.48}$$

Using equation (4.13), we obtain a simpler way for computing SB:

$$SB = \{[\textstyle\sum_k SE_k^2 \sum_j (1/lx_j)] \,/\, (mpn)\}^{1/2} \quad , \tag{4.49}$$

where l_{xj} is the jth eigenvalue and where the summation is done over the qx retained eigenvalues.

4.4. Comparison of the Methods

J. Guiot

The above-mentioned methods are compared using 15 standardized chronologies from the United Kingdom, Ireland, the Federal Republic of Germany, France, and Italy (*Table 4.1*). Three types of climate are involved: Atlantic, Alpine, and Mediterranean. Three predictands are used that have an MSSP, equation (4.41), of 64.68. They are summer temperature (June to August) in central England (Manley, 1974), Grand-St.-Bernard, and Marseille. These data were divided into the calibration interval 1851–1930 (80 observations) and the verification interval 1931–1960 (30 observations). The average temperatures for the calibration and verification periods were 14.0°C and 14.5°C, respectively. The presence of this 0.5°C difference is used to test the ability of each model to extrapolate beyond the range of the calibration period. To simplify the illustration, the calibration and verification periods were not switched as is often done in practice. In this example, the number of predictors is $m = 15$, the number of predictands is $p = 3$, the total number of years is $ny = 110$, the calibration years are $n = 80$, and the verification years are $n' = 30$.

There are an insufficient number of model replications to deduce definitive conclusions from this analysis. Nevertheless, the comparisons are instructive and useful to the extent that they illustrate the statistical methods described in this chapter.

Table 4.1. The predictors.

Code	*Location*	*Tree*	*Source*
RHIN	Trier (Germany, F.R.)	oak (*Quercus*)	Hollstein (1965)
BELF	Belfast (N.Ireland)	oak (*Quercus*)	Baillie (1977)
GLEN	Glenluce (Scotland)	oak (*Quercus*)	Pilcher and Baillie (1980)
RAEH	Raehills (Scotland)	oak (*Quercus*)	*ibid.*
LOCK	Lockwood (Scotland)	oak (*Quercus*)	*ibid.*
SCOR	Scorton (England)	oak (*Quercus*)	*ibid.*
OXFO	Oxford (England)	oak (*Quercus*)	*ibid.*
BLIC	Blicking (England)	oak (*Quercus*)	*ibid.*
BATH	Bath (England)	oak (*Quercus*)	*ibid.*
LUDL	Ludlow (England)	oak (*Quercus*)	*ibid.*
CALA	Massif Pollino (S.Italy)	pine (*Pinus*)	Serre-Bachet (1985)
MERV	Merveilles (French Alps)	larch (*Larix*)	Serre (1978)
VENT	Ventoux (S.France)	spruce (*Picea*)	Serre-Bachet (pers. comm.)
ITNO	Alps (N.Italy)	larch (*Larix*)	Bebber (pers. comm.)
ORGE	Orgere (French Alps)	larch (*Larix*)	Tessier (1981)

The computer time consumed by each method is tabulated for comparison. All the methods were run in FORTRAN 77 on an IBM PC-compatible microcomputer with a clock frequency of 4.77 Hz, an 8087 math co-processor, and a hard disk for input and output. The time for running each method was divided by the speed of the standard multiple regression analysis, which served as the computer time benchmark.

4.4.1. Analysis

Eight basic methods were applied to the same data set (*Table 4.1*). They were:

(1) Multiple regression.
(2a) All-possible-subset stepwise regression with three predictors selected according to an F ratio of 6.0.
(2b) Backward-elimination stepwise regression with two predictors selected according to an F ratio of 7.0.
(3) Regression-using principal components with the PCs computed from the predictor variables for the calibration interval and 12 PCs selected using the PVP criterion.
(4) Regression-using principal components including six PCs having eigenvalues exceeding 1.0.
(5) Canonical regression with PCs calculated from both the predictors and predictands and the retained PCs selected using the PVP criterion.
(6) Best analogs method with the Euclidean distance computed according to the US distance metric, equation (4.22), and with all $w_j = 1.0$ in equation (4.21).
(7) Best analogs method with the Euclidean distance computed according to the SD distance metric, equation (4.22), and with the weights w_j equal to the loadings of the first canonical variate between the predictors and the predictands.
(8) Multivariate autoregressive analysis with 19 predictors from 11 tree-ring series with lags indicated in parentheses: GLEN(1,3), RAEH(0,4), LOCK(1,4), BLIC(4), BATH(3), LUDL(4), CALA(1), MERV(0,2), VENT(0,1), ITNO(0,5), and ORGE(0,5). The predictands were also included in the regression with a one-year delay.

A small number of verification statistics were calculated to illustrate the procedures. More statistics would probably be used in actual practice. They include: 1) the DM statistic, which measures the variance of the differences between the actual and reconstructed means compared with the variance in the calibration period, equation (4.42); 2) the DSD, which measures the difference between the actual and reconstructed standard deviations, equation (4.43); 3) the $\bar{R}$, which is the average correlation coefficient; 4) the $\overline{RE}$, which is the average reduction in error; and 5) the SB, which is the mean standard error of the regression coefficients, equation (4.48) and (4.49). Tests 2, 3, and 4 are calculated for both the calibration and verification intervals. The $\overline{RE}$ for the calibration period is the same as the average of the square of the correlation coefficient. The most important observations and deductions that can be made from the results in *Table 4.2* are presented in the following paragraphs.

Table 4.2. The statistics for several methods for (*1*) the calibration period (1851–1930) and (*2*) the independent verification period (1931–1960): DM is the estimated minus actual mean in percentage of MSSP (a zero value indicates a complete agreement and a negative value indicates a systematic underestimation); DSD is the estimated minus actual variance in percentage of MSSP (a zero value indicates a complete agreement and a negative value indicates a systematic underestimation); $\bar{R}$ is the correlation between estimated and actual data; $\overline{RE}$ is the reduction of error defined in equation (4.39) (for the calibration interval $\overline{RE}$ is equivalent to the variance explained by the reconstruction); SB is the mean standard deviation of the regression coefficients.

		DM (%)	*DSD (%)*		$\bar{R}$		$\overline{RE}$		
Method	*Computer time*	*(2)*	*(1)*	*(2)*	*(1)*	*(2)*	*(1)*	*(2)*	*SB*
1 Multiple regr.	1	−16	−21	−17	0.55	0.32	0.30	0.17	0.125
2 Stepwise regr. (a)	192	−31	−37	−41	0.39	0.37	0.16	0.16	0.110
(b)	12	−25	−32	−37	0.43	0.24	0.19	0.13	0.106
3 Regr. + PC (PVP)	1	−20	−24	−20	0.52	0.47	0.27	0.31	0.092
4 Regr. + PC (1)	1	−26	−40	−46	0.37	0.53	0.14	0.28	0.052
5 Canonical regr.	3	−25	−39	−43	0.52	0.48	0.27	0.28	0.092
6 Analog (UW/US)	10	−21	−20	−25	0.05	0.34	0.26	0.19	–
7 Analog (W/SD)	11	−22	−36	−44	0.19	0.60	−0.02	0.34	–
8 Multiple AR.	10	−10	−8	−8	0.67	0.54	0.44	0.39	–

Method 1, which uses a multiple regression model, is the fastest technique. The means (DM) and standard deviations (DSD) are closer to zero than they are for most of the other techniques, indicating that these statistics are not seriously underestimated in the reconstructions. The $\bar{R}$ and $\overline{RE}$ statistics are reasonably

high for the calibration interval, but they are among the lowest for the verification interval. The SB statistic is the highest of any computed. Although the multiple regression method produces a good calibration, it lacks predictability in the independent period and has large standard errors in the regression coefficients.

The stepwise regression, method 2, includes case (a) with three predictors and case (b) with two predictors. They are presented because both models have very high F ratios using either the all-possible-subsets or backward-elimination method. The results would have been the same as method 1 if all candidate predictors had been forced into the model. However, the DM, DSD, $\bar{R}$, and $\overline{RE}$ statistics are all lower in the calibration interval owing to fewer variables in the stepwise models. This indicates that, with fewer variables in the model, there is an increase in the discrepancy between the estimated and actual means and additional unexplained variability. *Table 4.2* also shows that the $\bar{R}$ for the verification period has improved using method 2(a) ($\bar{R} = 0.37$ versus 0.32), and the standard deviations of the coefficients in both methods 2(a) and 2(b) are smaller. However, the $\overline{RE}$ values for both stepwise models are below that of the full multiple regression case. These data suggest that while there is an increase in the relative agreement of the actual and estimated data over the verification period, the means and/or variances are not well estimated.

Methods 3 and 4 are regression on the principal components of the tree-ring chronologies. The DM and DSD statistics indicate that this transformation of the data does not provide any better estimates of the means and standard deviations. This is most marked in method 4, which used only six PCs of the tree-ring chronologies. However, this same method has a larger $\bar{R}$ for the independent interval than for the dependent interval and a much reduced SB statistic.

For method 3, the PVP criterion selected 12 PCs. As a consequence of this treatment, there may be less correlation over the verification interval (although here the difference with the case of six PCs is weak and not significant). However, the underestimation of the mean and standard deviation is substantially less. In method 3, the errors of the regression coefficients (SB) are reduced from those of methods 1 and 2, which is the main effect of using the PCs rather than the original chronologies as estimators of climate. As shown by equation (4.49), the errors of the regression coefficients are amplified whenever eigenvectors with small eigenvalues are entered into the regression. That is why a stepwise regression with only three tree-ring variables, method 2(a), has a mean error of 0.110, which is considerably higher than the 0.052 error value for the regression with six PCs, method 4. These data provide strong arguments in favor of using PCs in regression analysis.

Method 5 uses canonical regression, which is a technique involving PCs of the covariance matrix (Section 4.2.4). It is most useful for analyzing larger numbers of predictor and predictand data sets than used in this test. Consequently, the method does not show improvements over methods 3 and 4, which used PCs in the analysis. A better illustration of the method is described in Section 4.5, which applies 65 tree-ring chronologies to estimate climate at 77 to 96 stations over a wide spatial grid.

The UW/US best analog, method 6, is now applied. The fact that the predictors are measured in the same units and have similar variability makes the standardization not absolutely necessary. The calibration interval provides the reference set for the analogs. Because the tree-ring series have much higher autocorrelation than the temperature data, the $\bar{R}$ and $\overline{RE}$ computed on the calibration period has no value. Indeed, the best analog of the observation i is often observation $i - 1$ or $i + 1$ if i belongs to the calibration interval. Whereas $i - 1$ or $i + 1$ are useful analogs for tree-rings, they are not adequate for temperatures. The fitting then appears inaccurate on the calibration interval. Consequently, this *autocorrelation effect* is not effective on the independent data because the best analogs are necessarily taken from nonadjacent observations. The $\overline{RE}$ on the calibration interval is not exactly the square of $\bar{R}$ in the example because the estimated means may be different from the actual ones. The method does not provide good results except for the DM and DSD statistics.

Method 7 is similar to 6 except that weights w_j, equation (4.21), are used, which are the loadings of the first canonical variable from the analysis between the predictors and the predictands. This modification improves the $\bar{R}$, but not the DSD. In fact, the analogs method, not being extrapolative, acts like a low-pass filter. The reason is that an estimate is given by a mean of a *best analogs* set. Using a smaller number of analogs increases the standard deviation of the estimates; the standard deviation becomes closer to that of the actual data (as it is for the UW/US case), but the correlation decreases. Evidently, it is better to emphasize the correlation and to correct the deficit of variability by a multiplying factor.

The multivariate AR, method 8, is applied to the 11 tree-ring series with a maximum lag or time delay of five years and each predictands with a one-year lag, giving a total of 19 predictors. A separate equation is calculated for each predictand. All of the results are improvements over the previous methods, with the DM and DSD statistics near zero and the $\bar{R}$ and $\overline{RE}$ statistics large. These results indicate that this method is superior, but the method is not easily applied to large sets of predictors. This problem follows from the need to estimate m^2 regression coefficients for each partial autoregression matrix. Thus, the number of coefficients to be estimated can quickly outnumber the available degrees of freedom. The multivariate AR estimates may also degrade if the method is extrapolated far away from the calibration interval, especially if the coefficient of the lagged predictand is large. Indeed, an estimate of the lagged predictand must be used as a predictor to make the extrapolation. Thus, the verification tests may be influenced by the distance of the estimate from the calibration period.

It must be noted that the other methods can be applied with lagged as well as unlagged predictors and predictands. Canonical regression analysis (Fritts and Gordon, 1982; Lough and Fritts, 1985) and stream-flow reconstruction models (Stockton, 1975) are such examples.

When the methods from *Table 4.2* are compared, the multivariate AR method seems to be the best. However, the potential extrapolation problems noted above for this method must be kept in mind in making this assessment. The regression with PCs and canonical regression appear to be equivalent when

analyzing this data set. The analogs method, using the canonical variate weights, appears useful when one wants to emphasize the low-frequency variations.

4.4.2. Bootstrapping the basic methods

To assess the robustness of the statistical estimates, bootstrap methods are applied to the PC and canonical regressions. The bootstrap method cannot be applied to the multivariate AR method because its time-domain structure cannot be preserved by that particular treatment. When bootstrapping is applied to the best analogs method the results do not differ significantly from the unbootstrapped case. However, it does provide confidence intervals for extrapolations (see example in *Figure 4.2*).

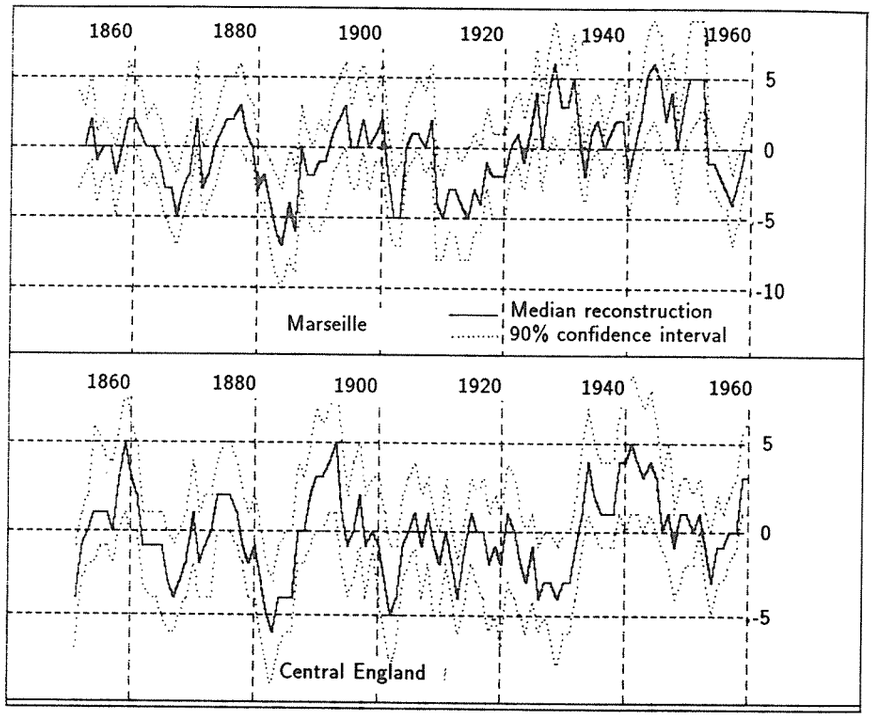

Figure 4.2. The reconstructions of summer temperature in Marseille and central England obtained from 15 chronologies (*Table 4.3*) using the bootstrap method. The dotted lines delimit the 90% confidence interval (the interval that includes 90 out of 100 replications) and the solid line is the median reconstruction.

Methods 3 and 5 from *Table 4.2* are tested, with the results in *Table 4.3*, to answer the following questions: what is the population error for the correlations between estimated and actual predictands; what is the population error in the standard deviation of the regression coefficients; and how many replications do we need to obtain reliable estimates?

Table 4.3. The statistics for several methods for (*1*) the calibration period (1851–1930) and (*2*) the independent verification period (1931–1960); SB is the mean standard deviation of the regression coefficients; $\bar{R}$ and SB are given with their standard deviation computed with bootstrap method (with a given number of replications). Computer time is in multiple regression units.

			(1)		(2)		
Method	*Computer time*	*Number of replication*	$\bar{R}$	*Std. dev.*	$\bar{R}$	*Std. dev.*	*SB*
1 Regr. + PC (PVP)	288	300	0.43	0.05	0.38	0.12	0.106
ibid.	100	100	0.43	0.05	0.38	0.14	0.103
ibid.	49	50	0.42	0.06	0.37	0.14	0.103
ibid.	11	10	0.43	0.06	0.36	0.13	0.091
2 Canonical regr. (PVP)	2,475	2,000	0.43	0.05	0.38	0.13	0.083
ibid.	372	300	0.43	0.05	0.38	0.13	0.083
ibid.	64	50	0.42	0.06	0.37	0.15	0.082
3 Canonical regr. (1)	59	50	0.33	0.07	0.45	0.15	0.049

The bootstrap method is used to obtain from 10 to 2,000 replicates of the two basic methods. The mean of the correlation coefficients and the associated errors are included in *Table 4.3* along with the errors of the regression coefficients. Method 1 is regression after using the PVP criterion to select the principal components. There is little change in the correlation statistics between 10 and 300 replications. These results indicate that this method has relatively stable correlation estimates. However, some change can be noted between 10 and 50 replicates, so a number of replicates of 50 would seem to be a good compromise between computation costs and efficiency (see Efron, 1979). The standard deviation of $\bar{R}$ does not seem to depend on the number of replications. The mean standard deviation of the regression coefficients is 0.106 for 300 replications, which is just a bit more than 0.092 obtained for this method in *Table 4.2*. This means that the statistical hypothesis (say normality of the residuals), which is the basis of the significance tests in the regression theory, agrees.

Method 2 in *Table 4.3* includes from 50 to 2,000 replications for testing the canonical regression. As was done in *Table 4.2*, the PCs were selected using the PVP criterion. The $\bar{R}$ values and their standard deviations are relatively stable. The canonical regression, with a mean error on the coefficients of 0.092, appears to be one of the most precise methods in *Table 4.2*. *Table 4.3* shows that this error is well estimated since it is close to those obtained by bootstrapping (0.082 to 0.083). These statements argue in favor of canonical regression over regression on PCs.

The standard deviations for the correlation coefficients of the independent interval for both methods 1 and 2 (*Table 4.3*) are larger than those for the

calibration interval. This may be due in part to the decrease in accuracy of the model when it is applied to the independent data. However, it may also be owing to the fact that fewer data points were used for verification than for calibration. Whatever the reason, the bootstrap method provides the means of assessing this accuracy in a direct manner.

As might be expected, method 3 (*Table 4.3*) shows that when only the six largest PCs (with eigenvalues > 1.0) are used, the $\bar{R}$ for the dependent interval is reduced to 0.33, the $\bar{R}$ for the independent interval increases to 0.45, and the SB terms are reduced to 0.049 indicating a greater stability.

It is clear from these examples that the bootstrap method, which is not really expensive, may be used to assess the accuracy of calibration and verification statistics. As few as 50 replications appear to be an adequate number for this type of analysis. Bootstrapping supports the contention that canonical regression provides a more realistic assessment of the errors in the equation than multiple regression on the PCs of the chronology variance.

4.4.3. Use of filters

Table 4.4 includes an example of a digital symmetric filter applied to separate low- and high-frequency components. The filtered series of z_i (where z_i may be x_{ij}, $j = 1, \ldots, m$; or y_{ij}, $j = 1, \ldots, p$) is defined as

$$z_i^L = 0.292\, z_i + 0.252\,(z_{i-1} + z_{i+1}) + 0.151\,(z_{i-2} + z_{i+2}) + 0.038\,(z_{i-3} + z_{i+3}) - 0.035\,(z_{i-4} + z_{i+4}) - 0.05\,(z_{i-5} + z_{i+5})$$

$$z_i^H = 0.708\, z_i - 0.252\,(z_{i-1} + z_{i+1}) - 0.151\,(z_{i-2} + z_{i+2}) - 0.038\,(z_{i-3} + z_{i+3}) + 0.035\,(z_{i-4} + z_{i+4}) + 0.05\,(z_{i-5} + z_{i+5}) \quad .$$

Table 4.4. See *Table 4.3.*

			(1)		(2)		
Method	*Computer time*	*Number of replication*	$\bar{R}$	*Std. dev.*	$\bar{R}$	*Std. dev.*	*SB*
1 All frequencies	128	100	0.43	0.05	0.38	0.14	0.083
2 Low frequencies < 1–7 yrs	126	100	0.70	0.03	0.45	0.18	0.089
3 High frequencies > 1–7 yrs	129	100	0.61	0.04	0.60	0.10	0.093
4 Sum 2+3	–	–	0.62	–	0.49	–	–

The low-pass filter (L) passes more than 50% of the original variance at periods of approximately seven years to infinity. The high-pass filter (H) passes high-frequency variance at periods from two to seven years. The cutoff at periods of seven years is an arbitrary choice.

In *Table 4.4* the bootstrap method with 100 replications is applied to canonical regression on unfiltered data 1, the low-frequency data 2, and the high-frequency data 3. In addition, the results of 2 and 3 are summed in method 4, equation (4.36), and the statistics of the sums calculated. It is especially important to use bootstrapping on the low-pass filtered series because they have so few degrees of freedom due to their high autocorrelation.

A correlation analysis at different lags (not displayed here) indicated a clear time delay of three years between the low frequencies of the summer temperature in central England (3rd predictand) and the low-frequencies of the English tree-growth series. When this delay, which is not apparent for the unfiltered and high-frequency data, is accounted for and the results are added to the high frequencies, the correlations for the dependent and independent interval (line 4, *Table 4.4*) improve considerably. The standard deviation for the low-frequency set appears to be low for the calibration interval (1), but this is a filtering effect, which also reduces the variance of the replications. The reduced number of degrees of freedom, equation (4.33), must be evaluated when interpreting the results for the low frequencies.

It appears from these data that spectral methods can improve the results in both the dependent and the independent interval. Bootstrapping is a complementary tool useful for assessing the accuracy of the estimates. This is especially helpful for evaluating filtered data because their degrees of freedom may not be estimated correctly. The bootstrap method also has the great advantage of providing confidence intervals for the estimates (*Figure 4.2*).

4.5. Statistical Reconstruction of Spatial Variations in Climate Using 65 Chronologies from Semiarid Sites

H.C. Fritts

Fritts (1976), Brubaker and Cook (1984), Hughes *et al.* (1982), Stockton *et al.* (1985), and many others show that climatic reconstruction from tree-ring series is moving forward on many fronts. Much activity has focused on extensive sampling to increase the coverage of the existing database, and a number of spatial grids of well-dated tree-ring chronologies have been developed that extend backward in time to the beginning of the 17th and 18th centuries (Hughes, 1987b). In the previous sections we have tried to describe the basic methods that we believe will become important parts of future analyses. The following is an example of canonical regression on PCs of large climate and tree-ring data sets. It represents a 10-year project that was originally designed to develop objective techniques for calibrating, verifying, and reconstructing large-scale variations in climate.

Tree-ring chronologies from 65 sites over western North America (*Figure 4.3*) are used as statistical predictors of seasonal and annual climatic conditions represented by grid points on a map (Fritts *et al.*, 1971). Even if the number of grid points is small, a large number of variables are sometimes needed to represent lags and leads in the model of the climate-growth relationships.

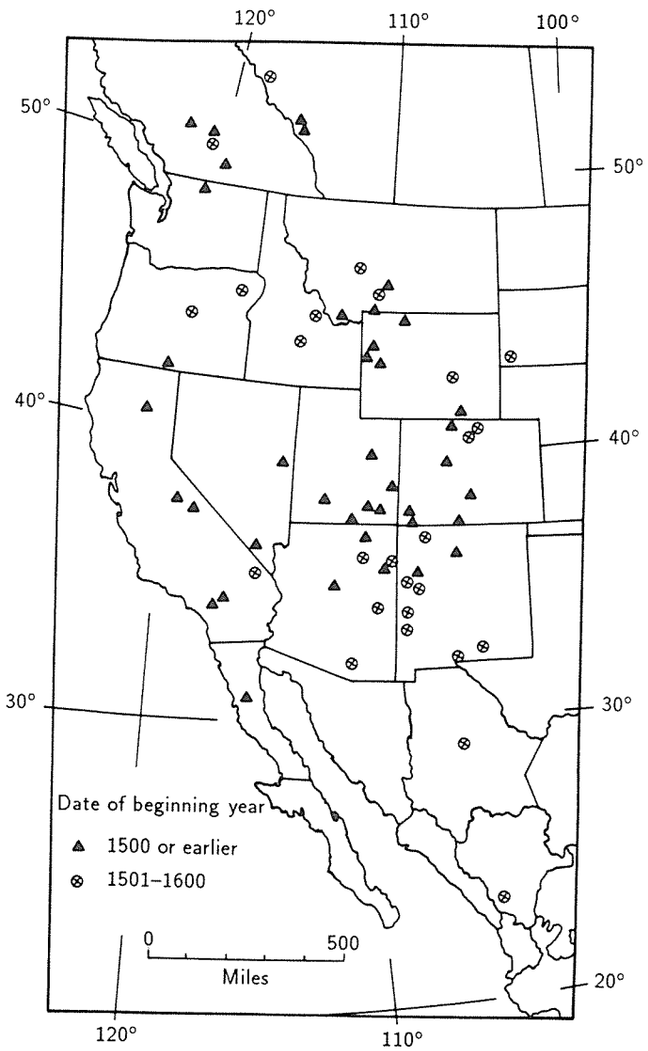

Figure 4.3. The locations of the 65 semiarid site chronologies selected by Fritts and Shatz (1975).

If there are a very large number of tree-ring chronologies or climatic stations, the most important spatial variations in either or both sets may be selected and used in regression by calculating the eigenvectors and extracting the largest PCs of the data sets. A complete matrix of m eigenvectors $m\mathbf{A}xm$ and

the corresponding eigenvalues $m\mathbf{L}xm$ are obtained [see equation (4.10) and (4.11)]. The first 10 columns represent the 10 eigenvectors that reduce the most variance from the grid of 65 western North American tree-ring chronologies (*Figure 4.3*) are mapped in *Figure 4.4(a)*. The computations are made on all available chronology data from 1602–1963.

The PCs time series or amplitudes are obtained by multiplying the qx selected eigenvectors by the normalized chronology data:

$$_{nx}\mathbf{Z}_{qx} = {}_{nx}\mathbf{X}_{m}\mathbf{A}\mathbf{x}_{qx} \quad . \tag{4.50}$$

The first 10 principal components for the 65-chronology grid are shown in *Figure 4.4(b)*. Each eigenvector portrays orthogonal patterns through space, and each principal component portrays orthogonal patterns through time.

Eigenvector 1, *Figure 4.4(a)*, reduces 25% of the chronology variance and reaches its most extreme (negative) value near the four-corners states of the USA. The magnitude of these elements decreases in all directions from this central point and changes sign for a small number of sites along the Canadian–United States border. It expresses the most important growth anomaly with the US chronologies of one sign and the Canadian chronologies of opposite sign. The PC for eigenvector 1, *Figure 4.4(b)*, shows large year-to-year variations in proportion to the amount of variance reduced. Low values represent times of high growth throughout the western United States, and high values represent times of low growth. A large and persistent negative departure occurs after 1900 when growth throughout the western USA was high. After 1920 this PC shows rising values representing declining growth over much of the west.

Eigenvector 2 reduces 10% of the chronology variance. It has large positive values for chronologies in the northwestern United States and Canada with negative values for chronologies in New Mexico and Arizona, *Figure 4.4(a)*. The zero line crosses central Colorado, southern Utah, and bends southward following the Colorado River to Baja. This eigenvector portrays a seesaw variation in chronologies at the northwest–southeast extremes of the tree-ring chronology grid. The plot of PC 2, *Figure 4.4(b)*, shows less variance and is marked by high values early in the 20th century with low values in the 1920s and 1930s.

Eigenvectors 3 through 10 show progressively more complicated spatial patterns in growth representing smaller-scale variations that may be added to eigenvectors 1 and 2 to account for the most important modes of variation in the 65 tree-ring chronology grid. The eigenvectors reduce less and less variance, which can be seen as less variation in the higher order PCs. The first 15 PCs, which accounted for 67% of the chronology variance, were used as the predictors of climate.

The predictands were the PCs of the seasonal climatic data. There were 77 stations with seasonal temperature, 96 stations with seasonal precipitation, and 96 Northern Hemisphere grid points with average seasonal pressure. Seasons

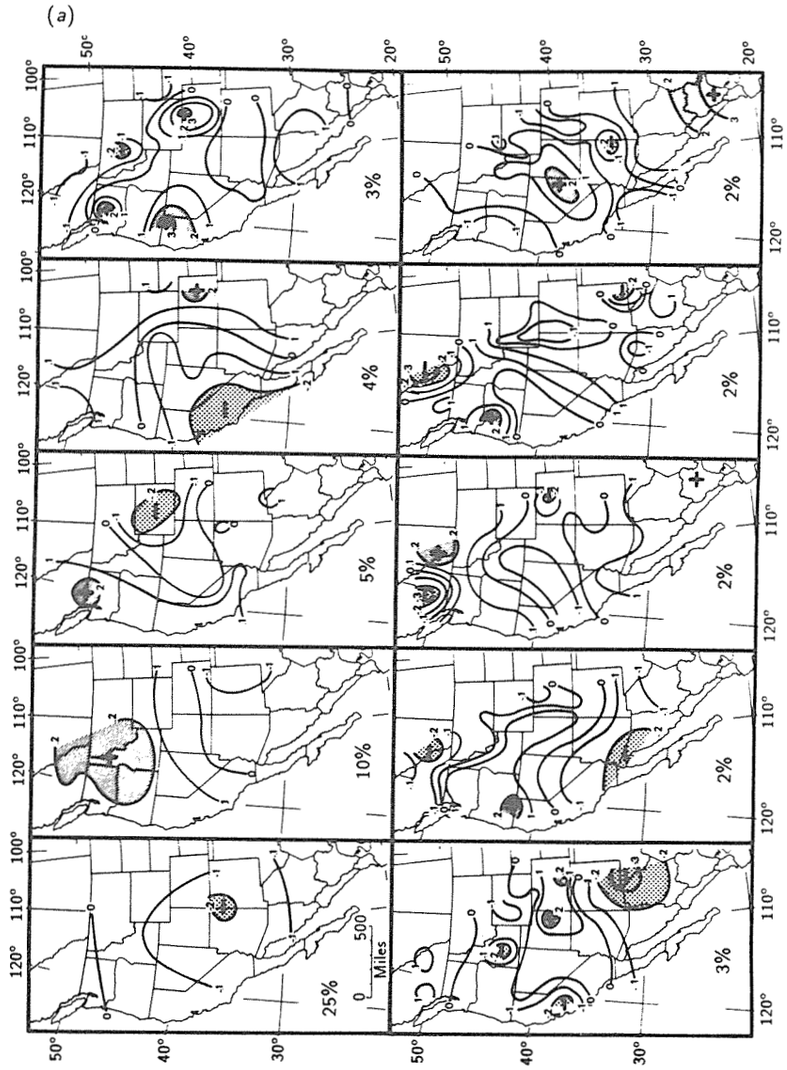

Figure 4.4. The first ten eigenvectors (*a*) and the corresponding principal components (*b*) of the 65 tree-ring chronologies shown in *Figure 4.3*.

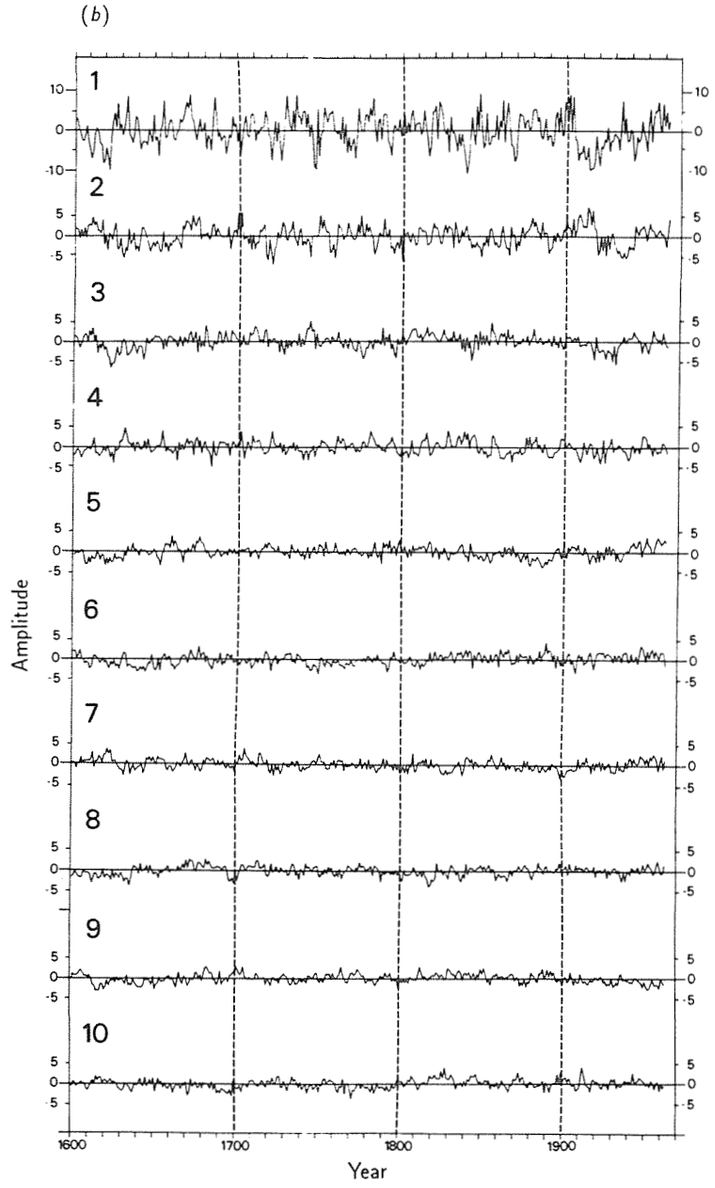

Figure 4.4. Continued.

rather than annual values were used because response function analysis had shown that the trees sampled for this selected grid differed markedly in their response to climate from one season to the next.

In addition, the chronologies differed in the amount of autocorrelation at different lags. Some of the low-frequency variations in the tree-ring data were removed from the tree-ring chronologies by estimating the first-order autocorrelation and subtracting it from the chronology index. In later work ARMA techniques were used to calculate the white-noise residuals. The eigenvectors and their PCs were also calculated from this data set. The first 15 of these PCs as well the first 15 PCs from the untransformed tree-ring data set were sometimes used as the predictors of a canonical regression analysis.

The period that was in common for these chronologies was divided into two parts. The outer portion beginning in 1901 and ending in 1963 was designated as the *dependent period* and the remaining period from 1602–1900 was designated as the *independent period* – the interval in which growth was to be transferred into estimates of climate. Some climatic data exist in the latter part of this period, and all available temperature and precipitation data prior to 1901 were used for verification. A modified jackknife method was used for verification of sea-level pressure (Gordon, 1982).

All calibrations involve statistically matching the PCs of climate data with the corresponding PCs of the tree-ring chronologies for the calibration interval of at least 61 overlapping years from 1901–1961. The PCs of the climatic data were estimated, and these data were transformed back to estimates of the instrumental climatic data at each point in the grid. Verification tests were calculated using the transformed data prior to 1901 whenever seven or more independent observations of the instrumental data were available for testing. Many statistical models were validated, so the verification data were used again to determine which of the competing models were the most successful ones (Gordon, 1982).

A stepwise version of canonical regression described by Blasing (1978) was used in the calibration. The coefficients for the canonical regression are estimated using the PCs of the chronologies and climate for the dependent period data. In fact the predictors $\mathbf{X}$ and the predictands $\mathbf{Y}$ in equations (4.14) to (4.17) are PCs and not the raw data; this was done explicitly to reduce the size of the problem for computer analysis. The PCs of the chronology data from both the dependent and independent periods were multiplied by the coefficients, and the products summed to obtain dependent and independent estimates of PCs of climate, equation (4.16). These estimates are multiplied by the eigenvectors of climate and scalers for the means, and variances are applied to obtain estimates of the individual station climatic data.

We did not know ahead of time what the structure of the model should be, so we varied the structure in various ways and used the calibration and verification statistics to determine which structures were appropriate. If the structure of the calibration model was adequate, it was assumed that the coefficients of the canonical variates may be able to accommodate some of the differences as well as the similarities between the chronologies and the varying effects of the climatic variables on growth.

4.5.1. Model structure notation

The values of the PCs of the tree-ring chronologies for different lags are designated as different matrices. Matrix $\underline{\mathbf{I}}$ contains the 15 PCs of the chronology data for the year immediately preceding and including year t, the season of growth (*Figure 4.5*). Matrix $\underline{\mathbf{B}}$ includes the PC for year $t-1$, the year before growth. Matrix $\underline{\mathbf{F}}$ is the year $t+1$ or the year following growth, while matrix $\underline{\mathbf{FF}}$ is year $t+2$ or two years following growth. The PCs for chronologies with autocorrelation removed are $\underline{\mathbf{M}}$, $\underline{\mathbf{M}}(\underline{\mathbf{B}})$, and $\underline{\mathbf{M}}(\underline{\mathbf{F}})$. PCs of chronologies with autocorrelation removed for year $t+2$ as well as chronology data at lags greater than 2 or less than $t-1$ were not used in the example presented here.

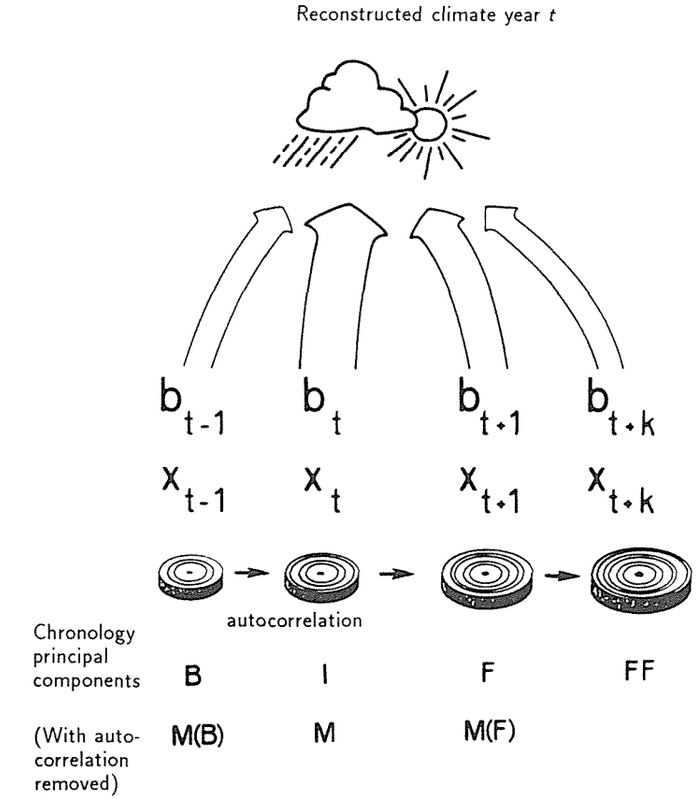

Figure 4.5. The coefficients of the transfer function b_{t-1} to b_{t+1} are multiplied by ring width or other types of tree-ring data x_{t-1} to x_{t+1}, and the products summed to obtain an estimate of year t climate. In this particular study the coefficients are actually multiplied by the PCs of the 65 tree-ring chronologies to estimate the PCs of climate.

The use of PCs not only reduced the size of the problem but excluded the smallest scale variations that are least likely to represent the signal of large-scale climatic variations. The structure of the calibration model was represented by using the above notations such as **B**, **I**, **F** and **FF** to indicate the lag of the PCs used as the predictor sets. Numbers preceding these notations designate the number of PCs included in the set. The first number in the model name gives the number of the climate predictand PCs used in the analysis. Generally, the first 15 PCs of the chronology set were used, and no more than two predictor sets of 15 PCs were used for any one calibration. The first model with 15 predictor PCs was called a *singlet*, and the second with 30 predictor PCs (15 from two different sets) was called a *couplet*. Different numbers of predictand PCs were used, however. The stepwise-selection procedure eliminated insignificant canonical variates and helped to preserve the degrees of freedom of the residuals available for significance tests.

4.5.2. Calibration and verification strategy

Experimentation with a number of reconstructions of the same variable using different calibration structures indicated that widely different structures sometimes yielded comparable calibration and verification statistics but significantly different reconstructions. This was assumed to reflect competing tree-growth response systems in the tree-ring data sets that could be used in reconstructing different versions of past climate. Thus, the structure was varied in a systematic fashion by varying the type of PCs used in the singlet and couplet models and then varying the number of predictand PCs from two to the total number of PCs that were significant (usually from 10 to 20).

A ranking system was developed to help in the identification, of which models provided the best reconstructions. Seven calibration statistics and 17 verification statistics were ranked for the competing models; the ranks were summed for each model, and those with the highest ranks were considered to be optimum.

The calibration statistics used in the ranking include: the calibrated variance percentage; the number of years in which the correlation between the reconstruction and instrumental data was > 0; the number of years in which the correlation between the reconstruction and instrumental data was > 0.3; the number of years in which the RE between the reconstructions and instrumental data was > 0; the number of years in which the RE between the reconstructions and instrumental data was > 0.09; the number of years in which the RE between the reconstructions and instrumental data was > 0.5; and the number of years in which the RE between the reconstructions and instrumental data was > 0.6.

The verification statistics include: the number and percentage of stations over the grid with $r > 0$ (r significant); the number and percentage of stations over the grid with RE > 0 (or a higher level); the number and percentage of stations over the grid with sign test significant; the number and percentage of stations over the grid with sign test of first difference significant; the number and percentage of stations over the grid with product means test significant; the number and percentage of stations over the grid passing one test (or two or three tests); total number and percentage of tests passed; the number of sign tests passed by year over all stations; the number of product means tests passed by year over all stations; and the similarity of reconstruction to a normal distribution as compared with the similarity of the instrumental data set.

To take advantage of differences as well as similarities of the high-ranking models, the reconstructions of two or three competing models were averaged; the averaged reconstruction is referred to as the merged model results for each variable and season. The annual values are simply the sum of the seasonal merged models for precipitation or the weighted average of the seasonal merged models for temperature and sea-level pressure. The weights were proportional to the number of months included in each season, with spring having four months and summer having two months. The autumn and winter seasons comprised three months each.

4.5.3. Rational

Almost all time series of climatic or tree-ring data from a geographical area are collinear because they reflect the largest-scale features of macroclimate. It was assumed that these large-scale common patterns are usually reflected in the variance of the highest-order and most important PCs. Yet, each chronology time series can express a considerable amount of individuality of its owner; it may share more with some neighboring chronologies and less with others. This information that is shared with some neighbors and not with others is likely to be reflected in the variations of the different eigenvectors and their PCs. As the order of the eigenvector and its PC increases, less shared information among the the chronology data would be expected along with proportionally more variance representing error and random variations in the chronologies unrelated to features of the macroclimate.

The largest-scale PCs also are analogous to the mean value of many data sets (LaMarche and Fritts, 1971; Fritts *et al.*, 1971); and as a mean, the larger PCs have a reduced error component. The effects of occasional extreme values and other minor abnormalities become a part of the smallest PCs that are left out of the analysis. Thus, the largest PCs are likely to be distributed normally even if some of the individual chronologies are not.

If the data are highly selected so that the chronologies respond to many of the same climate variables, the chronologies are similar and a large amount of the climatic variance may be reduced by a small number of eigenvectors and their PCs. However, sites that are sampled for general purposes by different workers often have wide differences in species, topography, elevation, exposure, and microenvironments; therefore, there are many different responses to the same climatic variables. Also, if a wide spatial grid is involved, more eigenvectors and PCs of a chronology set may be needed to express the important modes of climatic variations in the region as well as the differences in responses.

Because of this collinearity, multiple regression, canonical regression, or other related correlation techniques can underestimate the error and not provide

valid significance estimates. Stepwise multiple regression also enters individual chronologies as predictors, while at the same time it blocks the entrance of other chronologies that are highly correlated with the entered set. A small number of chronologies is usually selected along with the associated error terms to estimate climate, and the information in a much larger set of chronologies is completely left out. Such an approach implies that the chronologies, which are correlated, can be safely excluded because they may contain mostly redundant information that would not likely contribute significant variance to the statistical estimate.

Such a strategy might apply if the predictors were errorless and only one station climatic record is to be estimated. However, chronologies based on 10 or more trees can have large error components, particularly in the early years when the number of available trees was less (Wigley *et al.*, 1984). Every chronology in the area may contain useful climatic information as well as an error component. If a way could be found to factor out the variable response to climate, it would seem more reasonable to use the information from all related chronologies to reconstruct spatial variations in climate. The key to this approach is to select information that is meaningful from as large a number of chronologies as possible and to eliminate that information that is not meaningful, while at the same time maximizing the available degrees of freedom in the analysis.

It was thought that the eigenvectors of a chronology grid and their PCs provide a means of extracting the largest-scale (the most important) modes of variation from an array of climatic data or tree-ring chronologies. In addition, these transformations are mathematically constrained to be orthogonal to one another, which is optimal for multiple regression analysis. It is not necessary to interpret the eigenvectors, although the first few eigenvector usually have interpretable patterns.

4.5.4. Computations

Any relationship between the two types of data sets is not guaranteed even though PCs have been derived from the predictor and predictand data set. An assessment of the correlation between sets is accomplished by extracting the canonical variates (Clark, 1975). The regression equation is given by equation (4.16). The canonical analysis rearranges the correlations between predictors and predictands. This canonical rotation restores orthogonality that had been lost because of the following reasons: the PCs of both tree growth and climate were derived for the entire length of the record while the calibration was obtained using a shorter time period; the eigenvectors and PCs of the $\underline{\mathbf{I}}$, $\underline{\mathbf{M}}$, and $\underline{\mathbf{F}}$ tree-ring sets were computed independently, and therefore were correlated; the PCs of different lags were used as predictors, and the relationships between these lagged sets were not orthogonal.

The effect of any canonical correlation along with its corresponding elements in $\mathbf{Vx}$ and $\mathbf{Vy}$ can be eliminated without affecting the others by setting the corresponding canonical correlation to a zero value (Blasing, 1978). In canonical correlation analysis, the correlations are often tested through the Wilks' lambda statistic, equation (4.18). This test appears to be inappropriate for regression analysis because it gives equal weight to the variance in both the

predictand and the predictor sets. Since it is a problem of regression rather than correlation, we use the ratio between the explained and the unexplained predictand variance [see equation (4.7)], where the number of degrees of freedom of the residuals, $n - m - 1$, is eventually corrected, for the positive autocorrelation $r1$ of these residuals, by the factor $C=(1-r1)/(1+r1)$ (Mitchell *et al.*, 1966).

A stepwise-testing procedure was developed to enter one canonical variate at a time into regression starting with the largest canonical correlation (see Lofgren and Hunt, 1982). The canonical correlations for all other variables not to be considered at that step are set to zero, and the F value is computed: F_{inc}, which is the F ratio of the increase in explained variance from the last previously significant step.

Whenever the F_{inc} ratio is smaller than the theoretical value, that particular canonical correlation is set to zero and the F_{inc} ratio for the next smaller variate is calculated again using only the canonical variates found to be significant at previous steps in the selection sequence. If the F_{inc} ratio is equal to or greater than the expected value, the stepwise procedure leaves that canonical variate in regression. At that time it rechecks the variance ratios for variates that were rejected at all previous steps and enters them if the F_{inc} ratio is now large enough to be significant. After all previously rejected variables have been retested and either selected or rejected, the stepwise procedure continues by testing the canonical variate with the next smallest canonical correlation.

This forward and backward selection process continues until all canonical variates have been tested. Sometimes variables with high canonical correlations are excluded from the regression. At other times they are excluded at an early stage but are included at a later stage because the variance of the residuals declines with the inclusion of more and more significant variates. The variables retained in the final regression after all insignificant ones have been eliminated become the coefficients of the transfer function.

The reconstructions for all independent data are obtained by applying equation (4.16) including only the significant canonical correlation of C (the others are set to zero). Because the predictands are the PCs of the climate series, the estimates in equation (4.16) are multiplied by the climate eigenvectors. Indeed, by equation (4.50) we have:

$$_{nx}\hat{\mathbf{X}}_m = {}_{nx}\hat{\mathbf{Z}}_{qx}\mathbf{A}\mathbf{x}'_m \quad , \tag{4.51}$$

where $\hat{\mathbf{Z}}$ is the climate PC matrix estimated by canonical regression and *denormalized.* $\hat{\mathbf{X}}$, being normalized, must be also denormalized. In fact, the variance used in the above F test is calculated from the denormalized predictand estimates and from the variance of the climatic predictand set.

The percentages of variance reduced at each temperature station with canonical variates 2, 3, 4, 5, 6, 8, and 9 are shown in *Figure 4.6(a)*. The model was 16**T**15**I**15**M** in which 16 PCs of winter temperature were reconstructed from 30 PCs of tree growth. The variance reduced exceeded 50% for many stations in the southeastern United States and the southern Rocky Mountains and high

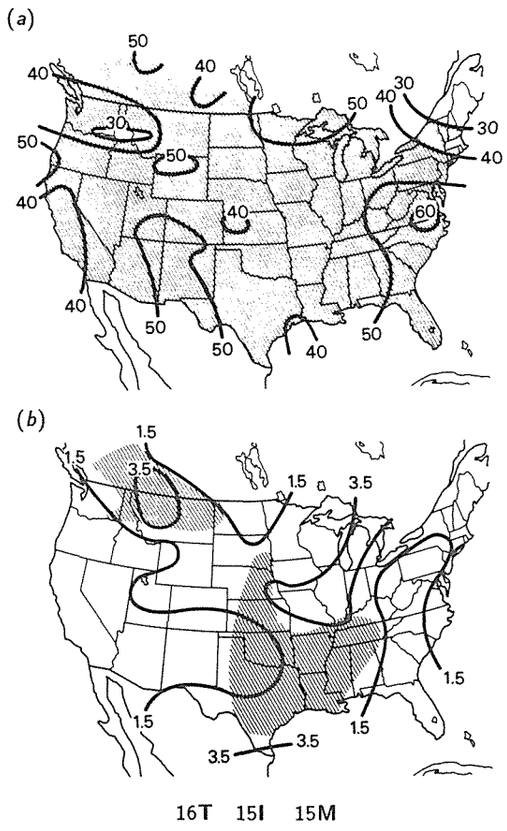

Figure 4.6. The percentage of explained variance, EV, (*a*) and the numbers of verification tests, out of 5, (*b*) that were significant for winter temperature model 16T15I15M over the reconstructed grid. Areas in (*b*) with RE greater than 1.0 are shaded.

plains. It is interesting that the highest variance reduced was 63% for the Lynchburg, Virginia, record. Such high values for such a distant station could well be a random result. It is especially important to check such results by applying verification statistics to independent temperature data from that record.

Figure 4.6(*b*) summarizes the verification statistics. The contours show the number of verification statistics out of a total of five that were significant. The 1.5 contour marks the area where the number of significant statistics are greater than that expected by chance. The shaded area shows where the RE statistic is greater than zero. Verification of this model appears to be good from the Rocky Mountains to the Great Lakes and south.

4.5.5. Spatial patterns in the statistics

The results from two or three individual models were averaged to form the seasonal models, and these seasonal models were averaged further to obtain the annual results. The spatial features in the calibration and verification statistics for annual temperature and precipitation are shown in *Figure 4.7*. The explained variance for annual temperature is a substantial improvement over the individual models (*Figure 4.7*). It exceeds 30% over most of the grid. The data were verified for many areas in the Plains states, the western Great Lakes area, and the upper Mississippi Valley, while verification was poor in many areas of the southwest and midwest states. The annual temperature data verified the best, but three areas of poor reconstruction were indicated: the Intermontane Basin of the west, the Ohio River Valley to the Atlantic coast, and Florida to south Texas. The results for the last two areas were expected because the regions are the furthest away from the tree-ring grid.

Good precipitation reconstruction was generally confined to the western states and was best for winter and spring. Calibration was poor in summer and autumn, but verification indicated that there was some success during these seasons in the far west, Central Plains, and Great Lakes. More than 30% variance in annual precipitation was reconstructed in California, the Rocky Mountains, and the Central Plains. The verification statistics suggested that some annual precipitation estimates could be better than chance for areas of the west extending through the Central Plains to the upper Mississippi Valley and the southern Great Lakes states, but the verification of precipitation in the Central Plains and upper Mississippi Valley was marginal at best.

The area of reliable annual precipitation reconstructions is more dependent on the proximity of the tree-ring grid than the reliability of annual temperature. The annual precipitation reconstructions appear of little value throughout the southern and eastern parts of the United States and west of Lake Superior to eastern North Dakota.

The spatial features in calibrated variance and verification statistics for annual sea-level pressure are shown in *Figure 4.8*. A maximum in calibrated variance is centered over the Canadian Arctic. Substantial pressure variance is both calibrated and verified for the southwestern United States, while little variance is calibrated and verified along the United States–Canadian border. Large areas over the North Pacific Ocean are both calibrated and verified. The areas of high calibration appear to be related to regions where anomalies in storms could influence the anomalies of precipitation and temperature in the area of the tree-ring chronology grid.

Some areas of Eastern Asia appear to calibrate and even to verify. Gordon *et al.* (1985) demonstrate a linkage between large-scale variations in reconstructed sea-level pressure over the North Pacific and winter severity in Japan. Lough *et al.* (1987) find sea-level pressure anomalies over the North Pacific that appear correlated with the occurrence of widespread drought or flood in both Asia and North America. The lowest verification of the annual pressure series can be noted from Central Asia through Siberia where the area of low verification turns southeast over southern Alaska, the Gulf of Alaska, and the

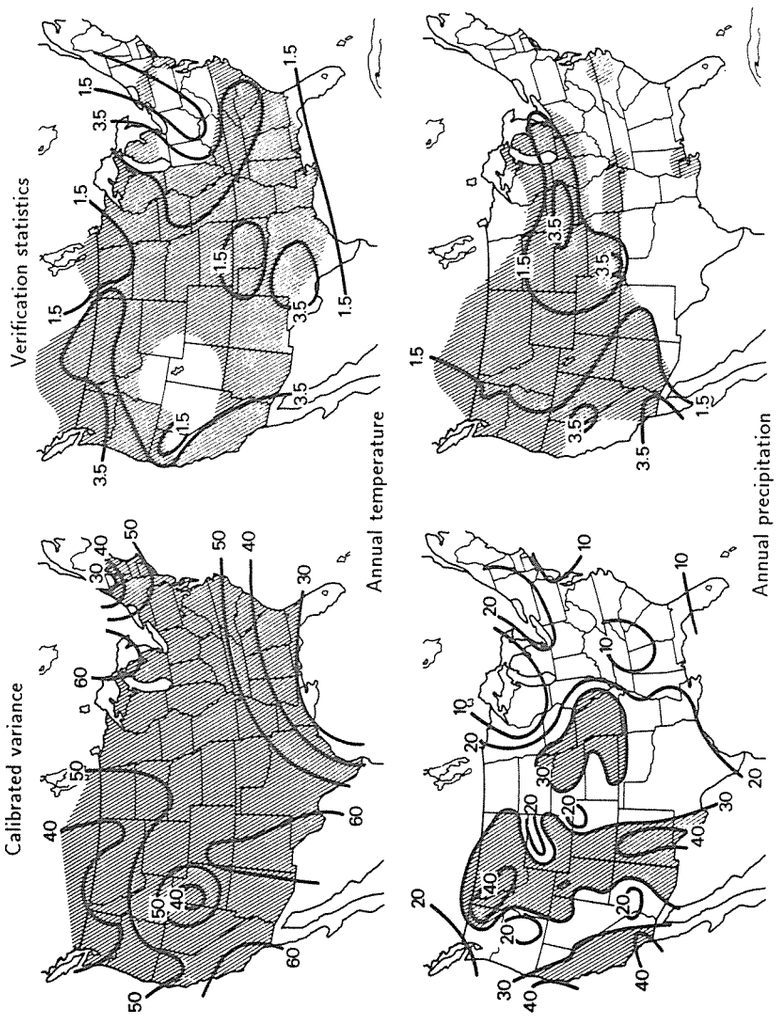

Figure 4.7. Same as *Figure 4.6* except the percentage of calibrated variance and verification statistics are for models of annual temperature and annual precipitation.

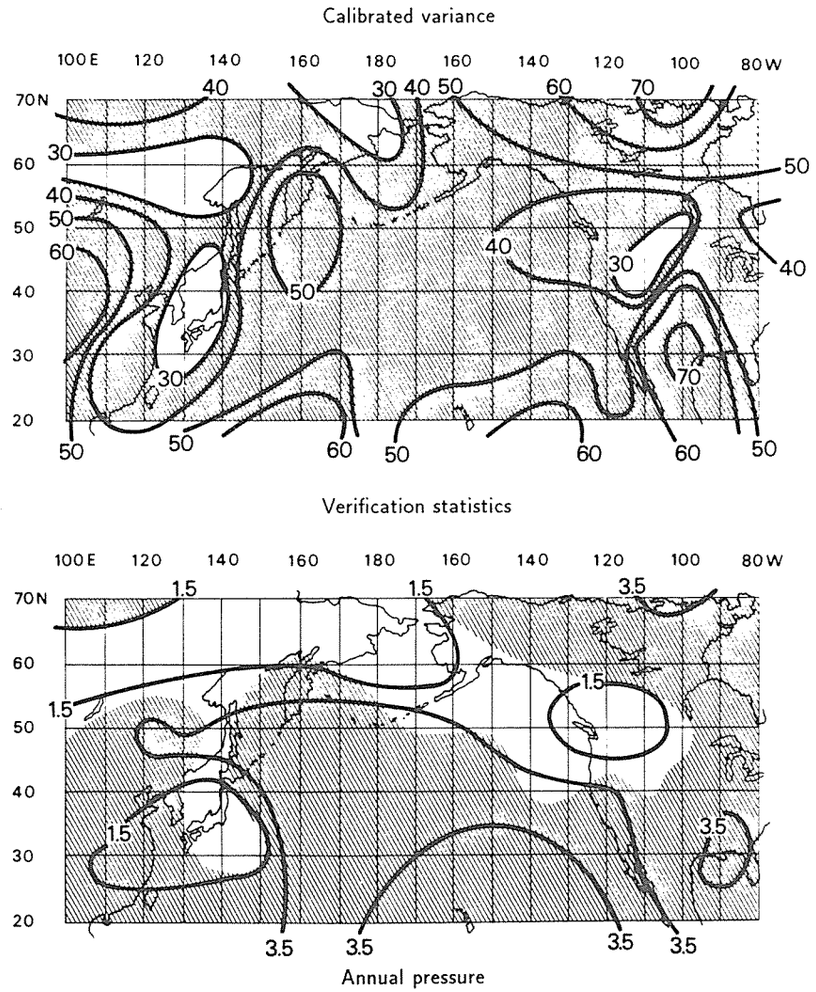

Figure 4.8. Same as *Figure 4.6* except the percentage of calibrated variance and the verification statistics are for the models of annual sea-level pressure.

Pacific northwest. This is an area of large pressure variations associated with the succession of cyclones and anticyclones that occur in the upper-level flow (Lamb, 1972). It is not clear why sea-level pressure in this area is so poorly reconstructed by this particular tree-ring chronology grid.

The calibration and verification statistics indicate that different variables can be reconstructed from the same tree-ring grid, and some reconstructions are possible beyond the area of the tree-ring chronology grid. However, the ability

to reconstruct generally declines with increasing distance from the tree-ring grid. The temperature reconstructions are more reliable than those for sea-level pressure and precipitation even though the chronologies used were primarily from semiarid sites. As indicated by the eigenvectors and PCs for the different variables, temperature exhibited more large-scale variability than precipitation, and the canonical analysis with PCs was effective in transferring the large-scale patterns of growth into large-scale variations in temperature. The large-scale patterns in sea-level pressure were also well calibrated, but accuracy was diminished because of the greater size of the grid compared with the size of the temperature and precipitation grid.

4.5.6. Effects of averaging on calibration statistics

All Seasons, Grids, and Variables Pooled

The above data as well as the theory of mean values suggest that substantial error variance can be reduced and the reliability of the reconstruction enhanced when data are averaged in some manner. In this climatic reconstruction, the results were averaged or combined in the following ways: the results from two to three component models of different structure for a variable, grid, and season were averaged (merged models) to form one set of grid-point reconstructions; the results from several grid points within a homogeneous climatic region were averaged (pooled by regions) to obtain one regional climatic signal; the regional averages were filtered (pooled and filtered) thus averaging the data over more than one year to enhance the low-frequency over the high-frequency climatic estimates; and the seasonal models were combined (merged) to form annual estimates. The statistics were used to assess the error changes. These annual estimates can be averaged for regions, filtered, and then tested for further signal enhancement.

The values of dependent and some independent data statistics from models reconstructing seasonal temperature, precipitation, and sea-level pressure were averaged from all seasons, variables, and grids. The reconstructions were then averaged as indicated above, the statistics recalculated to measure any improvements, and these data averaged. *Figure 4.9* shows the pooled results for EV, EV′, and RE′ values, equations (4.45) to (4.47). The plots for merged annual data are separated from the seasonal data shown on the left. As theory would indicate, the fractional variance estimated from EV was consistently higher than that of EV′, sometimes as much as 0.19. These data were in turn higher than the mean RE′ statistic. At each successive level of pooling there is an approximate increase of 0.10 fractional variance for the three statistics. The difference in EV′ progressing from left to right in *Figure 4.9* is 0.085, 0.104, and 0.077 for each change in level of the seasons and 0.120 and 0.156 for each change in level of the annual reconstructions. These data are averages of 48 different models that were calibrated with seasonal temperature, precipitation, or sea-level pressure. Each calibration utilized the growth data from more than 700 trees used in this particular analysis.

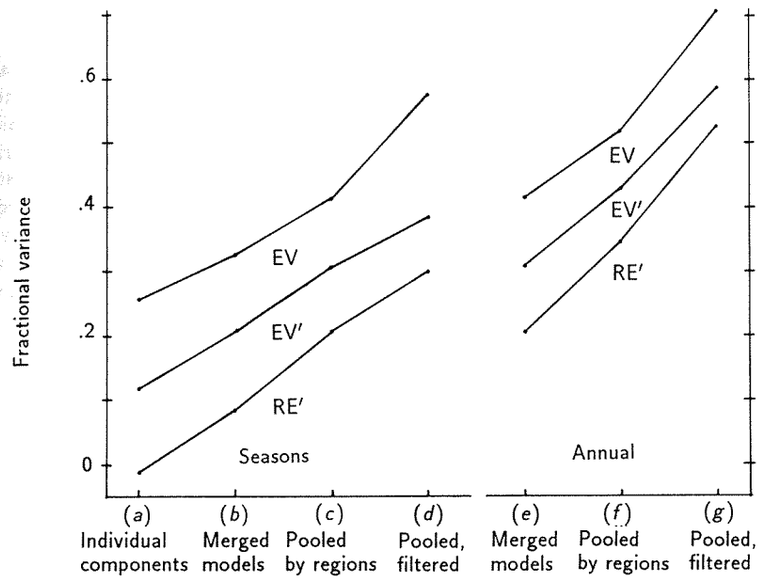

Figure 4.9. The explained variance (EV), adjusted explained variance (EV'), and estimated RE′ for all variables, seasons, and grids (*a*) averaged for individual seasonal component models, (*b*) averaged for seasonal merged models, (*c*) averaged for seasonal data pooled by region, (*d*) averaged for seasonal data pooled by region and filtered, (*e*) annual merged models, (*f*) annual merged data pooled by regions, and (*g*) annual merged data pooled by regions and filtered.

The annual estimates are clearly more reliable than the seasonal estimates, and the pooling and filtering of annual data are accompanied by a greater average improvement. The annual filtered regional average is 0.703 for EV, 0.585 for EV′, and 0.524 for RE′. This indicates that, on the average, 70.3% of the filtered climatic data was reproduced by the filtered estimates. This amounts to a population variance of 58.5% with an RE′ of 52.4%. These data also suggest that the annual estimates of climate, which have been summarized by regions and filtered, in the case of this study, have the highest SN ratio and provide the most reliable climatic estimate.

However, the degrees of freedom of the regionally averaged data and the filtered data were greatly reduced over the unfiltered data so many of the statistics for these series were insignificant or marginally significant. The more conservative population values for the explained variance, EV′, are used in the remaining analysis.

It should be noted that every increase in the agreement between reconstructed and estimated data due to averaging is accompanied by a corresponding decrease in total variance. Thus, the agreement must be expressed as fractional variance, percentage of the total variance or SN ratio.

Differences Among Climatic Variables

The statistics were categorized according to precipitation, temperature, and pressure, and the data were pooled to assess the fractional variance differences for reconstructions of different climatic variables. The results for EV′ are plotted in *Figure 4.10*. The precipitation reconstructions have a lower adjusted fractional variance than either temperature or sea-level pressure. The mean values for the individual component grid-point estimates for seasonal and merged models for precipitation are no larger than many noise-level estimates. However, when the seasonal estimates are pooled by regions and filtered or when they are combined to form annual estimates, the average fractional variance improves substantially reaching values just under 0.5.

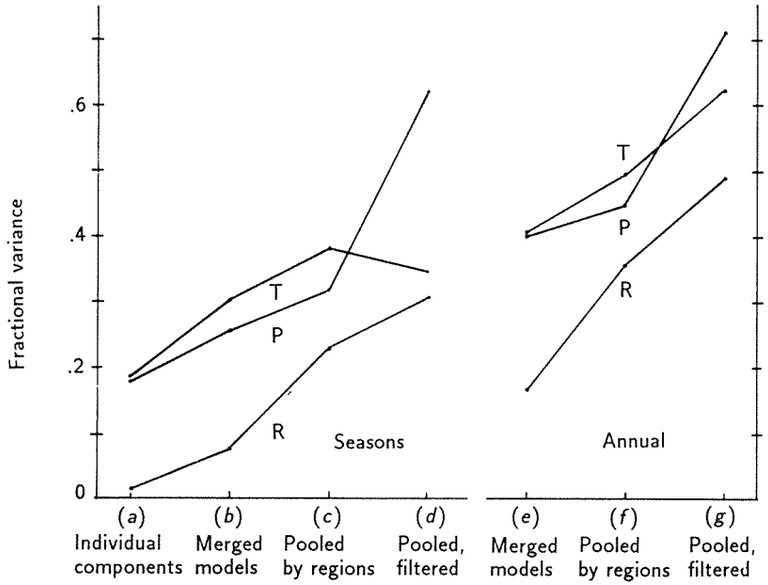

Figure 4.10. Same as *Figure 4.9* except for only EV′ and data categorized according to temperature (T), precipitation (R), and sea-level pressure (P) reconstructions.

The most reliable grid-point and regional estimates are those for seasonal and annual temperature. However, the filtered estimates for sea-level pressure are more reliable than either those for temperature or those for precipitation.

The merging of the component models resulted in an increase of 0.117 fractional variance for temperature, which was substantially higher than the fractional variance increases at the same level of 0.076 for sea-level pressure and 0.059 for precipitation. These data suggest that the pooling of temperature models resulted in a greater improvement than in those models when pressure and precipitation were pooled in the same manner.

The highest EV′ values for seasonal and annual reconstructions are those for the PCs of sea-level pressure with fractional variance values of 0.618 and 0.706 compared with 0.349 and 0.621 for temperature. The maximum values of the EV′s for the filtered pressure PCs are 0.857 and 0.879, and the corresponding RE′ values are 0.570 and 0.667, respectively. This suggests that the low-frequency and large-scale sea-level pressure changes are reconstructed more precisely than the high-frequency and small-scale changes. The greatest change in EV′ between pooling levels for precipitation occurs when data for merged models are pooled into regional averages. The difference in EV′ values is 0.156 for seasonal data and 0.189 for annual totals. This is more than twice the difference obtained for temperature and approximately three times the difference obtained for pressure. It, therefore, appears that the averaging of reconstructions from a number of stations within a climatologically homogeneous region is an effective way of increasing the reliability of a spatially inhomogeneous variable such as precipitation.

Differences Among Verification Statistics

The verification statistics can be classified, averaged, and compared in the same way as the calibration statistics, except that the independent instrumental record varies in length for each temperature and precipitation station. Therefore, comparable regional averages could not be computed for temperature and precipitation. However, they could be computed for sea-level pressure as independent PCs were available from the "Subsample Replication" (Gordon, 1982). The results for the five verification tests and the RE values > 0 for all variables, grids, and seasons were classified and averaged to show the changes associated with three levels of averaging (*Figure 4.11*). All six statistics show rising trends with each successive level of averaging.

The marked change in the percent of statistics is significant between the merged and annual models. These results indicate that calibrating one season at a time and then averaging seasonal estimates into annual values did appear to reduce the percentage of error substantially.

The two sign tests have the lowest percentages of tests passing. This simply reflects the fact that the nonparametric statistics are the least discriminating of the statistics. The product mean results were also low, but the percentage of change between the merged model and annual model for the product mean is as large or larger than any other verification statistic.

4.6. Visual Analysis

F. Schweingruber

The simplest but also most stringent assessment of the dendroclimatological quality of individual chronologies within a network is based on visual, year-to-year comparisons of anomalies in tree rings and climate. The measure of quality is the visual similarity of the patterns appearing on the maps. The comparison

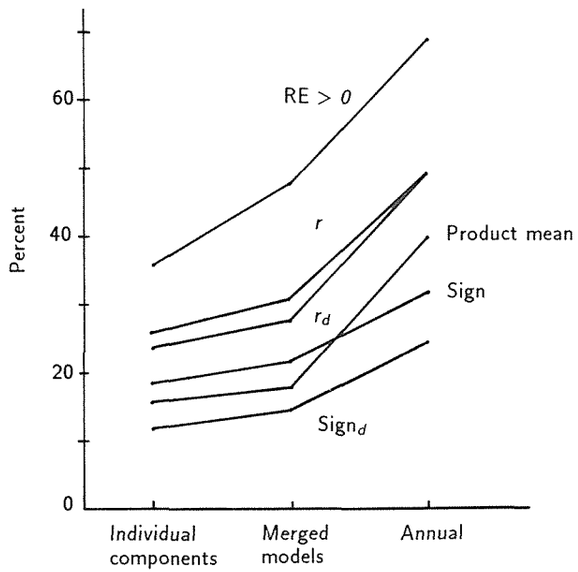

Figure 4.11. Same as *Figure 4.9* except for six independent verification statistics from individual components, merged models, and annual combinations.

reveals, in year-to-year terms, in which regions and to what degree the growth performance of the trees is directly influenced by climatic factors.

The prerequisite for such a stringent calibration of dendroclimatological data is that the network be ecologically uniform. The network discussed here comprises 101 indexed local chronologies of maximum density and ring width in Europe, which have been grouped to give 22 regional chronologies (Schweingruber, 1985). All the samples were taken from conifers with normal growth standing on moist cold sites in the summer near the upper or northern timberline. Selecting the samples according to these criteria maximizes the limiting effect of temperature, and it is to be assumed that the energy for cell wall formation in the latewood (maximum density) originates from photosynthetic production during the summer months of the current year. A section of the temperature network over the Northern Hemisphere constructed by Jones *et al.* (1982) provides a comparable climatological network.

To compare the data cartographically, the dendrochronological and climatic data were processed to produce year-to-year anomaly maps. In the dendroclimatological network, the 0 value (threshold between positive and negative anomalies) is the mean indexed value of every chronology over its whole length. In the climatological network it is the mean monthly temperature from July to September during the period 1881–1980. Within the anomalous fields, as many graduations as desired can be made. In the next step, the maps for each year are visually compared. The degree of similarity is subjectively assessed, i.e., it is

decided whether the match between fields in terms of border and size is good, fair, or poor. In the case of the European network, the patterns were first compared over the entire area, then over the eastern and western halves (division along the 10°E line of longitude) and the northern and southern halves (division along the 50°N parallel) for each parameter in each year from 1881 to 1976 (*Figure 4.12*).

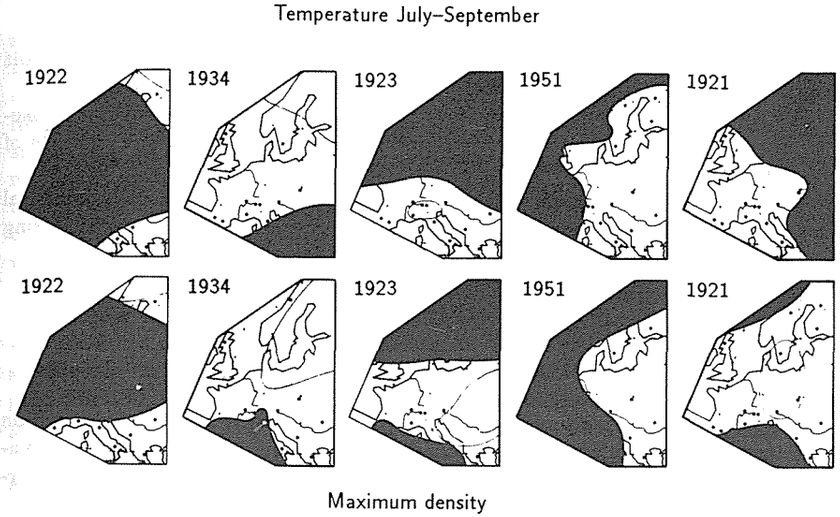

Figure 4.12. Examples of pairs of maximum density anomaly maps with differing degrees of similarity. Black areas are below-average temperature and maximum density values. White areas are above-average temperature and maximum density values.

1922: great similarity	size and shape very similar
1934: similar	size very similar, shape different
1923: similar	shape similar, size different
1951: similarity detectable	size or shape are somewhat similar
1921: dissimilar	no detectable similarity

The method allows year-to-year calibration of the values of all chronologies from the entire area. Verification is not necessary, as each map in a pair is statistically independent of the other. The measure of quality is the number of map pairs showing similarity or great similarity for each time unit. The quality and frequency of matching is not the same in all periods. A year with no detectable connections between maximum density and summer temperature (e.g., 1942, 1948, 1969, 1974) may be followed by a series of map pairs with great similarity, or a period with poor agreement may be succeeded by one with good agreement (e.g., 1881–1921 with 72% poor and 1922–1976 with 94% good). A lack of similarity in a particular year may be primarily owing to the effect of ecophysiological factors (e.g., extreme frosts) on maximum density. Poor agreement in periods of early meteorological records is probably owing to the low quality of

the meteorological data. Currently, the effect of pollution on the amount of agreement cannot be excluded. There is generally poor agreement between ring width and any single climatic factor. Since cambial activity is to a large extent dependent on the climatic-ecophysiological conditions of both the current year and the preceding years, hardly any direct influence of climate can be detected by means of mapping.

Visual calibration, i.e., comparison of anomaly maps of climatic factors and ring patterns in and around Europe, reveals the following points:

- Such calibration requires high-quality data, and is only successful where it is constructed on the basis of uniform criteria.
- Different ring parameters produce different patterns on the maps. Consequently, there seems to be little point in statistical analysis of a mixture of parameters.
- Map pairs are not similar on average but sometimes practically identical and sometimes completely dissimilar. This must be borne in mind during interpretation of statistically calibrated data series.

4.7. Conclusions

H.C. Fritts

Chapter 4 deals with methods that can be used to extract climatic information from tree-ring data. All methods assume that some kind of growth-climatic relationships are present and that the information in tree-ring features can be interpreted as or transferred to reliable estimates of past climatic conditions.

Most of the statistical methods are regression techniques assuming that the modeled relationships are time stable, analogs do indeed exist, the tree-growth and climate relationships have similar (linear) structures, and (for parametric statistics) the tree-ring and climate data sets are normally distributed.

Tree-ring and climatic data are calibrated over a particular time period. Most research designs require some type of quality control. It has been customary to validate the accuracy of the relationship by comparing estimates of climate from another time period with actual records of climate. A variety of verification statistics with different attributes can be used not only to verify the accuracy of the reconstruction but also to evaluate which of several promising models produce the most reliable results.

Bootstrapping offers an efficient alternative of verifying the reconstructions. In some instances it may be preferable to use all the data available to increase the chance of including a maximum range of climatic variations in the calibration. At each replication, the data, which are not randomly drawn, can be used for the independent verification. Finally, these verification statistics can be averaged over all the replications, and the confidence interval computed.

Multiple regression can be a useful calibration technique when the predictor data sets are not highly correlated and do not violate the assumptions of this method. Stepwise versions of multiple regression can be used to screen and select the predictor variables. The principal components can be extracted and a

subset of them used instead of the original predictor variable set. These *new* variables are orthogonal (uncorrelated), and the largest ones can be selected to simplify the analysis. Several criteria are described for deciding the number of principal components to include in an analysis. The PVP criterion is a good compromise between using all the PCs (which is equivalent to multiple regression) and using too few PCs with the associated underestimates of the predictand means and standard deviations.

Canonical regression differs from standard multiple regression in that there are more than one predictand variable, and an eigenvector analysis is made on the covariation matrix. The technique first involves a canonical correlation analysis, and then regression statistics are calculated and tested. Bootstrap method has shown that the errors of the canonical regression coefficients are small and well estimated. Canonical regression is found to be a promising method if a valid criterion is used to select the PCs and optimize the inversion of the correlation matrix. Criteria that remove too many PCs may increase the correlation between estimated and actual predictands on the independent interval but may underestimate the mean and standard deviation of the estimates.

Often principal component analysis is used on the input variables to reduce the number of variables, to orthogonalize the variations, and to reduce random variations by excluding the small principal components representing error and small-scale variations in growth and climate. It has been applied to consider lagging and autoregressive relationships with some success. One approach is to use predictor variables that lag behind the predictands. Another approach is to remove autoregressive-moving average processes by ARMA modeling or by applying filters. In addition, calibration with seasonal climatic data may allow the tree-response systems to accommodate for the changing relationships expected in different seasons. In such cases the annual response can be assessed by simply adding the reconstructions for each of the four seasons or, in the first case, summing the autoregressive or filtered estimates and the white-noise filtered estimates to obtain estimates for the entire spectrum.

Several characteristics are noted in the reconstructions of large-scale climatic patterns from a large number of tree-ring chronologies. The errors of the climatic estimates are reduced when the results from two or three well-verified seasonal models are averaged together or when the seasonal estimates from the four seasons are combined into annual values. Data estimates for different locations in a region are often improved by averaging and expressing them as a mean of the region. Estimates often appear to improve when the they are filtered but have too few degrees of freedom to be significant.

The canonical regression-using principal components show that different kinds of climatic information can be reconstructed from large grids of tree-ring chronologies. Temperature is reconstructed more reliably than either precipitation or sea-level pressure even when the chronologies are selected from sites where drought is thought to be limiting to growth. Generally, the climate from areas near the tree sites is best calibrated. However, for some regions the variations for temperature and sea-level pressure can be reconstructed at considerable distance from the tree sites. Low-frequency information appears to be more reliably reconstructed than high-frequency information.

The best analogs method reconstructs past climates by searching for years in which the growth patterns are similar to the present patterns. This method compares observations, not variables, and can deal with heterogeneous series such as the large differences between historical proxy data and pollen series or tree-ring data sets. It is a method that can enhance the low frequencies in a data set (Guiot, 1985b) and has been used to analyze pollen records (Guiot, 1987b).

Methods like spectral regression and AR modeling offer other viable alternative solutions depending upon the nature of the problem and the objective of the research. Bootstrapping is advised for the former because of the limited numbers of degrees of freedom in the low-frequency estimates.

Multivariate autoregressive analysis seems especially promising because it incorporates the strengths of ARMA modeling and multiple regression analysis. In one sense, the multivariate AR method works on more predictors than the number of tree-ring series that are present because it involves lagged predictors and predictands. This offers unique solutions to autoregressive and moving average processes but could be prohibitive in analysis of large climatic and tree-ring networks. It is optimal for analyzing a small number of long tree-ring chronologies and relating them to long-term variations in climate using a minimum of coefficients.

Some methods involve considerably more computation than the standard regression analyses. However, microcomputers are now available with so much memory and power that the one to two thousandfold increases in computing time that were reported in this paper would not limit the use of these methods.

Visual calibration by means of graphic techniques is described as an alternative to statistical calibration. The method requires that the tree-ring data be carefully sampled to assure that the network is ecologically uniform. Anomaly maps of growth and climatic data are compared and the year-to-year similarities and differences are assessed. It was concluded that there seems to be little point in statistical analysis of a mixture of parameters. Map pairs are not similar on average but sometimes practically identical and sometimes completely dissimilar. This must be borne in mind during interpretation of statistically calibrated data series.

In spite of some disagreements and differences in points of view, statistics provide an important and objective means to calibrate, verify, and reconstruct past climatic variations from the variations in tree-ring data. A variety of statistical models can be used to reconstruct a variety of climatic variables. Different kinds of tree-ring measurements can be calibrated in the same model to improve climatic estimation (Schweingruber *et al.*, 1978). However, some of the statistical models may never be successful if they do not adequately resemble the true biological cause and effect of climate on tree growth. A good calibration also requires that an adequate number of trees be collected from sites where climate has been limiting, that all the rings are dendrochronologically dated, and that nonstationarity is removed by some type of standardization process. In addition, a good calibration requires that accurate climatic data are available for enough years to make statistical tests of significance possible and to provide some independent data for verification purposes. Theoretically, the bootstrap method might appear to be an attractive alternative. However, the method assumes that

all the necessary information is contained in the sample. If this is the case, then it may not be as rigorous a statistic as a test on truly independent data.

In this chapter we have attempted to describe at least a few of the procedure of calibration and verification and some of the related statistics. We have tried to illustrate the basic ideas of calibration and verification by drawing from our own experience using our favorite statistics. It is a very large subject to cover completely, and we wish to acknowledge that our discussion is by no means an exhaustive one. It is obvious that more work is required to compare these statistics and to design effective strategies for hemispheric analysis of climate from tree-ring data. However, statistics can provide a powerful tool if they are used judiciously to test carefully constructed scientific questions and if the statistics adequately reflect the relationships that are to be evaluated.

CHAPTER 5

Tree-Ring/Environment Interactions and Their Assessment

Chapter Leader: D. Eckstein
Chapter Contributors: J. Innes, L. Kairiukstis, G.E. Kocharov, T.H. Nash, W.B. Kincaid, K. Briffa, E. Cook, F. Serre-Bachet, L. Tessier, D.J. Downing, S.B. McLaughlin, H. Visser, J. Molenaar, F.H. Schweingruber, D.A. Norton, and J. Ogden

5.1. Introduction

D. Eckstein

It is well known from history and prehistory that there are close relationships between environmental changes and the social, cultural, and economic development within a region. However, environmental impact assessment is a rather new field of research (e.g., Beanlands and Duinker, 1984), partly because of missing knowledge on the frequency and intensity of environmental changes in the past and of their causal mechanisms. Dendrochronology is one of several fields that can contribute to filling this gap.

The information on environmental changes can be recorded in a tree in various ways. Nevertheless, an individual tree represents only a single mosaic stone, whereas the whole picture becomes recognizable only if many trees are interpreted. In the most obvious case an environmental event of the past has injured some trees mechanically, e.g., through fire or rock slides, thus leaving a scar in the wood as a pointer of time. Visible signs can also be set through physiological pathways, e.g., by late frost. Harder to detect are those effects that are recorded but hidden in the width, wood density, and structure of the annual increment of trees. Only in exceptional cases are the deviations of these parameters, from what is assumed to be normal, so obvious that pure visual judgment will lead to a reliable result. In general, statistical procedures have to be applied to differentiate natural from man-made fluctuations. The annual increment of trees can also be analyzed for its chemical content derived from environmental

E. R. Cook and L. A. Kairiukstis (eds.), Methods of Dendrochronology, 219–288.

sources, particularly heavy metals. Like data on ring width, wood density, and structure, these data are measurable quantities. But rather than relying on statistics, a careful physiological interpretation is needed.

Another category of information in tree rings differs basically from the types mentioned above in the way that it is stored in the trees. For example, a record of the abundance of trees and their felling years from historical, archaeological, or geological material may indicate environmental changes, although the causal links may be difficult to recognize. Also, systematic changes in tree ages over time in a sufficiently large historical or archaeological wood collection, along with systematic changes in the average tree-ring width, may allow some consideration of the changing forest community as well as landscapes in general.

In this chapter various approaches to detect environmental changes of the past are introduced, in which the examples used for illustration are unavoidably subjective.

5.2. Qualitative Assessment of Past Environmental Changes
D. Eckstein

Man-made impacts on natural environments are as old as the human species itself, but the intensity of these impacts have increased during the past 10,000 years. Some of the early environmental changes can be detected in retrospect.

Becker (1983b) dated hundreds of subfossil oak trunks from Holocene gravel deposits along the Main valley in the Federal Republic of Germany. The dendrochronological dates cluster into groups separated by time gaps without any tree finds. These clusters indicate phases during which oaks from riverine forests were eroded and deposited into the valley fill. According to the dendrochronological dates, periods of increased fluvial activity occurred from 2200 to 1600 B.C. (sub-Boreal times), during the first two centuries A.D. (sub-Atlantic times), and between A.D. 550 to 750 (*Figure 5.1*). It was concluded that the buried trees originated from heavy and repeated floods whereby the river channels migrated laterally.

Sometimes floods reached oak sites far from the earlier flood plains. This is indicated by the fact that the deposition of trunks started with young trees in the second century B.C., includes 300-year-old oaks around the turn from B.C. to A.D., and 400-year-old oaks only 100 years later. The phases of heavy floods are assumed to reflect disturbances caused by forest clearances in the river catchment basin by prehistoric man resulting in accelerated runoff and an increased bed load. The sub-Atlantic deposits coincide with the settling of the Romans and Alemanni in southern Germany. Through this chain of events, the growth conditions in the valley must have improved due to the deposition of alluvial loam and a rise of the groundwater level. This is indicated by wider annual rings and higher autocorrelation in the tree-ring series.

Delorme *et al.* (1983) analyzed subfossil oaks from several bogs in northern Germany deposited between 350 to 150 B.C. They conclude from the clustering of the die-off years that the area became increasingly waterlogged resulting in the

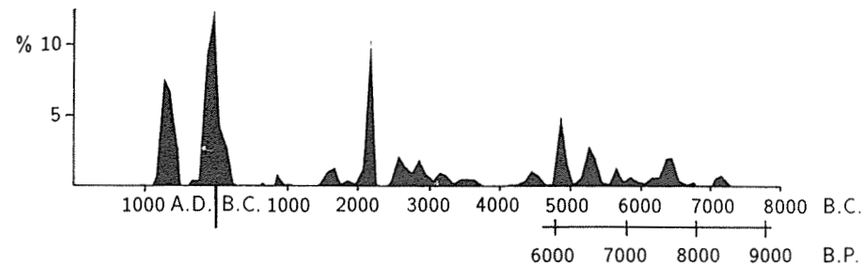

Figure 5.1. Clusters of dendrochronological dates from Holocene gravel deposits along the Main valley in the Federal Republic of Germany. The dendrochronological dates cluster into groups separated by time gaps without any tree finds. These clusters indicate phases during which oaks from riverine forests were eroded and deposited into the valley fill.

deposition of fen peat. This in turn was caused by the fact that the climate got increasingly humid during that period.

Pilcher and Munro (1987) present a graph of the distribution through time of the trees included in the Belfast 7,272-year chronology. This shows distinct periods of abundance and depletion in the population of oaks growing on wet fens in the north of Ireland. The depletions, particularly at 2450, 1900, and 950 B.C. may be interpreted as times when the fen lands became less favorable for tree growth owing to increased wetness.

Bartholin (1983) interpreted relative dendrochronological datings on oak (*Quercus*), basswood (*Tilia*), elm (*Ulmus*), and poplar (*Populus*) from an excavated pile construction near Lake Vattern in Ostergotland, Sweden, which according to ^{14}C dating belongs to middle Neolithic times (ca. 4430 B.P.). The trees cut down were very young, the oaks ranging from 20 to 70 years. All samples of oak could be cross-dated in a floating chronology that was applicable for dating samples of lime, poplar, and elm. According to the results all oaks started growing at the same time, irrespective of the time of cutting that spreads mainly over 17 years, and show an almost uniform growth pattern (*Figure 5.2*). It was therefore concluded that the forest grew up spontaneously in an open area. However, the cutting activity of the settlers did not result in an increase of the ring width of the remaining trees. Thus, a successive clearing of the woodland area was inferred rather than a selective cutting. From this study, an open landscape with scattered young apple (*Malus*) trees (identified from wood anatomy) and groups of elm (*Ulmus*) stump shoots is assumed to have existed before the forest emerged.

Heikkinen (1984) used tree-ring analysis to study the tree invasion of sub-Alpine meadows during the past 100 years and to find the factors controlling the dynamics of the upper timberline. To examine the progress of forest expansion, sample plots were chosen in an area on the west flank of Mount Baker, Washington, USA, and the 10 largest trees in each plot cored close to ground level. The annual rings were counted (and cross-dated), and the pith dates determined. The distribution of these dates over time illustrates the establishment dates of

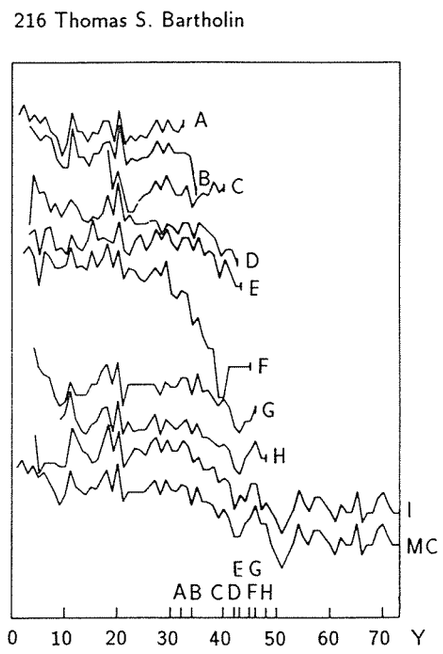

Figure 5.2. Relative dendrochronological datings on oak (*Quercus*), lime (*Tilia*), elm (*Ulmus*), and poplar (*Populus*) from an excavated pile construction near Lake Vattern in Ostergotland, Sweden. From these relative dates, a successive clearing of the woodland area was inferred rather than a selective cutting.

the seedlings in the study area. The most distinct concentrations fall within 1925–1934 and 1940–1944. This is in accordance with similar studies for western North America and thus hints at a general warming of the climate that reduced winter snow cover, promoted its melting, and lengthened the growing season.

Tree-ring analysis can also be applied to trace the fluctuations of glaciers, the occurrence of earthquakes, and the appearance of large meteorites. Holzhauser (1983) reconstructed the advances of the Great Aletsch Glacier in the Swiss Alps and determined that they occurred around A.D. 1100 and 1300 as well as at A.D. 1504 and 1588. The latter two dates will be dealt with in somewhat more detail. In *Figure 5.3* four trees are indicated with their locations of growth and life spans. The glacial surface at least between 1455 and 1588 (larch 1) was approximately as low as it was in 1920. Around 1504 the glacier approached larch 1, which responded with an abrupt decrease in wood production, but the glacier stayed more or less constant until 1588 when larch 1 was overridden and pushed down. This single event is an example of the more general situation at the end of the 16th century when the glaciers throughout the Alps advanced considerably and penetrated into cultivated areas.

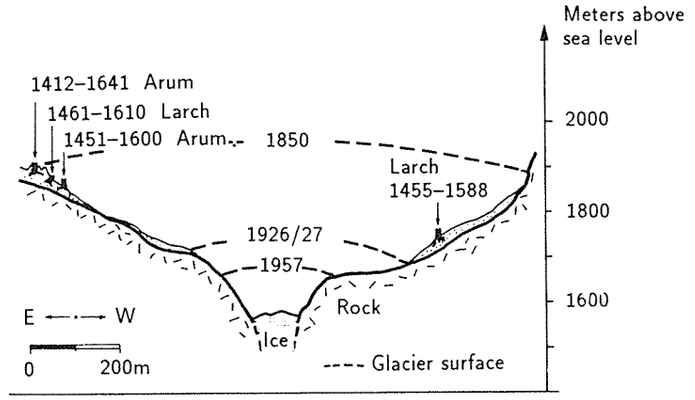

Figure 5.3. Advances of the Great Aletsch Glacier in the Swiss Alps have occurred around A.D. 1100 and 1300 as well as at A.D.1504 and 1588 based on dendrochronological dating of trees killed by glacial advances.

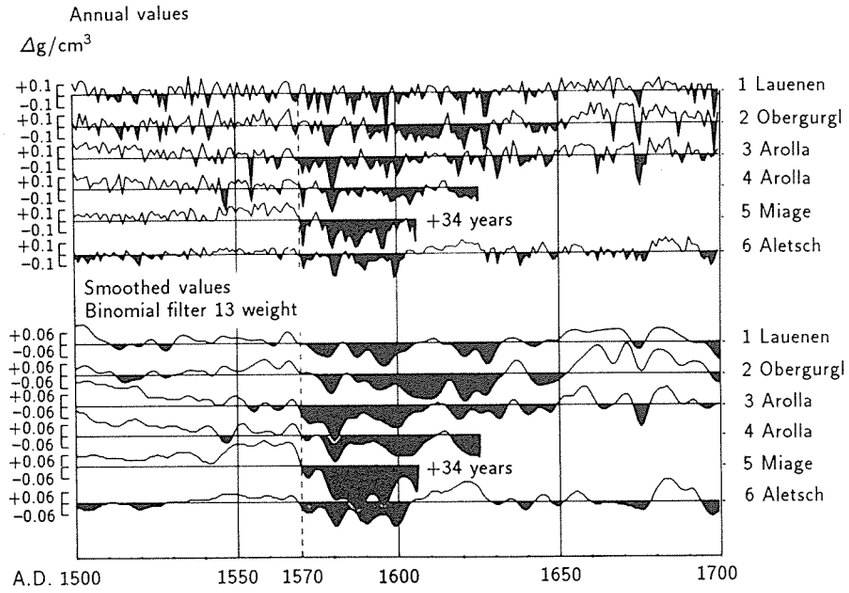

Figure 5.4. Climatic deterioration associated with the glacier advance can be seen in the latewood density series of conifers from the Alpine area, which show an obvious reduction until 1650.

This climatic deterioration can be seen in the latewood density series of conifers from the Alpine area, which show an obvious reduction until 1650 (*Figure 5.4*). After larch 1 was overridden in 1588, stone pine 1 was reached in 1600. Then, in 1610 larch 2 and in 1641 stone pine 2 were each pushed down. Thus, the Aletsch Glacier at that time achieved a new height that was reported also for 1850, the most recent maximum. The maximum around 1650 was so frightening for the farmers down in the valley that they performed a procession to the glacier's tongue in 1653.

Tree-ring analysis has also been used to assess the effect of the Tunguska meteorite impact on tree growth in Siberia (Lovelius, 1979). A considerable increase in ring width attributed to this event was found over a large territory.

The total range of qualitative assessment of environmental changes may be best described by pointing to one of the earliest and one of the most recent publications, *viz.*, Alestalo (1971) and Jacoby and Hornbeck (1987).

5.3. General Aspects in the Use of Tree Rings for Environmental Impact Studies

J. Innes

5.3.1. Introduction

There are several ways in which the environmental impact of pollution can be assessed using tree-ring analysis. The most important of these are the comparison of trees of the same species growing under similar environmental conditions but with different pollution loadings; the correlation of growth trends from a large number of sites with known patterns of pollution loadings; the removal of age trends and climatic effects from a particular chronology with the inference that any remaining trend can be attributed to air pollution; the comparison of a chronology prior to and after the onset of pollution; and the analysis of chemical ingredients in tree rings.

5.3.2. The traditional approach

The approach of comparing chronologies from polluted and unpolluted areas has been frequently used in studies of localized pollution (e.g., Pollanschutz, 1962; Vinš and Markva, 1973; Kreutzer *et al.*, 1983) (*Figure 5.5*). While it may be of considerable value in such situations, it is of little use when investigating the effects of long-distance pollution and has been dismissed by, for example, Eckstein (1985). This is because the technique relies on a number of assumptions, some of which are invalid. The most important of these is the assumption that differences between the two chronologies can be ascribed to differences in the level of pollution loading. In reality, a whole suite of factors are likely to be involved, ranging from different climatic conditions to different competitive environments. While it may be possible to control for some of these effects, the existence of complex interactive effects between pollution and environmental factors (e.g., Rehfuess and Bosch, 1987) makes such adjustments invalid.

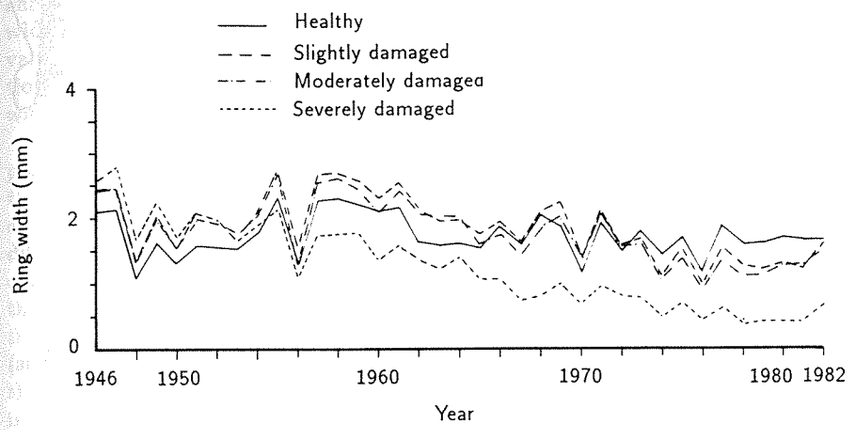

Figure 5.5. Annual increment of Norway spruce of varying condition in the Black Forest, Federal Republic of Germany. (From Kenk *et al.*, 1984.)

A variation of this approach involves the comparison of chronologies derived from trees growing in the same area with and without visible symptoms of decline. The method presupposes that trees without visible symptoms are less affected than those showing decline. This is questionable given that increment reductions are believed to have occurred prior to the onset of visible decline. The trees are obviously subject to approximately the same level of pollution stress and any difference in growth is likely to reflect differences in the responses of the individual trees due to genotypic variations. The technique has been strongly criticized by Athari and Kramer (1983); although it may provide an indication of the extent of the growth reduction, it cannot be used to obtain any quantitative information on the reduction.

5.3.3. Comparing tree-ring series from a large number of sites

The approach of comparing a large number of chronologies from a wide area suffers to a certain extent from the same limitations as the first one. The approach is typified by Strand (1980a, 1980b). In this work, 6,150 ring-width series of Norway spruce (*Picea abies*) and Scots pine (*Pinus sylvestris*) were collected from eight different regions in eastern Norway. The series were averaged into clusters of 1 km × 1 km, resulting in a reduction to 2,814 series. Using linear regression techniques, a *reaction coefficient* for each site was obtained. As these showed a great deal of site-to-site variation, they were averaged over 30 km × 30 km squares. The resulting patterns are shown in *Figure 5.6.* These maps were then compared with known patterns of sulfate deposition and rainfall pH. Strand concluded that there was no clear relationship between the pattern of coefficients and the pattern of sulfate deposition and rainfall pH.

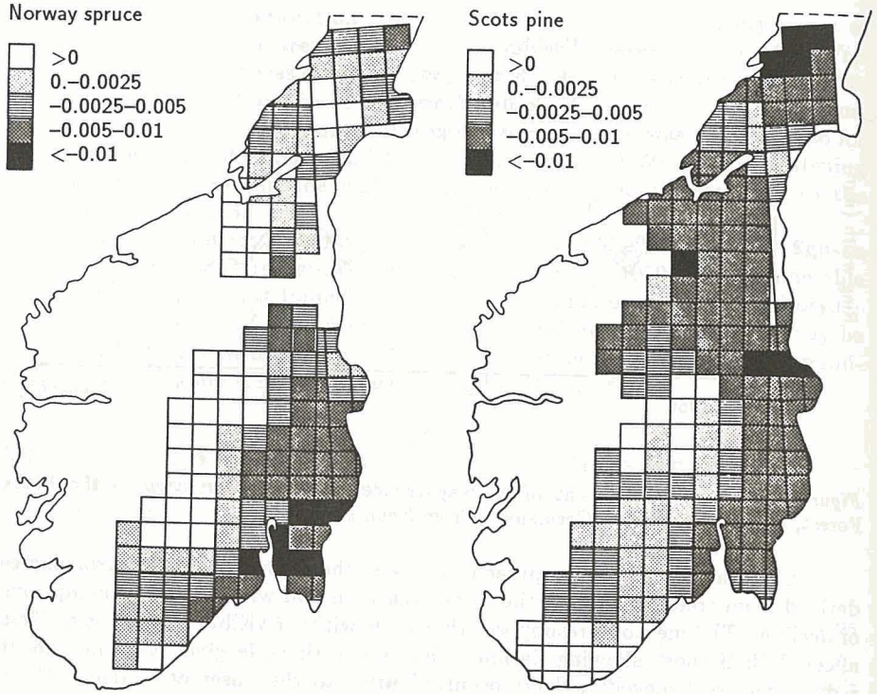

Figure 5.6. Reaction coefficients of Norway spruce and Scots pine in eastern Norway. (From Strand, 1980a, 1980b.)

One major drawback with Strand's technique is that, as described, it fails to take into account climatic differences between sites and also the soil type, which may play an important role. However, intuitively, the technique is attractive. It is possible that given a large enough data set or large enough territory, it would be feasible to identify anomalous regional trends in radial increment that were correlated with known trends in pollution levels. Alternatively, the technique could be used in a rather different fashion to establish the regional pattern of abrupt changes in increment, as done by Schweingruber (1986) (see Section 5.10).

5.3.4. Removing age trend and climatic effects

The method of removing the climatic, aging, and other effects and ascribing any remaining trend to the effects of pollution is illustrated by a recent example provided by Adams *et al.* (1985), working with red spruce (*Picea rubens*), balsam fir (*Abies balsamea*), and Fraser fir (*Abies fraseri*) in Virginia. They developed

chronologies by fitting a cubic spline function to the measured values, with ring-width indices being derived by dividing each ring width by its respective spline value. Climatic effects were removed using response function analysis (see Section 5.6.2). Residual values indicated that a decline in increment has occurred within the last 20 years.

There are problems with this particular approach. As Adams *et al.* (1985) point out, the regression analysis may fail to identify important climatic effects that are only operative in extreme cases (e.g., droughts). Furthermore, the effects of pollution and climate are known to be interactive; it may be very difficult to separate the two. In particular, pollution may alter the tree's climate-growth response (McClenahen and Dochinger, 1985; Mitscherlich, 1983), thereby creating problems for the response function analysis. One evidence of this is the inadequate increase of tree increment due to ameliorative measures (such as fertilization, land reclamation, thinning, etc.) when it takes place during the climatic-growth maxima period and, vice versa, an inadequate decrease of increment attributed to atmospheric pollution during the periods of climatic minima (Stravinskiene, 1981; Kairiukstis and Dubinskaite, 1987). Yet another difficulty is the separation of age trends from any decline associated with pollution. These all need to be resolved before this particular method can be used with confidence.

5.3.5. Comparing growth before and after the onset of an impact

The method of comparing increment before and after the onset of pollution appears to have a great potential. The efficacy of the technique has been illustrated by numerous studies of the impact of a particular source of pollution on increment. Essentially, it involves the calculation of response functions for the period prior to the onset of pollution followed by the application of those functions to the period with pollution (Cook *et al.*, 1987). The difference between the observed and the calculated indices are then used to gain an idea of the impact of pollution on tree growth at the site (e.g., Eckstein *et al.*, 1984).

An example of the technique using maximum latewood density rather than ring width is provided by Kienast (1982). The period 1875–1940 was used to obtain the calibrations and indices were extrapolated for the period 1940–1980. The difference between the computed indices and the measured ones are shown in *Figure 5.7.* There is a clear increase in the difference between the two indices in recent years. The increase is apparent in both healthy and damaged trees. To be more precise in looking for the causes of deviation of such indices, one may use the technique of harmonic analysis (see Chapter 6) to filter short- and long-term cyclic fluctuations apparent in tree-ring series. This may help to assess more precisely the impact of pollutants.

There are, however, considerable problems when investigating the recent decline in tree growth. First, the causes of a decline are mostly unknown and it is therefore not easy to identify a starting date for their onset. Second, the pollutants that are believed to be involved (namely, acidic substances) have been

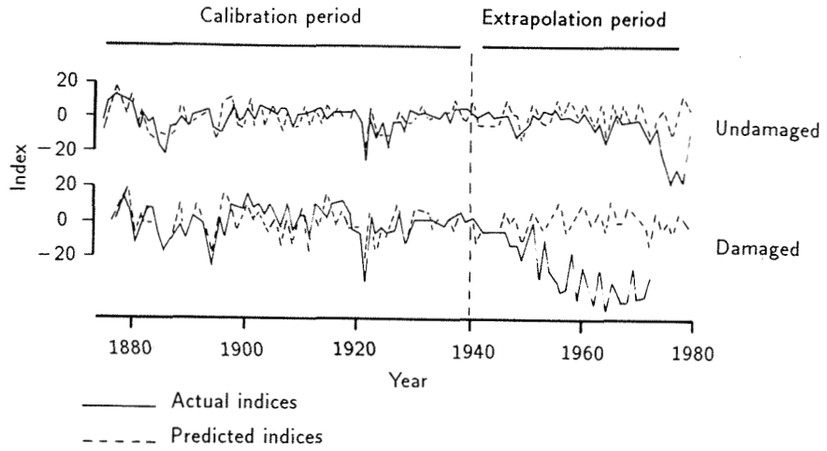

Figure 5.7. Actual and predicted indices for maximum latewood density of Norway spruce in Switzerland. The two series are for trees with and without visible damage. (From Kienast, 1982.)

present since the Industrial Revolution, although the proportions of the most important – sulfate and nitrate – have varied considerably through time. Ozone pollution is a more modern phenomenon, which has increased in recent years.

As a result of these complications, it may be necessary to make use of any observed change in the chronology to identify the start of the decline in growth. Numerous studies indicated that trees in both Europe and North America have been declining for much longer than is apparent from surveys of forest health (e.g., Kenk, 1983; Hornbeck and Smith, 1985; Greve *et al.*, 1986; Kairiukstis and Dubinskaite, 1986). This has important implications for establishing the cause of the decline because there has been a tendency to look for factors that correlate with the onset of the visible symptoms rather than with the onset of growth reductions.

Kairiukstis *et al.* (1987b) studied this problem in somewhat more detail. They ascertained that the tree's response to pollutants or other environmental changes depends on the initial stages of the tree and on the intensity of environmental changes themselves – i.e., the greater the environmental changes and the weaker the initial state of the tree (social class of the tree), the greater the impact on the tree. In detecting tree-growth change, three phases have been identified:

(1) Stress reaction phase can be detected immediately by measuring biochemical changes and biological potentials of cellular membranes.
(2) Growth suppression phase lasts for one or several vegetative periods during which morphometric analysis in tree crowns can be used to detect growth change.

(3) Only the adaptation phase takes place after one or several years when stress occurs due to pollutants. Dendrochronological records including chemical analysis of tree rings provide expedient retrospective information of tree growth in a changing chemical or physical environment.

A study by McClenahen and Dochinger (1985) has, to a certain extent, circumvented the problem of identifying the starting date for the onset of causal effects. They used several response functions to establish the presence of any discrepancies in the growth of white oak (*Quercus alba*) that could be attributed to relatively local pollution. They found that response functions for sites close to the pollution sources showed a strong non-climatic influence for the period 1930 to 1978 that was not present either at more remote sites or in the period prior to 1930. In addition, response functions derived for the period 1900 to 1978 declined through time in their reliability to predict indices from climate at sites close to the pollution sources.

5.3.6. Conclusion

It appears to a certain extent that there has been a lack of communication between dendroecologists and those concerned with forest decline. For example, in studies of pollution impact, considerable care is needed in the selection of the sample trees. In particular, attention should be paid to the crown height, diameter, and condition. The oldest trees at a site are not necessarily those that will provide the most information, and sampling design should be adjusted accordingly. Conversely, a general lack of awareness among those concerned with forest ecology and mensuration of the more advanced statistical techniques has recently developed in dendrochronology and dendroecology. Consequently, there has been a tendency to dismiss dendroecological techniques as a result of the perceived difficulties of analysis. Increment analysis provides a powerful tool for linking the interests of these groups and may well provide a valuable contribution to the understanding of the recent forest decline.

5.4. Measuring the Chemical Ingredients in Tree Rings

L. Kairiukstis and G.E. Kocharov

The analysis of chemical ingredients in tree rings can provide valuable information about environmental changes. At present more than 70 elements that can be taken up by plants are known. However, it is important that migration of elements from ring to ring does not occur; otherwise, the information about the year when a ring was formed would be distorted or lost. Several authors established that the vertical transport of food substances exceeds by a thousand times the horizontal one (e.g., Chavchavadze, 1979) and, that in a radial direction, complex insoluble compounds are formed by a number of elements (Holzman, 1970). Thus, the chemical memory of tree rings can be used to study environmental changes.

However, a further precondition is that the informative elements are accessible for measurement. A number of methods, such as neutron-activation, emission-spectral analysis, X-ray fluorescence, ionization and scintillation, beta-spectrometers, traditional mass-spectrometry, and the developing technique of accelerator mass-spectrometry, have been successfully applied to measure the abundance of various elements and isotopes.

Adamenko *et al.* (1982) studied 130-year-old larch (*Larix*) trees growing in Ary-Mas on the Taimir peninsula in the USSR. Owing to narrow tree rings (< 1 mm), the chemical composition was determined from a parcel of rings (not from each ring separately). The most representative elements in the wood ash were K and Ca (together 50%). The next most abundant element was Mn with a concentration of 1.3–2.2%. The concentration of Fe and Zn ranged from 0.3% to 0.8% and from 0.1% to 0.4%, respectively. There was a strong positive correlation between air temperature and the concentration of elements in the tree rings.

According to Vinnikov *et al.* (1987), the warming trend of the Northern Hemisphere beginning at the end of the 19th century had finished by 1940 and was followed by a hemispheric cooling from 1940 to 1960. Another warming trend appears to be taking place in the Northern Hemisphere since the mid-1960s. All these peculiarities are reflected in the variation of the K:Ca ratio in the tree rings of larch, in that it increased with the amelioration and decreased with the deterioration of the growth conditions of trees. An appropriate rapid method of early indication is described by Skuodiene (1987) and Kairiukstis *et al.* (1987c). Evidence shows that in years favorable for tree growth (extensive heat supply) at the upper tree line, the content of Ti, Mg, Sr, Mn, Fe, and Zn decreased and the content of Na, Cu, Al, and Si increased with the decreasing ash content and increasing tree-ring width and vice versa.

The chemical composition of tree rings reflects not only the change of heat or precipitation, but also the level of environmental pollution. The source of contamination selected was a factory of nitric fertilizers in the Lithuanian SSR, the emissions of which mainly consist of sulfurous anhydride, nitric oxides, fluoride combinations, ammonium, as well as formaldehyde, methanol, carbomide dust, nitrophosphate, and ammonium nitrate. A comparison of the potassium residue (K) and the tree-ring width of *Pinus sylvestris* was made for the period 1930–1985. From 1930–1967, which preceded the industrial emissions, the potassium residue agreed with the fluctuations of the tree-ring width reflecting physical environmental changes. For instance, the maximum content of potassium in the wood corresponded to the increase in the radial increment in 1935, 1950, and 1965 (*Figure 5.8*). There was a linear dependence between the data of the potassium residue and the radial increment in a control area (*Figure 5.8*, dashed line).

During the period 1967–1985, a new tendency appeared in the correlation between the parameters investigated. Significant rhythmic fluctuations of the radial increment (from 2.43 to 3.04 mm/year) occurred during the first eight years (1969–1977) caused by an overload of nitrates (fertilizers) and pollutants. However, the rest of the period was characterized by a considerable fall in increment. Owing to industrial emissions (overloaded with nitrogen compounds), the

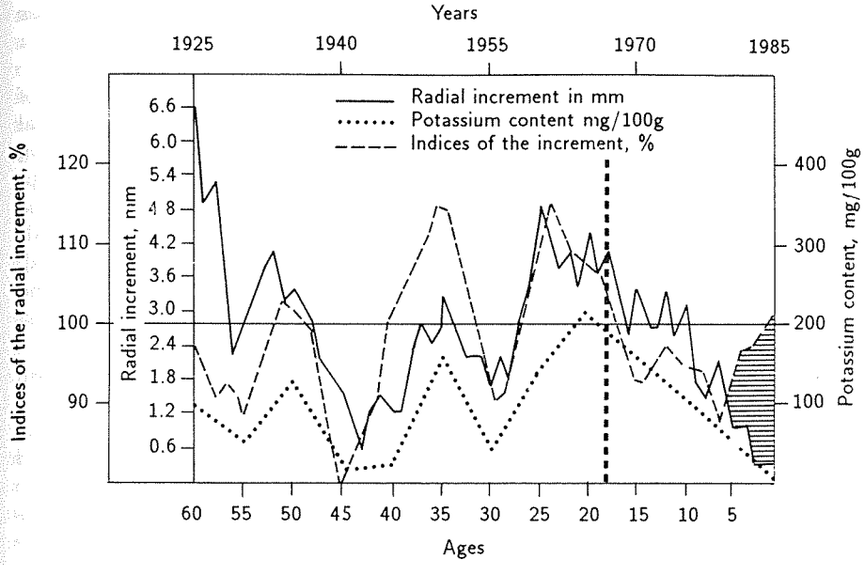

Figure 5.8. Characteristics of the potassium residue in tree rings in the background of climatic and air pollution changes.

quantity of the potassium residue in tree rings diminished distinctly as a result of the decreasing potential of substance transition. In the given period, a decline of both the potassium residue and the radial increment were noticed to have the same tendency. However, the dendrochronological indices from the unpolluted (control) area differed to a great extent, particularly for the last eight years (the shaded area in *Figure 5.8*).

These findings show that the potassium residue in tree rings caused by the penetration of K^+ ions via cell membranes may be used to evaluate the physical and chemical environment affecting trees. Adamenko *et al.* (1982) pointed out that the ratio of K:Ca in the polluted area sometimes decreased by 3.5 times. Such a decrease is from bursts of sulfur gases, powdery particulates, and possibly the change of the meteorological regime in the polluted zone (Pogocyan, 1974). The data correspond to results by Ilkun (1978), who found that with a high background of atmospheric pollution by fluoride and its accompanying chemical ingredients, the ratio K:Ca in larch and pine decreased from 2.5 to about 0.7.

A number of studies have been devoted to the abundance of heavy elements (Fe, Pb, Cr, Zn, Cd) in trees, growing at different distances from industrial sources (e.g., Holzman, 1970; Hampp and Holl, 1974; Rolfe, 1974; Hall *et al.*, 1975; Dollard *et al.*, 1976; Tian and Lepp, 1977; Symeonides, 1979; Baes and Ragsdale, 1981; Robitaille, 1981; Schweingruber *et al.*, 1983; Kazmierzczakowa *et al.*, 1984; Bauch *et al.*, 1985; Hagemeyer, 1986). Heavy elements penetrate into the trees through the soil and the root system, from the atmosphere through the leaves, and directly through the bark (Hall *et al.*, 1975; Robitaille, 1981). The

capacity of trees to accumulate metals was found to differ considerably. Baes and Ragsdale (1981) found the concentration of the same element to vary by a factor of 100 for trees growing in the same environment.

Meisch *et al.* (1986) studied the distribution of metals in the tree rings of beeches (*Fagus*) to get information on environmental changes in an industrial area in the southwest of the Federal Republic of Germany. Using trees ranging from 5 to 160 years old, they analyzed 14 elements by means of atomic absorption spectroscopy, whereby narrow rings were sometimes grouped. As to the temporal variation of the metals, three main trends were defined: metals without any tendency in their annual variation (Na, K, Pb, Cd, and others), metals with decreasing concentrations during the recent 15 years (Ca, Mg, and others), and metals with increasing concentrations (Fe, Al) during the last decades.

Kazmierzczakowa *et al.* (1984) studied heavy elements in beech in south Poland. This region is exposed to contamination from industrial pollutants to a variable degree. As a source of heavy elements for the trees, the soil was considered to be negligible compared with the atmosphere, which was considered most important. The analysis of heavy element concentrations in the tree rings from 1900–1980 showed that the penetration through the bark and radial migration into the tree rings is different for different metals and depends on the tree species. In beech, fast radial migration of Cd and Zn from new rings to the old ones was found. This spread in the radial direction increased with the concentration of these metals. The same effect for these elements holds true for other tree species (Robitaille, 1981; Symeonides, 1979). Consequently, these elements cannot serve as indicators of the environmental pollution dynamics. The high level of Pb in the youngest tree rings moves slowly (compared with Zn and Cd) into the central core of the tree; Fe and Cr behave the same as Pb. High concentrations of these trace metals in the tree rings during the last years is connected not only with the high assimilation during that time, but with direct penetration of Pb through the bark of the trees, where elements are stored to a great extent. The investigations using marked 210_{Pb} show that the penetration of Pb from the bark into the core is not metabolic in origin (Hampp and Holl, 1974; Lepp and Dollard, 1974).

As a whole, one can conclude that the method of measuring chemical and isotope abundances in tree rings enables one to carry out the spatial-temporal measurement of natural and anthropogenic factors of the environment.

5.5. Statistical Methods for Detecting Environmental Changes

T.H. Nash and W.B. Kincaid

5.5.1. Introduction

Much of the appeal of dendroecology for environmental change detection derives from the possibility of comparing affected tree-ring series with their expected

natural variation. Then, deviations from expectation may be indicators of, or responses to, some change in the environment. Rarely can dendroecological methods prove cause and effect. However, when combined with experimental results, they can provide evidence that will support the conclusion of environmental change. Here, we review methods for quantifying environmental change using tree rings that range from the simple difference methods to sophisticated time series analyses. Air pollution studies dominate the citations because they dominate the applications of dendroecology to detect environmental change.

Tree-ring analyses are facilitated by conceptual models of ring-width variation such as those described by Sundberg (1974), Fritts (1976), Graybill (1982), and Cook (1985). Basic assumptions of studies of environmental change are that all sources of natural variability can be accounted for and that their effects are uniform throughout the time series in question. In a number of studies using tree rings to detect environmental change, researchers have ignored dendrochronological principles. Frequently, these studies did not develop chronologies, but rather used raw ring widths or some function thereof. Although many of these studies produced useful results, they can be subject to problems of cross-dating, age effects, climatic effects, or inadequate sampling design. Here, we assume that tree age and undesirable disturbance effects have been removed by methods discussed elsewhere in this chapter, and, unless otherwise noted, the methods discussed are meant to apply only to appropriately formed chronologies. Hence, the problem of environmental change detection will frequently be reduced to distinguishing the effect in question from the ubiquitous climatic signal.

We have divided the quantitative methods to be discussed into those methods that rely on information from unaffected (*control*) sites and those that use surrogate predictors of natural variability in tree-ring chronologies. Methods that might fall into both categories will be discussed where they are most commonly applied with note of their alternative application.

5.5.2. Methods employing control sites

Many methods for predicting natural (climate) variability in a chronology rely upon the availability of unaffected or control sites. True controls are impossible to obtain in tree-ring studies because we can never assess (let alone manage) all possible sources of among-site variation. However, useful information on natural variability can be obtained from carefully chosen sites either that are known to be outside the range of the effect in question or that represent a gradient of the effect.

Whenever control chronologies are used, their adequacy must be assessed carefully. Beyond similarity of site characteristics and histories, the sites must occur within the same climatic region. Cropper and Fritts (1982) found that western North American chronologies within 161 km of each other will on average contain at least half of the common variance expected for chronologies from the same site. To verify adequacy, chronology variation should be comparable during periods when the environmental effect in question is known to be absent. In most cases, this will be a period prior to the environmental change to be

detected. This chronology comparison should be based on the method to be used as well as chronology statistics and plots.

A general method for detecting environmental change is to demonstrate a change in mean level of a chronology relative to some unaffected chronologies. This should be much more reliable than similar comparisons of raw ring-width series because of differential age-trend effects (see discussion of standardization in Chapter 3). However, care must be taken in choosing the type and degree of standardization applied. For example, a smoothing spline or high-order polynomial may mask or remove the signal trying to be detected if it is too flexible. Many standardization techniques are also subject to end effects from lack of information on subsequent behavior of the time series. It is also conceivable that, even in the absence of any environmental change, mean levels of short segments of a chronology differ. The magnitude of radial-growth responses to climatic variation often varies among trees within a site as well as among sites.

Peterson *et al.* (1987) used the control-site approach to test for effects of ozone on Jeffrey pine (*Pinus jeffreyi*) in Sequoia National Park and Kings Canyon National Park, both in California. In addition to a response function analysis (discussed below), they used paired *t*-tests to determine if there were significant differences in mean growth between control and exposed trees in two size and age classes (breakpoints 40 cm dbh and 100 years) and from time periods before and after a putative date when ozone became a serious air pollution problem (1965). During the pre-pollution period (1898–1964), there was no difference in mean index between control and exposed sites in any size or age class, which substantiated the similarity of the control and exposed stands. However, during the pollution period, growth indices of larger and older trees were significantly less in exposed stands than in control stands. Comparison of means of radial growth indices revealed a maximum of 15% growth reduction in the oldest trees and an 11% overall growth reduction. These results constitute the first evidence of long-term reduction in forest growth from ozone effects outside the Los Angeles basin.

Frequently, analyses are designed to detect a change in the climate-growth relationship under the assumption that a change in the non-climatic environment has altered this relationship. Chronology statistics have been used to characterize the sources of variance in tree-ring data. Mean sensitivity is a measure of the relative change in ring-width index from one year to the next and reflects the proportion of high-frequency variance (short period) in the chronology (Fritts 1976). Autocorrelation estimates the first-order autoregressive structure commonly present in tree-ring series and reflects the proportion of low-frequency variance (long period) in a tree-ring chronology. Standard deviation includes both low- and high-frequency components of variance. As the environment changes, the variance structure reflected by these statistics may be expected to change predictably from the situation observed in an unaltered site. Air pollution, for example, has been suggested to increase the proportion of low-frequency variance (autocorrelation) by substituting for the normally high-frequency (mean sensitivity) effects of climate as a limiting factor. Thompson (1981) and Fox *et al.* (1986) used chronology statistics to infer a deviation from the normal climate-tree growth relationship resulting from air pollution effects.

An alternative partitioning of variance in a chronology differentiates variance in common to all trees from error variance association with unique variation in individual trees or cores. The former is referred to as the signal (S), the latter is noise (N), and their ratio is the signal-to-noise ratio (SNR) (see discussion of SNR and its estimation in Chapter 3). Again, environmental change may produce predictable changes in SNR relative to an unaffected control. Some changes may break down the climatic signal reducing SNR, or some may constitute a major limiting factor dramatically synchronizing the affected trees and increasing SNR.

Cross-correlation and cross-spectral analyses are other procedures that may be useful for detecting a change in growth trend of an affected site relative to unaffected sites. One of the first applications of these techniques in tree-ring research was a comparison of bristlecone pine (*Pinus longaeva*) at ecologically contrasting sites (LaMarche, 1974). Swetnam (1987) applied these procedures to compare chronology variation between host and non-host species of the western spruce budworm. Cross-correlations for successive 20-year segments of the chronologies were reduced during periods of known and suspected budworm infestation. The cross-spectral analyses revealed reduced coherency between host and non-host chronologies at low frequencies relative to high frequencies. It was suggested that budworm effects were primarily manifest in the low-frequency variation of the host chronologies.

Response function analysis was developed by Fritts *et al.* (1971) to examine radial growth responses to climatic variation. Various regression techniques are used to calibrate a model predicting chronology variation from climatic variables such as monthly precipitation and temperature. In a classic paper for environmental-change detection, Ashby and Fritts (1972) attempted to detect tree responses to an increase in precipitation near LaPorte, Indiana, that had been attributed to increased industrialization and subsequent air pollution. They developed chronologies from six stands of white oak (*Quercus alba*), two of which were within the area of the precipitation anomaly. The four unaffected chronologies were averaged into a single regional tree-growth chronology.

A climatic database for the region (excluding LaPorte) was obtained by combining data from four stations. Stepwise multiple regression on principal components of climatic variation was then used to estimate a response function for the average of the unaffected white oak stands. Climatic data from the affected area was then used in this independent, regional response function to predict tree-ring chronologies for the LaPorte area. The anomaly in the LaPorte precipitation data lead to a prediction of relatively increased growth that was not observed in the actual indices of growth. On the contrary, relatively reduced radial growth was observed when the anomaly was supposedly most pronounced. Ashby and Fritts (1972) suggested that these results were from direct toxic effects of the increasing air pollution responsible for the precipitation effect.

Regardless of their inconclusive results, Ashby and Fritts (1972) established the response function approach as a standard that is still respected today. Subsequent applications have incorporated many variations on their theme. For example, both Thompson (1981) and McClenahen and Dochinger (1985) compared response functions among stands differing in pollution load and used a

single climatic station for both affected and unaffected sites. Both studies demonstrated increased importance of prior growth in the response functions for chronologies from the affected areas, which were attributable to non-climatic effects (i.e., air pollution).

Peterson *et al.* (1987) also applied the response function concept in their study of Jeffrey pine (*Pinus jeffreyi*) responses to a regional ozone problem. However, they did not use separate calibration and verification periods. Instead, they combined the period and included in the regression analysis an indicator variable reflecting years before and after the date of supposed pollution elevation as well as interactions of this variable with the climatic variables. In effect, this approach allowed them to test for the presence of a change in climatic response by testing the significance of these additional variables. Iterations of the analysis with different dates may allow identification of the year when the most significant environmental change occurred. However, care must be exercised to avoid biases from autocorrelation effects in the analysis (Monserud, 1986).

A procedure developed by Nash *et al.* (1975) eliminates the need for a climatic database by using the information in unaffected chronologies directly. It involves calculating *predicted residual indices* (PRI) according to the following formula:

$$\text{PRI} = \frac{\text{SD (affected)}}{\text{SD (control)}} \cdot [\text{Index (control)} - \text{Mean (control)}] \quad ,$$

where SD is the standard deviation, Index (control) is index values of the control chronology, and Mean (control) is the mean of the control chronology (about 1.0). Subsequently, *corrected indices* (CI) are calculated by:

$$\text{CI} = \text{Index (affected)} - \text{PRI} \, ,$$

where Index (affected) is index values for the affected chronology. For the study cited above, the control was defined as the average of several chronologies for stands located in a ring around the pollution source, but at a distance sufficiently great that no adverse pollution effect was anticipated.

No direct effects of air pollution were detected by Nash *et al.* (1975), but the procedure was successfully applied by Swetnam *et al.* (1985) and Swetnam (1987) in their studies of western spruce budworm effects in trees in the central Rocky Mountains of North America. In this case, Douglas fir (*Pseudotsuga menziesii*) and white fir (*Abies concolor*) are known host species for the budworm, and ponderosa pine (*Pinus ponderosa*) and pinyon pine (*Pinus edulis*) are non-host species. These four species are known to respond to macroclimatic variables in similar manners. Consequently, chronologies from Douglas fir and white fir were designated as the affected chronologies, and chronologies from ponderosa pine and pinyon pine were designated as control chronologies.

This study was enhanced by the fact that outbreaks of budworm infestation were well documented for three periods after 1920, and, consequently, the

behavior of the chronologies and corrected chronologies through these periods could be examined. Further analysis of the chronologies prior to 1920 led to the inference that five additional outbreaks occurred between 1750 and 1900. From these results, the western spruce budworm outbreaks were estimated to have an average duration of 14 years with an average interval of 35 years between them. Furthermore, the average maximum growth reduction was estimated to be 50.0% of potential growth, whereas the average periodic growth reduction was 21.6% of potential growth. In addition to applying the correction procedure to the affected chronologies, the correction procedure can be applied on an index-by-index basis and thereby calculate the percent growth reduction on a tree-by-tree basis for each year of concern.

Regression techniques may also be applied to account for control variation in affected chronologies. For example, Fox *et al.* (1986) used multiple regression to partition variation explained by climate and smelter emissions at tree-ring sites on a distance gradient from a smelter. Their general regression model included terms for annual sulfur emissions, the average of chronologies from three control sites, and two lagged values of the control average. The adequacy of the controls was assessed during a pre-pollution period.

They used coefficients of multiple determination (R^2) and coefficients of partial determination to assess the goodness-of-fit of the regression models and to examine their relationships to distance from the smelter. The former coefficient measures the proportional reduction in variation of the dependent variable (the polluted-site chronologies) achieved by the full set of independent variables, whereas the latter measures the marginal contribution of an independent variable (say, sulfur emissions of the control average) given that all other independent variables are already included in the model. Plots of these coefficients versus distance revealed that variation explained by sulfur emissions in the polluted-site chronologies decreased with distance from the smelter, and, concomitantly, variation explained by the control variables increased with distance. They also used regression on the control variables to produce climate-corrected tree-ring indices (residuals) that were inversely related to smelter emissions.

Regression techniques assume, among other things, that all observations are independent, which is certainly not the case with tree-ring series. Autocorrelation can inflate the variance of regression coefficients and, thereby, invalidate significance tests. For this reason, Fox *et al.* (1986) avoided significance testing and instead relied upon patterns related to the distance gradient to demonstrate a change in the forest environment from air pollution. Monserud (1986) recommended removal of the autocorrelation in tree-ring chronologies (i.e., prewhitening) to improve the results of techniques such as regression.

An alternative approach was taken by Kincaid (1987) to determine the responses in radial growth to ambient doses of SO_2 using a unique 32-year record of continuous SO_2 monitoring. Tree-ring data were available from three sites known to have been free of air pollution and from a site near the monitor. The statistical approach again assumed that tree-ring indices from the polluted site could be decomposed into climate and pollution components, but here an autoregressive AR(p) error component was incorporated that was jointly estimated with the structural components.

Under these assumptions, a stepwise autoregression procedure was employed to maximize use of available information. The SO_2 dose measurements were limited to a 32-year period, whereas the polluted and control chronologies were roughly equal in length. So, an autoregression of the polluted site on the average of the controls was performed first to estimate variation attributable to climate. Climate effects and an AR(1) error component were jointly estimated from a 77-year period. Then residuals were calculated for the 32-year period of SO_2 monitoring that excluded the contribution of the autoregressive error component. The AR(1) component was excluded because some of the autocorrelation in the time series may have been related to the pollution effect. Finally, an autoregression of the residual chronology (climate corrected) on SO_2 dose was performed to estimate the dose-response relationship while jointly re-estimating the AR(1) error process. A predictive relationship for relative losses in radial growth from SO_2 exposure was successfully obtained from this unique data set.

5.5.3. Methods applicable when control information is lacking

In the absence of ecologically similar sites, a number of surrogate variables have been used as predictors of natural variability. Most often these will be climatic measurements such as monthly or seasonal temperature and precipitation. Conceivably, any climatically driven variable could be used including stream flow, lake level, water table, snowpack, and even prior values of the chronology itself.

Some specific research questions suggest sources of these predictors. We have already mentioned the use of non-host trees to detect effects of insects on host trees (Swetnam *et al.*, 1985). Several air pollution studies have used asymptomatic trees (presumably from genetic resistance) to assess losses in symptomatic trees of the same species (Phillips *et al.*, 1977; Treshow *et al.*, 1987). Acid deposition studies have used differences in soil susceptibility to acidic inputs to estimate natural variation in trees on sensitive sites (Jonsson and Sundberg, 1972; Abrahamsen *et al.*, 1977). Equal care must be taken with these approaches when assessing adequacy of control sites to ensure their expected growth is the same as the affected sites.

Often the only available information on natural variation in radial growth comes from periods prior to the appearance of the affecting factor (disturbance). If the chronologies are long relative to the period of disturbance and the site histories are well documented, reasonable estimates of natural variation may be obtained. In a sense, the chronologies can serve as temporal controls for themselves. However, extreme caution must be exercised either to verify that the chronologies are stationary (time invariant) or to employ methods designed for nonstationary time series.

Cook (1987a, 1987b) developed a strategy for assessing regional air pollution effects on a stand of red spruce (*Picea rubens*) from northern New York. His analysis employed the response function methods previously discussed to create a prediction model of radial growth, which was them used to test for pollution effects. A chronology of more than two centuries was obtained that displayed the widely reported decline beginning in the 1960s. Tests failed to give

any evidence of end-effect bias from the standardization procedure that might account for the observed growth decline.

Mean monthly and daily temperature data from a regional database were used in the response function modeling. Available data from 1889–1976 were divided into sets before and after 1950 for calibration and verification purposes. And because of the potential effects of autocorrelation on response function modeling, all analyses were done with and without prewhitening of the chronology. Stepwise regression was applied to data from 1890–1950 to calibrate the response function, which was then used to predict the chronology during the later period for verification.

Verification was accomplished by computing differences between means of predicted and observed chronologies, product-moment correlations, and reduction of error statistics (see discussion of verification in Chapter 4). Verification statistics were computed separately for the periods 1951–1960, 1961–1967, and 1968–1976. The first period was considered to be pre-pollution and therefore assessed the time stability of the response function. In this period and the next (1961–1967), the model was well verified, whereas significant deviations from expectation were revealed in the last period. Cook (1987a, 1987b) concluded that the observed decline could not be explained by the verified climatic response model; however, a relationship to air pollution could not be established until the contributions of all natural growth-modifying influences have been taken into account.

Time series analysis provides great potential for detecting environmental change. Besides dealing with potential biases in modeling from autocorrelation effects alluded to above, time series analysis provides an additional avenue for characterizing natural variation in a tree-ring chronology. If we assume that any change in the growth environment will change the time series characteristics of the chronology, then we should be able to detect any environmental change by assessing the stationarity of time series models. The models in question will most often be specified as autoregressive-moving average or ARMA models as described in Chapter 3. Practical application of this approach may be limited to examination of environmental changes with long duration or dramatic effect and chronologies that are at least several centuries long because time series models frequently require extensive data to achieve an accurate fit.

Graybill (1987) has applied time series analysis to assess the effects of increasing atmospheric CO_2 on upper tree line bristlecone pine (*Pinus aristata*) from southern Nevada. The great longevity of these trees certainly facilitated this study by allowing him to work with chronologies from 1380–1980. ARMA models were first fit to the chronologies for the period prior to substantial elevation in CO_2 (1380–1859) and subsequently used to produce prewhitened or residual chronologies for the entire period (1380–1980). If the ARMA model was stationary and appropriate for the data, white-noise residuals should have been obtained. A principal component summarized common variation in five residual chronologies indicated a reasonable fir during the calibration period, but during the verification period an upward trend was appreciable. This increase in growth may be evidence for growth enhancement from elevated atmospheric CO_2.

5.6. Methods of Response Function Analysis

K. Briffa and E. Cook

5.6.1. Introduction

Relationships between tree-ring and climate data from many areas of the world have been explored through a variety of simple and multiple regression analyses. Most studies have used combinations of climate predictors to explain variations in a particular chronology. Many climate variables (defined over a variety of time periods) have been employed. In early studies, the variables were often chosen on *a priori* grounds with consideration being given to what was known of the physiology and phenology of the species under investigation. References to many uses of simple and multiple regressions in this context can be found in Fritts (1976).

Frequently, the situation may arise in which it is felt that there are insufficient grounds upon which to frame an *a priori* model of the climate/ring-width association, or where such an association is believed to relate only indirectly to the available climate data. In such cases it has become standard practice to use an empirical technique, designed to display the relationships between tree growth and climate in terms of monthly climate variables, thereby identifying the chronology *climate signal*. The technique has been termed the *response function* (Fritts *et al.*, 1971; Fritts, 1976). It is a form of multiple regression analysis where the predictor variables are principal components, usually of a number of monthly mean temperature and total precipitation values. These climate predictor variables are frequently supplemented with some value(s) of the tree growth in the previous year(s). Thus, both climate and prior growth variables are generally used to calculate the amount of chronology variance explained and to quantify the relative importance of the original individual climate variables. The total amount of the chronology variance explained is taken to be a measure of the strength of the climate-forcing signal. The sign and magnitude of the regression coefficients on individual monthly climate variables characterize the nature of the tree-growth/climate link.

The use of orthogonal predictor variables was originally suggested because statistical instability can arise in multiple regressions when the independent data are inter-correlated. In normal stepwise regression, this can lead to variables being excluded because others previously entering the regression share much of their variance. A comprehensive discussion of the technique as it was first used in dendroclimatology can be found in Fritts (1976), and a mathematical description of the first implementation of the technique is given in Fritts *et al.* (1971).

Though the approach is basically the same, various laboratories throughout the world have developed a number of response function programs. There are some differences among them. The differences relate mainly to the manner in which relatively unimportant predictor principal components are removed from consideration during the various regression screenings that form an important part of the programs. The following is a brief description that illustrates the salient details of the basic technique and highlights some of the specific variations in implementation to be found in different programs.

5.6.2. Details of response function implementation

A general expression for the response function is

$$W_i = \sum_{j=1}^{J} \mathbf{a}_j T_{ij} + \sum_{k=1}^{K} b_k P_{ik} + \sum_{l=-m}^{-1} c_l W_l \quad , \tag{5.1}$$

where i equals 1 to N years of the calibration period, W_i is the indexed ring width in year i, T_{ij} is the temperature datum (temperature variable j in year i), $\mathbf{a}_j$ is the coefficient on the temperature variables, P_{ik} is the precipitation datum, b_k are the coefficients on the precipitation variables, W_l is the number of lagged ring widths for up to m previous years, and c_l is the coefficient on the W_l. In matrix notation this can be expressed as

$$\mathbf{W} = \mathbf{X}\mathbf{b} \quad , \tag{5.2}$$

where $\mathbf{W}$ is the $N \times 1$ column vector of N standardized ring widths, $\mathbf{X}$ is the $N \times q$ matrix of standardized predictor data ($q = J + K + m$), and $\mathbf{b}$ is the $q \times 1$ vector of regression coefficients.

The calibration of the response function is essentially the calculation of the $\mathbf{b}$ along with the associated standard errors. Because of possible inter-correlations between the climate variables, the predictor data are first transformed using principal component analysis (PCA). The principal component scores (or amplitudes) are given by

$$\varepsilon_{ij} = \sum_{m=1}^{q} X_{im} \alpha_{mj} \quad , \tag{5.3}$$

where ε_{ij} is the value of the jth component in year i, X_{im} is the corresponding value of the mth original predictor variable, and α_{mj} is the loading of the jth normalized PC on the mth variable.

From a statistical point of view, it is preferable for the PCA to be carried out on all predictor variables, including prior growth. In the original response function program (Fritts *et al.*, 1971) only the climate variables were entered into the PCA. Considering previous growth separately removes the orthogonality of the total predictor data set and so negates one of the main computational and statistical advantages of PC regression.

The regression involves the standardized scores that are given by

$$\varepsilon_{ij}^{*} = \varepsilon_{ij} / s_j \quad , \tag{5.4}$$

where s_j is the standard deviation of ε_{ij} (where $i = 1$ to N). Note that s^2 is equal to λ_j where λ_j is the jth eigenvalue.

A common characteristic of all response function programs is that not all of the ε^* are necessarily offered as candidate predictors. Instead, some *a priori* noise-reduction criterion is used to identify nonsignificant predictors. This provides an objective means of eliminating high-order (noise) components. The various methods that have been used to delineate the candidate predictors include a simple percent variance threshold (e.g., retaining only those major PCs necessary to account for 95% of the variance of the whole set) or the alternative PVP criterion (Berger *et al.*, 1979). This retains those PCs whose cumulative eigenvalue product is greater than 1.0.

When the candidate predictors are not orthogonal (Fritts *et al.*, 1971), a stepwise multiple regression is used to arrive at a regression equation in terms of climate PCs and prior growth variables. Variables enter the regression in sequence according to the proportion of chronology variance that they explain. At each step the variance explained by the entry of a variable is compared with the error variance. When the F value falls below 1.0 (i.e., explained variance is less than the error variance), the regression is terminated.

The regression equation in terms of PCs is more easily derived when the candidate predictors are fully orthogonal. After the initial screening, the regression can be written in terms of the PCs as

$$\mathbf{W} = \varepsilon^* \mathbf{B}^* \quad , \tag{5.5}$$

where the values of ε^* are given by equation (5.4) and $\mathbf{B}^*$ are the standardized regression coefficients on the selected or candidate PCs. The $\mathbf{B}^*$ are given by

$$B_j{}^* = 1/N \sum_{i=1}^{N} W_i \varepsilon_{ij}{}^* \tag{5.6}$$

a result that follows from the fact that, as all predictor variables are orthogonal, $B_j{}^*$ is the simple correlation coefficient between W_i and $\varepsilon_{ij}{}^*$.

At this point a further selection of PCs is made on the basis of the regression significances, by using either a defined probability level (of rejecting the true hypothesis of null correlation when it is false, e.g., Guiot *et al.*, 1982) or the equivalent means of selecting only those PCs with simple correlations having t-values greater than a predefined threshold (Briffa, 1984).

Having calculated the $B_j{}^*$ and selected a final subset, the $\mathbf{b}$ [equation (5.2)] can be derived by

$$b_j = \sum_{m=1}^{q'} \alpha_{jm} B_m{}^* / s_m \quad , \tag{5.7}$$

where q' is used to denote that the summation is only over the selected components.

The standard errors (SEs) of the $\mathbf{b}$ are calculated by first calculating the standard errors for the $\mathbf{B}^*$. There are different methods of doing this. One may calculate the PC standard errors from

$$\mathrm{SE}(B_j{}^*) = [(1 - B_j{}^*)^2/(N-2)]^{1/2} \quad . \tag{5.8}$$

This method was proposed by Guiot (1981). Alternatively one may use

$$\mathrm{SE}(B_j{}^*) = [(1 - R^2)/(N - q' - 1)]^{1/2} \quad , \tag{5.9}$$

where R^2 is the coefficient of multiple determination for the equation that incorporates only the finally selected components (of which there are q'). This method gives a constant SE for all $B_j{}^*$ (Fritts *et al.*, 1971). Having calculated the PC standard errors, those for the $\mathbf{b}$ may be calculated by

$$\mathrm{SE}(b_j) = \sum_{m=1}^{q''} \mathrm{SE}(B_m{}^*)/s_m \cdot (\alpha_{mj})^2 \quad , \tag{5.10}$$

where q'' indicates that the summation is over the final selected PCs only.

In this second method, based on equation (5.10), there are also alternative methods for calculating the confidence levels for the individual response function elements. The standard errors must be multiplied by the appropriate t-value for the required confidence level but different t-values may be used. The t-value may be calculated using either of two values for the number of degrees of freedom (df): *viz.*, either

$$\mathrm{df} = N - q' - 1 \quad , \tag{5.11}$$

where q' is the total number of PCs from the initial selection, or

$$\mathrm{df} = N - q'' - 1 \quad , \tag{5.12}$$

where q'' is the final number of PCs with nonzero weights, i.e., after the second *a posteriori* selection has been made. If N is large there is effectively no difference between these options. In general, however, if N is low and the number of original climate variables is high, equation (5.11) will give a more conservative estimate of the confidence limits.

To avoid some of the uncertainties with regard to the use and sampling variability of PCA-based response functions, Cropper (1985) investigated the use of ridge regression as an alternative means of ameliorating the multicollinearity problem. In ridge regression, a biasing parameter, k, is added to the trace of the variance–covariance matrix of predictors with k usually falling in the range $0 < k < 1.0$. The resultant ridge regression coefficients are than estimated as

$$\mathbf{b}^*(k) = (\mathbf{X}'\mathbf{X} + k\mathbf{I})^{-1}\mathbf{X}'\mathbf{W} \quad , \tag{5.13}$$

where $\mathbf{I}$ is the identity matrix. If k equals 0, equation (5.13) reduces to the well-known formula for ordinary least squares (OLS) regression coefficients. The ridge parameter, k, is called a biasing parameter because it forces the coefficients toward zero. As a consequence, $\mathrm{E}[\mathbf{b}^*(k)] \neq \beta$, where $\mathrm{E}[\mathbf{b}^*(k)]$ is the expected value of $\mathbf{b}^*$ for a given k, and β is the true vector of coefficients. Thus, ridge regression estimates are biased. However in so doing, the main diagonal elements in the $(\mathbf{X}'\mathbf{X} + k\mathbf{I})^{-1}$ matrix, which are inflated by multicollinearity, will decrease. This results in smaller variance estimates for the regression coefficients. If the biasing influence of k is not too great, this translates into a regression model with smaller mean square error (MSE) than that obtained by OLS. This is possible because MSE = ${\sigma_e}^2$ + bias^2, where ${\sigma_e}^2$ is the error variance of the regression equation and bias = $\mathrm{E}[\mathbf{b}] - \beta$. For OLS estimates, which are unbiased, MSE = ${\sigma_e}^2$. For ridge estimates to have a smaller MSE, ${\sigma_e}^2$ must decrease faster than bias^2 increases.

The trick is to find the optimum value of k. In theory, a k can always be found that will produce a regression model with smaller MSE compared with OLS. This is based on an *existence theorem* of Hoerl and Kennard (1970). However, as Judge *et al.* (1985) point out, this theorem is based on k being fixed, not stochastic as it is in practice. Thus, in practice there is no guarantee that ridge regression will produce a model with smaller MSE compared with OLS. Numerous methods have been proposed for selecting the optimum k (e.g., the ridge trace, the Hoerl-Kennard-Baldwin estimator, the Lawless-Wang estimator, and the McDonald-Galarneau estimator). Judge *et al.* (1985) provide reviews of these methods.

Cropper (1985) and Fritts and Wu (1986) found that response functions estimated by ridge regression always produced wider confidence limits than those developed from principal components regression. Thus, ridge response functions seem to be much more conservative in their determination of statistically significant climatic and prior growth variables. Consequently, relatively few variables exceed the 95% confidence limits using ridge regression compared with PCA-based response functions. This difference reflects the overly narrow confidence limits of PCA-based response functions, as noted by Cropper (1985). However, the wider confidence limits of ridge response functions may also reflect difficulty in finding an optimum k for biasing the coefficients. Given this difficulty, it is not clear that ridge regression offers a significantly better solution to the multicollinearity problem confronting response function estimation.

5.6.3. A cautionary note

It is very important, as with all regression analysis, that the number of annual climate observations used in calibrating the response function exceed, as far as possible, the number of candidate predictors. This is necessary to guard against the possibility of over-calibrating the response functions.

Verification of response function equations, by comparing estimated and actual tree growth over an independent period, is strongly recommended (e.g., Briffa, 1984). Few areas have climate records shorter than 80 years. This means that 25 or 30 years could be routinely withheld for verification. Though it is generally accepted as fundamental in climate reconstruction work, verification is rare in response function work.

Attempts to compare the results of response function analyses of different chronologies (or for the same chronology over different periods) are fraught with problems: whether or not one wishes to compare the overall amount of chronology variance explained by climate (R^2) or the character of the tree/climate relationship in terms of significant response function coefficients. Such comparisons require detailed knowledge of the response function sampling distributions and confidence limits. R^2 depends on the number of predictors retained in the regression equation. It is therefore important, when comparing the results of different analyses, to use the same criterion (or criteria) for selecting the predictors. Ideally, the period of analysis should be standardized also; it should be of sufficient length to minimize sample-to-sample variability in the principal component loading patterns. Even when this is done, a problem of how to determine the confidence limits remains: both on R^2 and on each original climate predictor. Because the choice of final PC predictors is an *a posteriori* one, it is not clear what the correct degrees of freedom are. Use of the same approach to calculate significance in all analyses will allow more valid comparisons.

Even after adopting all of these suggestions, it is prudent to interpret only the gross features of individual analyses and not attempt to read too much into the finer details.

5.6.4. Analyzing groups of response functions

There are different ways in which the significant features characterizing a group of response functions can be expressed. Three illustrations are given here. The first method is concerned with summarizing only the statistically significant elements drawn from many individual analyses. The two remaining methods distill the salient features from all of the coefficients of a group of analyses.

Summary Response Function of Significant Elements

A summary response function can be constructed by plotting the total number of significant positive and negative response function elements from a group of separate analyses. Pilcher and Gray (1982) summarized the significant coefficients from 16 response functions, each expressing the growth of oaks (*Quercus*) chronologies in terms of temperature and precipitation for 14 months from the June preceding the growing season through the current July. Although they only later investigated the statistical significance of the monthly coefficient totals, they did note the general positive relationship between growing-season precipitation and growth and the inverse relationship between winter temperature, specifically for December and January, and growth in the following season.

In a later study, Briffa (1984) reworked this analysis using an expanded database of 36 *Quercus* chronologies. He also considered how to measure the statistical significance of the individual monthly totals of significant coefficients based on an earlier analysis of the statistical significance of the total number of significant elements in an individual response function (Gray *et al.*, 1981). Briffa (1984) confirmed a general relationship that existed from the November of one year to the November of the next. The strong relationship between increased growth of *Quercus* and lower than normal temperatures for previous Decembers and Januarys was also confirmed. March showed a similar relationship. The only month with a statistically significant total of positive temperature response function elements was May.

A recent analysis of 140 individual response functions led to the production of several summary response functions for ring-width and maximum latewood density chronologies for each of three genera of coniferous trees growing mainly at high altitude or high latitude sites in Europe (Briffa *et al.*, unpublished). These results highlight two things: the marked contrast between the densitometric and ring-width data in the extent and strength of temperature response; and the strong geographical variations of response functions between Northern, Central, and Southern European chronologies of the same genus.

Cluster Analysis of Response Functions

Fritts (1974) used cluster analyses to extract the major features of climate response in 127 ring-width chronologies from arid sites in western North America. His analyses enabled the individual responses to be classified into four major groups. The first three showed a generally positive growth response to above-average precipitation but differed from each other principally according to the time of year in which the precipitation influence was most marked. In the fourth cluster of response functions, temperature was shown to be as important a factor in influencing growth as precipitation and sometimes even more important. This group comprised mainly semiarid high altitude sites and contained 84% of all bristlecone pine chronologies analyzed.

Principal Components Analysis of Response Functions

An alternative approach to classifying the major modes of similarity in a number of response functions is to perform a principal components analysis (PCA) on the matrix of response function coefficients, where the monthly coefficients are the variables and the chronologies are the cases. This type of analysis has been applied to all of the coefficients of 36 response functions calculated for *Quercus* species (*Q. petraea, Q. robur*, and their hybrids) from sites in and around the UK and northern France (Briffa, 1984). This analysis reemphasized the relatively complex nature of climate/growth relationships in the comparatively moderate climates of this part of Western Europe. Nonetheless, the first five PCs explained 54% of the variance of all 36 response functions. The first three PCs accounted for 17%, 11%, and 10% of the variance in turn. The major modes of variation in the response functions were identified with the main modes expressing the spatial variance of the original chronologies. In particular, the

major north–south pattern of variation in the tree-ring data was shown to be explicable in terms of an opposite response to summer temperature variations between northern and southern chronologies.

5.6.5. Possible limitations of the response function approach

It is important to keep in mind that the response function is an empirical technique and even highly significant results achieved in terms of statistical probability do not necessarily reflect a genuine causal relationship. There is even a problem in calculating probability levels for response function results because of uncertainties associated with coefficients of the monthly climate variables. As was mentioned above, the primary difficulty in this regard stems from the uncertainty in knowing what the correct degree of freedom is.

One study using simulated tree-ring data with a known climate signal showed how easily misleading results can be achieved (Cropper, 1982), and a recent project using ridge regression techniques appears to confirm that all response functions underestimate the confidence levels on individual coefficients (Cropper, 1985).

Clearly the linear form of the response function is inappropriate if strong nonlinear interactions exist among the predictand and predictor data. In this regard, it has been suggested that cross products of various climate variables could perhaps be incorporated to allow for multiplicative effects. This, however, could "lead to significant loss of degrees of freedom and perhaps impair the ability to analyze individual months and sites" [Fritts (1976), page 401]. Some experimentation using nonlinear transformations of primary climate data have to overcome this problem to some degree (e.g., Brett, 1982).

Another approach to identifying nonlinear interactions in climate-related variables that influence tree growth is the use of response surfaces, more commonly used in palynological research (e.g., Bartlein *et al.*, 1986). A recent study of the growth of mountain hemlock (*Tsuga mertensiana*) and subalpine larch (*Larix lyallii*) in the Cascade Mountains, Washington, used response surfaces to demonstrate the nonlinear interaction between the growth of these trees and the variability of spring snow depth and summer temperature (Graumlich and Brubaker, 1986). There appears to be potential for experimenting with this approach in other areas.

5.7. Response Function Analysis for Ecological Study

F. Serre-Bachet and L. Tessier

5.7.1. Introduction

Response function analysis was developed and used for the first time (Fritts *et al.*, 1971) as a means for modeling climatic information in ring-width series in a more mathematically objective manner than simple or multiple regression analyses (Glock, 1950; Schulman, 1951, 1956; Glock and Agerter, 1962; Fritts, 1959, 1962, 1971; Fritts *et al.*, 1965; Serre *et al.*, 1966). The main objective of ring-

width studies, which made this information necessary, was the reconstruction of past climate.

Response function analysis has been and still is widely used for modeling tree-ring/climate relationships of numerous tree species growing in various habitats (e.g., Hughes *et al.*, 1978, 1982; Bednarz, 1981; Till, 1984, 1985; Aniol and Eckstein, 1984; Hughes and Davies, 1987). It is used both in ring-width studies and densitometric analyses (Schweingruber *et al.*, 1978; Conkey, 1979, 1986; Kienast, 1985; Kienast and Schweingruber, 1986; Hughes, 1987a). Discussion continues both on its computation and on its significance (Fritts, 1976; Guiot, 1981; Guiot *et al.*, 1982a, 1982b; Hughes and Milsom, 1982; Brett, 1982a; Cropper, 1982; Pittock, in Hughes *et al.*, 1982; Blasing *et al.*, 1984; Cropper, 1984; Till 1984, 1985; Fritts and Wu, 1986; Graumlich and Brubaker, 1986). Many improvements were proposed, especially for the construction of master chronologies (Peters *et al.*, 1981; Cook and Peters, 1981; Warren and MacWilliam, 1981; Guiot, 1986, 1987a; Guiot *et al.*, 1982c; Cook, 1985).

Its concept, its modeling considerations, the interpretation of its results, and its applications all place response function analysis in the field of ecology. One cannot argue against the fact that precipitation and temperature, which response functions often take into account, are environmental factors influencing tree growth. Yet, response function analysis has not often been used for autecology, i.e., dendroecology (Vinš, 1963). The term *dendroecology* was proposed for the first time by Vinš to expand the science of dendrochronology and dendroclimatology to the field of forest ecology with its broad spectrum of tree species and forest types. Defined as "a tool for evaluating variations in past and present forest environments" by Fritts and Swetnam (1986), dendroecology does not exactly correspond to Vinš' definition. In fact, the definition of Fritts and Swetnam (1986) is concerned more with the study of the impact of abnormal changes of the environment on tree growth due to forest pests, pollution, and forest damage and decline than with the analysis of normal environmental influences on tree growth. Dendroecology, in the sense of Fritts and Swetnam, does not use response functions as a main tool. Examples are detailed in Chapter 4.

We will present our use of response function analysis in the sense of Vinš (1963, page 195), who wanted to "apply the phytometric values of tree-ring thickness as indicators of growth of forest tree genera." As a matter of fact, like Fritts (1974), Pilcher and Gray (1982), and Till (1984, 1985), we consider response function analysis as a means of detecting the climatic-growth requirements of mature tree species in various habitats. This knowledge will lead to a better understanding of the ecological amplitude of tree species in general and to the better management of forests. Thus, response function analysis can "enlarge our knowledge about the biological properties of separate genera, about their ecological requirements and capacity of growth" (Vinš, 1963, page 195).

5.7.2. Materials and methods

The studies described here almost exclusively come from the French Mediterranean region or from North Africa, where summer drought is a frequent

occurrence (Emberger, 1971; Giaccobe, 1959, 1964–1965; Daget, 1980; Daget and David, 1962; Munaut, 1982). There, one or several tree species that are typical or interesting from a forest ecology point of view were analyzed. These species grow in pure or mixed stands distributed as several populations over more or less wide areas, and belong, at least with regard to a subgroup of the populations studied, to the same regional climate in the sense of Peguy (1970).

Except in some cases (Serre, 1978; Tessier, 1981), we related ring width to 24 climatic factors, i.e., the 24 response function variables corresponding to the monthly temperature and precipitation values from October of the previous year to September of the year of growth. The same 12-month period has also been used by Till (1984, 1985) in Morocco. The influence of prior growth has, with a few exceptions (*ibid.*), been removed from the chronologies by prewhitening techniques before regression was run. So, contrary to what is usually done (e.g., Fritts, 1976), prior growth at lags of 1, 2, and 3 years was not introduced in the calculation of the response function.

The response function of a population is most frequently calculated taking into account total precipitation and average mean temperatures. We also calculate response functions using average minimum and average maximum temperatures separately with precipitation because of the importance of extreme temperatures as limiting factors. Thus, the discussion of results generally concerns the synthesis of the three analyses (Serre-Bachet, 1982; Tessier, 1984, 1986; Guibal, 1984, 1985; Raouane, 1985). However, in some cases, response to only one of the temperature variables may be chosen because of its significance (Aloui, 1982; Tessier, 1987b).

A few attempts to utilize more complex regressors, i.e., various indices of climate such as evapotranspiration deficit (Thornthwaite and Mather, 1957; Turc, 1951) and summer drought indices (Emberger, 1971; Giacobbe, 1964–1965), did not lead to better results than those provided by discrete monthly data (Aloui, 1982; Tessier, 1984). This probably results either from excessive integration of those indices, even though it seemed that they might integrate climate in a similar way to the trees, or because the indices were inappropriate for forest stands that are more complex than the simple agronomic models (Thornthwaite and Mather, 1957) on which they are based. For Kienast (1985) too, evapotranspiration models "did not meet with the hoped-for success." However, Guiot *et al.* (1982a) successfully used the monthly water budget of four seasons in the period October–September. The number of eigenvectors entering the regression is defined by the eigenvalue product: PVP ≤ 1, according to Guiot (1985a).

Response functions can be calculated using the mean indices of raw data (the master chronology of indices of a population) in which the *persistence*, i.e., the influence of the autocorrelation or time-related interdependence between rings, is either corrected or left uncorrected in the regression model (Guiot *et al.*, 1982a). If autocorrelation is high and left uncorrected in the regression model, then the significance of the variance explained by climate (R^2) and of the partial coefficients in the response function will be difficult to assess. Response functions may also be calculated using the master chronology of residual resulting from the ARMA modeling of ring sequences from each analyzed core (Meko, 1981; Guiot,

1984, 1986, 1987a; Guiot *et al.*, 1982c; Tessier, 1984, 1986; Guibal, 1984, 1985; Raouane, 1985). This procedure is very effective in modeling tree-ring/climate relationships, especially as the master chronology only involves cores whose residual show a clear relation to climate.

Regression generally runs on a ring-width series in which length is at least equal to the number of variables. In the case of shorter ring series (< 24 years), for example, in the calculation of response functions of very young trees (Zhang, 1987), variables can be arranged in groups to reduce their number and thus make it suitable for the analysis.

In the type of ecological analysis presented here, the value of the response function is not questioned provided a plausible biological and physiological explanation can be given to the significant direct or inverse relationships it provides. For a group of scattered populations within a well-defined climatic region, it is quite obvious that the ***homogeneity*** of responses is a criterion for characterizing the climatic response of a tree species. Differences that appear may result from various site factors, such as exposure, elevation, slope, substratum, soil, and vegetation (Aloui, 1982; Tessier, 1984; Serre-Bachet, 1987). When response functions are used to help characterize the ecology of one or more species, this implies that a large number of populations representing various habitats must be compared (4 to 27 populations have been analyzed in each case so far).

The main elements for comparison are the significant partial regression coefficients of response functions. Some response functions that are insignificant (at the 90% level) are nevertheless taken into account on the basis of those coefficients. Of course, depending on the case, comparison of the R^2s of the response functions is especially significant. If appropriate, the R^2 explained by climate and that explained by prior growth are considered separately on account of the previously established model used to describe the chronology (see above).

Comparison of the significant partial regression coefficients of the different response functions is made directly and/or by calculation, especially when the number of populations studied is high. Instead of using the variable weights (Fritts, 1976), each response function is previously coded according to the significance of the partial regression coefficients. Nonsignificant coefficients are coded zero. Positive or negative coefficients whose significance may range from 0.90 to 0.95 and from 0.95 to 0.99 or is equal to or more than 0.99 are coded ± 1, ± 2, or ± 3, respectively.

A matrix is then established where ***variables*** are the different response functions to be compared and ***observations*** are the coded partial regression coefficients.

The matrix is analyzed using principal components analysis, and a hierarchical classification is made of response functions representative of the different populations (Serre-Bachet, 1982). This analysis may deal, for each population chronology, with the three response functions successively calculated with the P-minT, P-maxT, and P-meanT. A synthesis of the three responses functions, or only one of them, can also be used. When the number of populations is high and the results are confused, the responses related to temperatures are separated from those related to precipitation. Within each set of these results, one can distinguish the period prior to growth (October–March) from the period concurrent with growth (April–September) (Tessier, 1984, 1986; Guibal, 1984; Raouane, 1985).

Examples of autecological problems approached using responses functions will now be presented. These studies look at the definition of the behavior of either two or several species from a mixed-forest population at one site or one species in its natural or artificial distribution area. As will be shown, when genetic problems are involved (the subspecific definition of some populations, for example), the response to climatic factors may provide more diagnostic information. In addition, anatomical or biochemical features may also provide diagnostic information. When a species happens to present a certain longevity and when meteorological data are available, analysis can be made of its behavior through time; a spatiotemporal analysis is then necessary for reliable conclusions to be inferred.

5.7.3. Examples of the ecology of several species in a station

In some forest populations, the coexistence of several species suggests, for those species, fairly similar environmental requirements are needed. In the Mediterranean region some dynamic associations, for example, *Quercus ilex–Pinus halepensis* and *Quercus pubescens–Pinus sylvestris*, are probably based on similar requirements. These associations give an opportunity to compare the response of different species to the same climatic conditions.

This type of study has been made (Serre-Bachet, 1982) on seven populations representing five species (*Quercus pubescens*, *Pinus halepensis*, *P. pinea*, *P. pinaster*, and *P. sylvestris*) either in pure or in mixed formations, over a total area of only 5 km^2. The trees sampled are approximately 60 to 80 years old. The response functions with each P-maxT, P-minT, and P-meanT couple are calculated using meteorological data from the same station.

The factorial map 1 × 2 (*Figure 5.9*) explains 56% of the variance related to the response functions. Whenever a species is represented by two populations, as is the case for *Q. pubescens* or *P. halepensis*, the two populations are close together on the factorial map. Thus, the discrimination between response functions is actually not based on microstational conditions. Behavioral differences regarding climatic changes have to be ascribed to specific characters.

In the whole set of populations, the response function R^2 does not vary much from one population to another. However, it does contrast *P. pinea* ($R^2 = 0.68$) and *P. sylvestris* ($R^2 = 0.47$), which are also contrasted on the factorial map 1 × 2: these two species differ the most with regard to temperature and precipitation fluctuations.

From this first analysis, it appears that a particular subspecies status could be retained for the Euro-Asiatic species *P. sylvestris*, considering the marked Mediterranean character of the other species. However, it is obvious that the analysis of the only one site does not permit one to draw inferences about the autecology of the species as a whole. The spatial analysis of populations is required.

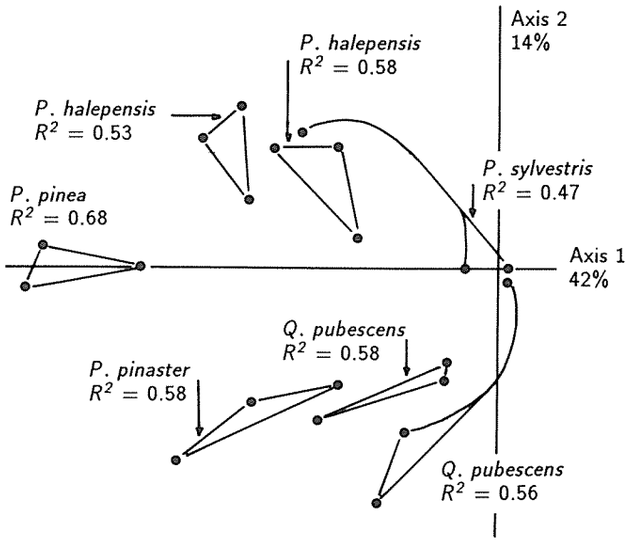

Figure 5.9. Distribution, on the factorial map 1 × 2, of the 21 response functions of 7 populations: three response functions per population with P-meanT, P-minT, and P-maxT. These response functions are characteristic of a population linked together. For each population, mean R^2 of the three response functions is given. (From Serre–Bachet, 1982.)

5.7.4. Spatial analysis

Spatial analysis can be made at different scales: several populations in different habitats under the same regional climate or a greater number of populations in a large area with more or less similar regional climates. The whole distribution range of the species can be the ultimate aim of the analysis.

Several Species Analysis

The analysis of several populations of a species under the same regional climate represents optimum conditions for an ecological interpretation of the response functions based on the role of the habitat in radial growth. Comparison of response functions highlights the importance of the ecotype in the response to climate, but the regional climate must be correctly represented by at least one of the meteorological stations available. The results of an analysis of tree-ring/climate relationships with all the meteorological stations available in a region are given below.

Six *P. sylvestris* populations were studied. They are located in three massifs some 20 km apart from each other and known to be under the same regional climate. To verify the uniqueness of this climate, the data from all six

meteorological stations nearest the massifs were utilized for the calculations of six response functions per population.

The cluster analysis of the 36 response functions (*Figure 5.10*) shows that the response functions differ from one another depending on the habitat. Response functions are clustered according to the massif and the population to which they belong. For each population, the use of different meteorological stations does not introduce differences. Hence, meteorological stations actually represent the same regional climate. The use of five more stations situated further away from the sites than the first ones disturbs the classification because the different stations do not represent the same regional climate. Moreover, response functions in this case are less significant, the correlations obtained express the transitiveness of the relationships between the regional climates; consequently, the ecological interpretation is more difficult.

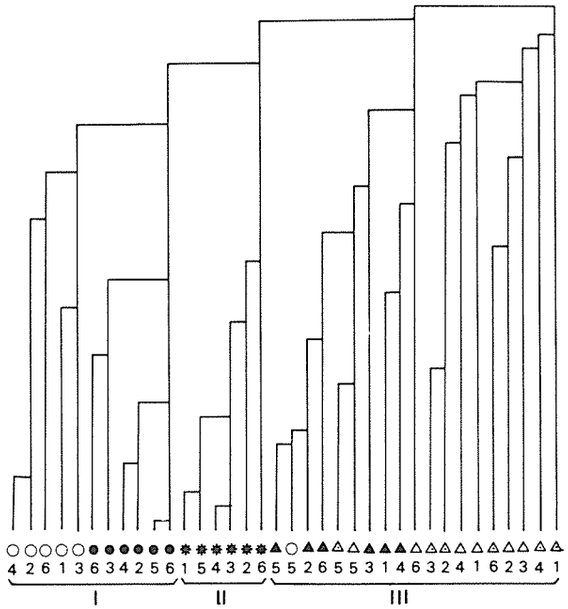

Figure 5.10. Hierarchial classification of 36 response functions on *Pinus sylvestris* populations representing the different combinations. Symbols indicate population; numbers 1 through 6 specify meteorological station; and Roman numerals I, II, III identify the forest massif of the Mediterranean region. (From Tessier, 1987b.)

When meteorological data clearly reflect the regional climate, a relationship can be established between the response functions and habitats. Thus, the global behavior of a species (its ecology) can be defined and its potential expansion estimated. It also makes it possible to interpret response functions from past periods and hence to reconstruct past habitats.

Spatial Scale Analysis

The scale of spatial analysis deals with the ecology of a species on all or part of its distribution area. Previous studies have been made on different species and genera: *Quercus* (Aloui, 1982; Pilcher and Gray, 1982; Raouane, 1985; Tessier, 1984;), *Larix decidua* (Serre-Bachet and Guibal, 1987), *Cedrus atlantica* (Guibal, 1984; Till, 1985), and *P. sylvestris* (Tessier, 1984). We shall take here the example of *P. sylvestris* (Tessier, 1984, 1986).

The area studied covers a large part of the French Mediterranean region, from the coast to the northern limit. In this area, the place occupied by *P. sylvestris* is important but marginal when compared with the whole range of species (Quezel, 1979). Three regional climatic units were defined, and 27 populations representing seven topographic areas provided the chronologies. To compare response functions in principal components analysis, it was necessary to separate the results of precipitation from the results of temperatures and to cut them into two phases as described above. The first phase (April–September) may be interpreted as resulting from direct physiological mechanisms. The second (October–March) involves the processes of water supplies that are always of great importance in the Mediterranean region.

As an example, an ecological interpretation has been advanced for the 1 × 2 factorial map (*Figure 5.11*) corresponding to the relation of growth with precipitation during Phase 1 (April to September). All response functions are grouped according to profile affinities that reflect ecotype affinities. There appears to be three types of response: a direct response to precipitation, practically over the whole summer (May–August); a direct response to precipitation, reduced or interrupted during full summer (June–July); and a poor or even zero response to summer precipitation. These three responses may be related to a range of habitats, from altitudinal and moist forest to habitats that are still far from the forest stage and drier, either because of the location of the population near the southern limit of the Mediterranean area or, in the case of more northerly populations, because of the substratum (marls). The response function merely expresses the particular response of the species to the hydric stress; that is to say, it reflects the strategy developed by the trees to escape unfavorable conditions (Aussenac and Valette, 1982). On marls, for example, *P. sylvestris* is able to survive severe xeric conditions and forms *durable pioneer* populations as long as the reduced activity of trees does not permit a rapid transformation of the habitat. Only when xeric conditions become less severe can *P. sylvestris* adopt a more normal behavior, as is now the case in nearly all of its forest populations.

These conclusions do not support the idea of any Mediterranean subspecies for *P. sylvestris*. Populations characterized by stunted trees merely reflect adaptive modifications due to reduced activity related to xeric habitats. The modulation of the response to climate according to the nature of the habitat also raises the problem of the evolution of response functions in time as a result of vegetation dynamics.

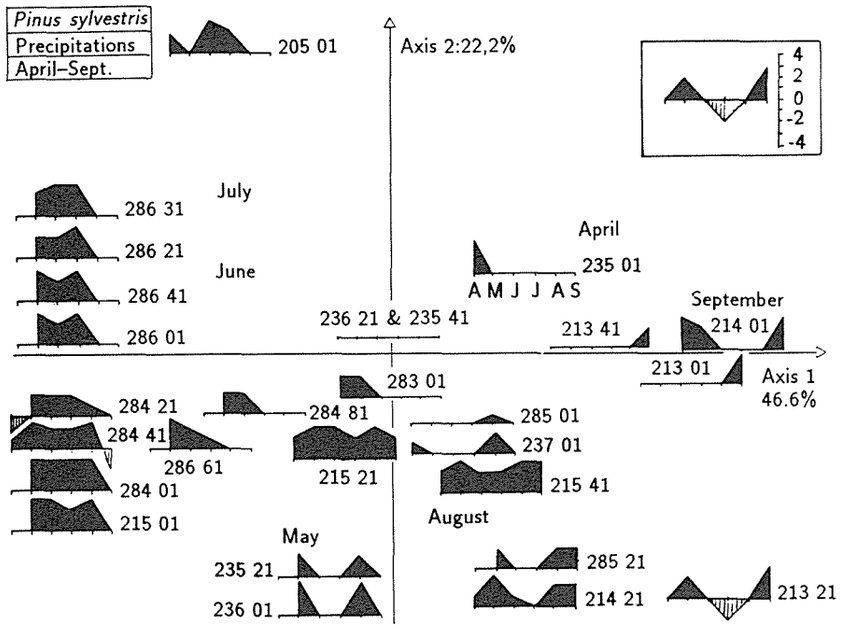

Figure 5.11. Distribution, on the factorial map 1 × 2, of the response functions of 27 *Pinus sylvestris* populations. (From Tessier, 1984.)

5.7.5. Temporal analysis

In the response function, each partial regression coefficient is interpreted as the average effect of the fluctuations of that monthly climatic parameter on tree growth.

The ecological interpretation of the response function, as well as its utilization for interpretations of the past, implies that the climate-growth system remains stable in time (Fritts, 1976). Any detected instability may be related to unstable climatic data (Gray *et al.*, 1981), to the occurrence of a new external factor [for example, air pollution (Puckett, 1982)], to the aging of trees (Pittock, 1982), or to the evolution of the habitat.

Whatever method is used – division of the chronology in two sequences and then comparison of response functions (Puckett, 1982; Gray *et al.*, 1981) or utilization of the Kalman filter (Visser and Molenaar, 1986) – it is difficult to find an explanation for this instability when only one population is analyzed. As a matter of fact, such an investigation generally requires the simultaneous use of spatial analysis.

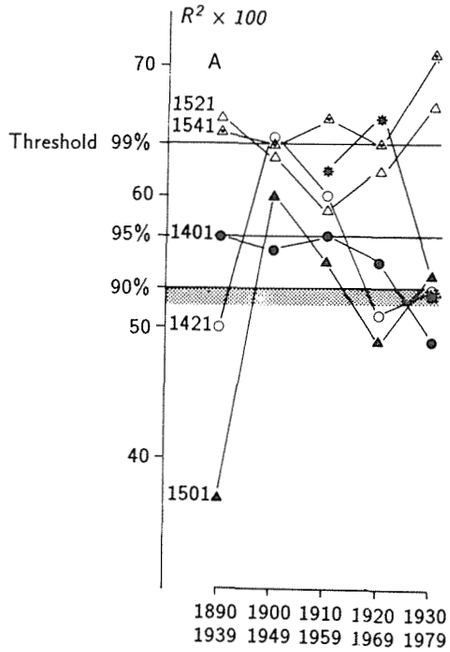

Figure 5.12. Evolution in time, in five overlapping time sequences, of the R^2 of response functions calculated using the P-maxT couple for each of six populations of *Pinus sylvestris*. (From Tessier, 1987b.)

5.7.6. Spatiotemporal analysis

This type of analysis made on six *P. sylvestris* chronologies from 1890 to 1980 gives the following results. The chronologies correspond to more or less forested populations. The six populations cover a limited area within the same regional Mediterranean climate.

Each chronology was divided into five overlapping sequences of 50 years, and a response function was calculated for each sequence. Climate data came from the same meteorological station, some 20 km away from the populations. The response function corresponding to P and maxT will be considered here. Response functions were compared on the basis of the significance of their percent variance reduced (R^2) (*Figure 5.12*) and of their profile (*Figure 5.13*).

The R^2 calculated varies depending on the population. For populations that are most forested today (15–21 and 15–41), R^2 remains significant and relatively stable during the five periods. However, for the two populations that have the least forest cover (15–01 and 14–21), the R^2 ranges between the significance levels 90% and 99%. The absence of parallel evolution between populations suggests that the cause of fluctuation is to be found in the differential change in

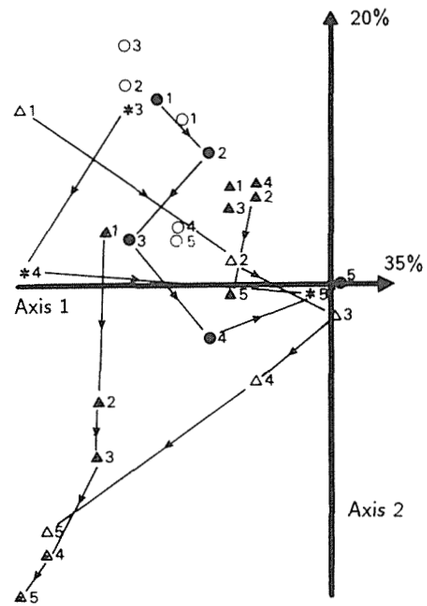

Figure 5.13. Distribution, on the factorial map 1 × 2, of response functions representing the different population–time sequence combinations. Symbols indicate populations, and numbers 1 to 5 specify time sequence. (From Tessier, 1987b.)

habitats rather than in a climatic evolution that would have affected all the populations in the same manner.

The response function profiles vary both in space and in time. Analysis of the 1 × 2 factorial map that explains 55% of the variance permits a spatial and a temporal comparison. For the present (period 5), there is an opposition between forest populations and non-forest ones. For the past (period 1) there appears to be an affinity between all the populations, including those at present that are forested. The profile of response functions for period 1 is similar to that of response functions of non-forest populations during period 5. Therefore, one can conclude that there has been a forest expansion since the beginning of the century. Only the two populations 15–21 and 15–41 reached the forest stage; classification in the factorial map of the five response functions corresponding to the five periods shows that this evolution took place gradually.

5.7.7. Discussion and conclusion

The examples presented show that response function analysis is an irreplaceable tool for the study of forest ecology. The few, exclusively autecological, analyses of one or several species that have been published until now were carried out under different and more or less contrasted climates, always less contrasted

anyway than those for which the response function was developed. However, valuable results have been obtained.

Response function analysis must be considered as the mean expression of the limiting factors experienced by a tree population for a certain time. This is only true if the meteorological data used in the analysis reflect the regional climate as experienced by the trees.

Within the same species, the different response to climate using the same meteorological data stations can always be explained by differences in habitats, as was pointed out by Fritts (1976) and other authors. Nevertheless, there appears to be a certain constancy in response that is related to the species or even the genus (Serre-Bachet, 1987). The difficulty in describing this constant depends on the ecological amplitude of the species. When a species or a genus has a weak ecological amplitude, as is the case for *Cedrus atlantica*, it is easy to find out this constant since climate is intrinsically the same over all the distribution area of the species. This is not the case for large amplitude species such as *P. sylvestris*. We chose to present only the aspect of response function analysis that, apparently, has not been widely used yet. But any investigation on tree rings (in particular climate reconstruction from one or several species in a more or less large area) implies using the same approach, even if the aim is different.

The present trend in the ecological interpretation of each year in a chronology (Till, 1985; Kienast, 1985) rests on the information directly available on the mean and most frequent climatic influences provided by the response function. The great number of stations involved in the analytical ecological approach, such as was used by Kienast (1985), is also a necessary element in the autecological study of species through response function analysis. In both methods the choice of stations is based on the widest and finest knowledge of local ecological factors. The two methods do not exclude each other but are used in different contexts. The aim of the research is primarily to clarify the so-called *normal behavior* of a species, so that this behavior may be used as a reference when analyzing for abnormal changes in tree growth.

5.8. Detecting Shifts in Radial Growth by Use of Intervention Detection

D.J. Downing and S.B. McLaughlin

5.8.1. Introduction

The time series of annual radial increments of forest trees examined in dendroecology provides a wide array of signals of varying frequency, duration, and intensity for examining responses of forest trees to environmental stress. Where hypothesized independent variables influencing growth are well documented over time, conventional modeling approaches may be used to test the strength of growth dependency on these variables. However, when both the identity and the mechanisms of action of independent variables are less clear, further analyses may be more efficiently performed by first identifying the nature and timing of significant changes in the long-term growth patterns.

Current emphasis on characterizing recent changes in growth patterns of forest trees in response to environmental stress has highlighted the need for such a stepwise approach involving specifically the systematic evaluation of the frequency, magnitude, and duration of past and recent shifts in those growth patterns. This need is perhaps most obvious in the case of the regional decline of red spruce (*Picea rubens*) in the USA.

The recent documentation of increased mortality and decreasing radial growth of red spruce in high elevation forests of the eastern USA (Siccama *et al.*, 1982; Scott *et al.*, 1984; Johnson and McLaughlin, 1986) has characterized what appears to be a regional-scale response to some regional-scale environmental stress. Climatic change, intensification of natural competitive stress, and atmospheric pollution have all been considered as possible influencing factors in contributing to observed changes, but to date there is no scientific consensus regarding the principal causal factor (McLaughlin, 1985).

In examining large-scale phenomena of this type in complex environmental systems, a wide range of influencing factors must be considered. However, the number of factors that can be considered logical contributors to observed changes may be substantially reduced by documenting the geographical pattern and timing of observed changes. Synchronous changes at many sites across a broad region may suggest that regional and not local site conditions are involved. Pattern analysis of candidate predictor variables may further indicate which variables are likely contributing factors and warrant closer study.

In initial studies aimed at examining the regional patterns of change in radial growth of several eastern tree species (McLaughlin *et al.*, 1983), a regional database on long-term growth patterns of more than 7,000 trees and associated changes in a variety of potentially related environmental variables was constructed (see McLaughlin *et al.*, 1986, for documentation). Our initial statistical analyses (McLaughlin *et al.*, 1987) of the regional growth patterns of red spruce from that data set has led us to explore a relatively new time series technique called *intervention detection* (Chang and Tiao, 1983) as a method of documenting the spatial and temporal homogeneity of observed changes. In the following discussion, the development and application of this technique is shown in an analysis of regional trends in radial growth of forest trees using red spruce as a case study.

In this application, the technique was used in analysis of 2,433 spruce cores in the FORAST database using an IBM-PC and a computer program written by Automatic Forecasting Systems, Inc. (AFS; see Reilly, 1984a). The program is written to analyze time series data and has the capability to construct Box-Jenkins models automatically. In addition, it can do transfer function analysis (relating exogenous time series – similar to multiple regression analysis), intervention analysis (similar to transfer function analysis except the exogenous series are binary sequences related to occurrence of some event), and intervention detection (a method to identify outliers). The AFS program was the ideal tool to analyze such a large data set, especially with the automatic intervention detection feature. Section 5.8.2 describes the basic Box-Jenkins models that are used in time series analysis. Section 5.8.3 introduces intervention detection, its relationship to Box-Jenkins time series modeling, and the use of intervention

detection. The results from the FORAST study concerning Box-Jenkins models and intervention detection with regard to the spruce cores are summarized in Section 5.8.4. Section 5.8.5 discusses the randomness of the interventions in time and space. Our conclusions of intervention detection as a statistical tool are provided in Section 5.8.6.

5.8.2. Time series models

Models that adequately describe several types of time series were introduced by Box and Jenkins (1970). These models are called autoregressive-integrated-moving average (ARIMA) models. The general model could be written:

$$\begin{aligned}&(1 - \phi_1 B - \phi_2 B^2 - \cdots - \phi_p B^p)\nabla^d (N_t - \mu) \\ &= (1 - \theta_1 B - \theta_2 B^2 - \cdots - \theta_q B^q) a_t\end{aligned} \tag{5.14}$$

or

$$\Phi(B)\nabla^d (N_t - \mu) = \Theta(B) a_t \quad ,$$

where

B = backward shift operator (i.e., $BN_t = N_{t-1}$);
∇ = difference operator = $(1 - B)$ [i.e., $\nabla N_t = (1 - B)\ N_t = N_t - N_{t-1}$];
N_t = value of time series at time t;
μ = unknown mean of the time series that must be estimated;
a_t = unobservable random variable taken to be white noise;
$\underline{\Phi}$ = $(\phi_1, \ldots, \phi_p)$ = unknown autoregressive parameters that must be estimated; and
$\underline{\Theta}$ = $(\theta_1, \ldots, \theta_q)$ = unknown moving average parameters that must be estimated.

The model given in equation (5.14) is usually called ARIMA (p, d, q). The p refers to the highest power of B in the autoregressive operator:

$$\Phi(B) = (1 - \phi_1 B - \phi_2 B^2 - \cdots - \phi_p B^p) \quad . \tag{5.15}$$

If we multiply N_t through the autoregressive operator and write $B^k N_t = N_{t-k}$, then we have

$$\Phi(B) N_t = N_t - \phi_1 N_{t-1} - \phi_2 N_{t-2} - \cdots - \phi_p N_{t-p} \quad . \tag{5.16}$$

One can think of equation (5.16) as a regression equation. Since the regression is on lagged values of the same variable, the term *autoregressive* is appropriate.

The value d is the power to which the difference operator, ∇, is raised. Usually d is 0, 1, or 2 in practice. To understand why the term *integrated* is used, consider the following. Let $d = 1$ and write

$$\begin{aligned}W_t &= \nabla N_t \\ &= (1 - B) N_t \\ &= N_t - N_{t-1} \quad .\end{aligned} \tag{5.17}$$

The series $\{W_t\}$ is generated from the original series by subtracting adjacent values. If we want to obtain the original $\{N_t\}$, what must we do? It is easy to see that

$$N_t = \sum_{j=-\infty}^{t} W_j \quad , \tag{5.18}$$

and, considering summation of the discrete analog of integration, we understand the reason for the term integrated. The q refers to the highest power of B in the moving average operator:

$$\Theta(B) = (1 - \theta_1 B - \theta_2 B^2 - \cdots - \theta_q B^q) \quad . \tag{5.19}$$

This operator multiplies the unobservable white-noise series $\{a_t\}$ and acts like an average of past errors, thus the nomenclature *autoregressive-integrated-moving average models.*

Procedures have been developed by Box and Jenkins (1970) that aid in identifying the form of the model, estimating the parameters of the model, and testing model adequacy. The procedure is iterative and moves through steps 1–3 until the model selected is found to be adequate. The widespread use of the Box-Jenkins modeling technique in the real world is proof of the technique and its wide applicability.

5.8.3. Intervention detection

Intervention detection began as an iterative technique to identify possible outliers and was proposed by Chang and Tiao (1983). A computer program written by Bell (1983) and developed into an automatic modeling procedure by Reilly (1984b) are the earliest uses of the intervention detection technique. We point out that intervention detection is normally used to identify outliers in the time series, remove their effects, and then specify a tentative model for the underlying process. Another aim is to identify the type of intervention (to be explained shortly) and its time of occurrence. Our interest was in the

randomness in time that these interventions occurred and in their direction (i.e., an increase or decrease in the ring-width increment).

Outliers can occur in many ways. They may be the result of a gross error, for example, a recording or transcription error, incorrect measurement reading, or faulty equipment. They may also occur by the effect of some exogenous intervention, for example, forest clearing, pollution, storm damage, or other climatological extremes. These can be described by two different generating models discussed by Chang and Tiao (1983) and by Tsay (1986). They are termed the innovational outlier (IO) and additive outlier (AO) models. An additive outlier can be defined as

$$Y_t = N_t + W\xi_t^{(t_0)} \quad , \tag{5.20}$$

while an innovational outlier is defined as

$$Y_t = N_t + \frac{\theta(B)}{\phi(B)} W\xi_t^{(t_0)} \quad , \tag{5.21}$$

where

Y_t = the observed time series,

W = the magnitude of the outlier, and

$$\xi_t^{(t_0)} = \begin{cases} 1 \text{ if } t = t_0 \\ 0 \text{ if } t \neq t_0 \end{cases} \quad ,$$

that is, $\xi_t^{(t_0)}$ is a time indicator signifying the time occurrence of the outlier, and N_t is an unobservable outlier-free time series that follows the model given by equation (5.14). Expressing equation (5.20) in terms of white noise in equation (5.14), we find that for the AO model

$$Y_t = \frac{\theta(B)}{\phi(B)} a_t + W\xi_t^{(t_0)} \quad , \tag{5.22}$$

while for the IO model

$$Y_t = \frac{\theta(B)}{\phi(B)} [a_t + W\xi_t^{(t_0)}] \quad . \tag{5.23}$$

Equation (5.22) indicates that the additive outlier appears as simply a level change in the t_{th} observation and is described as a *gross error* model by Tiao (1985). The innovational outlier represents an extraordinary shock at time t

since it influences observations Y_t, Y_{t+1}, ... through the memory of the system described by $\Theta(B)/\Phi(B)$. The subsequent analysis shall be concerned with the additive outlier case only. Those interested in the estimation, testing, and subsequent adjustment for innovational outliers should read Tsay (1986). Note that the above models indicate a single outlier while in practice several outliers may be present. This problem is discussed later.

The estimation of the AO can be obtained by forming

$$\Pi(B) = \Phi(B)/\Theta(B) = (1 - \Pi_1 B - \Pi_2 B^2 - \ldots)$$

and calculating the residuals e_t by

$$\begin{aligned} e_t &= \Pi(B)\, Y_t \\ &= \Pi(B)\{[\Theta(B)/\Phi(B)]a_t + W\xi_t^{(t_0)}\} \\ &= a_t + W\Pi(B)\xi_t^{(t_0)} \quad . \end{aligned} \tag{5.24}$$

By least squares theory, the magnitude W of the additive outlier can be estimated by

$$\begin{aligned} \hat{W}_{t_0} &= \eta^2 \Pi(F)\, e_{t_0} \\ &= \eta^2(1 - \Pi_1 F - \Pi_2 F^2 - \cdots - \Pi_{n-t_0} F^{n-t_0}) e_{t_0} \quad , \end{aligned} \tag{5.25}$$

where

$$\eta^2 = (1 + \Pi_1^2 + \Pi_2^2 + \cdots + \Pi_{n-t_0}^2)^{-1}$$

and F is the forward shift operator such that $Fe_t = e_{t+1}$. The variance of $\hat{W}_{t_0}$ is given by

$$\mathrm{Var}(\hat{W}_{t_0}) = \eta^2\sigma^2 \quad , \tag{5.26}$$

where σ^2 is the variance of the white-noise process a_t.

Based on the above results Chang and Tiao (1983) proposed the following test statistic for outlier detection:

$$\lambda_{t_0} = \hat{W}_{t_0}/\eta\sigma \quad . \tag{5.27}$$

If the null hypothesis of no outlier is true, then λ_{t_0} has the standard normal distribution. Usually, in practice the true parameters Π and σ^2 are unknown, but consistent estimates exist. Even more important is the fact that t_0, the time of

the outlier, is unknown, but every time point may be checked. In this case one uses the test statistic:

$$\lambda = \max|\lambda_{t_0}| \qquad \{t_0 : 1 \le t_0 \le n\} \tag{5.28}$$

and declares an outlier at time t_0 if the maximum occurs at t_0 and is greater than some critical value C. Chang and Tiao (1983) suggest values of 3.0, 3.5, and 4.0 for C.

The outlier model given by equation (5.22) indicates a pulse change in the series at time t_0. A step change can also be modeled simply by replacing $\xi_t^{(t_0)}$ with $S_t^{(t_0)}$ where

$$S_t^{(t_0)} = \begin{cases} 1 \text{ if } t \le t_0 \\ 0 \text{ if not} \end{cases} . \tag{5.29}$$

We note that $(1 - B)S_t^{(t_0)} = \xi_t^{(t_0)}$. Using $S_t^{(t_0)}$ one can apply least squares to estimate the step change and perform the same tests of hypothesis reflected in equations (5.26) and (5.27). In this way significant pulse and/or step changes in the time series can be detected.

The following procedure was used in the analysis of the FORAST spruce cores for intervention detection (we note that this is the method suggested by Tiao, 1985):

(1) Model the ring-width increment series, Y_t, assuming no outliers and from the estimated model compute the residuals:

$$e_t = \Pi(B)\, Y_t \quad .$$

(2) Compute the test statistic for the additive step outlier and additive pulse outlier at each time point and choose the one with the largest magnitude. If this value is greater than the upper 2.5% on the Student's t distribution, declare it to be an outlier. If not, stop and accept the model obtained in step 1.

(3) Given that there is an outlier, remove its effect by subtracting it from the residuals and defining new residuals given by

$$\tilde{e}_t = e_t - \hat{W}_{A,t_0}(B)\xi_t^{(t_0)} \qquad \text{(pulse outlier)} \tag{5.30}$$

or

$$\tilde{e}_t = e_t - \hat{W}_{A,t_0}\Pi(B)S_t^{(t_0)} \qquad \text{(step outlier)} \quad . \tag{5.31}$$

A new estimate of σ_a^2 is calculated from the new residuals.

(4) Repeat step 2 using the new residuals and new estimate of variance continuing through step 3 until no more outliers are found.

(5) Suppose that k outliers have been tentatively identified at times $t_1, t_2, \ldots, t_k$. Treat these times as if they are known, and estimate the outlier parameters $W_1, W_2, \ldots, W_k$ and the time series parameters simultaneously using models of the form

$$Y_t = \sum_{j=1}^{k} W_j X_t^{(t_j)} + \frac{\Theta(B)}{\Phi(B)}\, a_t \quad , \tag{5.32}$$

where

$$X_t^{(t_j)} = \begin{cases} S_t^{(t_j)} \text{ for a step outlier} \\ \xi_t^{(t_j)} \text{ for a pulse outlier} \end{cases} .$$

This model is simply an intervention analysis model developed by Box and Tiao (1975) where the interventions are either pulses or steps at the times corresponding to $t_1, t_2, \ldots, t_k$.

5.8.4. Modeling results

There were 2,433 spruce trees analyzed using the Automatic Forecasting System software. The program initially identifies an ARIMA model for the time series ignoring possible outliers. The summary of those models is given in *Table 5.1*, which gives a very general overview of the type of model. The table identifies the number of autoregressive (AR) and moving average (MA) factors in the model, but does not specify the actual orders of the AR and MA processes [the values of p and q in equation (5.14)].

Table 5.1 indicates that the majority of the ring-width series (1,438) was stationary in the mean and did not require differencing. Of these 709 (nearly 50%) are modeled by an ARIMA-type model. The next most frequent model is an AR model accounting for 609 (42%). The most complex models requiring two autoregressive factors account for nearly all the remaining models, 105 (7%). There were 995 series that required differencing. The first difference was the only differencing required to induce stationarity. In practice, after a difference is made the resulting series is well modeled by a moving average model. In these analyses we see the same behavior with 758 series (76%) being modeled with a pure moving average model. The next most dominant model is the ARIMA model with 91 series (9%) having this model.

Table 5.1. Frequency counts of ARIMA models ignoring outliers.

	Moving average factors			
Autoregressive factors	*0*	*1*	*2*	*Total*
Differencing value d = 0				
0	1(<1%)	7(<1%)	2(<1%)	10
1	609(42%)	709(49%)	5(<1%)	1,323
2	58(4%)	47(3%)	0(0%)	105
Total	668	763	7	1,438
Differencing value d = 1				
0	72(7%)	465(47%)	293(29%)	830
1	53(5%)	91(9%)	14(1%)	158
2	5(<1%)	2(<1%)	0(0%)	7
Total	130	558	307	995

Table 5.2. Frequency counts of ARIMA models for series having no outliers.

	Moving average factors			
Autoregressive factors	*0*	*1*	*2*	*Total*
Differencing value d = 0				
0	1(<1%)	2(<1%)	0(0%)	3
1	77(47%)	69(42%)	2(1%)	148
2	8(5%)	6(4%)	0(0%)	14
Total	86	77	2	165
Differencing value d = 1				
0	11(10%)	47(42%)	34(30%)	92
1	5(4%)	14(13%)	0(0%)	19
2	1(<1%)	0(0%)	0(0%)	1
Total	17	61	34	112

Table 5.3. Frequency counts of ARIMA models for series having at least one outlier.

	Moving average factors			
Autoregressive factors	*0*	*1*	*2*	*Total*
Differencing value d = 0				
0	0(0%)	19(2%)	12(<1%)	31
1	418(33%)	691(55%)	10(<1%)	1,119
2	40(3%)	56(4%)	3(<1%)	99
Total	458	766	25	1,249
Differencing value d = 1				
0	64(7%)	368(41%)	294(32%)	726
1	43(5%)	117(13%)	16(2%)	176
2	2(<1%)	3(<1%)	0(0%)	5
Total	109	488	310	907

Once the series is analyzed for outliers, and if any are found, then the previous model form is subject to change. Thus, a reanalysis is performed for series with outliers. The models for series having no outliers are summarized in *Table 5.2.* The percentage breakdowns are very similar to *Table 5.1*, which we might expect since the models for these series are a subset of those in *Table 5.1.* We note that 277 of the 2,433 (11.4%) tree-ring series did not have any statistically detectable outliers present. Of these, 112 (40.4%) were from northern sites and 165 (59.6%) from southern sites. A large percentage (48.7%) of these cores had series that were relatively short (from 50 to 80 years long). The majority (60%) of the series having no outliers did not require differencing, and of those that did the pure autoregressive models account for 52%. The majority of those series having no outliers, but requiring differencing, was well modeled by pure moving average models (72%).

Table 5.3 describes the frequency of models for those series having at least one outlier. The majority of the series (89%) had at least one outlier. Nearly 91% of the cores from the north experienced at least one outlier, while 86% of the southern cores had at least one outlier. The most recurrent model for cores requiring no differencing was an ARIMA model with one AR and one MA factor (55%). Another recurrent model for cores requiring no differences was the pure AR model accounting for 37% of the cores. For cores requiring a difference, the majority (73%) had pure moving average models. Another large percentage (13%) had models requiring both an AR factor and an MA factor.

By examining *Tables 5.1–5.3* on a percentage basis (figures in parenthesis) it is clear that a similar percentage of models appears in each category regardless of whether outliers have been found or not. This does not indicate that the models are robust to outliers, but it does indicate that making adjustments for them still leads to similar types of models.

5.8.5. Randomness in time and space

Our analyses of 2,433 cores in this study showed that approximately 76% of the tree cores exhibited step interventions and 81% had pulse interventions during their measured growth span. From the total population of cores examined, 62% exhibited at least one negative step intervention and 49% had positive interventions. Some had both. The number of observed interventions per core ranged from one to five.

The distribution of step interventions over time including total positive and negative changes as well as first-time negative changes are shown in *Figure 5.14.* Only the 488 cores for which the measurement record extended at least as far back as 1860 are shown. Data points plotted are for interventions occurring within successive five-year intervals. Beginning with the year indicated a strong upswing in positive steps is evident (1905, 1940, and 1955), each associated with a downswing in positive interventions occurring in the 1955 pentad.

The upswing in positive interventions in the late 1800s is a likely response of a residual population at some sites, which had been disturbed by logging and mortality of canopy trees at this time as reported previously. The very large

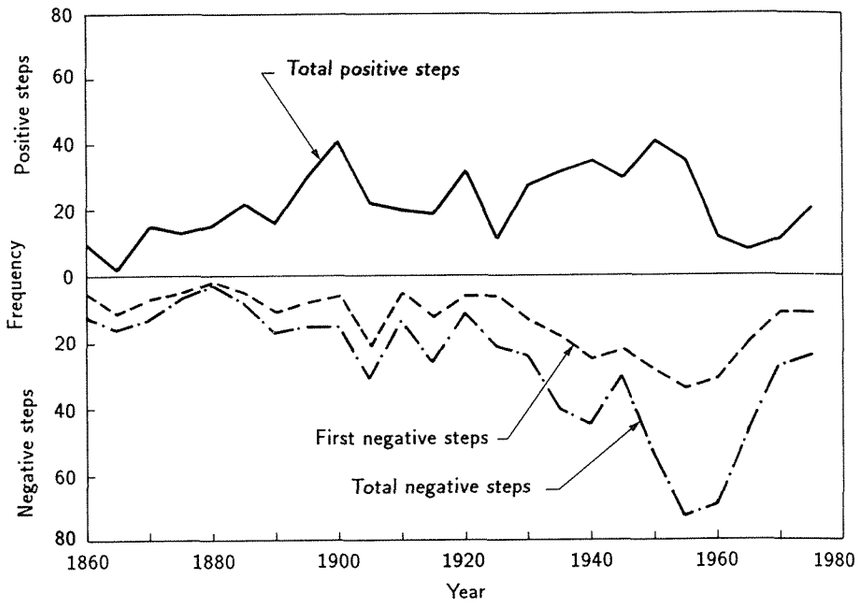

Figure 5.14. The distribution of step interventions over time including total positive and negative changes as well a first-time negative step changes for red spruce (*Picea rubens*) growing in the Appalachian Mountains of North America.

increase in negative steps in the interval 1955–1960 coincides with the observed radial growth decline and includes a large percentage of individuals that was responding negatively for the first time (*Figure 5.14*). The sharp decrease in negative steps in the past 10 years is a likely consequence of a diminished population of sensitive individuals that had not already experienced growth decreases by that time. An interesting feature of the recent period of declining growth is that the low frequency of positive steps provides no indication of competitive release of trees in these stands despite the fact that increased mortality occurred in many of the northeastern stands. Separate analyses of total number of cores measured back as far as 1900 (1,186 cores) and 1930 (2,078 cores) showed that this sharp upswing in negative responses and decrease in positive response occurred throughout the data set for all age classes.

Figure 5.15 focuses on comparisons between the total number of negative step interventions at northern and southern stands. For these analyses, the larger database of 1,186 (637 northern and 549 southern) cores for which measurements extended back at least to 1900 was used. These comparisons show that the maximum number of first-time negative steps occurred in northern stands during the 1955 to 1960 interval. This sharp increase in negative steps noted at northern sites was not replicated in the southern stands. The maximum response to southern sites occurred five to ten years later (1965 to 1969)

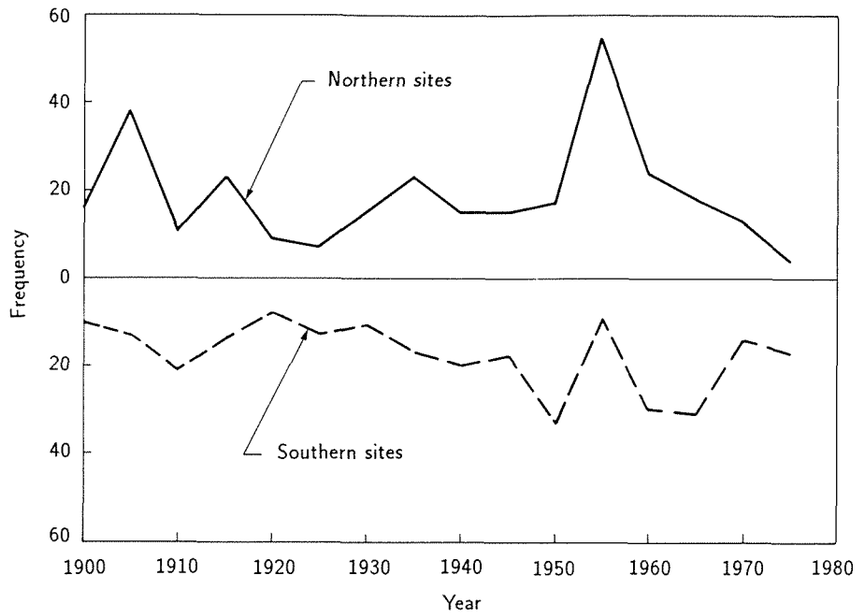

Figure 5.15. Comparison between the total number of negative step interventions at northern Appalachian and southern Appalachian red spruce stands.

and involved 11% of cores compared with 18% that responded at the 1955 to 1959 peak at northern sites. The secondary response in the southern stands in 1950–1955 is an apparent reflection of sharp reductions in growth during the 1952–1954 drought, a response that is obvious in nearly all spruce chronologies from the Great Smoky Mountains National Park.

In summarizing the long-term patterns of the spruce, it appears that during the past 20–25 years the noted decreases in radial growth represent a unique event in the available ring-width record of surviving trees based on duration of the pattern of decreasing growth and number of individual cores experiencing sustained downward shifts. The pattern of decrease appeared first, and most strongly, in northern stands during the interval from 1955 to 1960 and followed to a somewhat lesser extent five to ten years later in predominantly high-elevation southern stands.

5.8.6. Conclusion

As a statistical tool for characterizing biological phenomena we conclude that intervention detection is potentially a very useful approach for objectively and systematically examining large data sets for evidence of environmental influences. In the application we have described here, our focus has been on

sustained negative shifts that have typified the initiation of decline in radial growth of spruce. Positive steps may also be of interest, described by McLaughlin *et al.* (1987), as well as shorter-term negative or positive pulse interventions.

The documentation and characterization of changes in biological systems is obviously an important first step in determining what factors may be involved in contributing to those changes. Intervention analysis of patterns of change in associated environmental variables may similarly provide important answers regarding which chemical, physical, or biological factors showed synchronous patterns of change and hence are plausible contributing influences to the response of interest.

In our application we have arbitrarily used a 95% confidence level for discrimination of significant response. Other confidence limits (i.e., 75% significance) may also be useful for detecting meaningful patterns of change.

5.9. Detecting Time-Dependent Climatic Responses in Tree Rings Using the Kalman Filter

H. Visser and J. Molenaar

5.9.1. Introduction

In the early days, tree-ring chronologies of healthy stands were compared with those of stands affected by smelters and chemical industry to detect pollution effects. Today these comparisons cannot be made because tall stacks are used generating long-range transport of chemical compounds. Therefore, the only way to show relationships between tree growth and air pollution is to filter out all nonpolluting influences.

To determine growth–weather relationships several filtering techniques are available. In most cases the method of response functions is used (e.g., Ashby and Fritts, 1972; Strand, 1980a; Thomson, 1981; Arndt and Wehrle, 1982; Puckett, 1982; Phipps, 1983; Eckstein *et al.*, 1983, 1984; McClenahen and Dochinger, 1985). The model reads as follows:

$$\underline{y}_t = \alpha z_t + \underline{\xi}_t \quad . \tag{5.33}$$

The time index t runs over N successive years. Random variables are underlined. The dependent variable y_t represents a tree-ring index at year t. The vector z_t contains all selected meteorological variables and lagged indices at year t. All explanatory variables are standardized. Vector α contains the regression parameters. The noise process $\underline{\xi}_t$ is assumed to be normally distributed. The parameters are assumed to be constant over time. They are usually estimated by means of ordinary least squares (OLS).

The assumption of constant coefficients is a real disadvantage of this approach, because effects of aging, changes in climate, changes of groundwater levels, and increasing air pollution levels cannot be detected in this way. Puckett (1983), Phipps (1983), and McClenahen and Dochinger (1985) have tried to overcome this shortcoming by splitting up the available time series into two or three parts and applying the regression model to the respective time intervals. In this approach, however, the length of the intervals and the number of explanatory variables tend to be of the same order. The reliability of selection procedures such as stepwise regression is rather doubtful in that case. Another approach, introduced by Kienast and Schweingruber (1986), uses a dendroecological diagram to analyze tree growth on a year-to-year basis, thus allowing changes in tree response to weather. This method is, however, more descriptive than the time series approach described in the following sections.

5.9.2. The Kalman filter

To understand the time-dependent responses we introduce the Kalman filter technique. An application of this technique has been reported by Van Deusen (1987) and Visser (1986). The filter was developed by Kalman (1960) in the field of system and control theory. Since then it has been used in many other areas, but not yet in the present context. The idea of applying the filter to regression models with time-dependent parameters was introduced by Harrison and Stevens (1976) and perfected by Harvey (1984).

To get a time-dependent response, α must be made stochastic. The simplest model is the so-called *random walk*. Model 1 [equation (5.33)] changes in that case to:

$$\underline{\alpha}_t = \alpha_{t-1} + \underline{\eta}_t \tag{5.34a}$$

$$\underline{y}_t = \underline{\alpha}_t z_t + \underline{\xi}_t \quad . \tag{5.34b}$$

The noise vector $\underline{\eta}_t$ is assumed to be normally distributed with covariance matrix Q. The variance of $\underline{\xi}_t$ is denoted by R. It has been shown by Harrison and Stevens (1976) that model 2 [equations (5.34a, 5.34b)] can be estimated by the discrete version of the Kalman filter.

The mathematical formulation of the filter will not be given here, but are provided in Visser and Molenaar (1986). Some aspects of the filter, however, are important to mention here: the values of R and Q have to be known in advance. In most applications they are chosen by trial and error. In the present work these variances are estimated by maximization of the so-called *log-likelihood* function. This procedure yields an objective choice of noise variances and a different kind of changing behavior for every parameter.

A disadvantage of log-likelihood estimation, however, is the required amount of computer time (about one hour CPU time on a Univac 1100 to optimize a model with eight parameters). When Q is set to zero the estimates of $\underline{\alpha}_t$ are constant over time and equal the well-known multiple regression estimates of model 1. So model 1 is just a special case of model 2. The issue is, however, that one lets the data *choose* between constant or time-dependent parameters. In contrast to multiple regression analysis, no procedures are available to select a

small set of relevant explanatory variables among a large starting set. The selection procedure proposed by Visser and Molenaar (1986) yields a relatively simple scheme. Two kinds of selection criteria allow the selection of both variables with good prediction performance and variables that are significant only on a small part of the time axis. Minimization of the chance to select variables caused by fortuitous correlation is emphasized. Highly correlated explanatory variables give rise to problems such as inability to observe the parameters. This problem is analogous to the problem of multicollinearity in multiple regression models and can be solved by use of principal component analysis. The application of this technique is essentially no different from multiple regression.

5.9.3. Simulation

The use of simulation may not be underestimated in dendroclimatology. It is an important tool to verify the reliability and accuracy of mathematical modeling. Simulation can be used by generating simulated index chronologies, also called pseudo-chronologies. This idea has been proposed by Cropper (1982). A pseudo-chronology is obtained by multiplying *a priori* chosen meteorological time series by constant or time-dependent parameters. Artificially generated noise can be added to this series following model 2. The variance of ξ_t can be adjusted. In this way the reliability of selection procedures and the accuracy of parameter estimates can be determined. In general these two aspects highly depend on the length of the time series, the number of initial explanatory variables, and the amount of noise present in the data that cannot be attributed to the weather. When satisfactory simulation results are gained, this does not prove the correctness of the final growth model when estimated on real data. We used as a premise, the validity of model 1 or 2 to real data. Real relationships could be multiplicative instead of additive, for example. Correctness of response functions estimated on real data always has to be verified by biological interpretation of the model and by comparison of response functions of different ring-width series from the same stand.

We have tested the Kalman filter and the selection procedure extensively on pseudo-chronologies. An example is given in *Figure 5.16*. The underlying model was composed of eight time-dependent parameters multiplied by *a priori* chosen meteorological time series.

The initial set of explanatory variables consisted of 16 temperature series, 16 precipitation series, and two lagged indices. The *index series* run over the period 1897–1973. Four parameters had a step-form, and four parameters had a Z-form or a reversed Z-form as shown in *Figure 5.16* by thick lines. By varying the maximum parameter values a detection level could be determined: parameters with maximum absolute value smaller than this level were never detected.

Figure 5.16 shows that six variables are selected correctly, two parameters are missing, and one variable is selected due to fortuitous correlation. Moreover, sudden shocks are not followed directly but with a kind of delay. In few cases the real parameter values fall outside the 95% confidence limits for a short time.

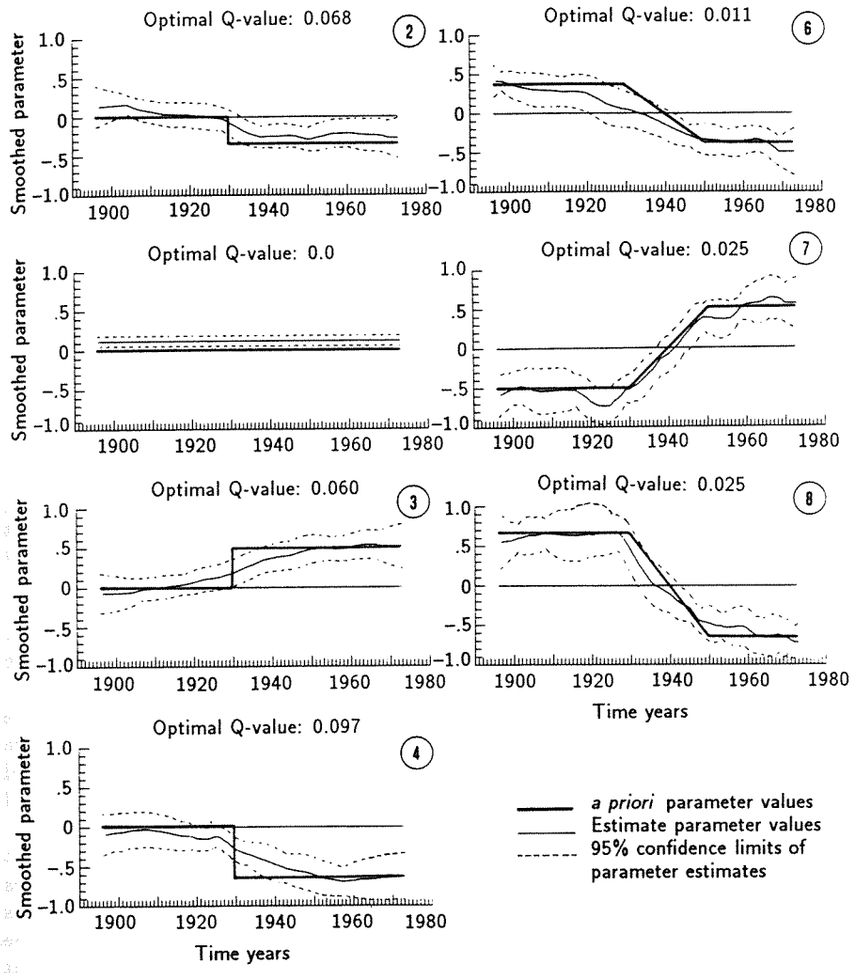

Figure 5.16. Response function of a pseudo-chronology composed of eight changing parameters (no additional noise). Six variables are selected correctly, one variable is selected incorrectly, and two variables are missing.

5.9.4. Two examples

As an illustration of the possibilities of the Kalman filter two examples will be discussed. *Figure 5.17* shows two ring-width series of European silver fir (*Abies alba*), grown in the Black Forest, Federal Republic of Germany. Publications based on these data are Brill *et al.* (1981) and Eckstein *et al.* (1983).

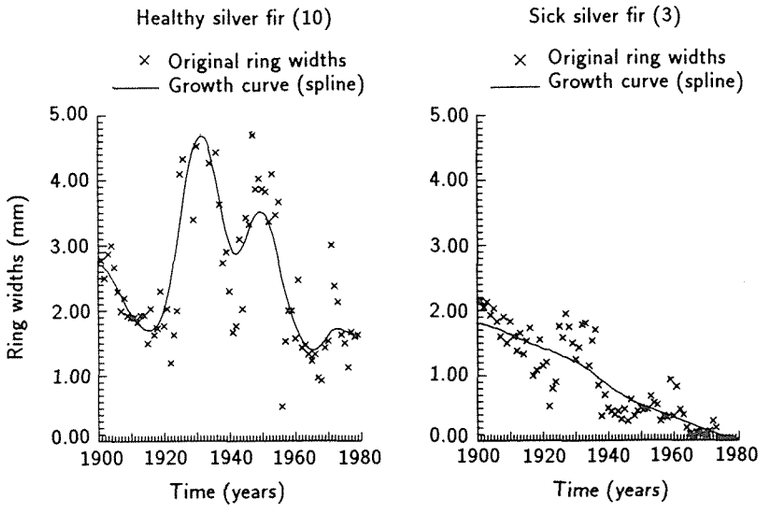

Figure 5.17. Ring-width series of European silver fir (*Abies alba*) from Bad Herrenalb. The numbers of the firs correspond to those of Eckstein *et al.* (1983). Both firs were cut in 1979. Fir 3 and 10 were 112 and 100 years old, respectively. Growth curves (solid lines) have been fitted by spline interpolation. (From Aniol, 1985.)

Fir 3 was classified as sick at cutting date, fir 10 as almost healthy. Growth of fir 10 has been heavily influenced by competition. Growth curves are determined by spline interpolation. Standardized index series are shown in *Figure 5.18* along with the corresponding residual series, i.e., the series where the influence of the weather and persistence has been filtered out. The response function of fir 3 and 10 are shown in *Figure 5.19*. The variables are selected from a starting set of 16 temperature series, 16 precipitation series, and 2 lagged index series.

The response function of fir 10 (the healthy fir) only shows time-dependent behavior for February temperatures (*Figure 5.19*, top left). This parameter has no statistically significant influence on growth apart from 1956. This coincides with a large negative index in 1956 (*Figure 5.18*(*a*), top). Inspection of the February time series shows that the average temperature was 10.6° C in that year, the highest February temperature of this century. Furthermore, temperature in March and April were low: 2.9° C and 4.4° C. Probably the extreme February temperatures falsely initiated the growing season. *Figure 5.18* bottom left shows that the index of 1956 has reduced to a small negative peak.

The response function of fir 3 is more complicated. All parameters seem to start changing after 1950, probably as a prelude to dying (*Figure 5.19*, right). April temperatures are influencing growth only in the years 1959, 1960, and 1961 (lower confidence limits above zero). This coincides with large positive indices in 1959 and 1961 and a zero index in 1960 [*Figure 5.18*(*b*), top]. Inspection of the April temperature time series shows high temperatures in 1959, very high

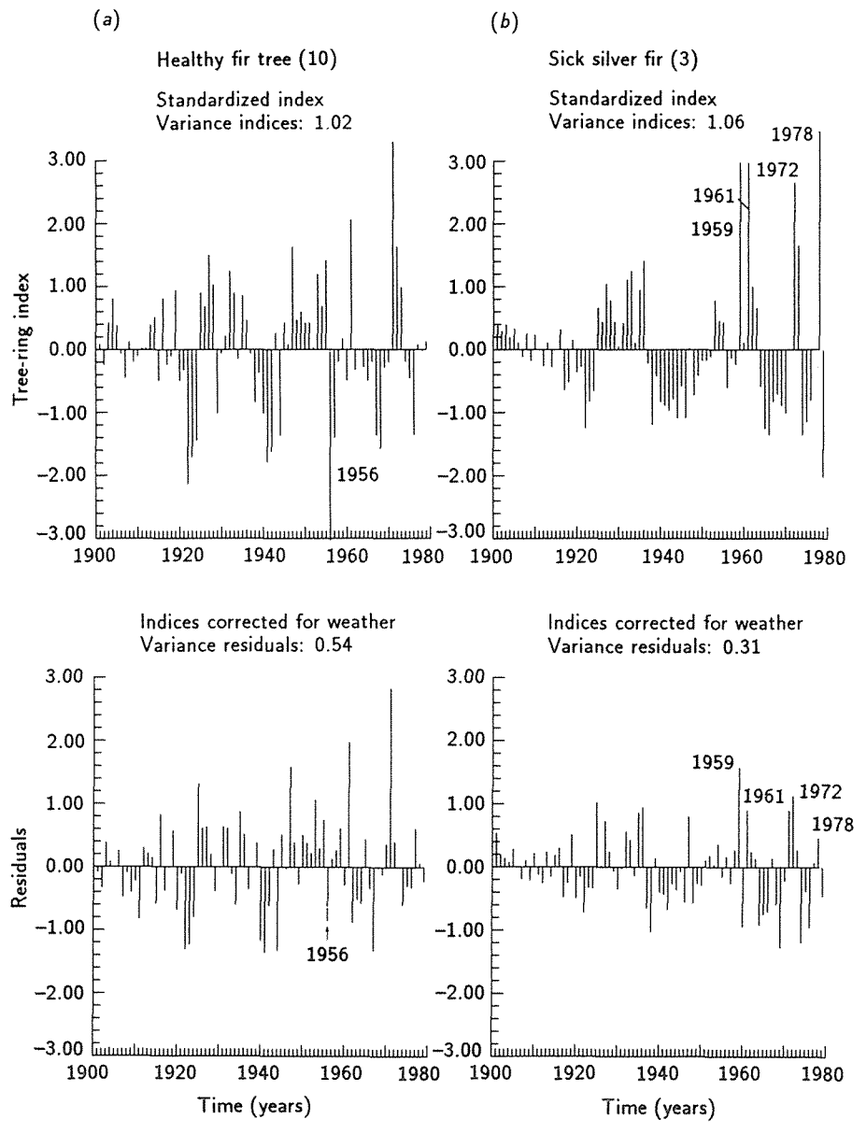

Figure 5.18. Index series of fir 3 (right) and fir 10 (left), along with the residual series after removing influence of weather and persistence. For fir 3, 61% of its variance has been explained. For fir 10, 47% of its variance has been explained.

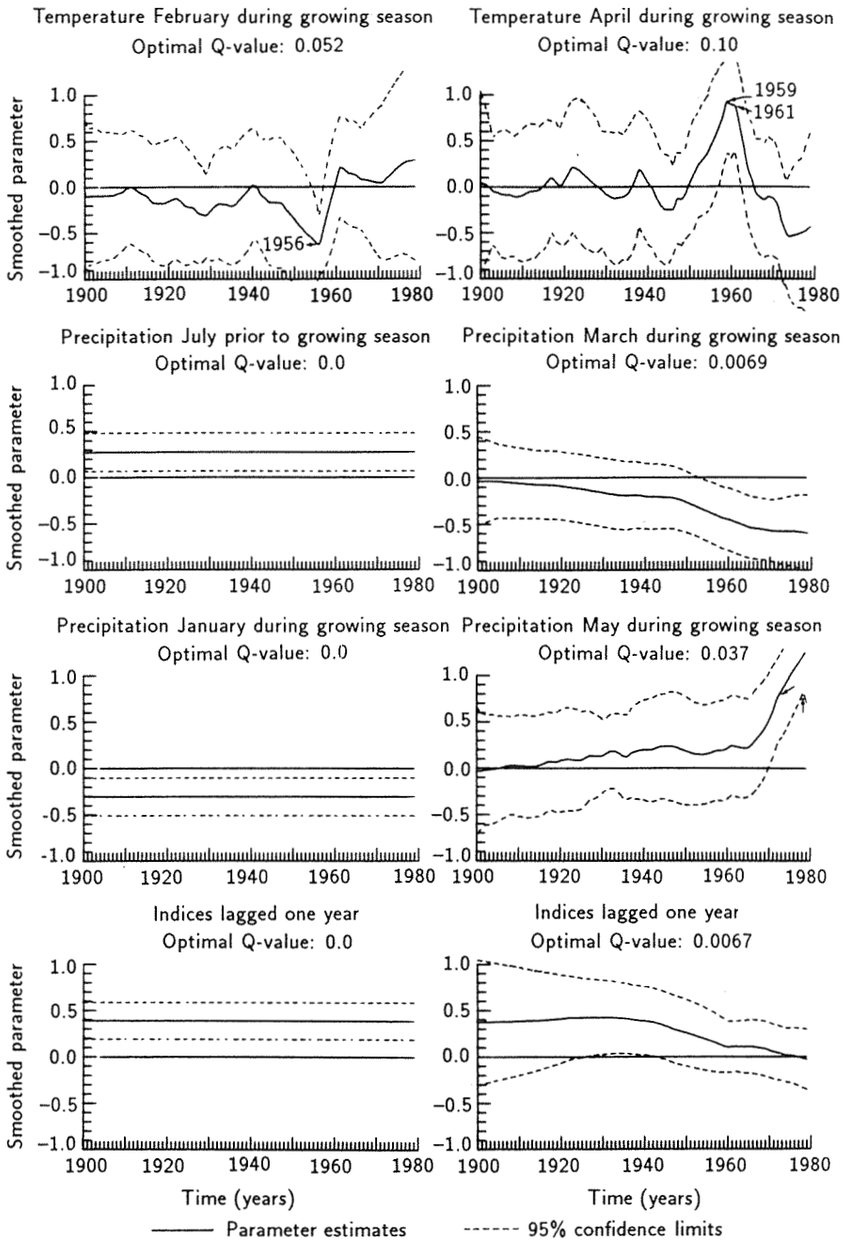

Figure 5.19. Time-dependent response functions of fir 10 (left) and fir 3 (right).

temperatures in 1961, and average temperatures in 1960. Probably the warm April months initiated the growing season earlier, thus lengthening the growing season. March precipitation is becoming significant from 1954 (upper confidence limits lower than zero). The reason is unclear. May precipitation is becoming significant from 1971, mainly caused by exceptional rainfall in 1978, coinciding with a large positive index in 1978 [*Figure 5.18*(*b*), top]. The influence of persistence, modeled by indices lagged one year, is damping out after 1945 (lower confidence limits become negative). This means that after 1945 the influence of the weather prior to the growing season has vanished completely.

Both firs show completely different responses to weather variations (*Figure 5.19*). One should interpret these results, however, carefully:

- The growth patterns of both trees are rather extreme and completely different (*Figure 5.17*).
- The construction of growth curves is far from being unique (*Figure 5.17*).
- It is dangerous to draw conclusions from an analysis of ring-width series of individual trees without knowing their history in detail. Information should be available about competition, thinnings, pathogens, etc.

5.10. Dendroecological Information in Pointer Years and Abrupt Growth Changes

F.H. Schweingruber

5.10.1. Pointer years

Pointer years are annual rings that differ visibly and markedly from the preceding and subsequent rings in some way. Some ring properties that can be used for identifying pointer years are larger or smaller total width, larger or smaller proportion of latewood, intraannual density fluctuations, tangential rows of resin ducts, traumatic tissue, or – in hardwoods – greater or lesser proportion of pores or pore size. *Figure 5.20* illustrates some examples of pointer years largely in agreement between two trees. Such rings, which are ecological indicators of local or regional factors and events that influence tree growth, form the basis for cross-dating and the skeleton-plot method of dating (see Chapter 2). As reflections of strong ecological influences, it is sensible to analyze these strong morphological signals for temporal and spatial patterns.

Pointer years have been analyzed in spruce (*Picea abies*), fir (*Abies alba*), and beech (*Fagus sylvatica*) from a climatically uniform area with moderately divided topography in northern Switzerland. The results, shown in *Figure 5.21*, indicated that the different species reflect climatic influences in different ways. Of the 14 pointer years between 1920 and 1985, only two (1959 and 1976) occurred in all three species. Winters with little precipitation (e.g., 1929), winters and springs with little precipitation (e.g., 1934), warm dry summers (e.g., 1945, 1979), extremely low winter temperatures following a few warm days (e.g., 1956), and reactions to unfavorable conditions from the previous year (e.g.,

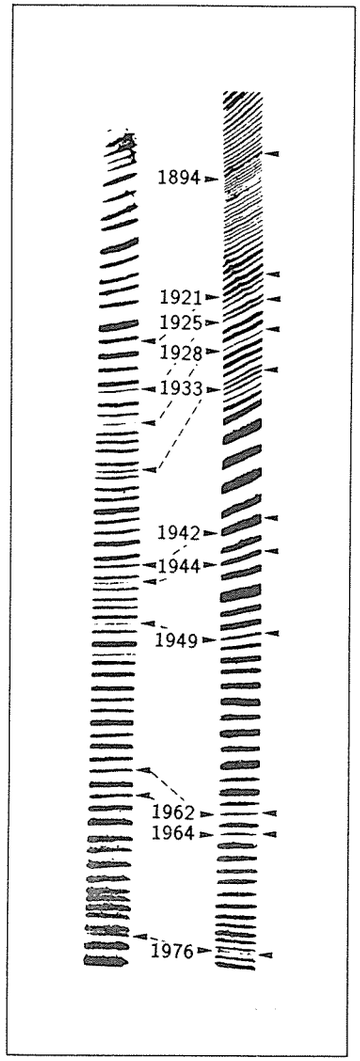

Figure 5.20. Visual synchronization of two ring sequences by means of pointer years. The ring for 1976 is narrow and has little latewood. The rings for 1962 and 1964 are of normal width, but have conspicuously narrow latewood. These samples are from the dry Rhone Valley in Valais, Switzerland. (From Kienast *et al.*, 1981.)

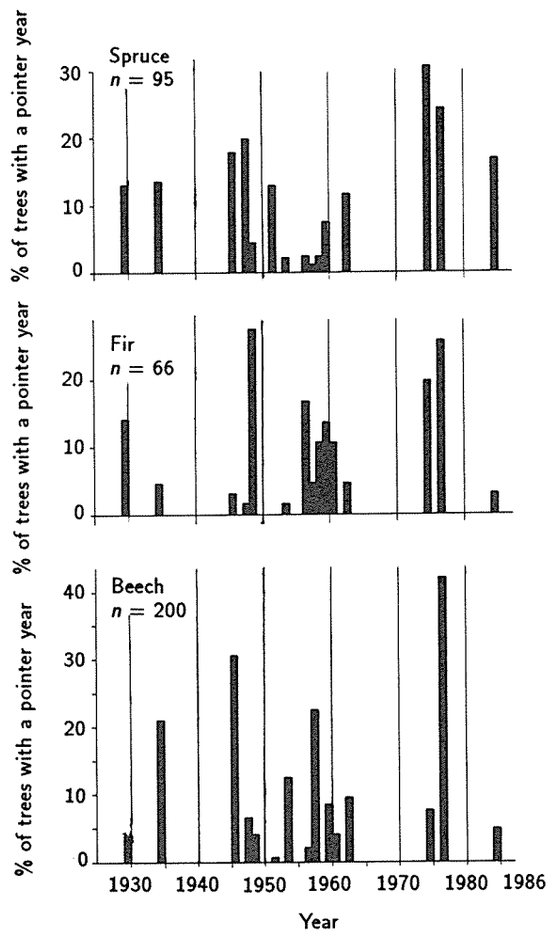

Figure 5.21. Percentage of trees with visible, marked pointer years in spruce, fir, and beech from the area of Liestal, canton of Basel Country, Switzerland. Under uniform climatic conditions, different species react differently to ecological influences. (From Spang, unpublished.)

1948) all produced pointer years in some trees. However, it was seldom possible to attribute all clear pointer years to climatic events.

Before time-consuming measurements and statistical analyses are begun, the information contained in the pointer years of tree rings should be investigated as an inexpensive means of preliminary analysis. This simple step may help prevent the failure of large-scale studies.

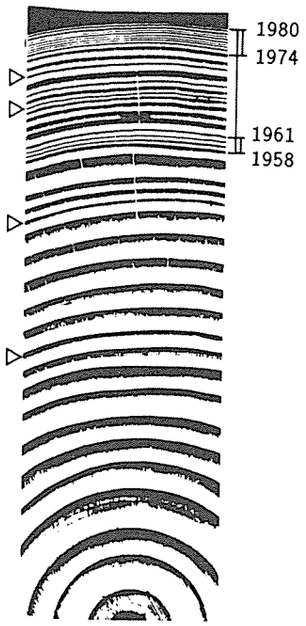

Figure 5.22. Ring sequences with two reduction phases beginning abruptly.

5.10.2. Abrupt growth changes

A further conspicuous feature of ring series is formed by abrupt growth changes (*Figure 5.22*). These, by definition, are sequences of more than three pointer years. In dendroclimatological research, they may be eliminated by means of special statistical filters on the assumption that they are not due to climate. In dendroecological research, geomorphology, pollution research, and forestry they should be maximized, i.e., they are given particular attention as indicators of local events such as soil movement and thinning. Like pointer years, abrupt growth changes persisting for some time reflect strong ecological influences. For each tree, the onset and duration of the growth reduction are determined. Where many stands are investigated in one area, the proportion of trees displaying a growth change at a given time is a measure of the intensity of the ecological event. To facilitate the analysis, the onset, duration, and frequency of the abrupt growth changes can be compiled in diagram form as shown in *Figure 5.23*.

Studies relating to suspected pollution injury have shown that abrupt growth changes occur much more frequently than was previously thought. The geographical and temporal distribution of growth changes, especially reductions, is affected by the characteristics of the species and the individual as well as local

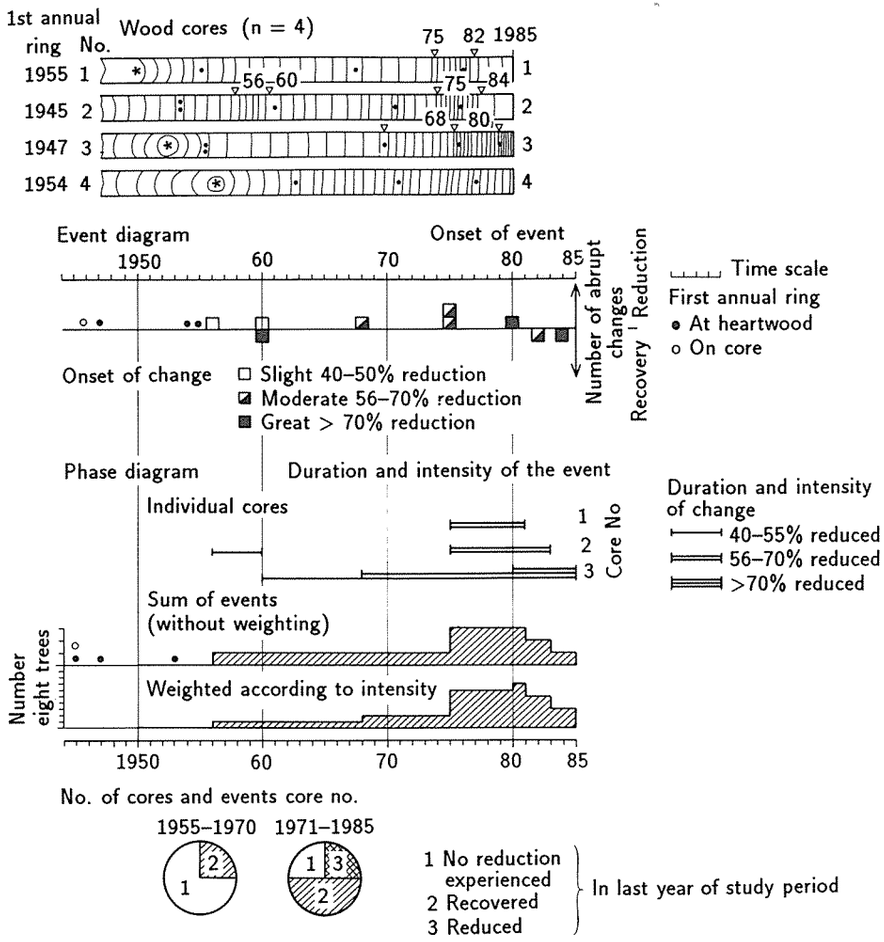

Figure 5.23. Schematic presentation of events and their duration in summation diagrams. The onset of the abrupt growth reduction or recovery is shown in event diagrams, the duration of the reduction in phase diagrams, and the proportion of trees with reduction per site in pie charts. (From Schweingruber *et al.*, 1986.)

and regional natural and anthropogenic factors. To identify the distribution patterns, a large number of trees must be investigated. As the technique is simple and quick, however, 500 trees or more can easily be analyzed, even in simple studies.

A study of 480 spruces and 464 firs from the Swiss Jura illustrates the value of abrupt growth change analysis. The firs display far more growth reductions in past years than spruces (*Figure 5.24*). Within the 27 fir sites

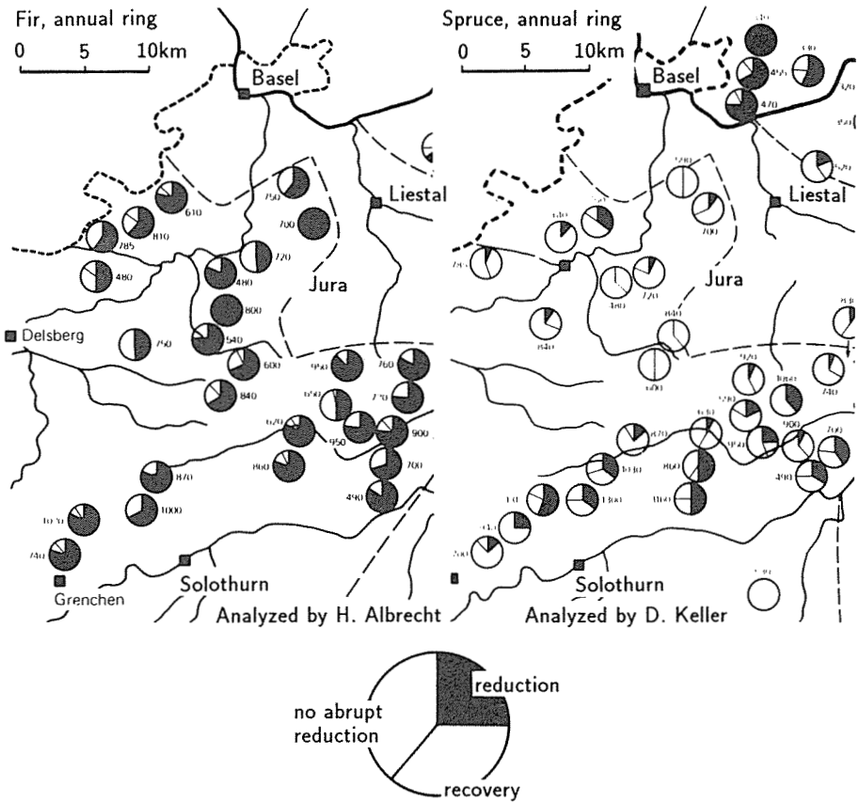

Figure 5.24. The geographical distribution of growth reduction in fir and spruce in the central Jura of Switzerland.

investigated, there is no pattern of geographical distribution. Spruce, in contrast, exhibits many growth reductions in the stands around Basel, a fair number in the densely settled southern part of the Jura, and a few in central Jura. The two species also behave differently in terms of time (*Figure 5.25*). In spruce, *Figure 5.25*(*a*), the percentage of trees with growth reductions varies periodically. This may be related to phases with little summer rain. However, in fir, *Figure 5.25*(*b*), the percentage leaps up in 1944, remains almost constant until 1972, and peaks in 1976. The sudden increase was presumably due to the fir dieback known to have occurred. The effects of precipitation are reflected in waves superimposed on the general trends, e.g., 1944–1953 and 1973–1982.

The simple techniques of analysis using pointer years and identifying abrupt growth changes, both based on observation, should be accorded a permanent, basic role in dendrochronological research.

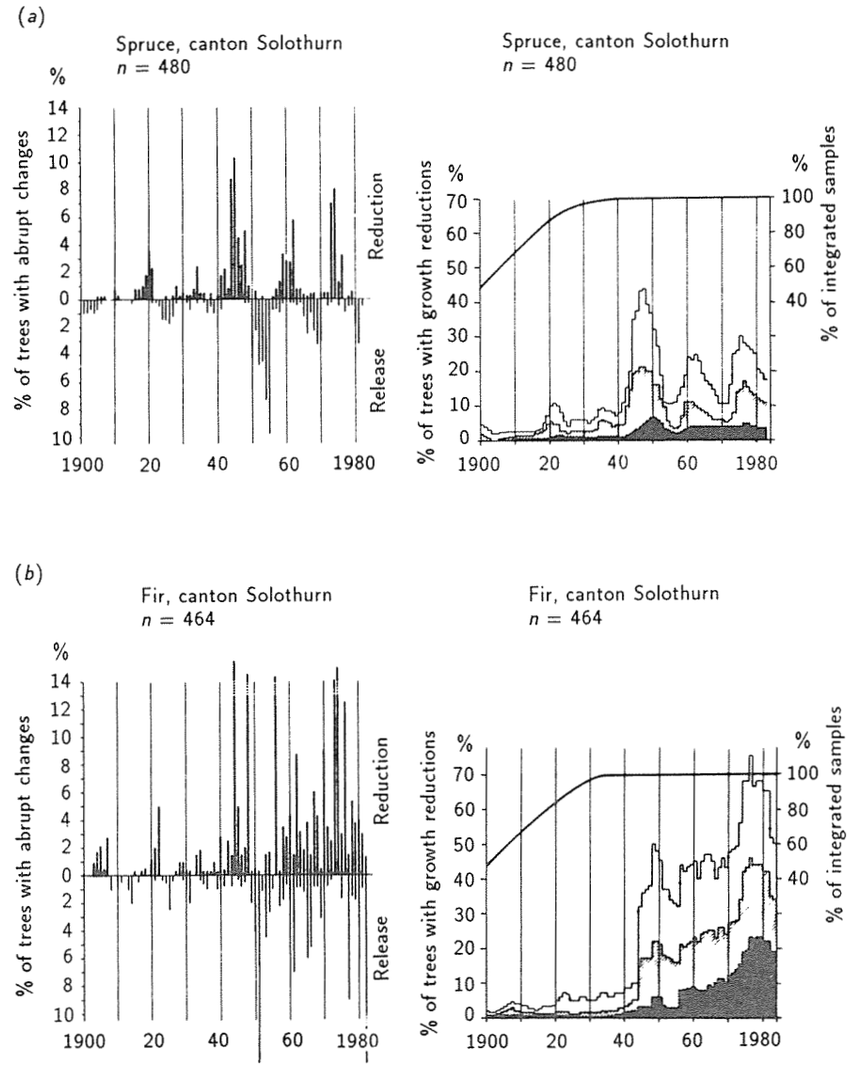

Figure 5.25. Event and phase diagrams for spruce (*a*) and fir (*b*) from northern Switzerland. In spruce, the variations in frequency reflect climatic conditions; in fir, in constrast, the abrupt increase is due to disease. (From Schweingruber *et al.*, 1986.)

5.11. Problems with the Use of Tree Rings in the Study of Forest Population Dynamics

D.A. Norton and J. Ogden

5.11.1. Introduction

Experience gained in dendrochronological studies can be of considerable benefit for investigating the dynamics of forest tree populations (cf., Lorimer, 1985). Too often, studies of forest population dynamics are characterized by simplistic assumptions about tree-growth rates and relationships between tree ages and diameters. We see difficulties occurring at two levels: first, in aging individual trees and, second, in predicting the age structure of tree populations using size-class data. This section illustrates the extent of these problems.

5.11.2. Problems in aging a single tree

Three main sources of error occur in estimating the age of an individual tree: anomalous growth rings, extrapolation of tree ages from partial cores, and estimation of the time it takes a tree to grow to sampling height.

Anomalous Growth Rings

Tree ages are usually determined from ring counts on cores or cross sections from trunks, although occasionally bud scars may be used to age young trees (e.g., Herbert, 1977). However, before a tree can be accurately aged it has to be assumed that growth-ring formation is annual. Annual formation of growth rings has been demonstrated for many temperate zone trees (e.g., Palmer and Ogden, 1983; Norton, 1984a, 1984b); whereas in the Tropics, trees with annual growth rings are less common (Ogden, 1981). Even in some temperate zone areas, the annual nature of growth-ring formation has been questioned and examples of continuation of growth through the winter has been shown (e.g., Haase, 1986).

Anomalous growth rings (false and locally absent annual rings) can complicate ring counts even in species with annual growth. False rings usually result from the occurrence of extreme environmental conditions such as drought (Fritts, 1976) or cold temperatures (Schweingruber, 1980) during the growing season and cause the formation of diffuse bands of smaller thick-walled cells (resembling latewood) in the middle of the growth ring. These can be distinguished from true annual growth rings; for example, an abrupt change from small thick-walled latewood cells to large thin-walled earlywood cells occurs at the growth-ring boundary. It has been suggested that some species are more predisposed toward forming false rings than others (LaMarche, 1982). The New Zealand species *Agathis australis* and *Phyllocladus glaucus* are commonly characterized by sequences of alternating narrow and wide growth rings. These may represent two growth flushes during one season or relate to a biennial flowering cycle. Failure to recognize false rings can lead to substantial overestimations of tree age.

Locally absent rings are a common feature of many tree-ring sequences and appear to occur for two reasons (Norton *et al.*, 1987). In trees growing near the environmental limits of their range, growth rings are often incompletely formed during environmentally limiting years. For example, Norton (1985) found that the percentage of locally absent rings in *Nothofagus solandri* increased from nearly zero at low altitudes to 2.3% at 1,300 m, near the alpine timberline. Often the growth ring is present in the upper bole near the photosynthetic tissue but is absent from the lower bole (Fritts *et al.*, 1965; Norton, 1986). These locally absent rings can, however, be detected by cross-dating ring-width series between trees.

The second type of locally absent rings occurs because of *ring wedging* (Norton *et al.*, 1987). Ring wedging occurs when rapid radial growth occurs over several years in certain segments of the tree's circumference, while being extremely slow or absent in others. Ring wedging may be caused by the development and death of major branches and by consequential variations in food and growth regulator supplies (Fritts *et al.*, 1965). Ring wedging appears to be particularly pronounced in gymnosperms (e.g., in the New Zealand Podocarpaceae species *Dacrydium cupressinum*, *Podocarpus totara*, and *Prumnopitys taxifolia*, Norton *et al.*, 1987). Examination of complete cross sections can help overcome this problem, and for some species accurate age counts must be based on cross sections rather than increment cores.

The problems associated with anomalous growth rings often make it difficult to obtain reliable age estimates unless cores or cross sections are carefully examined. The problems are compounded by the narrow growth rings typical of many mature trees. In New Zealand, ring widths are frequently less than 1 mm (Norton *et al.*, 1987), and it is common in some trees to find bands of very narrow growth rings separated by wider growth rings. With a cursory inspection, many of these narrow growth rings are easily missed and can lead to substantial underestimates of tree age.

Even with careful preparation of a core, it is not always possible to recognize some of these anomalies. Accurate ages in many cases can be obtained only from complete cross sections, and even then only through cross-dating ring-width sequences between trees. Annual ring counts made from cut stumps in the field, or from improperly prepared cross sections and cores are likely to be inaccurate. Without the use of cross-dating techniques, it is probable that for many species, age estimates will differ from true ages – in some cases substantially so.

Partial Cores

It is usually difficult and often impossible to obtain sections from trees, and consequently most tree-age estimates are based on increment cores. However, cores can fail to reach the center of the tree. This occurs because of incorrect borer alignment, because the borer is too short, or because the tree center is rotten. In such situations it is usual to estimate the number of missing growth rings and thus obtain an estimate of tree age. Although methods have been proposed to make this estimation more objective (Applequist, 1958; Liu, 1986), it would appear that these techniques are only appropriate for fast-growing trees with

concentric growth rings (e.g., some Northern Hemisphere conifer species). In many temperate forest trees, especially in the Southern Hemisphere, growth rings are very irregular (because of ring wedging, eccentric growth, etc.), and it would seem that these techniques are of limited value.

In a study of the errors associated with estimating tree ages from partial cores in four New Zealand tree species, Norton *et al.* (1987) obtained mean errors in age estimates for cross sections of known age ranging from 3.7% to 63.9% (based on samples of 5 to 15 trees per species). Errors for individual trees were considerably larger; in one case the estimated age was 78% greater than the true age. It was found that the error decreased as the length of the partial core increased, but only when the partial core was 90% of the radius of the tree did the mean error consistently drop below 10%. Of greater concern was the observation that the direction of the error (above or below the true value) is unpredictable, being largely dependent on growth rates while the tree was young thus making it difficult to adjust systematically for the error. These errors in age estimates appear to occur for three reasons: eccentric growth (i.e., the chronological and geometric centers of trees are not the same), age-dependent-growth variations, and other growth variations (e.g., due to competition).

Partial cores ending during periods of slow growth tend to overestimate tree age, while those ending in periods of rapid growth underestimated age. Unfortunately no magic formula can correct these errors, but their existence shall be acknowledged in any study using partial cores to estimate age.

Estimation of Time Taken to Grow Sampling Height

Sampling is rarely at ground level, so any estimate of tree age needs to include an allowance for the time taken for the tree to grow to sampling height (between 1.3 and 1.4 m). Such estimates are usually made from a sample of seedlings and saplings taken from the study area. Seedling growth rates are affected by a number of environmental variables (light, moisture, etc.), while competition between seedlings can be intense. It is therefore not surprising that seedlings show a great variability in age at the same height. For example, age ranges of 35–103 years for subalpine *Libocedrus bidwillii* seedlings and 8–29 years for *Agathis australis* seedlings have been measured for growth to 1 m (Norton, 1983d; Ogden, 1983).

A further difficulty in estimating the time taken to grow to sampling height relates to whether or not the seedlings measured are representative of those that grew to become mature trees. Many more seedlings are produced than ever grow to maturity, and it can be argued that seedlings that become trees are a select group of *winners*, either of superior genetic composition, or those that have some local advantage over their neighbors early in life. It is therefore unlikely that a random selection of current *ordinary* seedlings will accurately reflect the growth rate of those seedlings in the past that grew to become mature trees. More significant than this, however, is the likelihood that the present trees may have established themselves under very different conditions from those under which the present seedlings are growing. It is now widely recognized that many temperate forest trees establish after some form of disturbance (Ogden, 1985a, 1985b; Runkle, 1985; Veblen, 1985), with seedling recruitment and early growth often occurring under very different environmental conditions from those existing under a mature canopy. In *Arthrotaxis selaginoides* (Ogden, 1985a) the present mature trees in the sampled stand reached a diameter of 5 cm in 15–30 years, while current seedlings in the stand take 60–110 years to reach the same diameter. The growth rates of the present mature trees during the first few years of their lives are similar to those of seedlings presently growing in post-fire regenerating vegetation. Similar examples can be found for other species.

5.11.3. Problems associated with the use of diameter to predict age

In most studies of forest tree dynamics it is common practice to age a sample of the trees studied. Using the resultant age-diameter relationship, the ages of the remaining trees are then estimated based on their diameters. There are, however, some serious limitations associated with this approach (Ogden, 1985b). Because of the considerable uncertainties involved in determining the age of individual trees, an unavoidable error is built into the age-diameter model. The magnitude of this error is usually unknown.

In many cases age and diameter are not closely related (e.g., Clayton-Greene, 1977; Herbert, 1980; Norton, 1983d; Ogden, 1983). This arises largely because competition among trees causes marked differences in growth rates and is often best seen in even-aged stands where a wide variation in diameters can be found (e.g., Hough, 1932). Clearly there are very real limitations in the use of size class data to determine age structures. Even if the relationship between age and diameter is statistically significant, as it often is (e.g., Ogden, 1978b; Norton, 1983d), it may still be misleading to predict diameter from age because of the large variance in age for any diameter class. For example, Norton (1983d) measured age ranges of over 200 years for 10 cm diameter size classes in *Libocedrus bidwillii*, despite the existence of statistically significant age-diameter relationships. The problems associated with using diameter to predict tree age have been elegantly summarized by Harper (1977, page 634):

> It is wholly unrealistic and very dangerous to assume any relationship between the size of trees and their age, other than the vague principle that the largest trees in a canopy are likely to be old. However, it cannot be argued conversely that small trees are likely to be young: they may be as old as the main occupants of the canopy. If a tree is very young it is likely to be small, but if it is small it may be of any age.

5.11.4. Discussion

In this section we have outlined a number of sources of error that can occur in aging a single tree and in estimating the ages for a population of trees. Although some of these errors may cancel themselves out, it would seem more likely to us that in most instances the errors will compound although their final magnitudes are difficult to assess. Furthermore, it appears that it is often difficult to predict

the sign of the error (either overestimate or underestimate of true age). These difficulties clearly highlight the need for careful sampling and sample analysis in age determinations. Where possible, the utilization of cross-dating techniques will greatly increase the accuracy of the age estimates. A minimum requirement of any study presenting tree-age estimates is to acknowledge the possibility of errors in the estimates.

The errors can present serious limitations in studies of the dynamics of tree populations. As has been suggested by Ogden (1985b) it is quite conceivable that a small sample of inaccurately aged trees from widely separated size classes may provide a highly significant age-diameter relationship but obscure a multiple cohort age structure derived from several episodes of regeneration. However, the recognition of these potential errors and the use of dendrochronological techniques such as cross-dating will assist in obtaining more accurate information on the ecology and dynamics of forest trees.

CHAPTER 6

Tree Rings in the Study of Future Change

Chapter Leaders: L. Kairiukstis and S.G. Shiyatov
Chapter Contributors: G.E. Kocharov, V. Mazepa, J. Dubinskaite, E. Vaganov, T. Bitvinskas, and P.D. Jones

6.1. Tree Rings: A Unique Source of Information on Processes on the Earth and in Space

G.E. Kocharov

6.1.1. Introduction

The various ground-based and space-borne sensors in use today offer the possibility of detecting practically all the major kinds of corpuscular and electromagnetic radiation emanating from processes occurring on the Sun and in interplanetary and interstellar space, in real time. It would be difficult to overemphasize the importance of such studies. At the same time direct methods do not permit one to establish the characteristics of the astrophysical and geophysical processes over a large time scale. To solve these problems, which are essential for both theory and practice, one has to have eyewitnesses of the past who would be capable, as it were, not only of recording a phenomenon but of retaining the relevant information in their memory in its original form as well. Such outstanding eyewitnesses of the past are trees, which contain in their annual rings information both on the local conditions of growth and on the global properties of the Earth's atmosphere as a whole and of interplanetary space and solar activity.

Photosynthesis makes each annual ring a documentary indicator of atmospheric carbon dioxide and available soil water. The isotopic composition of wood-bound carbon depends on the dynamic characteristics of the carbon exchange reservoir and temporal variations of the cosmic ray flux incident in the Earth's atmosphere. By measuring the ^{13}C:^{12}C and ^{14}C:^{12}C ratios in tree rings, it is possible to reconstruct the variation of cosmogenic radiocarbon content in the Earth's atmosphere over a large time scale in the past. This, in turn,

E. R. Cook and L. A. Kairiukstis (eds.), Methods of Dendrochronology, 289–340.

provides data on solar activity, the geomagnetic field and galactic cosmic ray flux in interstellar space. Variations in the soil chemical composition manifest themselves directly in the tree-ring composition. Therefore, the tree represents a unique detector of variations in the chemical composition of the environment both in time and in space. The information on paleotemperature becomes recorded in tree rings via the concentration ratios of the stable isotopes of hydrogen, carbon, and oxygen.

This section touches on some results obtained by *interrogating* the trees, these truly unique eyewitnesses of the past, with the aim of using the past to provide a glimpse of the future.

6.1.2. Tree rings and the deep minima of solar activity

The coordinated approach to studying tree rings (Kocharov *et al.*, 1985, and references therein) involving the radiocarbon and dendrochronological methods provides an insight into the spatial and temporal variations of the pattern of solar-terrestrial relationships. Note that while the ^{14}C content in tree rings reflects global astrophysical and geophysical phenomena (solar activity, geomagnetic fields, and climatic variations), the tree-ring width is sensitive not only to global but also to regional and local components of the environment.

The influence of the Sun on the tree-ring width can manifest itself clearly in some regions of the globe while remaining practically undetectable in other areas. This can be accounted for, on the one hand, by spatial features in the manifestation of the solar–climatic relationships. On the other hand, there are intrinsic biological reasons for the selective response of trees to qualitatively identical changes defined by the Law of Limiting Factors (Odum, 1975; Fritts, 1976); namely, if an external factor (e.g., climatic) is close to the tolerance range for a given species, it is this factor that determines the activity of the species by narrowing the tolerance range to another ecological (e.g., solar) factor. This means that under climatically extreme conditions (e.g., in temperature or precipitation), typical of the northern boundary of forests in subpolar latitudes and the upper elevation boundary of forests in mountainous areas, the sensitivity of trees to solar variations should, in principle, be higher. Therefore, we have studied (Kocharov *et al.*, 1985; Kocharov, 1986) tree-ring width variations in time from the trees that grew under extreme conditions (northern latitudes and mountainous regions). The time range studied spanned three deep minima of the solar activity, namely, the Maunder (1645–1715), Spörer (1390–1550), and Wolf (1280–1350) minima.

The data obtained are presented in *Figure 6.1.* One immediately notices deep minima in ring width that appear synchronously in all the series and coincide in time with the solar activity minima. It should be pointed out that radiocarbon content in tree rings reveals clearly pronounced maxima during deep minima in the solar activity, which can be accounted for by reduced modulation of the cosmic ray flux by the Sun. The fact that the dramatic decrease in the sunspot number, the increase of radiocarbon content, and the depression of ring width of the trees, which grew in different regions, occurred simultaneously gives

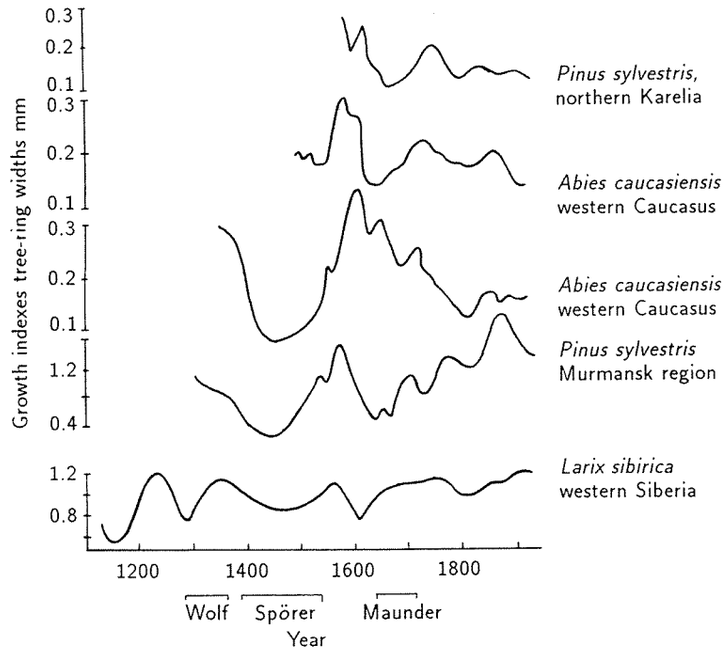

Figure 6.1. Secular variations of tree-ring width.

grounds to conclude that the observed variations originated from the physical processes occurring in the solar system. The problem of the nature of the global minima is very complex and still far from being understood. We are only in the initial stage of finding an approach to its solution. The development of a coordinated method based on reconstructing the characteristics of tree rings and of the cosmogenic isotope content in the Earth's atmosphere over a large time scale is a promising step. This method offers a possibility of establishing the characteristics of many solar activity minima and the corresponding features of the underlying natural process in question that may eventually form a basis for a concrete theoretical model.

6.1.3. Solar rhythms and trees

We have studied tree-ring growth of pine (*Pinus*) in 38 sites distributed along the Murmansk–Carpathian profile (49°–69°N), corresponding to dry valleys. For each point along the profile, a yearly series of ring widths was obtained by averaging data from 20 to 600 trees that grew in identical local environmental conditions and were about the same age.

The major rhythm in each series has been found to decrease from ~20 years in the north down to ~10 years in the south (*Figure 6.2*). A study of the

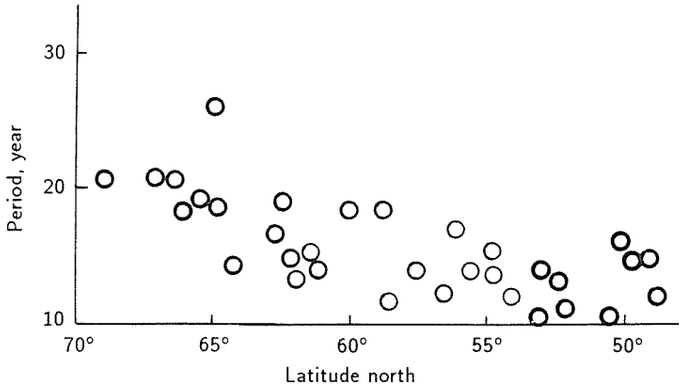

Figure 6.2. Change of period with latitude along the Murmansk–Carpathian profile.

dynamics of rhythm formation for the recent 200 years has permitted us to separate the northern latitudes as areas having synchronous rhythms of ~10–20 years in length, which apparently implies that these rhythms are generated by a common mechanism.

The isolation of large-scale tree-ring trends along the Murmansk–Carpathian profile and a study of their dynamics during the period 1910–1959 has revealed a remarkable change; namely, the pine ring-growth records before 1930 exhibit a significant internal consistency, whereas in the subsequent period the profiles can be divided into northern and southern regions with the boundary crossing southern Karelia. These features can be attributed to the effects of atmospheric circulation in the Atlantic–European sector. That is, the zonal (westerly) circulation prevalent in the beginning of the 20th century reduced the differences between the northern and southern regions resulting in a substantially similar tree-ring growth pattern along the profile. However, in the second period, blocking and meridional circulation in the troposphere becomes more pronounced; as a consequence, the differences between the climatic conditions in the north and south become enhanced, dividing the dendroprofile into two regions.

The 250-year tree-ring growth record obtained by us from northern Karelia has been studied using various techniques. A spectral analysis has been carried out with the results presented in *Figure 6.3*. Shown for comparison in the same figure are the results of a spectral analysis made on Wolf sunspot number series. One clearly sees that three spectral features manifest themselves in different degrees in both series. First, there is a secular cycle that dominates the power in the series. A 22-year cycle stands out reliably in the tree-ring growth series while being hardly distinguishable in Wolf sunspot numbers. An 11-year cycle is seen to exist in both the series. Its amplitude for the tree-ring growth record is a tenth of that for the 22-year cycle. It should be noted that all three spectral features are manifested in tree-ring radiocarbon content series too.

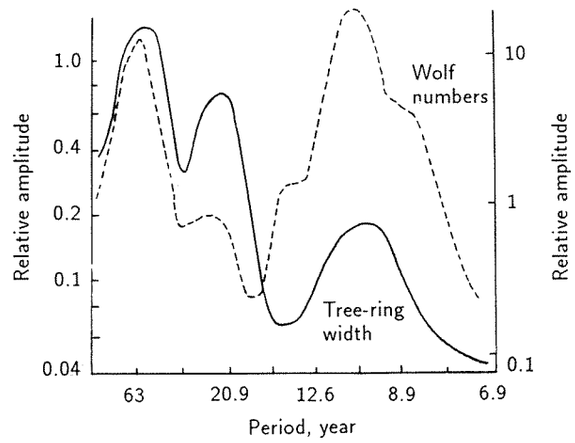

Figure 6.3. Spectra of the Wolf sunspot numbers and tree-ring width.

We have studied the trend in the amplitude of the 22-year pine ring growth rhythm obtained from northern Karelia for the past 250 years. The corresponding data are presented in *Figure 6.4* together with the envelope of the Hale sunspot cycle. Also shown are the 22-year drought rhythm amplitude variations from the data of Mitchell *et al.* (1979), who carried out extensive reconstructions of drought records from tree rings. Regional drought area indices (DAI) were compiled on an annual basis, each reconstructed from a 40 to 65 site tree-ring grid covering an area from Canada to Mexico and from the West coast to the Plains states. Each DAI is expressed in terms of the relative area hit by droughts of a specified intensity. Variance spectrum analysis of the DAI series provided reliable evidence for a close-to-22-year drought rhythm starting from 1700. A study of the DAI series revealed phase locking between the 22-year drought rhythm and the Hale sunspot cycle. Indeed, the drought maxima were found to occur predominantly in the first 2–3 years following the Hale sunspot minima.

An analysis of the dependences presented in *Figure 6.4* leads to the following conclusions:

- All three records reveal clearly pronounced deep minima around A.D. 1700 and 1900, as well as ~A.D. 1800.
- In each record, there are two close maxima between deep minima.
- There is a tendency for the epochs of large-amplitude drought cycles in the western USA to lead those of large-amplitude sunspot cycles by 10 or 20 years. At the same time, the maximum amplitudes of the 22-year northern Karelian tree-ring growth rhythms and of the 22-year sunspot cycles practically coincide in time.
- The amplitude of both the 22-year drought rhythm and the tree-ring cycle was quite large going into the Maunder minimum while decreasing toward

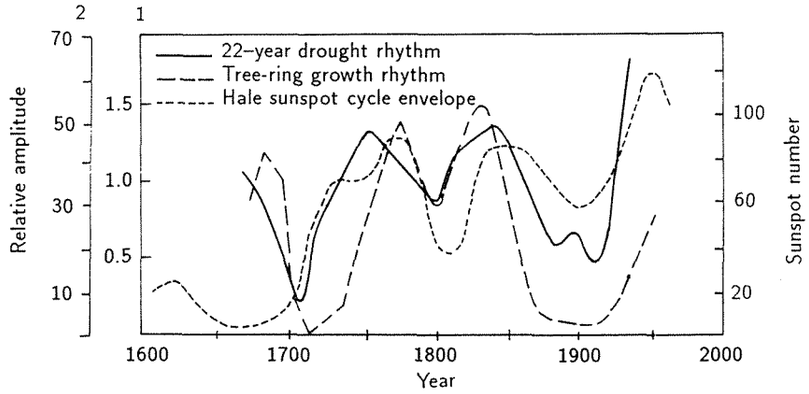

Figure 6.4. Amplitude variation of 22-year drought rhythm, tree-ring growth rhythm, and Hale sunspot cycle envelope.

the end. Around A.D. 1900, amplitudes of these rhythms turned out to be as low. This suggests the existence of a long-period modulation of drought maxima in the western USA and of tree-ring growth amplitude in northern Karelia on time scales of the solar magnetic cycle.

Thus, the magnitude of radial tree-ring growth is a sensitive indicator of the level of solar influence. This opens up unique possibilities for investigating the solar activity and the pattern of solar-terrestrial relationships over a large time scale. A coordinated study of the tree response to environmental changes and of the cosmogenic isotope content in reliably dated samples (tree rings, polar ice cores, etc.) is a promising method of establishing the history of the physical processes responsible for solar activity and the nature of solar-terrestrial relationships in time and space.

6.1.4. Atmospheric radiocarbon as an indicator of heliospheric processes

Kocharov *et al.* (1983) were the first to reconstruct, based on Suess' radiocarbon series (Suess, 1978), the variation of the galactic cosmic ray flux over 8,000 years, i.e., over a time scale 200 times that of direct cosmic ray observations. Within this time interval, more than 10 cosmic ray flux maxima have been found in addition to those corresponding to the known minima of solar activity, namely, the Maunder, Spörer, and Wolf minima. It is natural to assume that the maxima thus found originate from deep solar activity minima. This implies that states characterized by extremely low activity occur regularly in the sun. As already pointed out, the Maunder, Spörer, and Wolf minima manifested themselves in depressed tree-ring growth for the trees that grew in extreme conditions. To check this conclusion, we have carried out a combined analysis over a

long time scale of our data and the chronology reconstructed by Stockton (1981) from ring-width records of 1,000-year-old pine and samples of wood from dry mountainous areas in the USA. *Figure 6.5* presents a dendrochronological series of pine (*Pinus longaeva*) and the cosmic ray flux profile for a time interval spanning 6000 years B.C. One sees that, on the whole, the cosmic ray flux increases and the tree-ring growth depressions are phase locked. This suggests the existence of a common factor affecting the atmospheric radiocarbon level and tree-ring growth. An obvious candidate appears to be the solar activity that modulates the cosmic ray flux and influences tree-ring formation. The actual mechanism by which the sun acts on tree-ring growth has not yet been revealed. This could occur either indirectly through the inertial climatic system or directly via perturbation of the electromagnetic field near the Earth's surface (this effect should be more clearly pronounced in high latitudes and on mountains) that manifests itself in physical–chemical processes occurring in the trees.

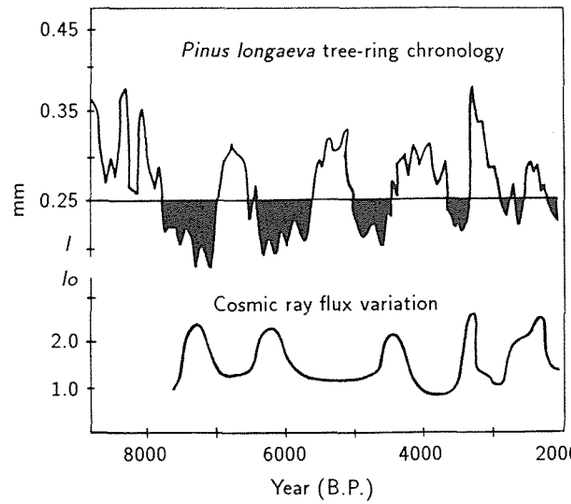

Figure 6.5. Cosmic ray flux variation and *Pinus longaeva* tree-ring chronology.

For the theory of the origin of cosmic rays, their spectrum in interstellar space both at present and in the past is of paramount importance. As follows from *Figure 6.5*, the average cosmic ray flux in the vicinity of the Earth practically did not change in the last 8,000 years. At the same time, in some periods that presumably correspond to deep minima in solar activity, the flux increased by about a factor of two. We may assume that in the epochs of deep minima the characteristics of the cosmic ray flux are close to interstellar. It is not possible to say, however, to what extent they approach the interstellar characteristics. Detailed studies of cosmic ray flux dynamics during deep depressions of solar activity are necessary. Note that it is essential to determine the energy spectrum of cosmic rays in addition to their flux variations.

The second problem has been solved for the Maunder minimum by making high-precision yearly measurements of radiocarbon content in tree rings (Kocharov *et al.*, 1985; Kocharov, 1986 and references therein). As for the energy spectrum, it can be derived by simultaneous measurement of the content of several cosmogenic isotopes (^{10}Be, ^{14}C, ^{36}Cl) in dated samples (Kocharov, 1986). Our data on the evolution of radiocarbon content in the Earth's atmosphere during the Maunder minimum reveal considerable fluctuations against a generally rising ^{14}C content level, which implies that even during deep solar activity minima the mechanism of galactic cosmic ray modulation continues to operate. Fourier analysis reveals two peaks in the spectrum, with a confidence level above 80%, at the frequencies corresponding to periods of 11 and ~22 years. Note that a period close to 11 years is more clearly seen in the years preceding the Maunder minimum while during the minimum proper a 22-year oscillation is more manifest. Our analysis suggests that the 22-year modulation of cosmic rays found to have existed during the Maunder minimum is most probably related to a change of the solar polar magnetic field. One can thus conclude that the solar dynamo does not stop during deep minima of solar activity. The nature of the Maunder minimum is apparently associated with the existence of several long-period solar variations, the superposition of their minima having resulted in a dramatic drop of solar activity.

6.1.5. Conclusion

We have succeeded in analyzing only a fraction of the wealth of available information from studies of astrophysical, geophysical, and ecological phenomena making use of cosmogenic isotopes. We hope, however, that this report demonstrates the richness, uniqueness, and importance of the information on heliospherical processes recorded in tree rings, both in theory and in practice. This information can provide a basis for the reconstruction of past and the prognosis of future physical and chemical environmental changes.

6.2. Outline of Methods of Long-Range Prognosis on the Basis of Dendrochronological Information

L. Kairiukstis and S.G. Shiyatov

For the natural sciences, which deal with the study of uncontrollable or hardly controllable phenomena and processes (climatology, hydrology, ecology, etc.), prediction is the fundamental and frequently the only possible method of obtaining scientific results in the sphere of practical applications. In connection with working out long-term plans for the rational utilization and protection of natural resources in the last decades, there has been a sharply rising need to devise and elaborate long-term (from one year to several decades) ecological predictions. Such precautionary information is necessary to improve the effectiveness of adopted solutions.

Because dendrochronology is a scientific discipline in the ecological sphere, predictions based on the use of dendrochronological information could be placed in a separate class of ecological prognosis as dendrochronological predictions – particularly when one takes into account the fact that a tree-ring chronology contains information about the past that is unique in its duration and accuracy.

The basic task of dendrochronological prognosis is to forecast changes in the growth index of arboreal plants. Nevertheless, on the basis of knowledge about the functional and correlational ties between the growth index of trees and factors of the environment and with the course of various natural processes, it is also possible to provide qualitative and quantitative predictions of environmental factors themselves. The extensively practiced reconstruction of natural past conditions (climatic conditions in particular), on the basis of dendrochronological information, may also be given the name of prediction in the past or retrodiction.

The general methods of ecological prediction and the methods used in the prediction of dynamic systems are applicable to dendrochronological prognoses. In this case, it is necessary to take into account the specificity of the dendrochronological series, which are discrete time series reflecting principally the changes in external limiting factors, primarily of a climatic nature, that are common for a given aggregate of trees. The specific character of these series is also year-to-year persistence, i.e., the influence of the size and conditions of growth during the previous year on the size of the growth of the current year, and also the possibility for statistical evaluation of the growth indicators for the individual calendar years.

Although the problem of dendrochronological prediction had been studied as early as the end of the 19th century and the beginning of the 20th century by Shvedov (1892) and Douglass (1919, 1928, 1936), we cannot compliment ourselves on much success in this field. The attention of dendrochronologists has so far been focused mainly on reconstruction of the climatic conditions of the past, i.e., retrodiction.

The approaches used in making predictions in dendrochronology may be divided into two large groups: intersystemic and intrasystemic. The essence of the intersystemic approach lies in using the dynamics of an external system of variables (the predictors) to predict, with a certain probability, the change in a dependent system of causally linked tree-ring variables (the predictands). The intrasystemic approach is based on the existence of persistence or autocorrelation within the dendrochronological series, which also allows predictions to be made without the need for external predictor variables.

The intersystemic approach is the most promising one and is most frequently used in dendrochronological prognosis. It is necessary to link both systems to one another either functionally or correlatively, such that the response of the tree rings takes place after the occurrence of the predicting variable in time. The predicting systems are most frequently the chronological series of solar activity and the tide-forming forces of the Moon and Sun that influence growth-limiting factors of the environment on tree growth.

Interest in the establishment of the correlational ties between the growth of trees and solar activity has arisen from the very beginnings of the science of dendrochronology and has not diminished (Douglass, 1919, 1928, 1936; Erlandsson,

1936; Kostin, 1961; Kolischuk, 1966; Komin, 1969; Bitvinskas, 1974, 1986; Olenin, 1976; Mitchell *et al.*, 1987). This interest is far from accidental. The establishment of such a connection is additional evidence in favor of the hypothesis about the influence of solar activity on the course of geophysical and biological processes. For example, Currie (1980) found an 11-year cycle in temperature records from North America at locations east of the Rocky Mountains and north of 35°N, which he attributed to the 11-year sunspot cycle. Besides that, the series of indicators of solar activity (sunspots) possesses sufficient duration to enable cyclical fluctuations of various durations to be readily surveyed in it. We also have much experience in long-term prediction of solar activity (Vitinskiy, 1983).

An analysis of the literature on clarifying the correlation between the indicators of solar activity and the growth of trees shows that in certain regions the connections are fairly strong, in other regions they are weak, while in still other regions they are not evident at all. The nature and closeness of the connections differ for the different phases of solar activity. For example, Bitvinskas (1986) used solar activity (the Wolf sunspot numbers for hydrological years) as pointer years to which radial tree growth could be *attached* to forecast the ecoclimatic background fluctuations responsible for forest growth. Those areas with sufficiently stable connections in time between the variable quantities examined can be used fully for the purposes of dendrochronological prediction. But until we have discovered the physical mechanisms responsible for the influence of solar activity on natural process on the Earth, it would be difficult to expect any great successes in the utilization of this method of prediction.

A promising method for the prediction of tree growth from the biggest anomalies of hydrometeorological indicators derives from the distribution of the maxima of solar and lunar gravitational tidal forces on Earth. These tidal forces lead to the formation of blocking anticyclones and to changes in the character of the atmospheric circulation (Yavorskiy, 1977). Drought appears in the zone of such anticyclones, with considerably increased precipitation observed around its periphery. The width of the zone of maximum tidal effects amounts to 300–500 km in longitude. When the atmospheric tides are formed over regions of precipitation formation, e.g., above the North Atlantic, then the drought may be manifested over very large territories. The change in the amount of precipitation and in the air temperature can be observed on the growth of the trees, since there exist sufficiently strong connections between the growth indices, climate, and the intensity of the atmospheric tides. Long-term dendrochronological series are helpful in establishing such connections (Yavorskiy, 1977).

Calculations of the tide-forming forces of the Moon and of the Sun can be made for many years in advance. Using this method, it was possible to predict successfully the disastrous drought that occurred in the USSR in 1972 and 1975. In connection with the responsiveness of the atmosphere to the action of tide-forming forces, it is possible to explain the origin of a fairly large number of cyclic fluctuations in the growth of trees with the duration of two to several hundred years. The analysis of 102 recent tree-ring chronologies made by Currie (1984) confirms earlier evidence for 18.6-year tidal drought–flood induction (Currie 1981, 1984) and led to the discovery of the 11-year solar-induced drought–flood cycle for western North America. Bistable phasing in terms of geography was also found, with epochs of maxima in lunar nodal 18.6-year drought in western Canada out of phase with those in western United States and northern Mexico for the past two centuries. As for prognostical use, this approach awaits further studies because the climatic response of solar cyclicity is highly dependent on the atmospheric chemistry.

If we had at our disposal reliable predictions about the factors of the environment that determine tree growth, it would have been possible to make predictions of growth in a comparatively easy and reliable manner, particularly in those regions where the number of tree-growth limiting factors is low. Since long-term predictions of the hydroclimatic factors are unreliable, it is not possible to use them as predictors for the time being. Currently, on the basis of dendroclimatic models, a basic reconstruction, or retrodiction, is possible for the most important climatic factors, as well as an evaluation of the adequacy of the prediction models (Fritts, 1982; Fritts and Gordon, 1982). Self-organizing regression models (Ivaxenko, 1975; Rosenberg and Feklistov, 1982) can be of great help in developing hydroclimatic models, and they could also be useful for the purposes of long-term prediction. These models make it possible to evaluate both the contribution of the individual factors and the aggregate influence of a set of factors.

In the reconstruction of the environmental conditions of the past, the dendrochronological series appears in the capacity of predictors. The dendrochronological series could also be used as predictors of the future behavior of other time series if a stable and reliable connection exists between them, though with a shift in time. In this case, it would be useful to carry out a cross-correlation analysis.

In using the intrasystemic methodological approach, it is necessary to know the extent that the series can be represented by deterministic, stochastic, and purely random components. There is no unity of view on whether there is a deterministic component in dendrochronological series. Some authors believe that the cyclic components may be considered as deterministic. Others do not agree with this point of view and use methods from the theory of random stationary processes for analyzing the cyclical components. The theoretical prediction of the probability component must be made on the basis of the probability model of the process. Because no such models have yet been adequately worked out in dendrochronology, predictions make use of deterministic models in which the observable fluctuations are approximated and extrapolated by sinusoids. The purely random fluctuations in the dendrochronological series (white noise) are composed of random properties of the series and with methodological errors and, therefore, cannot be predicted. They determine the objective limit of predictability in the series.

The study of intraseries laws and principles of development and their utilization for the purposes of prediction are impossible without the availability of sufficiently continuous and homogeneous series. In this respect, the dendrochronological series are favorably different from the hydroclimatic series. Of great significance is the establishment of continuous fluctuations of the growth index, and in this connection, it is necessary to use appropriate methods of standardization of the tree-ring series. It is also necessary to account for the fact that the

intrasystemic methods of prediction are not very appropriate in those cases when an essentially qualitative change occurs in the predicted system, for example, a change in the pattern of rhythmical fluctuation in tree-ring series (Kairiukstis and Dubinskaite, 1986).

The cyclical method of prediction is the one most frequently used in dendrochronology. It is based on the identification, approximation, and extrapolation of the most important cyclical components (Siren, 1963; Komin, 1978a, 1978b; Mazepa, 1985; Shiyatov, 1986). Several such cycles are usually identified in each series. We are now in possession of sufficiently powerful analytical methods and computing equipment to enable us to determine the necessary parameters of the cycles. Mention must be made of the promising nature of the joint utilization of maximum entropy spectral analysis and narrow-band digital filtering (Section 6.3).

The questions raised by Douglass (1919, 1928, 1936) about the reality of the cycles, about their stability in time, and about the mechanism of their formation are still topical. As long as the mechanism of cycle formation remains unknown, the reliability of such prognoses is restricted by the initial quantity of cycles more or less of one order, i.e., one type. With cycle change of the highest order, the type of cycles of the lowest order is changed as well. Then, the prognosis makes no sense. A paradoxical phenomenon occurs: the more accurate the prognosis, the less reliable it is (Kairiukstis, 1981). We come across such phenomena by processing tree-ring chronologies of many countries presented by different authors. Nevertheless, the only method of evaluating the reality of the cycles will be the analysis of their occurrence in sufficiently large numbers of continuous dendrochronological series obtained for one region or another. In any case, if the dendrochronological series contains well-expressed cycles that are stable in time, it could be fully utilized for the purposes of extrapolation. An attempt has also been made to establish and utilize the highest frequency cycles that are found by means of spectral decomposition. In this case, it is possible to give not only long-term climatic background predictions but also to predict short-term (seasonal) climatic fluctuations as well (Mazepa, 1985).

One of the methods of eliciting and using hidden periodicities for the purposes of long-term prediction was proposed by Berry *et al.* (1976). This method was tested on a sufficiently large number of dendrochronological series and produced fairly good results (Berry *et al.*, 1979; Kairiukstis, 1981; Kairiukstis and Dubinskaite, 1986). The essence of the method lies in that, by means of sorting out, the approximation of the series is carried out by single harmonics that are simple multiples of the sampling interval of the time series, and a selection is made of the most representative among them.

In dendrochronology, there is practically no use made of prediction based on the use of autoregressive functions. Since the dendrochronological series possesses a higher degree of autocorrelation compared with the climatic ones, it might be expected that autoregressive predictions for several years in advance could be effective in many instances.

Thus a definite, quantitative, and methodological basis exists for carrying out dendrochronological prediction. This is possible because of the knowledge of

the laws of arboreal plant growth, the system analysis approach, and the theory of random stationary processes. With regard to the prediction of dendrochronological series, successes in this area are still modest.

Of great significance is the determination of the limits of predictability, i.e., an evaluation of how well and how far in the future it is possible to predict the change in the index of tree growth. In dendrochronological predictions such matters have not yet been studied extensively. Obviously, predictability must be higher in those series that have been obtained from extreme conditions of growth for arboreal vegetation. It is possible to expect higher predictability in regional average series, in comparison with single-site tree-ring chronologies. Nevertheless, experience gained in the Lithuanian SSR shows that indices of tree growth, as well as agricultural crops, forecast in the late 1970s (Kairiukstis, 1981) for normal growth conditions and boggy soils are still proving themselves. It is possible to expect higher predictability in regional average series, in comparison with single-site tree-ring chronologies.

The mathematical tools used today for the purposes of prediction are based on the assumption that the tree-ring series are stationary. But there are no purely stationary processes in nature. How is it possible to remove that apparent contradiction? It is possible that a theory will be developed for nonstationary random processes up to the level of practical application. At any rate, the probability approach to prediction is more promising than the deterministic one, although it is desirable for prediction to have a more concrete approach. Apparently, it will never be possible to eliminate completely the indeterminateness of prediction.

Finally, we wish to stress that it is desirable to use different methods of prediction. At least both of the intersystemic and intrasystemic approaches mentioned above must be linked to one another functionally or correlatively to improve our ability to make predictions. But what is most important to the successful development of prediction is the development of reliable, homogeneous, and continuous dendrochronological series, which would also contain continuous fluctuations of the growth indexes.

In connection with the increase in the anthropogenic load on forest ecosystems and with the appearance of new limiting factors (e.g., pollution of the air and soil), the problem of dendrochronological prediction is becoming more urgent and still more complex. We must no longer rely on the continuity of the properties of the data from the past to the future. It is necessary to adopt other methods to assess non-climatic influences and to use past cyclicity to predict the future. More advanced prognostic models must be worked out that would include anthropogenic factors. Promising approaches to solving this problem have been made using climatic response models (Cook, 1987; Eckstein *et al.*, 1984).

That is how dendrochronological prediction is both possible and necessary. The elaboration of predictions is not only of great practical significance, but of cognitive value as well, because it enables us to gain better insight into the mechanism of change in tree growth.

6.3. Spectral Approach and Narrow Band Filtering for Assessment of Cyclic Components and Ecological Prognoses

V. Mazepa

Progress in the study of stochastic processes has resulted in the distinction of stationary stochastic processes as a separate class. Significant contributions to the study of their properties have been made with the help of the spectral theory formulated in the 1930s and developed by Khintchine (1934), Kolmogorov (1941), Cramer (1942), and Wiener (1949). In particular, the problem of predicting stationary processes was solved on the basis of these works. Further progress in this field is credited to Kalman (1960) and involves accounting for the dependence of the autoregression coefficient on time, which has also been given detailed consideration in the literature (Hannan, 1970).

However, a number of factors obstruct the practical application of this theory. The most important of these is lack of knowledge of the spectral function of the process under consideration. Even if we assume the spectral function as known, the resulting numerical calculation may be very complex. This fact accounts for few applications of these techniques except in very simple cases. However, the spectral theory is useful because it provides the optimal mathematical solution of the prediction problem, which can be compared with less systematic but practically more useful procedures.

This section discusses an approach to the description of the cyclical dynamics of annual tree rings. The impetus for studying the cyclicity in annual tree-ring chronologies was given at the beginning of this century. This problem has been considered very extensively by American dendrochronologists. The first comprehensive studies on the annual growth dynamics and its connection with solar activity were undertaken by Douglass (1919, 1928, 1936). Subsequently, however, the interest in cyclicity dropped (Glock, 1941) because of the methodological difficulties arising during the investigation and detection of cycles in tree rings and many other natural phenomena as well.

In spite of these difficulties, which have not been eliminated completely, the cyclicity in tree growth remains a subject for study (Kolischuk, 1966; Galaziy, 1967; Komin, 1970a; Shiyatov, 1986; Kairiukstis and Dubinskaite, 1986; Bitvinskas, 1987). The importance of this problem is not only in its connection with the urgency for ecological forecasts. The cyclical dynamics of forest productivity have a great ecological significance because they ensure stability and productive functioning of the forest ecosystem over a wide range of environmental variations (Komin, 1981).

Having reviewed the papers on the problem of cyclicity, we have concluded that dendrochronologists are aware in principle of the possibility of splitting the tree-ring series into cyclical components. Unfortunately, the terms and concepts used are poorly defined, and misunderstandings and misusages are frequent. In general, the quantitative characteristics of the cycle (the amplitude, phase, and period) provide a rather inadequate picture of the essential features of these components, since occasional breaks in the regularity of the cycle occur.

The existing definitions of the cycle are descriptive and phenomenological, which do not allow the cycle to be identified and distinguished. There is no acceptable definition of the cycle, which is regrettable because the causes of cyclicity are often unknown.

A prominent place in such investigations is given to the cyclical component estimation techniques. The traditional methods are the visual analysis of time series, smoothing, and filtering, and a number of statistical methods – the results of correlation and spectral analyses. It should be noted that spectral analysis methods are not widely used in dendrochronology mainly due to difficulties in drawing statistical inferences about the estimates of the spectral density. In statistical theory, when testing the value of the spectral function, the underlying model generating the time series is assumed to be known. This assumption is hardly plausible in practical dendrochronological studies at the present time. The literature does not support such a choice in terms of the substantial interpretation of the model parameters. We think that such models are used only for the purposes of approximating dendrochronological series. Nevertheless, information on spectral analyses is being collected.

We have carried out a number of computer experiments to study the cyclical structure of dendrochronological series using spectral analysis and narrow band-pass filtering techniques. We have had at our disposal mean dendrochronological series and series of tree-ring indices for the individual trees that have been included in the mean chronologies. The series were obtained from individual trees of *Larix sibirica* found during excavations of Mangazeya town and those living at present (Shiyatov, 1980).

The estimates of the spectral density have been analyzed without accounting for the type of parametric model generating these time series. It is to be assumed, however, that the series under consideration is a realization of stochastic processes that are stationary in the broad sense of the term.

A proviso should be made here. One main principle in dendrochronology is the principle of cross-dating. Mean values of indices of sample trees are significantly different from year to year. Thus, stationarity of the mean-value function is out of the question with regard to this. However, if we abstract from dating chronologies of sample trees and assume the time to be an ordinal number in the time series observed, then the series of separate sample trees may be considered as realizations of a stochastic process. In this case, we may hope, it is possible to treat such a process as a stationary one. Hereafter, stationarity is assumed to exist in the general sense of the term (i.e., the existence of the second-order moments and dependence of serial correlation only upon the time lag).

We shall call the process defined above *the formation of relative wood growth* over sufficiently large areas, where the cross-dating principle acts locally. Stationarity of the mean-value function of this process has been tested (over different time intervals) by means of an analysis of variance. The results obtained for five mean chronologies show that the conventional time does not affect the mean values. The variance equality hypothesis has been tested with the help of the Bartlett criterion (Bolshev and Smirnov, 1968). The corresponding statistics do not exceed the value of chi-square with the required degrees of

freedom at a 5–10% level of significance. The covariance structure of the process has been determined by the spectral density of individual tree-ring series that are combined into a mean chronology. It has been necessary to confirm the existence of important narrow frequency bands over different time intervals. By the importance of these bands we mean increased spectral density values at these frequencies as compared with the neighboring ones for the majority of the series of the sample trees included in the mean chronology and independence of spectral density on the time interval represented by the tree-ring series. *Figure 6.6* presents part of the results of this test. Testing for a peak in the spectral function was analyzed visually because the type of parametric model generation of the time series was not assumed. One modification of the statistical problem of testing for a peak in the spectral function of a stationary time series was considered by Hannan (1961).

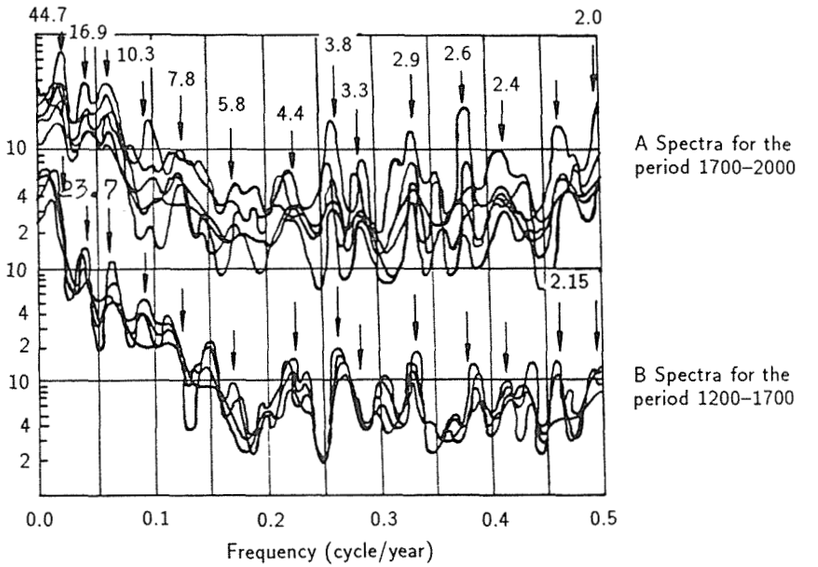

Figure 6.6. The maximum entropy power spectra of the individual tree-ring series that are combined into a mean chronology.

The spectral density functions are commonly estimated using the fast Fourier transform (FFT). This approach to spectral analysis is effective from the calculation standpoint. However, there are limitations inherent to it – poor frequency resolution and *leakage* by the spectral window. In the last decade many alternative spectral estimation procedures based on parametric models have been postulated to reduce these limitations. A summary of many of these new techniques for spectral analysis of discrete time series was presented by Kay and Marple (1981). An examination of the underlying time series model

assumed by each technique serves as the common basis for understanding their differences among the various spectral analysis approaches.

In this paper, two principal methods are used: the Blackman-Tukey method (Blackman and Tukey, 1958) and the maximum entropy method (Anderson, 1974). The Tukey-Hamming (Hannan, 1960) and Parzen (Parzen, 1961) spectral windows are used for the first method, while in the second case Tukey-Hamming multipliers are applied (Swingler, 1979).

To extract certain frequency bands, narrow band-pass filtering has been applied employing a filter, using truncated Fourier series coefficients of the Π-shaped function (Mazepa, 1986), and an optimal filter in the Chebyshev sense for approximating the Π-shaped frequency response function (McClellan *et al.*, 1973).

The results of the analysis are summarized in the following statements:

- The spectral density estimator used provide an adequate picture for the frequency pattern of the series constructed using the trees growing under extreme climatic conditions. The growth-index series for trees growing in homogeneous ecological conditions display similar spectra. The estimates of the spectra derived for intervals of the time series spanning from 200 to 1,010 years do not suffer significant changes within a time interval of 300–500 years. This allows the spectral methods to be used successfully for the analysis of stationary random sequences.
- The spectral density of dendrochronological series includes important frequency bands for which the variance is significantly higher compared with neighboring frequencies (*Figure 6.6*). The width of these bands is approximately 0.02–0.05 cycles per year. These frequency bands may be characteristic of the cyclicity in the wood-growth dynamics.
- The spectral densities do not change abruptly when going from one important frequency band to another. No discrete changes in frequency powers are observed. We may speak only of dominant frequency bands (making large contributions to the variance of a series as compared with other bands). Variance does not disappear at frequencies between the dominant ones (*Figure 6.7*).

Based on these statements we can define the principal features of the cycle. The cycle is defined as the component of the mean chronology that corresponds to an important narrow frequency band in the spectral density, if these frequencies are significant for the majority of the series of separate sample trees included into the mean chronology. By the fractional cycle periods we mean the average of close cycle lengths over the period of observation, since growth is, in fact, a discrete process. The vegetation periods are separated by dormant periods.

This definition is practically convenient. Purposeful narrow band-pass filtering with a prescribed frequency response function becomes possible. Once the important frequency bands are found they can be analyzed by choosing an appropriate filter.

One practical objective of analysis of the cyclicity in dendrochronological series is the prediction of the climate-dependent dynamics of wood plant growth.

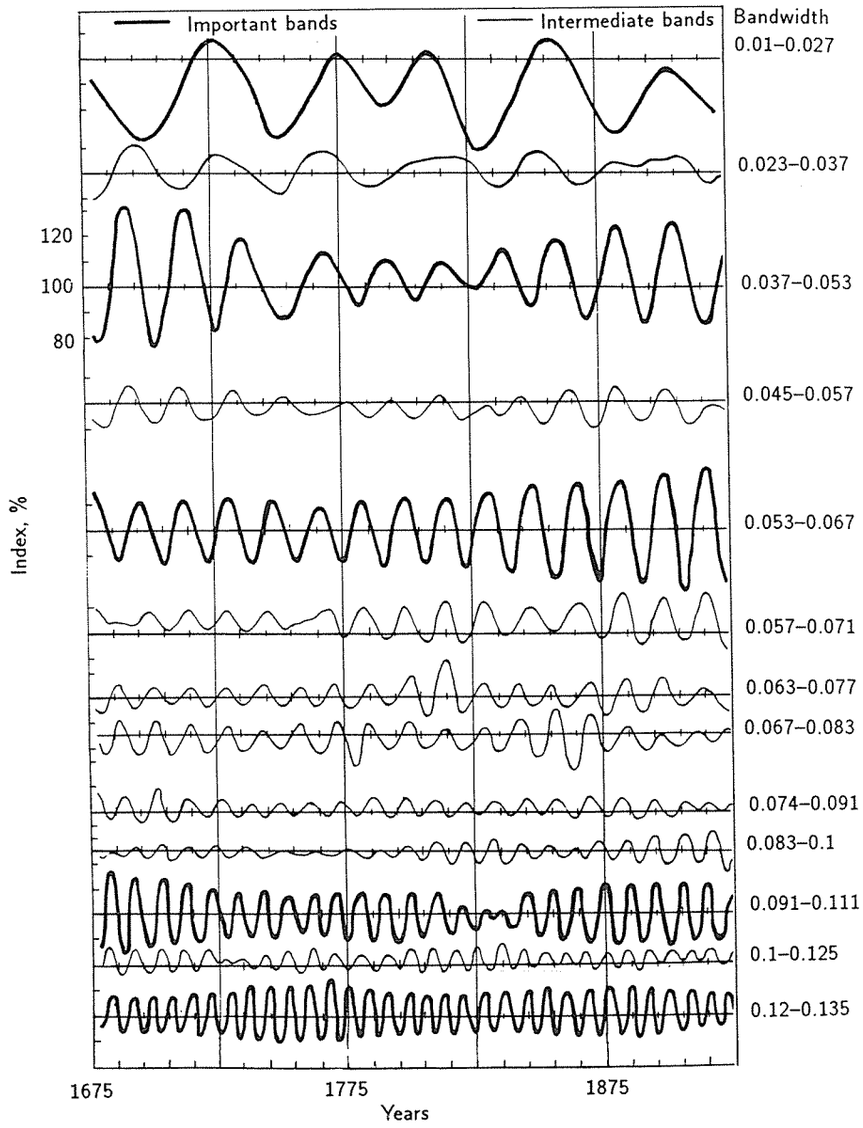

Figure 6.7. Successive series output after the band-pass filtering.

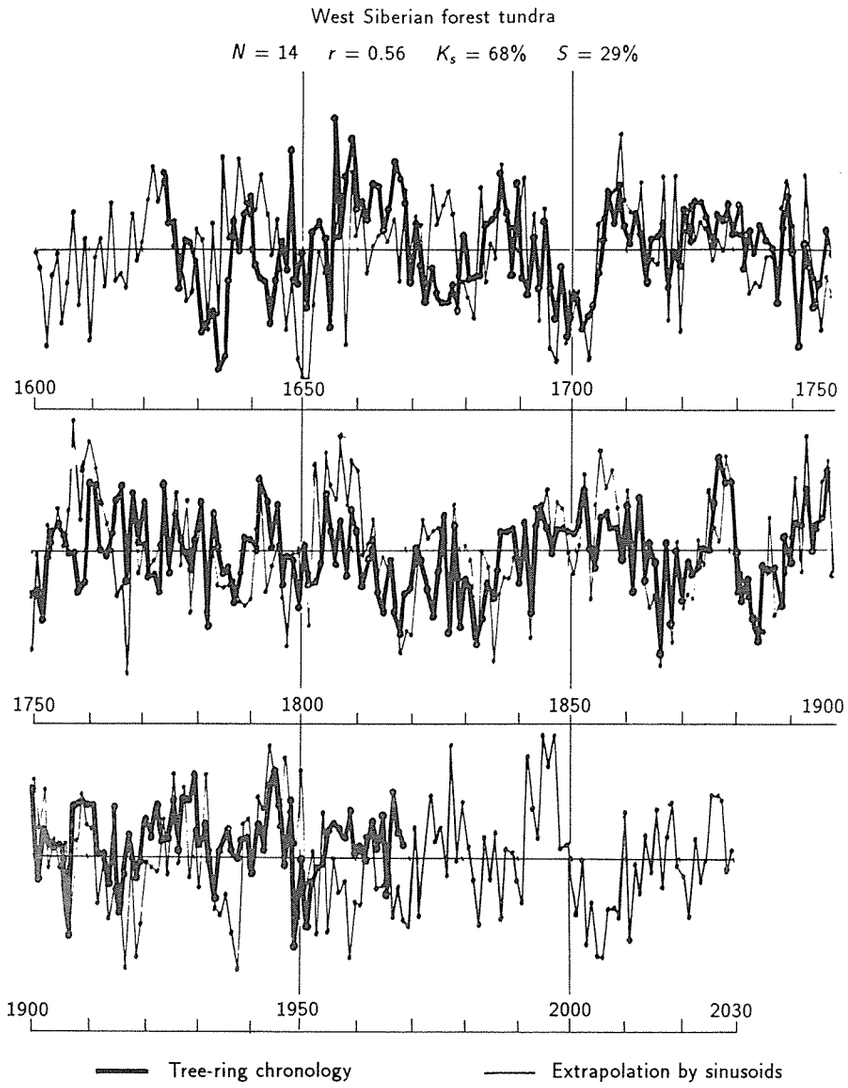

Figure 6.8. Tree-ring chronology and its approximation and extrapolation by sinusoids. N is the number of sinusoids in the approximation, r is the correlation coefficient, K_s is synchroneity coefficient, and S is the mean-root-square error.

It is known from the theory of stationary random processes that if we pass this process through sufficiently narrow band-pass filters, then the outgoing fluctuations over a large number of periods are approximated with high accuracy by the sinusoid of a certain frequency. Of course, the filtered component is not strictly periodic even for the narrowest band width: two intervals of a long time series separated by a long time interval will be well approximated by the sections of sinusoids of the same frequency, but, generally speaking, the amplitudes and phases of these sinusoid sections will differ.

Our experience in the approximation of the cyclical components of dendrochronological series corresponding to important frequency bands suggests that the sinusoid phases, at least for the greater part of the detected cycles, do not change significantly. Thus, thermal conditions were predicted for growth periods of woody plants growing at high altitude and high latitude boundaries in the following regions: the northern and southern Urals and the lower reaches of the Pechora and Taz rivers. Forecasts of woody-plant growth dynamics were made also for other regions of the USSR (Shiyatov and Mazepa, 1985). This was done as follows: the series was filtered to extract only those frequency bands over which increased spectral density estimates were observed; the extracted cycles were approximated by sinusoids; the forecast of the tree-ring indices was presented in the form of the sum of fitted sinusoids.

The amplitudes and phases of the sinusoids were estimated by the least squares method. To avoid negative features of the solution of a poorly conditioned set of linear equations (Tikhonov and Arsenin, 1979), the sinusoid frequencies were estimated by an exhaustive search method in every important frequency band.

The quality of approximation for the initial tree-ring series was characterized by the coefficients of correlation and synchronization (the number of adjacent parallel trends divided by total trends) that were equal to 0.5–0.8 and 66–68%, respectively. *Figure 6.8* presents an example of approximation and extrapolation of the dendrochronological series constructed for Siberian larch (*Larix sibirica*) growing in the lower reaches of the Taz River.

6.4. Harmonic Analysis for Ecological Prognoses

L. Kairiukstis and J. Dubinskaite

6.4.1. Introduction

Currently, a large number of models are used to approximate and predict temporal series (see Section 6.3). However, for the successful application of any model to a given temporal series, the model selection must be well grounded. We shall give the reasons for proper selection of a cyclical model for approximating dendrochronological series.

Cyclical fluctuations are peculiar to dendrochronological series of short duration. Even a visual evaluation of the series (*Figures 6.9* and *6.10*) enables us to confirm that they are all the realization of stationary random processes. In these series, the fluctuations similar to the behavior of the sum of periodic

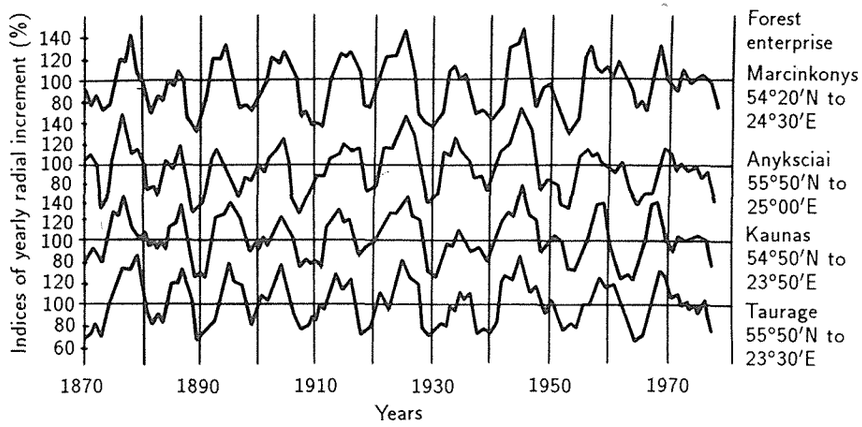

Figure 6.9. Annual tree-ring indices of *Caricoso-sphagnosum* type of *Pinus sylvestris* forest stand.

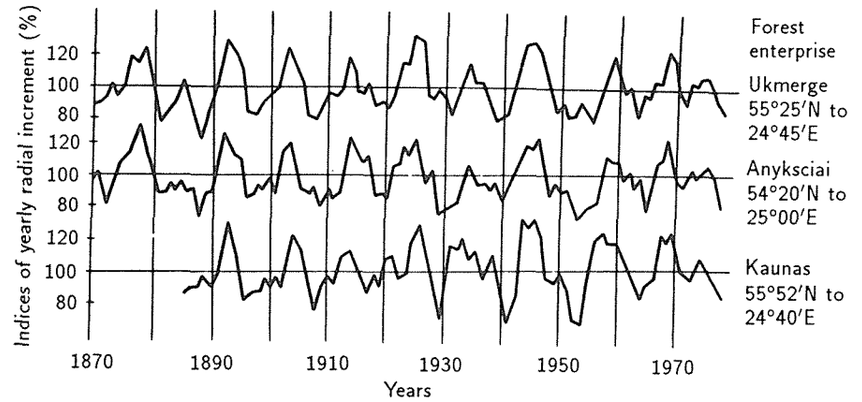

Figure 6.10. Dynamics of radial increment of yearly indices of *Pinus sylvestris* type of *Vaccinium myrtillus-sphagnosum* forest stand.

components can be detected visually. The process x_t is said to be stationary when the distribution of random values $x_{t1}, x_{t2}, \ldots, x_{tn}$ coincide with the distribution of $x_{t1+t}, x_{t2+t}, \ldots, x_{tn+t}$ for any integer numbers $t_1, t_2, \ldots, t_n$, etc. Therefore, for a stationary random process x_t, the mathematical expectation $E[x_t]$ does not depend on t (Anderson, 1971). It must be noted that temporal series are also random processes. Only here the parameter t is discrete. For instance, in the tree-ring chronology constructed from a large number of trees from moist sites (*Figure 6.9*), the maxima and minima repeat every 9–12 years. Significant peaks (95% significance) corresponding to the periods 10–13.3 and 20–24 years are indicated in power density spectra of all series. The order of

significant coefficients of the autocorrelation function exceeds 15. To estimate power density spectra, the method of Parzen and Tukey (Anderson, 1971) was applied. The 95% confidence limit for this estimation is the following:

$$\left[\hat{f}_t(v)\, e^{-1.96\tau\sqrt{K_T/T}},\ \hat{f}_T(v)\, e^{1.96\tau\sqrt{K_T/T}}\right] ,$$

where T is the length of a series; $v = 2\pi j/T$ is the frequency, $j = 1, 2, \ldots [T/2]$; $\hat{f}_t(v)$ is the estimation of density spectra with frequency v; and τ and K_T are the coefficients depending on the smoothing window (*Figure 6.11*).

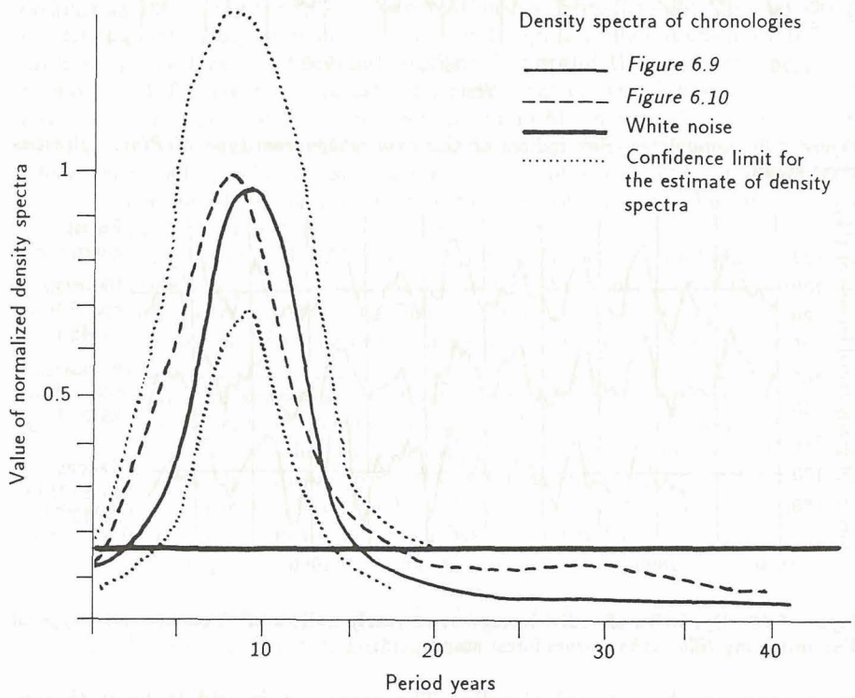

Figure 6.11. Normalized density spectra of chronologies for *Figure 6.9*, *Figure 6.10*, normalized density spectra of white noise, and confidence limit for the estimate of density spectra; $\tau = 0.73$, $K_t = 20$ (number of autocorrelations used to estimate spectra), $T = 109$, and $a = 10$ (number of degrees of freedom).

The peaks of density spectra are significant, if the 95% confidence limits lie higher than the spectra of white noise $\sigma^2/2\pi$, where σ^2 is the variance of chronologies. For the purpose of this study, a white-noise null continuum has been assumed for ease of calculation. Theoretically, the null continuum is more of a red-noise process.

The autocorrelation function $r(k)$ of order k for series x_t is determined as

$$r(k) = \frac{\sum_{t=1}^{T-k} (x_t - \bar{x})\,(x_{t+k} - \bar{x})}{\sqrt{\sum_{t=1}^{T} (x_t - \bar{x})^2 \sum_{t=1}^{T-k} (x_{t+k} - \bar{x})^2}} ,$$

where $\bar{x}$ is the arithmetic mean of the series, and T is the series length.

The results discussed above allow one to assert that dendrochronological series (i.e., *Figures 6.9* and *6.10*) may be the sum of cyclical components of the form

$$f(t) = A_0 + \sum_{j=1}^{n} A_j \cos\,(2\pi t/T_j - Y_j) \quad , \tag{6.1}$$

where A_j, T_j, and Y_j are the amplitude, period, and phase of the jth harmonic; n is the number of cyclic components; and T_j is the integer number.

Also, dendrochronologies may be a process of autoregression of a larger order.

6.4.2. Methods

We shall briefly describe the methods of singling out a cyclic component of the form of equation (6.1). Let $x_1, x_2, \ldots, x_t$ be the mean-corrected series of tree ring indices. According to the following equation

$$\rho_v = \sqrt{A_v^2 + B_v^2} \quad , \tag{6.2}$$

where

$$A_v = \frac{2}{T} \sum_{j=1}^{T} x_j \cos \frac{2\pi_j}{v}, \qquad B_v = \frac{2}{T} \sum_{j=1}^{T} x_j \sin \frac{2\pi_j}{v}$$

are the trigonometrical amplitudes ρ_v for experimental periods $v = 2, 3, \ldots, [T/2]$, which are to be estimated. To verify whether a cyclical component with period v is in a series $\{x_i\}$, a characteristic statistical test is applied:

$$P_v = \rho_v^2 \left(\frac{T}{v} - 0.5\right) .$$

This test for singling out a cyclical component (I) is described by Berry *et al.* (1979). The larger P_v is, the greater the probability that a periodic component with period v is in the series $\{x_t\}$.

A cyclical component

$$\sum_{j=1}^{n} A_j \cos (2\pi t/T_j - Y_j)$$

in series $\{x_t\}$ is singled out in the following way: ρ_v, P_v (as defined above), and

$$Y_v = \begin{cases} \arctan (B_v/A_v) , & \text{if } A_v \geq 0 \\ \arctan (B_v/A_v) - \pi , & \text{if } A_v < 0 , B_v < 0 \\ \arctan (B_v/A_v) + \pi , & \text{if } A_v < 0 , B_v \geq 0 \end{cases}$$

are calculated for all $v = 2, 3, \ldots, [T/2]$. Further, the integer number k (usually $k < 20$, to obtain useful prognoses) of the largest numbers P_{v1}, $P_{v2}, \ldots, P_{vk}$ from series $\{P_v\}$ are selected.

According to the equation

$$f_j(t) = \sum_{l=1}^{j} \rho_{v_l} \cos \left(\frac{2\pi t}{v_l} - Y_{v_l}\right) , \quad j = \overline{1,k} \tag{6.3}$$

k series of prognoses are derived. Now the criterion for selecting the best prognosis from the k cyclical components $\{f_j(t)\}$ must be determined. One of the most widely used criteria of proximity between an actual series $x(t)$ and the series estimated by harmonics $\hat{x}(t)$ is the sum of squares of deviation:

$$\text{SSE} = \sum_{t=1}^{T} (x_t - \hat{x}_t)^2 .$$

In dendrochronology, the extent of agreement between the series of indices and their prognoses can be estimated by the coefficient of synchronization (Bitvinskas, 1974):

$$\frac{2}{T-1} \sum_{t=2}^{T} \Big[\text{sign} \{[\Delta x(t)] - [\Delta y(t)]\} + 1\Big]$$

where Δ is the difference between successive values of the x_t and y_t.

Hence, for an approximation of indices $\{x_t\}$ of a series, it is recommended that a cyclical component $f_j(t) = f(t)$ is taken that meets the condition:

$$\sum_{t=1}^{T} [x_t - \bar{x} - f(t)]^2 = \min_{1 \leq j \leq 20} \sum_{t=1}^{T} [x_t - \bar{x} - f_j(t)]^2$$

or $f_j(t) = f(t)$ for which the coefficient of synchronization between x_j or $f_j(t)$ is largest. It must be mentioned that by increasing the number of harmonic components, the coefficient of synchronization does not necessarily increase. Usually, this coefficient is largest when 7–15 components are summed.

6.4.3. Harmonic analysis method to single out cycles of 10–24 years in duration

We shall present the results obtained in applying the aforementioned methods for prognostic purposes.

The aim is to predict the behavior of tree-ring chronologies for 10 to 15 years. For this purpose, we shall make use of 76 dendrochronologies covering 88–160 years for *Picea abies*, *Quercus robur*, *Pinus sylvestris*, and *Alnus glutinosa* from the Lithuanian SSR. The dendrochronologies were constructed by Stravinskiene (1979, 1981) and Kairaitis (1978, 1979). For the construction of the dendrochronologies discussed below, 25–30 and 50–70 trees were used, respectively.

In these dendrochronologies $\{x_t\}$ and in series of indices $\{lnx_t\}$ obtained logarithmically according to the approach described above, a cyclical component [equation (6.1)] has been singled out. T_j represents integer numbers. To single out the cyclical components, we applied the methods described above because the length of the cycles determined according to the peaks of density spectra or according to the significance of the Fourier analysis depends on smoothing and are fractional numbers. The assumption that the length of the cycles is an integer number conforms more to reality.

The correlation function of residuals $U_t = x_t - f_j(t)$ or $V_t = lnx_t - f_j(t)$ (here the index x_t refers to a series of indices) decreases very slowly. The order of autoregression U_t and V_t ranges from 5 to 10. In 70% of the dendrochronological series investigated, residual variance exceeds the variance of series U_t or V_t by 70%. These series are not approximated to the series of autoregression because we need models for prediction purposes for a period of 10 to 15 years.

The results discussed above enable one to assert that the dynamics of indices $x(t)$ of the tree-ring series covering the 90–150 year records are reflected best by the models

$$x(t) = A_o + \sum_{j=1}^{n} A_j \cos (2\pi t/T_j - Y_j) + E_j , \tag{6.4}$$

and

$$x(t) = \exp \left\{A_o + \sum_{j=1}^{n} A_j \cos (2\pi t/T_j - Y_j) + E_t\right\}, \tag{6.5}$$

where E_t is a random autocorrelated time series and n is selected in such a way that the actual and approximating series might show a higher level of agreement while the sum of squares of deviation might be as little as possible. T_j, $j = 1, 2, \ldots, n$ are usually selected from the intervals 7–14 and 20–25 years (*Figure 6.12*).

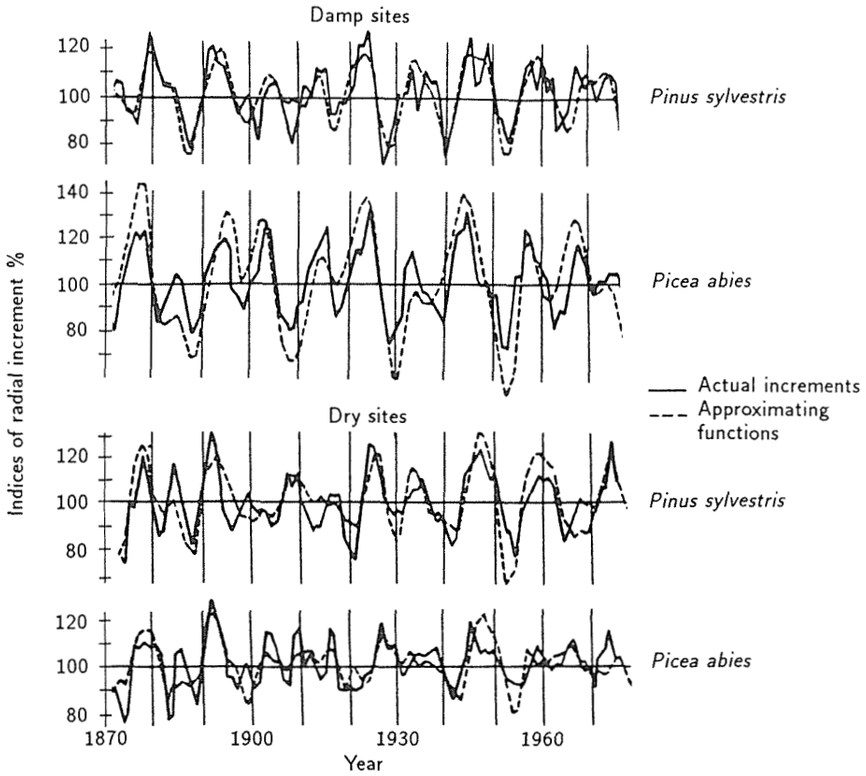

Figure 6.12. Actual increment indices and values of the approximating function for *Pinus sylvestris* and *Picea abies* on very damp and dry sites from the Lithuanian SSR, according to dendrochronologies A (Stravinskiene, 1981) and B (Bitvinskas, 1974, 1981).

With regard to the adequacy of models as shown in equations (6.4) and (6.5), in at least 90% of the series, the approximating function explains 85–90% of the significant fluctuations while in master chronologies from damp sites of the range is 95–100% using the coefficient of synchronization. It must be noted that considerable rises and falls (8–22 years in duration) in each dendrochronology characterize the generally favorable or unfavorable growth conditions. Therefore, the prediction of these rises and falls is of paramount importance.

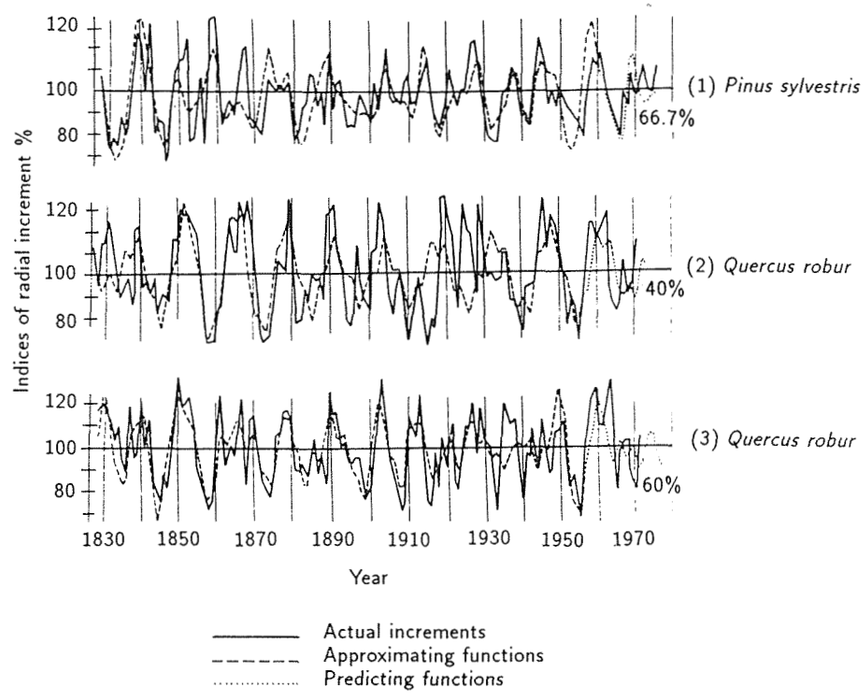

Figure 6.13. Actual increment indices, values of approximating function, and predicting function for *Pinus sylvestris* stand of *Sphagnum* forest type from the Kaunas region and *Quercus robur* stands of *Oxalis* forest type from the Kaunas and Vilnius regions of the Lithuanian SSR [according to dendroscales (Stravinskiene, 1979) (1) and (Kairaitis, 1979) (2) and (3)]. The prognoses in (1) are calculated according to equation (6.5) and in (2) and (3) according to equation (6.4). The coefficient of synchronization (%) between the actual and predicted data are indicated on the right.

The actual and approximating series of the tree-ring chronologies incorporating a large amount of material from damp sites (Stravinskiene, 1981) were compared with those of the dendrochronologies from dry sites (Bitvinskas, 1974, 1981). Their agreement ranges from 74–84%. The residual variance is less than half the variance of the original series. Whole calculations (i.e., assessments T_j, A_j, Y_j) were made on published dendrochronologies without smoothing. For a comparison of important fluctuations (maxima and minima), we used a three-year unweighted moving average. In 66 of 76 dendroscales studied, the agreement between the approximating and actual filtered series exceeds 65%. In 80% of the dendrochronologies covering the past 100–150 years for other regions of the USSR, between-series agreement averages over 65%.

Calculations reveal that the models shown in equations (6.4) and (6.5) are not applicable for dendrochronologies with great variance (800% of the mean and more). The coefficient of synchronization and a sum of squares of deviation in

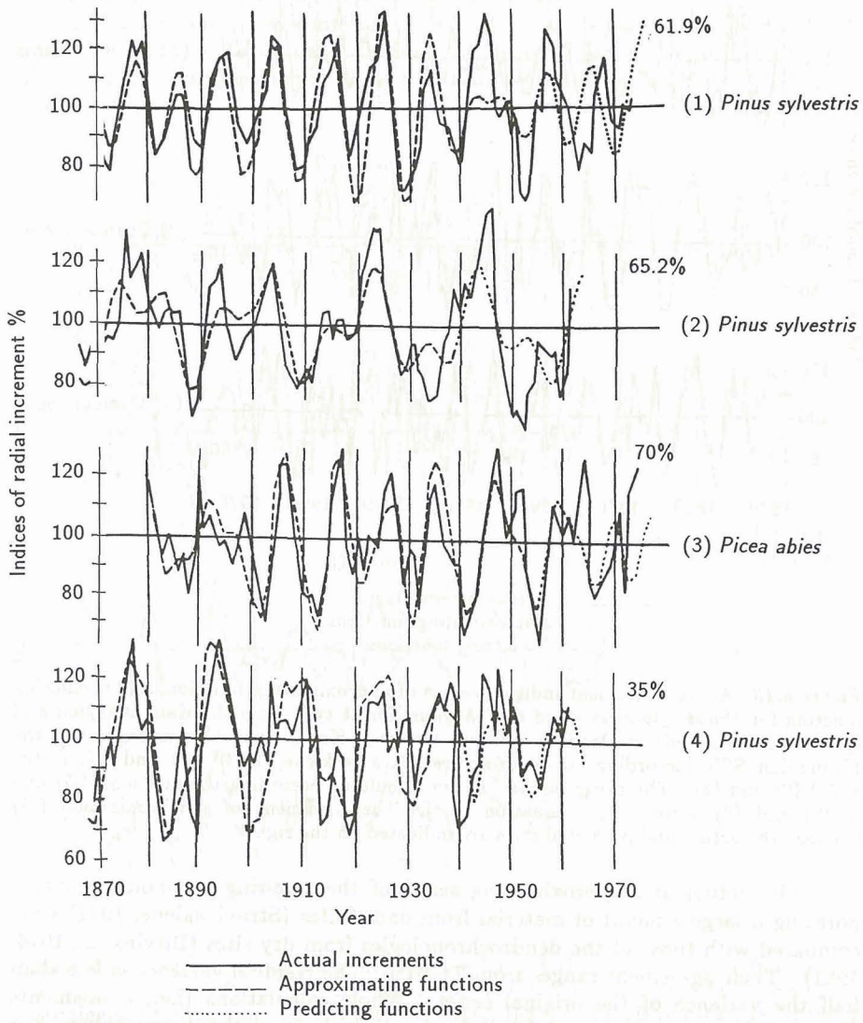

Figure 6.14. Actual increment indices, values of approximating function, and predicting functions for (1) ***Pinus sylvestris*** stand from very damp sites (master chronology for the whole Lithuanian SSR); (2) ***Pinus sylvestris*** stand of *Sphagnum* forest type from the Svencioneliai region of the Lithuanian SSR; (3) ***Picea abies*** stand of ***Vaccinium myrtillus*** forest type from the Anydsciai region; and (4) ***Pinus sylvestris*** stand of ***Vaccinium myrtillus-Oxalis*** forest type from the Kaunas region of the Lithuanian SSR [according to dendroscales (Stravinskiene, 1981) (1) and (3); (Bitvinskas, 1974) (2) and (4)]. The agreement values (%) between the actual and predicted data are indicated on the right.

this case are not convenient characteristics for the adequacy of the models. It is not difficult to find some series that reflect the fluctuations very similarly. However, they have only 50% agreement.

Since the dendrochronologies $x(t)$ covering the years 100–150 are approximately stationary, it is feasible to predict $x(t)$ for 10–15 years by equations (6.4) and (6.5). To verify this statement, we calculated the predicted values of the indices of 23 series of dendroscales without the last 10–15 (*Figure 6.13*) and 20–30 years (*Figure 6.14*), using the parameters of approximating functions (4) and (5). The results were compared with the actual data. In 19 series, significant fluctuations (8–22 years) were reflected properly, although the agreement of the ends of some series was less than 50%.

6.4.4. Harmonic analysis method for singling out cycles of long duration

A question arises as to whether it is possible to apply harmonic models [equations (6.4) and (6.5)] to approximate and predict fluctuations in dendrochronologies over long periods, for instance 200–450 years. Such dendrochronologies, as a rule, are not stationary; for example, in some series this may be noted visually (*Figure 6.15*). In these series, the spectral and harmonic analysis of non-overlapping intervals of 100–150 years resulted in changing dynamics of short cycles (8–13, 20–25 years in duration). Therefore, these cycles are revealed best in dendrochronologies covering only 100–150 years. If T_j, A_j, and Y_j are determined in the whole series of dendrochronologies covering the 200–450 years, these models are not appropriate for an approximation and prediction of series with such cycles.

Let us consider long-term cycles. Suppose that long-term cycles reflect the generally favorable or unfavorable climatic background of a region. Then, short-term (8–13, 20–25 years in duration) cycles of growth will be superimposed on the background of a favorable or unfavorable impact of long-term fluctuations. To elucidate the general tendency for the changing environmental background of the northern parts of the Eastern and Western Hemispheres (approximately the taiga zone of the USSR and North America), we attempted to single out long-term cycles (35 and more years in duration) in dendrochronologies from these regions. For this purpose, we have investigated 14 chronologies from the northern parts of the USSR (the Urals, Karelia, and west Siberia) (Bitvinskas, 1978a; Lovelius, 1979; Shiyatov, 1972, 1975, 1979) and 18 chronologies from Canada and the USA (Washington, Oregon) (Cropper and Fritts, 1981; Stokes *et al.*, 1973; Drew, 1975a, 1975b). Each has a span of more than 260 years (*Tables 6.1* and *6.2*).

To single out long-term cycles, we calculated the trigonometrical amplitudes in each series for the periods from two years to one-half of the length of the series. Calculations also included density spectra with different bandwidths of smoothing using the Tukey and Parzen windows (Anderson, 1971). It turned

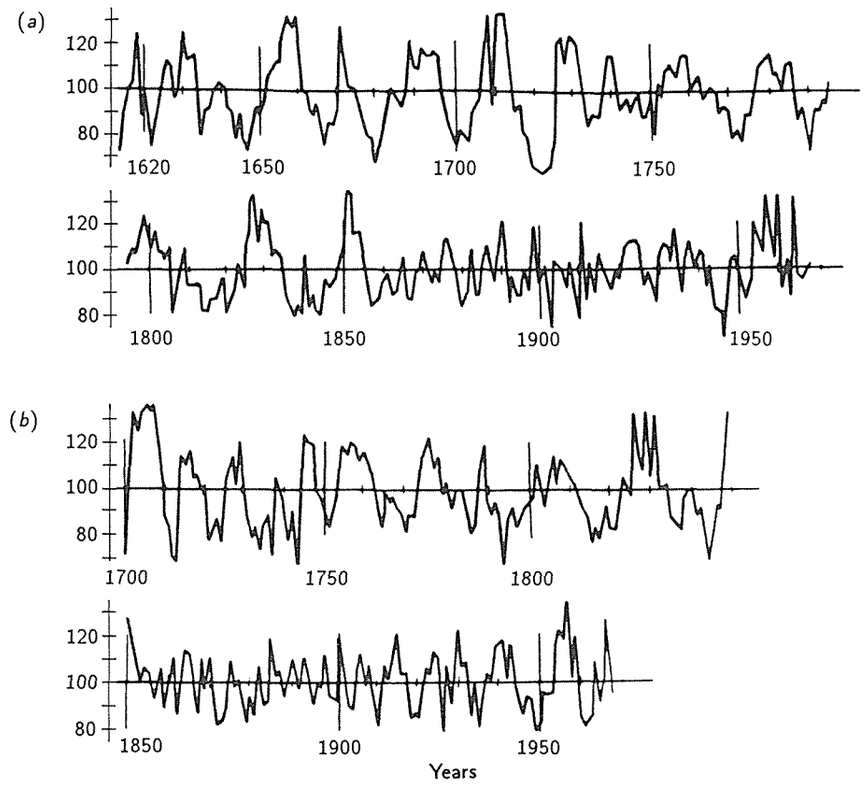

Figure 6.15. Examples of distinctly nonstationary dendrochronologies of *Pinus sylvestris* stands from the Kola Peninsula (*a*) and the Karelia ASSR (*b*) (Bitvinskas and Kairaitis, 1979). Absolutely different dynamics of indices' fluctuations are noted in the intervals 1650–1850 and 1850–1960 (*a*) and 1750–1850 and 1850–1960 (*b*).

out that the maxima of the trigonometrical amplitudes and density spectra are revealed with a frequency corresponding to the following cycles: 35–40, 50–54, 58–60, 76–84, 90–93, 110–117, and 171–176 years in duration in the tree-ring chronologies from the USSR. In the chronologies from the USA and Canada, the maxima of the trigonometrical amplitudes and density spectra are also revealed with a frequency corresponding to the very similar cycles: 37–39, 46–53, 58–62, 72–78, 98–105, and 178–192 years in duration (*Figure 6.16*).

A synchronization is observed in all groups of cycles. The peaks of the trigonometrical amplitudes appear at points of maxima and minima in at least 90% of the cycles in the time interval 1880–1980. There is a phase shift of no more than 20% of the length of the period of the estimated rhythm. It must be noted that almost half of the maxima of the trigonometrical amplitudes and density spectra lie below the 95% confidence limit.

Table 6.1. Chronologies obtained for selected long-term cycles from northern parts of the USSR.

No.	*Species*	*Place of publication*	*Growing location*	*Years*
1.	*Pinus sylvestris*	Bitvinskas, Kairaitis, 1979, 56 p., table 2	Kola Peninsula	1614–1971
2.	*Pinus sylvestris*	Bitvinskas, Kairaitis, 1979, 59–60 pp. table 3	Karelia ASSR	1648–1973
3.	*Pinus sylvestris*	Bitvinskas, Kairaitis, 1979, 60 p., table 3	Karelia ASSR	1702–1973
4.	*Pinus sylvestris*	Bitvinskas, Kairaitis 1979, 61–62 pp., table 6	Karelia ASSR	1695–1971
5.	*Pinus sylvestris*	Britvinskas, Kairaitis 1979, 62–63 pp., table 7	Karelia ASSR	1684–1973
6.	*Pinus sylvestris*	Britvinskas, Kairaitis 1979, 63 p., table 8	Karelia ASSR	1673–1973
7.	*Pinus sylvestris*	Britvinskas, Kairaitis 1979, 64 p., table 9	Karelia ASSR	1617–1971
8.	*Larix sibirica*	Shiyatov, 1975, 50–51 pp.	West Siberia	1103–1969
9.	*Larix sibirica*	Lovelius, 1979, 62 p., table 14	North forest bound	1459–1975
10.	*Larix sibirica*	Lovelius 1979, 81 p., table 17	Tamir	1704–1970
11.	*Larix sibirica*	Shiyatov, 1979, 108 p., table 1	North Ural	1541–1968
12.	*Larix sibirica*	Shiyatov, 1979, 109 p., table 2	Arctic Ural	1691–1969
13.	*Larix sibirica*	Shiyatov, 1979, 109 p., table 3	North Ural	1590–1969
14.	*Pinus sibirica*	Shiyatov, 1979, 110 p., table 4	North Ural	1557–1969

Being concerned as to whether the maxima might or might not be a consequence of short-term cycles, we created several tree-ring chronologies covering the years 300–400 according to equation (6.4). We assume that $E_t = 0$, and T_j, A_j, and Y_j are the cycle periods, amplitudes, and phases adequate to the predicted parameters of series of 100–150 years. For such series, we calculated trigonometrical amplitudes and density spectra. It turned out that the peaks of these functions were not observed with a frequency corresponding to the long-term cycles. Thus, the aforementioned results confirm the presence of long-term cycles and establish the period of T_j and phase of fluctuation Y_j where $j = 6$ or 7. Visual observations of dendrochronologies discussed above and observations made by other authors (Berry *et al.*, 1979; Komin, 1978b) indicate that the amplitude A_j of each cycle is directly proportional to its period T_j. Because of this, we selected an amplitude for each rhythm appropriate to its length. With the aid of the equation

$$\sum_{j=1}^{n} A_j \cos\left(2\pi t/T_j - Y_j\right), \quad n = 6 \text{ or } 7, \quad t = 1,2,\ldots, \tag{6.6}$$

Table 6.2. Chronologies obtained for selected long-term cycles from Canada and the USA.

No.	*Place of publication*	*Chronology number*
1.	Stokes *et al.*, 1973	071540
2.	Stokes *et al.*, 1973	526547
3.	Stokes *et al.*, 1973	064649
4.	Stokes *et al.*, 1973	525547
5.	Drew, 1975a	057540
6.	Drew, 1975a	066400
7.	Drew, 1975a	067540
8.	Drew, 1975a	106640
9.	Drew, 1975a	062649
10.	Drew, 1975a	056540
11.	Drew, 1975b	205749
12.	Drew, 1975b	057549
13.	Drew, 1975b	060540
14.	Drew, 1975b	058540
15.	Drew, 1975b	058540
16.	Cropper and Fritts, 1981	422880
17.	Cropper and Fritts, 1981	646749
18.	Cropper and Fritts, 1981	478749

where the index t refers to time (years), we determined the average variation of conditional change in the environmental background. The year 1500 was considered to be the start of fluctuations in ascertaining Y_j with $j = 1, 7$.

Equation (6.6) describes fluctuations with regard to some average value (for example, 100%). These values during the last century have some similarity (*Figure 6.17*), particularly for cycles of long duration in both groups of tree-ring chronologies [from the northern parts of the USSR (i.e., in the eastern part of the Hemisphere) and North America (i.e., in the western part of the Hemisphere)]. Hence, the background impact of long-term ecoclimatic fluctuations on the rhythm of short-term fluctuations may be similar in the whole Northern Hemisphere during the corresponding periods (for instance, 1920–1980). This means that for this period of time, the average long-cycle (735 years) variations of actual increment (ecoclimatic background fluctuations) (>35 years) can be used for larger regions in the Northern Hemisphere then when short-term fluctuations are considered. Such examples of approximation and forecasting in very damp and comparatively dry sites of the Lithuanian SSR are shown in *Figure 6.18.*

6.4.5. Conclusions

Fluctuations in tree-ring chronologies reflect ecoclimatic changes. To the extent that these fluctuations have a cyclical character, they can be used for practical purposes to forecast the main trends in wood increment dynamics due to ecoclimatic changes.

The variations of long-term cycles of dendrochronologies may be used to characterize the general tree-growth baseline and the baseline activity of other

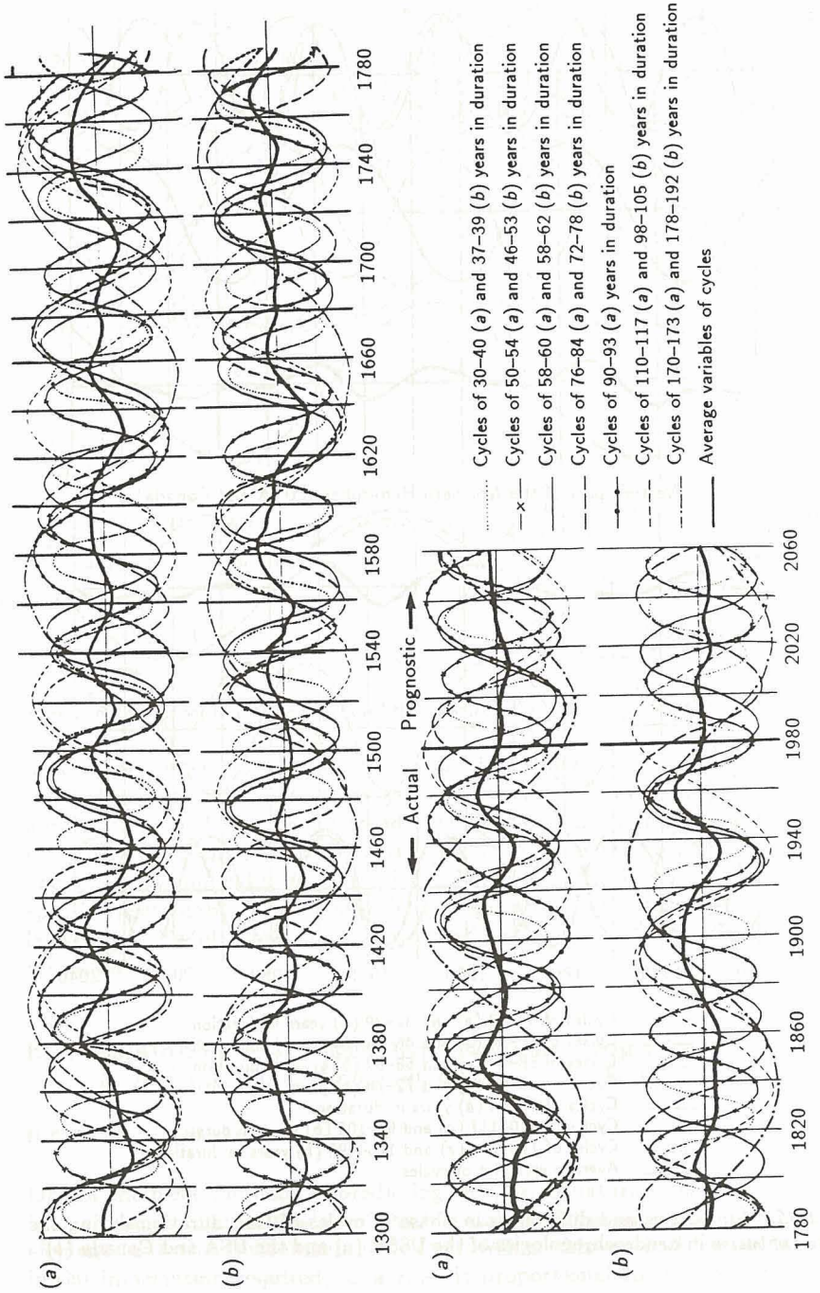

Figure 6.16. Cyclical fluctuations in the dendroscales of the USSR (*a*) and the USA and Canada (*b*).

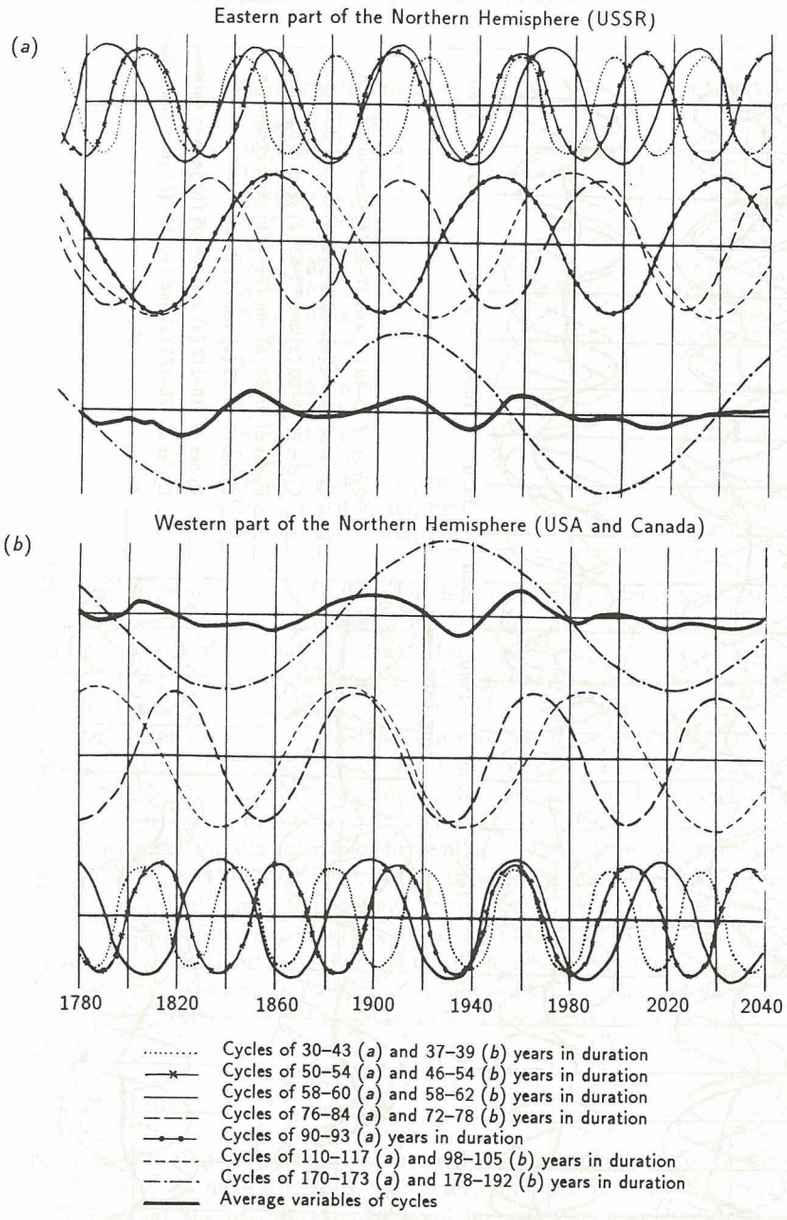

Figure 6.17. Similarities and differences in phase of cycles of long duration during the past two centuries in dendrochronologies of the USSR (*a*) and the USA and Canada (*b*).

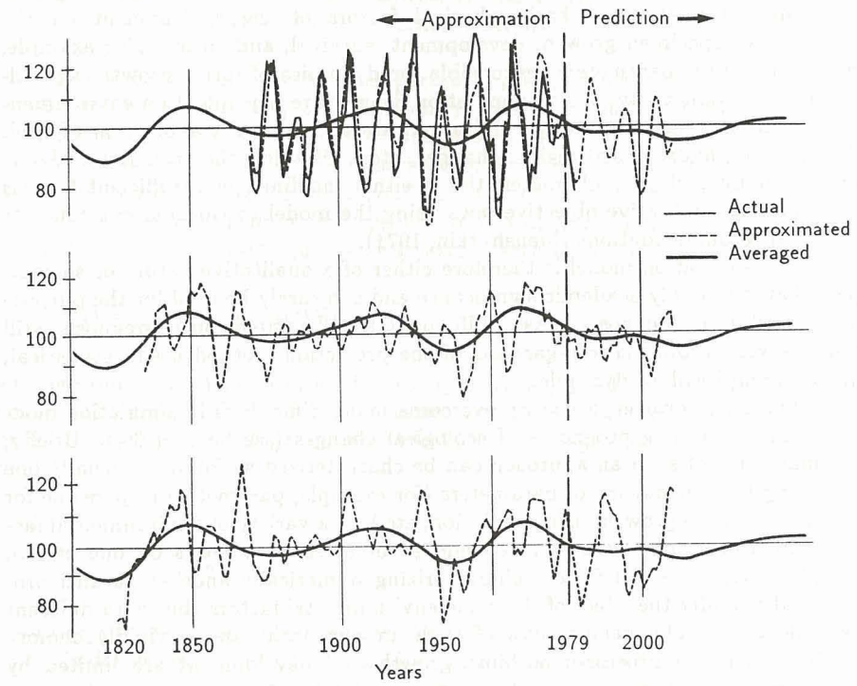

Figure 6.18. Ecoclimatic background fluctuation in the Lithuanian SSR.

production processes in the Northern Hemisphere. Short cycles of cyclical fluctuations of 8–13 and 20–25 years in duration proved that they could be applied to predict the current trend of tree growth and yield of agricultural crops in a given region. Apparently the cyclicity in dendrochronologies discussed above is also applicable to create a number of scenarios associated with the perspective sustainability of forest growth, regeneration of natural resources, assimilative capacity of plant cover, and changes in the CO_2 concentration in the atmosphere.

6.5. Examples of Dendrochronological Prognoses

L. Kairiukstis, E. Vaganov, and J. Dubinskaite

6.5.1. Introduction

One of the basic methods of predicting changes in natural ecosystems at present is to create simulation models of the interactive processes between the ecosystem elements and the environmental factors. When this method is used, the entire initial information required, as a rule, is proportional to the complexity of the

ecological system. Usually there is a shortage of experimental data, mainly that concerning the effect of basic physical factors of the environment on the processes of specimen growth, development, survival, and so on. For example, many important parameters responsible for dynamics of forest growth, agricultural crop productivity, or fish population density are dependent on environmental conditions (temperature, precipitation, abundance and composition of feed, illumination, hydrological regime changes, etc.). Besides, the accuracy of determining many ecological characteristics is either indefinite or insufficient to pass from finding qualitative objective laws using the model to working out concrete practical recommendations (Menshutkin, 1971).

The simulation model is therefore either of a qualitative nature or so complex that it has only academic significance and can rarely be used for the purpose of quantitative prognosis. As Williams (1977) pointed out, prognosis still remains very problematic regardless of the prediction method used: statistical, physical-empirical, or dynamic.

There is, however, a way to overcome many difficulties in simulation modeling and composing prognoses of ecological changes (see Section 6.4). Briefly, the main idea of such an approach can be characterized as follows. Usually one is looking for dependency of parameters (for example, parameters responsible for dynamics of crop growth, fish population, etc.) on a variety of environmental factors. Instead, one should find dependency of these parameters on one or two complex environmental factors characterizing numerically another parallel process that is under the effect of the same environmental factors (but with different dependencies). The perspectives of such an approach can be vividly demonstrated when the processes of biota growth and development are limited by environmental factors.

We will attempt to show the application of such methods that partially overcome simulation modeling difficulties by constructing ecological prognoses on the basis of the correlation between two biological processes: tree growth dynamics, on the one hand, and agricultural crop productivity, forest, or fish growth dynamics, on the other.

6.5.2. Prediction of the yield of agricultural crops in a given region

The models shown in Section 6.4, and particularly in equations (6.4) and (6.5), approximate well the generalized dendrochronologies for different species over various sites. Thus, it is feasible to use them to predict the future trends in the carrying capacity of ecological systems for 5–15 years. Such predictions can be considered only as the most probable scenario. Its probability is limited, on the one hand, by the validity of dendrochronologies being used and, on the other, by the assumption that the cyclical regularities in the future will remain the same as those in the past. Let us therefore discuss the application of dendrochronological predictions in agriculture.

Such a prognosis has, for example, been calculated for the Lithuanian SSR. We investigated the dependency of the dynamics of grain crops on the fluctuations of dendrochronological series $x_1(t)$ and $x_2(t)$, where $x_1(t)$ refers to a series

of increment indices of the *Pinus sylvestris* master (regional) chronology from comparatively dry sites of the Lithuanian SSR while $x_2(t)$ refers to that from very damp areas.

The same climatic factors (temperature, precipitation, etc.) affect the tree increment on dry and damp sites differently. It is possible to assume that vector $[x_1(t), x_2(t)]$ reflects the impact of the ecoclimatic background of the given region. To begin, from the yield of series of agricultural crops $y(t)$ (tons/ha), we estimated the technological trend $D(t)$ due to such factors as an increase in the use of fertilizers and improved agricultural practices. For this purpose we applied the model of least squares. Further, in accordance with the equation

$$w(t) = [y(t)/D(t)] \cdot 100\% \quad ,$$

we determined $w(t)$ main crop (barley, rye, wheat) yield indices free from the trend. These depend only upon weather conditions. To evaluate the climatic background impact $[x_1(t), x_2(t)]$ on yield indices, we applied a lagged regression model:

$$w(t) = a + \sum_{j=2}^{2} [a_j x_1(t+j) + b_j x_2(t+j)] + e_i \quad , \tag{6.7}$$

where $\{e_i\}$ refers to independent normal errors.

To derive equation (6.7), we used a stepwise procedure (the method of stepwise regression) of the statistical package BMDP (Biomedical computer programs, *P*-series, 1977, the Program P2P, Dixon, 1983). Initially, we estimated coefficients a, a_j, b_j, $(j = -2, 2)$, and for each variable $[x_1(t+j), x_2(t+j)]$ we calculated particular coefficients of the correlation and used the F-test to select variables for removal. From equation (6.7), we removed the variable, shown by the F-test to be least important and nonessential. Then, we again estimated a, a_j, b_j coefficients with the remaining variables and calculated particular coefficients of the correlation and repeated the F-test. We continued the procedure of removing variables until the F-test no longer removed variables. This resulted in an approximation $w(t)$ of the following series:

$$w(t) = 146 + 1.07\tilde{x}_2(t-1) - 1.54\tilde{x}_1(t+2) \, , \tag{6.8}$$

where

$$\tilde{x}_i(t) = A_o + \sum_{j=1}^{n} A_j \cos(2\pi t/T_j - Y_j) \, , \quad i = 1, 2 \quad ,$$

which refers to the approximation of the climatic background of the given territory $[x_1(t), x_2(t)]$. Approximating series by equation (6.8) explains 72% of the variance. Relying on the prognoses of the trend of yields and on those of the

climatic background $x_1(t)$, $x_2(t)$ as well as of equation (6.8), it is feasible to calculate exemplary yield (tons/ha) prognoses. For example, in the late 1970s this agricultural crop scenario was calculated for the Lithuanian SSR (Kairiukstis and Dubinskaite, 1986), and subsequent agricultural yields verified the scenario forecasts (*Figure 6.19*).

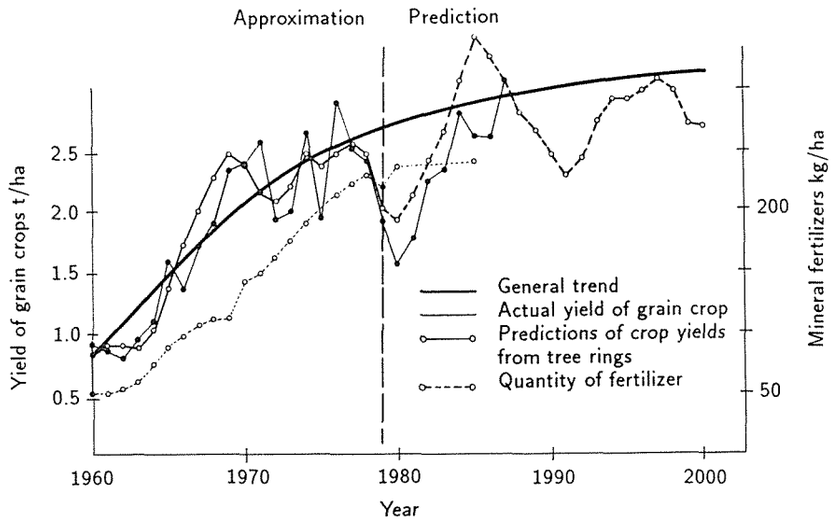

Figure 6.19. Yield of grain crops in the Lithuanian SSR.

6.5.3. Forecasting fish population dynamics and fish catch

The dynamics of fish growth, fish catches from the Chatanga River, and dendrochronological characteristics of dauric larch (*Larix gmelini*) growing along this river were studied. We have found the dendrochronological series to be a complex parameter of the seasonal growth rate. At the same time, these series were found to be integrated parameters of seasonal temperature dynamics (Vaganov *et al.*, 1985). The scale-curve method (Vaganov, 1978) was used to determine fish age and to analyze the dynamics of linear fish growth. Data treatment by statistical methods (spectral analysis) allowed us to obtain a reliable estimation of the yearly growth rate. The data of more than 40 years of vendace (*Coregonus sardinella*) catch were used. These series were first transformed into index series from initial data by the removal of the component determined by fishery organizations, fishery conditions, and other factors of a nonbiological origin (*Figure 6.20*).

Spectral analyses of the initial data on the catch of every species of sigs, pike, and burbot, as well as on larch-growth dynamics, were carried out. The

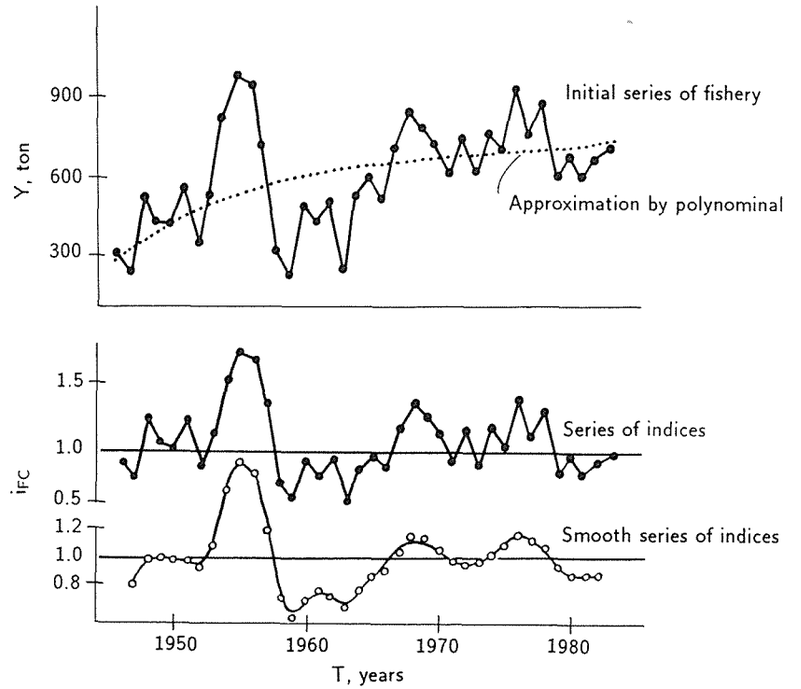

Figure 6.20. Example of vendace (*Coregonus sardinella*) catch dynamics.

results showed the presence of a considerable 20-year cyclical component. Various fish species reaching maximum size corresponding to the maximum cell size of the larch tree-ring [reflecting perennial variance temperature conditions (Vaganov *et al.*, 1985)] were compared with smoothed curves of fish catch. This comparison (*Figure 6.21*) showed that catch curves are qualitatively similar to the dendrochronological series, shifted by a different number of years (depending on the fish species). There is coincidence not only of the main 20-year cycle, but also of small variations in some cases.

Since the cell size curve characterizes temperature variations, one can assume that the temperature regime also determines different age-class populations of fish species. The time shift between the curves is sufficiently constant. It means that temperature conditions of a specific year are responsible for the initial age-class populations of fishes for a given year. Therefore, the value of the delay time interval should be consistent with a period of mass fish maturity. Thus, the rising temperature, and consequently the warming of the water and prolongation of growth season, increases the population of spawned fish. Evidently, with the improved temperature conditions the increased number of fish reflects the decreased mortality of young fish by accelerating the process of fish development and growth. It also decreases the time period of strong *pressure* from predators and increases the availability of food for the growing young fish.

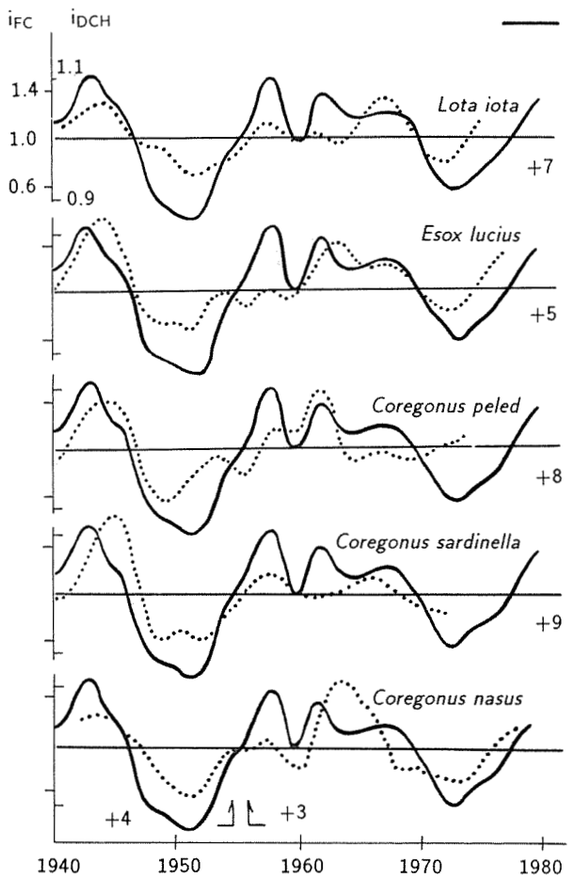

Figure 6.21. Comparison of smoothed curves of fish catch indices with dendrochronological series of larch cell size indices.

The analysis of annual scale curves chosen from a random sample of spawning vendace from a two-year catch showed that the ninth year class predominates. If we assume that the first arrival for spawning makes the main contribution to the fishery, then the large population of this class was determined by the improved temperature conditions affecting the first year class nine years ago. The catch-index curve is shifted against dendrochronological series by the same number of years. The analysis of the scale curve allows us not only to estimate the age, but also to measure the yearly growth rate. The corresponding measurement showed (*Figure 6.22*) a good agreement between larch cell size variability and linear growth of vendace for certain years (correlation coefficient = 0.91).

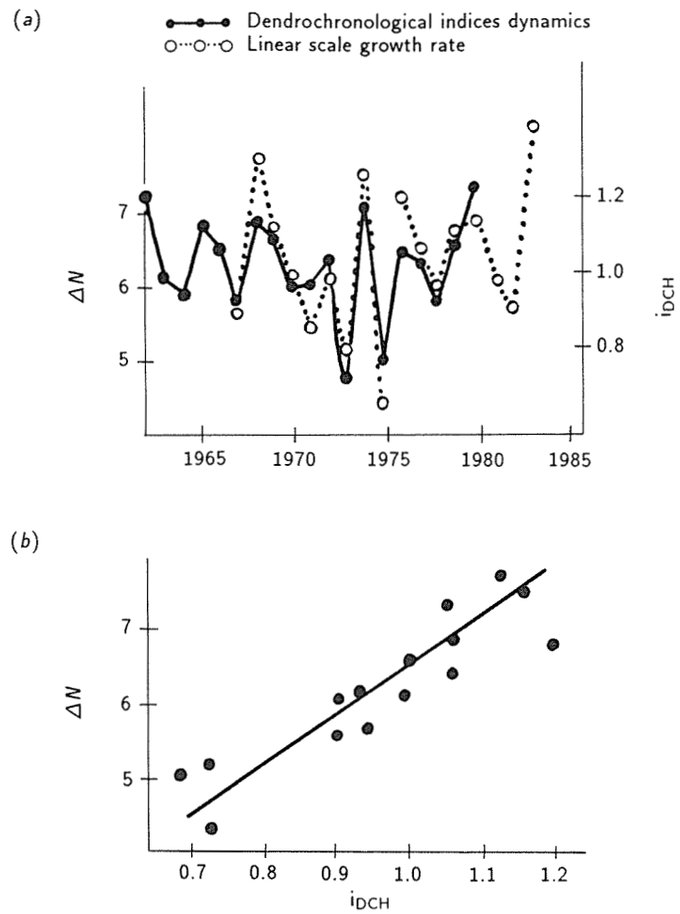

Figure 6.22. Comparison of dendrochronological indices dynamics with the vendace linear scale growth rate for the same years (*a*) and correlation between them (*b*).

Thus, both the population of each vendace generation involved in the fishery and the dynamics of linear and weight growth are closely connected with changes in the temperature regime, characterized by a complex dendrochronological index that is the cell size in tree rings of larch. Therefore, when creating a simulation model of vendace fishing, there is no need to consider the effect of a variety of environmental factors (water temperature, estimation of feed, feed heterogeneity, duration of life span, and so on). It is possible to introduce, in a simple age-structure model of fish population, a dendrochronological index as one environmental factor. The index is characteristic of the environmental effect

on fish survival and the rate of fish growth. We shall demonstrate this using the model.

To consider the dynamics of age structure and fish population, the generally accepted model (Svirezgev and Logofet, 1978; Fedorov and Gilmanov, 1980) is used with the following assumption: only mature species of reproductive age are considered for harvest; and survival of young fish (first year class fishes) in the first year of growth is correlated with the value of a complex dendrochronological index.

Let us take $x_i(t)$ for a number of fishes and $y_i(t)$ for mean weight of fishes of age i at time t (a year), n for a number of age groups in a population. Then, dynamics of age structure can be described by the following system of equations:

$$x_i(t+1) = s_o x_o(t) = s_o \frac{A}{2} \sum_{j+1}^{n} x_j(t) y_j(t)$$

$$x_2(t+1) = s_1 b^2(t+1) x_1(t)$$

$$x_3(t+1) = s_2 x_2(t)$$

$$x_1(t+1) = s_{l-1} x_{l-1}(t)$$

$$x_{l+1}(t+1) = s_l x_l(t) \cdot k$$

$$x_n(t+1) = s_{n-1} x_{n-1}(t) \cdot k \quad .$$

Here, l = the age of maturing, s = the coefficient of survival of corresponding age class, k = the coefficient characterizing fish yield, A = the quantity of roe per unit of weight of a mature fish (female), $b(t)$ = the value of dendrochronological index that shows that survival of young fish is higher during years with a favorable temperature regime.

Besides the age model, the simple model of weight growth is used with the assumption that the weight increase per year depends on age in correspondence with a parabolic law of growth (Vaganov, 1978), on current weight, and on the complex dendrochronological index (*Figure 6.22*). The dynamics of mean weight of fish of a separate age group is

$$y_{i+1}(t+1) = b(t+1) y_i(t) \quad .$$

This expression for vendace considering the data from literature on the subject is

$$y_{i+1}(t+1) = [1 + 1.2b(t+1)/i] y_i(t) \quad .$$

The coefficients s and A are obtained experimentally from the single analysis of vendace population of the river Hatanga (Lukjanchikov, 1967). These coefficients as well as coefficient k are constant in the calculations of the model even though there are no restrictions to consider their dependence on the current conditions of the complex dendrochronological index.

In correspondence with the representation of dynamics of fish number and fish mean weight, withdrawal was calculated for each year:

$$Y(t) = (1 - k) \sum_{j=1}^{n} x_j y_j \quad .$$

Representation of a small number of coefficients of the model obtained experimentally makes it possible to compute numerical calculations of vendace fishing using known dendrochronological series. Corresponding calculations made according to the conventional age model demonstrated a good correlation between calculated and real curves of catch (*Figure 6.23*) with a high correlation coefficient (+0.875).

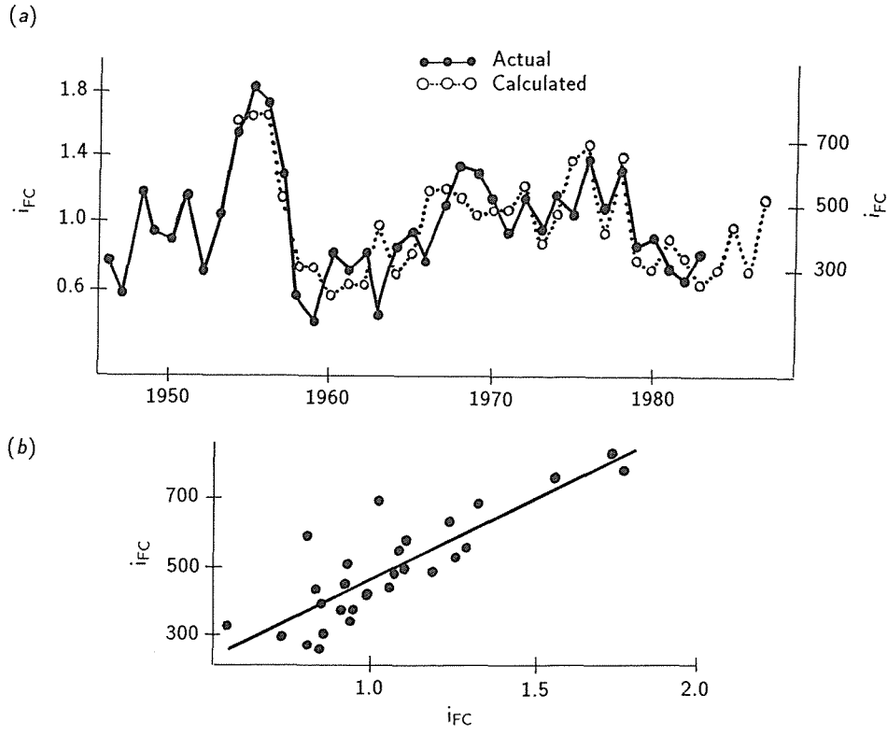

Figure 6.23. Comparison of dynamics of actual and calculated values for vendace fishing (*a*) and correlation between them (*b*).

Apparently, this approach to ecological forecasting may be used not only for ecosystems with one factor of growth limitation. Actually, in each year, the growth rate may be influenced by several environmental factors; therefore the correlations between the growth parameters and environmental factors are multiple. The left part of the time-sequence data can then be used to create a multiple regression model to calculate the characteristics of one process using independent characteristics from the other. The right part of the sequence (series) can be used to verify the regression model and forecast.

6.5.4. Prediction in forest practice

Predictions of ecoclimatic fluctuations of short duration have already found applications in the practice of forestry. For example, in the Lithuanian SSR, fertilizers in the forest are applied two years before the predicted maximum increment for the same forest under ideal conditions, using the 11-year cyclicity in dendrochronologies. Also, timing of forest thinning is rescheduled according to the maximum increment predicted. The thinning effect is higher when thinning is applied two to three years before the predicted maximum increment. Forest reclamation is also applied one to two years after the maximum forest increment on the same soils predicted by dendrochronologies. Using these measures has made it possible to obtain an additional 15–30% wood increment.

The ability to predict ecoclimatic fluctuations of long duration for entire regions opened up new spheres for the application of dendrochronology in planning forest use as well as in the practice of regional management.

For example, as was stressed in the resolution drawn up at the Workshop on Forest Decline and Reproduction: Regional and Global Consequences (Krakow, Poland, 1987), the long-term ecological background changes influence to a considerable extent the sustainability and productivity of forest ecosystems, sometimes strengthening and sometimes weakening them. The long-term changes of forest-system productivity as illustrated in *Figure 6.17* can lead to further decline and changes in the amount of estimated forest use, particularly when short rotation is being applied. There are scenarios calculated for allowable wood cutting until the year 2135 for the Lithuanian region using long-term dendrochronological cycles (Kairiukstis *et al.*, 1987a). Scenarios revealed a decrease in available wood by the middle of 21st century in the Baltic region due to unfavorable climatic changes and long-term forest decline.

6.6. Prognosis of Tree Growth by Cycles of Solar Activity

T. Bitvinskas

In the Dendro-climato-chronological Laboratory of the Institute of Botany (Lithuanian Academy of Sciences) some pointer or registration years were used to which radial tree growth could be *attached* to forecast environmental conditions of forest growth. Solar activity expressed by the number of sunspots (according to Wolf) for hydrological years was chosen as the basis for selecting

pointer years. It was shown that in certain regions of the USSR there is a clear correlation between the amplitude of the 22-year cycles and the radial tree growth during the same period (Bitvinskas, 1967, 1971). In different phases of the solar activity at maxima marked *a* and *b* and minima marked *c* and *d* as well as in time periods of increasing and decreasing solar activity marked *ac* and *cb* and *bd* and *da* (*Figure 6.24*), forest growth in varying regions and under various growth conditions is very different.

Research was based on the assumption that at certain phases of solar activity, we can expect – with certain probability – extreme radial tree growth (maximum or minimum) for given periods of time. The method conceived involved all the processes that have affected tree growth during certain phases of the solar activity.

Hydrological years (September–December of the previous year through January–August of the present year) of the highest and lowest solar activity are considered pointer years for *attachment* of dendrochronological data. The central year of the three years with extreme values of the Wolf sunspot number are considered pointer years. We attached yearly data of tree-rings and their indices to the pointer years of the solar activity and studied the growth trend for given regions, sites, and species. Confirmed data can date the Wolf sunspot number as far back as 1749, which at present form twenty-one 11-year and eleven 22-year cycles. Solar activity series in the pointer years systems were checked according to Shove's system (see Vitinskiy, 1963; Vitels, 1977). Ecological forecasting is based upon the definite prognoses of 11-year and 22-year cycles of the solar activity. It is known that the prognosis of the solar activity is guided by mathematical modeling of regularities of variability of the Wolf sunspot number (Vitinskiy, 1963, 1983; Vitels, 1977). We tried to use the method of overlapping epochs while making up generalized series of the solar activity for the hydrological year to reveal the distinctive features in time for the 22-year cycles as well as the 44-year and 88-year cycles. *Table 6.3* shows the pointer years of the solar activity according to the first and second maxima (*a, b*) and the first and second minima (*c, d*) of the solar activity including prognosis collated statistically.

The average data on solar activity allow one to calculate the average variability and to use it as the standard. We can thus forecast and reconstruct (*Figure 6.24*).

With this pointer year system, it is easy to make tables of the relationships between dendroclimatological data and the pointer years of past solar activity. If there are long enough series of natural phenomena (e.g., tree-ring indices, air temperature, precipitation, complex climatic indices, earthquakes), the method can be used to process this information and reveal whether there are some regularities connected with solar activity. The width of tree-rings or calculated yearly indices can be easily attached to the maximum and minimum of the 22-year cycles of the solar activity from 1745 to the present. This numerical and graphical method enables one to link the different increments of a tree's different phases to solar activity. For example, the distribution of dendrochronological indices of *Pinus sylvestris* in western Lithuania, according to the years in relation to pointer years of the first maximum solar activity, is shown in *Table 6.4*.

Table 6.3. Pointer years of the solar activity.

Cycle no.	Phases of the solar activity: a First maximum	c First minimum	b Second maximum	d Second minimum
0			1751	1755
1	1761	1765		
2			1770	1775
3	1779	1784		
4			1788	1798
5	1804	1811		
6			1817	1823
7	1829	1834		
8			1837	1843
9	1849	1856		
10			1860	1867
11	1871	1876		
12			1884	1889
13	1894	1900		
14			1907	1913
15	1918	1923		
16			1928	1933
17	1937	1944		
18			1948	1954
19	1958	1964		
20			1969	1976
21	1980	(1987)		
22			(1991)	(1997)

Table 6.4. Distribution of yearly indices of pine (*Pinus sylvestris*) in Neriga, western Lithuania (soil site: *Pinetum Oxalidosa-myrtilosum*); to the years of the first maximum of solar activity.

Group of cycles	Cycles	Value of yearly indices											
1	1	108	103	84	128	108	127	103	97	124	107	89	80
2	3	118	98	104	117	138	45	36	62	76	85	116	119
1	5	88	111	130	141	34.5	29	49	67	90	70	67	77
2	7	127	90	76	106	120	85	71	116	113	89	90	77
1	9	49	116	117	96	81	100	110	64	37	62	122	160
2	11	155	104	74	53	77	112	133	108	90	116	128	118
1	13	102	111	98	88	126	181	102	85	115	71	34	48
2	15	28	82	121	160	132	114	125	91	91	90	84	109
1	17	97	83	78	93	104	137	123	132	64	142	117	94
2	19	102	80	92	86	107	94	140	76	59	54	83	114
I gr.	M	89	105	101	109	91	115	97	89	86	90	86	92
II gr.	M	106	91	93	104	115	90	101	91	86	87	100	107
M	Aver.	97	98	97	107	103	102	99	90	86	89	93	100
		−5	−4	−3	−2	−1	0	+1	+2	+3	+4	+5	+6

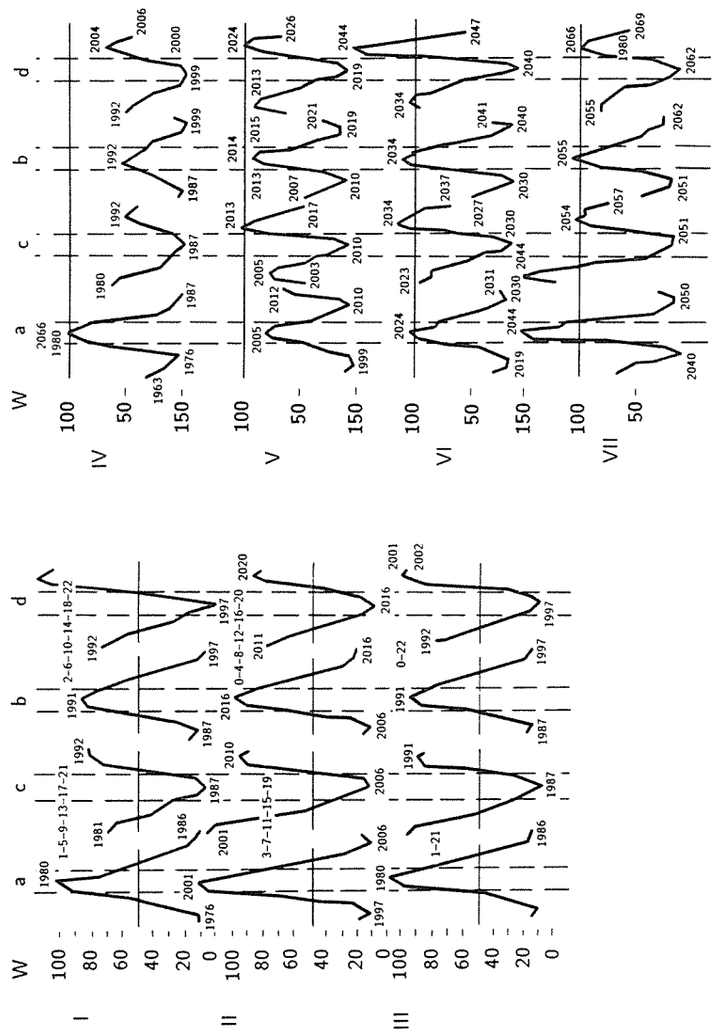

Figure 6.24. Conditional prognoses of 22-year (I, II), 44-year (III), and 88-year (IV, V, VI, VII) cycles of solar activity, calculated according to adequate variability of values of the Wolf sunspot number: W (Wolf sunspot number averaged for adequate cycles); *a,b,c,d* (pointer years of solar activity); 1-5-9-,... (cycles numbers, see *Table 6.3*); 1976, 1980,... (calendar years, 1–21 for whole single and 0–22 for whole even cycles).

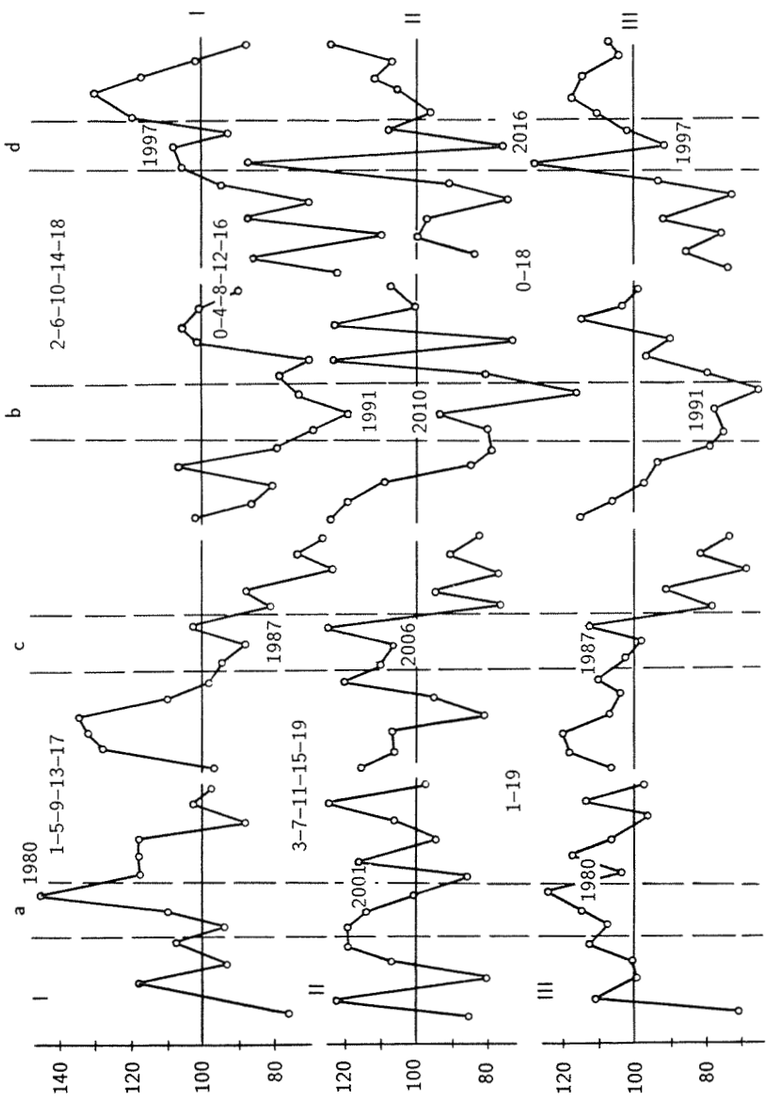

Figure 6.25. Current and anticipated tree-growth indices for *Larix sibirica* in the polar Ural Mountains attached to pointer years forecast from solar activity. (From Shiyatov, 1986.)

Regularities of growth thus revealed from the past are transferred to the future and attached to anticipated pointer years (a,b,c,d) of solar activity. Thus, for instance, current and anticipated tree-growth indices calculated by the method above are presented in ***Figure 6.25*** for polar Ural Mountains, according to dendrochronologies of *Larix sibirica* published by Shiyatov (1986). By comparing these results with the prognosis of forest growth in the west Siberian forest tundra derived by approximation and extrapolation by sinusoids (***Figure 6.8***), great similarity can be found.

Summing up we can state that the pointer year system of the solar activity is one method that allows one to foresee the future trend of tree growth according to the regularities of the growth in the past.

6.7. Possible Future Environmental Change

P.D. Jones

6.7.1. What major environmental changes are expected over the next century?

The major change in the environment over the next 50 to 100 years is expected to result from changes in the climate due to increasing concentrations of carbon dioxide and other gases in the atmosphere. Since about 1750, and particularly since the middle of the 19th century, CO_2 concentrations have increased as a result of the activities of man. CO_2 concentrations in 1985 were 345 ppmv, a value that is almost 25% more than the level that is now thought to have existed in the 1850s (Neftel *et al.*, 1985; Raynaud and Barnola, 1985). Apart from carbon dioxide, concentrations of other radiatively active trace gases, such as CH_4, N_20, 0_3, and CFCs (which act like CO_2), have been increasing rapidly over the last 25 years. Based on projected future energy use scenarios, it is to be assumed that these gases will continue to increase and the concentration of CO_2 and other trace gases (converted to equivalent CO_2) will double the 1850 preindustrial level by as early as 2030 (Bolin *et al.*, 1986).

The potential climatic effects of this increase in CO_2 and other trace gases in the atmosphere, as estimated by numerical models of the global climate system, would constitute a major alteration to the present climate regime and have far-reaching economic and social implications. The latest model results indicate that the global mean temperature would increase by between 1.5 and 4.5° C as a result of the CO_2 and other trace gas increases (MacCracken and Luther, 1985; Bolin *et al.*, 1986). The rise will not be rapid but will occur gradually, albeit with increasing speed, over many years. Because of the nature of the climate system and the inherent lag of the system to forcing, the full effects will not be evident until many years after equivalent CO_2 levels have doubled. The latest projected rise over the next 25 years (i.e., to 2010) is for an increase of between 0.3 and 0.6° C. Such a rise is of the same magnitude as the rise in global temperatures that has occurred during the last 100 years.

The increase in global mean temperature will not be uniform over the Earth. Most areas will warm, but some may even cool. General Circulation

Models (GCMs) suggest that the greatest warming will occur in polar latitudes and be amplified during the winter half of the year. Such projections are based on an instantaneous equilibrium response to increased CO_2 levels. In the real world CO_2 concentration will increase gradually and the transient response may be different from the equilibrium response with its fixed CO_2 level.

Overall temperature rise is not the only response of the climate system to the change in the thermal regime of the Earth caused by the adjustment to the radiation budget of the planet. There will be associated alterations in the present precipitation and pressure patterns affecting almost all aspects of the climate system. However, just as the spatial pattern of the temperature response can only be estimated, the spatial nature of the changes in these other parameters can also only be projected – with varying degrees of uncertainty.

Two types of analysis have been used to try to assess possible future changes in the climate. Both have their limitations, and both must be considered as guides or scenarios as to what might happen. They are not forecasts but best possible projections that fit the facts as we currently know them. Scenarios can be developed using either past instrumental or proxy data from previous warm periods or GCM model projections of what the climate might be in a higher CO_2 world. Instrumentally or proxy-based scenarios have some advantages because they occurred in the past. They are based on the assumption that any pattern of warming will be similar whatever the cause. Warm periods from the past can therefore be used as analogs to the future. The arguments against such scenarios are that the projected increase in global mean temperatures, likely to occur in the future, is much greater than any previous warm period and the response of the climate system may not be linear. The argument against GCM-based scenarios is that GCMs do not model present-day climate well; therefore, confidence cannot be placed in their projections.

The use of the scenario approach has been widespread. Potential implications for agriculture have been discussed by Warrick *et al.* (1986a, 1986b) for water resources by Callaway and Currie (1985), for forestry by Shugart *et al.* (1986) and by Solomon and West (1985), and for climate by Webb and Wigley (1985) and by Wigley *et al.* (1986).

For forestry, Solomon and West (1985) identified the following five important areas:

(1) The life spans of trees are long; unlike crops, experimentation in the field throughout the life of the tree is not possible. We therefore require complete understanding of tree dynamics.
(2) Although management is important, forests are dominated by the stability of the climate and any climatic change. It is therefore vital to understand this if forest management techniques might ameliorate the effects of climatic change.
(3) The direct effects of increasing atmospheric CO_2 concentrations range from growth enhancements to growth retardations.
(4) Combined with the indirect effects of climatic warming, air pollution, and other environmental factors, forests can respond by enhancing growth or by forest dieback.

(5) Two types of models (empirical and conceptual) may be used to resolve the many issues. Both have their place, and neither can be discounted.

6.7.2. What might be the effects on tree rings of increased levels of carbon dioxide?

Enhanced carbon dioxide levels are often used by horticulturalists and market gardeners to increase plant growth. In small-scale growth-chamber experiments, levels of CO_2, higher than those normally in the atmosphere, have been shown to increase plant growth and the yield in C-3 plants (see Strain and Cure, 1985). Increases in CO_2 levels are often of the order of two to four times greater than present levels in experimental chambers in order for increases in yield to be measurable.

If the measured level of CO_2 in the atmosphere can be taken as a proxy for ambient CO_2 levels in forests, the increase in the real world is only 25% above levels in the mid-19th century. Actual levels measured in forest stands vary widely from season to season and within the day. Global average CO_2 levels may not be related to or be relevant to those in forest stands. The relationship between local and global levels of CO_2 requires further study.

The effects of increasing carbon dioxide ought to be evident by increased tree-ring widths. This is a direct effect that may be observed in chambers with fixed conditions. Most experiments are undertaken with agricultural crops, and it is to be assumed that increases in growth seen in these crops also apply to forest trees. There are two indirect effects. First, trees and other plants use water more efficiently at higher CO_2 levels. They should therefore be less susceptible to drought. They also use nitrogen more efficiently and growth is not as severely limited by nitrogen deficiency. Second, in most areas of the world higher CO_2 levels are expected to increase air temperatures. When combined with greater water efficiency and similar or slightly lower than normal precipitation, growth increases are likely.

If we are seeking to detect the effect of increasing CO_2 levels, we must be aware of this potential combination of factors. It would seem unlikely that we will ever be able to distinguish between the direct and indirect effects.

6.7.3. How might these changes be detected?

Detection of changes in tree growth requires a rigorous statistical approach that seeks to isolate effects that may be induced by factors other than those occurring naturally. Possible factors include the rise of carbon dioxide concentrations in the atmosphere and the rate and amount of acidic deposition and other pollutants. Both factors are new and are the direct result of industrialization in the last 150 years.

To claim detection we must either isolate a known signal in the tree-ring series or show that *unprecedented* changes have occurred in the series (Wigley *et*

al., 1986). Knowledge of the signal implies that we have an expectation of what might happen and that this is what we are looking for. From growth-chamber experiments we would expect the rise in atmospheric CO_2 concentrations to lead to an increase in tree growth. Whether this increase is the direct or indirect effect discussed earlier is probably immaterial to detection. We should, however, be aware that the possibility of combined effects exists.

In the unprecedented case we do not know what to expect. We have, however, a long record of tree-ring behavior (ring width, density, variability, etc.) against which to test recent growth changes. The idea behind this approach is that if unprecedented changes in tree-ring series have occurred recently then some new forcing factor is affecting tree growth. Attribution of these changes to a potential factor is only possible once all other factors have been considered. In general it is difficult to consider every possibility and give reasoned explanations why a factor is not important. For example, although climate might explain some of the variance of the tree-ring patterns it may be that the unprecedented changes resulted from one extreme event not present in the record before.

In any detection strategy it is always better to start with some knowledge of what the effects might be. In the CO_2-fertilization case we have an undisputed hypothesis based on experimentation. In the acidic deposition case, there is no accepted theory or model of what the effects might be. Effects will probably differ from site to site depending specifically upon soil type and species.

Three detection strategies have been considered by Wigley *et al.* (1986): noise reduction, signal maximization, and fingerprint studies. Before any strategy can be put forward it is important to understand the effects on tree-ring parameters of any form of indexing or filtering that has been used on the tree-ring data (Briffa *et al.*, 1987; Wigley *et al.*, 1987; this volume Chapter 3). The effects of the CO_2-fertilization factor on tree growth might be to increase tree growth slowly. The effect will therefore probably be seen in the lower frequency part of the chronology. Any indexing procedure that has been shown clearly to affect the low-frequency part of the tree-ring series would be most inappropriate. It is therefore important to have a good knowledge of the frequency aspects of any indexing procedure. In general these aspects are hardly ever discussed (Briffa *et al.*, 1987). Furthermore, if detection is sought in the low-frequency parts of tree-ring series it is important to have some idea of the statistical confidence in the series, especially when the average is made up of few samples (Wigley *et al.*, 1987).

In noise reduction studies an attempt is made to factor out the effects of one or more known factors to enable the effects of other factors to be seen more clearly. The most appealing variable to factor out is the high-frequency variation due to climate. Signal maximization seeks to detect the effect in the area most likely to be affected by theoretical studies. It has been suggested that CO_2 fertilization might be enhanced at high elevations where pressure is reduced markedly. LaMarche *et al.* (1984, 1986) have used this approach to see if growth changes can be seen in long-lived pines from the southwestern United States at elevations higher than 3,000 m. Fingerprint studies seek to detect a combination of effects all of which might be expected to occur from theoretical or modeling studies.

Appendix A

List of Tree Species Known to Have Been Used to Build Tree-Ring Chronologies

Scientific name	*Common name*
Abies alba	Fir, European
Abies balsamea	Fir, Balsam
Abies concolor	Fir, White
Abies lasiocarpa	Fir, Alpine
Abies pindrow	Fir, Himalayan Silver
Abies procera	Fir, Noble
Abies spectabilis	Fir, Silver
Acer rubrum	Maple, Red
Acer saccharum	Maple, Sugar
Agathis australis	Pine, Kauri
Araucaria araucana	Pine, Chile
Artemisia tridentata	Sagebrush, Big
Arthrotaxis cupressoides	Pine, Pencil
Arthrotaxis selaginoides	Pine, King William
Austrocedrus chilensis	Cedar, Chilean Incense
Betula alleghaniensis	Birch, Yellow
Betula carpatica	Birch, Carpathian
Betula papyrifera	Birch, Paper
Betula pubescens	Birch, White
Callitris robusta	Pine, Rottnest Island
Carya illinoensis	Pecan
Cedrela angustifolia	Cedar
Cedrus atlantica	Cedar, Atlantic
Cedrus deodara	Cedar, Himalayan
Cryptomeria japonica	Cedar, Japanese
Dacrydium biforme	Pine, Pink
Dacrydium colensoi	Pine, Silver
Dushekia viridis	
Fagus grandifolia	Beech, American
Fagus sylvatica	Beech, European
Fitzroya cupressoides	Alerce
Fraxinus americana	Ash, White
Juglans australis	Walnut
Juniperus occidentalis	Juniper, Western
Juniperus osteosperma	Juniper, Utah
Juniperus scopulorum	Juniper, Rocky Mountain
Juniperus turkestanica	Juniper, Turkestan
Juniperus virginiana	Cedar, Eastern Red
Larix decidua	Larch, European
Larix laricina	Larch, Tamarak
Larix lyallii	Larch, Subalpine
Larix occidentalis	Larch, Western
Larix sibirica	Larch, Siberian
Libocedrus bidwillii	Cedar
Libocedrus chilensis	Cedar, Chilean
Libocedrus decurrens	Cedar, Incense
Liriodendron tulipifera	Tuliptree
Nothofagus gunnii	Beech, Tanglefoot
Nothofagus menziesii	Beech, Silver
Nothofagus obliqua	Beech, Southern
Nothofagus solandri	Beech, Mountain
Phyllocladus alpinus	Pine, Alpine Celery-top

Phyllocladus asplenifolius	Pine, Celery-top
Phyllocladus glaucus	Toatoa
Phyllocladus trichomanoides	Tanekaha
Picea abies	Spruce, Norway
Picea engelmannii	Spruce, Engelmann
Picea excelsa	Spruce, Norway
Picea glauca	Spruce, White
Picea mariana	Spruce, Black
Picea obovata	Spruce, Siberian
Picea orientalis	Spruce, Oriental
Picea rubens	Spruce, Red
Picea schrenkiana	Spruce, Schrenka
Picea sitchensis	Spruce, Sitka
Picea smithiana	Spruce, Himalayan
Pilgerodendron uviferum	Cipres de las Guaitecas
Pinus albicaulis	Pine, Whitebark
Pinus aristata	Pine, Bristlecone (Rocky Mountain)
Pinus balfouriana	Pine, Foxtail
Pinus banksiana	Pine, Jack
Pinus cembra	Pine, Stone
Pinus cembroides	Pinyon, Mexican
Pinus contorta	Pine, Lodgepole
Pinus echinata	Pine, Shortleaf
Pinus edulis	Pinyon, Colorado
Pinus flexilis	Pine, Limber
Pinus gerardiana	Pine, Gerard's
Pinus halepensis	Pine, Aleppo
Pinus jeffreyi	Pine, Jeffrey
Pinus koraiensis	Pine, Korean
Pinus lambertiana	Sugar, Pine
Pinus leiophylla (chihua.)	Pine, Chihuahua
Pinus leucodermis	Pine, Besnian
Pinus longaeva	Pine, Bristlecone (Great Basin)
Pinus monophylla	Pinyon, Singleleaf
Pinus mugo	Pine, Mountain
Pinus nigra	Pine, Black
Pinus palustris	Pine, Longleaf
Pinus pinaster	Pine, French Maritime
Pinus pinea	Pine, Umbrella
Pinus ponderosa	Pine, Ponderosa
Pinus pumila	
Pinus quadrifolia	Pinyon, Parry's
Pinus resinosa	Pine, Red
Pinus rigida	Pine, Pitch
Pinus roxburghii	Pine, Chir
Pinus sibirica	Pine, Siberian
Pinus strobus	Pine, White
Pinus sylvestris	Pine, Scots
Pinus taeda	Pine, Loblolly
Pinus uncinata	Pine, Mountain
Pinus wallichiana	Pine, Kail
Platanus occidentalis	Sycamore, American
Populus balsamifera	Poplar, Balsam
Populus fremontii	Cottonwood, Fremont

Populus grandidentata	Aspen, Bigtooth
Populus tremuloides	Aspen, Quaking
Prunus serotina	Cherry, Black
Pseudotsuga macrocarpa	Spruce, Bigcone
Pseudotsuga menziesii	Fir, Douglas
Quercus alba	Oak, White
Quercus lobata	Oak, Valley White
Quercus lyrata	Oak, Overcup
Quercus macrocarpa	Oak, Burr
Quercus petraea	Oak, Durmast
Quercus pontica	
Quercus prinus	Oak, Chestnut
Quercus pubescens	
Quercus robur	Oak, English
Quercus rubra	Oak, Red
Quercus stellata	Oak, Post
Quercus velutina	Oak, Black
Sequoiadendron giganteum	Sequoia, Giant
Taxodium distichum	Cypress, Bald
Tectona grandis	Teak
Thuja occidentalis	Cedar, Northern White
Tilia americana	Basswood
Tsuga canadensis	Hemlock, Eastern
Tsuga caroliniana	Hemlock, Carolina
Tsuga heterophylla	Hemlock, Western
Tsuga mertensiana	Hemlock, Mountain
Ulmus rubra	Elm, Slippery
Widdringtonia cedarbergensis	Cedar, Clanwilliam

Appendix B

Sample Site and Tree Information Forms for Tree-Ring Collections

Site Information Sheet
INTERNATIONAL TREE-RING DATA BANK
Laboratory of Tree-Ring Research
University of Arizona
Tucson, Arizona 85721, USA

DO NOT WRITE HERE:
Data Classification:
ITRDB only
Permission only
ITRDB No.: DB

Site name Date collected / /

Species name common scientific

Genus/Species code

Location Country State/Province

County or other

Latitude (deg) (min) (sec) N or S (circle)

Longitude (deg) (min) (sec) N or S (circle)

Elevation feet or meters

Sample Source of collection (check all applicable): Living trees

Remnants Archaeol/Historical Other

Number Total sample Total trees measured

Total radii measured

Types of measurement: Total ring width (AA)

Earlywood width (AB) Latewood width (AC)

Minimum density (BD) Maximum density (BE)

Other (specify)

Unit of measurement: 100th mm Other

Site ID X X X

Date RWLIST run / /

Personnel Collector:

Name and institution

Dater:

Name and institution

Measurer:

Name and institution

Principal investigator:

Name and institution

Submittor's classification of data 1) Available to all Data Bank users.
2) Available by permission of submittor only.

I acknowledge that all materials within the site do cross-date and that actual measurements have been submitted.*

Signature of submittor *Date*

*Averaged indices of the final chronologies are requested but cannot be accepted without the original dated ring-width measurements.

Chronology Information Sheet
INTERNATIONAL TREE-RING DATA BANK
Laboratory of Tree-Ring Research
University of Arizona
Tucson, Arizona 85721, USA

DO NOT WRITE HERE:
Data Classification:
ITRDB only
Permission only
ITRDB No.: DB

Identification I.D. # Database #

Type: (Climatic) (Statistical) (Merged) (Other)

If Merged, List Component IDs / /

Type of raw data: (Ring Widths [AA]) (Other)

Statistics First Year Last Year Total Years

Total number included: Trees Radii

Index/SUMAC Date run /

Serial r Stan Dev. Mean sens.

Standard error Mean index

Mean Ring Width % Missing Rings

Curve Fit Option Used (2 most common)

Neg. exponential (0) Neg. exponential (3)
Horizontal line (1) Polynomial (4)
Straight line (2) Other

ANOVA Date run / Common period /

% var. Y % var. YT % var. YC

% var. YCT Var. comp. of Y Error Y

Mean Ring Width % Missing rings

XCORR Date Run / Common Period /

r all series / r within trees /

r among trees

RESPONS Date run /

% due to climate % due to prior growth

Step used Variable type Intervals

Earliest and latest month

Comment

DATE: / /	ESPECE:	ARBRE No.
LIEU:		CODE:

MILIEU PHYSIQUE	Altitude m	Topographie Versant Plateau Depression	orientation exposition pente %	Remarques
	Substrat			
	Sol	Type Epaisseur Horizons		

VEGETATION	Recouvrement Description Composition floristique

DESCRIPTION	Hauteur m	Circonf. cm	1ere brche. vivante m	Plan de situation partiel
	Port et particularités:			
	Carottes: 1 Amont ou N 2 (D) 3 (G)	Orientation	Hauteur cm cm cm	Anomalies

Positionnement de l'arbre dans le schema general !!!!

Appendix C

Sources of Tree-Ring Measuring Programs and Measuring Stages

Belfast Tree-Ring Programs

Dr. J.R. Pilcher
Palaeoecology Centre
Queen's University
Belfast BT7 1NN
Northern Ireland

CATRAS (Computer Aided Tree-Ring Analysis System)

Institut für Holzbiologie
Universität Hamburg
Leuschnerstrasse 91
D-2050 Hamburg 80
Federal Republic of Germany

TRIMS (Tree-Ring Incremental Measuring System)

Madera Software
2509 North Campbell Avenue, #386
Tucson, Arizona 85719
USA

CompU-TA Tree-Ring Measuring System

Mr. Robert Evans
CompU-TA
9533 Grossmont Boulevard
La Mesa, California 92041
USA

Measuring Stages (Laboratory and Field Models) Digital Display Units, Dry Wood Corers, etc.

Fred C. Henson Co.
P.O. Box 3523
Mission Viejo, California 92690
USA

MEASU-CHRON Digital Micrometer – Measuring Stage

Micro-Measurement Technology
P.O. Box 120
Bangor, Maine 04401
USA

System Digital-Positiometer (Laboratory and Field Models) – Measuring Stage

Leopold Kutschenreiter
Siccardsburggasse 64
A-1100 Vienna
Austria

ADDO Tree-Ring Measuring Machine

Parker Instrument
S 216 17 Malmo
Sweden

References

Abraham, B. and J. Ledolter. 1983. *Statistical Methods for Forecasting.* John Wiley and Sons, New York, NY, USA.

Abrahamsen, G., R. Horntvedt, and B. Tveite. 1977. Impacts of Acid Precipitation on Coniferous Forest Ecosystems. *Water, Air, and Soil Pollution* **8**: 57–73.

Adamenko, M.F. 1978. Growth Dynamics of Larch as Indicator of Thermal Regime of Summer Seasons in the Gorny Altai. In: *Regional Geographical Investigations in Western Siberia.* Nauka Publishing House, Siberian Division, Novosibirsk, USSR [in Russian].

Adamenko, M.F. 1986. Reconstruction of Thermal Regime Dynamics of Summer Seasons During XIV-XX Centuries in the Gorny Altai. In: *Dendrochronology and Dendroclimatology.* Nauka Publishing House, Siberian Division, Novosibirsk, USSR [in Russian].

Adamenko, V.N. 1963a. On the Similarity in the Growth of Trees in Northern Scandinavia and in the Polar Ural Mountains. *Journal of Glaciology* **4**(34): 449–451.

Adamenko, V.N. 1963b. Experience of Glacial Occurrence Conditions in the Polar Urals During of 260 Years Period on the Data of Dendrochronological Analysis. In: *Glaciological Investigations.* Section IX. International Geophysical Year Programme, No. 9. Publishing House of the USSR Academy of Sciences, Moscow, USSR [in Russian].

Adamenko, V.N., M.D. Masanova, and A.F. Chetverikov. 1982. *Indication of Climatic Change.* Hydrometizdat Publishing House, Moscow, USSR [in Russian].

Adams, H.S., S.L. Stephenson, T.J. Blasing, and D.N. Duvick. 1985. Growth-Trend Declines of Spruce and Fir in Mid-Appalachian Subalpine Forests. *Environmental and Experimental Botany* **25**: 315–325.

Ahmed, M. and J. Ogden. 1985. Modern New Zealand Tree-Ring Chronologies 3. *Agathis australis* (Salisb.) – Kauri. *Tree-Ring Bulletin* **45**: 11–24.

Akaike, H. 1974. A New Look at the Statistical Model Identification. *IEEE Transactions on Automatic Control* **AC-19**: 716–723.

Alestalo, J. 1971. Dendrochronological Interpretation of Geomorphic Processes. *Fennia* **105**: 1–140.

Aloui, A. 1982. *Recherches dendroclimatologiques en Kromirie (Tunisie).* Thesis Dr Ingenieur. Université d'Aix-Marseille III, Marseille, France.

Andersen, N.O. 1974. On the Calculation of Filter Coefficients for Maximum Entropy Spectral Method Analysis. *Geophysics* **39**(1): 69–72.

Anderson, T. 1971. *Time Series Analysis.* John Wiley and Sons, New York, NY, USA.

Anderson, R.L., D.M. Allen, and F.B. Cady. 1972. Selection of Predictor Variables in Linear Multiple Regression. In: T.A. Bancroft (ed.), *Statistical Papers in Honor of George W. Snedecor.* Iowa State University Press, Ames, IA, USA.

Methods of Dendrochronology

Applications in the Environmental Sciences

Edited by

E. R. Cook
Tree-Ring Laboratory, Lamont-Doherty Geological Observatory, Columbia University, New York, U.S.A.

and

L. A. Kairiukstis
IIASA, Laxenburg, Austria and Lithuanian Academy of Sciences, U.S.S.R.

Only recently have tree rings been fully recognized as a valuable tool in detecting environmental changes. For example, tree-ring measurements have been critically important in studies of forest decline in Europe and North America. There are also attempts to use tree-rings analysis for ecological prognosis to solve large-scale regional problems including the sustainability of water supplies, prediction of growth of agricultural crops, and adoption of silvi-cultural measures in response to ecological changes. More speculatively, dendrochronological methods are also used for dating and evaluating some astrophysical phenomena and for indicating possible increase in the biospheric carrying capacity due to increased atmospheric carbon dioxide.

Such a wide range of application of modern dendrochronology beyond its traditional field has resulted in the development of various approaches. This has placed heavy demands on methodological unification and improvement. This book is a review and description of the state-of-the-art methods of tree-ring analysis with specific emphasis on applications in the environmental sciences.

It is a reference for foresters, climatologists, and broad-profile environmental scientists who are interested in applying the techniques of tree-ring analysis.

From the same publisher: *Tree Rings*, by Fritz Hans Schw
HB 90–277–2445–8; PB 0–7923–0559–0

KLUWER ACADEMIC PUBLISHERS

ISBN 0–79